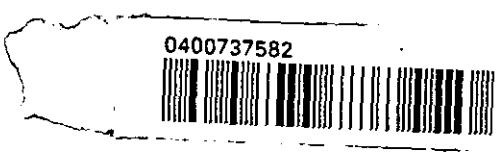

Crossflow Microfiltration Modelling

And Mechanical Means To Prevent Membrane Fouling

by

Guan Mei Zhang B Sc

A DOCTORAL THESIS

SUBMITTED IN PARTIAL FULFILMENT OF REQUIREMENTS

FOR THE AWARD OF

DOCTOR OF PHILOSOPHY OF LOUGHBOROUGH UNIVERSITY OF TECHNOLOGY

December 1992

Dedicated To

My Wife And Son
For Their
Love, Tolerance And Encouragement

CERTIFICATE OF ORIGINALITY

This is to certify that I am responsible for the work submitted in this thesis, that the original work is my own except as specified in acknowledgements or in footnotes, and that neither the thesis nor the original work contained therein has been submitted to this or any other institution for a higher degree.

Guan Mei Zhang

ABSTRACT

The definition, history and applications of Microfiltration (MF) are briefly reviewed in Chapter 1. The physical mechanisms and mathematical models of the filtration process including concentration polarization (CP), gel polarization (GP) and pore blocking are given in Chapter 2.

Crossflow microfiltration membrane fouling and the deposition of solids onto the filter surface have been investigated using a process fluid (seawater), latex and a ground mineral. The performance of various membrane materials has also been studied, including: acrylonitrile, polypropylene, PTFE, ceramic and stainless steel. The seawater filtration work showed in Chapter 3 that good filtrate flux rates can be maintained if material fouling or depositing on the membrane can be prevented from entering the membrane structure. A surface deposit may be removed by mechanical means such as backflushing with permeate or compressed air. This aspect of the work indicated that a more comprehensive study of fouling was required. Existing crossflow filtration membrane models did not adequately represent even the simplest filtration when penetration of the membrane structure applied. Such conditions occurred during latex filtration in Chapter 4.

Latex of varying sizes and density were manufactured and filtrations using acrylonitrile membranes were performed. Considerable deposition of latex inside the membrane pores occurred despite the nominal rating of the membrane being less than the latex particle diameter. Thus the membranes relied on a depth filtration mechanism rather than a surface straining mechanism for filtration effectiveness. A standard filtration blocking model was modified for use in crossflow microfiltration, coupled with a mass balance on the amount of material filtered. This mathematical model was then used to predict and correlate the rate of filtration flux decay with respect to filtration time during crossflow filtration. The model provided acceptable accuracy and is an improvement on existing empirical models for the flux decay period.

Under the circumstances of membrane penetration it is advisable to minimise the amount of material entering the membrane structure. Mechanical means to achieve this were investigated and a novel anti-fouling method using a centrifugal field force and enhanced shear stress at the membrane surface was developed. The filtration of limestone slurries with three different tubular filters are presented in Chapter 5, in which one filter was conventional, the other two novel ones were specially designed for the separation of particles with a density different from that of the liquid, one used a helical channel around the filter, and the other had tangential inlet and outlet endcaps. The centrifugal force produced by the spinning flow around these two filters retarded the approach of particles towards the membrane surface so that the particle deposition was reduced. The results showed such a system was energy efficient, saving 20 % of the energy required to effect a separation of mineral material compared with using the membrane in a more conventional way.

ACKNOWLEDGEMENTS

I wish to express my sincere gratitude and appreciation to my supervisor Dr. R G Holdich for his valuable guidance and support throughout the study. I should also like to thank Dr. I W Cumming for his useful help.

Thanks are also due to Mr. M R Kerry, Mr. S G Graver and Mr. G P Moody for the particle analysis; Mr. R G Boyden, Mr. F Page and Mr. J S Bates for the photographs; Dr. Y Z Lu, Mr. I Sinclair, Mr. T M Neale and Miss. A M Braithwaite for the computer and electronics work; Mr. L Moore, Mr. M J Amos, Mr. A R Eyre, and Mr. J B Powell for the mechanical work; Mr. J Wang and Mr. A Milne for their help in producing latex suspensions.

Further, I should also like to pay my tribute to all the staff of Chemical Engineering for their help, advice and friendship.

I am grateful to the Loughborough University of Technology for the financial support and CVCP (Committee of Vice-Chancellors and Principals of the Universities of the United Kingdom) for an ORS award for the past three years.

CONTENTS

ABSTRACT
ACKNOWLEDGEMENTS

1	**Introduction**	1
1.1	Microfiltration (MF), Ultrafiltration (UF) and Reverse Osmosis (RO)	2
1.2	History	4
1.2.1	Early history	5
1.2.2	Development in later years	5
1.2.3	MF in the 1980s	7
1.2.4	Aspects of MF literature	7
1.3	Membranes	8
1.3.1	Requirements	8
1.3.2	Types	8
1.3.3	Characteristics	13
1.4	Membrane configurations	15
1.4.1	Tubular	15
1.4.2	Hollow fibres	16
1.4.3	Spiral-wound	16
1.4.4	Flat	16
1.4.5	Pleated	19
1.5	Operation systems	19
1.5.1	Single-pass and cascade	20
1.5.2	Batch	21
1.5.3	Continuous	22
1.6	Applications	23
1.6.1	Laboratory tests and medical analysis	23
1.6.2	Effluent treatment	24
1.6.3	Food industries	25
1.6.4	Engineering processes	26
1.6.5	Pharmaceutical and biochemical industries	26
1.7	Permeate flux rate decline and prevention techniques	27
1.7.1	Resistances to the permeate flow	27

1.7.2	Membrane fouling mechanisms	28
1.7.3	Adhesive and removal forces	30
1.7.4	Techniques to prevent the flux rate decline	31
2	**Mathematical Models of Crossflow Microfiltration**	33
2.1	Mathematical models for deposit distribution	33
2.1.1	Models with R_C	33
2.1.2	Models with R_{PB}	35
2.1.3	Model with R_{AD} - Standard blocking model	36
2.2	Mathematical models of deposit resistances	36
2.2.1	Gel-Polarization (GP) model	36
2.2.2	Osmotic pressure model	40
2.2.3	Resistance model	41
2.3	Prediction of permeate flux rate	44
2.3.1	CP and GP resistance modelling	44
2.3.2	Cake resistance modelling	47
2.3.3	Membrane fouling model	49
2.4	Other Methods of prediction	53
2.4.1	By supplying a correction factor	53
2.4.2	By experimental data expressed in process parameters	53
2.4.3	By numerical method	56
2.4.4	By considering the effects of other forces	57
2.5	Brief summary	71
3	**Crossflow Microfiltration of Seawater**	73
3.1	Crossflow filtration of seawater	73
3.2	Experiments with challenge materials	75
3.2.1	Test rigs	75
3.2.2	Computer programs	78
3.2.3	Challenge materials	78
3.2.4	Membranes	80
3.2.5	Calibrations	81
3.2.6	Test items	85
3.2.7	Data acquisition and expression	86
3.2.8	Test results and discussions	87
3.2.9	Comparisons of membrane types	100

3.3	Experiments with North Sea seawater	104
3.3.1	Test rig and control programs	104
3.3.2	Test items	107
3.3.3	Test procedures	107
3.3.4	Test results and discussions	107
3.4	Brief summary	109
4	**Crossflow Microfiltration of Latex Suspension (Investigation of Membrane Fouling Process)**	112
4.1	Test rig	112
4.2	Latex suspensions	115
4.2.1	Equipment and materials	115
4.2.2	Preparation procedures	115
4.2.3	Relevant properties of the produced latex	117
4.3	Calibration and system performance tests	119
4.3.1	Equipment	119
4.3.2	Leakage tests	119
4.3.3	Flow distribution test	121
4.3.4	Channel equivalent height test	124
4.3.5	Membrane selection	124
4.3.6	Minimum pressure difference test	126
4.4	Experimental procedures	127
4.4.1	Rig cleaning and tap water filtration	127
4.4.2	Transmembrane pressure measurement	127
4.4.3	Membrane resistance test	128
4.4.4	Flux rate decay tests	129
4.4.5	Latex particles concentration measurements	130
4.4.6	The investigation into the early stage of membrane fouling	130
4.5	Test results and discussions	131
4.5.1	The particle concentration variation during filtration from Hiac/Royco sizing equipment	134
4.5.2	The effects of the membrane pore sizes on the flux rate	137
4.5.3	Structure of membranes and foulants observed by SEM	139
4.6	Mathematical modelling and predictions	146
4.6.1	Mathematical modelling of particle deposition	

	during filtration	146
4.6.2	Estimation of membrane characteristics	151
4.6.3	Prediction of permeate cumulative volume or flux rate with process time	156
4.6.4	Discussions on the predictions	163
4.7	Brief summary	165
5	**Crossflow Microfiltration Incorporating Rotating Fluid Flow (Anti-Fouling Technique)**	167
5.1	Test rig and experimental procedures	167
5.1.1	Test rig	167
5.1.2	Experimental procedures	170
5.2	Test results and discussions	174
5.2.1	Effect of temperature	174
5.2.2	Membrane resistance	175
5.2.3	Effect of filtration pressure	182
5.2.4	Effect of shear rate	182
5.2.5	Effect of particle size, concentration and centrifugal acceleration	187
5.2.6	Comparison of models and rotating velocities	190
5.2.7	Depth of the deposit	194
5.2.8	Energy efficiency	194
5.3	Brief summary	197
6	**Conclusions and Recommendations**	198

NOMENCLATURE

REFERENCES

FIGURES

Fig	1	The place for MF, UF and RO as separation processes [Osmotic Inc., 1985]	3
Fig	2	The configurations of crossflow and dead-end filtration	4
Fig	3	Sharp & diffusive cutoff vs. retention efficiency	15
Fig	4	Membrane configurations	17
Fig	5	Dead-end filtration cells	19
Fig	6	Basic operating diagram	20
Fig	7	Single-pass and cascade system	21
Fig	8	Batch system	22
Fig	9	Continuous system	22
Fig	10	Resistances to the filtration	28
Fig	11	Two filtration models	35
Fig	12	The schematic diagram of "Three-Zone" model .	46
Fig	13	The interaction between turbulent burst and particles	67
Fig	14	Layout of laboratory test rig	76
Fig	15	Size distribution of solids in seawater and silica	79
Fig	16	Size distribution of seawater algae in cleaned tap water	80
Fig	17	Shedding effect of the rig at 25 l/min	84
Fig	18	Shedding effect of the rig at 12.5 l/min	84
Fig	19	Flux rate of PTFE and ceramic membranes with tap water	88
Fig	20	Flux rate with clean water (Fairey and Enka)	88
Fig	21	Water flux rate of ceramic filter	90
Fig	22a	Flux rates of metal membranes (Re 8500)	91
Fig	22b	Flux rates of metal membranes (Re 42500)	91
Fig	23	Flux rate of clean water (Versapor)	92
Fig	24a	Permeate flux rate at 5 mg/l of lipid	93
Fig	24b	Permeate flux rate at 10 mg/l of lipid	94
Fig	24c	Permeate flux rate at 20 mg/l of lipid	94
Fig	25	Flux rate of Enka filter at different concentrations	96
Fig	26a	Flux rate of ceramic filter at low pressure	97
Fig	26b	Flux rate of ceramic filter at high pressure	97
Fig	27	Flux rate of Versapor membrane at high pressure	98
Fig	28	Flux rate of algae on metal membrane	99

Fig	29	Flux rate of algae on polymer membrane	99
Fig	30	Polymer membrane	102
Fig	31	Metal fibre membrane	103
Fig	32	Layout of seawater filtration rig	105
Fig	33	Flux rate for different filters	108
Fig	34	Flux rate of ceramic filters over several days	108
Fig	35	Flux rate of metal filters with or without precoating	109
Fig	36a	Top plate of the module (unit: mm)	113
Fig	36b	Bottom plate of the module (unit: mm)	113
Fig	36c	Inlet side connector (unit: mm)	114
Fig	36d	Outlet side connector (unit: mm)	114
Fig	36e	Configuration of the filter module	114
Fig	37	Particle size distributions of test latices	118
Fig	38	Streamlining leakage test	120
Fig	39	Dyed flow distribution during the minimum flow rate test	122
Fig	40	Channel flow rate distribution test	123
Fig	41	Filtered tap water test results	125
Fig	42	Minimum pressure test	126
Fig	43	Pressure distribution test	128
Fig	44	Membrane resistance test	129
Fig	45a	Variation of particle counts of six channels during filtration	136
Fig	45b	Variation of total particle counts of six channels during filtration	136
Fig	46	Permeate rates with different membrane pore sizes	138
Fig	47a	Photographs of fouled membrane G by SEM	140/1
Fig	47b	Photographs of fouled membrane H by SEM	142/3
Fig	48	Photographs of 1.2 μm membranes with No 11 latex by SEM	144
Fig	49	Photographs of 0.45 μm membranes with No 11 latex by SEM	145
Fig	50	Photographs of 0.45 μm membranes with No 9 latex by SEM	146
Fig	51	The relationship between permeate flux rate and	

		transmembrane pressure	147
Fig	52	Mathematical analysis of test G4	149/50
Fig	53	Comparisons of measured and predicted permeate flux rate	159/62
Fig	54	The layout of test rig	168
Fig	55	The configuration of filter module	168
Fig	56	Endcaps of tangential and normal modules	169
Fig	57	The side view of the filter with helically wound o-ring	170
Fig	58	Inlet pressure (P1) as a function of feed flow rate for different endcap types	171
Fig	59	Pressure inside the membrane module (P3) and downstream of the filter (P2) for different endcap types	172
Fig	60	Permeate flux rate decay with time and the effect of variable temperature	173
Fig	61	Particle size distributions of fine and coarse powders	174
Fig	62	Cumulative permeate volume with time and use of initial rate for membrane resistance	176
Fig	63a	Equilibrium permeate flux rate with pressure using different endcaps (1.5% coarse powder)	183
Fig	63b	Equilibrium permeate flux rate with pressure using different endcaps (1.6% fine powder)	183
Fig	64a	Equilibrium permeate flux rate with pressure using different endcaps (4% coarse powder)	184
Fig	64b	Equilibrium permeate flux rate with pressure using different endcaps (3% fine powder)	184
Fig	65a	Equilibrium permeate flux rate with pressure at various crossflow velocities using normal endcaps (coarse powder)	185
Fig	65b	Equilibrium permeate flux rate with pressure at various crossflow velocities using normal endcaps (fine powder)	185
Fig	66a	Equilibrium permeate flux rate with pressure at various crossflow velocities using tangential endcaps (coarse powder)	186
Fig	66b	Equilibrium permeate flux rate with pressure at various crossflow velocities using tangential endcaps	

(fine powder) 186
Fig 67 Schematic diagram of particles in stationary orbit around filter due to balance of centrifugal field and liquid drag force 187
Fig 68a Permeate flux rate with tangential endcaps at different particle sizes (1.5%) 191
Fig 68b Permeate flux rate with tangential endcaps at different particle sizes (3 %) 191
Fig 69 The deposits on the filter with different endcaps 192
Fig 70a Equilibrium flux rate as a function of power requirement (1.5% coarse powder) 195
Fig 70b Equilibrium flux rate as a function of power requirement (1.6% fine podwer) 195
Fig 71a Equilibrium flux rate as a function of power requirement (3% coarse powder) 196
Fig 71b Equilibrium flux rate as a function of power requirement (4% fine powder) 196

TABLES

Table 1	Early history of membrane research	5
Table 2	Commercial developments of MF	6
Table 3	Comparison of configurations	18
Table 4	Levich's "Three-Zone" model	46
Table 5	Parameters in Mehanc's (1986)model	56
Table 6	Hiac/Royco readings vs. solids concentration	82
Table 7	Particle retention efficiencies of Fairey filters	92
Table 8	Lipid concentration in the feed and filter at different lipid concentration in the tank	95
Table 9	Metal membrane resistance	101
Table 10	Polymer membrane resistance	101
Table 11	Seawater particle size distribution and solid concentration during trial period	106
Table 12	Some properties of the produced latices	119
Table 13	Test conditions with filtered tap water	125
Table 14	Test results of latex suspensions with Versapor membranes	132/3
Table 15	Latex particle concentrations of all tests	135
Table 16	Particle concentrations in Test H5	137
Table 17	Test results and pore size estimation of membranes G,H and I	154
Table 18	Membrane resistance, pore length and density of membranes G, H and I	156
Table 19	Prediction of flux rate with process time	158
Table 20	Membrane resistance at 1.5% solid concentration (Coarse powders)	177
Table 21	Membrane resistance at 4 % solid concentration (Coarse powders)	178
Table 22	Membrane resistance at 1.6% solid concentration (Fine powders)	179
Table 23	Membrane resistance at 3% solid concentration (Fine powders)	180
Table 24	Conditions of membrane surface according to models based on free and hindered dispersions	193

APPENDICES

Appendix 1 Photographs of microfiltration membranes

Appendix 2 Mass transfer correlations by Gekas and Hallström (1987)

Appendix 3 Test results in Chapter 3

Appendix 4 Files in Table 14 of Chapter 4

Appendix 5 Files in Tables 20 to 23 of Chapter 5

Appendix 6 Relevant published papers

<<Crossflow Filtration of Seawater>>
Holdich R G, Zhang G M, Boston J S
Filt & Sep Mar/Apr (1991) pp117-120

<<Seawater Crossflow Filtration>>
Holdich R G, Zhang G M
Filtech'91 pp19-27 Karlsruhe, Germany

<<Crossflow Microfiltration Incorporating Rotational Fluid Flow>>
Holdich R G, Zhang G M
Trans IChemE v70 Part A Sept(1992) pp527-536

CHAPTER 1

Introduction

The definition, history and applications of Microfiltration (MF), the types of MF membrane, filter modules and operating modes, the fouling and re-entrainment mechanisms as well as anti-fouling techniques are briefly reviewed in Chapter 1.

The physical mechanisms and mathematical models of the filtration process including concentration polarization (CP), gel polarization (GP) and pore blocking are surveyed in Chapter 2. This survey was comprehensive in order to test as many mathematical models as possible with the later observed phenomena. Subsequently some theories were not used later if the model on which the theory was based did not agree with the experimental results.

The crossflow microfiltration of simulated and real seawater with various membranes and conventional filter modules is described in Chapter 3; the results showed that membrane fouling, especially with real seawater, was one of the major causes of flux rate decline during the process in spite of the application of some conventional anti-fouling techniques. Further investigation, therefore, was carried out in Chapter 4 to explore the mechanism of the membrane fouling process.

The initial stages of membrane fouling were investigated by the crossflow filtration of latex suspensions in Chapter 4. The results showed that the fouling process started with partial pore blocking if particles smaller than the pore size existed. The crossflow could reduce the particle deposition on the membrane surface which, on the other hand, facilitated the pore blocking process as happened in this study as well as in the seawater filtration in which the membrane was fouled by "clean" seawater. Therefore, it is important to prevent the particles from approaching the membrane surface to block the pores under the condition of maintaining reasonable permeate flux rates. One such novel technique is presented in Chapter 5.

The crossflow filtration of limestone with three different tubular filters is described in Chapter 5, in which one filter was conventional, the other two were novel ones which were specially designed for the separation of particles with a density different

from that of the liquid; one had a helical channel around the filter, and the other had tangential endcaps. The centrifugal force produced by the spinning flow around the filter retarded the approach of particles towards the membrane surface so that particle deposition was reduced. The results also showed that the filter with tangential endcaps could save as much as 20 % of the energy compared to the conventional one.

Conclusions and the recommendations for the further work are put forward in Chapter 6.

1.1 Microfiltration (MF), Ultrafiltration (UF) and Reverse Osmosis (RO)

Microfiltration (MF) is a pressure-driven membrane separation process in which the membrane plays the role of a material boundary to control the transport of matter across it - it remains impermeable to a specific substance or groups of substances depending on the properties and working conditions of the system. The other two pressure-driven membrane separation processes are Reverse Osmosis (RO) and Ultra-filtration (UF).

All these processes are attractive for industries due to their following advantages [Cartright, 1991]:

Continuous process - resulting in automatic and uninterrupted operation.
Low energy consumption - involving neither phase nor temperature changes.
Modular design - no significant size limitations.
Maintenance - minimum of moving parts with low maintenance requirements.
Efficiency - discrete membrane barrier to ensure clear separation;
Purity - no chemical additions required.

The distinctions between these three processes are quite arbitrary, the operating principles are similar and applications overlap. Some differences are, however, clear and these will be discussed in the following sub-sections:

1) Separation range

They can be distinguished by the size of the particles or molecules retained by the membranes, so that each process can be defined by the rated pore size shown in Fig 1, in which RO is less than 0.001 μm, UF is 0.001 - 0.1 μm, MF is 0.1 - 20 μm. These figures are used here only for the purpose of illustrating the range of membrane

separation processes. Some authors have different definitions for the range of micro-filtration, e.g. 0.02 - 14 μm [Ballow & Porter, 1980], 0.05 - 20 μm [Porter & Billiet, 1986], 0.01 - 10 μm [Boonthanon et al, 1991], and 0.1 - 10 μm [Cartwright, 1991] etc.

2) Solubility

MF can only separate suspended particles (pollen, starch, DNA, bacteria), UF can separate macromolecules (protein, red blood cells) as well as particles, whereas RO can separate small molecules and ions.

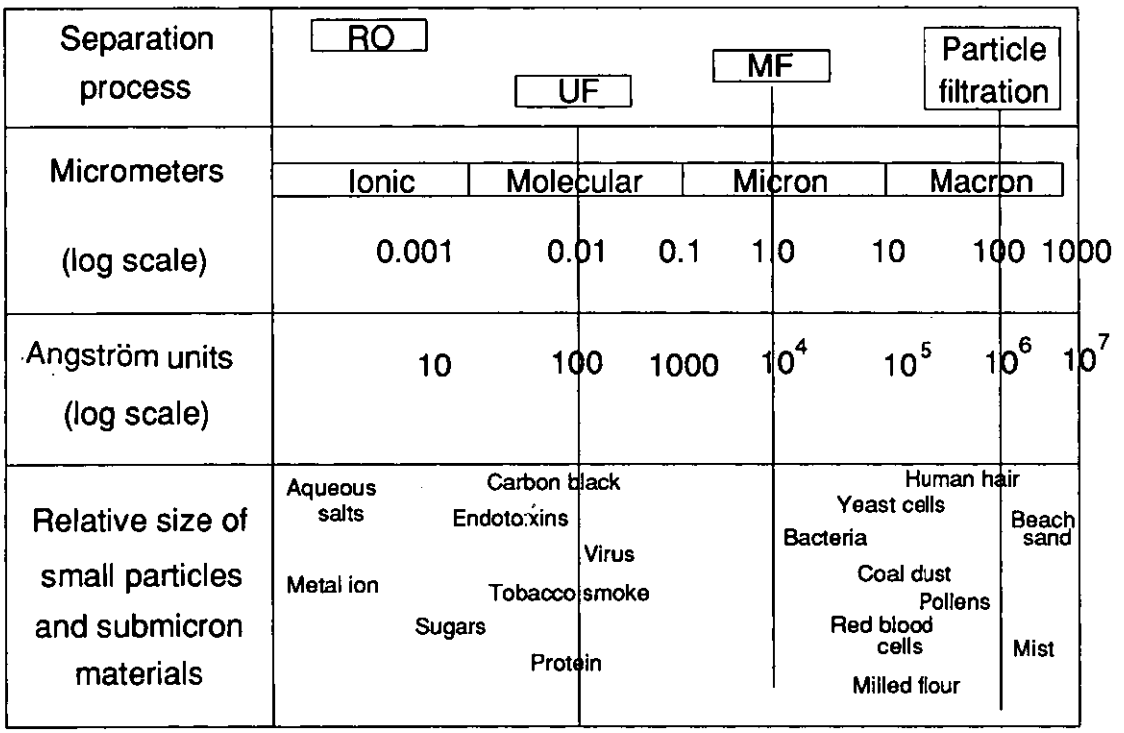

Fig 1 The place for MF, UF and RO as separation processes [Osmotic Inc., 1985]

3) Operating flow types

In most cases the feed flow of RO, UF and MF is crossflow in which the feed flow is parallel to the membrane surface as shown in Fig 2a, however, UF and MF are also operated under dead-end configuration in which the feed flow is normal to the membrane surface as shown in Fig 2b, the latter configuration is not only common in laboratory studies but is also found industrial applications as cartridge filtration which will not be discussed any further here.

4) Operating pressure

RO needs a high hydraulic pressure (20 - 100 Bar) to overcome osmotic pressure; whereas MF and UF work under lower pressure (0.1 - 10 Bar) because the macromolecules solutes and colloidal species in these two processes usually have insignificant osmotic pressures.

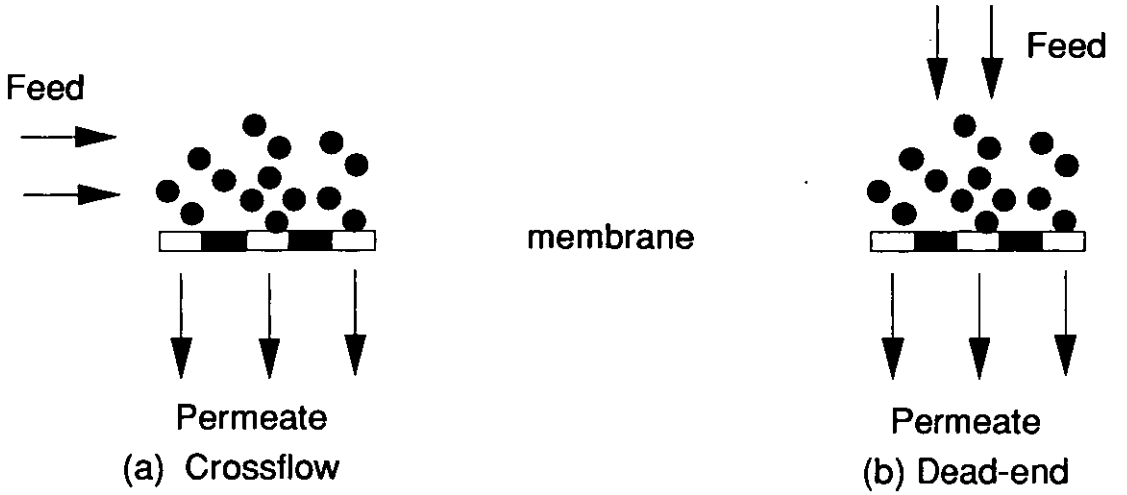

Fig 2 The configurations of crossflow and dead-end filtration

5) Separation mechanisms

The mechanism of MF and UF is "sieving" and "sorption", the permeate selecting process is pore-suspended species interaction, the permeate flow is viscous type, whereas the permeate selecting process in RO is membrane material-permeate interaction, the permeate flow is diffusive.

6) Chemical property

MF changes none of the chemical properties of the fluid whereas in UF and RO , separation of the dissolved species modifies the chemical potential and creates a gradient which tends to make the separated solvent diffuse back in the reverse direction.

1.2 History

As a process, membrane separation is as old as any living organism; as a subject, it has been studied for hundreds of years; however, as a practical technique, it is new and has a history of only 30 years; as a science, there is still more to explore.

1.2.1 Early history

The first documented membrane experiment was described by the friar Nollet in 1748 regarding the semipermeability of pig bladder to wine. Some of the earliest artificial membrane preparations have been attributed to Fick who discovered the collodion membrane (cellulose nitrate) in 1855 or so.

The early history of membrane technology was reviewed in detail by Ferry (1936). The milestone of developments of the pioneers are listed in Table 1, reproduced from Porter & Billiet (1986).

Table 1

Early history of membrane research

1748	Nollet	Osmosis through semipermeable animal bladder
1845	Matteucci & Cima	Asymmetric permeability difference
1855	Fick	First synthetic membrane (nitrocellulose)
1872	Baranetzky	First synthetic membrane
1887	van't Hoff	Osmotic pressure equation
1890	Sanarelli	Improved the filter characteristics
1906	Bechhol	Determining pore size, produced graded pore sizes by varying collodion concentration
1907	Bigelow & Gemberling	Regulated pore size by varying evaporation time
1911	Schoep	Regulated pore size by non-volatile additives in casting solution
1915 & 1917	Brown	Regulated pore size by varying alcohol in quench water
1921	Eggerth	Regulated pore size by varying alcohol/ether ratio in casting solution
1925	Asheshov	Regulated pore size by volatile additives
1930	Elford	Studied gel structure-produced highly permeable membrane using amyl alcohol, acetone, acetic acid and water

1.2.2 Development in later years

The inventions of Bechhol, Bigelow & Gemberling, Schoep (1911) and Brown (1915 & 1917) were soon used by Zsigmondy & Bachmann (1918) in Germany to develop the technology of manufacturing nitrocellulose and cellulose-ester membranes on a

semi-commercial scale and the product was named "membrane-filter". This kind of filter was first produced on a small commercial scale by Sartorius-Werkes in 1927 and found its application in laboratory research work.

Table 2

Commercial developments of MF

1918	Zsigmondy & Bachmann	Developed commercial process
1927	Sartorius-Werkes	Began commercial production
1947	Mueller	Membrane filter method for culturing bacteria [Mueller, 1947a]
1950	Goetz	Improved production method and grid-marked membrane [Goetz, 1947 & 1951]
1952	Lovell Chemical Co	Designed and constructed large scale equipments production
1954	Millipore Corp	First membrane company formed
1962	Gelman Instrument Co	Cellulose tri-acetate membrane
1962	Sartorius Co	Regenerated cellulose membrane
1963	Millipore, Gelmann, Sartorius, S & S	PVC and nylon membranes
1963	Fleischer, Price & Walker(G.E.)	Track-etch membrane [Feischer et al 1963,1964 & 1969]
1964	Gelman Sciences	Fabric reinforced membrane
1964	Selas Flotronics	Silver membrane [Minneci & Paulson, 1988]
1970	Celanese	Polypropylene membrane [Druin et al, 1974]
1970	Gore Corp	PTFE membrane [Gore, 1976a & 1976b]
1975	Hydronautics & Membrane	Thermal-inversion process
1979	Gelman	Polysulfone
1980	Millipore	Polyvinylidene fluoride
1981	Nuclepore	Polyester
1984	Norton Co., Ceraver	Alumina

No significant developments in MF, either academic or commercial, were achieved during the following 20 years until the late 1940s when it was used to detect the microbial contamination of water in Germany [Mueller, 1947a & 1947b].

In the early 1950s, membranes began to be recognized for their value and commercial potential through the use of microfiltration for air monitoring, laboratory analysis, and diagnosis testing. Several European and USA companies were formed in the mid 1950s and early 1960s to explore the above technologies and for other filtration industries including UF for dialysis and RO for desalination.

Activities were accelerated in the mid 1960s and early 1970s, MF was applied for parenteral drug filtration for injectable substances, manufacturing particle- and bacteria-free rinsing water for the semiconductor industry, and medical devices such as intravenous filters and spike vents.

Numerous types of materials, mainly polymers, have been employed in manufacturing MF membranes during this period. The milestones of the developments are listed in Table 2, also reproduced from Porter & Billiet (1986).

Although MF was the first commercialised membrane separation technology, it was not as competitive as UF and RO were to other traditional technologies, because it was usually carried out in dead-end style plate and frame devices or pleated cartridges due to the fragility of the porous membranes. This configuration, which results in low permeate flux rate, short membrane lifetime and high cost of running, seriously limited its application in industries.

1.2.3 MF in the 1980s

The 1980s started a new era for MF, during this decade MF had significant developments brought about by two major achievements.

The emergence of many new inorganic membranes and novel techniques in manufacturing polymer membranes broadened the applications of microfiltration, some of which were thought impossible just a few years ago.

The shortcomings caused by dead-end configuration were overcome by crossflow operation in which the high shear force reduces the materials depositing onto the membrane surface, and therefore yields higher permeate flux rates, long membrane lifetime, low cost and the process can be time saving and highly efficient.

It is now not only a major subject studied by most laboratories engaged in separation processes but also an important business.

1.2.4 Aspects of MF literature

A great deal of literature on MF have been published since the 1960s. These contributions can be roughly catalogued into two groups:

1) Highly theoretical literature on the transport mechanisms of the process. Most of the topics were about concentration polarization and membrane fouling since these are the most unfavourable factors for membrane filtrations. The theories in this field have not dramatically changed since Brian (1965) and Johnson Jr et al (1966) published their first and rather simple equations. A large number of minor extensions to the original ones have been presented. The introduction of computer technology for numerical calculation and process simulation in the 1980s facilitated the research in this field.

2) Literature about membrane manufacturing, commercial applications, operating techniques, plant designs and market research has been available. Computer technology has also been widely used for system controlling and data analysis. These papers occupy a larger part of the publications on MF.

1.3 Membranes

1.3.1 Requirements

Since the membrane is the key element of a microfiltration process, it must have:

- high hydraulic permeability to liquid (water) and high retention efficiency to particles;
- good mechanical durability, chemical and thermal stability as well as relatively long lifespan;
- ease of restoration of the initial permeability after cleaning/sanitizing;
- low cost and large scale for manufacture.

1.3.2 Types

The MF membranes can be catalogued into three groups by their nature: natural (biological), polymeric (organic) and mineral (inorganic).

a) Natural

Animal membranes (e.g. pig and fish bladders) were the first ever used isotopic membranes [Michael, 1968]. Because of their poor performances and limited sources, they are not used for MF nowadays.

Fabric materials have been used for filtration for a long time, and still are [Dahlheimer et al, 1970; Hunt et al, 1987a, 1987b].

Metal material should be sorted into this group, however, due to their costs and manufacturing processes, they are listed in the mineral group.

b) Polymeric

The first polymer membrane was commercialized by Zigmondy & Bachmann in Germany in 1918. It was a nitrocellulose film based on the solution cast method.

There are many different membranes today based on different synthetic processes. Some membranes manufactured by these processes are shown in Fig 1 of Appendix 1 respectively.

1) Phase inversion or wet/dry cast method

Both methods use a solvent to dissolve the polymer and a non-solvent material as the pore-former. The solution is then spread on to the surface of the pore former on which the solvent will then evaporate under carefully controlled temperature, volumetric air flow and humidity. During the initial loss of the solvent, the concentration of the pore former begins to affect the solubility of the polymer. At this point, the initially homogeneous colloidal (sol) becomes a gel. The two methods differ from this stage: in the wet process, complete solvation is restricted by immersing the formed film into a quench bath to remove the remaining solvents and pore forming agents, while the dry process allows complete evaporation of both solvent and non-solvent and no quench stage is involved. The membranes from this method are asymmetric due to the differences in the rate of evaporation of solvents from the upper and lower side of the cast film [Goetz, 1947]. The asymmetry ranges from 2:1 to 5:1.

Various kinds of materials may be used for this method: nitrocellulose, acrilic copolymers, polyvinylidene difluoride (PVDF), mixed-esters of cellulose, cellulose triacetone (CTA), nylon, polypropylene and polysulphon polymers (POS).

They can be either hydrophilic or hydrophobic, and the forms can be tubular, sheet or hollow fibres or pleated into any cartridge, they are usually 100 μm thick, and become 3 - 8 mm thick when supported by a felt of nonwoven cloth [Le & Ward, 1984] or a weft [Schiele & Alt, 1978; Knibbs, 1981; Tanny et al, 1982]. The pore size can be rated as low as 0.2 μm.

This is the oldest and most common method, however, the membranes by this method have about 90% of the membrane market share.

2) Stretch method

This is the second most common method for manufacturing MF membranes with about 10% of the polymer membrane market share.

It is based on stretching a polymer film such as polypropylene (Celgard) or Teflon - polytetrafluorethylene (PTFE) (Goretex) [Brock, 1983] to form the pores.

They are 1-2 mm thick and hydrophobic, but wettable by applying surfactants. The pore size can be as low as 0.1 μm

3) Thermoplast method

These membranes consist of more or less graded powders. The grains are either fixed by heating or bonded by porogenic agents [Rivet, 1979]. The materials for this method are polyvinylchloride (PVC), polythylene, polystyrene and polymids.

The rated pore size can be as low as 0.1 μm.

Since the shape, porosity, thickness, pore-size distribution can be precisely controlled by the process, they can be used alone without supporting substrates.

4) Track-etch method [Porter, 1975]

The film is exposed to a collimated beam of fission-fragments which produces tracks across the entire thickness of the film, and subsequently the film is etched to produce pores. Polycarbonate and polyesters are used to make the so-called "Track-etch" or "capillary-pore" membranes.

The membranes made in this way are only 100 μm thick and offer extremely homogeneous morphology, the pores are rectilinear cylindrical and therefore have a sharp "cutoff" on particle size retention.

5) High-speed method

The so called Sunbeam process creates membranes by crosslinking monomers and oligomers under either an ultraviolet or electron-beam source. The membranes may be either hydrophilic or hydrophobic, 2 - 4 mm in thickness when supported by nonwoven fabric materials [Tanny, 1986]

The main advantage of this process is that it can yield 1.5 - 2.4 m wide webs at 105 - 180 m/min speed comparing to the conventional process which usually works at 1.5 - 4.5 m/min for 0.3 - 0.9 m wide webs.

6) Sintering method

PTFE may be sintered like metal to obtain hydrophobic membranes with an absolute rating of 0.1 μm [Societe Belge de Filtration, 1975].

7) Laser method

This new method was developed in the late 1980s for manufacturing membranes. The membrane is comprised of a flat foil of polymers, with cylindrical or funnel-shaped pores formed by pulsed laser beams. The pores are perfectly round and their positions, density (numbers in unit area) can be controlled by the laser. [Flottmann & Trezel, 1990].

This membrane can improve separation by particle size, resistance to blinding, and the rate of permeate flux.

8) Composite method

When two microporous films are layered together, the resulting pore size distribution will be narrower. The pore size may be as low as 0.01 μm which is already the lowest limit of MF by any definition [Steadly & Laccetti, 1988].

c) Mineral

The first filtration equipment with mineral materials was nothing but a cracked jar [Mason, 1991]. However, it was the late 1950s when the synthetic mineral membranes were originally developed by Oak Ridge National Laboratory in USA and CEA in France. In the early 1960s, a nickel membrane was made by plating nickel on nickel wire mesh with pore sizes 0.05 to 0.3 μm. The first commercial mineral membrane was a silver one by Selas Flotronics in 1964 based on the similar process. The real application of mineral membranes started in the early 1980s as a result of new powder metallurgy. Their emergence has greatly increased the potentials of MF in industries due to their unique features:

- Thermal stability
- Mechanical stability
- Chemical resistance
- Controlled, defined, stable pore structure
- Microbiological resistance
- Backflush capability
- Reduced fouling/flux loss

- High throughput/volume.

The commercial mineral membranes can be roughly divided into three groups: ceramic, metal and composite. Some ceramic membranes are shown in Fig 2 and metal membranes in Fig 3 respectively in Appendix 1.

1) Ceramic

The ceramic membranes can be made by sintering method. They are formed by the use of layers of different particle sizes. The smaller the pore size, the thinner the layer. The matrix is a few hundredths of a micron thick and consists of grains of some tenths of a micron. A layer of some tenths of a micron with even finer grains is then deposited on the matrix surface to obtain the desired absolute ratings. The details of the process can be obtained in the paper presented by Charpin et al (1988) and its references 15-18.

The materials can be metal oxides, nitrides, and carbides, e.g. α-Al_2O_3, γ-Al_2O_3 [Hsieh et al, 1988], glass (90% SiO_2) [Ogasawara et al, 1991], silicon carbide (SiC) [Charpin et al, 1988].

Most of the ceramic membranes are asymmetric in structure and have a porosity of 50%. They are excellent in chemical, thermal and mechanical properties, and used in tubular or monolithic multichannel modules, it was recently reported that ceramic membranes in sheet form had been commercially manufactured [Cowieson, 1992]. The disadvantages include small-scale production and higher costs than polymeric membranes.

2) Metal

Porous metals for metal membranes are available in a variety of forms including sintered powders, wire mesh, sintered mesh, sintered fibres, and photo etched screens. The porosity is also about 50% and pore size can be 1 μm. They can be operated with the help of electric or magnetic fields to enhance particle rejection ability.

The materials may be stainless steel by sintering; silver by plating [Druin et al, 1974], or by temperature induced phase separation [Minneci & Paulson, 1988], or by electron or ion irradiation [Japanese Patent Application, 1986]; aluminium by double-sided etching [Bailey, 1991], copper, metal fibres and sintered metal fibres

[de Bruyne, 1990 & 1991].

Metal membranes are tougher, but more expensive in cost and less resistant to acid or alkaline than ceramic ones.

3) Composite

Most ceramic membranes are composed with several layers different grain size. However, mineral membranes can be further made into composite with itself or another material by sintering, e.g zirconia on inconel 600 [Davidson et al, 1990], carbon on sintered metals [Boudier, 1990]. The resulting membranes have a better mechanical durability than the ceramic membranes.

1.3.3 Characteristics

a) Permeate rate

Permeate rate (or flux rate) is pressure dependent but often less so than in RO, it also normally increases with increasing feed flow rate and temperature, decreases with concentration and with operating time until a force balance is set up on the membrane surface. The mechanism for this will be discussed in the following chapter.

b) Surface charge

Most MF membranes are negatively charged, however, some membranes like fibrous asbestos can be made into positively charged in order to increase its retention efficiency [Blosse, 1982]. A type of charged membrane has been reported in the manufacture of ultrapure water [Yasminov et al, 1990].

c) Lifespan

Membrane life normally decreases with increasing temperature and depends on the time-temperature condition of exposure to cleaning/sanitizing methods.

d) Hydrophilic and hydrophobic

The hydrophobic membranes are especially suitable for oil/water separation, and it can be wetted by surfacant agents for the separation under aqueous conditions.

e) Symmetric and asymmetric

Most MF membranes are asymmetric in structure except the screen type ones although the ratio of asymmetry is usually less than five [Gutman, 1987]. In some

applications, the asymmetric membranes are used in a reverse way as those in RO and UF: the opening side faces the feed flow to work as an inherent prefilter for the membranes.

f) Retention efficiency

1) Porous filter

Most MF membranes have a "nominal" retention efficiency due to the broad pore size distribution - some pores are even several times as large as the rated values so that they can only retain some percentage (e.g. 90%, 95%, 98%) of all particles which are equal to the rating of the membrane. Furthermore, the retention efficiency depends on the depth and tortuosity of the matrix which also trap a number of particles below the rated pore size. By this means, these membranes have a "diffusive cutoff" characteristic. The membranes are catalogued by some authors as "porous media filter".

2) Screen filter

The membranes made by etching or laser method have unique pore size and therefore their retention efficiency is "absolute". They can retain as high as 99.9999% of the particles equal to or larger than their pore ratings. So that they have a "sharp cutoff" and catalogued as "screen filter"

The relationship between the retention efficiency and different "cutoff"s is schematically shown in Fig 3.

However, the above definitions are nominal since there are other factors which determine the retentivity, e.g. the size, shape, charge and deformability of the particles, and therefore, the flake or linear flexible particles are less prone to clog the pores than the shephrical hard particles with the same nominal size. Fluid shear stress near the pores, electrostatic forces, van der Waals force, pH values of the fluid and the dynamic membrane formed from particles or solutes will also affect the retentivity.

The retention is largely pressure independent for incompressible deposited film or cake, but somewhat sensitive to flow rate.

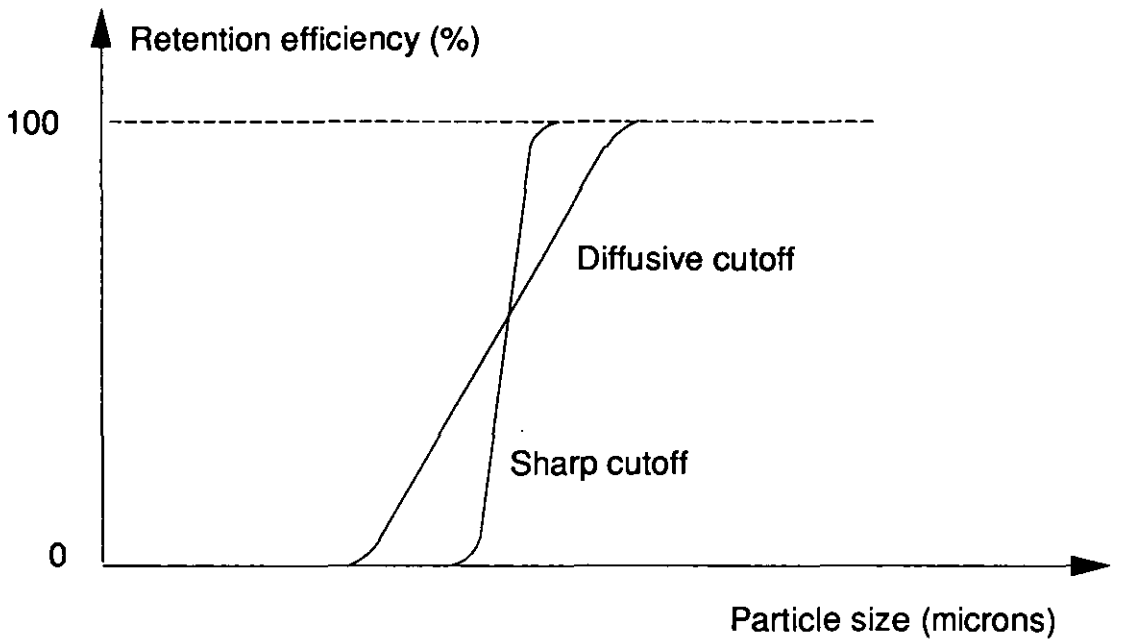

Fig 3 Sharp & diffusive cutoff vs. retention efficiency

1.4 Membrane configurations

Membranes are manufactured in modular forms which are the basic elements of any membrane system. Membrane systems essentially consist of series and/or parallel arrangements of these modules. A number of MF modules have been developed differing principally in the size and shape of the flow channels in which the membranes are mounted.

1.4.1 Tubular (Fig 4a)

The tubes usually have an internal diameter (ID) between 4 and 25 mm. The feed solution is pumped through the tube. There are two forms of tubes:

1) Inside feed - this is the most popular form, the membrane is on the inside of the tube by casting, inserting or gluing. This tube is then fixed solely or in bundle into a permeate collection shell which is usually made of stainless steel or plastics, or left open so that the permeate drips continuously and is collected in a drip tray or tank.

2) Outside feed - the membrane is on the outside of the tube. The feed flow passes between the outside of the tube and the shell, the permeate leaves from the internal side of the tube.

Tubular membrane is the simplest form, they are not prone to blockage, easy to clean chemically and physically, and easily removed or replaced. Its disadvantages are large space for installation of a given membrane area, the high "hold-up" volume, difficult to check leakage if in bundles and relatively high energy costs for pumping.

1.4.2 Hollow fibres

They are formed as self-supporting tubes with 0.05 to 1.2mm ID. A bunch of such fibres are placed in a shell and the ends are sealed in a plastic end block provided with fittings. The flow is usually fed inside of the fibres for MF applications. (Fig 4b)

This configuration results in small overall dimensions, low hold-up volumes, and low process pumping costs. The disadvantages are prone to blockage, difficult to clean, plus impossible to determine the leakage of single fibres.

1.4.3 Spiral-wound

Two rectangular flat membranes are placed one on the top of the other, separated by a porous material, and sealed together on three sides. The fourth side is separately sealed along the length of a tube perforated to form a header for removing the permeate which passes through the membranes from the outside. A spacer is laid on the top of the two membranes which are then rolled round the header tube to form the spiral. The spiral is sealed into a cylindrical housing and the process fluid is fed from one end to the other through the region occupied by the spacer and across the membrane surface. Permeate will enter the porous membrane interspace and spiral round to the header. The flow through the module is basically laminar although a degree of turbulence is promoted by the spacers. (Fig 4c)

They are cheap, very compact and have low pumping costs, but are easily blocked.

1.4.4 Flat

A flat membrane is supported by a porous plate through which the permeate leaves. The feed is passed at high speed across the surface of the membrane between the spacers or flow channels, which are 0.2 to 4 mm high. Permeate passes to the interspace between the coupled pairs of membranes and is led out through a header.

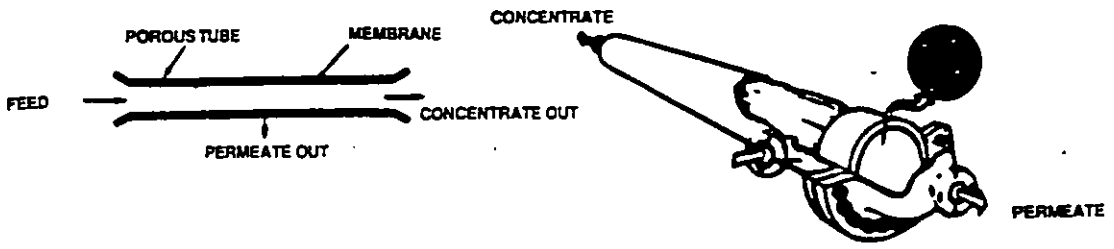

(a) Tubular (b) Hollow fibres

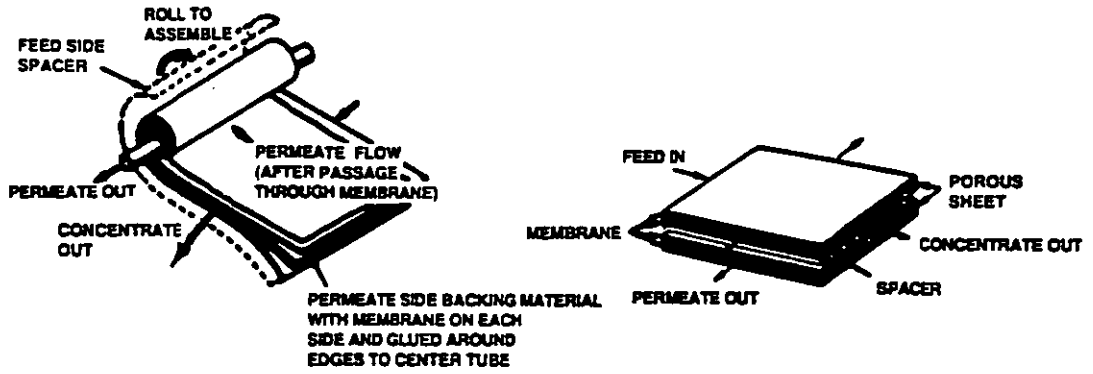

(c) Spiral wound (d) Plate & Frame

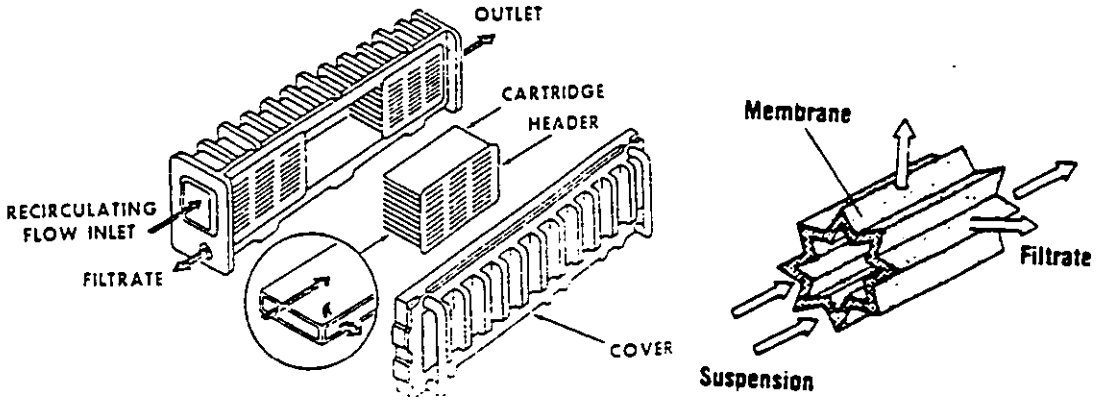

(e) Leaf (f) Pleated

Fig 4 Membrane configurations

There are two main types of this form:

1) Plate & Frame - a series of circular, rectangular or oval plates of membranes are mounted parallel to each other and interspersed with spacers or plates. The whole system is assembled by a frame on which the feed, concentrate and permeate pipes are connected. (Fig 4d)

2) Leaf - a series of parallel plates are formed from a double sheet of membranes sealed on three sides. The envelope formed by the sealed double membranes is formed on a porous support of carboard-like material and attached to a square section metal or plastic header. Several such membrane envelopes are attached in parallel to the same header so that the resultant end-section resembles a comb. The feed is passed longitudinally through the system, i.e. parallel to the envelopes. (Fig 4e)

Table 3
Comparison of Configurations

Type	Tube	Hollow Fibres	Spiral Wound	Plate Frame	Leaf
Flow type	T	La	La/T	T	T
Simplicity of flow path	G	F	F	P	F
Resistance to mechanical damage	G	G	P	G	P
Lack of suspects to blockage	G	P	P	P	P
Hold-up volume	P	G	G	G	G
Ease to mechanical cleaning	G	F	P	F	P
Ease of isolation of small volume	G	P	P	G	P
Power costs of unit permeate rate	P	G	G	G	F
Prefiltration	N	Y	Y	Y	Y
Field replacement	G	G	G	F	F
Typical module life (years)	2-6	1	1-2	1-2	
Membrane surface vs. volume	Lo	H	H	M	M
Investment cost	H	M	Lo	H	H

Notes: G - Good F - Fair H -High La - Laminar Lo - Low
N - No P - Poor Y - Yes T - Turbulent M - Medium

1.4.5 Pleated

Membranes can be casting or gluing on to the surface of irregular shaped tubes for form filters. There are also inside and outside forms for filtration (Fig 4f).

The advantages and disadvantages of this form are the same as hollow fibres, but the uneven flow pattern may result in sanitary problems.

The characteristics of different configurations are listed in Table 3.

There are also dead-end configurations: stirred and unstirred batch cells (Fig 5), which are mainly used for laboratory or for shear force sensitive materials. Since they are not related to crossflow, they will not be discussed here.

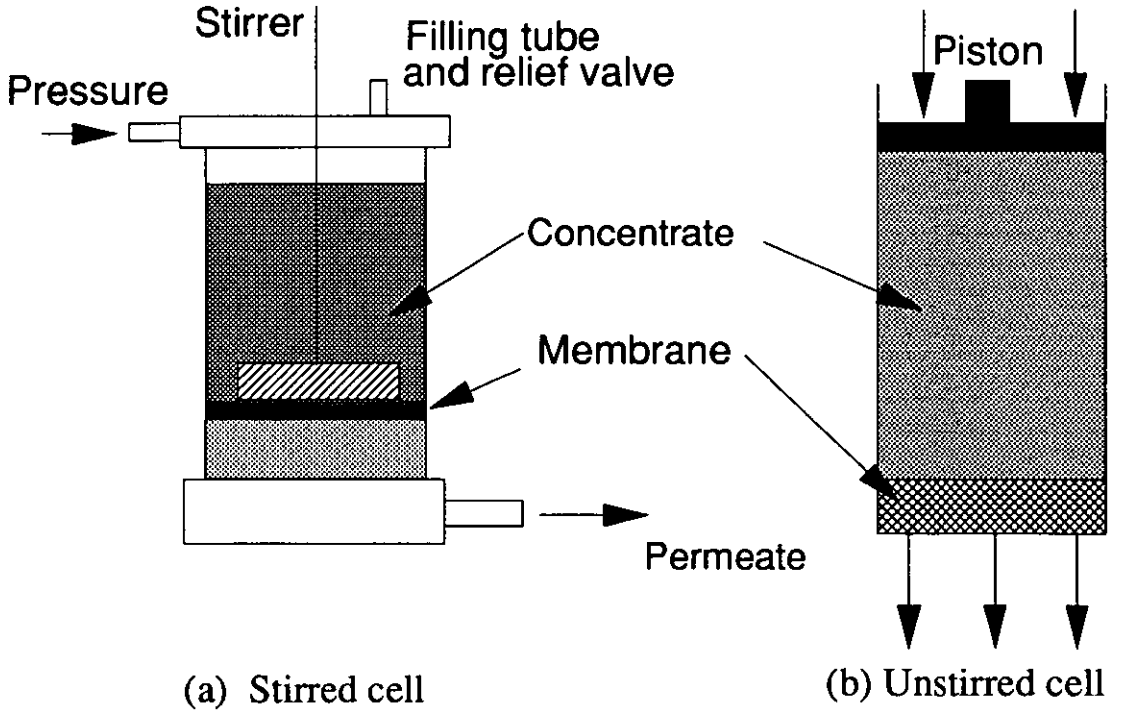

Fig 5 Dead-end filtration cells

1.5 Operation systems

There are three major crossflow type operating systems for commercial uses. The feed solution, either turbulent or high-shear laminar, flows tangentially over the membrane surface. The difference among them is that if and where the concentrate flow is fed back. (Fig 6)

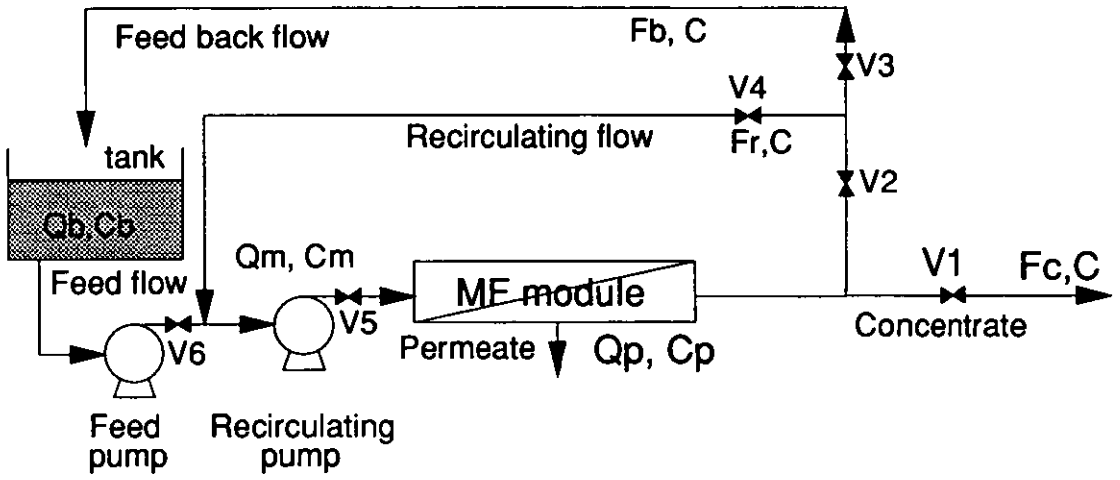

Fig 6 Basic operating diagram

1.5.1 Single-pass and cascade

In a single-pass system, the concentrate is not fed back (i.e. Fr = Fb = 0), it flows directly either into the modules of the next stage or is collected as a product. Maximum feed rate is defined by the acceptable pressure drop along the modules while minimum feed rate depends on the flow required to reduce flux rate decay. In order to meet flow requirements, one or more stages are installed in series. Each stage contains an adequate number of modules in parallel or in series (Fig 7). Booster pumps are usually required between the stages.

It is ideal for the control of microbial growth owing to its short residence time, the mechanical stress on the liquid and required energy is also smaller than other systems. But its flexibility is low, and it is very difficult to get a high final concentration.

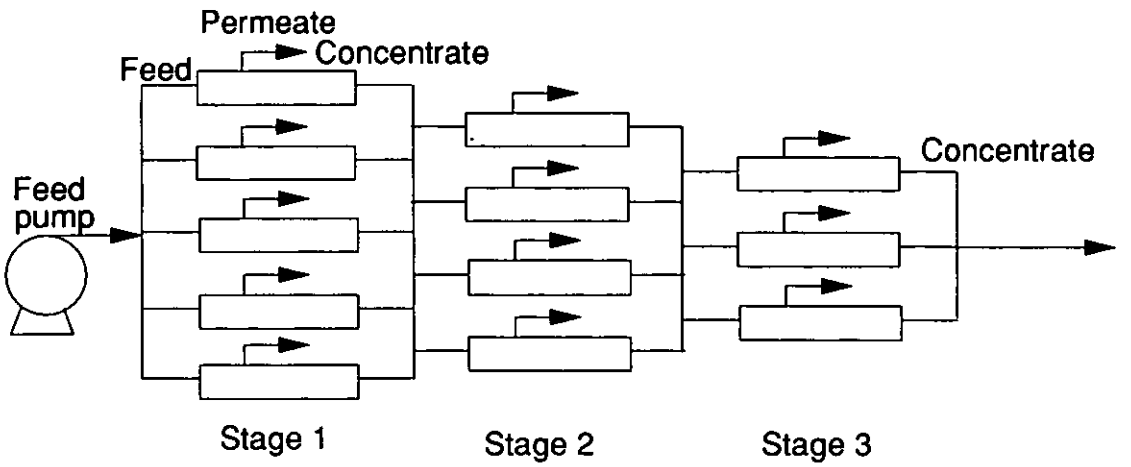

Fig 7 Single-pass and cascade system

1.5.2 Batch (Fig 8)

In a batch system, the length of the module is shorter than that in a single-pass system. When the permeate is being removed, the level in the tank keeps falling and concentration increases until it reaches the desired or limited degree. It is simple in design, easy to control, and theoretically no minimum required membrane area. The permeate flux will be high for quite a long operating time since the entire system works at a low concentration for a long time. It is economical and flexible. The disadvantages are the potential microbiological growth due to long residence time, a large feed tank and discontinuous process. The batch system can also be multistaged to shorten the residence time, the number of the modules in each stage are equal.

The batch system can be either open looped or closed looped.

If the recirculating valve (V4) in Fig 8 is closed, (i.e. Fr = Fc = 0), it is an open loop. Otherwise it is a closed loop (i.e. Fc = 0, Fr >0), the closed loop is also called semi-continuous system by some authors.

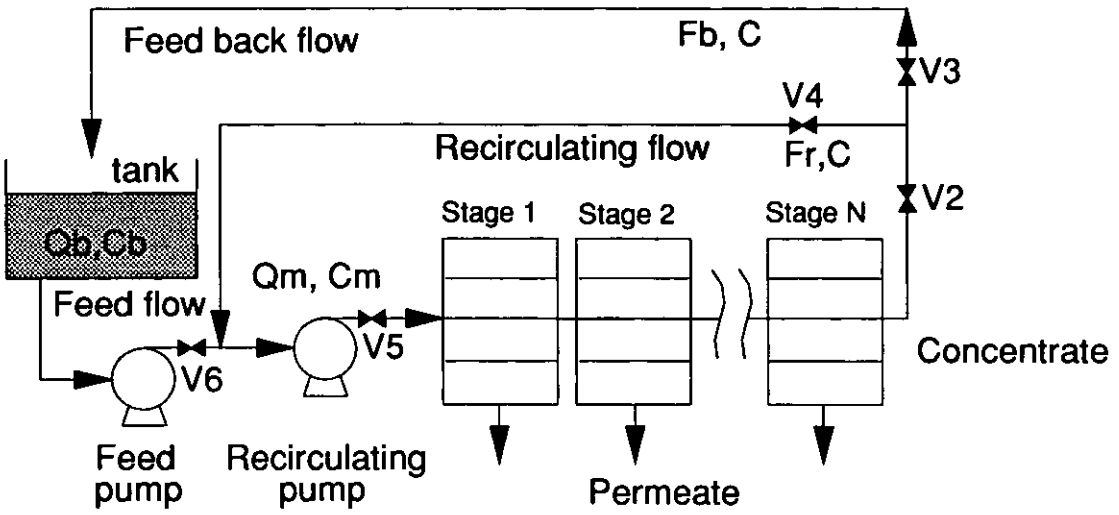

Fig 8 Batch system

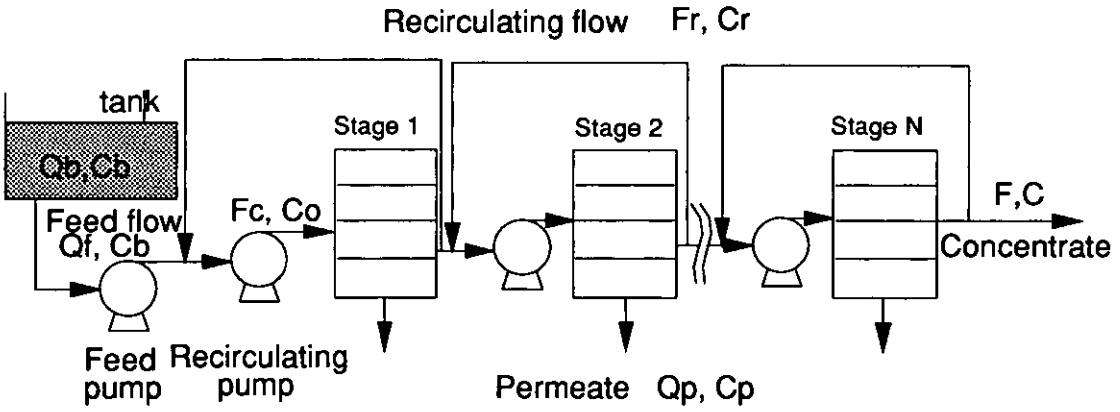

Fig 9 Continuous system

1.5.3 Continuous

A small pump feeds dilute liquid into a circuit in which a large pump recirculates it continuously through the membranes. The concentration takes place totally within the recycling loop and none of the concentrate is returned to the tank, (i.e. the feed back flow Fb = 0). The concentrates within the loop will, therefore, increase to the desired degree. Then the concentrate is bled from the system. The rate of the feed must be equal to the sum of the bled and permeate so that the concentration within the circulating loop is the same as that of the concentrate product.

In a single continuous system, the residence time of the product is short (only a few minutes), significantly reduces the possibility of product deterioration, however,

since the system is running at high concentration, the permeate flux is low, the required membrane area will be higher and the yields of retained species lower than that for a batch system of the same overall capacity.

A multistage system (Fig 9) will overcome this shortcoming since only the final stage will be operated at the highest concentration, the total permeate will increase, the residence time shorter, but it is more expensive because of the necessity of process control.

1.6 Applications

The main performances of MF can be roughly divided into following aspects:

1) purification - removal of impurities from the fluid;
2) concentration - removal of water from the fluid;
3) separation - separation of particles by their sizes;
4) fractionation - separation of macromolecules with different types (with UF);
5) retention - retention of particles larger than the rated pore size.

With these performances, MF is usually used solely or as an important part for following applications:

1.6.1 Laboratory tests and medical analysis

The main purpose of using MF in this field is either removing particles to purify liquid or detecting bacteria in fluid by culturing process.

The first academic application of MF was removing particles, microorganisms and virus from liquids for diffusion study and sizing of proteins in the late 1920s.

The first industrial application of MF was for bacteriological analysis of water supplies and air contamination control in the 1930s.

This method was widely used in Germany after World War II meanwhile the Americans used it for culturing coliform and Sallmonella for military uses.

In the 1950s, it was used for enumerating a wide variety of microorganisms, e.g. yeasts, moulds, algae, protozoan, virus and bacteria.

In the 1970s, the "track-etch" membranes were used for trace element analysis, microscopic analysis [Davis et al, 1974], blood rheology studies [Chien et al, 1971] and crossflow plasmapheresis [Castino et al, 1978; Zydney & Colton, 1984].

In the 1980s, MF membranes were used as a bioreactor [Cabassud & Aim, 1986; Michaels, 1987] or for chromatography [Davies, 1990].

1.6.2 Effluent treatment

A lot of suspension or emulsion effluents contain hazardous or useful materials. They may be treated by MF. Although it is relatively expensive, it is worthwhile when the waste stream can be re-concentrated without contaminating or damaging it, leading to recycle and re-use of a component.

a) Effluent from the electronic industry

A large amount of high purity water is used for rinsing semiconductors, printed circuits, TV tubes [Klein & Hoelz, 1982], etc. The water used can be recovered for reusing by MF combined with other technologies such as UF, ion exchange, activated carbon adsorption etc [Cartwright, 1991].

b) Effluent from the metallurgy industry

MF is used to recycle grinding water [Peters & Pedersen, 1990] to remove particular wastes (e.g. metal hydroxides) [Klein & Hoelz, 1982], and separate oil/water emulsions generated during cutting, lubrication, cooling, quenching and heat treatment [Klein, 1982; Johnson, 1986].

c) Effluent from the chemical industry

The diluted latex from alkaline waste water can be concentrated by MF up to 10% by weight [Ostermann et al, 1986], insoluble salts can be removed from wax solution in acetone [Klein & Hoelz, 1982], and recuperation of valuable suspended solids (paints) [Gillot et al, 1990].

d) Effluent from the sewage systems

A microfiltration plant was used in Poland to yield of 100 m^3/day of water from sewage for a mountain recreation centre [Grabska-Winnicka & Winnicki, 1991].

e) Effluent from the fish industry

The applications of MF in fishing industries and aquacultural farming have

been reviewed by Jaouen et al (1990). MF is used as a means to reduce pollution of surface waters generated by the effluent of fish farms [Schmidt & Wulle, 1988; Watanabe et al, 1986].

f) Effluent from the food industry

Recycling of cleaning solution (e.g. filtration of potato washing water [Peters & Pedersen, 1990]) and filtration of waste water to reduce BOD.

g) Effluent from the paper industry

MF with mineral membranes were used as first step of removing the coloured compounds in bleach plant effluent. The results showed the performances of the following UF had been greatly improved [Afonso & Pinho, 1991].

h) Effluent from the nuclear power industry

The effluent from nuclear power plant contains radioactive materials due to the corrosion of a reactor core or as fission products. MF with mineral or polymer membranes can be used to reduce the particle concentration in the effluent for more efficient waste treatment and management with other technologies [Assadi, 1990].

i) Effluent from the textile industry

MF combined with UF for dyehouse wastewater treatment was investigated by Polish scientists [Szaniawski et al, 1990]. MF was used as a prefiltration step for UF. The membrane used was an alumina ceramic tube.

j) Effluent from the oil industry

To separate oil from water to reduce hydrocarbon concentration to an environmental acceptable level [Gillot et al, 1990]

1.6.3 Food industries

The applications of MF in this field concentrate on two main industries:

a) Dairy food

MF was used to remove lipids in the whey [Hanemaaijer, 1985] and skimmed milk [Bernard & Largeteau, 1990] so as to enrich the protein concentration.

b) Beers, wines and beverages

MF is used to recover the beer yeasts from the tank bottom [Meunier, 1990],

clarify musts [Drioli & Molinari, 1990] and wines [Peters & Pedersen, 1990], harvest yeasts from cider [Taddei et al, 1990], prepare fruit juices (apple, citrus, etc) for fermentation, sweetening, sterilizing and concentration [Kilham, 1987].

Besides the above, MF is also used for the purification of sugar solution [Punidadas & Decloux, 1990] and vinegar [Ebner, 1981].

1.6.4 Engineering processes

a) Chemical - MF can be used to recover the dispersed catalyst particles, produce clean liquids, remove particle products, protect heat-exchanger surfaces against fouling. A lot of such applications in chemical processes are listed by Ostermann (1986).

b) Electronic - Perhaps the largest amount in quantity and most rigorous requirements in quality for the application of MF is the electronic industry. Ultrapure deionised water with a resistivity of 18 megohm-cm and as few as possible particulates, is used as a solvent for cleaning silicon wafers, printed circuits and TV tubes [Yaeger, 1987].

c) Water - MF can be used as a pre-treatment for RO on the desalination of sea water, or to produce drinking water [Butcher, 1990], or as an alternative method of oxidation and sand filtration on removing irons from the groundwater [Pain et al, 1990], or to treat water for boiler feeding [Greiner, 1986].

d) Oil - MF can be used to separate petrol or gasoline from the water by hollow fibres membrane [Klein & Hoelz, 1982], filtration of water (freshwater or seawater) which is injected into the oil-bearing formation to maintain the oil under pressure. The technique of seawater microfiltration will be described in detail in Chapter 3.

1.6.5 Pharmaceutical and biochemical industries

The typical application in this area is for fermentation processes. It is believed that MF has more potentials in it than other fields in the future.

It has been used for processing fermentation broth by filtration and diafiltration for cell recovery, product removal, filtration in conjunction with continuous fermentation and substrata purification, such as:

- remove pyrogens or bacterial endotoxins from the liquids for pharmaceutical use [Blosse, 1982];

- recover enzymes from process [Kröner et al, 1984];

- separate yeast cell suspensions from fermentation slurries [Kavanagh & Brown, 1987],

- filter Aspergillus Niger fermentation broth [Sims & Cheryan, 1988];

- isolate casein from milk for pharmaceutical use [Noël & Fermier, 1990];

- separate fungal cells and purify the produced polysaccharide [Haarstrick et al, 1990];

- separate plasma of bovine blood [Ogasawara et al, 1991];

- control suspensions of E Coli [Fane et al, 1991].

1.7 Permeate flux rate decline and prevention techniques

1.7.1 Resistances to the permeate flow

During the course of filtration, particles are brought by convection towards the membrane, some of them may be retained on the surface to form a concentration layer (cake, concentration polarization or gel polarization), some may block the membrane pores externally or internally. These deposits exert resistance to the filtrate flux and sometimes can severely limit the flux.

According to the history of formation, positions within the membrane, and influences to the filtration, these resistances may be divided into five groups (Fig 10):

1) R_m (Membrane resistance) - this is the intrinsic characteristic of the membrane. It depends on the nature, structure and history of previous operation of the membrane. It is thought to be constant during the process if the membrane is incompressible, the value of which can be determined by pure water filtration test,

2) R_{CP} (Concentration polarisation resistance) - caused by the increased concentration of retained materials next to the membrane surface,

3) R_g (Gel polarisation resistance) - also caused by retained materials,

R_{CP} and R_g can alternatively be thought as R_C of cake resistance,

4) R_{PB} (Pore blocking resistance) - caused by the blockage of the pore by particles at the membrane surface, and

5) R_{AD} (Adsorption resistance) - caused by the partial blockage inside of the membrane pore due to the interaction between the particles and pore wall.

If the blockage can not be removed by cleaning, R_m will increase and it is difficult to distinguish R_m from R_{PB} and R_{AD}, therefore, for a set of tests with same membrane, R_m ($R_m = R_m + R_{PB} + R_{AD}$) must be determined *in-situ* for better data analysis.

The membrane resistance always exists during the filtration, other resistances may or may not exist depending on the properties of the processed materials and membrane as well as the operating conditions.

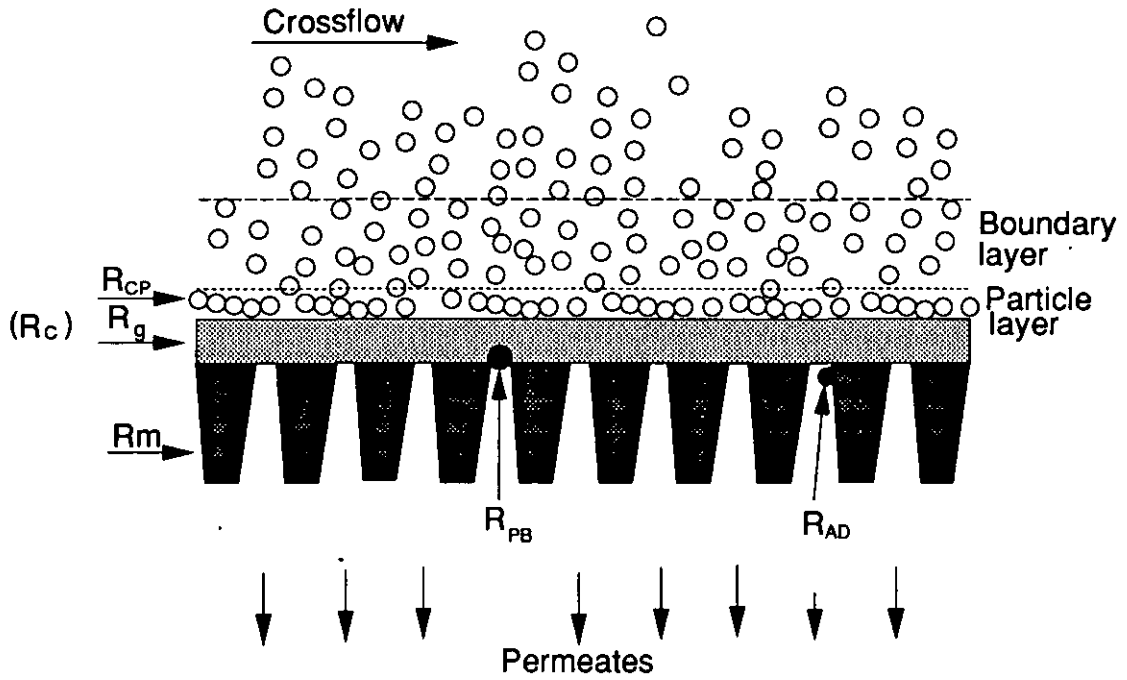

Fig 10 Resistances to the filtration

1.7.2 Membrane fouling mechanisms

If the deposits can not be removed by possible methods, the membrane is thought to be fouled and these deposits are called foulants. The foulants can be macromolecular solutes, suspended solids, colloidal materials, oil/grease, scales, metal oxides and biological microorganisms [Cartright, 1985]. The fouling mechanisms involved in the crossflow filtration are complicated and include:

- precipitation when the solubility of the foulants is exceeded;
- agglomeration which combines the "gel-like" foulants such as colloids, proteins, fats, pectin, human acids and other organic materials;
- sieving mechanism which causes simple hydraulic deposition;
- adsorption which causes particles to be attracted onto the membrane.

These mechanisms are the resultant of multiple forces such as shear, diffusion, electrostatic attraction and repulsion etc., depending on the characteristics of the fluid, particles, membrane and the operating conditions.

a) By fluid-particles-membrane interaction

The fouling may be caused by the interaction between the solutes or particles and the membrane due to the differences in the distribution of electrons in their atoms or molecules [Jonsson & Kristensen, 1980]. This will result in the formation of a number of different types of bonds like ion-ion, ion-dipole and dipole-dipole bonds:

Jackson & Landolt (1973) found that a nucleation-growth mechanism controlled the membrane fouling;

Bhattacharyya & Grieves (1979) found that the detergent-water system caused reversible detergent-membrane interaction which led to flux rate decay;

Hopfenberg et al (1973) found that ion characteristics, surface activity of solute molecule and surface charge of the membranes are vital to the occurrence and magnitude of fouling;

Palmer et al (1973) concluded from their UF experiments that solute-membrane interaction occurred at low solute concentration;

Kesting (1971) found that hydrolysis existed for cellulose acetate membrane which also caused flux rate decay.

b) By mechanical effect

Due to the structure of the membrane and the shape of the particles, the particles may clog the pore externally and internally by impingement.

High pressure will also increase the fouling if the membrane or foulant is compressible.

c) By membrane properties

The membrane properties such as pore size distribution, pore shape, length and tortuosity, zeta potential [Freeman, 1976] and surface tension, surface charge, surface potential [Lee, 1977] may influence the fouling process.

d) By salts in the fluids

Salts may affect the fouling by changing the solubility of the foulant, or interacting with the membrane, or increasing the osmotic pressure [Lee & Merson, 1976; Lee, 1977].

e) By pH value or temperature

pH value will change the charge of the foulant and result in the change of ionic strength and solubility. It also influences the particle sizes [Winfield, 1973; Lee,

1977].

High temperature may change the nature of the foulant and therefore influence the fouling [Hayes et al, 1974; Muller et al, 1973].

1.7.3 Adhesive and removal forces

a) Adhesive force

When the particle has been trapped by the membrane, there are three adhesive forces which may hold up the particles:

1) van der Waals force

It occurs between the molecules.

$$F_W \propto \frac{a_W d_s}{L^2} \tag{1.1}$$

where F_W is the van der Waals force (N)

d_s is the particle diameter (m)

a_W is the van der Waals constant which is a function of particle, membrane surface composition and surrounding medium

L is the separation distance between the particle and the membrane (m).

2) Electrostatic (electronic double layer) force

It occurs upon particle-surface contact because of the formation of contact potential difference due to the differences in the local energy of states.

$$F_\zeta \propto \frac{\zeta^2 d_s}{L} \tag{1.2}$$

where F_ζ is the electrostatic force (N)

ζ is the zeta potential (V).

3) Surface tension (capillary) force

It occurs when a liquid becomes condensed between the particle and the surface from a humid atmosphere, it can also occur when particle-surface system is immersed in a liquid and then withdrawn from the liquid to leave a small amount of liquid between the surface and particle.

$$F_\sigma \propto \sigma d_s \tag{1.3}$$

where F_σ is the surface tension force (N)

σ is the liquid surface tension coefficient ($N \cdot m^{-1}$).

b) Removal forces

Apparently, the surface tension force is not a major force in crossflow membrane system, therefore, the principle of improving the flux rate decay is how to remove the attached particles from the membrane by overcoming the van der Waals force and the electrostatic attractive force. The removal forces can be divided into two main groups: vertical forces and axial forces. The vertical forces include increasing the backward movement of the particle by diffusion, electrostatic or magnetic repulsion and mechanical vibration; the axial forces aim at dragging the particles away from the surface by increasing the shear force of the fluid or sweeping with scouring materials. Besides, pretreatment of the particle, fluid or membrane to reduce the adhesive force is also effective.

1.7.4 Techniques to prevent the flux rate decline

According to the above analysis, the decay can be reduced but not eliminated by changing the operating conditions such as increasing the crossflow velocity or decreasing the transmembrane pressure. However, the flow velocity can not be too high (usually less than 5 m/s) and in some cases, there is a threshold of velocity above which the flux rate is unaffected, and the transmembrane pressure can not be too low otherwise the flux rate will be too poor, and therefore, not practical.

Considerable research efforts, other than simply changing the operating conditions, have been directed towards the techniques, which are based on the chemical, physical and hydrodynamic principles, to overcome the adhesive forces and recover the flux rate.

These techniques are used before, during or after the filtration depending on the nature of the foulants, membranes, products and the used equipments. Some of these techniques are listed here:

1) Electric fields [Bowen & Sabani, 1992; Wakeman & Tarleton, 1987];

2) Acoustic and electro - acoustic fields [Wakeman & Tarleton, 1991];

3) Backflushing [Holdich et al, 1990; Jaffrin et al, 1990];

4) Turbulence promotors [Dejmek et al, 1974; Shen & Probstein, 1979; Light & Tran, 1981; Poyen et al, 1987];

5) Pulsating feed flow [Boothanon et al, 1991];

6) Baffles [Finnigan & Howell, 1989];

7) Filtration aids such as foam ball or abrasive particulate material added [Milisic & Bersillon, 1986];

8) Precoat the membrane with solids [Holdich & Zhang, 1991] or liquid [Le & Howell, 1984];

9) Pretreat the feed flow with magnetic force [Lin, 1990], with coagulants and flocculents [Applegate & Saskinger, 1984; Bedwell et al, 1988], with oxidatives, or change its pH values to affect the zeta potential [Bedwell et al, 1988], or cause agglomeration [Koglin, 1983].

10) Pretreat the membrane surface to be polar, nonpolar, hydrophilic or hydrophobic [Belfort & Altena, 1983];

11) Cleaning the fouled membrane with chemicals [Holdich & Zhang, 1991; Belfort & Altena, 1983], or steam sterilization, autoclavation [Hsieh et al, 1988; Gillot et al, 1984], or ignition [Minneci & Paulson, 1988];

12) Optimize the filter/module geometries [Belfort & Altena, 1983], and operating techniques [Nonogami et al, 1986];

13) Moving the membrane or a surface near to the membrane by rotation [Rushton & Zhang, 1988; Murkes & Carlsson, 1988; Belfort, 1989], or by vibration [Borre et al, 1988; Culkin & Armando, 1992].

Some of the above methods: backflushing, precoating, chemical agents cleaning, flow geometries and operating techniques optimization were used in this study, their operating principles, procedures, effects as well as limitations in each application will be discussed in the corresponding chapters.

It looks as if the scientists have done a substantial amount to assist the utilisation of MF, however, it is certain that with the developments in the membrane manufacturing technology and anti-fouling techniques, MF will have more applications open to it.

CHAPTER 2

Mathematical Models of Crossflow Microfiltration

2.1 Mathematical models for deposit distribution

The filtration process may be described by modelling the flow resistances described in § 1.7.1.

2.1.1 Models with R_C

Both submodels assume that R_m does not change during the process and therefore it is the deposit layer on the membrane surface which affects the flux rate ($R_t = R_m + R_C$).

a) Cake-Filtration Model (Fig 11a)

This model is based on Darcy's law of flow in a porous medium. It relates the pressure drop to the superficial velocity through the membrane by assuming that the concentration of the particles in the deposit layer are the same everywhere, and can be pressure dependent; its thickness is proportional to the total filtrate volume. The permeate flux rate is therefore:

$$J_v = \frac{P_t}{\mu \cdot R_t} \tag{2.1a}$$

where J_v is the permeate flux rate ($m^3 \cdot m^{-2} \cdot s^{-1}$)

P_t is the transmembrane pressure (Pa)

μ is the dynamic viscosity of the liquid (Pa•s)

R_t is the total resistance which is the sum of R_i (m^{-1})

The concentration layer in unstirred dead-end filtration belongs to this type and hence the flux is proportional to the reciprocal of the square root of processing time t:

$$J_v \propto \frac{1}{t^{0.5}} \tag{2.1b}$$

If pore blocking is concerned [Karpov & Zhuzhikov, 1981], then

$$J_v \propto \frac{1}{t^b} \tag{2.1c}$$

where a is a constant $b = \frac{1-a}{2-a}$ ($b \neq 0.5$).

b) Film Model (Fig 11b)

The concentration of the deposit layer decreases with distance from the membrane surface until it is same as that in the bulk flow. The total resistance takes place in a film (concentrated layer) near the membrane where there is no turbulence.

This type can be mathematically described by a diffusional mass balance equation in the form:

$$\frac{\partial C_l}{\partial t} + J_v \frac{\partial C_l}{\partial x} = \frac{\partial}{\partial x}\left(D \frac{\partial C_l}{\partial x} \right) \tag{2.2a}$$

where C_l is the film layer concentration ($kg \cdot m^{-3}$)

D is the diffusion coefficient ($m^2 \cdot s^{-1}$)

x is the distance from the membrane (m)

$J_v \frac{\partial C_l}{\partial x}$ is convective transport towards membrane

$\frac{\partial}{\partial x}\left(D \frac{\partial C_l}{\partial x} \right)$ is back-diffusion caused by a concentration gradient.

On the assumption that the filtration is under steady state and D is a constant, Eq 2.2a can be solved to obtain:

$$J_v = \frac{D}{x} \ln \frac{C_l - C_p}{C_b - C_p} \tag{2.2b}$$

where C_p is the concentration of the filtrate ($kg \cdot m^{-3}$)

C_b is the concentration of the bulk flow ($kg \cdot m^{-3}$)

D/x is the mass transfer coefficient represented by k later ($m \cdot s^{-1}$)

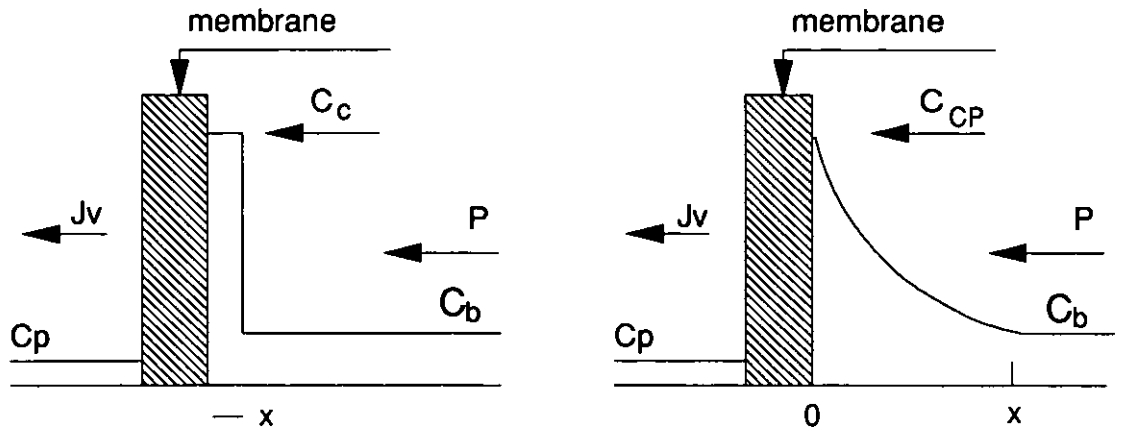

Fig 11 Two filtration models

2.1.2 Models with R_{PB}

a) Complete blocking model

This model assumes that when the particle reaches the pore, it completely seals it and all the particles do not overlap each other. The pore size and length do not change, the change in flow resistance is caused by the change in pore density ($R_t = R_m + R_{PB}$). For constant pressure, this model can be expressed as:

$$t \propto -\ln\left(\frac{J}{J_0}\right) \tag{2.3a}$$

b) Intermediate blocking model

This model assumes that particles do not necessarily completely block the pores on reaching the membrane surface, they can superimpose upon other particles to form layers. This is the combination of cake filtration and complete blocking models ($R_t = R_m + R_{PB} + R_c$), and for constant pressure [Hermia, 1982], it can be expressed as:

$$t \propto \left(\frac{1}{J} - \frac{1}{J_0}\right) \tag{2.3b}$$

2.1.3 Model with R_{AD} - Standard blocking model

This model assumes that pore volume decreases proportionally to the filtrate volume by particle adsorption or collection on the pore walls. Since the pore length (or membrane thickness) and pore density are assumed constant, the decrease in pore volume is looked upon as the decrease in pore diameter as the result of partial blockage of the flow path ($R_t = R_m + R_{AD}$). For constant pressure, this model can be expressed as:

$$\frac{t}{W} \propto t \tag{2.4}$$

where W is the permeate volume (m^3).

2.2 Mathematical models of deposit resistances

Deposit resistance models can be divided into three major groups:

1) Gel-Polarization Model

2) Osmotic Pressure Model

3) Resistance Model

2.2.1 Gel-Polarization (GP) model

This model assumes that as long as the concentration at the membrane surface reaches its maximum value C_g, the increase in the applied pressure will not have an effect on flux but will on the thickness of the gel layer, therefore the pressure term can be neglected. The distribution of particle concentration in the boundary layer is a combination of both types - the gel layer is a cake where cake theory dominates, the non-gel layer is a film where convective - diffusive force dominates.

For an unstirred dead-end system, the solution to Eq 2.2a results in an equation similar to cake theory except a diffusion coefficient is involved:

$$J_v \propto \quad (const)\left(\frac{D}{t}\right)^{0.5} \tag{2.5}$$

For stirred dead-end and crossflow systems,

$$J_v = k \ln \frac{C_g - C_p}{C_b - C_p} \tag{2.6}$$

where k is mass transfer coefficient ($m.s^{-1}$) and equals to D/x where x is the diffusional distance.

If $C_p = 0$, then:

$$J_v = k \ln \frac{C_g}{C_b} \tag{2.7}$$

a) In laminar flow

The Graetz (1885) or Leveque (1928) solutions for convective heat transfer in laminar flow channels, suitably adapted for mass transfer, can be used to calculate k for retained materials diffusing away from the membrane surface. Furthermore, when diffusivity is very low, the CP boundary layer is much smaller than the channel height when axial distance is small compared with the entrance length. Under such conditions (usually applicable to macromolecular solutions whose diffusivities are of the order of 10^2 m^2/sec) the rigorous solution for the prediction of k can be approximated by Leveque solution [Leveque, 1928]:

$$k = A\left(\gamma \frac{D^2}{L}\right)^{1/3} \tag{2.8}$$

where A is the constant ~ 0.816

L is the channel length (m)

γ is the fluid shear rate at the membrane surface (s^{-1}), its value depends on the flow geometry.

The followings are the values of γ in some geometries [Blatt et al, 1970]:

Rectangular slit $$\gamma = \frac{3U}{H} \tag{2.9a}$$

Circular tube $$\gamma = \frac{4U}{d/2} \tag{2.9b}$$

Triangular channel $$\frac{30U\left(\left(5\frac{b}{a}\right)^2+12\right)}{a}\left(\left(27\frac{b}{a}\right)^2+20\right) \qquad (2.9c)$$

where U is the flow velocity ($m.s^{-1}$)

d is the diameter of the channel (m)

H is the height of channel (m)

a, b are the height and the base of the cross-sectional area (m)

However, in a very long channel, Eq 2.8 inadequately describes the mass transfer. The length of the "concentration entrance region" where the cubic-root relationship can be expected to hold is nearly ($0.1\gamma d_h^3/D$). This ensures the validity of Leveque solution used for analysis of some systems (e.g. polymer in solution).

The average limiting flux for a macromolecular solute is [Blatt et al, 1970]:

$$J_v = 1.18\left(\frac{UD^2}{d_h L}\right)^{0.33} \ln\frac{C_g}{C_b} \qquad (2.10)$$

where d_h is the equivalent hydraulic diameter of the conduit (m).

Shen & Probstein (1977) considered that the difference between theory and experiments could be due to variable transport properties of the macromolecular solution normal to the membrane surface in the concentration boundary layer. The results of their theoretical analysis were that the concentration dependence of viscosity has little effect on the limiting flux but the diffusivity dependence of the concentration could not be ignored. Probstein et al (1978) found out, by means of an integral method, that the appropriate diffusivity defining the flux in the gel-polarized region was that at the gelling concentration, rather than at the bulk concentration. This means that the diffusivity coefficient calculated at the bulk concentration in Eq 2.10 should be replaced by one evaluated at the gel concentration to give:

$$J_v = 1.31\left(\frac{UD_g^2}{d_h L}\right)^{0.33} \ln\frac{C_g}{C_b} \qquad (2.11)$$

The formula apparently agreed well with the experimental data they quoted when the gel concentration was large compared to the bulk concentration in macro-molecular solutions.

Trettin & Doshi (1980) claimed that the disagreement between theory and experiments was due to the inaccuracy in the film theory. They used, instead, an integral method to solve the mass balance equation:

$$V\frac{dC}{dx}+U\frac{dC}{dy}=\frac{d}{dx}\left(D\frac{dC}{dx}\right) \tag{2.12a}$$

where V is the radial flow velocity ($m \cdot s^{-1}$)

y is the axial distance (m)

x is the radial distance (m)

By assuming linear velocity and a second order polynormal concentration profile, they obtained a closed solution expressed in dimensionless variables:

$$J_v^+=\frac{F_g-1}{F_g}[\kappa F_g]^{\frac{1}{3}}(\dot{D}_g)^{\frac{2}{3}} \tag{2.12b}$$

where J_v^+ = dimensionless permeate velocity

$$= J_{v(\lim)}(3x)^{0.33}(D_b^a)^{-0.33}$$

$$\dot{D}_g=\frac{D_g}{D_b}$$

$a = 3V/d_h$

F_g = CP modulus Cg/C_b

$\kappa = 2b^2/(b+1)(b+2)$ $b=f(F_g)$

When b=2 $\kappa = 2/3$, Eq 2.12b equals Eq 2.11. When C_g/C_b <4, the theoretical solution agrees well with the experimental data, while C_g/C_b >4, the real flux is lower than that predicted by the model [Trettin & Doshi, 1980].

b) In turbulent flow

There are numerous correlations involving the Sherwood (Sh), Schmidt (Sc), Stanton (St) and Reynolds numbers (Re) such as:

$$St = \frac{0.5\sqrt{f}}{19.12Sc^{0.67} + 12.74Sc^{0.33} - 21.64lnSc} \quad \text{[Vieth et al, 1963]} \qquad (2.13a)$$

$$St = \frac{0.5f}{1.18 + 0.5\sqrt{f}[11.8(Sc-1)]Sc^{-0.33}} \quad \text{[Hannah \& Sandall, 1972]} \qquad (2.13b)$$

$$St = \frac{\sqrt{f/2}}{12.527Sc^{-0.67} + 1.24lnSc + \frac{2.78}{n}\ln\left(\frac{Re\sqrt{f/2}}{90}\right)} \quad \text{[Metzner \& Friend, 1959]} \qquad (2.13c)$$

where n = power index of non-Newtonian fluid

2.2.2 Osmotic pressure model

The concentration difference of the liquid across a membrane is relatively small in microfiltration, and D_i is not a function of C_i, therefore, the liquid flux can be expressed as:

$$J_v = -\frac{D_v \cdot C_v \cdot \upsilon_v}{R \cdot T \cdot \delta}(\Delta P - \Delta\Pi) \qquad (2.14)$$

where υ is the partial molecular volume

$\Delta\Pi$ is the osmotic pressure (Pa)

R is the gas constant.

Although the osmotic pressure in MF is insignificant, some authors including Goldsmith (1971), Zawicki et al (1981), Forström et al (1975) have suggested that osmotic pressure in filtration of macromolecular solutions is an important factor, especially when the gel has been formed.

a) Unstirred dead-end system [Vilker et al, 1981a]:

$$J_v = f(C^o, C_b)\left(\frac{D}{t}\right)^{0.5} \qquad (2.15)$$

where C^o is the concentration for which $\Delta P - z \cdot \Delta\Pi = 0$,

ΔP is the applied pressure (Pa or Bar)

z is the reflection coefficient.

b) Stirred dead-end [Jonsson, 1984] or crossflow system [Goldsmith, 1971]

$$J_v = \frac{\Delta P - z\Delta\Pi}{\mu R_t} \tag{2.16}$$

where $\Delta\Pi = \Pi(C_l) - \Pi(C_p) = \frac{RT}{M}\sum_{i=0}(a_i C_l^{i+1} - b_i C_p^{i+1})$

M is molecular weight ($kg \cdot mol^{-1}$)

a_i, b_i are virial coefficients which can be calculated as a function of parameter such as excluded volume, hydration and Donnan effects [Vilker et al, 1981b; van den Berg et al, 1987].

2.2.3 Resistance model

This model calculates the total resistance of the deposit layer to the permeate flux and can be further described by two sub-models.

a) Filtration models

This submodel assumes that solids which are larger than the membrane pore size will be retained. The flux in the pore is mainly viscous and can be expressed by Poiseuille's law:

$$J_v = \frac{N_m \cdot \pi \cdot d_m^4 \cdot P_t}{128\mu \cdot \delta_m} = \frac{\varepsilon_m \cdot d_m^2 \cdot P_t}{32\mu \cdot \delta_m} \tag{2.17}$$

ε_m is the membrane porosity

d_m is the pore diameter (m)

δ_m is the pore length (m)

N_m is the pores density (number of pores per unit area) (m^{-2}).

The total resistance R_c in the boundary layer can be expressed by deposit layer thickness x_l and specific resistance r_l (m^{-2})in the form:

$$R_l = \int_0^{x_l} r_l \cdot dx \qquad \text{(film type)} \qquad (2.18a)$$

$$\text{or } R_c = x_l \cdot r_l \qquad \text{(cake type)} \qquad (2.18b)$$

In either type of distribution, $\mathbf{r}_l$, which is the reciprocal of the hydraulic permeability ($\mathbf{p}_s$) of the deposit layer, can be described by the Kozeny-Carman relationship:

$$r_l = \frac{180(1-\varepsilon_s)^2}{d_s^2 \cdot \varepsilon_s^3} \qquad (2.19)$$

Assuming that the mass of the deposits can be determined, then

$$x_l = \frac{m_s}{\rho_s \cdot (1-\varepsilon_s) S_s} \qquad (2.20)$$

where m_s is the mass of deposited particles (kg)

ρ_s is the density of the deposits ($kg \cdot m^{-3}$)

ε_s is the porosity of the deposit layer

S_s is the deposit layer surface area (m^2).

The relationship between $\mathbf{r}_l$ and P_t under dead-end filtration was empirically found to be:

$$\frac{r_l}{C_l} = \left(\frac{r_l}{C_l}\right)_0 P_t^q \qquad (2.21)$$

where sub *0* represents the original conditions

q is the compressibility factor which varies between 0.5 to 0.7 for the solutes BSA and silica [Chudacek & Fane, 1984; Dejmek, 1975].

This model has been used for various of types of filtration. [Chudacek & Fane, 1984; Howell & Velicangil, 1980; Baker et al, 1985; Fane, 1984].

During this sieving mechanism, some particles which are smaller than the pore sizes may be retained by either impingements on the edge of a pore, or by interaction with the pore walls. The steric effects and friction interaction with the pore walls can be expressed by the Férry - Faxén equation [Férry, 1936; Faxén, 1922a & 1922b]:

$$\frac{S_a}{S_D}=\left[2\left(1-\frac{d_s}{d_m}\right)^2-\left(1-\frac{d_s}{d_m}\right)^4\right]\cdot\left[1-2.104\left(\frac{d_s}{d_m}\right)+2.09\left(\frac{d_s}{d_m}\right)^3+0.95\left(\frac{d_s}{d_m}\right)^5\right] \quad (2.22)$$

where S_a is the pore area available for transporting particles (m^2)

S_D is the total cross-sectional area of the pore (m^2)

The first square bracket is the steric factor, the second one is the Férry - Faxén friction factor. This equation is only suitable for monosize particles loading fluid.

b) Boundary layer resistance model - Sediment coefficient

This model is analogous to the situation in a sedimentation process. The hydraulic permeability is related to the layer concentration C, partial specific volumes of the solids and liquid v_1 and v_0, and a sedimentation coefficient s{C}:

$$p_s=\frac{\mu s\{C\}}{C\left(1-\frac{v_1}{v_0}\right)} \quad (2.23)$$

where s{C} is a function of concentration C

$$\frac{1}{s}=\frac{1}{s_0}\left(1+\sum_{i=1}^{3}a_iC^i\right) \quad (2.24)$$

where s_0 is the original condition of s(C) and a_i's are constants.

van den Berg & Smolders (1988) found in their experiment with BSA in an unstirred UF system that:

$$\frac{1}{s}=\frac{1}{4.412\text{x}10^{-13}}(1+7.051\text{x}10^{-3}C+3.002\text{x}10^{-5}C^2+1.173\text{x}10^{-7}C^3) \quad (2.25)$$

Therefore, the total resistance R_t in crossflow is:

$$R_t=\frac{D}{J_v\cdot\nu\cdot s_0}\left[C_l-C_b+\sum_{i=1}^{3}\frac{a_i}{i+1}(C_l^{i+1}-C_b^{i+1})\right]\left(1-\frac{v_1}{v_0}\right) \quad (2.26)$$

C_l is difficult to measure directly, however, if k is known, C_l can be calculated from:

$$J_v=k\ln\left(\frac{C_l}{C_b}\right) \quad (2.27)$$

2.3 Prediction of permeate flux rate

2.3.1 CP and GP resistance modelling

These two resistances can be modelled by mass transfer correlations of ***k***. A lot of such models have been proposed for both laminar and turbulent flow in pipes or flat ducts. The general correlation of ***k*** has the empirical form:

$$Sh = k\frac{d_h}{D} = (a_1)Re^{a_2}Sc^{a_3} \tag{2.28}$$

where a_1 is a constant or function;

a_2, a_3 are constants.

For non-slip conditions and laminar flow in ducts where the length of the entry region:

$L^* = 0.029\ Re \cdot d_h$

$L < L^*$ $Sh = 0.664Re^{0.5}Sc^{0.33}(d_h/L)^{0.33}$ [Grober et al, 1961] (2.29a)

$L > L^*$ $Sh = 1.86Re^{0.33}Sc^{0.33}(d_h/L)^{0.33}$ [Harriot & Hamilton, 1965] (2.29b)

For non-slip conditions and turbulent flow, the most popular correlations used are based either on the Chilton-Colburn (1934) or on the Deissler (1959) analogies.

$Sh = 0.023Re^{0.8}Sc^{0.33}$ $Sc < 1$ (2.30a)

$Sh = 0.023Re^{0.875}Sc^{0.25}$ $1 \le Sc \le 1000$ (2.30b)

Harriot & Hamilton (1965):

$Sh = 0.0096Re^{0.91}Sc^{0.35}$ $Sc > 1000$ (2.30c)

a) For Newtonian fluids

For a Newtonian fluid, there are six further groups of correlations derived by different approaches, some of them are listed in **Appendix 2** according to the work of Gekas & Hallström (1987).

1) Based on momentum, mass, heat transfer analogies

The most famous correlation of this type is the Chilton-Colburn analogy in

which k is correlated with the friction factor f. In this treatment it is usual to substitute Sh for Nu and Sc for Pr [Bird et al, 1960].

$$j_D = \frac{k}{U} Sc^{\frac{2}{3}} = \frac{f}{2} \tag{2.31}$$

2) Based on eddy diffusivity models

This model assumes that eddy diffusivity $D_{eddy} = D_{eddy}\{x^+\}$ varies with the distance from the wall and how the duct is sectioned [Harriott, 1962].

In some of these sections molecular or turbulent or both types of transfer are considered effective. The resultant Sh correlation by this model can be described by the asymptotic form (at high Sc number)

$$Sh \sim f^{1/2} Sc^a \tag{2.32}$$

where a is 0.25 to 0.33.

This model suffers from the drawback that D_{eddy} can not be experimentally observed or measured.

3) Based on surface renewal model

This model (sometimes referred to as the penetration model) assumes that both momentum and mass are transferred by whirls and by molecular diffusion between the whirls and the wall. The whirls are stochastical in frequency and penetration depth [Harriott, 1962; Eriksson, 1980]. This model predicts a dependence of the mass transfer coefficient on $f^{1/2}$ like the eddy diffusion model. The simplified versions of this model approximately met their experimental data while the comprehensive ones failed to do so.

4) Based on Levich's "Three-Zone" model (1962)

In this model, the boundary layer is subdivided into three zones: developed turbulent, turbulent boundary layer and viscous sublayer (restricted turbulence) as shown in Table 4 and Fig 12.

Table 4
Levich's "Three-Zone" model

Zone	Value of coordinate	Characteristics of the zone	Mechanism of transfer		Concentration distribution
			Momentum	Mass	
1	$x > x_1$	developed turbulent	turbulent	turbulent	C = constant
2	$x_0 < x < x_1$	turbulent boundary layer	turbulent	turbulent	$C = \frac{j_D}{bU_0} \ln \frac{x}{x_1} + C_0$
3	$0 < x < x_0$	viscous sublayer	molecular viscosity	molecular diffusion	$C = \frac{j_D}{D} x$

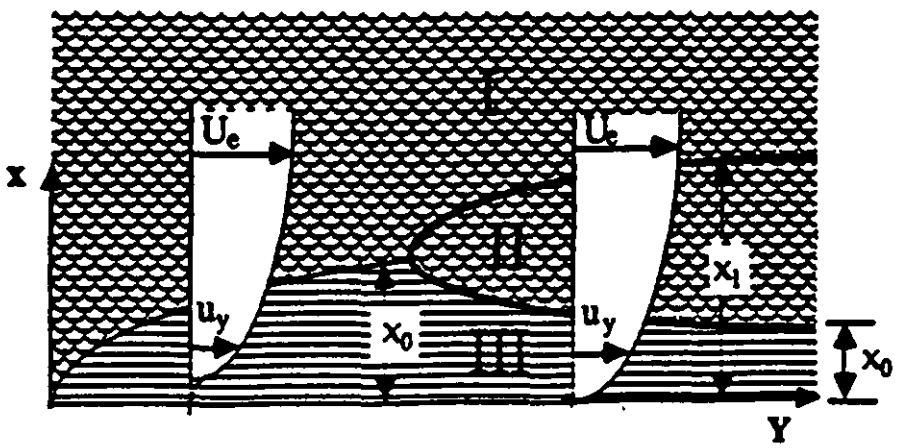

Fig 12 The schematic diagram of "Three-Zone" model

5) Based on new turbulence concepts (coherent structures)

With the development of experiment techniques, the flow near the wall can be visualized and measured. The existence of coherent structure close to the wall characterized by a lateral dimension and a period in a dimensionless form has been proved [Brodkey et al, 1978; Wood & Petty, 1983]. The extent of the influence of the coherent structures on mass transfer has been studied and will be discussed later (turbulent burst).

However, under high Sc number conditions, the turbulent mass transfer to a solid boundary is very little controlled by those velocity fluctuations which contain most of the turbulent energy.

6) Based on experimental data

b) For viscoelastic fluids

In this type of fluid, the friction factor f has to be measured, since the lower the f, the lower the mass transfer coefficient k ($k \sim f^{a}$). Some results according to the work of Gekas & Hallström (1987) are also listed in **Appendix 2**.

In fact, the empirical correlations agree with most of the theoretical models with a Re exponent in the region of 0.71 - 0.73 and a Sc exponent of 0.33. The lower value of Re in comparison with values of 0.75 - 0.90 for Newtonian fluids can be explained by friction factor decrease.

c) For power-law fluids

Due to CP, it is possible for some solutions to show non-Newtonian behaviour. In the power-law cases, the flow index n must be known. Some results on this can be found in **Appendix 2** according to the work of Gekas & Hallström (1987).

2.3.2 Cake resistance modelling

a) By conventional cake filtration model

For dead-end cake filtration, the permeate flux can be well described by following formula:

$$\frac{dt}{dQ} = \frac{2}{a} Q + \frac{2}{b} \tag{2.33}$$

where Q is the permeate flow rate ($m^3 \cdot s^{-1}$)

a and b are integration constants

$$a = \frac{C \cdot r \cdot \mu}{2S \cdot P_t}$$

$$b = \frac{\mu \cdot R_t}{S \cdot P_t}$$

S is membrane surface area (m^2).

Nakao et al (1990) found that initial permeate flux decay within 5 to 10 minutes can be well predicted by above equation.

Rushton & Aziz (1984) concluded from their filtration experiment of dilute suspensions of various mineral slurries that this equation might be used to describe the process of particulate polarisation.

b) By specific resistance

Since $$J_v = \frac{P_t}{\mu \cdot R_t} \tag{2.1a}$$

in this method $R_t = R_m + R_c$

and $R_c = x_s \cdot r_c$ (cake type) (2.18b)

it is possible to predict permeate flux rate by modifying r_c in the Kozeny-Carman formula.

Zuk & Rucka (1987) calculated r_c of the gel layer based on dead-end filtration from their filtration of casein solution and obtained:

$$r_c = \frac{30\pi \cdot d_s}{m_s} \cdot \frac{1-\varepsilon_s}{\varepsilon_s^3} \tag{2.34}$$

Sabuni (1990) assumed that only certain particles will be retained at the membrane surface to form the cake as those in the traditional cake filtration, other particles will be re-entrained into the bulk suspension. He modified R_c as:

$$R_c = \frac{r_c \cdot Q_0 \cdot C}{S}\left(1 - e^{\left(-\frac{\varrho}{\varrho_0}\right)}\right) \tag{2.35}$$

Mikhlin et al (1982) assumed that both turbulent eddies and shear force had an effect on moving deposits. They presented:

$$\left(\frac{J_0}{J_\infty}\right)^2 \ln\left[\frac{1-\left(\frac{J_\infty}{J_0}\right)}{1-\left(\frac{J_\infty}{J}\right)}\right] - \left(\frac{J_0}{J_\infty}\right) \cdot \left(\frac{J_0}{J} - 1\right) = \frac{r_c \cdot \mu \cdot C \cdot J_0^2 \cdot t}{P_t} \tag{2.36}$$

Baker et al (1985) concluded that under crossflow conditions

$$r = a \cdot r_c P_t^n \tag{2.37}$$

where a is a coefficient which increases with increasing feed velocity (U). ($1 < a < 10$)

2.3.3 Membrane fouling modelling

When fouling has occurred, the membrane resistance will be changed due to the blockage or shrinkage of the pores, therefore, R_t should be expressed with the models described in §2.1: cake filtration model, Complete blocking model, Intermediate blocking model and Standard blocking model. Most of such expressions were deduced from RO and UF since fouling is prominent in these processes, the mathematical models for MF have been little studied so far. However, by proper modification, these models may be used to describe the fouling process in MF.

a) By cake filtration model

Kimura & Nakao (1975) predicted the flux rate based on the fouling of CA tubular RO and UF membranes based on the gel polarization model of Michael (1968):

$$J_v = \left[k \cdot \ln\left(\frac{C_g}{C_b}\right) + \frac{\rho_b}{C_b}\frac{dx}{dt} \right] \cdot \frac{1}{C_b} \tag{2.38a}$$

Hiddink et al (1980) predicted the flux rate in the RO of whey and skimmilk accounting on the resistances caused by fouling, R_c and R_m:

$$J_v = \frac{\Delta P}{R_m} - \frac{\Pi_1}{R_m} e^{\frac{J_v}{k_1}} - \frac{\Pi_2}{R_m} e^{\frac{J_v}{k_2}} \tag{2.38b}$$

where sub **1** and **2** refer to the resistance caused by fouling and CP.

Belfort & Mark (1979) converted the cake filtration model into a modified gel filtration model by adding a third item (**a/W**) on the right side of the equation and then normalized different membranes with fouling and compaction.

For the initial transient period:

$$\frac{t}{W} = a_1 W + a_2 + \frac{a_3}{W} \tag{2.39a}$$

For the later stage of the initial period:

$$\frac{t}{W} = a_1 W + a_2 \tag{2.39b}$$

For steady-state period:

$$\frac{t}{W} = a_4 W + a_5 + \frac{a_6}{W} \tag{2.39c}$$

When W approaches ∞:

$$\frac{t}{W} = a_4 W + a_2 (1 + b) \tag{2.39d}$$

where a_i (i=1 to 6) are constants

b is the constant characteristic of the membrane.

b) By Complete blocking model

Carter & Hoyland (1976) described the build up of rust fouling layers on RO membranes in turbulent flow and predicted the effective deposit layer as a function of kinematic viscosity of the fluid and channel height and irrelevant to the flux rate and particle concentration:

$$r_l = \frac{4H^2}{a_1 a_2 \rho_b \nu^2} \tag{2.40}$$

where a_i (i=1,2) are constants.

Gutman (1977) predicted the flux rate based on turbulent burst theory, his model will be discussed in § 2.4.

c) By Intermediate blocking model

Bhattacharyya et al (1979) predicted the flux rate of a UF oil-detergent-water system with a noncellulose tubular membrane:

$$J_v = \frac{P_t}{R_m} e^{-\frac{kC_f}{C_{det}}} \tag{2.41}$$

where subscripts *f* and ***det*** refer to foulants and detergent respectively.

Bhattacharya et al (1988) found that at higher concentration and relatively higher pressures the cake filtration model replaced the Intermediate blocking model in their experiments of settling sedimentation and vacuum filtration on manganese nodule leach slurry of Indian Ocean origin.

d) By Standard blocking model

In the Standard blocking model the values of the pore length (δ_m) and density (N_m) are assumed constant, only the pore size decreases due to particle deposition.

Nonaka (1986) presented an expression based on the Standard blocking model to estimate the variation in pore diameter with permeate volume (W) and processing time (t):

$$d_m = \left(d_{m_o} - \frac{2W}{3\delta_m} \Sigma\left(d_{s_i}^3 C_{b_i}\right)(1-\exp(D\,t)) \right)^{\frac{1}{2}} \tag{2.42}$$

Sharma & Yortsos (1987) predicted the pore size variation with time:

$$\frac{d\,(d_m)}{dt} = -2\,\rho_s V_s \left(\frac{4\,U\,D^2}{d_m \delta_m} \right)^{0.33} \tag{2.43}$$

Grace (1956) made a thorough study of the Standard blocking model and derived the formula for calculating the pore length and density based on a mass balance equation and Poiseuille's law on the assumptions that:

1) parallel pores of equal length and radius,

2) during a certain period, the initial pore diameter must be at least several times greater than the particle diameter whatever the solid concentration, and

3) the capture is a direct interception of particles from the streamlines adjacent to the pore walls, and the volume of major flow channel through the pores decreases in direct proportion to the volume of filtrate passing the pores.

$$\delta_m \cdot N_m = \frac{4C_{pore}}{\pi S\, d_m^2 (1-\varepsilon_s) \cdot \rho_s A} \frac{1}{A} \tag{2.44a}$$

$$\frac{\delta_m}{N_m} = B \frac{\pi d_m^4 S\, P_t}{128\mu} \tag{2.44b}$$

δ_m and N_m can be obtained as:

$$\delta_m = \sqrt{(\delta_m \cdot N_m) \cdot \left(\frac{\delta_m}{N_m}\right)} = \sqrt{\frac{C_{pore} \cdot d_m^2 \cdot P_t \cdot B}{32\mu \cdot (1-\varepsilon_s) \cdot \rho_s \cdot A}} \tag{2.44c}$$

$$N_m = \sqrt{\frac{(\delta_m \cdot N_m)}{(\delta_m / N_m)}} = \frac{1}{\pi \cdot S \cdot d_m^3} \sqrt{\frac{512 C_{pore} \cdot \mu}{P_t (1-\varepsilon_s) \cdot AB}} \tag{2.44d}$$

where C_{pore} is the particle concentration of the fluid inside the pores ($kg \cdot m^{-3}$)

A and ***B*** are the gradient and intercept in Eq 2.4f:

$$t/W = A \cdot t + B \tag{2.44e}$$

Apparently, ***A*** is the packed volume of solids removed per volume of filtration $C_{pore}/[(1-\varepsilon_s)\rho_s]$ divided by the effective pore volume of the membrane effective filtration area ε_m which is $(S\, \delta_m N_m \pi d_m^2)/4$. It is a function of the deposited material (C_{pore}, ρ_s and ε_s).

The expression for ***B*** is an upside down version of Poiseuille's law. B stands for the time required to filter unit volume of permeate. It is independent of deposited material but a function of transmembrane pressure P_t.

A and ***B*** should be experimentally determined. The procedures of experiment and data processing will be described in Chapter 4.

When δ_m, N_m, ***A*** and ***B*** have been obtained, the initial pore size of the current run can be estimated with the intercept ***B*** by Eq 2.44b:

$$d_m = \left(\frac{128\, \delta_m \cdot \mu}{\pi N_m S\, P_t B}\right)^{\frac{1}{4}} \tag{2.44f}$$

or alternatively with the gradient ***A*** by Eq 2.44a if C_{pore} and ε_s are available too:

$$d_m = \left(\frac{4 C_{pore}}{\pi N_m S \delta_m (1-\varepsilon_s) A} \right)^{\frac{1}{2}} \qquad (2.44g)$$

Shirato et al (1979) and later Hermia (1982) applied the four blocking models to the constant flux rate or constant pressure filtration with power-law non-Newtonian flow.

2.4 Other methods of prediction

2.4.1 By supplying a correction factor

Some of the mass transfer correlations in § 2.3.1 are transplanted from non-porous smooth duct flow so that their applications in membrane separation are limited because neither the properties (e.g. pore size and shape, length, density, tortuosity and the matrix) of the membrane, nor the change of physical properties of the fluid (e.g. viscosity and diffusivity) due to filtration, are taken into consideration. Several methods for modifying the correlations have been put forward.

A general correction for the effect of flux on the mass transfer coefficient is the Stewart correction [Bird et al, 1960]. Recently Gekas & Hallström (1987) suggested the introduction of an *Sc* correction factor $(Sc/Sc_w)^{0.11}$ in an analogy with heat transfer correlations.

2.4.2 By experimental data expressed in process parameters

Some authors used empirical process parameters such as velocity (U), pressure (P), concentration (C) and temperature (T or θ) to describe the flux (J_v) since these factors are easily measured and controlled.

Baker et al (1985) correlated flux rate with feed flow rate by:

$$J_v = 7.4 \cdot 10^{-5} U^{0.6} \qquad (2.45a)$$

Nakashima & Shimizu (1989) related J_v with Re based on their microfiltration of an oil/water emulsion:

$$J_v = a\, Re^{1.43-1.77} \qquad (2.45b)$$

Shishido et al (1988) tested the relationship between J_v and operation parameters (d_h, U, P, C) in their experiment with ferric hydroxide suspension:

$$J_v \propto \left(\frac{d_h}{2}\right)^{-0.4} \quad d_h = 0.002 - 0.11 \text{ m}$$

$J_v \propto U^{1.2}$ U = 1 - 3 m•s^{-1}

$J_v \propto \overline{P}^{1.0}$ P = 10000 - 30000 kg•m^{-2}

$J_v \propto C^0$ C = 0.51 - 30 kg•m^{-3}.

Yan et al (1979) presented six models with four parameters (J,C,U,θ) to describe the flux rate of cows' milk within the pressure plateau area. The following one was thought to be the most reliable:

$$J_v = (133.8748 + 1.6496C_r)U^{-52.7383}e^{\frac{-0.6723\theta}{1.987}} \qquad (2.45c)$$

where C_r is the concentration ratio C_b/C_{bo}

θ is the temperature (°C).

Peri & Setti presented a four parameter model (J,U,C,P) on the flux of skimmed-milk (1976a) and sweet whey (1976b) under constant temperature.

for sweet whey:

$$J_v = 28.362e^{-0.284C_b}PU^2\left(1 - 0.09Ue^{-0.02C_b}\right)(1 - 0.5U) \qquad (2.45d)$$

for skimmed-milk:

$$J_v = 19.8U^{1.315}e^{-0.15C_b - 0.0015C_b^2} + (1.44lnP - 1)(1.20 - 0.075C_b)e^{1.1(U-1.7)} \qquad (2.45e)$$

Cheryan & Nichlos (1980) presented a four parameter (J,U,T,P) model of the flux in processing water extracts of soybeans:

$$J_v = 0.782 + 0.026(T - 273) + 0.009U + 0.105P \qquad (2.45f)$$

Lafailli et al (1987) obtained their empirical expressions of flux of bovine albumin, dextran and PVP in laminar flow (Re<800)

$$J_v = AU^aC_b^b \qquad (2.45g)$$

Detran	$A=3.08\ 10^{-5}$	a=0.4	b=-0.4	C_b= 1 - 150 g•kg^{-1}
Albumin	$A=5.60\ 10^{-5}$	a=0.4	b=-0.4	C_b= 1 - 100 g•kg^{-1}
PVP	$A=2.32\ 10^{-5}$	a=0.62	b=-0.22	C_b= 1 - 40 g•kg^{-1}

Matthews et al (1978) used cake theory to present a two parameter (J,W) model of sulphuric acid casein whey:

$$J_v = J_0 W^{-a} \tag{2.45h}$$

where J_o is the initial permeate flux rate

Kiviniemi (1972) suggested the permeate flux rate for skimmed-milk:

$$J_v = a_1\, a_2\, e^{\frac{a_3}{\theta}} \left(\frac{U}{500} \right)^{a_4} \tag{2.45i}$$

where $a_1 \sim 10^5$ $a_2 << 1$ $a_3 \sim 3000$ $a_4 \sim 1$

Hunt et al used the term of eddy diffusivity and developed two four parameter models (U, P, C_b, d) for steady-state (1987a) and unsteady-state (1987b) microfiltration with short tubular modules:

For steady-state:

$$J_v = d_h \cdot D_{eddy} \cdot \ln\left(\frac{C_s}{C_b} \right) [r_h^2 - (r_h - x_c)^2]^{-1} \tag{2.45j}$$

For unsteady-state:

$$J_s = \frac{C_b - C_s \cdot \exp[-a(r_h^2 - (r_h - x - x_l)^2)]}{1 - \exp[-a(r_h^2 - (r_h - x - x_l)^2)]} (J_s + J_v) \tag{2.45k}$$

where $a = \dfrac{J_s + J_v}{D_{eddy} \cdot d_h}$

where $r_h = d_h/2$ (m)

Their models were adapted by Pillay et al (1989) for computer simulation and the results agreed with experiments in a long tube.

Mahenc et al (1986) proposed an empirical relationship of J and operating parameters for tubular system based on Matthews et al (1978):

$$J_v = a_1 U^{a_2} C_b^{a_3} L^{a_4} \qquad (2.451)$$

Table 5

Parameters in Mahenc's (1986) model

Solute	a_1 (10^{-5} g m/kg)	a_2	a_3	a_4	Mean Deviation	Validity of a_1
Albumin	3.27	0.4	-0.4	-0.33	3.3	1 - 150
Dextran	1.80	0.4	-0.4	-0.33	2.3	1 - 120
Blood Plasma	1.27	0.5	-0.33	-0.33	3.7	1 - 150
PVP	1.35	0.62	-0.22	-0.33	1.5	1 - 40

2.4.3 By numerical method

Most of the models (suction or injection) have been for slits, tubes and annuli since they are the common geometries for membrane systems. Two categories of problems have been solved: fully developed flow where the shape of the non-dimensional velocity profiles is considered similar or constant with axial distance, and the developing flow at the duct entrance where the shape of the non-dimensional velocity profile is changing with axial distance. Most of the work except Galowin et al (1971, 1974) and Terrill (1983) assumed that k is constant along the duct. Numerical solutions assuming constant wall suction and similarity of velocity profiles are summarized by Berman (1958) and White (1974).

Most of the studies have been conducted for turbulent flow of air [Weissberg & Berman, 1955; Weissberg, 1956; Wallis, 1965; Aggarwal et al, 1972; Brosh & Winogard, 1974] and for laminar flow of air [Bundy & Weissberg, 1970] in porous tubes.

Singh & Laurence (1979a & 1979b) used numerical methods to solve the flux under slip velocity conditions for slit and tubular systems. They solved the equation of motion in 2-dimensions by a first-order perturbance method and diffusion equation by a finite difference technique. They concluded that CP decreased with an increased slip coefficient since slip velocity enhanced back-diffusion of solutes. The flux rate, on the other side, will increase.

Some work in this field during 1934 to 1986 has been surveyed by Belfort (1986) and interested readers are referred to this work for further details.

2.4.4 By considering the effects of other forces

For particles and macromolecules it has been found that the back transport of solutes was well beyond the ability of diffusional force or shear stress. In order to explain this phenomenon, other forces are considered. These forces can be either parallel or vertical to the membrane surface.

a) Vertical forces

There are four sources which are considered able to make the particles move perpendicular to the local direction of flow [Cox & Mason, 1971].

1) Body forces e.g. gravity and buoyancy force if the membrane is horizontally placed, or centrifugal force.

It is no doubt that for the range of microfiltration, both gravity and the buoyancy forces are too weak to remove the deposit from the membrane surface.

Centrifugal force is strong enough as long as the rotating speed is high, it has been one of the conventional technologies of separating solids from gas or liquid in the cyclone and hydrocyclone. However, this force only exists in rotating flow which is induced, and therefore is considered later in another chapter.

2) Self Induced Hydrodynamic Diffusion (SIHD) [Goldsmith & Mason, 1967; Karnis et al, 1966; Eckstein et al, 1977].

This model assumes that the transfer of momentum between different streamlines and the rotation of the particles caused by shear force will affect the motion of neighbouring particles and eventually form a back-diffusion like movement of particles.

Eckstein et al (1977) experimentally determined the self-diffusion coefficients for lateral dispersions of spherical and disk-like particles in linear shear flow of a slurry at very low Reynolds number. They obtained self-diffusion coefficients by means of random-walk theory:

$$D = 0.02\nu \cdot d_s^2 \cdot \gamma \qquad \text{for} \quad \nu < 0.2 \tag{2.46a}$$

$$D = 0.025 d_s^2 \cdot \gamma \qquad \text{for} \quad 0.5 > \nu > 0.2 \tag{2.46b}$$

where ν is the kinematic viscosity ($m^2 \cdot s^{-1}$)

The values of γ for some geometries have been listed in Eq 2.9.

The values of D are not of high accuracy but are correct to within a factor of two.

Leighton & Acrivos (1987) measured viscosity of particles in their experiment and obtained:

$$D = k \frac{\nu^2 d\mu_s}{\mu_s d\nu} \gamma d_s^2 \tag{2.47}$$

Taddei et al (1990) expressed their correlation based on SIHD theory:

For a clean membrane $$J_v = 1.7 \cdot 10^{-3} \gamma^{1.09} \tag{2.48a}$$

For a fouled membrane $$J_v = 3.25 \cdot 10^{-3} \gamma^{0.25} \tag{2.48b}$$

The shortcoming of this model lies in that there is no experimental evidence in the microfiltration range to confirm its correctness. Besides, the model is based on laminar flow, in turbulent flow the turbulence will destroy the concentration gradient and the back transportation by diffusion will be questionable. All the flows in this study are turbulent, therefore, this model is not applied to our study.

3) Lift forces [Karnis et al, 1966; Ho & Leal, 1974]

It is believed that some of these forces might play an important role in the difference between predicted and experimental data. The "Tubular Pinch Effect" is thought to be one of such effect caused by inertial force near the membrane.

Segré & Silberberg (1962) first published their observations of the tubular pinch effect on dilute suspensions of rigid spheres in a solid wall tube where the particles migrated away both from the tube wall and tube axis, reaching equilibrium at an eccentric radial position. This phenomenon was reported by Karnis et al (1966) from their experiments on many kinds of particles in various conditions and flowing media.

The extensive surveys of both experiments and theories of this effect have been made by Brenner (1966), Goldsmith & Mason (1967), Cox & Mason (1971), and later by Leal (1980).

1) Radial migration velocity owing to slip-spin Magnus force

It is known that particles flowing in a shear field of a laminar or turbulent flow spin due to the unequal fluid velocity on either side. Rubinow & Keller (1961) suggested the existence of a transverse force which arises from a slip-spin force akin to Magnus force and derived the expressions of lift velocity

$$V_L = \frac{1}{9} URe \left(\frac{d_s}{r_h}\right)^4 \left(\frac{x}{r_h}\right) \tag{2.49}$$

where V_L is the lift velocity ($m.s^{-1}$).

However, others found that even non-rotating particles also migrate [Theodore, 1964; Oliver, 1962], hence, this theory can not cover everything.

2) Radial migration velocity owing to inertial effect (slip-shear force)

Saffman (1956) obtained his expression from a solution of the Navier-Stokes equation retaining the inertial terms:

$$V_L = 0.86U\,Re \left(\frac{d_s}{r_h}\right)^4 \left(\frac{x}{r_h}\right) \tag{2.50a}$$

In his expressions, the slip-shear force is independent of the angular velocity of a sphere and occurs in both laminar and turbulent flows.

In order to explain the two-way migration of the particles, Cox & Brenner (1968) obtained a first-order solution of the Navier-Stokes equation and computed the lateral force required to maintain the sphere at a fixed x:

$$V_L = \frac{1}{2} U\, Re \left(\frac{d_s}{r_h} \right)^3 f\left\{ \frac{x}{r_h} \right\} \tag{2.50b}$$

where $f\{x/(r_h)\}$ is a function of the radial position of the particle in the tube or slit.

This equation is close to the empirical equation used by Segré & Silberberg (1962) to correlate their data:

$$V_L = 0.17 U\, Re \left(\frac{d_s}{r_h} \right)^{2.84} \frac{x}{r_h} \left(1 - \frac{x}{x_e} \right) \tag{2.50c}$$

where x_e is the equilibrium radial position of the particle which decreases as (d_s / r_h) increases [Karnis et al, 1966a & 1966b].

Ho & Leal (1974) and Vasseur & Cox (1974) performed the most complete theoretical analysis of the lateral migration phenomenon, valid for infinitely dilute suspensions, by explicitly including inertial effect in the presence of the flow boundaries and gave the form:

$$V_L = \frac{\gamma^2 d_s^3}{\nu} f\left\{ \frac{x}{r_h} \right\} \tag{2.50d}$$

The position dependence $f\{x/r_h\}$ is a maximum at the wall with a value of 0.095 [Vasseur & Cox, 1974] or between 0.26 and 0.42 [Ho & Leal, 1974].

All the works above have dealt with particle motion in a non-porous duct. It was Porter (1972) and Henry (1972) who applied the theory of "Tubular Pinch Effect" to explain the higher flux in experiments than predicted.

Madsen (1977) suggested that the lift velocity and filtration velocity estimated from polarization theory are additive, with the filtrate flux given:

$$J_v = V_L + k \ln \left(\frac{C_w}{C_b} \right) \tag{2.50e}$$

Green & Belfort (1980) proposed a model which explicitly considers the build-up of an immobile particle cake at the membrane that limits the flux according to

$$J_v = \frac{P_t}{\mu R_C} \tag{2.1a}$$

where $R_C = 5(1-\varepsilon_s)^2\delta_l\varepsilon_s^{-3}\left(\frac{S_s}{v_s}\right)^2$

where (S_s/v_s) is the particle specific surface to volume ratio (m^{-1}), this expression is, in fact, the Kozeny-Carman equation.

They obtained the lift velocity as

$$V_L = a\overline{U}Re\left(\frac{d_s}{r_h}\right)^b f\{x\} \tag{2.50f}$$

where $\overline{U}$ is the average axial velocity ($m.s^{-1}$)

b is close to 3

a is the dimensionless empirical coefficient

This model for a latex suspension was in order of magnitude agreement with experimental data of Porter (1972) but the calculated cake thickness indicated that the cake occupied over 70% of the channel. This model failed to predict a pressure independent value for the flux or a dependence on bulk particle concentration.

Ishii & Hasimoto (1980) used the resistance model with integration and obtained:

$$J_L = -abx^2\left(\frac{\overline{U_m}^2 d_s}{2\mu}\right)\left(\frac{x_e - x}{r_h^2}\right) \tag{2.50g}$$

where a = 5

$b = d_s/r_h$

x_e = -0.7 for best empirical fit.

Zawicki et al (1981) employed Saffman's (1956) analysis in their model, led to a formulation known as deposition theory [Forström et al, 1975] in which the drag force due to filtration is balanced by hydrodynamic lift force. Particle diffusion is entirely

neglected. They assumed that there is a particle free layer immediately adjacent to the membrane when the lift force exceeds the drag force. The maximum flux is thus given by:

$$J_v = V_L = 0.34 \frac{d_s^2 \dot{\gamma}^{\frac{3}{2}}}{\lambda \mu^{\frac{1}{2}}} \tag{2.50h}$$

where λ is a correction factor for the drag force on a spherical particle in a concentrated suspension [Trettin & Doshi, 1980]. The deposition theory did not agree well with the experimental data [Werynski et al, 1981; Zydney & Colton, 1984].

Belfort & Altena (1983) presented a gel-polarization lateral-migration model:

$$J_v\left\{x \ll \frac{d}{2}\right\} = \left[1.295\left(\frac{D^2}{L r_h}\right)^{\frac{1}{3}} \ln\frac{C_w}{C_b}\right]\overline{U}^{\frac{1}{3}} + ab^2\left(\frac{d_s}{2}\nu\right)\left(1 - \frac{x_e}{r_h}\right)\overline{U}^2 \tag{2.50i}$$

Diffusive term Lateral migration term

where a is an empirical coefficient ~ 5 [Ishii & Hasimoto, 1980]

$b = d_s / d_h$.

Altena & Belfort (1984) studied spherical rigid neutrally buoyant particles moving in a laminar fluid flow in a slit with one porous wall, where the wall flux was constant and independent of the axial coordinate. By extending the analysis of Cox & Brenner (1968), the effect of the wall porosity had been taken into account, they obtained the lift velocity in dimensional form.

$$V_L = Re\left(\frac{d_s}{d_h}\right)^2 U_{max} f\{\beta\} \tag{2.53}$$

where U_{max} = maximum undisturbed fluid flow velocity at the entrance to a porous channel ($m \cdot s^{-1}$),

$f\{\beta\}$ is the result of a numerical integration involving the undisturbed velocity profile and the Green's function. They calculated it with the expressions of Vasseur & Cox (1974) by the means of DO1FCF (Numerical Algorithms Group, Oxford, OX26NN, UK).

However neither this model, nor that of Madsen (1977), and Green & Belfort (1980) incorporated any correction in the lift velocity expression for the presence of other particles in a concentrated suspension.

Most of the existing models on the "Tubular Pinch Effect" were derived for laminar flow although Porter (1972) proposed that this effect should be greater in turbulent flow because of the larger inertial effects caused by radial migration velocity will increase with the Reynolds number, fluid velocity, and particle size but will decrease with increasing channel dimensions. Most CFMF applications use turbulent flow and have small particles suspended, hence radial migration should not be a dominant force.

4) Turbulent burst

Turbulent burst is a natural physical phenomenon which occurs in the turbulent sublayer boundary. It is the result of the evolution of small streaks along the wall ($x^+ < 100$, where x^+ is the normalized vertical distance from the wall). Since it is responsible for most of turbulent energy production from the boundary layer towards central flow, particles suspended in the boundary layer will certainly be affected by it. Most of the studies on turbulent burst have been concentrated on experimental observations and the determination of the average time between two bursts [Antonia, 1981]. The development of the theoretical nature is relatively slow due to the complexity of the mathematical expressions. The details on turbulent burst has been surveyed by Bogard (1982).

Grass (1971) observed that sand particles were carried up from sea bed region through virtually the total turbulent boundary layer thickness.

Sumer & Deigaard (1981) traced the motion of a single 3.0 mm diameter particle suspended in a horizontal water channel. They found the particle motion to be in accordance with available information on the burst phenomenon and deduced that turbulent burst might be the mechanism which maintains particles in suspension.

Roger & Eaton (1989) observed that the particles did not closely follow the fluid fluctuations in the normal direction and also the presence of particles tended to suppress turbulence.

Cleaver & Yates (1973) were the earliest authors who attributed particle re-entrainment to the turbulent burst:

$$F_L = 0.076\,\rho_b\,\nu^2\left[\frac{d_s u^*}{\nu}\right]^3$$

$$= 0.076\,\rho_b\,\nu^2 (Re^*)^3 \qquad (2.51)$$

where F_L is the lift force,

u^* is wall friction velocity $= \sqrt{\tau_w / \rho_b}$

and by O'Neill (1968):

$$F_D = 8\,\rho_b\,\nu^2\left(\frac{d_s u^*}{\nu}\right)^2 \qquad (2.52)$$

where F_D is the drag force for steady flow parallel to the wall past a sphere and in this case $F_L = 0$.

From Eq 2.51 and Eq 2.52, if the particles are small, $d_s u^*/\nu \le 1$, then $F_L << F_D$, which is coincident with observations [Clark & Markland, 1971]. The lift force will only remove those particles whose sizes are larger than $(0.005/\tau_w)^{-0.75}$ (where τ_w is the wall shear stress).

The rate of lifting will be

$$\frac{dF_L(0)}{dt} = -\frac{u^{*2}}{75\nu}\log\left(1-\frac{a}{270}\right) \qquad (2.53)$$

where a is a constant and supposed to be 0.01.

The time between bursts is about $100\,\nu / u^{*2}$, so that the number of particles remaining on the membrane surface per unit area [Cleave & Yeates, 1976]:

$$N = N_o \exp\left[-\frac{u^{*2} T_t}{100\nu m_B}\right] + N_s m_B\left[1-\exp\left(-\frac{u^{*2} T_t}{100\nu m_B}\right)\right] \qquad (2.54a)$$

where T_t is the duration from 0 to the m th burst (s)

N is the total number of particles remained on the per unit membrane surface area at time T_t (m^{-2})

N_o is the original number of particle per unit area (m^{-2})

m_B is the number of bursts per unit area (m^{-2})

N_s is the number of particles deposited between bursts (m^{-2}).

For clean surfaces, $N_o = 0$ and T_t is very small,

$$N \approx n_B \frac{u^{*2} T_t}{100\nu} \tag{2.54b}$$

therefore

$$n_B = \dot{N}_B \frac{100\nu}{u^{*2}} \tag{2.54c}$$

$$N = \dot{N}_B T_t \qquad (\tau_w < \tau_{w_c}) \tag{2.54d}$$

where $\dot{N}_B$ is the fixed depositing rate (s^{-1}).

τ_{w_c} is the critical wall shear stress

$$N = \dot{N}_B \frac{100\nu m_B}{u^{*2}} \left(1 - \exp\left(-\frac{u^{*2} T_t}{100\nu m_B} \right) \right) \qquad (\tau_w > \tau_{w_c}) \tag{2.54e}$$

Gutman (1977) related the theory of turbulent burst to the fouling mechanism of crossflow membrane filtration. Based on the postulation of Cleaver & Yates, he proposed a mathematical model for particle removal from RO membrane surfaces:

$$\frac{J}{J_F} = 1 + \frac{\beta C_F}{A u} \left[1 - \exp\left(- \frac{\frac{J}{J_F} - 1 - J A u t}{1 + \frac{\beta C_F}{A u}} \right) \right] \tag{2.55a}$$

$$(for \quad J_F > 2k_s)$$

$$\frac{J}{J_F} = 1 + \frac{\beta C_F}{A u} \left[1 - \left(\frac{\frac{2k_s}{J_F} + 1}{\frac{2k_s}{J} + 1} \right)^{-\frac{JAu}{2k_s(Au + \beta C_F)}} \exp\left\{ -A u \left[k_s + \frac{J A u}{2(A u + \beta C_F)} \right] t \right\} \right] \tag{2.55b}$$

$$(for \quad J_F < 2k_s)$$

where J is the flux of water through the membrane ($m \cdot day^{-1}$)

J_F is the flux of the fouled membrane ($m \cdot day^{-1}$)

C_F is the concentration of foulant ($kg \cdot m^{-3}$)

k_s is the mass transfer coefficient of liquid away from the membrane surface ($m \cdot day^{-1}$)

β is the parameter ($m^2 \cdot kg^{-1}$))

$$\beta = \frac{R_F}{R_m} \tag{2.55c}$$

where R_F is the hydraulic resistance of fouling layer per unit mass;

A is the parameter ($s \cdot m^{-2}$)

$$A = \frac{\rho_b S_B}{100 u_B} \tag{2.55d}$$

where S_B is the fraction of surface cleared by turbulence burst (m^2);

u_B is the superficial liquid velocity ($m \cdot s^{-1}$).

Knibbs (1984) applied this model to the UF of a ferric hydroxide floc and found the rate of mass re-entrainment was the product of a bursting rate coefficient and deposited mass. The bursting re-entrainment was an increasing function of crossflow velocity.

However, Yung et al (1989) modified Cleaver & Yates' models (1973 & 1976) by pointing out that the rate of re-entrainment is not directly proportional to the frequency of the bursting actions and the residence time of the deposited particles will be much higher as suggested in Cleaver & Yates' (1976) theory. They concluded that for particle sizes smaller than the viscous sublayer thickness, the tangential drag force is the dominant re-entrainment force, the removal criterion for small particles where adhesive forces dominant becomes:

$$\tau_w \propto d_s^{-1} \tag{2.56a}$$

and for large particles where particle weight dominates:

$$\tau_w \propto d_s^{1} \tag{2.56b}$$

According to their experimental results, turbulent burst is insignificant in the re-entrainment of those particles completely submerged within the viscous sublayer.

Rashidi et al (1990) further studied the particle - turbulence interaction in the wall turbulent flow.

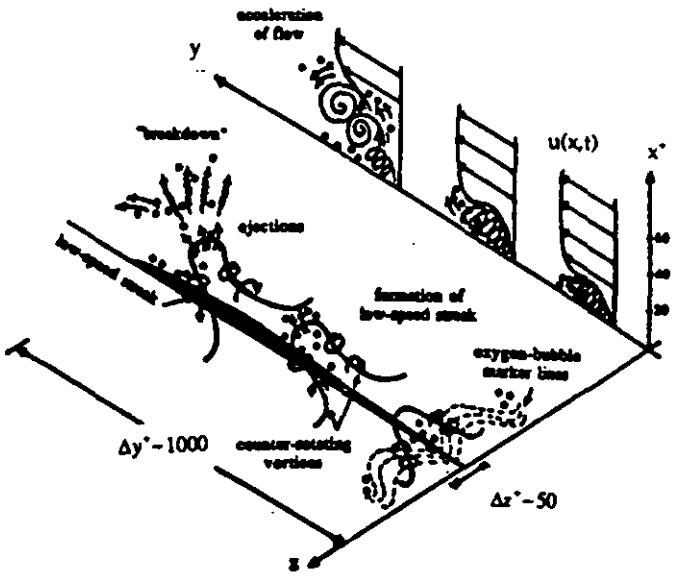

Fig 13 The interaction between turbulent burst and particles

They concluded that for particles with $d_p^+ > 1$, the transport is controlled mainly by ejections originating from the lifting up and breakdown of the low-speed streaks in the wall regions. When the particles are introduced into the flow, they mostly accumulate in the low - speed streak of the wall structures. These particles are then lifted up (depending on their size and density) by the inclined vortex - loops of the wall regions and are ejected into the bulk flow. The ejected particles with a greater density than that of the fluid, will eventually come back to the wall region, where some of them encounter the wall ejections which have already been in progress and will be lifted up before reaching the wall regions. The bursting process repeats itself and dominates the particle transport, while the particle presence affects the mechanism by which the turbulence energy is transported from the wall region to bulk flow.

The reported bursting process causes the transport of the particles in the flow direction. $\Delta z^+ \approx 50$, and inclined angles of the vortices are about $20 \sim 50^\circ$ to the boundary at $x^+ < 20$. (Fig 13)

They also found that the particle-burst interaction is very dependent on the density, size and flow Re of the particles. The angle and maximum elevation lifting up decrease with increasing particle size and density. Meanwhile the lifting process increases with increasing Re.

The particles with size $d_s^+ < 1$ have no response to burst, which meets Yung et al's (1989) conclusions.

Therefore, although some authors have made positive conclusions, the significance of turbulent burst on the membrane fouling mechanism is still not yet clear since the phenomenon of permeation is similar to wall suction which will suppress the turbulent burst by reducing the probability of the breakdown of low-speed streaks and therefore increasing the period between two ejections; the existence of particles will also reduce turbulent bursts. Besides, the particle size will be important to the interaction with turbulent burst, the small particles will not be influenced by the occurrence of turbulent burst - they only "roll" along the wall surface.

b) Axial force

There are three types of models which owe the removal of particles to the axial forces.

1) Axial convection force

Vassilieff et al (1985), Leonard & Vassilieff (1984) proposed a model based on solely convective transport which also explicitly considered the hydraulic resistance provided by the particles at the membrane surface. Particle diffusion and lift force were entirely neglected. Convection perpendicular to the membrane is balanced by axial convection parallel to the membrane to give

$$J_v = \left(\frac{C_w}{C_b} - 1\right)\left(\frac{\gamma}{2L}\right)H^2 \qquad (2.57)$$

where H is the cell layer height (cm or μm)

By solving Eq 2.1a and Eq 2.57 simultaneously with the particle layer

resistance which is a function of H, and after some approximations, they found that by assuming $H \geq 25\,\mu m$, the predicted values of this model met with selected plasmapheresis results but still gave some discrepancy.

Davis & Birdsell (1987) developed this model by using the parabolic velocity profile and predicted that a flowing cake thickness is a function of axial position x.

Hoogland et al (1990) assumed that the removal of solids towards the membrane is accomplished by converting these solids into axial directions and finally out of the filter module. They used Kozeny-Carman equation and obtained:

$$J_v = \frac{(1-\nu_c)^2}{2\nu_c^2}\left[\frac{(1-\nu_s)\tau_w}{\nu_s \mu_c L}\right]^{\frac{1}{3}}\left[\frac{d_s^2 P_t}{60\mu}\right]^{\frac{2}{3}} \tag{2.58}$$

However, it has been confirmed that a packed static cake has more influence on the permeation and therefore this model has limited significance.

2) Scouring force

This model is based on an analogy between the flow across the cake and the motion of a sediment-laden stream over a layer of settled sediment. Under steady state, the convection velocity of the particle towards the membrane is equal to the rate of scouring a particle from the membrane surface, which is proportional to the shear rate.

Fane et al (1982) used the idea of an "erosion coefficient" which is a function of bulk concentration and set up the relationship between permeate flux rate , bulk concentration and velocity:

$$J_v \propto C_b^{a_1} U^{a_2} \tag{2.59}$$

They further developed their model (1984) by intuitively combining the three forces (Brownian diffusion, lift and scour) together:

$$J_v = a_1 \ln\left(\frac{C_w}{C_b}\right) + a_2 V_l + a_3 C_b^{a_4} U^{a_5} \tag{2.60}$$

This model was comprehensive and met well with their experimental results.

3) Force balance

This model is based on the balance between the resultant axial force, which tends to remove the particles, and normal force which tends to retain the particle. The axial force is thought to be constant since the bulk velocity is constant, and the normal force will decrease due to the decay of the permeate flow rate. In the initial stage, the normal force is stronger than the axial one and hence causes the deposition. The steady state occurs when the two forces are balanced and results in constant cake thickness and permeate flux rate.

Shirato et al (1970) analysed the forces acting upon a particle which sits at the surface of the particulate bed, they proposed that during permeation, there exists a critical axial velocity at the bed surface, over which the particle can no longer keep static and removal is possible.

Rautenbach & Schock (1988) showed from their tests with the crossflow filtration of 2 - 2.5 micron clay and quartz powders in tubular and thin-channel modules that:

$$J_v = aRe^{1.26}\left(\frac{\nu}{d_h}\right)\left(\frac{d_s}{d_h}\right)^{0.44} \tag{2.61}$$

Lu & Ju (1989) obtained the similar conclusion but by considering moments acting on a particle at a rough surface. Their expression also well met their experiment results.

Blake (1990) analysed all the above models (axial and radial). He developed a force balance model and simplified Rautenbach & Schock's formula (1988) into:

$$J_v = a_1 d_s \tau_w + a_2 \tag{2.63}$$

His model has been supported by Cumming et al (1991) in their filtration of slurries.

The weakness of this model is that filtration is a multibody system, the interaction between particles must be taken into account, and the existence of the cake

also complicated the estimation of a friction coefficient and boundary layer velocity profile. The continuum theory forwarded by Willis et al (1986) and statistical mechanics theory by Mason & Longsdale (1990) might be helpful to solve this problem.

2.5 Brief summary

The theory for CFMF has evolved from the traditional cake filtration and concentration polarization theory of ultrafiltration because of the same operating principles and considerable overlapping applications, with some modifications in the results based on experimental data.

It seems that the cake-filtration model is mostly suitable for the situation where a concentration gradient is insignificant, the film-filtration model is suitable for the macromolecules or suspensions whose concentration gradient plays an important role in the transport mechanism.

Navier-Stokes equation is the basic equation for CFMF. The various solutions to it provide different expressions for the filtrate flux depending on the assumptions made.

Concentration polarisation is studied by most authors working on membrane separation experimentally and theoretically. There is substantial discrepancy between experimental data and theoretical prediction in most cases.

None of existent models, neither the famous "Tubular Pinch Effect", nor the popular "Self Induced Hydrodynamic Diffusion" or other mechanisms have successfully explained the origin of the discrepancy between equilibrium flux rates based upon particle diffusion coefficients calculated by means of a modified Stokes-Einstein equation and experimental measurement.

Pore blocking, on the other hand, is also an important factor for flux decline, especially because it affects membrane resistance. The blockage can not be simply improved by crossflow since the pore flow is essentially laminar and the adhesive force in the micron or submicron range is very strong. A major task for all workers interested

in membrane separation processes is how to eliminate or at least to reduce fouling caused by pore blocking. It is evident from the above discussions that if the pore blocking can be prevented, the prediction of MF will depend on the nature of the suspended material being filtered: cake, film theories, pinch effect, force balance, etc.. Under such circumstances mechanical membrane cleaning may be effective. Pore blocking is important because it is not reversible and is a progressive effect which is common in most microfiltrations. Despite its evident importance it has received less experimental and theoretical attention than those in RO and UF. Thus if pore blocking can be better understood and efficient membrane cleaning means to prevent it be developed, the application of microfiltration in the process industries will be furthered.

CHAPTER 3

Crossflow Microfiltration of Seawater

Many possible applications have been described in § 1.6 for the uses of microfiltration, such as ultra-pure water production, fermentation product processing, precipitate concentration, etc..

The technique would appear to be well suited to a process in which a substantial volume of retained material (say up to 20 or 30%) can be discharged into a receiving water with little or no effect on the environment. The crossflow filtration of seawater for off-shore use would seem to fit this requirement very well. The retained materials could be discharged into the sea at only a slightly higher solids content than the water drawn into the process.

The process scale requirement is appreciably large for the duty of seawater filtration, yet the specification of the particle retention is not very demanding, when compared with biological or ultra-pure water applications. Under these circumstances seawater filtration was thought to provide a good challenge to both the existing mathematical models of the process and the robustness of the crossflow filtration technology.

During the experimental programme, it was discovered that the interaction between the membrane material and the finely divided and suspended materials undergoing clarification was critical. Membrane fouling which was irreversible to mechanical cleaning methods resulted from penetration of fines into membranes of significant depth. This leads to the later investigation of the internal membrane fouling processes and methods to prevent or minimise the penetration of fine particles, as described in Chapter 4 and 5 respectively.

3.1 Crossflow filtration of seawater

The most well-known application of crossflow filtration of seawater is RO, during which more than 98% of the salt is rejected. RO has become an important source of fresh water supplies in some Gulf countries. Large scale plants are running nowadays yielding desalinated water flows as high as millions of gallons per hour [Gutman, 1987].

Another case of crossflow filtration of seawater is in the fish industry in which a combination of UF and MF for waste water treatment is used as described in Chapter 1 [Jaouen et al, 1990; Schmidt & Wulle, 1988; Watanabe et al, 1986].

The offshore oil industry also requires large amounts of filtered seawater to inject into the oil reservoir rocks to maintain the pressure and displace the oil. 98 % of the particles larger than 2 μm in the injected water must be removed before injection, so as to prevent deposition and blockage within the oil reservoir rocks [Mitchell & Finch, 1981]. This specification assumes a constant feed suspension and an alternative specification is less than 2000 particles per ml greater than 2 μm and absolute filtration at 5 μm [Holdich et al, 1990]. The required volume of water flood will be as high as 2600 m^3/hr for a field and rarely less than 650 m^3/hr [Abdel-Ghani et al, 1988]. Some production platforms now employ RO on the injection water to reduce the concentration of sulphate ions present, thus reducing the precipitation of barium sulphate in the rock formation. Crossflow microfiltration could be employed to pretreat the water before RO.

Filtration is also used to protect equipment which uses seawater on the oil platform: RO, water sealed pumps, cooling, etc. On some platforms over 50% of the water drawn up from the sea is used for duties other than injection.

These tasks are currently being carried out mainly by backwashable deep bed or disposable cartridge filters [Kaiser, 1983; Cubine & Randolf, 1973]. These facilities work adequately over a large part of the year, but do not perform well during periods of algae bloom since they are run in the dead-end mode and usually suffer from clogging and low flux rates due to the retained particles. Water used for cooling duties is at present filtered on 80 μm coarse screens.

The North Sea seawater used in reservoir injection is reasonably clean, containing between 0.2 and 0.8 mg/l of suspended solids [Mitchell, 1978; Carlberg, 1979], a consequence of having been pumped up from a depth of 60 m [Mitchell, 1978].

The major contaminates are clays, sand, bacteria and plankton which are usually filtered out in deep bed or cartridge filters. The seawater solids loading is highly seasonal: the quantity of suspended solids increases considerably during spring and autumn due to the "bloom" of plankton. It has been reported that the major foulant found in seawater cartridge filters is the lipid content of plankton [Edyvean & Lynch, 1989], which is

released into suspension when the organisms are crushed by the pumps and filters. The resulting lipid concentration can rise to as high as 20 mg/l during a bloom period [Edyvean & Sneddon, 1985; Volkmann et al, 1980]. The lipids are fatty materials which act as a glue to stick the suspended solids to the filter surface and cause blockage [Edyvean & Lynch, 1989].

Since the 1980s, with developments in the technology of manufacturing and applying membranes, there has been an increasing interest in utilizing crossflow membrane microfilters to replace conventional filters.

During crossflow filtration, the operating pressure will be lower than that during conventional filtration, the feed flow is parallel to the membrane surface, therefore the shear force will greatly reduce the deposition at the membrane surface and result in higher flux rates, longer membrane lifespan, lower costs and easier maintenance.

One purpose of this study was to investigate the feasibility of using crossflow microfilters for offshore applications and to obtain information on potential fouling problems.

3.2 Experiments with challenge materials

3.2.1 Test rigs

a) Rig of one inch pipeline (referred to later as Rig 1)

This rig was constructed out of one inch PVC pipes and was designed to accommodate the sheet membrane in a plate and frame module [Carter, 1982]. The use of PVC enabled a light-weight filter, resistant to chemical attack, easily constructed - these are the essential factors in offshore use. The membranes on each plate are 0.2 x 1 m (width x length), 25 channels on each plate, each channel has a dimension of 5x5x1000 mm (width x depth x length).

This rig was significantly refurbished in 1990 for seawater filtration. It can accommodate tubular modules in different sizes, numbers and materials as well as the plate and frame ones.

b) Rig of 3/4 inch pipeline (referred to later as Rig 2)

This rig was developed in 1989 for the purpose of studying crossflow micro-

filtration of simulated seawater. It used PVC pipes of 3/4 inch. It can accommodate either tubular or capillary membrane modules .

The principles of the layout of the two rigs are the same as shown in Fig 14.

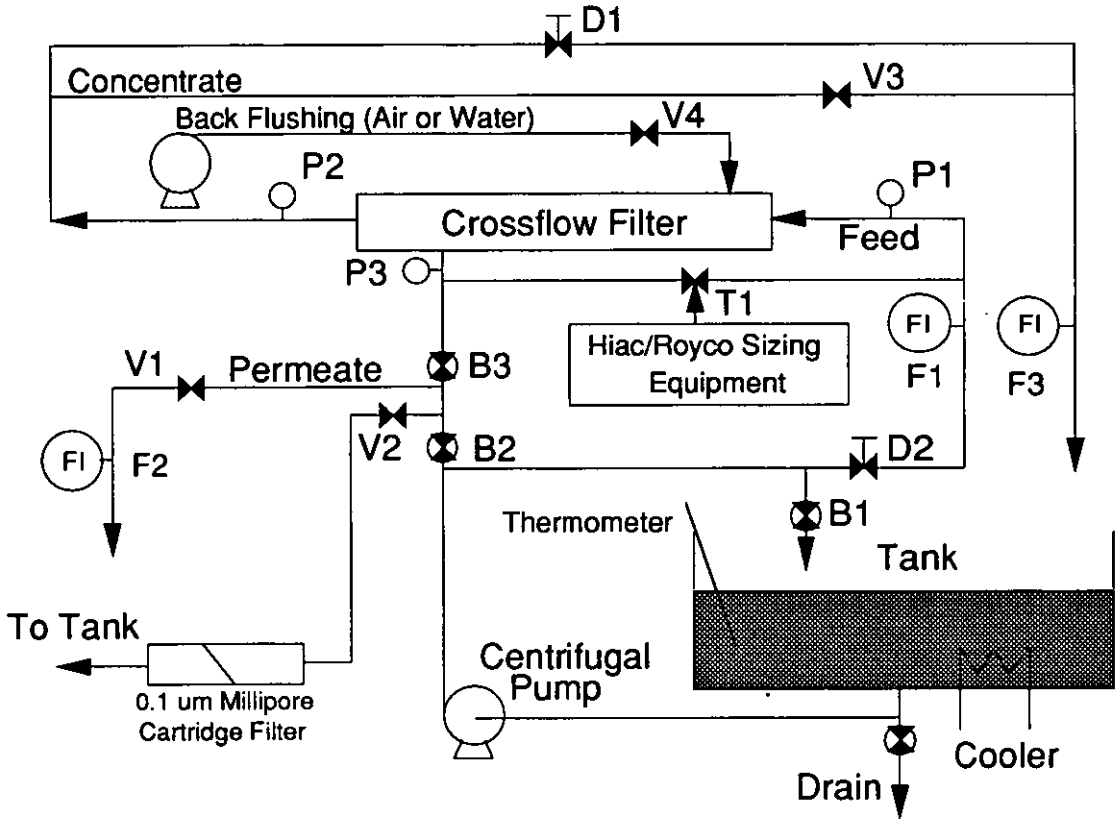

Fig 14 Layout of laboratory test rig

In Fig 14:

B1 to B3 are ball valves. B1 controls the by-pass flow, B2 only opens for system cleaning together with opened V2, B3 is used to control the permeate side pressure.

D1 and D2 are diaphragm valves. D1 controls the outlet pressure while D2 regulates the inlet flow rate.

P1 to P3 are pressure gauges. P1 and P2 are used to measure the pressure at the inlet and outlet of the module, P3 is used to measure the pressure at the permeate side, the pressure range is 0 - 6 Bar.

The inlet flow meter F1 is a rotameter, its measuring range is 0 - 22 l/min. The other two flow meters are both Litre Meter electrical type with different ranges: 1 - 65

l/min for the F3 which is on the concentrate side and 1 - 12 l/min for F2 which is on the permeate side. They are alternatively connected to a CR450 chart recorder depending on the requirements of the tests.

T1 is a three way valve which alternates the permeate and feed flow through the Hiac/Royco sizing equipment.

V1 to V4 are solenoid valves.

V1 is a normally opened type, only closed during system cleaning and back-flushing.

The others are all normally closed type:

V2 is only opened for system cleaning.

V3 is only opened during backflushing to relieve the outlet pressure so as to enhance the efficiency of backflushing.

V4 is also only opened during backflushing to let the cleaning media (air or water) enter the shell and backflush the filter.

A 0.1 μm Millipore cartridge filter is fixed after V2 for system cleaning.

There is a cooler and a thermometer (0 to +110 °C) in the tank whose capacity is 100 litres with a 3/4 inch hose at the bottom.

In the case of air backflushing, only one centrifugal pump is used for feeding the flow throughout the system. The air is supplied by the pipeline and its pressure is set at 3.5 Bar. The air is filtered with a 0.1 μm cartridge air filter before it enters the module, this filter is not included in the figure.

If water backflushing is involved, another pump and another tank are needed. The required water comes either from the permeate or from the 0.1 μm cartridge filter. It backflushes at 2.8 Bar. The layout of the backflushing part has not been shown in the figure except for the pump and the solenoid valve.

A Hiac/Royco laser light particle sensor (model 346-BCL) and a counter (model 4100/4150) are used. The sampling rate is set at 100 ml/min, the channel settings vary with the sizes of the challenge materials.

3.2.2 Computer programs

Rig 1 is controlled by an ITT microprocessor whose program was written when the rig was assembled in 1982 and later modified in 1989. It was rewritten in 1990 to control the solenoid valves for backflushing during on-site seawater tests.

Rig 2 is controlled by an IBM PC with programs written in Turbo Basic language. Several programs were composed for different purposes.

One program is used to switch on/off the solenoid valves separately or simultaneously to check the performance of the solenoid valves, it is also used for system cleaning by switching on/off V1 and V2.

One program is uniquely set for studying the efficiency of backflushing, by which the period and length of backflushing can be individually set, so that the optimum period of backflushing to recover the flux rate can be obtained.

The main program can collect the results from the Hiac/Royco counter, record the permeate flux rate and set the backflushing starting time, frequency and duration.

3.2.3 Challenge materials

a) Tap water and cleaned tap water

The solids concentration of tap water was very high, therefore, the tap water had to be filtered before it was used for the tests. This process was carried out by the Millipore cartridge filter which was cleaned with hydrogen peroxide if there was suspicion of microorganism growth in it.

The system cleaning started with the rig being cleaned with 0.1% of Ultrasil 50 (pH 4.9) or Ultrasil 11 (pH 10.4) for a few hours depending on the water quality and previous history of filtration. Then the residual detergent in the rig was washed away with tap water. The rig was again filled with 50 litre tap water and filtered by the Millipore cartridge filter until it was clean.

During system cleaning, the filter was replaced by a pipe and dipped in solvent for 30 minutes. When the system had been cleaned, the filter was put back and backflushed by air or water for several times, each time lasted 2 - 3 seconds.

Between each two test runs, the crossflow filter was also backflushed for several times, each one lasted 2 seconds.

The cooler was on during this operation. The Hiac/Royco sizing equipment was used only at the end of the process to check the solids concentration.

b) Silica powder mixture (3 - 20 μm with d_{50} = 7 μm) was used to simulate the solids in real seawater [Knibbs, 1985], the size distribution of the both are shown in Fig 15. The silica powder was mixed in 200ml deionized water from the Milli-Q water system (referred to as deionized water later) and was ultrasonically vibrated for 30 minutes before it was put into the tank.

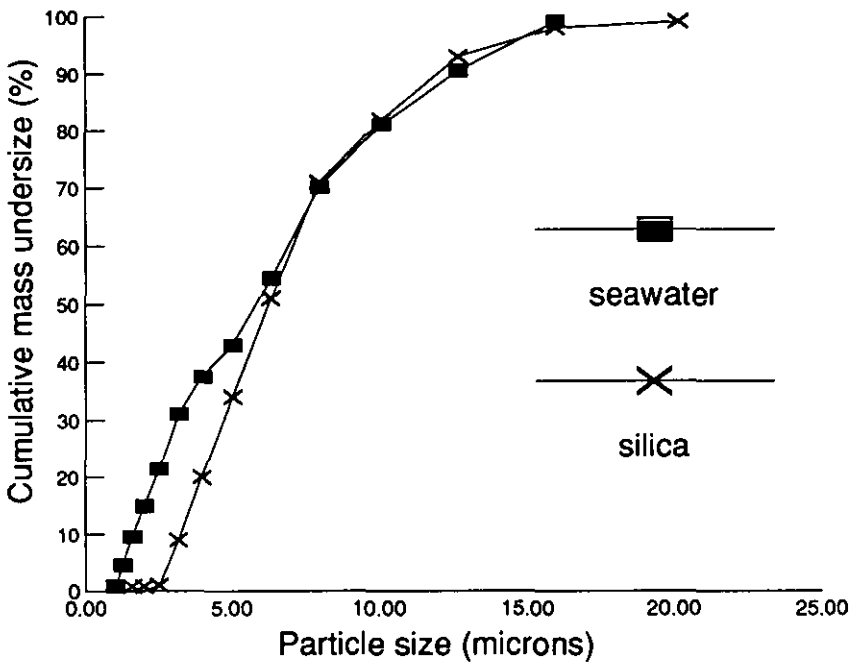

Fig 15 Size distribution of solids in seawater and silica

c) Seawater algae suspensions containing *Dunaliella tertiolecta* (CCAP 19/6B); a seawater algae cultured from Norwegian Fjord. The size distribution is shown in Fig 16. Its concentration used in the system was approximately 1 mg/l.

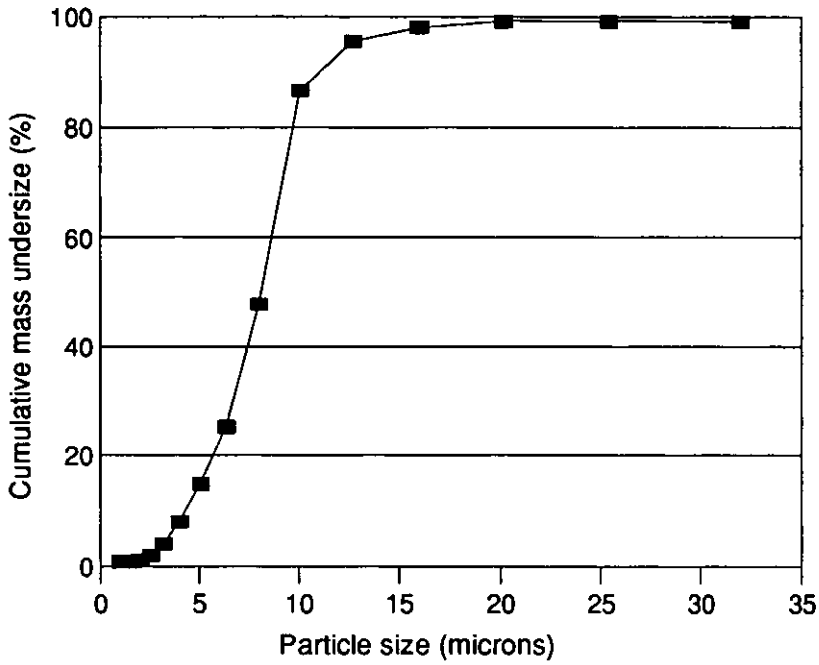

Fig 16 Size distribution of seawater algae in cleaned tap water

d) Seawater containing lipids was simulated with fish lipid concentrate capsules containing eicosapentaenoic and docosahexaenoic acids, purchased from *Boots the Chemists Ltd.* The lipid was mixed with 200 ml deionized water before it was put into the system, but it had not been ultrasonically vibrated since the ultrasonic energy might break the lipid structure.

After the mixture had been put into the tank, it was circulated for 5 minutes in the recycling lines to ensure that it was homogeneously distributed in the tank.

3.2.4 Membranes

a) Metal fibre tubular filters (Fairey)

Three such filters were used for the tests. Each of them has 0.014 m ID and 0.01 m^2 inner surface area. The absolute pore size is 3 μm. The flow is fed inside of the tube and permeate leaves from the shell side.

b) Capillary filter (Enka)

42 polypropylene capillary tubes are in parallel in a shell. Each has a 0.0018 m ID, and the total surface area is 0. 1 m^2. The absolute pore size is 0.2 μm.

c) Ceramic tubular filters (Ceraflo, Norton, USA)

The filter is in the monolithic arrangement with 19 tubes in parallel. The absolute pore size is 1 μm. The ID is 0.0027 m, and the total surface area is 0.13 m^2.

d) Sheet membrane (Versapor 3000, Gelman)

The acrylonitrile membrane has 0.2 m^2 of filtration surface area in the plate and frame module. The absolute pore size is 3 μm.

e) PTFE capillary (Gore)

19 tubes in parallel, each tube is 0.004 m ID and 0.7 m long. Two of these modules were run in parallel on Rig 1. The absolute pore size is 0.8 μm and the total surface area is 0.334 m^2.

f) Metal sheet (3 AL 3 , Bekaert)

The stainless steel sheet membrane has an absolute pore size of 3 μm and total surface area of 0.0255 m^2.

3.2.5 Calibrations

a) Pressure gauges

The calibration was carried out with cleaned tap water on a weekly base.

The three gauges are the same model. When the pump is off, they all display 0, when the pump is on, the inlet valve is opened, outlet and permeate valves are closed, they also display same pressure readings.

Due to the positions where the gauges were situated, the pressures indicated from the outlet and permeate sides were lower than those in the modules, therefore it was necessary to carry out pressure distribution tests for each filter to check if the displayed value represented the real situation. This was done by fully closing the permeate valve (B3) and fully opening the outlet valve (D2), recording the readings from all the gauges under different flow rates (varied from 4 to 20 l/min). If the difference between (P1 + P2)/2 and P3 is great, where P1, P2 and P3 are the inlet, outlet and membrane feed side pressure respectively, then corrections were made. The details of the corrections will be described in the next two chapters.

b) Hiac/Royco readings vs. solids concentration in the flow

Since the Hiac/Royco is a very sensitive particle sizer and the signal processing saturates at too high a solid concentration, this test was devised to check the concentration up to which it could be used on-line to measure the solids concentration.

The six channel thresholds were first set at 0.7, 1.1, 2, 3, 5 and 9.8 μm. 50 litres of tap water was cleaned with the 0.1 μm Millipore cartridge filter until the total counts of particles larger than 1.1 μm were less than 10 per ml, the system was then regarded as clean.

Table 6

Hiac/Royco readings vs. solids concentration

Silica	Counts per 100 ml in the following channels (μm)						
(mg/l)	0.7	1.1	2	3	5	9.8	19.8
0	290	76	10	5	6	4	
1.25	18706	26667	357	204	133	8	
2.5	36211	4903	531	280	148	7	
3.75	48769	6888	717	346	174	8	
5	59355	9006	835	389	176	8	
6.25	69954	11999	1036	463	219	4	
7.5	Fail	14917	1199	512	218	3	2
8.75		18461	1373	591	248	3	2
10		23367	1661	676	291	5	4
11.25		27593	1924	770	304	6	6
12.5		32222	2159	842	335	4	4
13.75		35682	2257	871	335	6	7
15		40982	2721	996	387	7	8

1 g of silica suspended in 400 ml deionized water, well mixed ultrasonically, was used. The concentration of silica in the tank was increased by 1.25 mg/l each test.

The lower channels which responded to smaller sizes saturated first, the channel settings were then adjusted to a larger size. The highest concentration was 15 mg/l, which was much higher than that of seawater. The results are shown in Table 6, the particle concentrations are in counts per 100 ml.

The Hiac/Royco readings essentially increased linearly with the solids concentration for small particles. For large particles (≥ 9.8 μm), the counts fluctuated at low readings. This was due to the low concentration of large particles in the silica mixture. From the above test, the Hiac/Royco was shown to be capable of monitoring the solids concentration in the tests.

This test was carried out only once. The Hiac/Royco sizing equipment was self-calibrated against cleaned tap water several times a day.

c) Flow meters and chart recorder

Flow meters and chart recorder were calibrated on a monthly base against a known volume collected in a measured time.

d) Temperature fluctuation

The experiments were usually run with 50 litres of water for two hours. The variation of temperature during this process period was within 1 °C and therefore the change in permeate flux due to the temperature variation was neglected.

e) Particle shedding effect of the rig

It was necessary to investigate the particles produced by the rig itself during the process. Only Rig 2 was tested since both rigs were made of same materials. When the water in the rig had been purified by the Millipore cartridge filter, the system was run at 25 l/min and 12.5 l/min for two hours respectively with the Hiac/Royco monitoring the variation of particle counts.

The number of counts in a channel, between particle sizes (μm) given by the legend shown in Figs 17 (25 l/min) and 18 (12.5 l/min) respectively was monitored with respect to time.

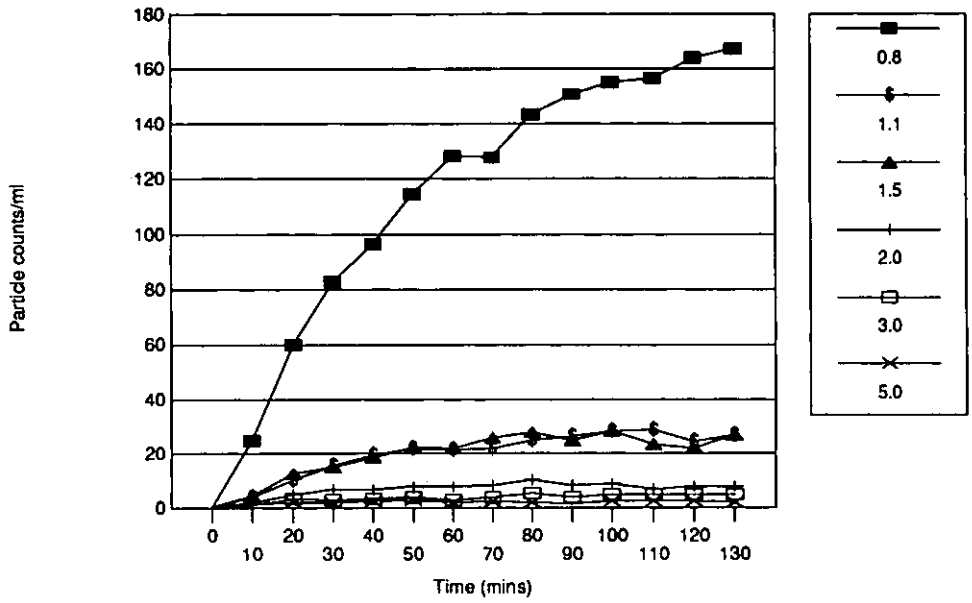

Fig 17 Shedding effect of the rig at 25 l/min

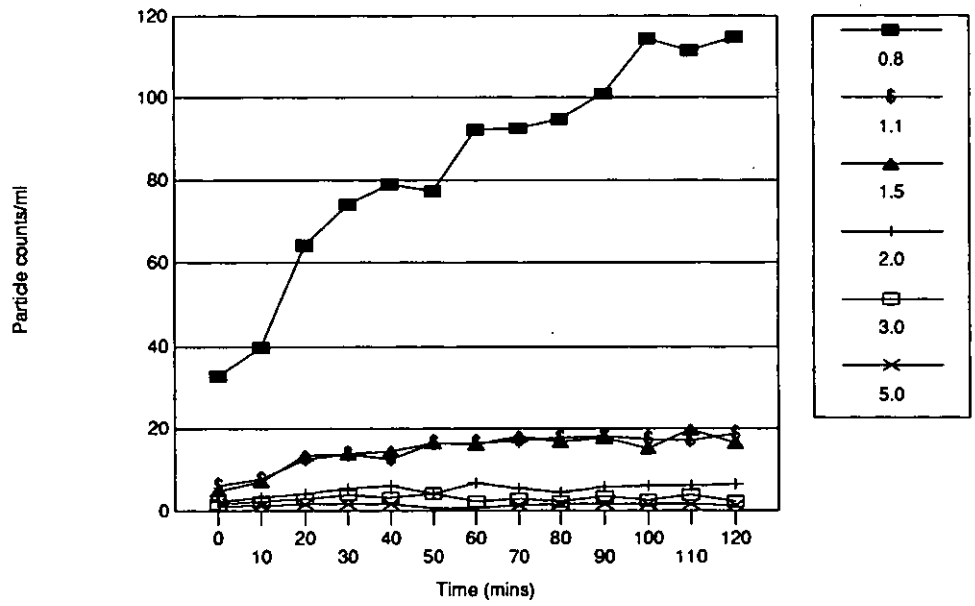

Fig 18 Shedding effect of the rig at 12.5 l/min

From the above figures we can see that the rig does not produce any significant particles in the range of 2 - 5 μm which we are interested in, therefore, the shedding effect of the rig can be ignored.

3.2.6 Test items

All the tests were run in batch mode.

a) Effects of membrane types and geometries on the permeate flux rate

Three metal fibre tubular filters (Fairey, No 97, 98, 99), one polymer capillary filter (Enka) and one ceramic tubular, were tested on Rig 2.

Versapor sheet, PTFE capillary and ceramic filters were tested on Rig 1.

b) Effect of solids concentration on the permeate flux rate

All the filters were tested with the following items:

Membrane resistance with cleaned tap water; the flux rate decay and recovery with solids in the same water at different concentrations and finally flux rate decay and recovery with 2mg/l solids plus lipids at different concentrations.

In addition to the above items the metal and polymer sheet membranes were also tested with solids plus seawater algae to investigate the fouling process. The PTFE and ceramic filters were tested with tap water to investigate the effectiveness of back-flushing and chemical cleaning.

c) Effects of operating pressure and feed flow rate on the permeate flux rate

For each concentration, 3 sets of tests were conducted:

Transmembrane pressure by changing the flow rate with P2 fully opened, then the effects of shear force on filtration by changing the flow rate with constant pressure. Finally the effects of pressure on the permeate flux rate by varying the transmembrane pressures at constant feed flow rate.

e) Effect of backflushing on the permeate flux rate

The backflushings were commenced when the permeate flux rate became constant. Then it was carried out at constant frequency and duration till the end of the run.

e) The membrane retention efficiency (MRE) to the particles and lipids

For solids concentration, only the Fairey and the Enka filters were tested.

For lipids concentration, only one metal filter (No 98) was tried because other

types of filter were not suitable to be tested due to their sizes or structures.

For algae with solids, Scanning Electron Microscope (SEM) was used to investigate the form of deposit layer on the membrane surface.

f) The membrane resistance

Only tested with Versapor and Bekaert membranes. The permeate flux rates at different pressures under constant flow rates and concentrations were measured.

3.2.7 Data acquisition and expression

a) Pressure

Recorded from the three gauges in psi, since the difference between (P1 + P2)/2 and P3 is not great, the transmembrane pressure (P_t) is expressed as (in Bar):

$$P_t = \frac{(P1 + P2)}{2} - P_p \tag{3.1}$$

where P_p is the permeate side pressure.

b) Feed flow rate

Recorded from the rotameter, and expressed in l/min;

c) Solids concentration

Recorded from the Hiac/Royco sizing equipment in counts/ 100 ml/min, and expressed in counts per ml;

d) Membrane retention efficiency

The retention efficiency to the solids was examined by Hiac/Royco during the process. A three way valve let the flow from permeate or feed side pass the sampling cell alternatively so that the difference between two flows could be obtained.

The retention efficiency to the lipids was only investigated during each test of the Fairey No 98 filter, 100 ml of permeate or feed was mixed with 45 ml chrolo-form/methane mixture (2: 1), and the filter was submerged in 75 ml of solvent for 30 minutes. The solution was then evaporated and put in the oven at 50 °C until its weight did not further decrease and part of the yellow oil-like material had been dehydrated. The lipid concentration in tap water and in the filter before fish oil was put in were also tested. The results were 0 mg/l for both cases.

The retention efficiency to the algae was observed by SEM on a piece of membrane, comparison was made between the pictures of the clean and the fouled ones.

e) Permeate flux rate

Recorded at 2 minute intervals, each reading taking 10 seconds, essentially by beaker, stop watch and scale due to the low quantity and for improved accuracy, expressed in $m^3/m^2 \cdot hr$.

The permeate flux rates were not recorded during solids sampling periods.

The permeate flux rate was recorded two minutes after backflushing.

3.2.8 Test results and discussions

The test results of PTFE, Fairey, Enka and ceramic filters are listed in Appendix 3. Table A for PTFE, Table B to E for Fairey filters, Table F for Enka and Table G for ceramic filter.

The test results with PTFE and Enka filter are tabulated in detail.

Due to the extensive data taken during the tests with the Fairey and ceramic filters, the details of the permeate flux rate variation with time during the process have not been included, only those at the start of the process, and right before/after the backflushing are listed.

a) With tap water

Since tap water contains many solids, it was the first object studied experimentally. PTFE and ceramic membranes were tested. The tests were carried out on Rig 1 only. The transmembrane pressure varied between 0.7 Bar and 1.1 Bar. Backflushing with air at 2.8 Bar was initiated at the 16th minute during each test with a frequency of 1 sec/min. The flux rate dropped very quickly - it reached the "plateau" region within 10 minutes and air backflushing could not recover it efficiently. Ultrasil 50, Ultrasil 11 and nitric acid were used as chemical cleaning agents. For each cleaning material, the rig was cleaned for 20 minutes at the same operating pressure. Then the rig was drained and washed by tap water to get rid of the residual chemicals, the filtration was then run again.

It was found that only nitric acid (0.1 pH) could effectively recover the flux rate with the aid of air backflushing. The flux rate recovered from 0.086 $m^3/m^2 \cdot hr$ up to 0.431 $m^3/m^2 \cdot hr$ after backflushing. The results of the tests were listed in Table A of Appendix 3 and shown in Fig 19.

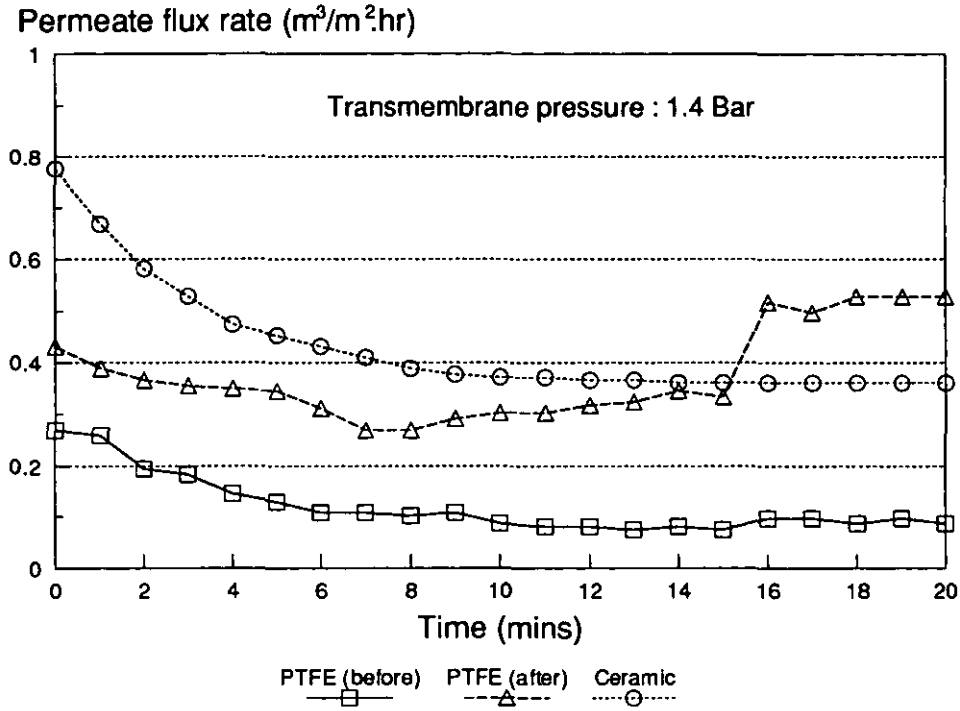

Fig 19 Flux rate of PTFE and ceramic membranes with tap water

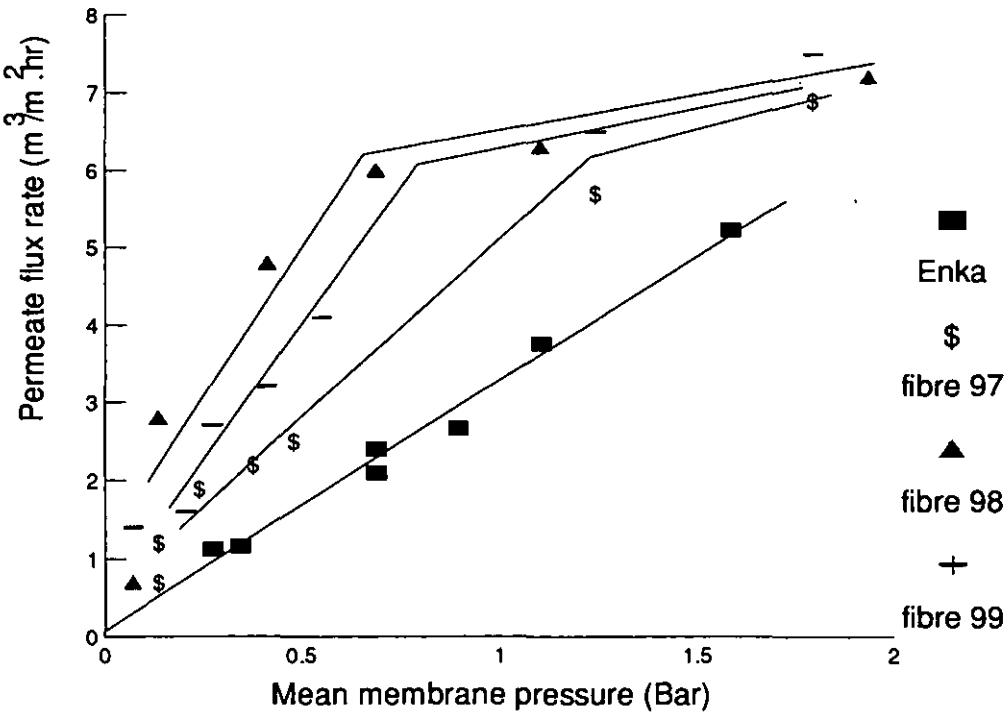

Fig 20 Flux rate with clean water (Fairey and Enka)

In Fig 19, *PTFE (before)* refers to the flux rate before nitric acid was used, it is evident that backflushing had no effect on the flux rates.

PTFE (after) refers to the flux rate after nitric acid cleaning, the flux rate was high at the beginning and could be improved further by backflushing;

The *ceramic* refers to the Norton Ceraflo filter which was tested following the same procedures, the effect of backflushing after nitric acid washing was not as prominent as that on the PTFE filter

Since nitric acid was not ideal for offshore use, it was clear that unfiltered tap water was not suitable for direct use for the laboratory study, all the tests afterwards were carried out with cleaned tap water if not specified.

b) With cleaned tap water

All the filters demonstrated that, up to a flux rate of 6 $m^3/m^2 \cdot hr$, the permeate flux rate was a unique function of transmembrane pressure, and independent of crossflow velocity. This can be true only when filtering clean water. It obeys Darcy's law for flow in porous media in the form of:

$$J_v = \frac{\Delta P}{\mu \cdot R_m} \tag{3.2}$$

The test results of Fairey and Enka filters are given in Fig 20.

The results for the Ceramic filter are shown in Fig 21. It shows that the permeate flux rate linearly increased from 0.08 to 4.5 $m^3/m^2 \cdot hr$ with transmembrane pressure increasing from 0.07 to 1.17 Bar at a 12 l/min feed flow rate.

The permeate flux rate of Versapor 3000 sheet membrane also linearly increased from 2.1 to 9.2 $m^3/m^2 \cdot hr$ with transmembrane pressure increasing from 0.4 to 0.8 Bar.

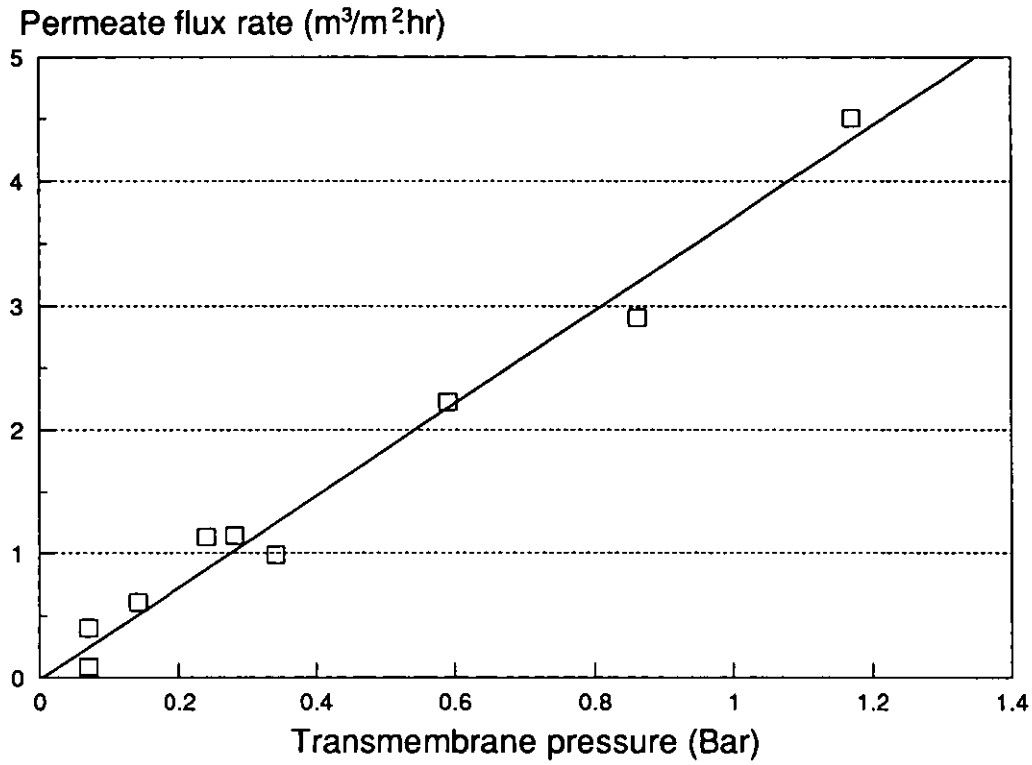

Fig 21 Water flux rate of ceramic filter

c) With solids and lipids

During a bloom period, the concentration of suspended solids in seawater can rise to as high as 10 mg/l, therefore, the initial series of membrane tests were devised to use this concentration of silica suspended in cleaned tap water.

Three Fairey filters on Rig 2 and Versapor sheet membrane on Rig 1 were used for this item.

The flux rates and the retention efficiency of the membranes under different flow rates and pressures were examined. Two sets of such tests are shown in Fig 22.

Also shown in Fig 22 is the effect of backflushing with compressed air at 3.5 Bar, it indicates that backflushing can recover the flux rates to as high as 80 -90 % of their original.

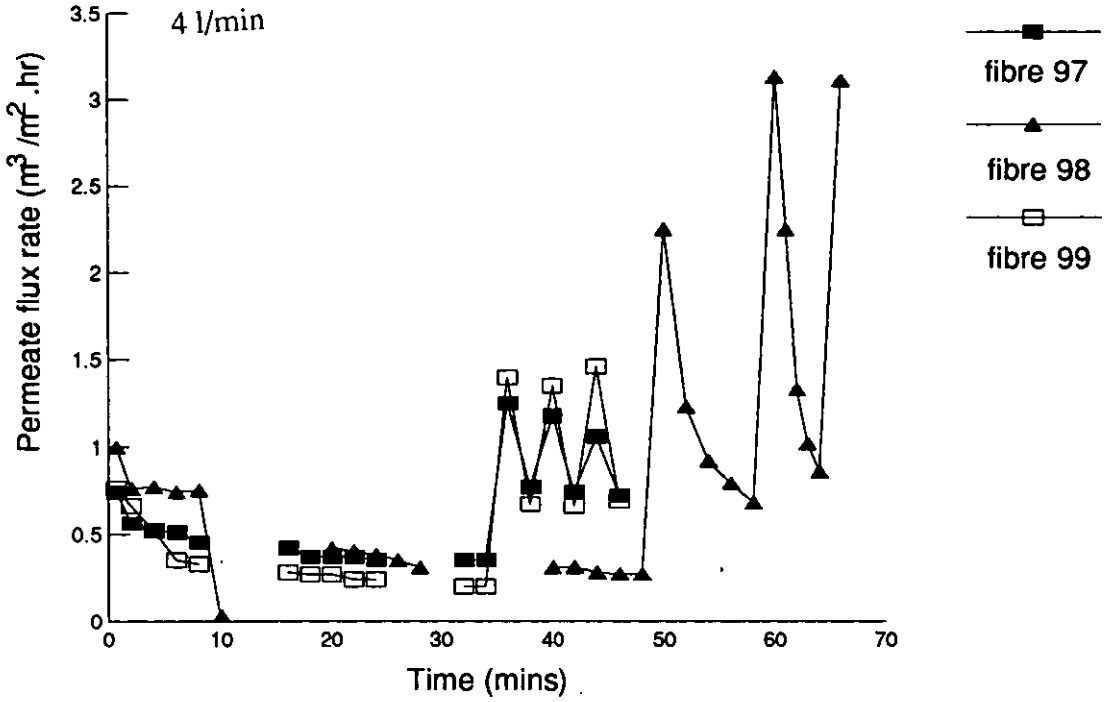

Fig 22a Flux rates of metal membranes (Re 8500)

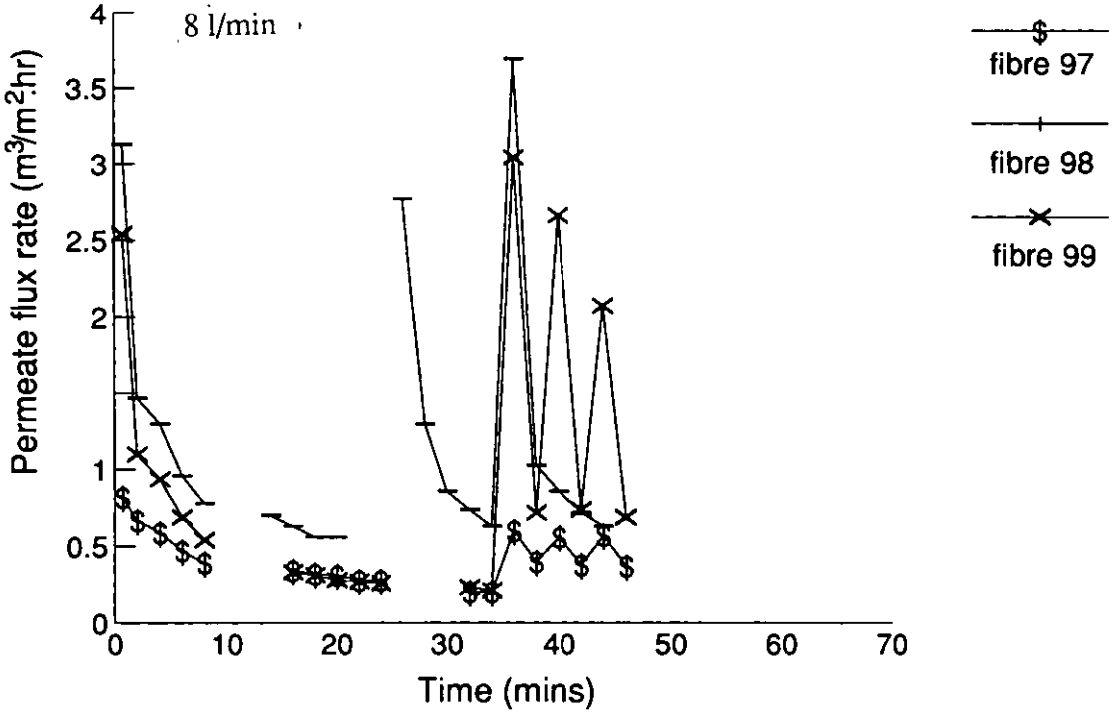

Fig 22b Flux rates of metal membranes (Re 17500)

Membrane retention efficiency are tabulated in Table 7.

Table 7
Particle retention efficiencies of Fairey filters

Filter No	Flow rate l/min	Retention efficiency (%) in grade (μm)			
		> 3	3 - 2	2 - 1.1	1.1 - 0.72
97	4	100	100	99.9	99.9
97	8	100	99.9	99.9	99.9
98	4	100	99.7	99.7	99.7
98	8	100	99.9	99.9	99.9
99	4	100	100	100	99.9
99	8	100	99.9	99.9	99.9

The test result of Versapor 3000 sheet membrane is shown in Fig 23. Back-flushing was performed using compressed air at 3.5 Bar, the duration of the reverse flow was 1 second.

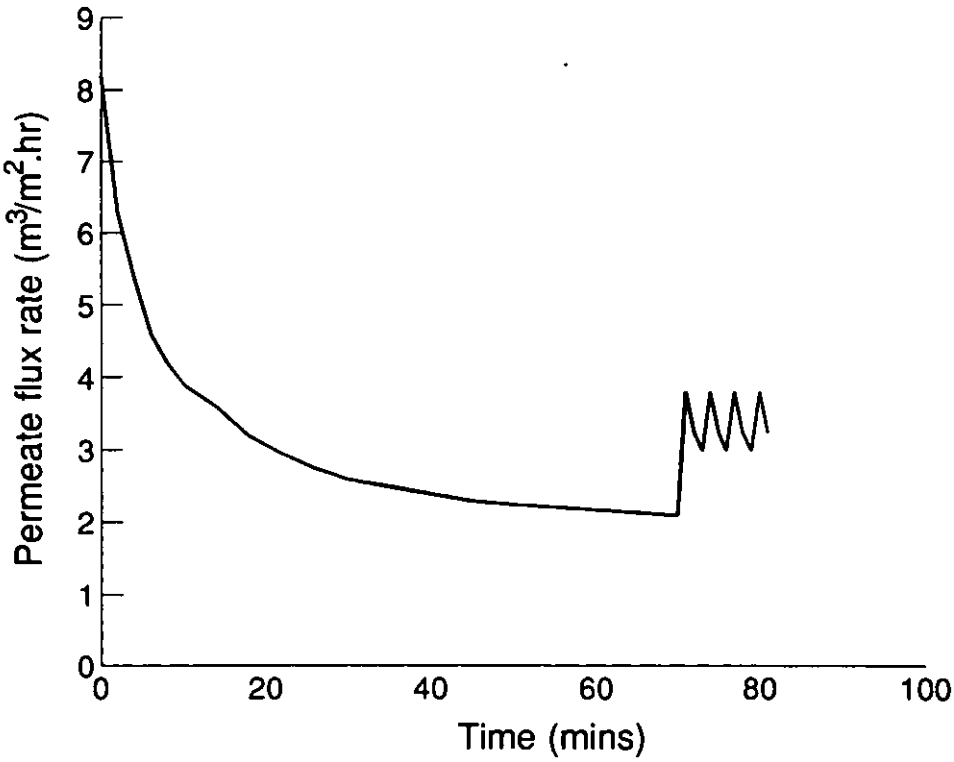

Fig 23 Flux rate of 10 mg/l solids (Versapor)

The above tests indicated a reasonable flux rate, sufficient for offshore use. Thus these membranes were subjected to challenge suspensions containing lipids (fish oil). The literature suggests that lipid containing suspensions represent the most fouling fluids that the membranes will have to operate on, therefore, tests with 2 mg/l solids and/or different concentrations of lipids were carried out with four different membranes.

The tests on Fairey filter (No 98) were carried out under 12 l/min flow rate (Re 25500) and 1.2 Bar transmembrane pressure. Three lipid concentrations were used: 5, 10, 20 mg/l. Before the lipid was added to the tank, the flux rate with clean water, and water with 2 mg/l silica, which was still a relatively high concentration of solids for offshore seawater filtration, were checked. The results are shown in Fig 24.

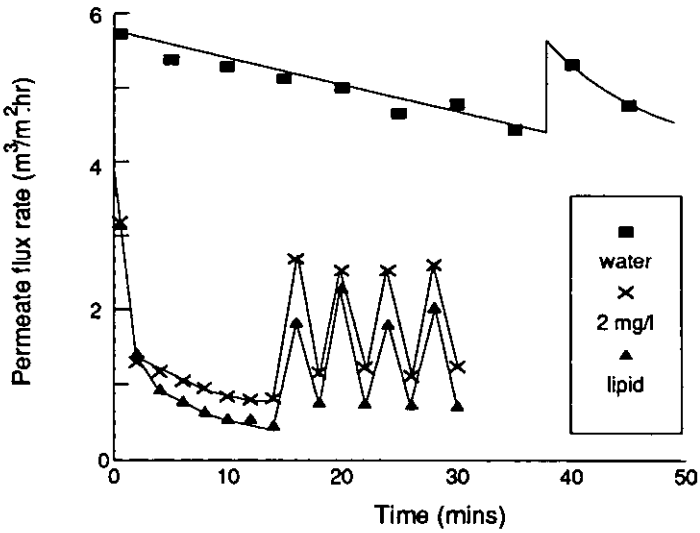

Fig 24a Permeate flux rate at 5 mg/l of lipid

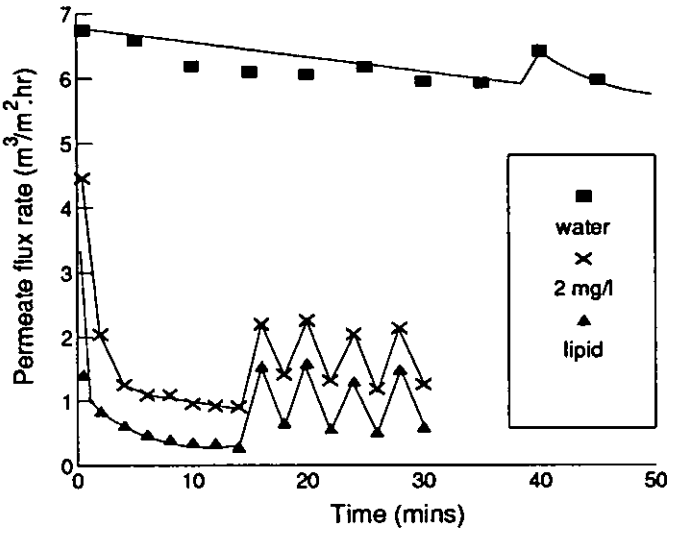

Fig 24b Permeate flux rate at 10 mg/l of lipid

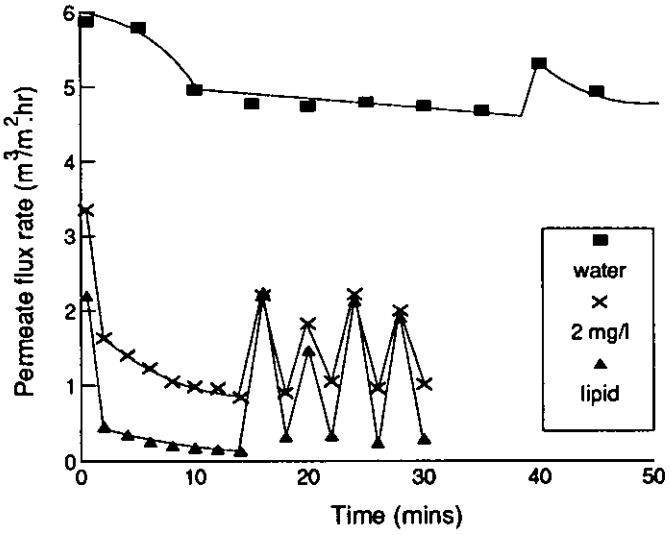

Fig 24c Permeate flux rate at 20 mg/l of lipid

These figures show that *clean* water flux rate, was between 5 - 7 $m^3/m^2 \cdot hr$. Increasing the lipid concentration decreased the permeate flux rate and caused the flux to decay more rapidly after backflushing. Backflushing with compressed air at 3.5 Bar considerably restored the membrane flux rates, even on filtering a suspension containing 2 mg/l of silica and 20 mg/l of lipids.

After test, the membrane was removed from the module for lipid retention efficiency tests. Table 8 is the results of lipid concentration tests by the means of extraction, evaporation and oven drying. The lipid concentration of the feed was

approximately the same as the calculated values shown in column 1. The appearances of all samples were milk-like liquids after evaporation, but they were different after drying. For the samples from the feed, they dried and turned into white spots on the flask wall. For the samples from the filter, they became a yellow oil with a strong fish-oil smell after drying, further drying only resulted in dehydration without any weight reduction.

Table 8

Lipid concentration in the feed and filter
at different lipid concentration in the tank

Calculated in the tank	Measured in the: (mg/l)	
mg/l	Feed	Filter
5	5	34.8
10	13	81.9
20	25	192.4

Since the polypropylene Enka filter is hydrophobic, the membrane was wetted with IPA before it was used and backflushed with water at 2.8 Bar during the process.

The tests with solids and lipids were all carried out under 0.7 Bar transmembrane pressure and 12 l/min feed flow rate. The results are listed in Table F of Appendix 3 and shown in Fig 25.

The figure shows that increase in the concentration of challenge materials did not significantly change the flux rate, but change in challenge materials brought about significant change in flux rate.

Although the flux rate dropped when challenge materials were added in, the flux rate was still high: up to 0.7 $m^3/m^2 \cdot hr$, therefore it was a good candidate for seawater filtration if backflushing with water is acceptable under offshore situation.

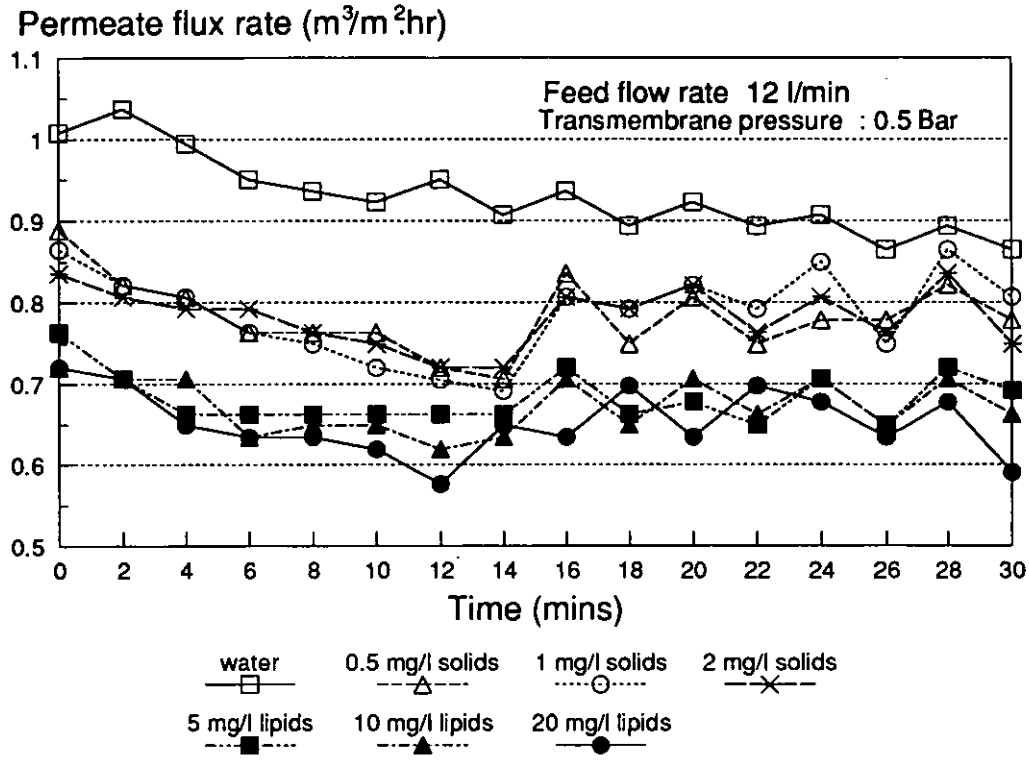

Fig 25 Flux rate of Enka filter at different concentrations

50 tests were run with ceramic filters on Rig 2. The results are listed in Table G of Appendix 3. The backflushing was commenced at the 48th minute for 1 second. The results of test No 7, 17, 25, 35 and 45 are shown in Fig 26a, which were under similar test operating conditions but different concentrations, another set of such test results, but at higher transmembrane pressure, from tests No 10, 20, 30, 40 and 50 are shown in Figure 26b. From the two figures, we can see that the increase in the pressure greatly increased the flux rate. The flux rate decayed more quickly when lipid was added in, this confirmed the conclusion by other authors that lipid is the major foulant to seawater filtration.

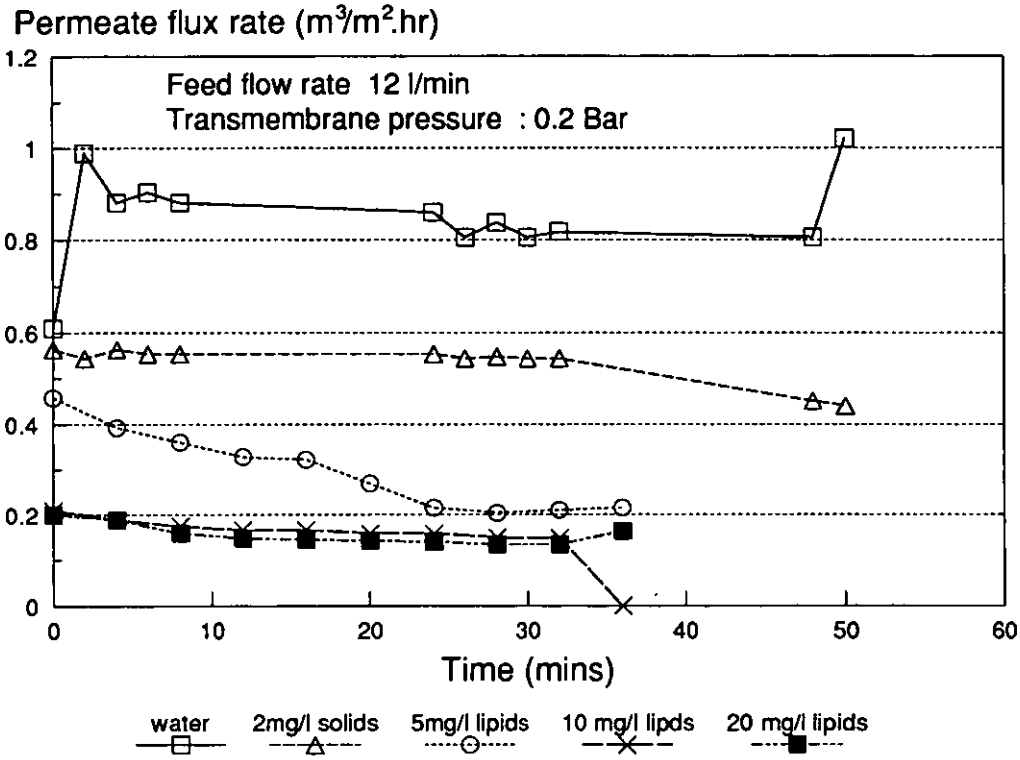

Fig 26a Flux rate of ceramic filter at low pressure

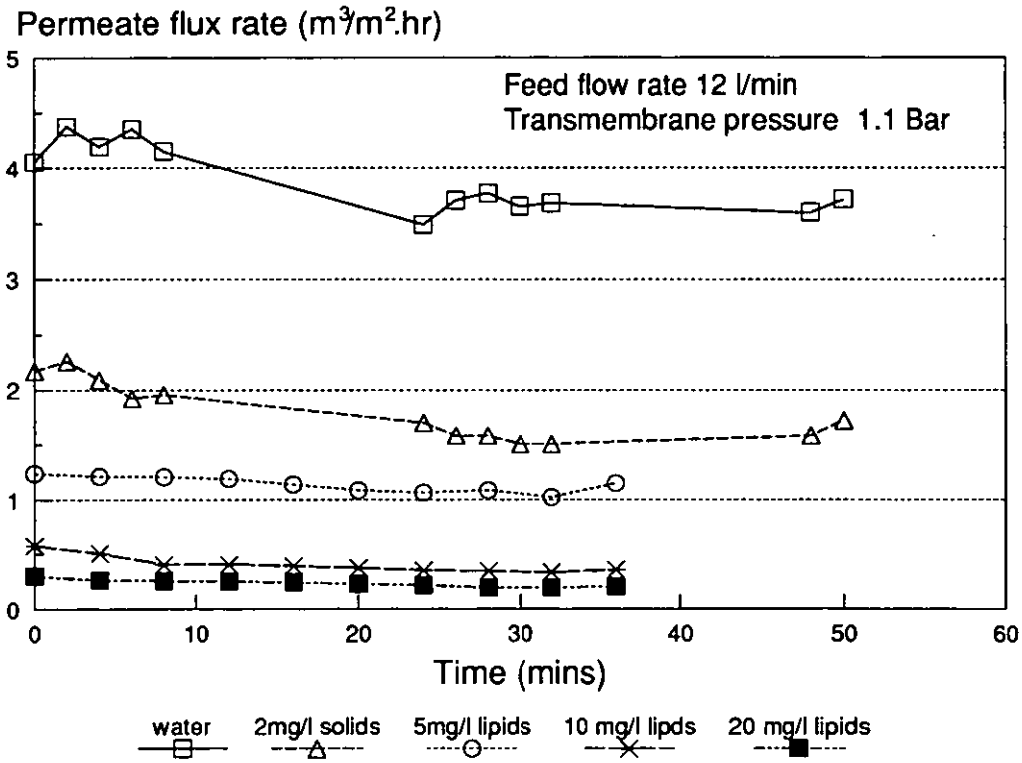

Fig 26b Flux rate of ceramic filter at high pressure

The tests with Versapor 3000 sheet membrane were run on Rig 1 only.

Fig 27 shows the flux rates obtained from various lipid concentration tests at 80 l/min feed flow rate and 0.7 Bar transmembrane pressure. Also shown in this figure are the flux rates using tap water and a 2 mg/l silica concentration.

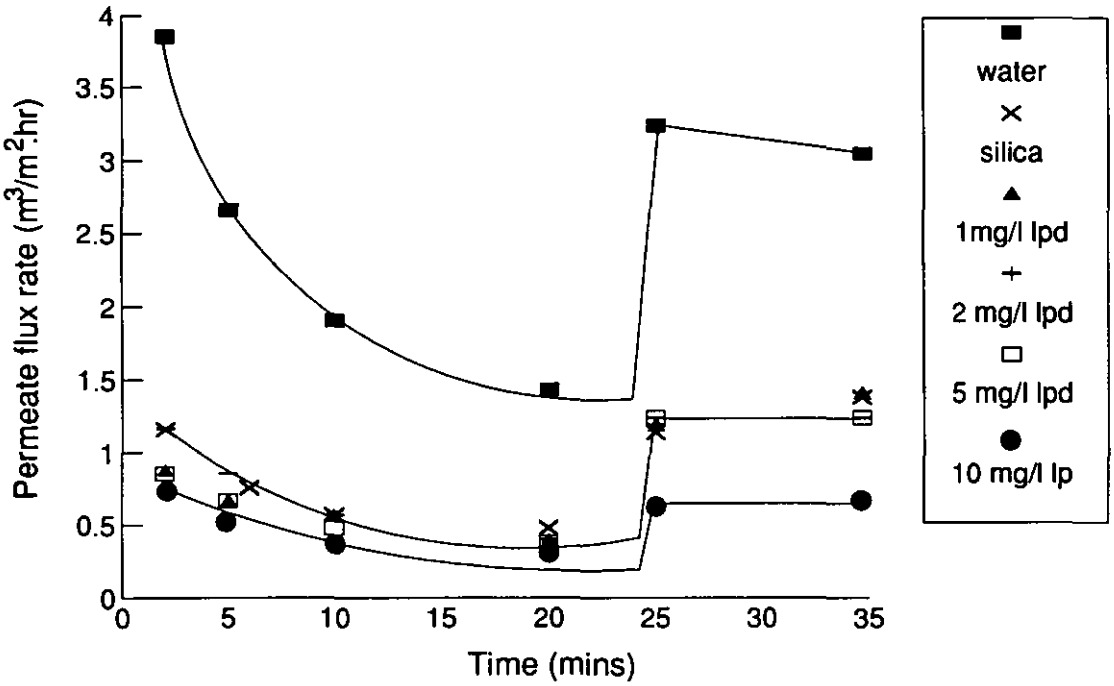

Fig 27 Flux rate of Versapor membrane at high pressure

d) With algae

The tests were run on Rig 1 only.

Two types of membranes were used, they were Bekaert metal sheet and Versapor 3000 polymer membranes.

The test results with two membranes are shown in Figs 28 and 29 respectively.

It was clear that changes in feed flow rate did not greatly affect the flux rate.

The permeate decayed very quickly due to the clogging of membrane pores with algae and solids.

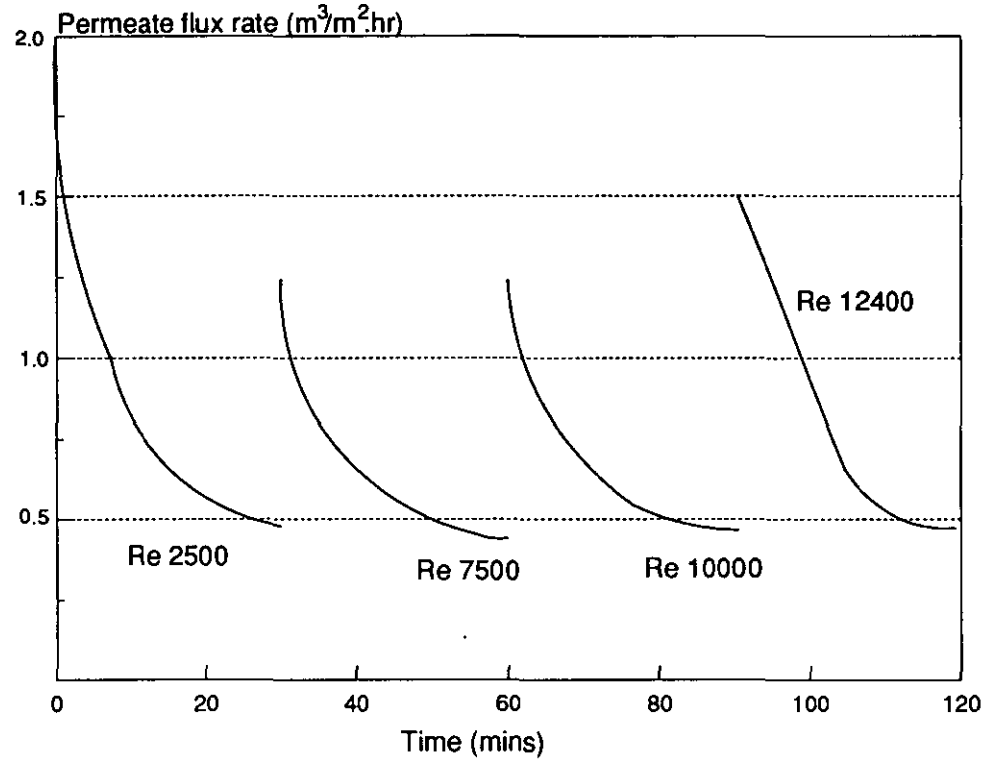

Fig 28 Flux rate of algae on metal membrane

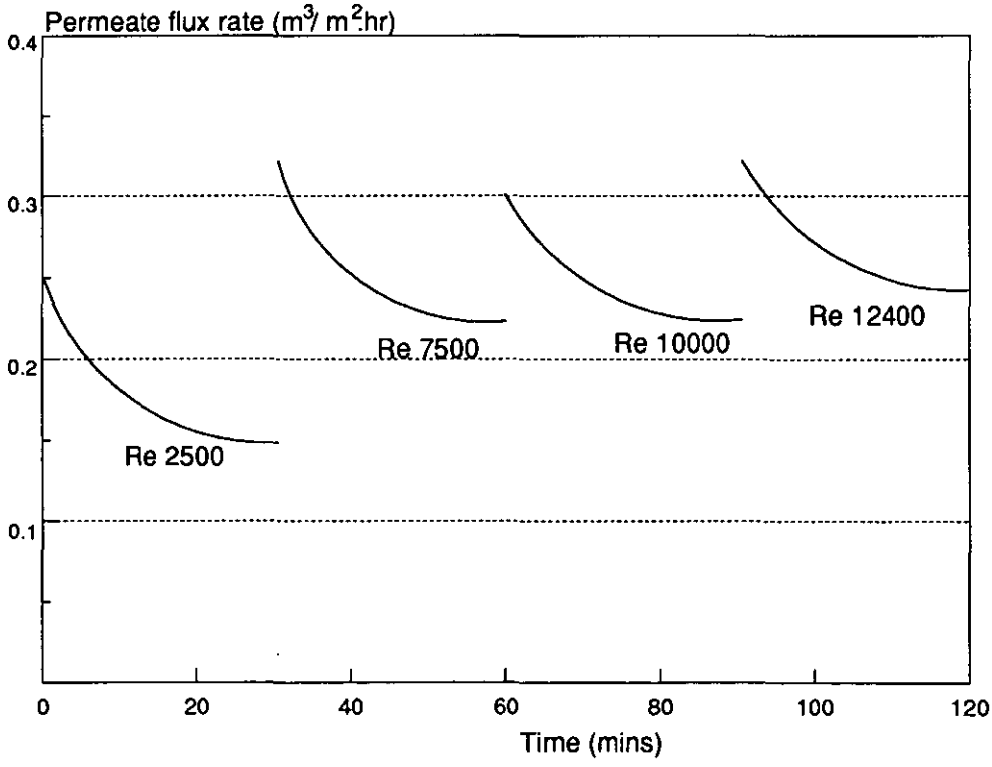

Fig 29 Flux rate of algae on polymer membrane

3.2.9 Comparison of membrane types

a) Lipid content

All these membranes gave similar flux rates when operating on suspensions containing highly fouling materials as solids and lipids or algae. This might have been due to the formation of a dynamic or secondary membrane which controlled the resistance and rejection of the further filtration process [Holdich & Boston, 1990].

The Enka filter had the highest flux rate of all the filters at 2 mg/l of solids and 20 mg/l lipids which means it was least affected by the presence of oil in water, and the Fairey was the lowest.

b) Operating conditions

Increase in operating pressure or feed flow rate increased the flux rate, but the former had more effect on the flux rate than the latter within a certain range.

c) Backflushing

It is clear that backflushing is capable of restoring the permeate flux rate to 80 - 90% of its original amount, but the flux rate will drop very quickly within 2 minutes; so that it is necessary to keep on backflushing during the whole process at certain frequency such as 1 second per minute.

d) Membrane resistance

The membrane resistance was analysed only on the algae test results. It was calculated according to the "cake" filtration theory as applied to microfiltration:

$$J_v = \frac{\Delta P}{\mu (R_c + R_m)} \tag{3.3}$$

The results, determined in *in-situ*, are listed in Table 9 for the metal membrane and Table 10 for polymer membrane.

The tests indicate that the presence of algae did not affect the metal membrane resistance, but significantly increased the polymer membrane resistance. It is also noticeable that the polymer membrane resistance increased with increasing pressure and decreased with increasing shear rate.

Table 9

Metal membrane resistance

Challenge suspension	Membrane resistance ($x10^{10}$ m^{-1})
filtered tap water	0.3 - 1.0
2 mg/l silica	0.5 - 2.2
10 mg/l silica	6 - 13
above plus algae	6 - 11

Table 10

Polymer membrane resistance

Challenge suspension	Re	Transmembrane pressure (Bar)	Membrane resistance ($x10^{10}$ m^{-1})
filtered tap water	2500	0.6	51
filtered tap water	2500	1.7	94
filtered tap water	2500	2.2	101
filtered tap water	2500	2.8	110
filtered tap water	7500	0.6	59
filtered tap water	7500	1.1	78
filtered tap water	7500	1.7	91
filtered tap water	7500	2.2	88
filtered tap water	12400	0.3	10
filtered tap water	12400	1.0	18
filtered tap water	12400	1.5	21
filtered tap water	12400	2.1	21
with algae	12400	0.28	32
with algae	10000	0.34	44
with algae	7500	0.48	64
with algae	2500	0.55	97

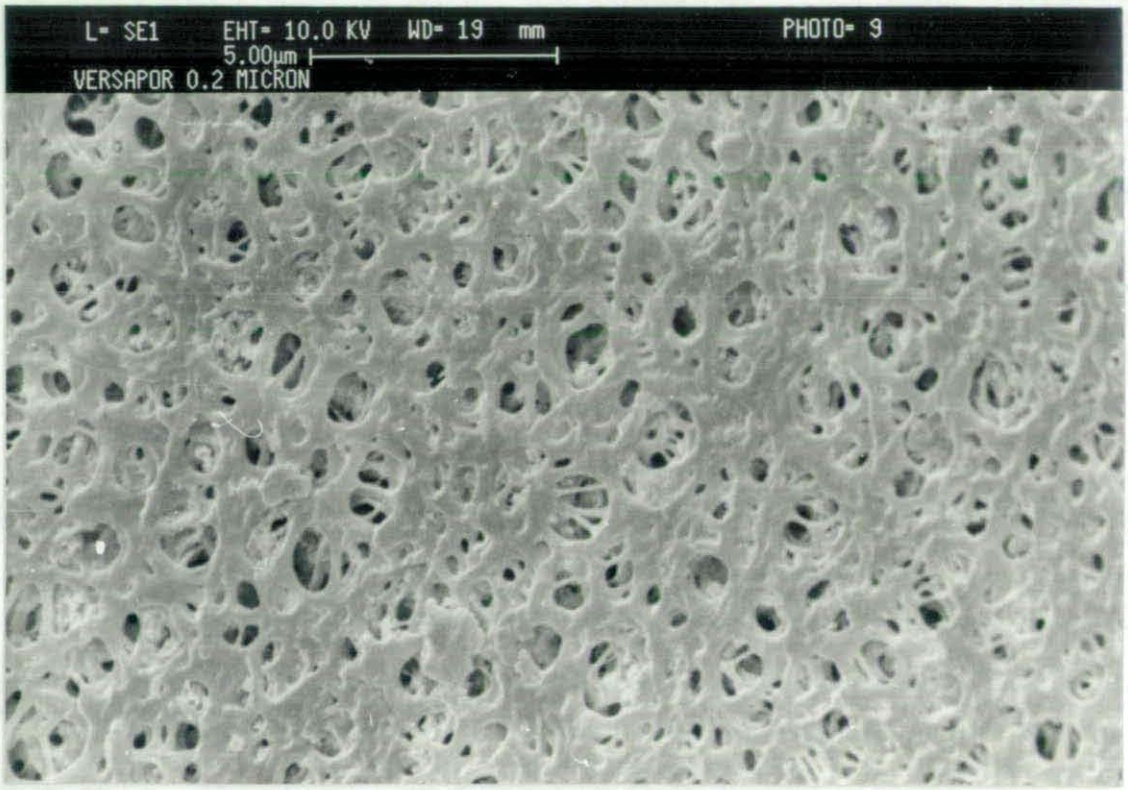

a) Clean

b) Clogged with algae and solids
Fig 30 Polymer membrane

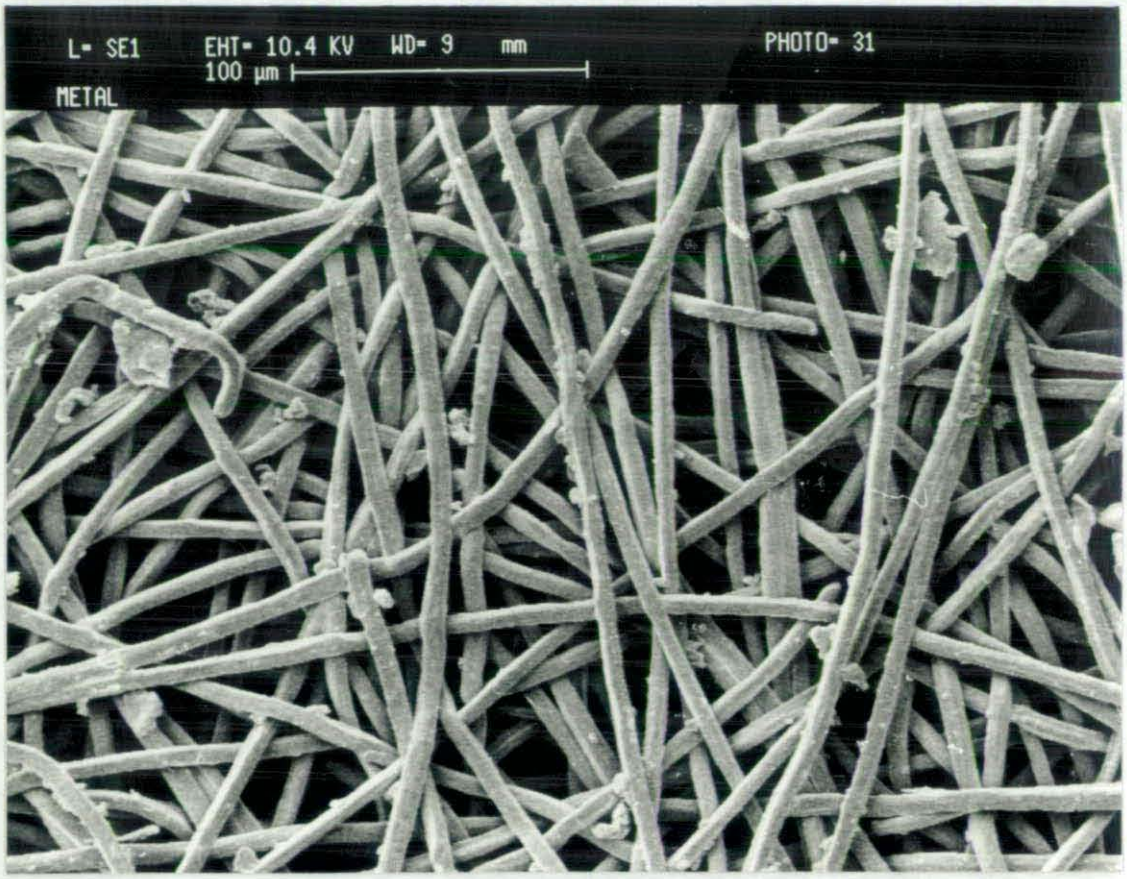

a) Clean

b) Clogged with algae and solids
Fig 31 Metal fibre membrane

All the above resistances are membrane resistances ***only***, i.e. not including the cake or deposit resistance. It is clear that there are still some suspended materials in the filtered tap water, they will deposit onto the membrane during filtration. These deposits must have combined with the membrane to provide the additional resistance. We learned from this test, that membrane resistance cannot, therefore, be assumed constant and equal to that given by a clean water test, especially in the case where particles are close to or even smaller than the pore size. The membrane resistance must be determined ***in-situ***, a similar situation to that of classical cake filtration. The details of the method of building this model will be discussed in Chapter 5.

e) Fouling mechanisms

The SEM photographs of the two fouled membranes from algae tests are reproduced in Figs 30 and 31.

It is apparent that the fouling on the surface of the polymer membrane is in the form of a contiguous gel coating. This blocks all but the largest surface pores, and severely restricts flow through those remaining open. The surface porosity of the clean metal membrane is much higher than that of polymer, but the presence of low concentrations of inorganic materials will clog it with algae acting as a binder. In both instances it is likely that the materials released by algae cells form a gel layer which exerts the major resistance to the permeation.

f) On-site operation consideration

Since the rig will be fixed on the platform, the membrane packing density, the necessity of coarse filtration, convenience and cost of maintenance and replacement, the feasibility and effectiveness of anti-fouling techniques, and the optimum layout of rigs must be taken into account. These have been discussed in another paper [Holdich et al 1990].

3.3 Experiments with North Sea seawater

The above tests showed promise for seawater filtration, further trials with North Sea seawater were carried out at Orkney Water Test Centre, Flotta, Orkney, Scotland.

3.3.1 Test rig and control programs

The rig was refurbished in July 1990 for the purpose of seawater filtration as shown in Fig 32.

In Fig 32 there is no sizing equipment, no cooler and no Millipore cartridge filter. B2, B3 and T1 are removed; a ballcock valve was installed in the tank to control the seawater level; V2, which is a normally opened type solenoid valve, was repositioned next to D1 and closed during backflushing so that the flushed deposits will not go back to the tank; only F1 and F2 are used. The operation was run in semi-continuous mode since the concentrates after backflushing with air at 3.5 Bar were disposed by opening V3; two PTFE capillary filters (Gore) in parallel, five ceramic filters (Ceraflo, Norton) in parallel and one metal tubular filter (Fairey) were used for the tests. The ITT program was rewritten so as to control the backflushing frequency and solenoid valve on/off duration.

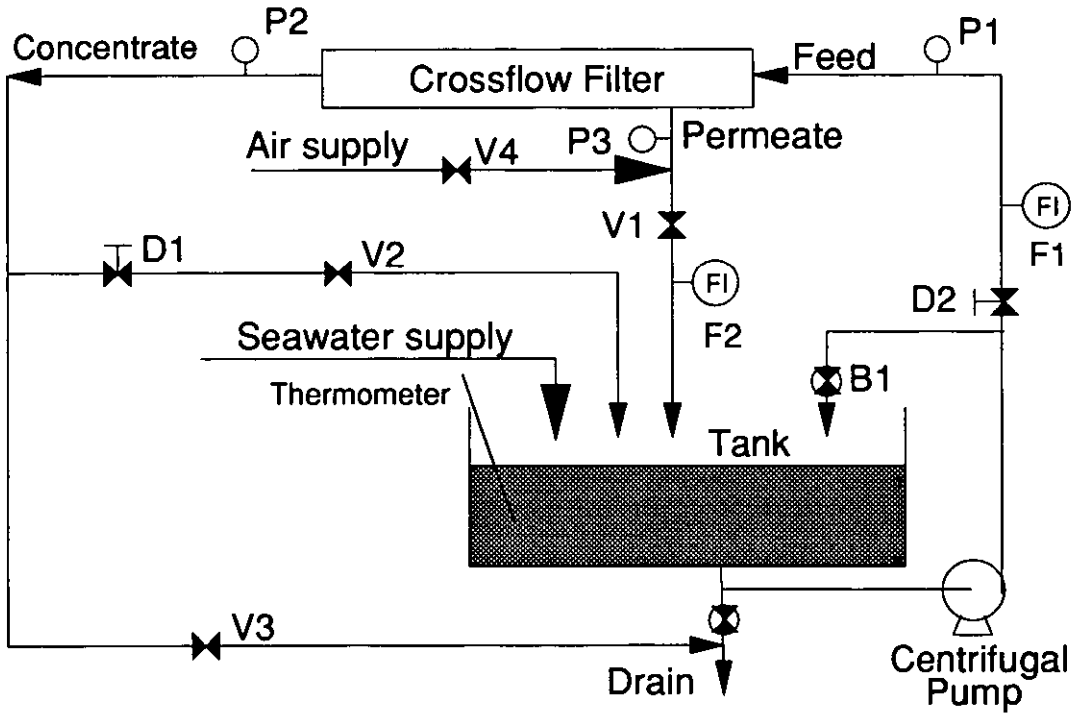

Fig 32 Layout of seawater filtration rig

The seawater used at the Test Centre is pumped from Scapa Flow which is fully marine and the main water mass has the characteristic of the flow round the north of Scotland into the North Sea. Plankton levels (blooms) are similar to those found offshore, with some local coastal enhancement. Natural mineral particulate concentration is usually very low. Since during the bloom period, the plankton found adjacent to Flotta

often slightly precede those which cause filtration problems offshore, the experiment was carried out over late August and the whole of September in 1990, which was not a bloom season.

The seawater was pumped from a depth of 15 metres at the Southend pier which is 150 metres away from the coast. The water was coarsely filtered with 80 - 100 μm filters to prevent seaweed or any possible large living organisms from getting into the reservoir.

Nine samples of seawater were taken from the hose through the trial period, and the Coulter Counter analysis for these samples are shown in Table 11.

Variation in the trial fluids was inevitable whilst undertaking field trials, but the variation between samples show below is not substantial. More than 80% of the particles are below 20 μm, therefore the challenge solids used in the laboratory were close to the distribution in North Sea seawater by their sizes. Meaningful comparison between the filter performance can, therefore, be made.

Table 11

Seawater particle size distribution
and solid concentration during trial period

No	Concentration	Cumulative mass % less than size (μm)				
	(mg/l)	32	20	10	5	1.3
1	0.7	88	81	76	68	20
2	1.3	98	88	69	42	6
3	1.5	98	93	76	45	6
4	4.7	91	84	48	14	2
5	0.8	99	95	85	69	13
6	1.1	86	70	52	28	8
7	0.9	89	82	63	43	11
8	2.2	92	78	54	34	4
9	0.9	92	83	63	46	14

3.3.2 Test items

Since the performance of these filters under different pressures, flow rates and concentrations had been comprehensively investigated in the laboratory, the tests at Flotta were targeted on the feasibility of filtering real seawater.

a) Operating conditions

The temperature was constant for all tests, it was 15 °C.

All the tests were operated under the same transmembrane pressure, which was 1.1 Bar since it was not possible to test under identical conditions of Reynolds (Re) number.

b) Air backflushing

It was used at 5 Bar at a frequency of 1 second per 10 minutes when the flux rate curve became flat.

c) Cleaning chemicals

Ultrasil 50 and Ultrasil 11 (0.1%), and citric acid (5%) were used to clean the filters.

d) Precoating method

Filter aid materials (dicalite) were tried on the metal filters so as to examine the effectiveness of precoating on fouling prevention. The system was first run at a concentration of 0.5 g/l and then seawater was introduced at a solids content of 1 mg/l. After 2 hours, backflushing was used.

3.3.3 Test procedures

Each filter was first cleaned by one of the cleaning chemicals in order to compare the effectiveness. Then it was run under different flow rates. The rig was left running overnight with the flux rate recorded by the chart recorder. There was no backflushing during the night so as to study the decay process.

3.3.4 Test results and discussions

a) Flux rate

It was possible to achieve an average flux rate over 1 $m^3/m^2 \cdot hr$ if the membrane fouling could be controlled.

The change in Reynolds number did not significantly affect the flux rate.

All the filters had a serious flux rate decay within a short period as shown in Fig 33.

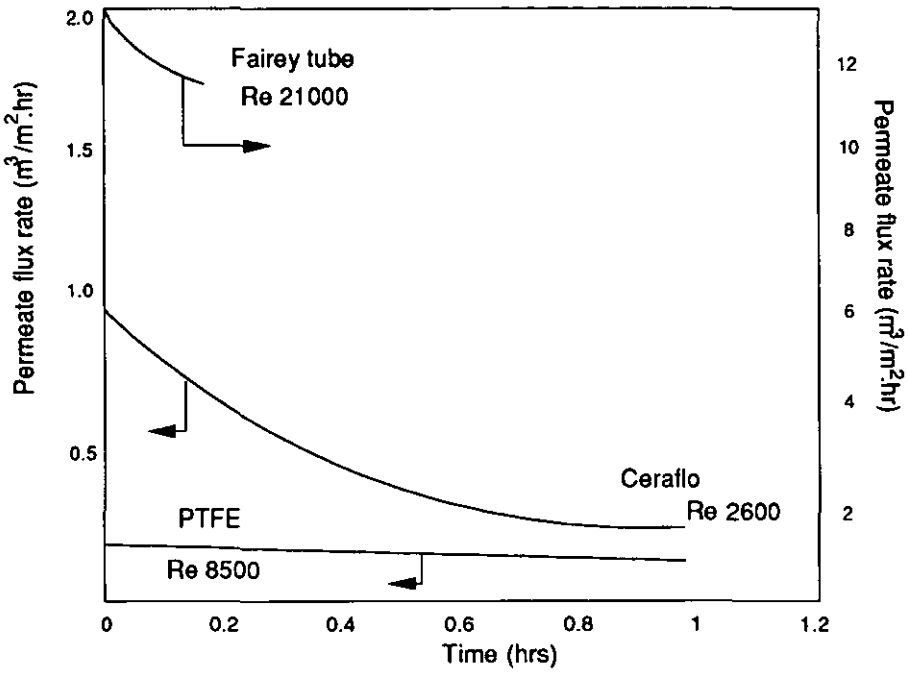

Fig 33 Flux rate for different filters

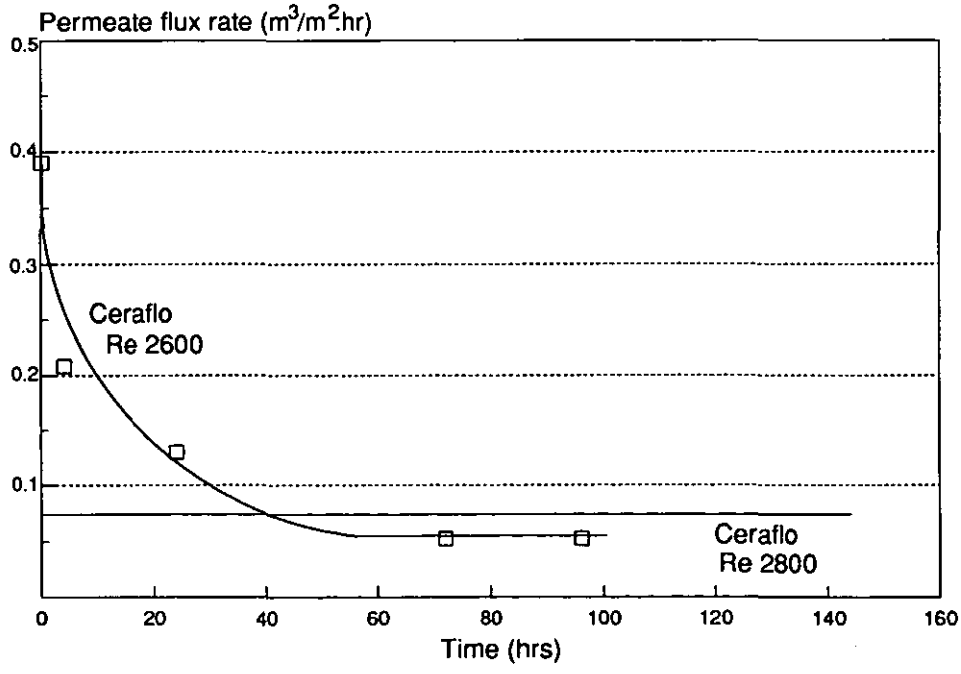

Fig 34 Flux rate of ceramic filters over several days

b) Flux rate recovery

The fouling was irreversible, neither the increase in the frequency and duration of air backflushing, nor the increase in the concentration and cleaning period of either chemicals, or the combination of both, could efficiently recover the flux rate. One of the trials on a long time base is shown in Fig 34.

c) Precoating

Fig 35 shows the effect of mixing dicalite speedplus with seawater. After precoating, the flux rate decayed as other filters did, however, backflushing resulted in a flux rate of over 30 $m^3/m^2 \cdot hr$, which subsequently decayed to 0.4 $m^3/m^2 \cdot hr$ within two hours. Backflushing could not restore the flux rate at that stage. Clearly, the precoating protected the metal membrane from intrusion of fine suspended material and irreversible fouling. Also shown in Fig 35 is a new metal membrane which had not been precoated, the flux rate dropped from 50 down to 0.4 $m^3/m^2 \cdot hr$ within 1.5 hours and backflushing had no effect on recovering the flux rate.

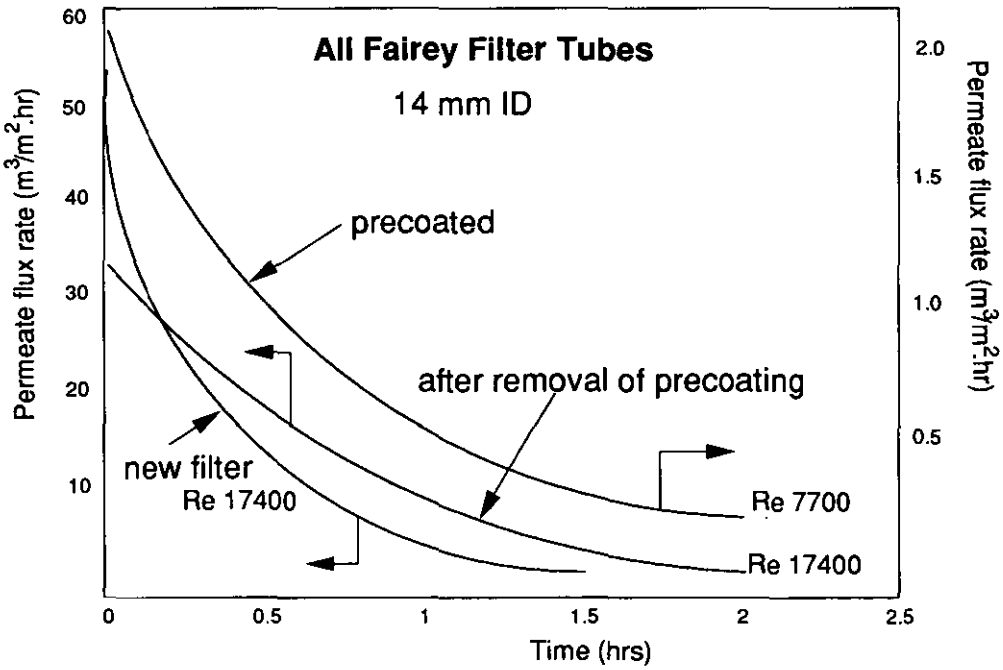

Fig 35 Flux rate of metal filters with or without precoating

3.4 Brief summary

The results of experiments with challenge materials or North Sea seawater show

the following:

Good filtration performances could be achieved when filtering suspensions of high mineral content with a mechanical membrane cleaning technique.

Transmembrane pressure had more influence than flow rate on the flux rate, however, high pressure would result in quicker deposition and less effective back-flushing.

Variation in the concentration of the suspended material was not very prominent since it was the deposit on and in the membrane surface and not the solids in the bulk flow which resisted the permeation, the higher concentration shortened the decay period, but the flux rates at the steady-state were similar.

Since the membranes were reused after cleaning, the membrane resistance of the same membrane varied in different cases, it should be estimated on *in-situ* base.

Fouling inside the membrane was the most important problem for seawater crossflow filtration. The major foulant was the lipid which acted as a glue combining other low concentration mineral materials to foul the membrane internally and externally.

Backflushing is an effective method to restore flux rate in many cases, however, it is not strong enough to recover the flux rate if there is a certain physico-chemical force (e.g. adhesive force) as in the presence of algae or lipid, since the flow within the membrane pores is essentially laminar which exerts less force than the shear force produced by turbulent flow on the membrane surface. Hence, backflushing is not effective at removing the internal clogging.

Chemical cleaning methods are also effective in many cases, however, two factors must be considered before applying them: the environment, and possible change to the properties of the membrane and materials. The chemicals used in seawater filtration (Ultrasils and citric acid) might not be suitable to get rid of these foulants.

Precoating can provide protection to the membrane, but it may be expensive and unacceptable from environmental standards. Precoating with sand may be an acceptable alternative for seawater filtration.

A coarser filter of screen type may be a better candidate than the finer ones for seawater filtration. The use of ultrafiltration membranes would not help to yield higher flux rates since the fouling is due to an organic gel of molecular weight proportions

(fatty acids) - thus flux rates similar to microfiltration would be expected. However, although the coarser membrane can reduce the possibility of building up gel bridges across the membrane pores, the finer particles may still penetrate into the membrane and be retained there unless a true surface filter is used.

Thus the most effective membrane for seawater filtration is one in which mechanical cleaning (backflushing) is effective. Organic fouling is clearly inevitable with any membrane. The required duty on oil platforms is reasonably coarse, over 50% of the water drawn from the sea needs to be filtered at only 10 μm. Thus an asymmetric or surface filtering membrane with high porosity and large pore size could be used. This could provide a sufficiently large pore to prevent complete pore blockage, or one in which mechanical cleaning is more likely to be successful.

A combination of crossflow and dead-end filtration may be suitable for the complete duty: crossflow filtration replaces the coarse filter to screen out particles which may foul the finer cartridge filter which could be used to filter water to below the 2 μm requirement. Such a crossflow filter arrangement would prove to be useful in the protection of the cartridge filters during an algae bloom period. When the solid content of seawater is increased the crossflow filter is easier to clean as the particles are retained on the filter surface. Cleaning only proved difficult at low suspended solid concentration due to the penetration of particles into the filter structure - under these conditions the cartridge filters will perform adequately [Holdich & Zhang, 1991].

It may be worthwhile to test more chemicals and other anti-fouling techniques to improve the flux rate since the crossflow filter has an intrinsic advantage over dead-end filters.

All the tested membranes afforded reasonable flux rates, the geometries and types of filter did not significantly change the flux rate, this was a consequence of the formation of a dynamic or secondary layer on the membrane surface or inside the pores. The offshore operation with crossflow filters is feasible if the membrane fouling can be minimised. The principle of selecting appropriate membranes is based on a multitude of factors such as ease of operation and service, recovery ability after cleaning, membrane packing density and robustness, and operation costs.

This work very clearly demonstrated the importance of the finely suspended material entering the membrane filter matrix. This is the subject of Chapter 4.

CHAPTER 4

Crossflow Microfiltration of Latex Suspensions
(Investigation of Membrane Fouling Process)

It was apparent from the crossflow microfiltration of seawater that fouling inside the membrane is a major cause of flux rate decay. Therefore, further study was concentrated on this internal fouling process using well characterised latex suspensions and membranes.

4.1 Test rig

Rig 2 was used for this study, its layout is shown in Fig 16, water backflushing (2.8 Bar) was used if necessary.

The rig was modified to use a plate and frame module because sheet membrane is more easily investigated than other geometries, for example by SEM after the test. Gelman Versapor acrylonitrile membranes were used, they were the same as those used in seawater filtration except the pore sizes were slightly larger.

The module consisted of three parts: top plate, bottom plate and two flow connectors. The structure of the these parts are shown in Fig 36. The two plates were made of perspex so that the flow in the channels could be observed during filtration. The connectors were made of PVC so as to facilitate connection with the pipeline.

Fig 36a is a diagram of the top plate. The fluid flows in the channels, the geometries of each channel were 3 x 3 x 500 mm (width x height x length). There were 10 channels in the plate, but only six are displayed in the diagram because the four side channels were not used during the experiments.

Fig 36b is the diagram of the bottom plate, three layers of different sheets were placed on the ridges. The bottom one was a brass sheet mesh, its opening size was 1 mm; the middle one was a stainless steel membrane, its pore size was 3 μm, the top one was the Versapor membrane. The lower sheets were used to support the top one. The total thickness of the three sheets were about 1 mm, however, since they were sealed by silicon rubber at their edges, the total thickness of the sheets increased, the membranes intruded into the channels, and therefore, the depth of the channels was slightly reduced.

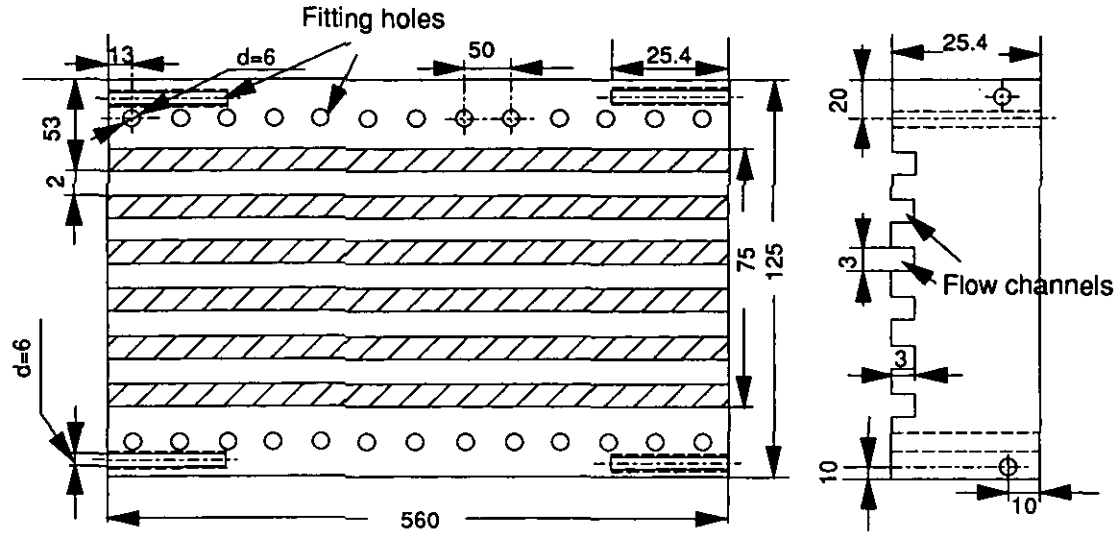

Fig 36a Top plate of the module (unit: mm)

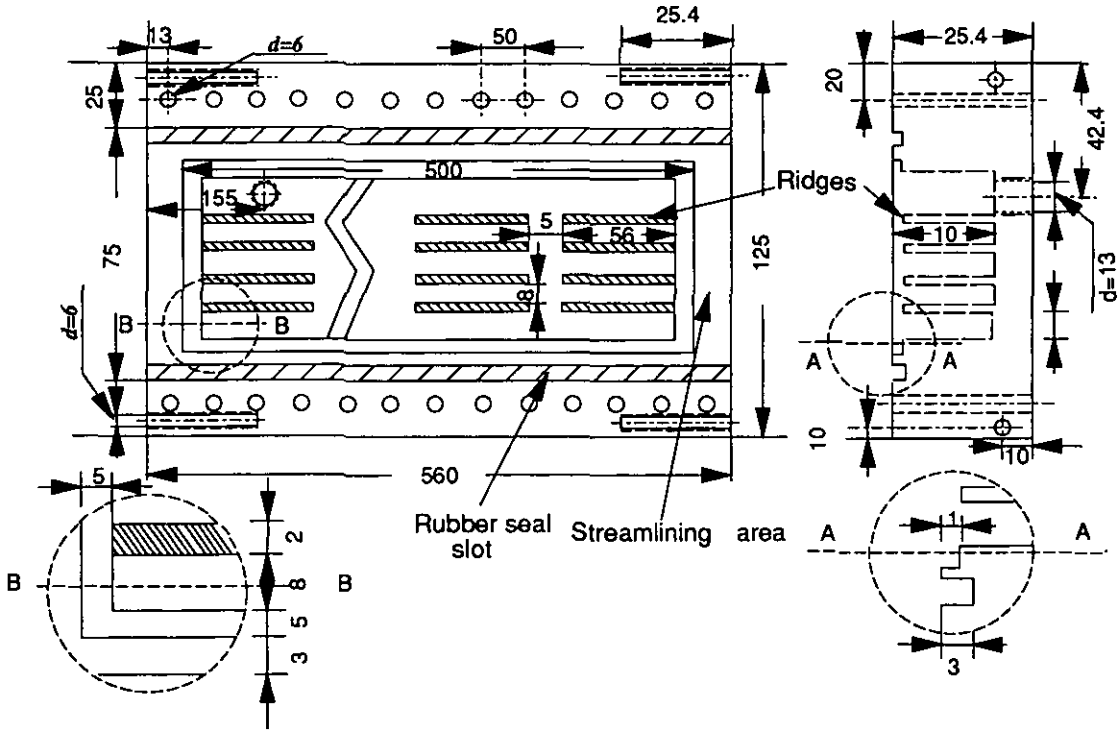

Fig 36b Bottom plate of the module (unit: mm)

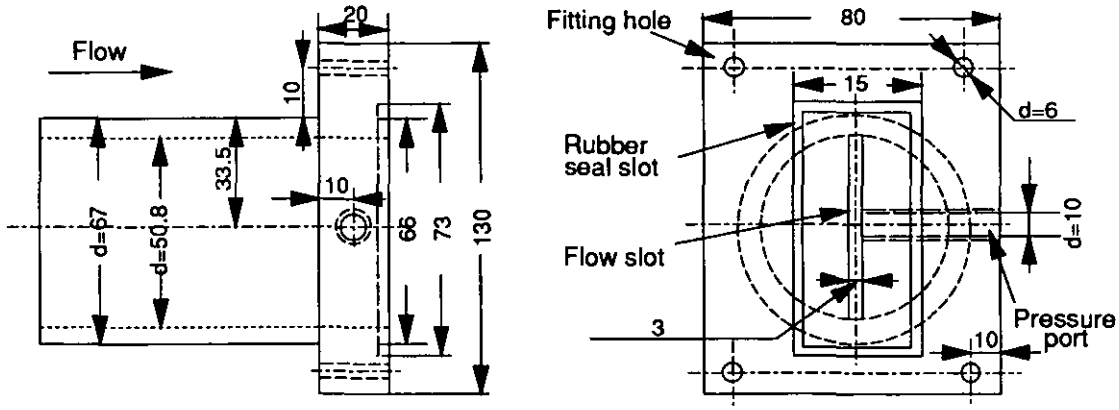

Fig 36c Inlet side connector (unit: mm)

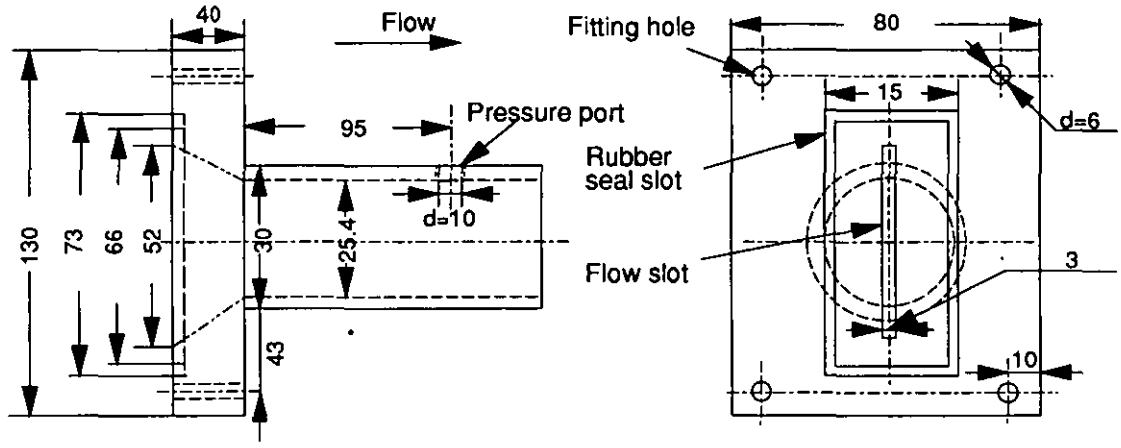

Fig 36d Outlet side connector (unit: mm)

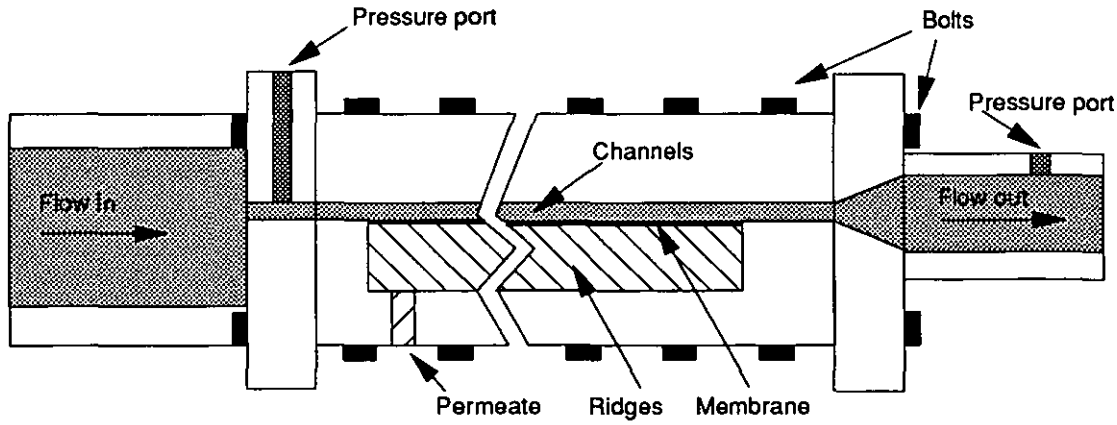

Fig 36e Configuration of the filter module

The streamlining areas were designed to be a region to minimize the effects of entrance and exit on the flow inside the channels.

The two connectors were used to produce a flat velocity profile entering the channels (plug flow), and also minimize the flow rate differences between the neighbouring channels.

4.2 Latex suspensions

Latex was chosen as the foulant due to its spherity, uniform size and well-defined properties such as density, viscosity and zeta-potential.

The latices were produced in the laboratory by the Balance Swell Method (BSM) based on Goodwin et al. (1974)

4.2.1 Equipment and materials

a) Equipment

One vacuum pump, two 100ml round-bottom flasks, two thermostats, one large beaker, one 1000ml four-neck round-bottom flask, two water baths, two thermometers (0 to 100 °C), one electrical stainless steel stirrer, two condensers, one catchpot, rubber pipes for connecting water and gas, some cylinders, beakers and flasks for measuring, glass wool and Visking tubing.

b) Raw materials

Deionized water, BDH General Purpose Reagent grade styrene (99.5% purity) BDH AnalaR NaCl, BDH AnalaR potassium persulphate ($K_2S_2O_8$), BDH phylatol.

Compressed oxygen-free nitrogen gas (99.5% purity) and tap water.

4.2.2 Preparation procedures

a) Distillation of styrene

The impurities in the styrene, i.e. inhibitors, polymers and peroxide [Goodall et al, 1979], were removed by the method of vacuum distillation. The styrene was distilled in a 100 ml flask which was placed in a water bath containing 40 °C water. After condensing, the styrene was collected in another 100 ml flask which was placed in a large beaker containing ice-water mixture. The purified styrene was used on the day it was distilled.

b) Latex seed production

50 ml of distilled styrene, 440 ml of deionized water and 0.41 g of NaCl were put into a 1000 ml four-neck flask which was fixed in a water bath containing 60 °C water. Its central neck was used for the stirrer, the other three were used for the condenser, thermometer and nitrogen gas respectively.

The nitrogen gas was supplied through a manifold from outside the building, therefore, a glass catchpot was used to remove the impurities from the pipelines. A glass nozzle was used to introduce the nitrogen gas near the bottom of the flask so as to expel other gases out of the reactor.

The stirrer rotated at low speed because high shear force might destroy the structure of the latex particles.

When the temperature of the contents in the flask reached 60 °C, 0.373 g $K_2S_2O_8$ which had been mixed with 10 ml of deionized water was added into the reactor to initiate the polymerization.

This process lasted 24 hours, the produced latex was then filtered by glass wool and dialysed in the boiled Visking tubing against deionized water, the water was changed several times until its electrical conductivity was less than 30 μs/cm.

The particle size of the latices at this stage were usually much less than 2 μm in diameter. They could be used as seeds for swelling if larger sizes were required.

c) BSM for larger particles

The amount of styrene required for this method could be calculated from the following formula which was based on the assumption that all the charged styrene was polymerized on seed particles (i.e. no new particles were formed).

$$m_{styrene} = \frac{m_{seed}(d_{latex}^3 - d_{seed}^3)}{d_{seed}^3} \tag{4.1}$$

where m is the weight (kg)

subscripts **latex** and **seed** for product and seed respectively.

It was found that the amount of $K_2S_2O_8$ was crucial to the swelling - overdose would cause scattered particle size distribution and underdose would lead to non-swelling. From the results of several tests, 0.22 g $K_2S_2O_8$ for 100 g solution was the optimum.

The temperature should not be less than 57 °C, otherwise no reaction happened, and the optimum range was 60 to 65 °C.

This process lasted 24 hours, the first few hours were the most important since more than 50% of reaction occurred during that period.

The products were also filtered and dialysed. They were stored in the glass reagent bottles with one drop or two of phylatol in it to prevent the possible growth of microorganisms.

4.2.3 Relevant properties of the produced latex

A total of 19 latex emulsions were made by this method, their particle size distribution, percentage dry weight, density and zeta-potential were measured. Only three of these latices, two with diverse particle size distribution (No 6 and 11) and the other with relatively uniform particle size distribution (No 9), were used for the experiments. Some of their properties are tabulated in Table 12.

a) Percentage of dry weight (wt%)

The percentage dry weight of latex was determined by the oven drying method.

b) Zeta (ζ) potential (at pH 7)

The Zeta potential of latex particles suspended in deionized water were determined by Particle Micro-Photophoresis Apparatus (Ranker Brothers, Mark II).

c) Density

The density of latex was measured by density bottle.

d) Viscosity

The suspension was essentially an Newtonian fluid up to 58 wt% solids according to Blake's test results [Blake, 1990] The relative viscosity of suspension could be expressed by Krieger's equation [Krieger, 1972]

$$\mu_{rela} = (1 - k_{cr} v_s)^{-\frac{\mu_{intr}}{k_{cr}}} \qquad (4.2)$$

where μ_{rela} is the relative viscosity,

μ_{intr} is the intrinsic viscosity (2.5 for non-interacting spheres)

v_s is the volume fraction of particles,

k_{cr} is a crowding factor (the inverse of the maximum volume fraction of particles).

Due to the limitation of the maximum concentration of the Hiac/Royco sizing

equipment used to monitor the filtration, the latex concentration for the experiments was very low - less than 0.3 mg/l - the viscosity of the suspension was therefore taken to be that of water, which is 0.001 Pa•s (20 °C).

e) Particle size distribution

The particle sizes distribution of latex was investigated by Malvern Laser Diffractometer (Series 2600). Since this Malvern sizer could not provide the size distribution less than 1.2 μm, Coulter LS130 equipment was used for No 9 and No 11 latex. The cumulative particle size distributions of No 6, 9 and 11 from these equipments are shown in Fig 37.

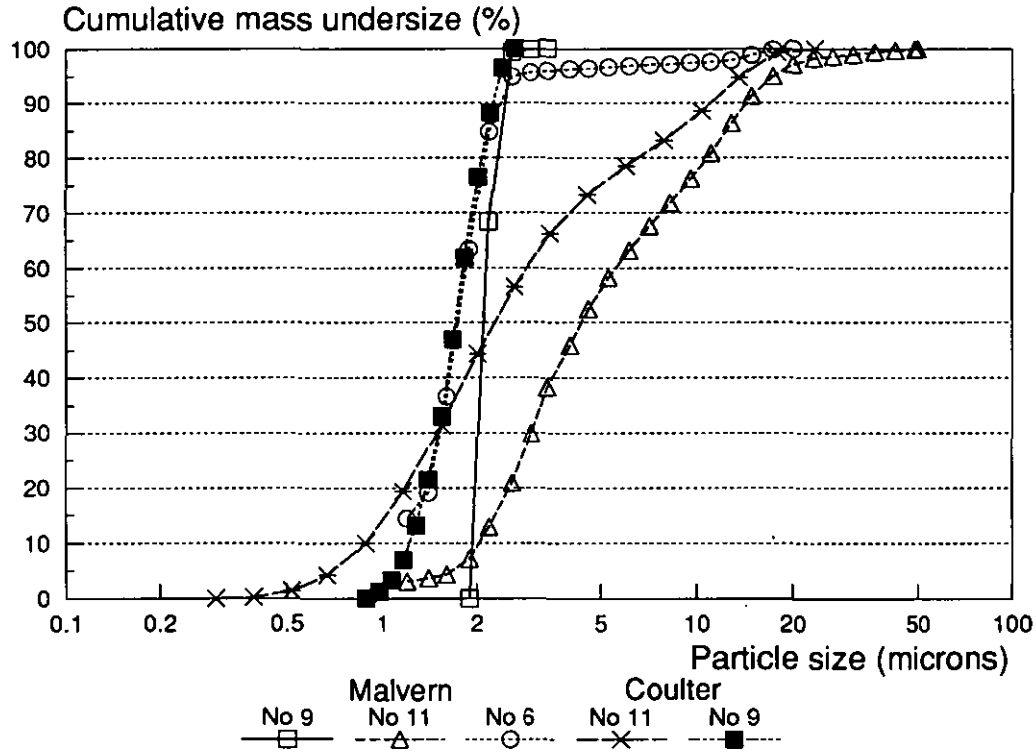

Fig 37 Particle size distributions of test latices

There is some discrepancy between the size distributions, especially for No 11 latex. The solid content of No 6 and No 11 latex was very low (0.13% and 1.96% respectively), compared with that of the No 9 latex, due possibly to excess initiator which may have stabilized more smaller particles. These smaller particles contribute to a wider particle size distribution of the No 11 and No 6 latex.

f) Filter cake compressibility

The filter cake compressibility was apparently low during filtration [Blake, 1990].

Table 12

Some properties of the produced latices

No	Particle Size Distribution (μm)						Dry weight	Density	ζ
	< 90%		< 50%		< 10%				
	Mlvn	Cltr	Mlvn	Cltr	Mlvn	Cltr	wt%	kg/m^3	mV
6	2.3	/	0.9	/	0.13	/	1.8	989	-51.82
9	2.3	2.3	2.1	1.7	2.0	1.2	13.2	1250	-29.78
11	14.6	11	4.4	2.3	2.1	0.9	1.96	1450	-53.72

4.3. Calibration and system performance tests

4.3.1 Equipment

Flow meters, chart-recorder, Hiac/Royco sizing equipment and pressure gauges (0 - 2 Bar) were calibrated following the same procedures in Chapter 3. The computer programs for system control and data collection were also the same.

The performance of the Hiac/Royco equipment with the concentration of latex suspensions was tested. It was found that the Hiac/Royco sizing equipment could only count particles at relatively low concentration, otherwise the optical signal became saturated; the lowest channel setting used was 0.7 micron, this helped to limit signal saturation.

The shedding effect of the rig under clean water condition was also tested. The rig shedded out small amounts of minute particles, but it would not affect the counting results if the lowest channel setting of the sizing equipment was larger than 0.7 micron and the total counts per ml of the six channels were high (i.e. about 3000).

4.3.2 Leakage tests

a) Edge leakage test

During the filtration of latex suspension, the particle concentration in the bulk

and permeate flow was counted by the Hiac/Royco, and compared with each other. Only when the particle concentration of the permeate flow was as low as the cleaned tap water, could the module be thought well sealed.

b) Inter-channel leakage test (inside the module)

When the module had been assembled, the three sheets, which were used to seal the neighbouring channels as well as to filter the suspension, were pressed by the ridges of the two plates. Since there were no sealing materials between the sheets and the plates, and sheets themselves, it was necessary to check the possibility of inter-channel leakage.

This was achieved by using dyed water. After the dyed water had run along the membrane for several hours without filtration, the module was disassembled. If only the filter channel portions had been dyed, there was not any inter-channel leakage.

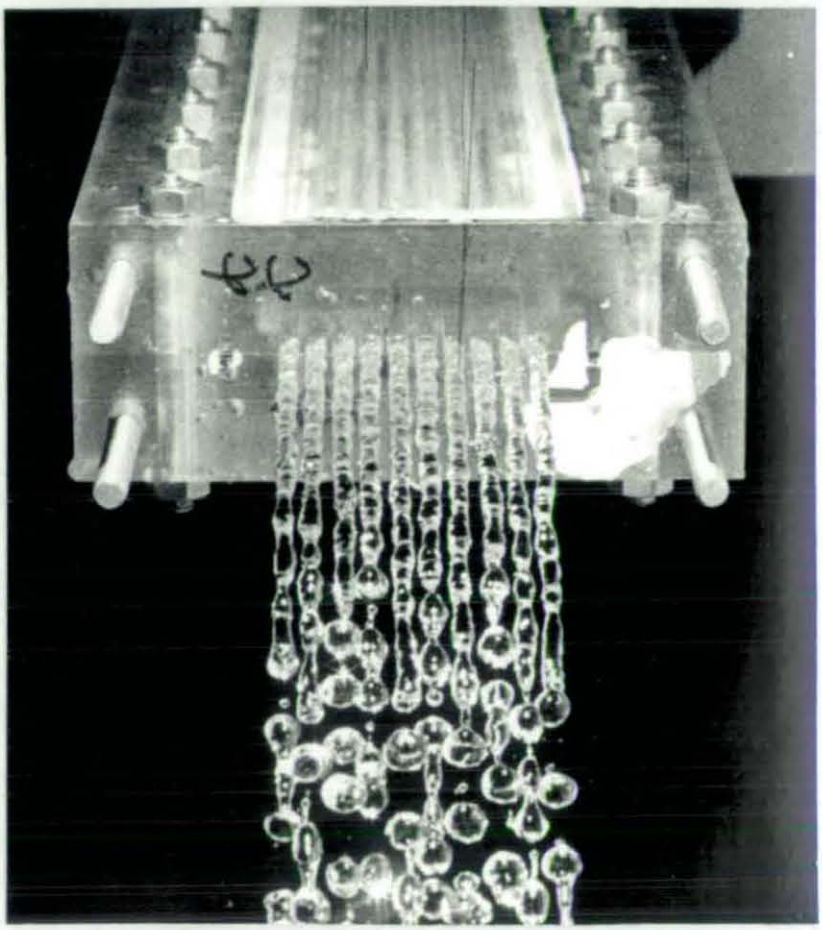

Fig 38 Streamlining leakage test

c) Streamlining leakage test

The possible leakage between the channels in this part was tested. The module was horizontally placed, the flow connector was taken off, if there was no leakage, the jet from each channel would not connect and its isolation was visible as shown in Fig 38.

4.3.3 Flow distribution test

It had been noticed during the filtration of seawater that the flow distribution in the channels of the plate and frame module were not uniform - the flows in the central channels ran much faster than those on the both sides.

Although the flow distribution had been greatly improved by using the flow connectors and streamlining areas, it was still necessary to investigate this further.

a) Minimum feed flow rate test

The module was set in the operating position, i.e. one channel was over another on its side, pulsed blue dye was injected into the module through the inlet pressure port by the backflushing pump. The front line of blue waves were then photographed as shown in Fig 39. It was found that the minimum channel flow rate should be more than 1 l/min, otherwise the top channels would not be fully filled; when the channel flow rate was more than 2 l/min, photographs could not display the channel flow distributions. The photographs also showed that the velocities of bottom channels were faster than the top ones, thus the distribution needed to be further improved, therefore, another test was carried out.

b) Channel flow distribution measurement

This time the module was horizontally placed so that each channel was at the same height. One flow connector was taken away and the flows from this exit were photographed as shown in Fig 40.

The flow rate of each jet was measured by a stop watch, beaker and scale. The results showed that the flow rates of the central six channels were almost the same while those of the two channels on each side were much lower. These four channels were then sealed with silicon rubber, further tests with the remaining six channels gave an evenly distributed flow profile, all further experiments were carried out with six channels only.

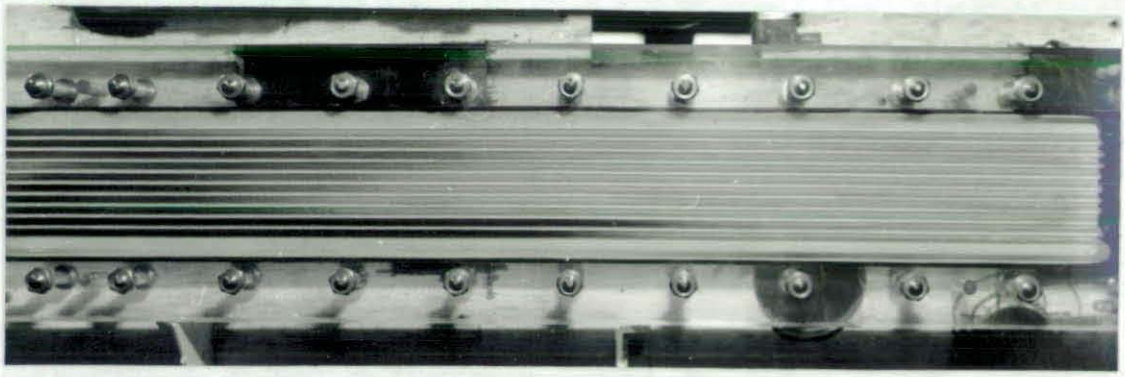

(a) 1 l/min

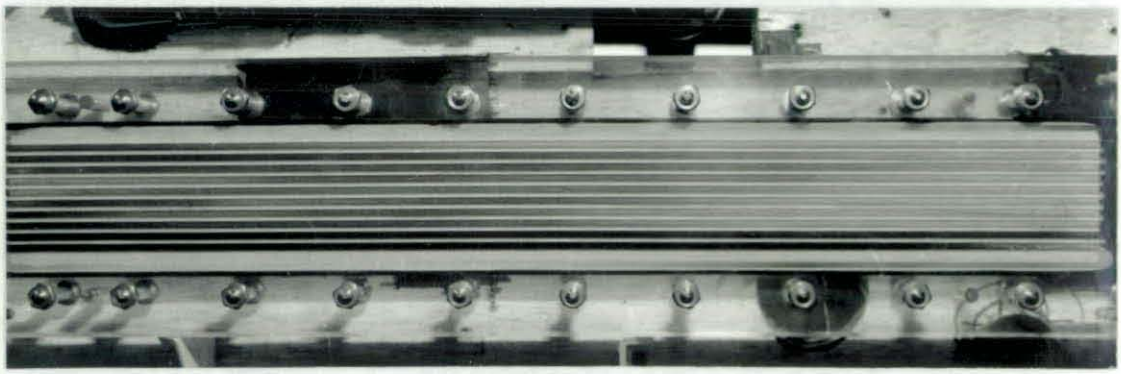

(b) 1.6 l/min

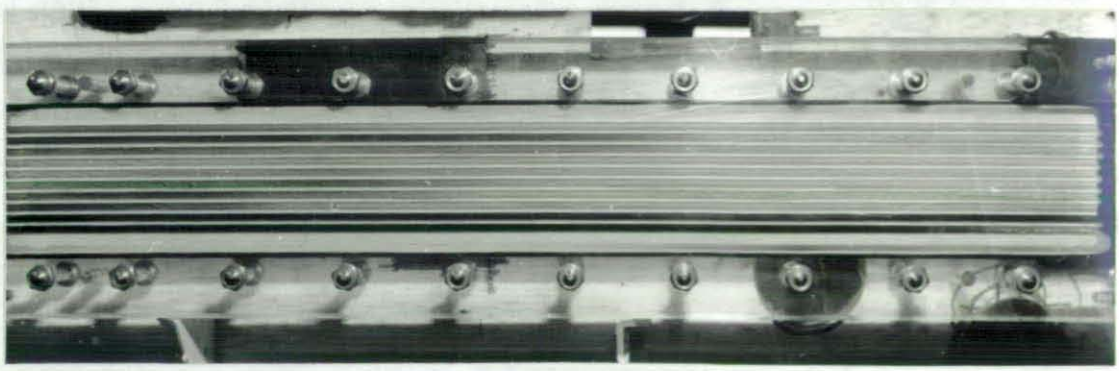

(c) 2 l/min

Fig 39 Dyed flow distribution during the minimum flow rate test

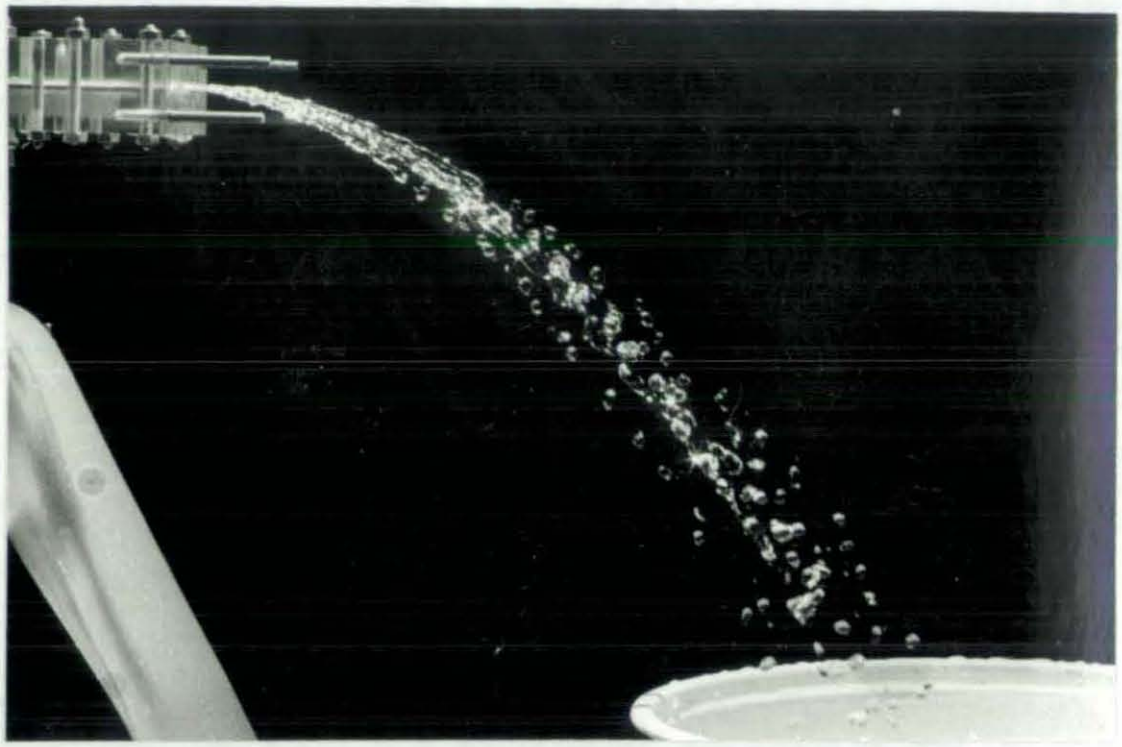

(a) 1 l/min

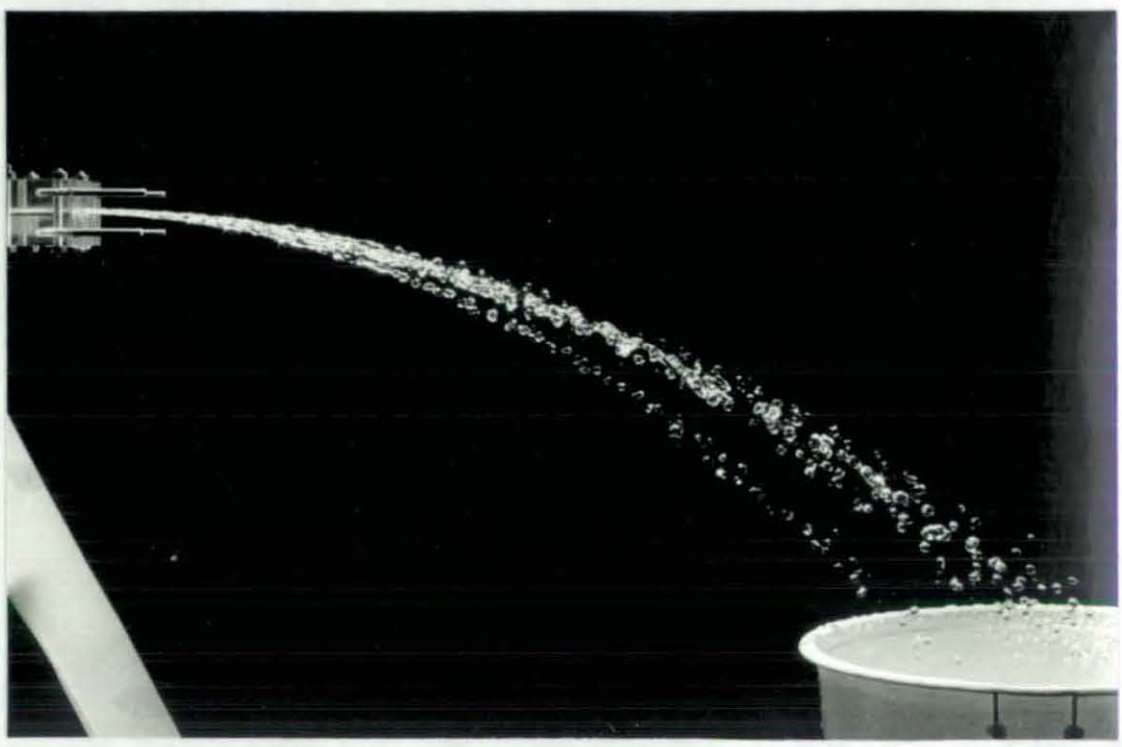

(b) 2 l/min

Fig 40 Channel flow distribution test

4.3.4 Channel equivalent height test

Due to the intrusion of membrane into the channel, the channel height was certainly less than 3 mm. Therefore, it was important to estimate the channel equivalent height when a new membrane had been placed into the module.

The height could be measured by the ruler before the connector was assembled. However, considering the unevenness along the membrane surface due to assembly, further measurements were carried out under kinetic conditions.

The module was placed in the same way as that for the streamlining leakage test. Since the flow rate (Q), the flying distance (L) and the falling height (X) of each jet could be measured as shown in Fig 40, the equivalent cross sectional area (S) could be obtained:

$$X = \frac{1}{2} g\, t^2 \tag{4.3a}$$

$$L = U\, t \tag{4.3b}$$

$$U = L\sqrt{\frac{g}{2X}} \tag{4.3c}$$

$$S = \frac{Q}{U} = \frac{Q}{L}\sqrt{\frac{2X}{g}} \tag{4.3d}$$

Since the width of the channel was not changed by the membrane (3mm), the equivalent height of the channel (H) could be obtained:

$$H = \frac{S}{3} = \frac{Q}{3L}\sqrt{\frac{2X}{g}} \tag{4.3e}$$

where g is the gravity (9.81 m/s^2)

From the tests, the equivalent height was about 2.95 mm, which was very close to the measured height.

4.3.5 Membrane selection

Four different rating pore size membranes were tested with cleaned tap water. The test conditions are tabulated in Table 13 and the results in Fig 41, in which the 1.2 μm membrane was under higher pressure than the 3 μm membrane.

Table 13

Test conditions with filtered tap water

Membrane pore size	Channel flow rate	Transmembrane Pressure	Temperature
(micron)	(l/min)	(Bar)	(°C)
0.2	2	0.41	20
0.45	1.67	0.41	28
1.2	1.16	0.2	30
3	1.16	0.12	30

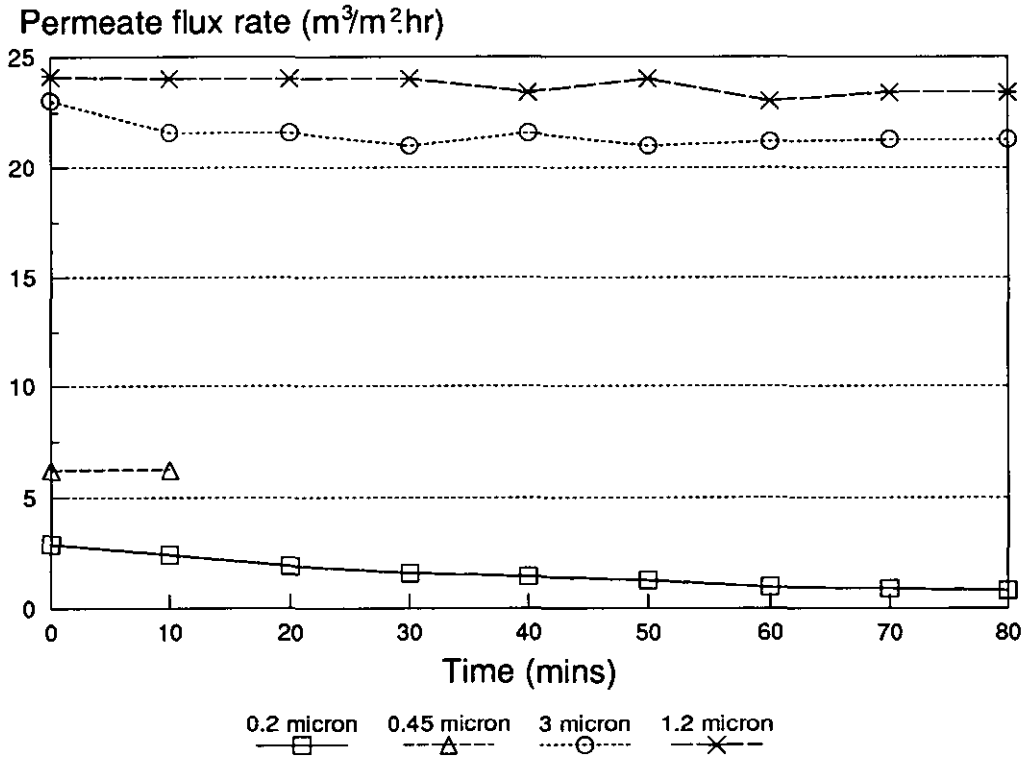

Fig 41 Filtered tap water test results

The flux rate of the 0.2 μm membrane was too low and declined quickly within 2 - 3 hours. Since it was easily fouled by filtered tap water, this kind of membrane was not used for further tests.

The flux rate of the 3 μm membrane was steady with the time but it was not practical because No 9 latex could completely penetrate this membrane.

The flux rates of the 0.45 μm and 1.2 μm membranes were moderate and the decline was not serious, therefore they were selected.

4.3.6 Minimum pressure difference test

The design of the filter module was such that the pressure difference due to flow down the module's channels could be greater than the transmembrane pressure. This could cause flow reversal from the permeate back into the bulk flow. Thus a minimum pressure had to be maintained at the filter outlet to ensure that the full membrane area was used for filtration.

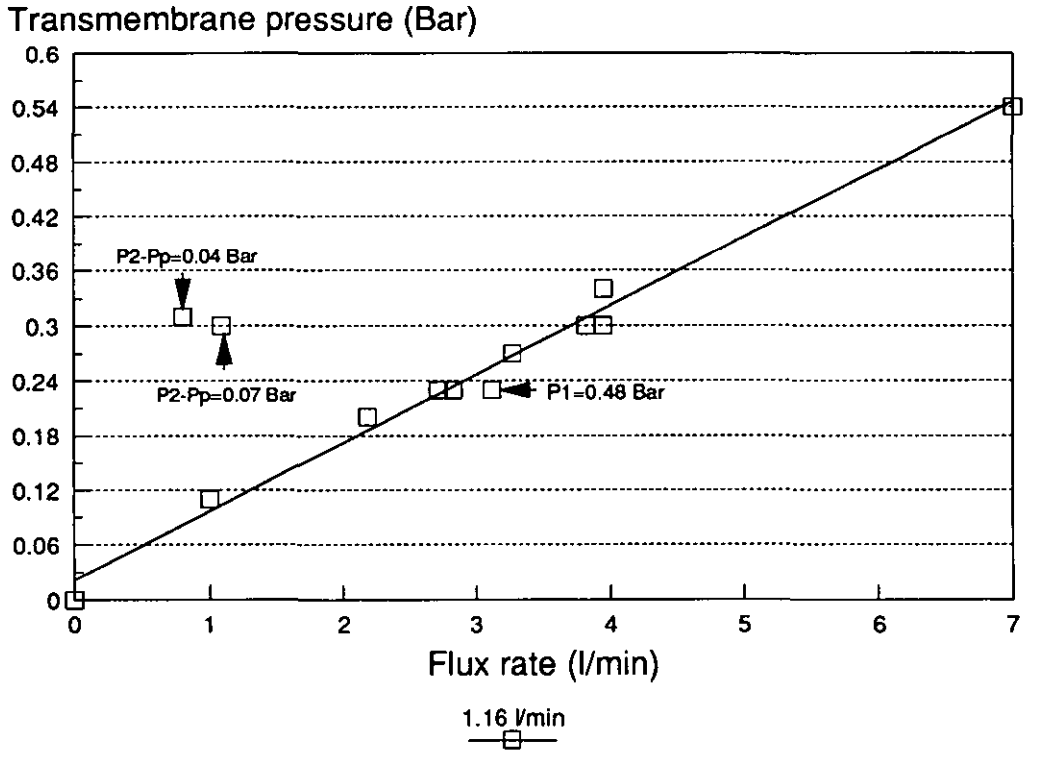

Fig 42 Minimum pressure test

The test to determine the minimum required pressure was carried out with filtered tap water, different flux rates against pressures under the same feed flow rate were measured as shown in Fig 42. They indicate that the minimum pressure difference between P2 (outlet side) and Pp (permeate side) should be no less than 0.2 Bar and P1 (inlet side) should be greater than 0.5 Bar.

4.4 Experimental procedures

Each membrane underwent the following tests:

4.4.1 Rig cleaning and tap water filtration

The rig was cleaned with tap water after each test. Then the tank was filled with tap water which was filtered by a 0.1 μm Millipore cartridge filter. The cleaning procedure was the same as that given in Chapter 3.

Since it took several runs to foul one membrane, the module was replaced by a tube during the system cleaning so that the deposition on the membrane surface would not be reduced by cleaning or contaminated by tap water.

4.4.2 Transmembrane pressure measurement

The system was run in batch mode for this test.

The structures of the two flow connectors and the position of the pressure gauges cause the real transmembrane pressure to be different from the results calculated from the values given by Eq 4.4:

$$P_t = \frac{(P1 + P2)}{2} - P_p \tag{4.4}$$

Therefore, the transmembrane pressure must be determined for each run experimentally.

The values of the inlet, outlet and permeate gauges at different flow rates with the permeate valve fully closed and outlet valve fully opened were measured. The values on the permeate gauge in this case is equivalent to the pressure on the feed side of the membrane. The relationships between the flow rates and pressure were found to be of the form:

$$P_i = a_i Q^{b_i} \tag{4.5}$$

where a and b are constants, but vary for different runs

sub i refers to 1 (inlet), 2 (outlet) and 3 (membrane feed side) respectively.

The results of one such test with membrane H are shown in Fig 43.

It was found that all the three pressures increased when the outlet valve was throttled, and the increase in P3 could be obtained from the difference between the

displayed value on the pressure gauges and the value calculated from the Eq 4.5, therefore, the transmembrane pressure P_t is:

$$P_t = \Delta P_i + P3 - P_p \tag{4.6}$$

where sub *i* refers to 1 (inlet) or 2 (outlet) respectively.

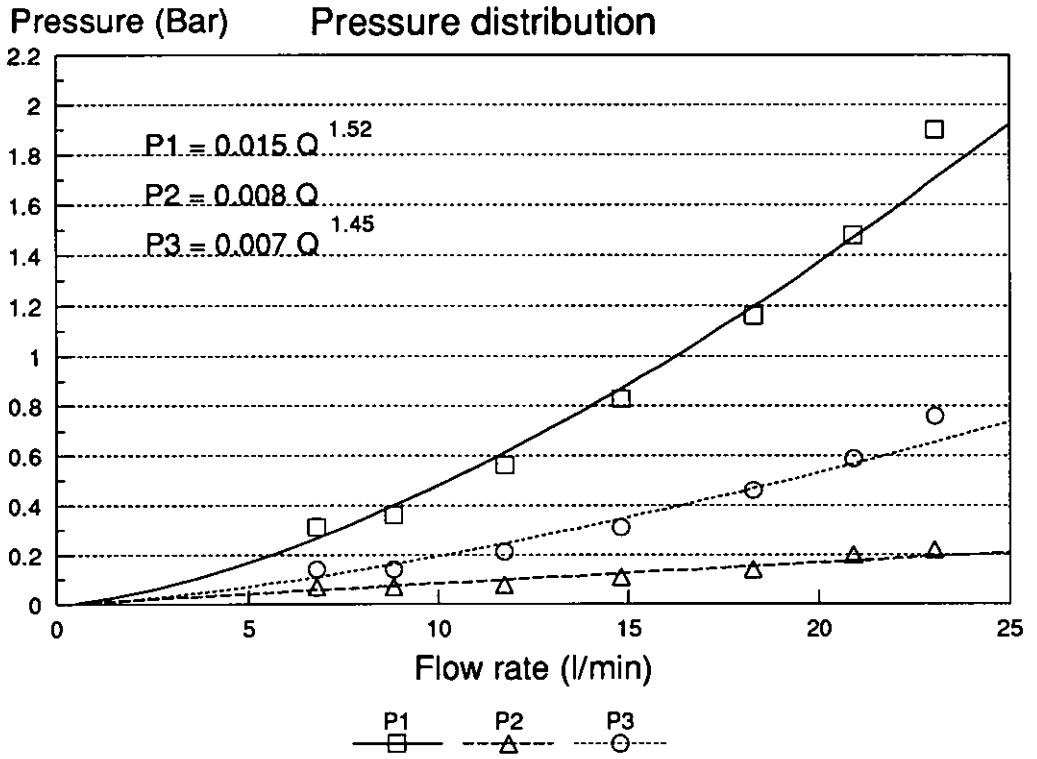

Fig 43 Pressure distribution test

4.4.3 Membrane resistance test

The system was also run in batch mode for this test.

The resistance of the newly fixed membrane was tested with filtered tap water. By changing the feed flow rate and transmembrane pressure, the membrane resistance was obtained by regressing the transmembrane pressure $\mathbf{P_t}$ against the permeate flux rates $\mathbf{J_v}$. This test was carried out before latex had been added into the tank. The membrane resistance can be calculated from following formula:

$$R_m = \frac{P_t}{\mu J_v} \tag{4.7}$$

Eq 4.7 is the transformed expression of Eq 2.1a:

$$J_v = \frac{P_t}{\mu R_t} \qquad (2.1a)$$

Fig 44 shows one result of Test H1/1 which indicates that P_t based on P1 was more linear and closer to the origin than those based on either P2 or Eq 4.4. This was also true of membranes G and I as shown in the diagrams of Appendix 4, therefore, all P_t in the tests were based on P1.

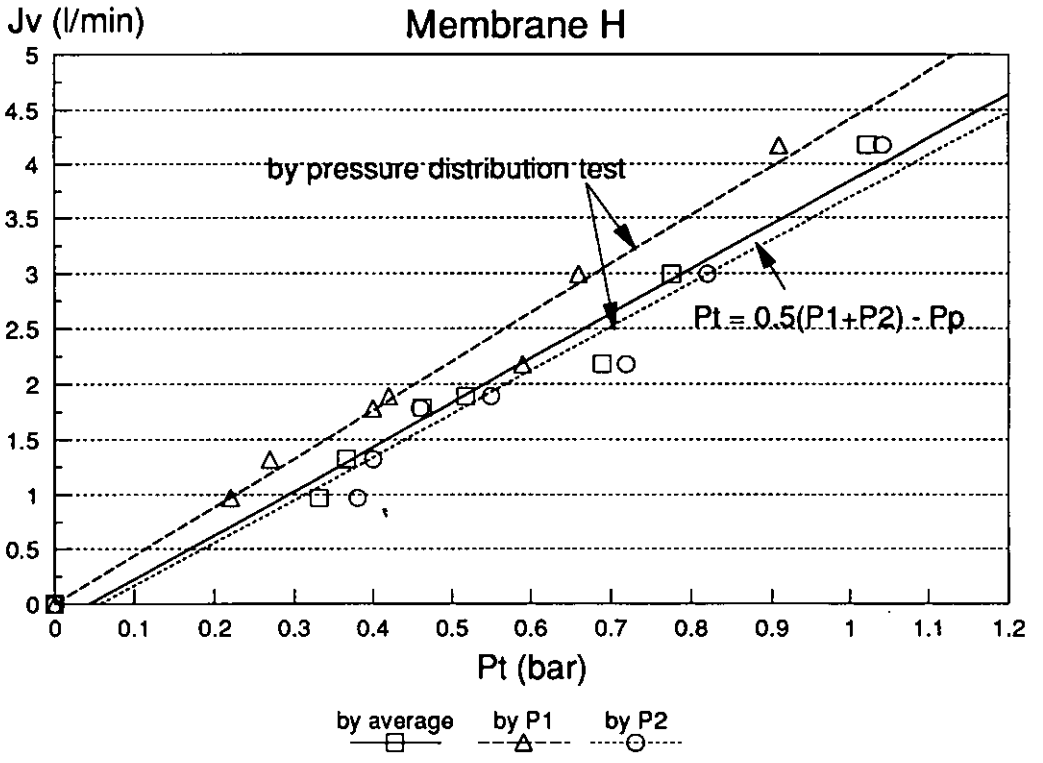

Fig 44 Membrane resistance test

4.4.4 Flux rate decay tests

After the above tests, the latex suspension was added into the tank and the system ran several minutes without filtration until the suspension had uniformly distributed throughout the system. The latex had been diluted and sonicated for several minutes before it was put in.

The system was run in single pass mode during filtration, the cumulative permeate volume was measured periodically and the flux rate was obtained by the following formula:

$$J_{v_t} = \frac{1}{S}\frac{W_{t+1} - W_{t-1}}{t_{t+1} - t_{t-1}} \tag{4.8}$$

4.4.5 Latex particle concentration measurements

The amount of added latex suspension varied for the tests of the same membrane so as not to saturate the sizing equipment which resulted in very low concentration by wt % in some tests although the readings by Hiac/Royco remained high.

The numbers of latex particles in different size ranges in the bulk flow were recorded by Hiac/Royco equipment in the unit of counts per ml, then they were multiplied by the volume of the suspension left in the rig so that the total number of the particles of different sizes could be monitored. The concentration of latex suspension in mg/l was calculated by following formula:

$$C_b = \frac{\pi \cdot \rho_s}{6} \sum_{i=1}^{6} (d_i^3 \cdot N_i) \tag{4.9}$$

where d_i is the channel setting size (m)

N_i is the counts per ml of each channel.

The particle concentration in the filtrated tap water and permeates was also monitored by Hiac/Royco. The particle concentration of fresh tap water was too high to be measured.

4.4.6 The investigation into the early stage of membrane fouling

Flux rate decay during filtration is the result of an increase in the flow resistance, i.e. the formation of deposits on the membrane surface and pore blocking inside the membrane. By analysing the flux rate and process time with the mathematical models presented in Chapter 2, the fouling process can be investigated.

In order to investigate the early stage of membrane fouling, some tests consisted of several runs, each run finished when 15 to 20 litres of permeate had been collected, the system was then turned into batch mode without filtration to test the pressure distribution as done in §4.4.2, after that the system was switched back into single-pass

mode to initiate another run. Some deposit on the membrane surface may have been swept away by the increased shear force or backflushed by permeate during the pressure distribution tests, therefore, the flux rate may recover to some degree.

Some tests lasted as long as 160 minutes in order to see if a deposit layer or film could be formed under crossflow conditions and if the pore blocking still occurred after the formation of a deposit layer.

When the permeate flux rate had become steady at the lowest possible level, the membranes were taken out and investigated by SEM to see which was the main reason for the flux rate decay for this type of experiment.

4.5 Test results and discussions

11 Versapor membranes with different rating pore sizes were tested for the above items. The results are tabulated in Table 14 chronologically which means membrane J was the first tested, followed by membranes K and M, and then membranes A to I.

The detailed contents of the tests are listed alphabetically in Appendix 4.

In Table 14, the first item is the membranes and tests carried out with this membrane, in which letters ***A*** to ***M*** refer to the membrane used, the first number refers to the order of the test, and the second number refers to the order of the run during this test. For example, H1/2 means the second run of the first test with membrane H, and H3 refers to the third test of membrane H and there was only one run for this test.

d_m refers to the rating pore size of each membrane. For membranes G, H and I, the variation in d_m due to pore shrinkage has been investigated based on the Standard blocking model and the results are tabulated in Table 17.

The ***Pressure*** item, P1, P2 and P_p are the displayed values of the pressure gauges, P_t of membranes G, H and I are based on P1 by pressure distribution tests, P_t of other membranes are based on Eq 4.4 (see § 4.4.2). This is why only the details of tests with membranes G, H and I have been analysed in Appendix 4. The cause of low permeate rate under high transmembrane pressure - due to flow reversal through the membrane - was discovered with membrane E, and membrane F was used to find the optimum value of transmembrane pressure as described in § 4.4.2.

The words ***Start*** and ***End*** in permeate ***Flux rate*** item refer to the highest and lowest rate of each run.

Table 14a

Test results of latex suspensions with Versapor membranes

Membrane		Pressure				Flux rate		Te	Flow rate		Ti	Latex		
Test	d_m	P1	P2	Pp	Pt	J_v		θ	Q	Re	t	No	C_b by	
		in	out	per	trns	Start	End						Oven	Hiac
	µm	Bar				$m^3 \cdot m^{-2} \cdot hr^{-1}$		°C	l/m		min		$mg \cdot l^{-1}$	
J1	0.20	0.69	0.14	0.00	0.41	2.88	0.30	20	2.00	11224	140	W		
J2		1.38	0.83	0.00	1.10	2.72	0.83	20	2.00	11224	160	W		
J3		2.07	1.52	0.21	1.59	3.94	1.12	25	2.00	11224	150	W		
L	0.20	2.07	0.83	0.00	1.45	2.10	0.15	20	3.60	20203	180	W		
M	0.20	0.17	0.00	0.00	0.09	2.10	0.15	25	1.37	7689	330	6	0.152	0.014
K1	0.45	0.83	0.28	0.00	0.55	2.22	0.73	20	1.56	8755	190	6	0.019	0.006
K2		0.69	0.21	0.00	0.45	3.59	0.20	20	1.73	9709	130	6	0.018	0.012
K3		0.51	0.21	0.00	0.36	10.7	8.15	24	1.73	9709	20	6	0.018	0.013
A1	0.45	0.83	0.53	0.30	0.68	10.8	6.97	24	1.33	7464	40	6	0.015	0.017
A2/1		0.86	0.54	0.30	0.40	3.51	2.25	23	1.40	7857	60	6	0.015	0.030
A2/2		0.94	0.51	0.30	0.42	2.27	1.22	23	1.80	10102	50			
A2/3		1.21	0.22	0.30	0.41	1.22	0.75	23	2.50	14030	60			
A3/1		1.15	0.52	0.07	0.77	1.49	0.54	23	2.45	13750	60	6	0.072	0.008
A3/2		0.83	0.60	0.07	0.64	2.31	0.07	23	1.18	6622	50			
B1/1	0.45	1.21	0.33	0.52	0.26	1.67	0.64	22	2.50	14030	60	11	0.040	0.006
B1/2		1.04	0.47	0.52	0.24	2.24	1.43	24	2.00	11224	60			
B1/3		0.91	0.63	0.52	0.25	3.54	1.78	26	1.17	6566	60			
B1/4		1.01	0.48	0.52	0.23	4.56	2.94	14	0.83	4675	40			
B2/1		1.21	0.33	0.37	0.40	4.80	2.72	28	2.50	14030	20	W		
B2/2		1.00	0.61	0.40	0.41	7.86	6.23	28	1.67	9372	10			
B2/3		0.87	0.73	0.37	0.43	5.21	5.78	28	0.83	4675	10			
B3/1		1.17	0.90	0.33	0.70	1.19	0.67	25	2.50	14030	30	11	0.038	0.010
B3/2		1.00	0.41	0.30	0.40	1.92	1.72	26	2.00	11224	30			
B3/3		0.91	0.63	0.37	0.40	7.59	5.38	28	1.16	6510	30			
D	3.00	1.45	0.69	0.55	0.52	23.0	21.0	30	1.16	6510	120	W		
E1	1.20	2.07	1.31	0.55	1.14	24.8	22.7	30	1.16	6510	120	W		
E2/1		1.43	0.59	0.77	0.23	1.75	1.35	26	2.50	14030	60	11	0.022	0.006
E2/2		1.01	0.47	0.53	0.21	3.28	2.17	30	2.00	11224	60			
F1	1.20	0.62	0.48	0.31	0.24	16.5	8.22	28	1.15	6454	35	11	0.109	0.034
F2		0.62	0.48	0.31	0.24	14.0	5.72	29	1.15	6454	50	11	0.022	0.007
F3		0.62	0.48	0.31	0.24	10.7	5.27	29	1.15	6454	70	11	0.002	0.002

Table 14b

Test results of latex suspensions with Versapor membranes

Membrane		Pressure				Flux rate		Te	Flow rate		Ti	Latex		
Test	d_m	P1	P2	Pp	Pt	J_v		θ	Q	Re	t	No	C_b by	
		in	out	per	trns	Start	End						Oven	Hiac
	µm	Bar				$m^3 \cdot m^{-2} \cdot hr^{-1}$		°C	l/m		min		$mg \cdot l^{-1}$	
G1	1.2	0.54	0.41	0.26	0.15	36.6	31.7	29	1.22	6847	15	11	0.22	
G2/1		0.69	0.48	0.31	0.16	20.3	6.73	29	1.22	6847	10	11	0.22	
G2/2		0.69	0.48	0.31	0.17	9.47	4.73	29	1.22	6847	20			
G2/3		0.69	0.48	0.31	0.17	6.00	2.40	29	1.20	6734	30			
G2/4		0.69	0.48	0.31	0.17	4.87	1.80	29	1.22	6847	30			
G3/1		0.69	0.48	0.31	0.20	8.47	3.33	29	1.15	6454	30	11	0.22	
G3/2		0.68	0.48	0.31	0.18	6.93	2.53	29	1.15	6454	30			
G3/3		0.68	0.48	0.31	0.15	5.40	1.53	29	1.18	6641	40			
G3/4		0.68	0.48	0.31	0.17	3.73	0.93	29	1.18	6622	50			
G4/1		0.68	0.48	0.31	0.17	3.73	1.20	29	1.16	6510	40	11	0.20	
G4/2		0.68	0.48	0.31	0.19	2.33	0.87	29	1.17	6566	40			
H1/1	0.45	0.90	0.76	0.14	0.64	13.9	11.3	29	1.18	6622	12	11	0.25	
H1/2		0.90	0.76	0.14	0.61	11.9	8.80	29	1.18	6622	12			
H1/3		0.91	0.76	0.14	0.64	9.73	6.13	29	1.28	7183	16			
H1/4		0.90	0.76	0.14	0.60	7.33	3.53	29	1.20	6734	20			
H2/1		0.90	0.76	0.14	0.62	4.40	2.27	26	1.22	6734	32	11	0.33	
H2/2		0.91	0.76	0.14	0.64	2.80	1.40	26	1.23	6903	48			
H3		0.90	0.76	0.14	0.65	2.67	1.29	25	1.17	6547	130	11	0.20	0.002
H4		0.90	0.76	0.14	0.61	2.48	1.00	26	1.17	6547	130	11	0.12	0.006
H5		1.38	1.03	0.14	0.91	2.81	1.43	29	1.94	10859	130	11	0.12	0.008
H6		1.86	1.03	0.14	0.95	2.91	0.95	29	3.08	17304	130	11	0.12	0.004
I1	0.45	0.76	0.62	0.41	0.26	9.04	4.93	29	0.95	5331	80	9	0.03	0.008
I2		0.81	0.62	0.41	0.23	4.13	1.37	25	1.22	6828	130	9	0.03	0.022
I3		0.77	0.62	0.41	0.16	2.83	0.97	25	1.28	7161	160	9	0.02	0.003

Te is the temperature in the tank. This was kept between 25 to 29 °C, therefore, the variation in density and viscosity due to temperature were neglected.

Flow rate includes feed flow rate and Reynolds numbers of each channel, the equivalent hydrodynamic diameter of the channel was 2.98 mm. The Reynolds numbers in all tests were greater than 4000, so that all channel flows were turbulent.

Ti item in Column 12 is the period of each run.

Latex item includes the latex types and their original bulk concentrations of each test by OVEN and HIAC methods, word ***W*** refers to tests with water.

4.5.1 The particle concentration variation during filtration from Hiac/Royco sizing equipment

Table 15 is the latex concentration of all tests obtained by OVEN and HIAC methods. The values by HIAC were close to those by OVEN method at low concentrations, but much lower than those at high concentrations. This is because the Hiac/Royco could not count particles smaller than 0.7 μm and only six particle sizes were used in Eq 4.9 to calculate the concentration, therefore, the concentrations by OVEN method were used for analysing the results from membranes G, H and I.

The results of the measurements of the particle concentrations in the fresh tap water, filtered tap water, original bulk flow and permeates with Hiac/Royco equipment of Test H5 are tabulated in Table 16. The details of latex suspension variation during the test are shown in Fig 45.

It is evident from Table 16 that particle concentration in the fresh tap water is very high and the 0.1 μm cartridge filter can effectively get rid of these particles. The particle concentration in the permeate is low so that the loss of particles in the permeate can be neglected during calculation of the bulk flow concentration.

Since the tests were run in single pass mode and the permeates were very "pure", the concentration in the bulk flow should have increased with time, This phenomenon is demonstrated in Fig 45a where the particle concentration in six channels increased, however, Fig 45b shows that the total amount of particles in the system decreased. The only reason for the loss of particles was that they had been trapped inside the membrane pores since a filter cake did not form as shown in Fig 47.

Table 15
Latex particle concentrations of all tests

Test	C_b (mg/l)		Latex	Water	Channel settings (μm)					
	Oven	Hiac	ml	litres	counts/ml					
No 6	10 ml latex in 100 ml water				0.9	1	1.1	1.5	1.8	2.3
M	0.212	0.012	10	85	554	581	386	404	755	1327
K1	0.257	0.006	5	35	205	230	175	140	314	729
K2	0.255	0.012	8.5	60	230	263	214	303	981	1259
K3	0.252	0.012	7	50	169	194	165	217	918	1359
Change channel settings					1.1	1.3	1.5	2.3	3	5
A1	0.201	0.018	9.5	85	149	317	1024	516	303	132
A2	0.210	0.027	10.5	90	195	282	989	913	405	200
A3	0.100	0.008	5	90	105	168	656	309	128	43
No 11	1 ml latex in 110 ml water				1.1	1.3	1.5	1.8	2.3	3
B1	0.040	0.011	20	90	27	106	951	589	291	167
B3	0.038	0.018	14	65	37	176	1370	829	460	309
Change channel settings					0.7	0.9	1.5	1.8	3	5
E2	0.022	0.010	10	80	220	366	789	498	103	39
10 ml latex in 100 ml water					0.7	0.9	1.5	1.8	3	5
F1	0.109	0.087	5	90	1009	1073	2838	4837	1205	341
F2	0.022	0.013	1	90	261	344	1027	777	146	41
F3	0.002	0.001	0.1	90	60	63	86	49	13	6
G1	0.022		1	90						
G2	0.218		10	90						
G3	0.218		10	90						
G4	0.196		5	50						
H1	0.245		10	80						
H2	0.327		10	60						
H3	0.002		0.1	80						
Change channel settings					0.9	1.1	1.5	1.8	3	5
H4	0.012	0.010	0.3	50	159	74	81	663	172	33
H5	0.012	0.015	0.3	50	210	86	60	998	255	50
H6	0.012	0.010	0.3	50	128	54	112	781	153	28
No 9	5 ml latex in 250 ml water				0.9	1.1	1.5	1.8	3	5
I1	0.330	0.010	10	80	285	137	161	1789	150	30
I2	0.293	0.017	10	90	314	128	175	1779	354	82
I3	0.018	0.006	0.4	60	293	136	124	911	68	15

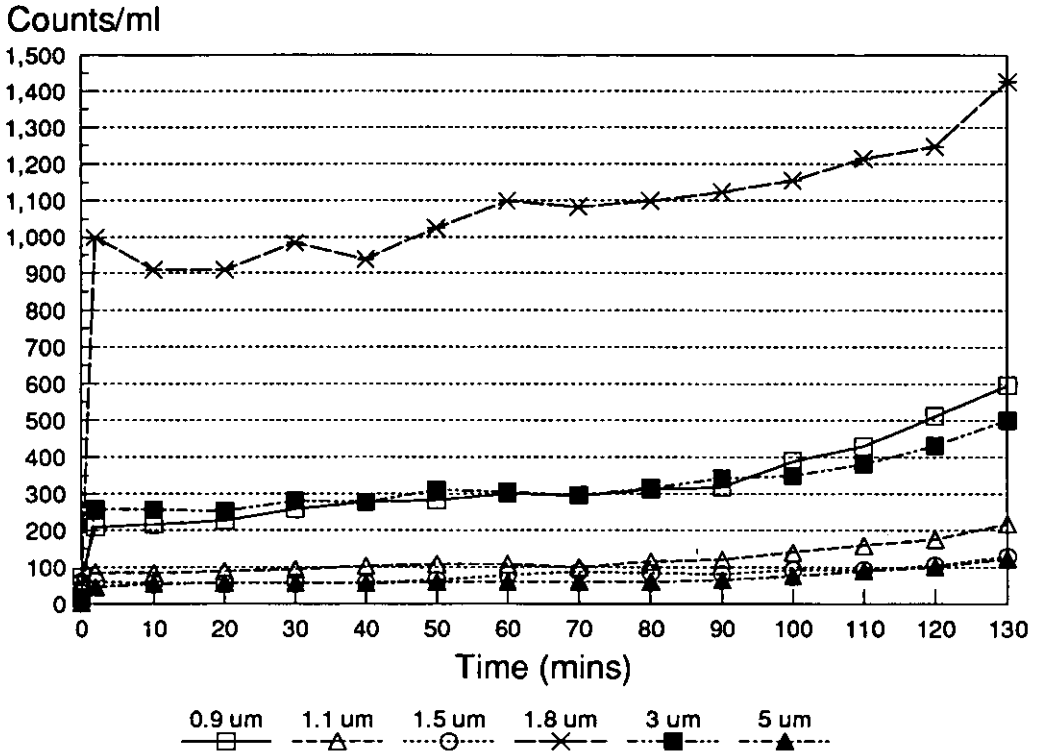

Fig 45a Variation of particle counts of six channels during filtration

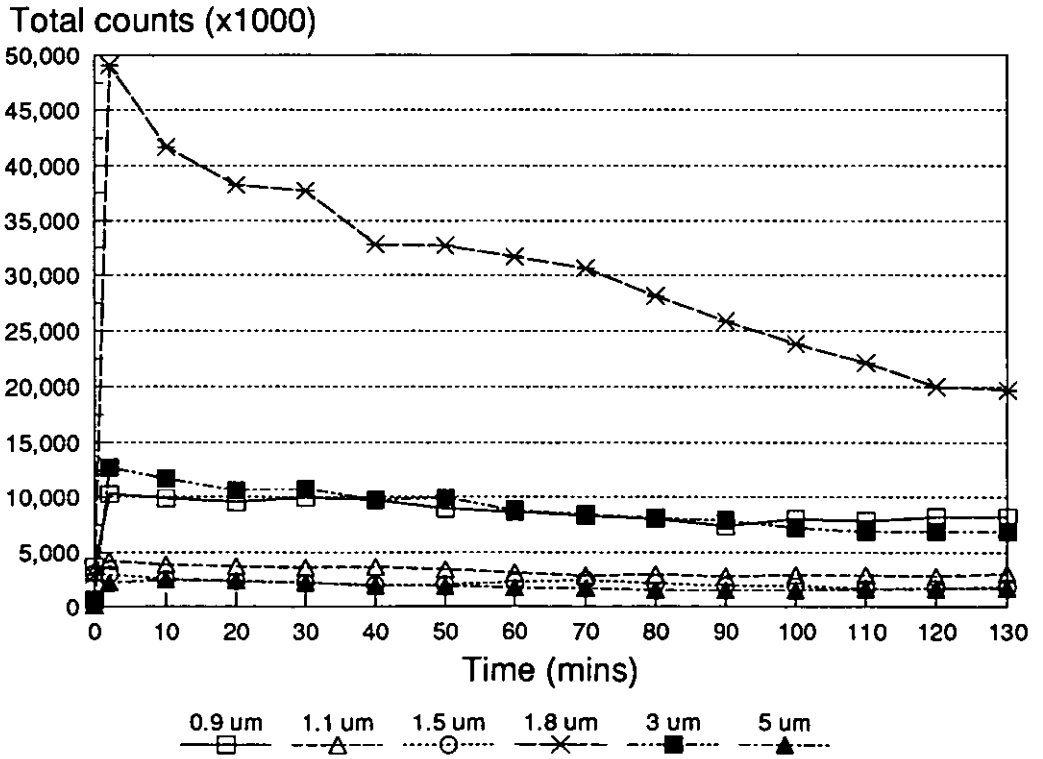

Fig 45b Variation of total particle counts of six channels during filtration

It was noticed that the sampling rate of Hiac/Royco equipment dropped from 100 ml/min to 80 ml/min within 10 minutes, which led to low counts, and the counts would also jump after adjusting the sampling rate. This resulted in a fluctuation of counts for the six curves in Fig 45a. This error was later prevented by fixing a nozzle at the exit of the sampling pipe and progressively reducing the pressure drop across the sampling cell. The counts then increased steadily. The particle counts at time 0 are for clean water, the latex was added in at the 2nd minute which resulted in the jump in the counts.

One of the intentions of this work was to find out the relationship between the flux rate and the thickness of the deposits, however, due to the pore size distribution, the particles larger than 0.7 μm also penetrated into the membrane and were retained there. This greatly reduced the flux rate without forming any deposits on the membrane surface, therefore this relationship has not been quantitatively investigated by this experiment.

Table 16

Particle concentrations in Test H5

Fluid types	Channel settings (μm) and counts/ml						
	0.9	1.1	1.5	1.8	3	5	Total
Fresh tap water	System saturated						
Filtrated tap water	45	15	7	19	7	2	87
Latex bulk flow	210	86	60	998	259	46	1659
Permeate	73	9	1	13	12	25	118

4.5.2 The effects of the membrane pore sizes on the flux rate

Although the variations in the concentration of minute particles during the filtration could not be observed because the Hiac/Royco sizing equipment did not respond correctly to the particles less than 0.7 μm in diameter, the results of the Coulter analysis showed that their concentration in the latex suspension was very low as shown in Fig 37, therefore, the membranes were apparently fouled by particles whose sizes were up to the largest membrane surface pore which, as shown in Figs 48a and 49a, is about 5 μm for membrane G which covers 80% of No 11 cumulative particle size distribution,

and 1.7 μm for membrane H and I which covers 40% of No 11 latex and 80% of No 9 latex cumulative particle size distribution respectively, therefore, considerable amount of particles will enter the membranes during filtration which makes the assumption (2) in Grace's theory valid [Grace, 1956].

Fig 46 shows the results of the permeate flux rate of tests G2/1 and H1/1 respectively.

The concentrations and channel velocities for both tests were similar but test H1/1 was under higher pressure. Membrane G which had a larger pore size provided higher flux rate at the beginning, but it dropped very quickly: within 10 minutes, it was surprisingly lower than that of membrane H. The results indicate that the larger pore membrane is prone to be fouled at the beginning of the process due to high flux rate which brings more small particles into the pores and leaves them there. Therefore, J_v can not be restored by flushing the surface even if it is run under low pressure.

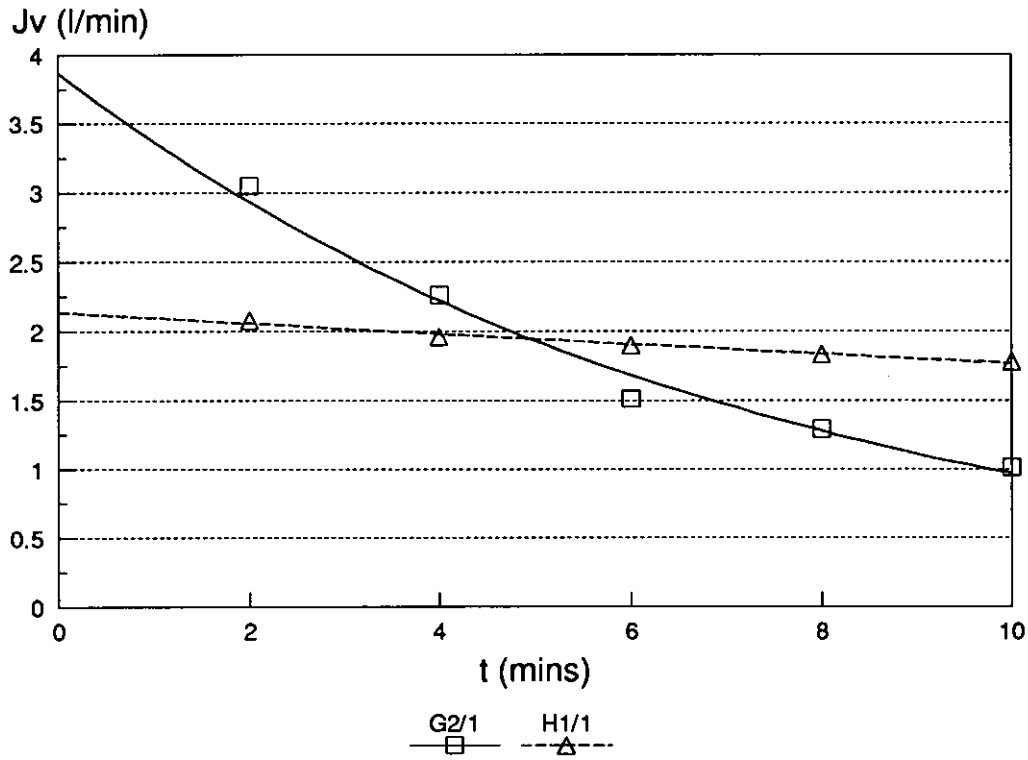

Fig 46 Permeate rates with different membrane pore sizes

4.5.3 Structure of membranes and foulants observed by SEM

Photographs in Figs 47 to 50 were taken by SEM.

In order to make comparison, new clean membranes before and after dead-end filtration with the same amount of latex suspensions used for each membrane were examined by SEM. The results are shown in Figs 48, 49 and 50 respectively. The membranes after crossflow filtration of latex suspensions are shown in Fig 47.

Fig 48a and 49a show that the Versapor membrane has a wide pore size distribution. For 1.2 μm membrane, the pore size can be as large as 5 μm, for 0.45 μm membrane, it can be as large as 1.7 μm, both are about four times greater than the rating values. The rated pore size results from overlapping of the pores to provide a tortuous flow path. Therefore, particles larger than the rated pore size will be trapped. Since this is common to all "diffusive" type of membranes, it is essential to have a comprehensive knowledge on the membrane pore size distribution so as to give better information for the analysis of the test results. This test has not be carried out in this study due to the lack of available facilities, e.g. a Coulter porometer.

All the structures of foulants in either type of filtration do not differ from each other significantly whatever the difference in the latex and membrane pore sizes.

The pore size distribution of the "diffusive type" membrane is wide, the membranes with different pore sizes will give similar flux rates when fouling has started, because the membrane with large pores will be fouled more quickly than that with the finer pores even if the larger pores had been only partially blocked.

There were filter cakes on the surface after dead-end filtration as shown in Figs 48b, 49b and 50 and the particles agglomerated, but there were no such cakes on the surface and particle agglomeration was not so evident after crossflow filtration as shown in Fig 47 in which most particles were separated whether on the surface or inside the wholly or partially blocked pores.

The indented parts in Figs 47a(3) and 47b(3) are the positions of a filter ridge, there are no latex particles on it which indicates excellent isolation between the channels.

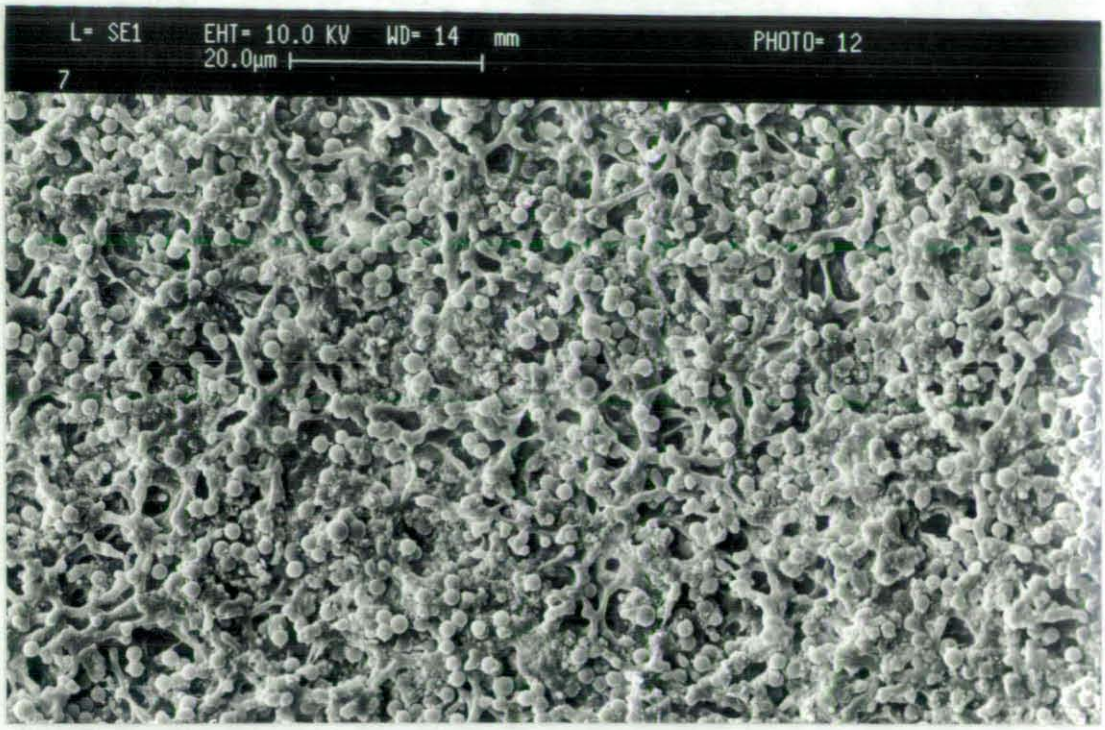

(1) 5 cm from the entrance

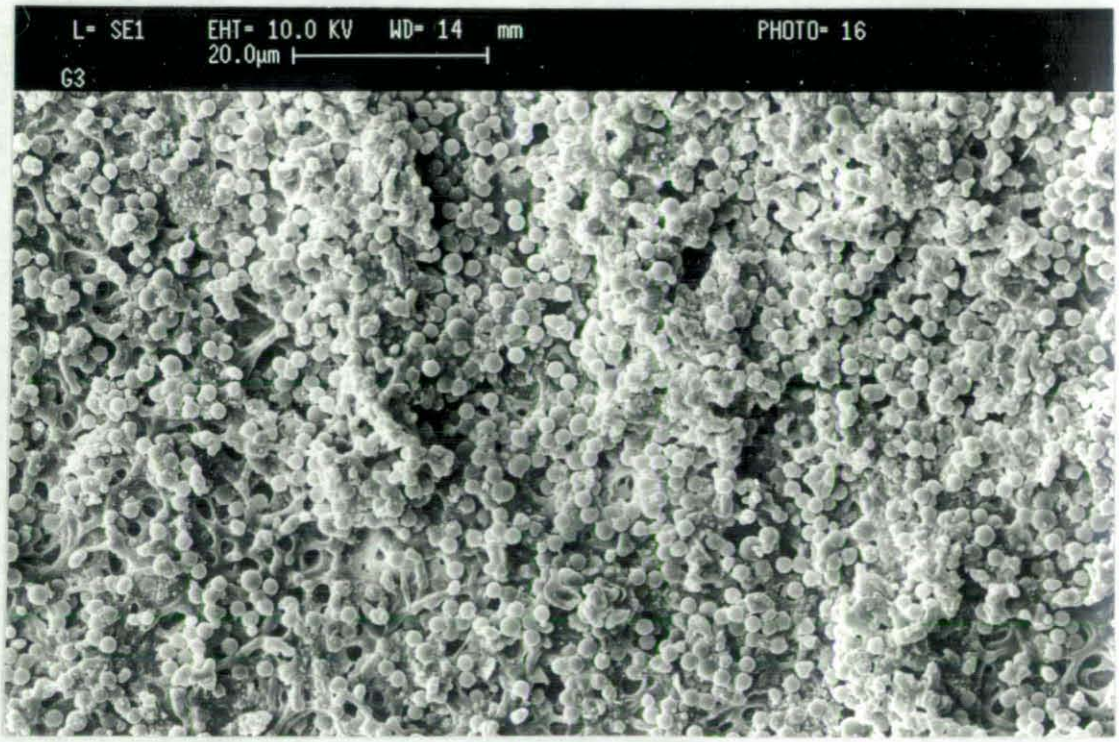

(2) 20 cm from the entrance

Fig 47a Photographs of fouled membrane G by SEM

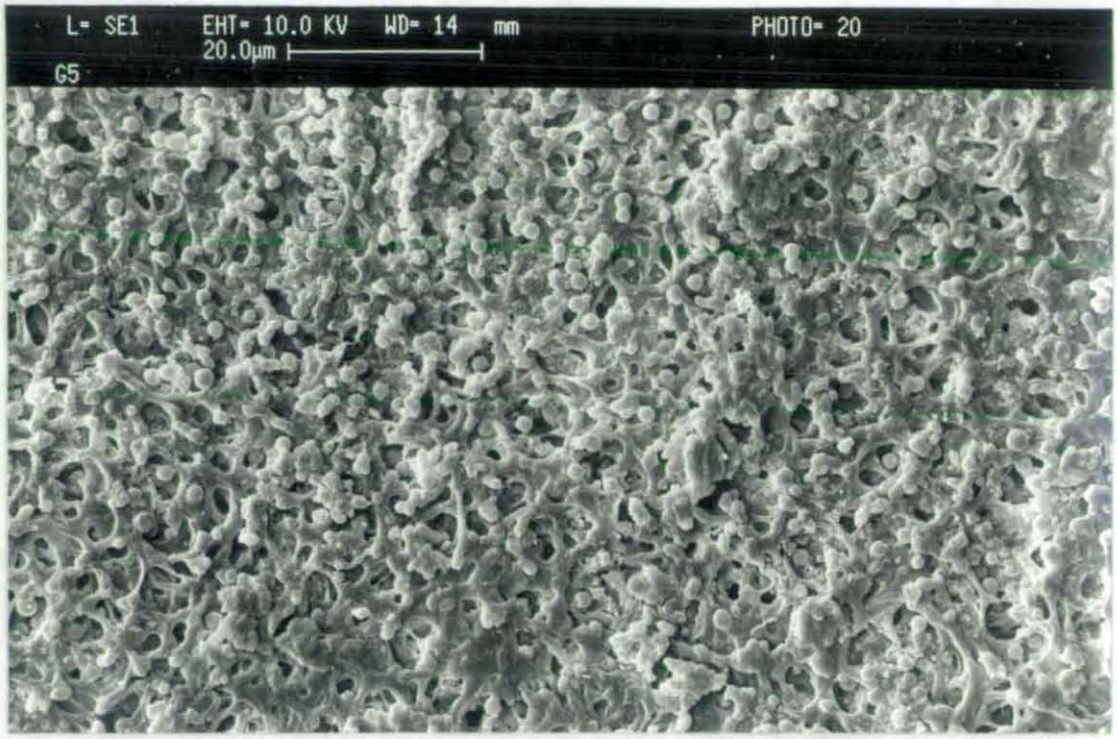

(3) 35 cm from the entrance

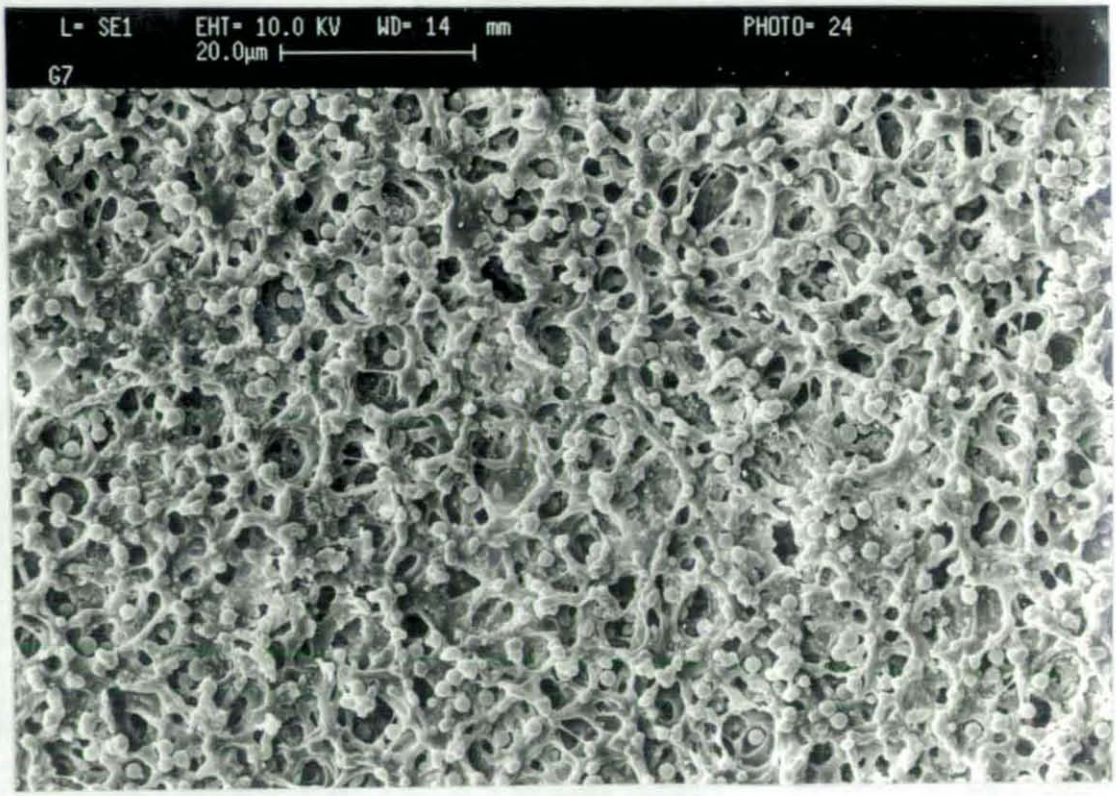

(4) 5 cm from the exit

Fig 47a Photographs of fouled membrane G by SEM

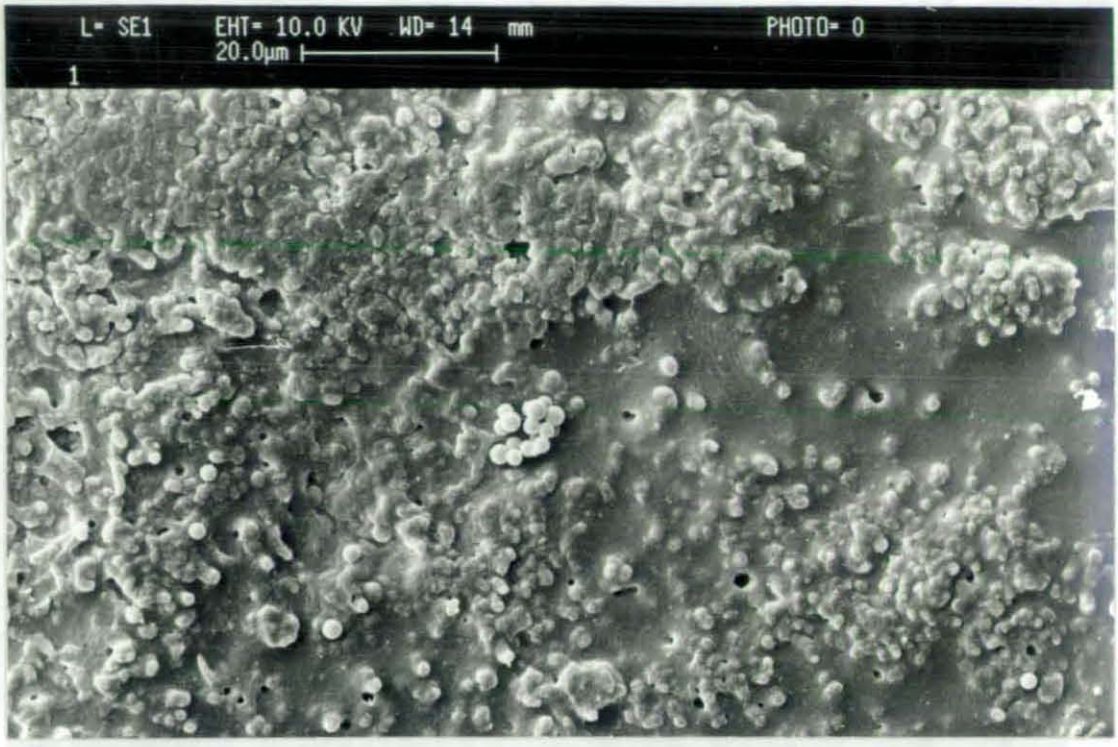

(1) 5 cm from the entrance

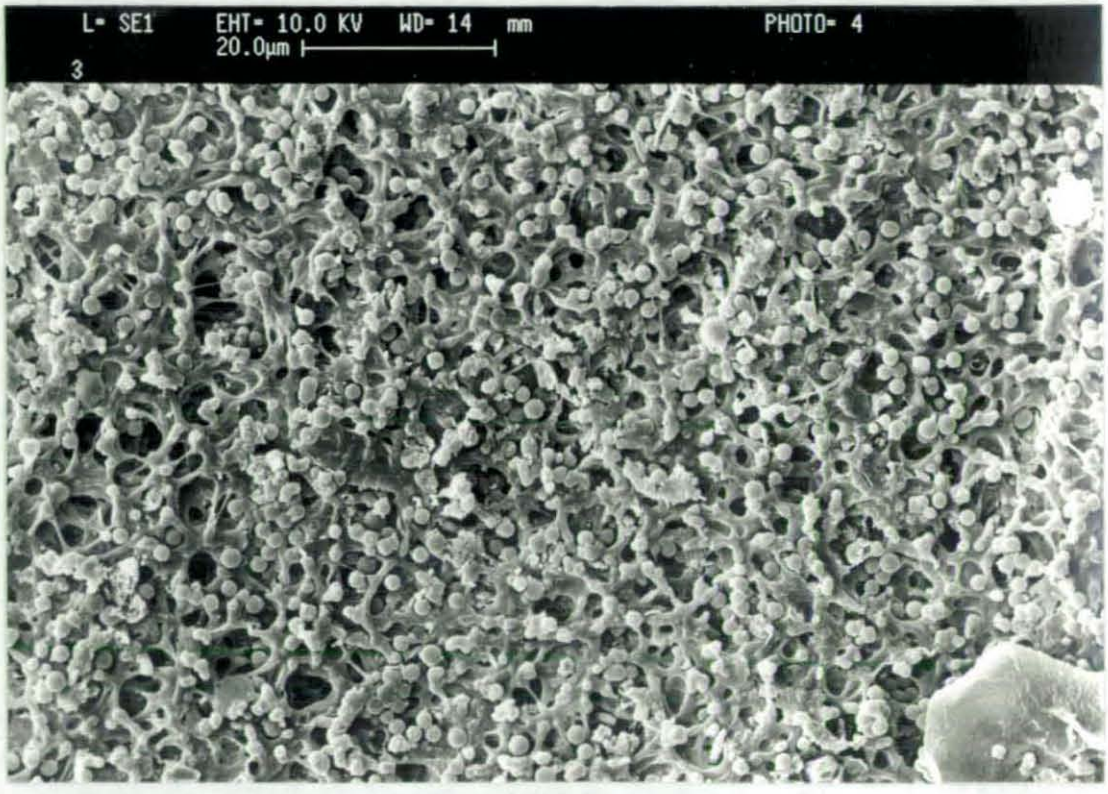

(2) 20 cm from the entrance

Fig 47b Photographs of fouled membrane H by SEM

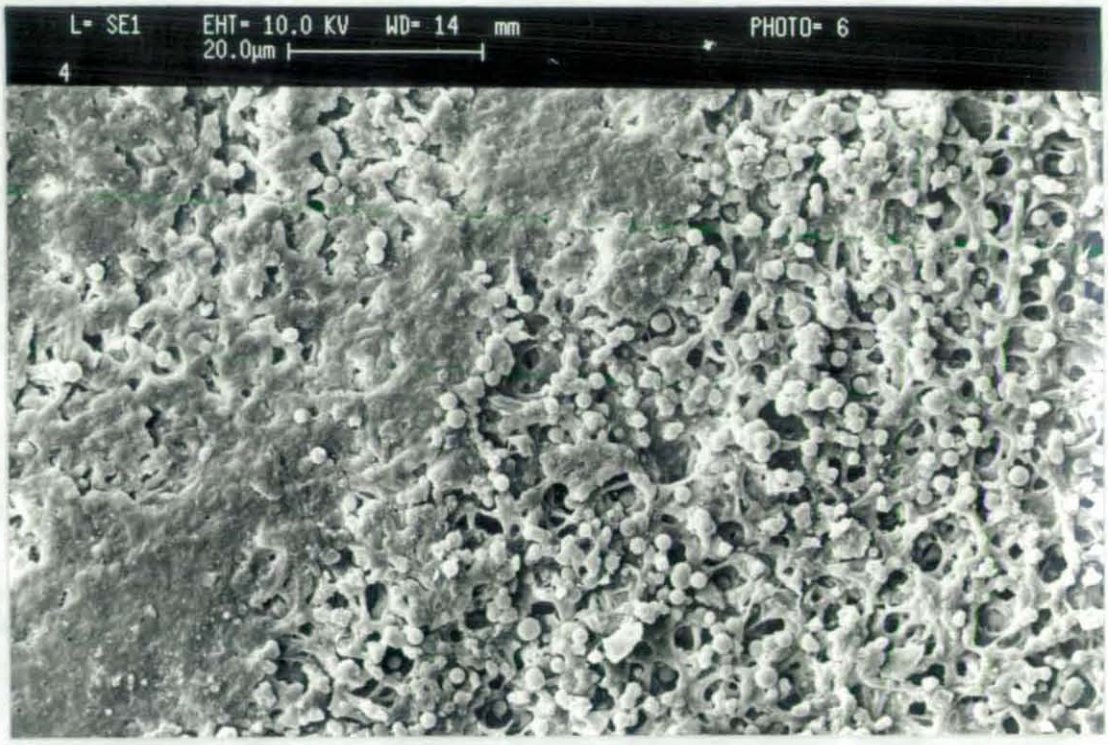

(3) 35 cm from the entrance

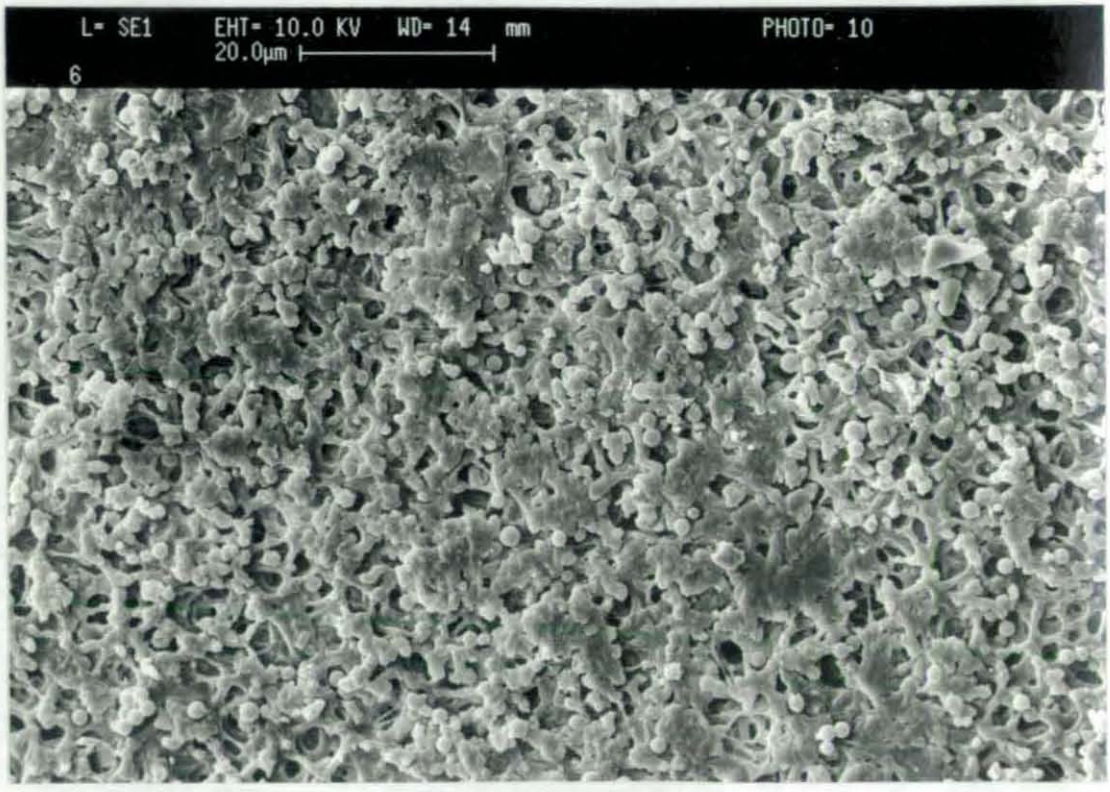

(4) 5 cm from the exit

Fig 47b Photographs of fouled membrane H by SEM

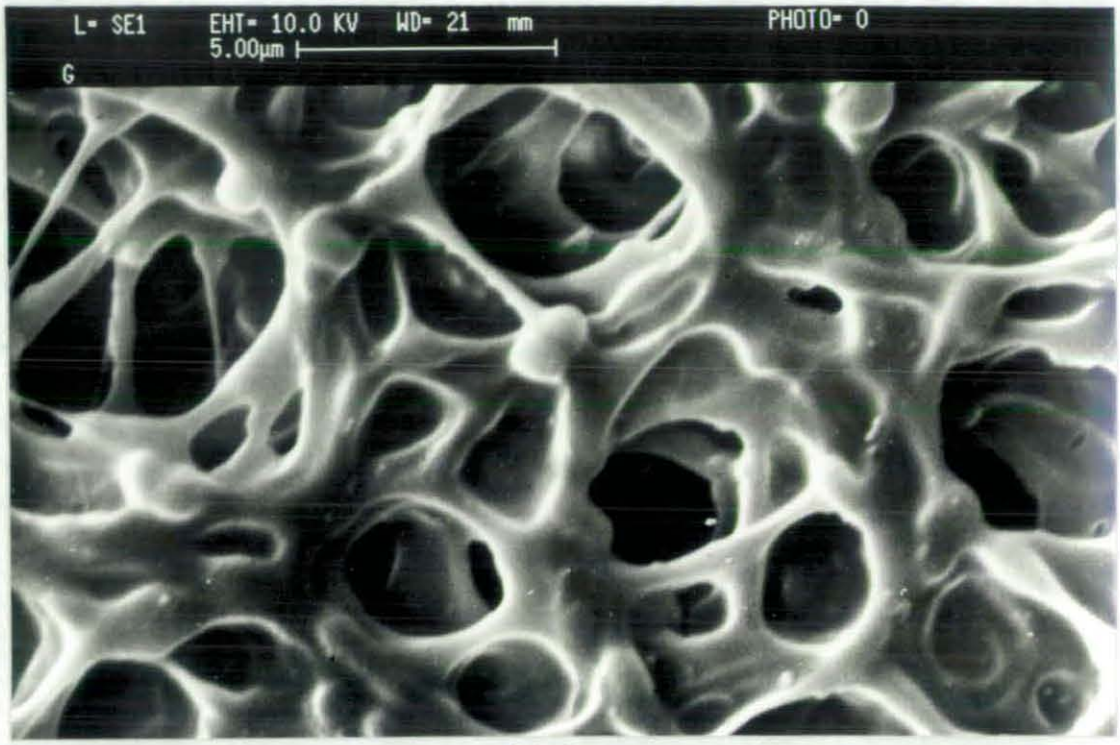

(a) clean

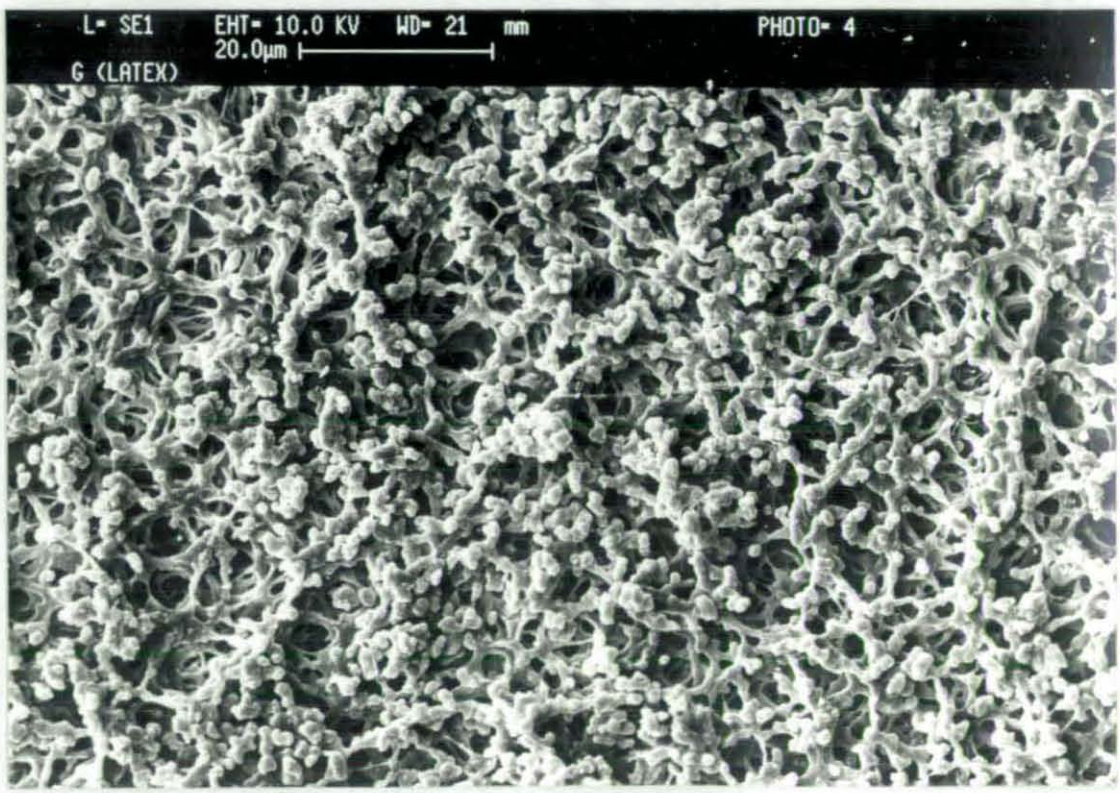

(b) after dead-end filtration

Fig 48 Photographs of 1.2 µm membranes with No 11 latex by SEM

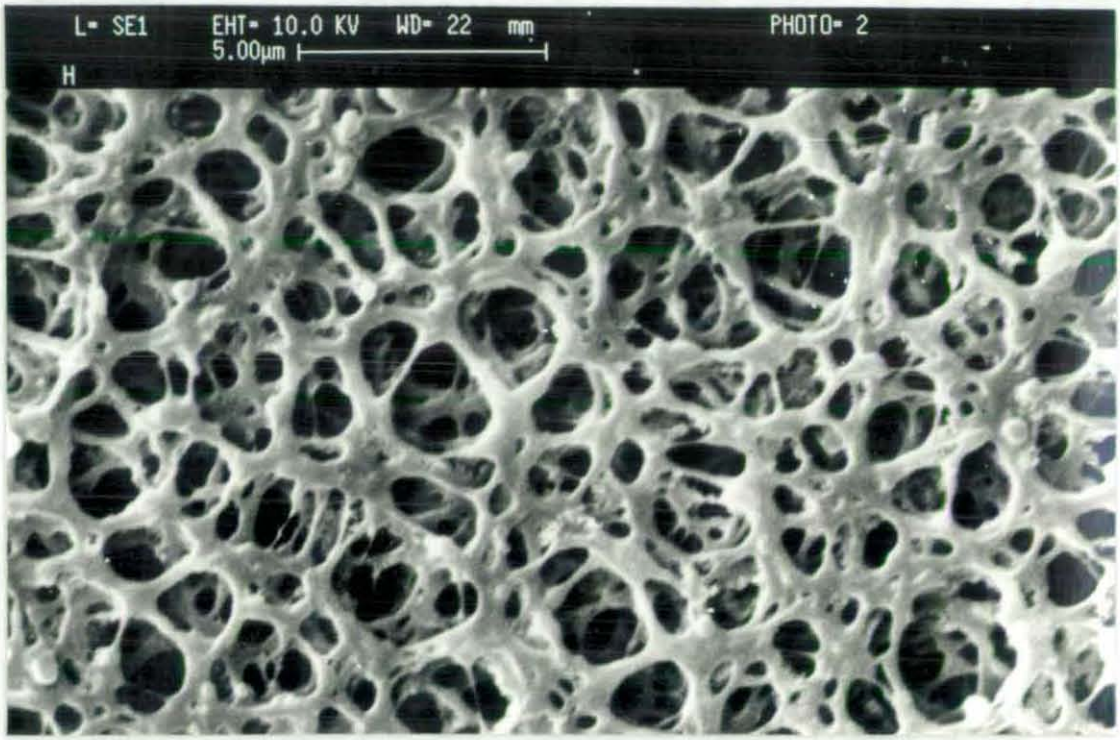

(a) clean

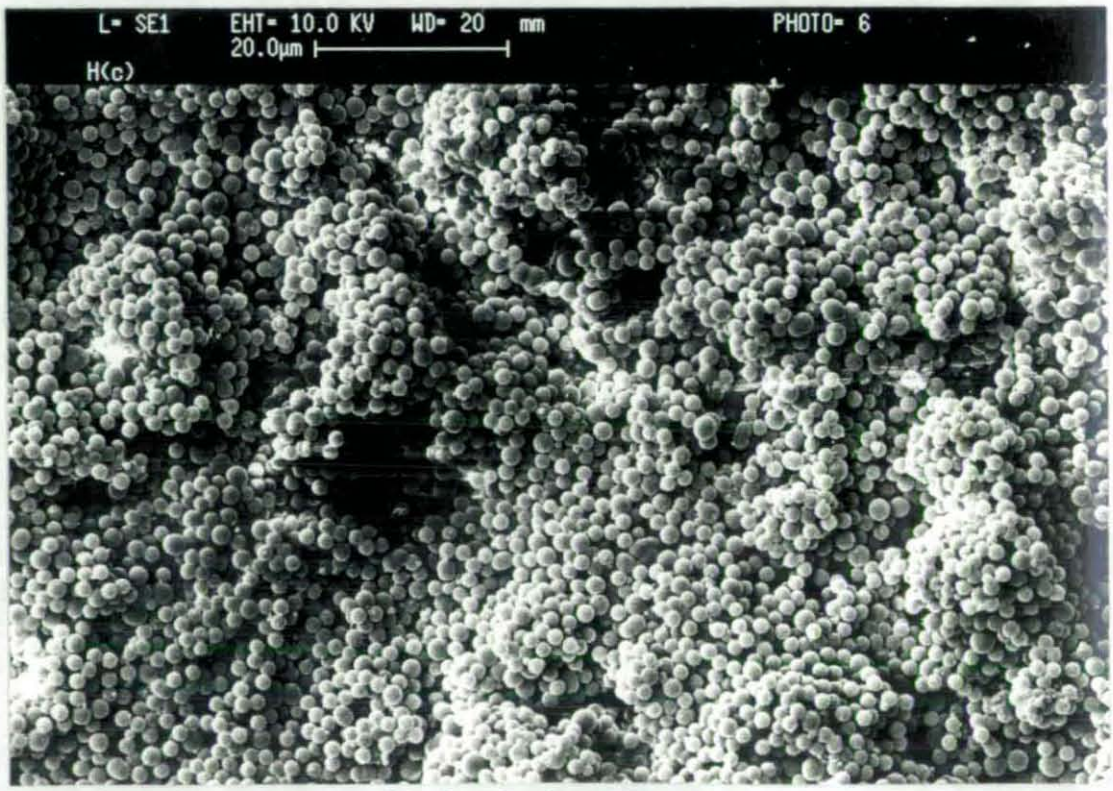

(b) after dead-end filtration

Fig 49 Photographs of 0.45 µm membranes with No 11 latex by SEM

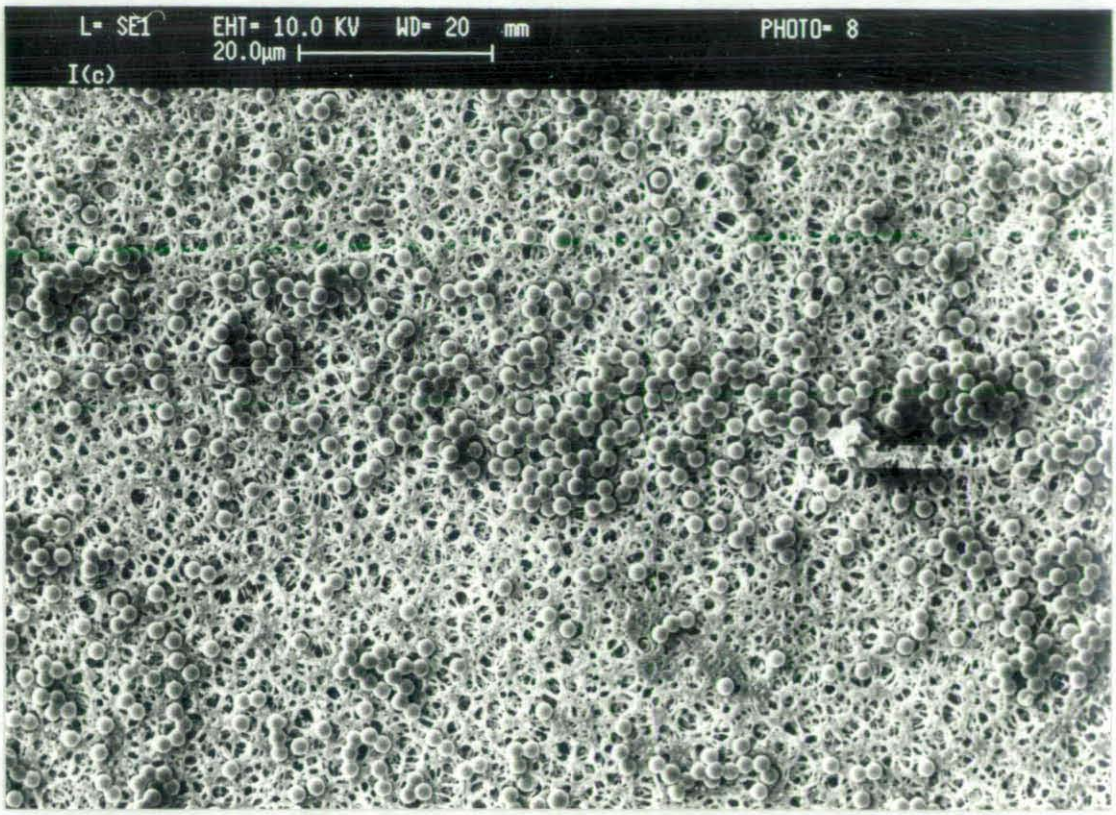

after dead-end filtration

Fig 50 Photographs of 0.45 µm membranes with No 9 latex by SEM

4.6 Mathematical modelling and predictions

4.6.1 Mathematical modelling of particle deposition during filtration

a) Film model (Eq 2.27 for R_C)

In the film model, the equilibrium flux rate (J_e) is independent to the trans-membrane pressure (P_t) but proportional to the mass transfer coefficient (k) as shown in Eq 2.27:

$$J_v = k \ln\left(\frac{C_l}{C_b}\right) \tag{2.27}$$

Fig 51 is the relationship between J_e and P_t of Tests H3, H4 and I2, I3 respectively. These tests were not run with new membranes and they ran for at least 130 minutes so that the film might be formed during the process. Fig 51 suggests a dependency of J_e on P_t when P_t is less than 0.9 Bar. Besides:

$$k \propto \frac{D}{x} \tag{4.10a}$$

and $$x \propto 1/Re \tag{4.10b}$$

therefore $$k \propto Re \tag{4.10c}$$

since $$Re \propto U \tag{4.10d}$$

in which U is the channel velocity therfore:

$$k \propto U \tag{4.10e}$$

However, it was found that flux rate did not increase with increasing channel velocity. This indicated that film model for R_C is not applicable in this study.

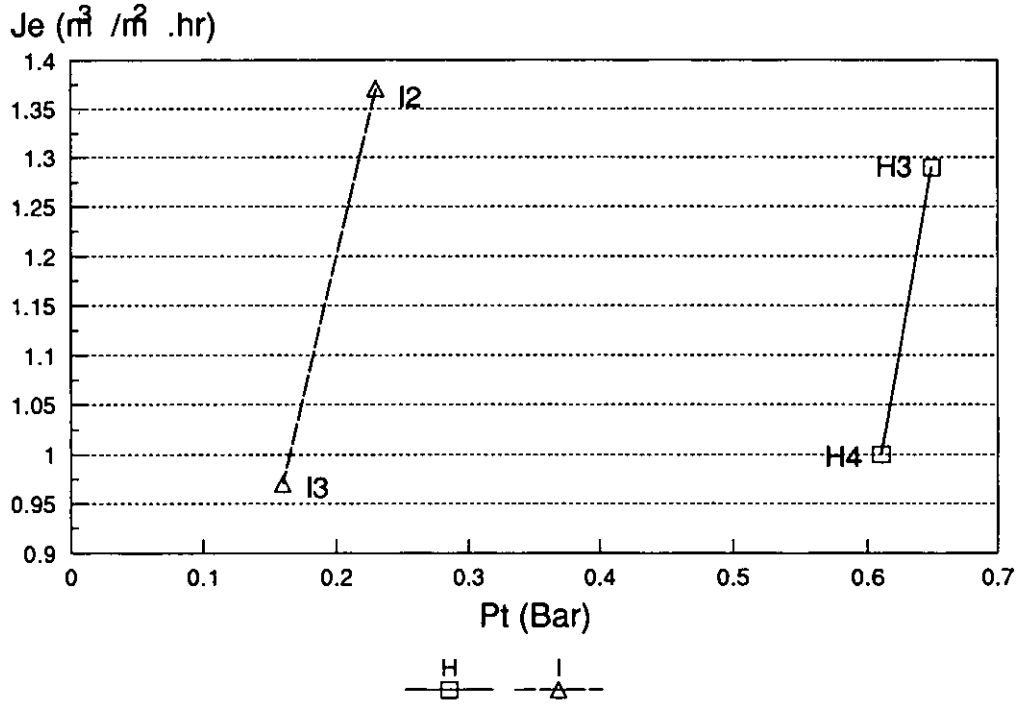

Fig 51 The relationship between permeate flux rate and transmembrane pressure

Several models for particle distribution during filtration were presented in § 2.1 corresponding to the flow resistances R_C, R_{PB} and R_{AD} respectively. Some blocking models were used to analyse the test results of membranes G, H and I. The details of the analysis are shown in diagrams in Appendix 4. Since all the four models have linear

expressions, the experimental data were linearly regressed, if the regression line meets the experimental data well, the model is assumed to be valid. Some results of test G4 by these models are presented in Fig 52 for illustration. All the diagrams with relevant models are similar and lead to the same conclusion.

b) Complete blocking model and Intermediate blocking model (Eq 2.3 for R_{PB})

The Complete blocking model is expressed as:

$$-\ln\left(\frac{J}{J_o}\right)=A \cdot t+B \tag{4.11a}$$

and the Intermediate blocking model is expressed as:

$$\frac{1}{J}=A \cdot t+B \tag{4.11b}$$

Both models indicate that the pore is wholly blocked by a single particle, but the photographs in Fig 47 show that the pore is not wholly blocked by a single particle but partially blocked by many particles inside the pores. The analysis results in Figs 52a and 52b also show that the Complete blocking model and the Intermediate blocking models do not fit the experimental data. Therefore, these two models are not applicable in this study.

c) Cake filtration model (for R_C)

The cake filtration model for normal flow is expressed as:

$$t/Q=A \cdot Q+B \tag{2.33}$$

where A and B are experimentally determined constants

It is usual to replace Q with cumulative vlome of filtrate (W):

$$t/W=A \cdot W+B \tag{2.44e}$$

It was evident in Fig 47 that there was no filter cake on the membrane surface. The elimination of the filter cake was caused by the shear force produced by crossflow since there were filter cakes in Figs 48 to 50 after dead-end filtration. Fig 52c shows that the prediction by the Cake filtration model did not meet the test results very well. However, this model fits better than either the Complete blocking model or the Intermediate blocking model.

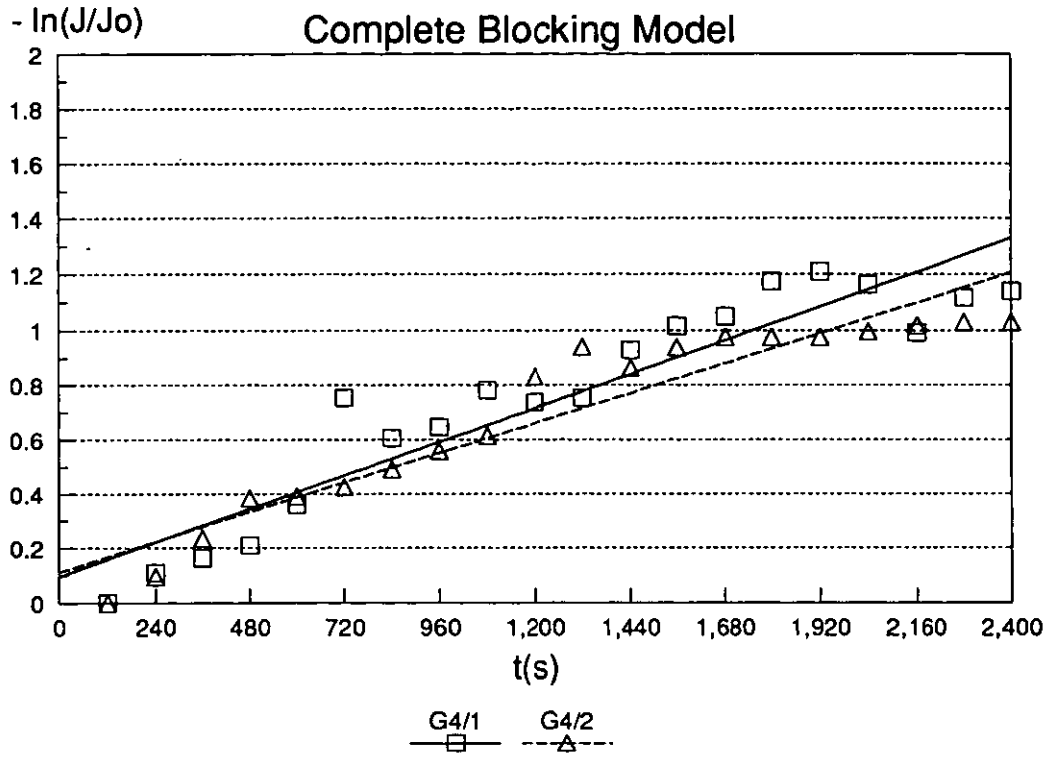
- ln(J/Jo)
Complete Blocking Model
2
1.8
1.6
1.4
1.2
1
0.8
0.6
0.4
0.2
0
0
240
480
720
960
1,200
1,440
1,680
1,920
2,160
2,400
t(s)
G4/1
G4/2

(a)

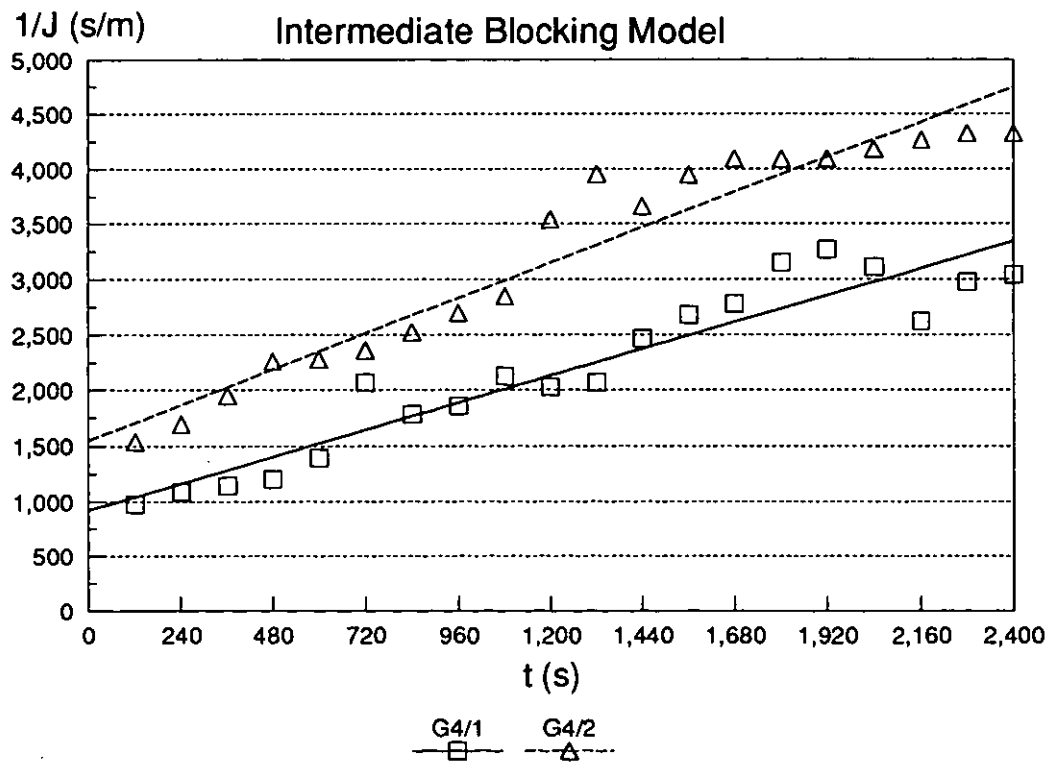
1/J (s/m)
Intermediate Blocking Model
5,000
4,500
4,000
3,500
3,000
2,500
2,000
1,500
1,000
500
0
0
240
480
720
960
1,200
1,440
1,680
1,920
2,160
2,400
t (s)
G4/1
G4/2

(b)

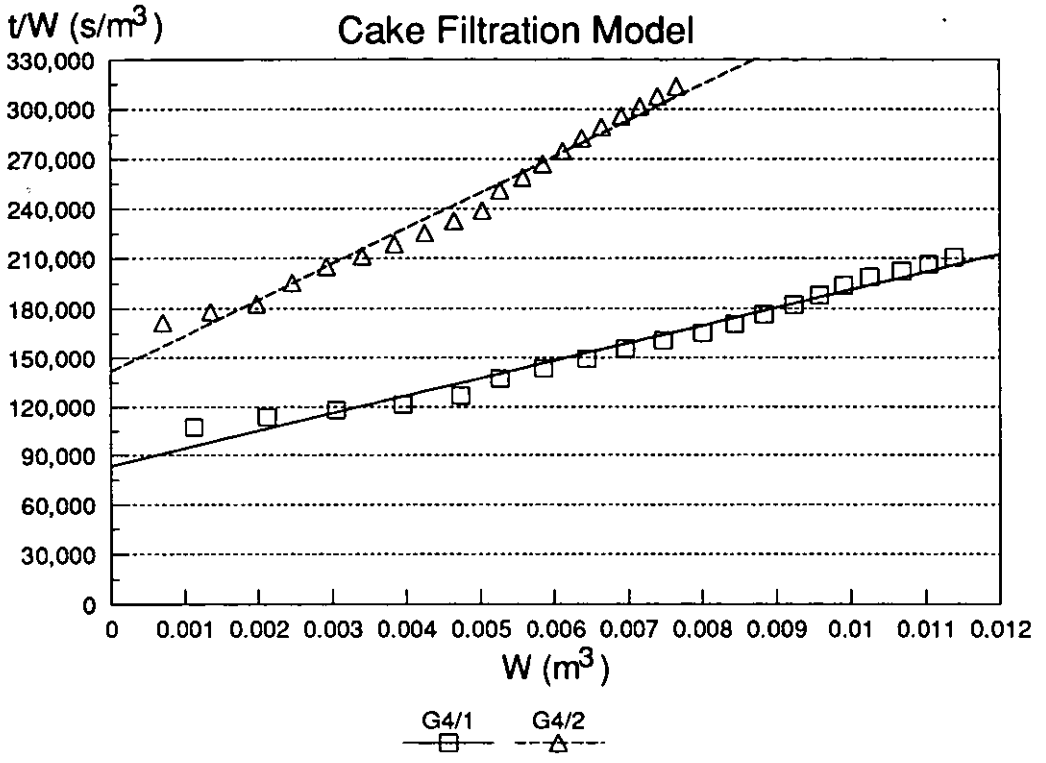

(c)

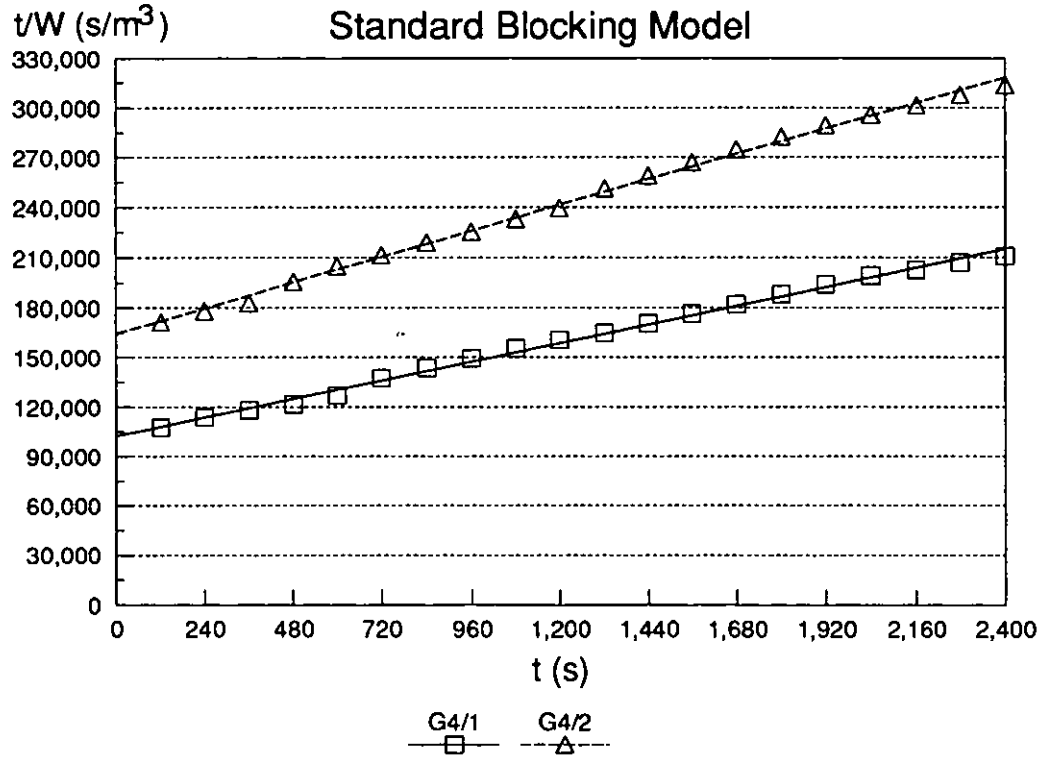

(d)

Fig 52 Mathematical analysis of Test G4

There was no direct indication in Table 14 that the increase in channel velocity brought about an increase in flux rate. This was because the increase in flow velocity only resulted in the increase of shear force on the membrane surface. Increasing the flow velocity will not help to increase the permeate flux rate if the fouling was due to internal pore blocking, as shown in Fig 47. It was also found that the flux rate recovered slightly after a pressure distribution test during which the channel velocities had been changed without filtration.

d) Standard blocking model (Eq 2.4 for R_{AD})

This model is expressed as:

$$t/W = A \cdot t + B \qquad (2.44e)$$

The results from this fit the experimental data very well as shown in Fig 52d which means pore sizes were affected by small particles adhering on to the pore walls. This is in agreement with the photographs shown in Fig 47 where the particles inside the pores can be clearly seen.

4.6.2 Estimation of membrane characteristics

It is clear that the shear force on the membrane surface, produced by the crossflow, swept away larger particles so that the whole blockage of the pore by single particles at the surface did not govern the process, the cake filtration process was also not dominant due to the shear force and low particle concentration. The membrane surface, therefore, was more exposed. The small particles migrated into the pores and were retained there by adhesive force as discussed in §1.7.3 and thus the filtration process in this study can be described by the Standard blocking model. It is feasible to use this model to estimate some membrane characteristic such as pore length, density and variation in size.

a) Pore size variation (d_m)

The Standard blocking model assumes that the pore size decreases during the process while the pore length and density remain constant, therefore, it is likely that

if δ_m and/or N_m can be directly obtained from Eq 2.44c and 2.44d by the first run of the new membrane with the rated pore size d_o as d_m:

$$\delta_m = \sqrt{\frac{C_{pore} \cdot d_m^2 \cdot P_t \cdot B}{32\mu \cdot (1-\varepsilon_s) \cdot \rho_s \cdot A}} \qquad (2.44c)$$

$$N_m = \frac{1}{\pi \cdot S \cdot d_m^3} \sqrt{\frac{512 C_{pore} \cdot \mu}{P_t \rho_s (1-\varepsilon_s) \cdot A B}} \qquad (2.44d)$$

then d_m of the following run of the same membrane can be calculated with the same δ_m and/or N_m if **A** and **B** of these runs are known.

Where μ is the dynamic viscosity of the water (0.001 Pa•s)

ε_s is assumed to be 50% for all runs

C_{pore} is the particle concentration of the fluid inside the pores (kg/m^3)

ρ_s is the density of the latex particle (kg/m^3)

A and **B** are the gradient and intercept in Standard blocking model respectively [Grace, 1956], which can be obtained by linear regression of test results as shown in Fig 52d.

It is impossible to determine δ_m and N_m directly by either of the above equations with other runs because d_m is smaller than d_o due to pore shrinkage. Therefore, it is essential to estimate the variation of d_m for obtaining δ_m and N_m. It is also impossible to obtain d_m directly from above two equations since there are three unknown variables: d_m, δ_m and N_m there. However, the membrane resistance test with pure water offers a relationship of d_m, δ_m and N_m based on Poisueille's law:

$$\frac{P_t}{\delta_m} = \frac{128\mu}{N_m \pi d_o^4 S} Q \qquad (4.12a)$$

which means:

$$Q = \frac{N_m \pi d_o^4 S}{128 \delta_m \mu} P_t = a \cdot P_t \qquad (4.12b)$$

where a is the gradient of the Q vs. P_t regression line by P1 as shown in Fig 44.

Therefore:

$$\frac{\delta_m}{N_m} = \frac{1}{a}\frac{\pi d_o^4 S}{128\mu} \tag{4.12c}$$

$$a\frac{\delta_m}{N_m} = \frac{\pi d_o^4 S}{128\mu} \tag{4.12d}$$

From Eq 2.44b:

$$\frac{\delta_m}{N_m} = B\frac{\pi d_m^4 S P_t}{128\mu} \tag{2.44b}$$

we can have:

$$B_i = \frac{\delta_m}{N_m}\frac{128\mu}{\pi d_i^4 S}P_{t_i} \tag{4.13a}$$

where d_i is the pore size at the beginning of the *i*th run.

Since δ_m and N_m are assumed constant, $\delta_m \cdot N_m$ and δ_m/N_m are also constant. Therefore, δ_m/N_m in Eq 4.13a can be substituted with that in Eq 4.12c to obtain:

$$d_i^2 = \frac{d_o^2}{\sqrt{a \cdot B_i \cdot P_{t_i}}} \tag{4.13b}$$

The results from Eq 4.13b are tabulated in the Table 17 as $\mathbf{d_m}$. The values of the rated pore sizes (d_o) for each membrane are those as listed in Table 14, i.e 1.2 and 0.45 μm respectively. Also tabulated are the experimental data such as transmembrane pressure ($\mathbf{P_t}$), the particle concentration of fluid in the pore ($\mathbf{C_{pore}}$), cumulative permeate volume (**W**) and the constants **A**, **B** obtained based on Grace's (1956) model. The estimated pore sizes of clean membranes H and I obtained from Eq 4.13b are similar to each other and smaller than the rated values while the estimated pore size of membrane G is greater than the rated value. It is also clear that all pore sizes of the three membranes all generally decreased with ongoing runs during each test, they drop quickly during the first several runs and slowly during the last several runs. There are also exceptions between some tests such as G3, G4 and H3, where the pore size is greater than or equals to that of previous run due to smaller values of $B \cdot P_t$, the reason for this will be discussed later.

Table 17

Test results and pore size estimation of membranes G, H and I

Test	A	B	P_t	C_{pore}	W	d_m	ε_m	$\delta_m \cdot N_m$	δ_m	N_m
	m^{-3}	$s \cdot m^{-3}$	Pa	$mg \cdot l^{-1}$	m^3	µm	%	m^{-1}	µm	10^{11} m^{-2}
G1	1	11484	15227	0.22	0.0679	1.36	21.1	23048616	56	4.15
G2/1	28	16206	23448	0.22	0.0188	1.12	14.3	1213455	13	0.95
G2/2	22	39977	16595	0.22	0.0187	0.98	10.9	2040619	17	1.23
G2/3	25	64375	18103	0.22	0.0167	0.85	8.19	2380043	18	1.33
G2/4	27	75352	17678	0.22	0.0142	0.82	7.66	2356086	18	1.33
G3/1	17	45775	19224	0.22	0.0235	0.91	9.43	3041432	20	1.51
G3/2	27	54329	17255	0.22	0.0178	0.90	9.13	1976517	16	1.21
G3/3	34	69423	14951	0.22	0.0162	0.87	8.68	1651577	15	1.11
G3/4	50	110464	16623	0.22	0.0119	0.76	6.53	1493778	14	1.06
G4/1	47	102195	17279	0.20	0.0162	0.77	6.65	1388355	14	1.02
G4/2	64	164127	18856	0.20	0.0119	0.67	5.03	1349768	13	1.00
H1/1	5	28442	63629	0.25	0.022	0.43	21.3	51838813	27	19.5
H1/2	10	32550	61703	0.25	0.018	0.42	20.2	27305244	19	14.2
H1/3	14	39604	63734	0.25	0.018	0.40	18.1	21864750	17	12.7
H1/4	23	51810	59566	0.25	0.015	0.38	16.3	14716197	14	10.4
H2/1	20	94590	61725	0.33	0.014	0.32	11.9	31068642	21	15.1
H2/2	21	143588	64291	0.33	0.013	0.29	9.44	37206085	22	16.5
H3	10	128200	64705	0.20	0.037	0.29	10.0	45299591	25	18.3
H4	13	160024	61294	0.12	0.030	0.28	9.16	22734781	18	12.9
H5	10	137023	90514	0.12	0.038	0.27	8.15	33234352	21	15.6
H6	19	163783	94726	0.12	0.027	0.25	7.28	19563565	16	12.0
I1	4	41712	25517	0.033	0.079	0.41	13.5	10146749	8	12.4
I2	7	91053	22681	0.029	0.053	0.35	9.63	7796236	7	10.9
I3	10	154973	14594	0.018	0.038	0.34	9.21	3544822	5	7.33

b) Pore length (δ_m) and density (N_m)

$\delta_m \cdot N_m$ of each run can be obtained by rearranging Eq 2.44a with subscript *i*:

$$(\delta_m \cdot N_m)_i = \frac{4C_{pore_i}}{\pi S \rho_s (1-\varepsilon_s) d_i^2 A_i} \frac{1}{A_i} \tag{4.14a}$$

$\delta_m \cdot N_m$ can also be obtained by combining Eq 4.14a and 4.13b:

$$(\delta_m \cdot N_m)_i = \frac{4\sqrt{a}}{\pi S \rho_s (1-\varepsilon_s) d_o^2} \left(\frac{C_{pore_i}}{A_i} \sqrt{B_i P_{t_i}} \right) \tag{4.14b}$$

δ_{m_i} and N_{m_i} can be calculated with the results from Eq 4.12c and 4.14:

$$\delta_{m_i} = \sqrt{(\delta_m \cdot N_m)_i \cdot (\delta_m / N_m)} \tag{4.15a}$$

$$N_{m_i} = \sqrt{\frac{(\delta_m \cdot N_m)_i}{(\delta_m / N_m)}} \tag{4.15b}$$

The results of the above calculations are tabulated in the last three columns of Table 17. The values of δ_m are in the micron range which are reasonable for this type of membrane.

It is clear that $\delta_m \cdot N_m$, δ_m and N_m differ from run to run. Therefore, it is necessary to average $\delta_m \cdot N_m$, δ_m and N_m for further work.

$$\overline{\delta_m \cdot N_m} = \frac{\sum_{i=1}^{n} (\delta_m \cdot N_m)_i}{n} \tag{4.16a}$$

$$\overline{\delta_m} = \frac{\sum_{i=1}^{n} \delta_{m_i}}{n} \tag{4.16b}$$

$$\overline{N_m} = \frac{\sum_{i=1}^{n} N_{m_i}}{n} \tag{4.16c}$$

The values of *a*, δ_m / N_m, $\overline{\delta_m \cdot N_m}$, $\overline{\delta_m}$, $\overline{N_m}$ and R_m of membranes G, H and I as well ρ_s of the latex used are tabulated in Table 18.

c) Fraction open to flow (ε_m)

The membrane fraction open to flow (ε_m) can be estimated as:

$$\varepsilon_{m_i} = \frac{100 \cdot \overline{N_m} \cdot \pi \cdot d_i^2}{4} (\%) \qquad (4.17)$$

The results from this calculation are tabulated in Table 17.

The values are much less than 100% which in turn confirm that N_m is reasonable.

Table 18

Membrane resistance, pore length and density of membranes G, H and I

Test	Latex	ρ_s	R_m	a=Q/P_t	δ_m/N_m	$\overline{\delta_m \cdot N_m}$	$\overline{\delta}_m$	$\overline{N}_m$
		$kg \cdot m^{-3}$	10^{11} m^{-2}	10^{-10} m/Pa•s	10^{-17} m^3	m^{-1}	μm	10^{11} m^{-2}
G	11	1450	2.8	34.2	13.4	3812750	19	1.45
H	11	1450	13.5	6.67	1.36	30483202	20	14.7
I	9	1250	7.64	13.7	0.66	7162603	7	10.6

4.6.3 Prediction of permeate cumulative volume or flux rate with process time

The validation of the Standard blocking model also makes it possible to predict the cumulative permeate volume (W) or flux rate (J_v) with process time if δ_m and N_m are known. It can be achieved by three steps:

a) Predict **A** and **B**

The gradient (**A**) and intercept (**B**) in that model (Eq 2.44e) of the first run of a new membrane can be obtained with Eq 2.44a and 2.44b with d_o as d_i:

$$t/W = A \cdot t + B \qquad (2.44e)$$

$$A_i = \frac{4}{\pi \overline{\delta_m \cdot N_m} d_i^2 S \rho_s (1-\varepsilon_s)} \frac{C_{pore_i}}{} \qquad (4.18a)$$

$$B_i = \frac{\delta_m}{N_m} \frac{128\mu}{\pi d_i^4 S P_{t_i}} \qquad (4.18b)$$

A and **B** of the following run can be predicted by using the final pore size of the current run as d_i. However, considering the effect of pressure distribution test on the

pore size in our study, d_i used in predicting **A** and **B** are those estimated values listed in Table 17.

b) Predict **W** and $\mathbf{J_v}$

The permeate volume W vs. time t can be obtained by rearranging Eq 2.44e into

$$W_i = \frac{t}{A_i \cdot t + B_i} \tag{4.19a}$$

and J_v is the gradient of W with time t:

$$J_{v_i} = \frac{1}{S}\frac{dW_i}{dt} = \frac{1}{S}\frac{B_i}{(A_i t + B_i)^2} \tag{4.19b}$$

c) Predict the initial pore size of next run $\mathbf{d_{i+1}}$

The initial pore size of the following runs can be calculated based on a mass balance equation by assuming that particles in the permeate all deposit uniformly on to the pore walls. This assumption is supported by the negligible latex concentration in the permeate as shown in Table 15 and a non-existent filter cake on the membrane surface as shown in Fig 47. Thus the relationship between the mass of the deposit layer and that of cumulative permeate can be expressed as following:

$$\frac{\pi}{4}(d_i^2 - d_{i+1}^2) \cdot \overline{\delta_m \cdot N_m} \cdot S \cdot \rho_s \cdot (1-\varepsilon_s) = W_i \cdot C_{pore_i} \tag{4.20a}$$

therefore,

$$d_{i+1} = \sqrt{d_i^2 - \frac{4 W_i \cdot C_{pore_i}}{\pi \cdot \overline{\delta_m \cdot N_m} \cdot S \cdot \rho_s \cdot (1-\varepsilon_s)}} \tag{4.20b}$$

where d_i is the initial pore size of the ith run which is calculated from the d_{i-1} of the i-1th run listed in Table 17.

C_{pore_i} is the concentration of latex suspension (by oven drying method) in the pore. It should be equal or close to the bulk concentration (C_{b_i}) if the pore size is several times greater than the particle size according to assumption (b) in Grace's model (1956).

ε_s is also assumed to be constant (50%).

The constants in Eq 4.20b can be replaced by that in Eq 4.14a to obtain:

$$d_{i+1} = d_i \sqrt{1 - W_i A_i} \qquad (4.20c)$$

where A_i is the predicted values.

The results of the predicted $\mathbf{d_m}$, ε_m, **A**, **B**, **W** and $\mathbf{J_v}$ are tabulated in Table 19 together with measured $\mathbf{J_v}$ for comparison, and predicted graphically in Fig 53.

Table 19

Prediction of flux rate with process time ($m^3 \cdot m^{-2} \cdot hr^{-1}$)

Test	Predictions								Measured	
	d_m	ε_m	A	B	t	W	J_v ($m^3 \cdot m^{-2} \cdot hr^{-1}$)			
	μm	%	m^{-3}	$s \cdot m^{-3}$	min	m^3	Start	End	Start	End
G1	1.36	21.0	6	11645	15	0.052	34.3	15.9	36.6	31.7
G2/1	1.05	12.5	10	21458	10	0.021	18.6	11.3	20.3	6.73
G2/2	1.03	11.9	11	33042	10	0.015	12.1	8.49	9.47	4.73
G2/3	0.86	8.47	15	60263	10	0.008	6.64	5.02	6.00	2.40
G2/4	0.73	6.06	21	120586	10	0.004	3.32	2.72	4.87	1.80
G3/1	0.72	5.85	22	119000	10	0.004	3.36	2.73	8.47	3.33
G3/2	0.75	6.42	20	109864	10	0.004	3.64	2.96	6.93	2.53
G3/3	0.78	6.86	19	111214	10	0.004	3.60	2.97	5.40	1.53
G3/4	0.76	6.61	19	107703	10	0.005	3.71	3.03	3.73	0.93
G4/1	0.66	5.00	23	180696	10	0.003	2.21	1.91	3.73	1.20
G4/2	0.65	4.81	24	179277	10	0.003	2.23	1.92	2.33	0.87
H1/1	0.43	21.4	8	28303	12	0.021	14.1	9.56	13.9	11.3
H1/2	0.39	17.3	10	44381	12	0.014	9.01	6.59	11.9	8.8
H1/3	0.38	17.0	11	44792	16	0.017	8.93	5.91	9.73	6.13
H1/4	0.36	14.8	12	63137	20	0.015	6.34	4.17	7.33	3.53
H2/1	0.34	13.6	18	71977	32	0.018	5.56	2.56	4.4	2.27
H2/2	0.27	8.49	29	177829	48	0.011	2.25	1.05	2.8	1.4
H3	0.23	6.30	24	320886	130	0.015	1.25	0.50	2.67	1.29
H4	0.20	4.48	20	667839	130	0.009	0.60	0.40	2.48	1
H5	0.24	6.50	14	215493	130	0.024	1.86	0.83	2.81	1.43
H6	0.20	4.77	19	381666	130	0.015	1.05	0.55	2.91	0.95
I1	0.41	13.5	6	41438	80	0.067	9.65	3.27	9.04	4.93
I2	0.32	8.14	9	127482	130	0.039	3.14	1.30	4.13	1.37
I3	0.27	5.74	8	398132	160	0.020	1.00	0.71	2.83	0.97

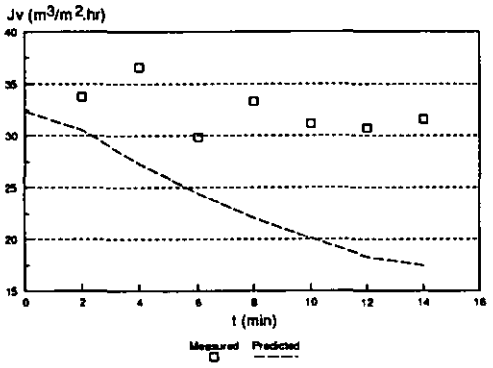

Test G1

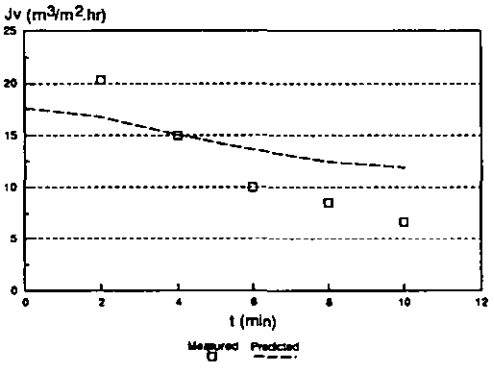

Test G2/1

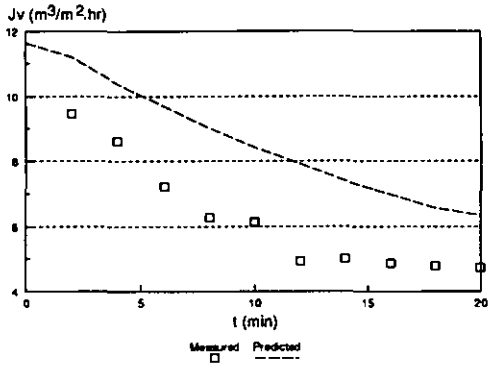

Test G2/2

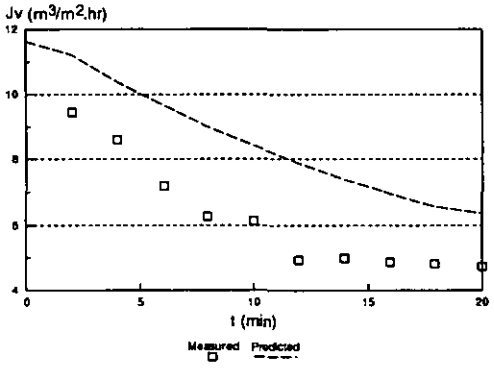

Test G2/3

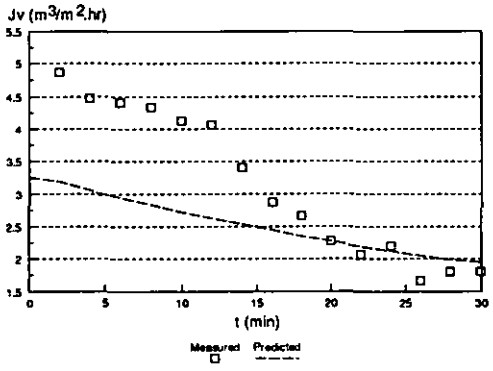

Test G2/4

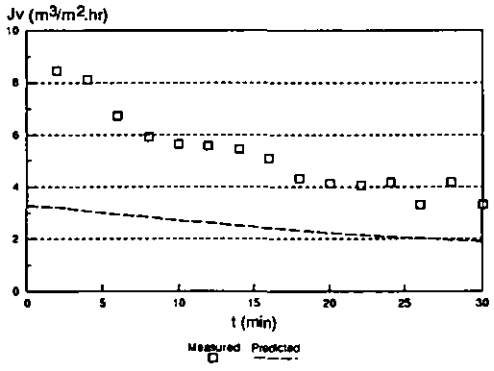

Test G3/1

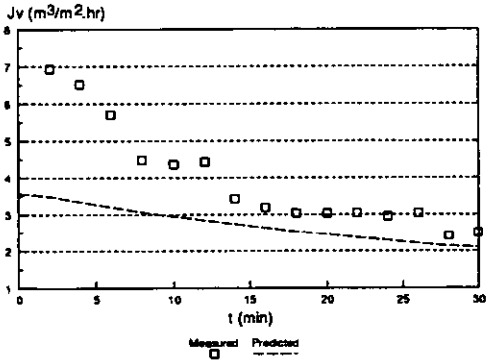

Test G3/2

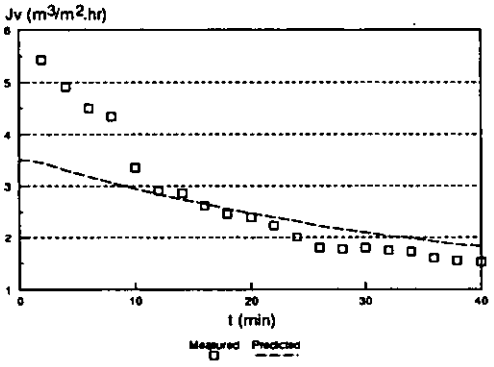

Test G3/3

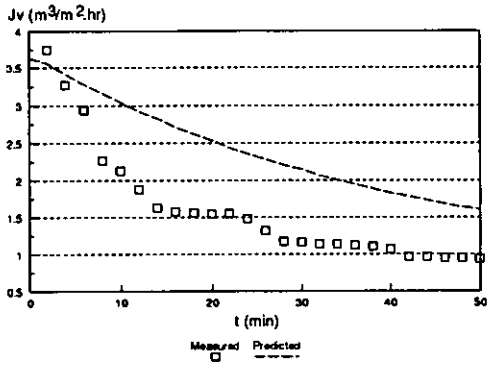

Test G3/4

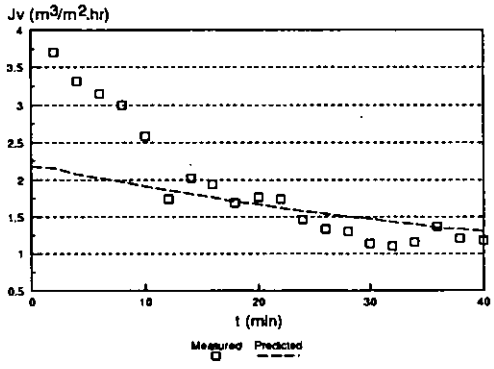

Test G4/1

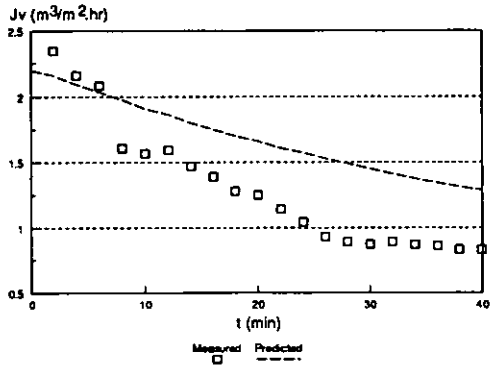

Test G4/2

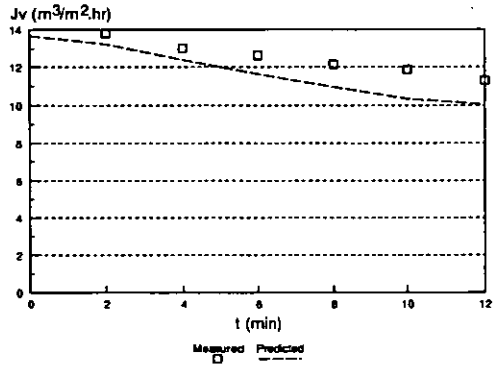

Test H1/1

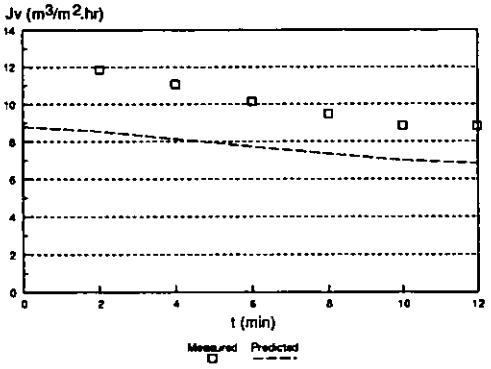

Test H1/2

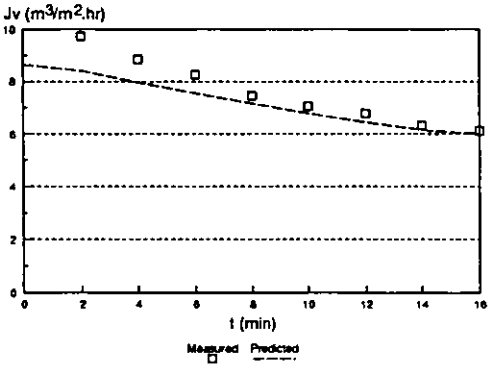

Test H1/3

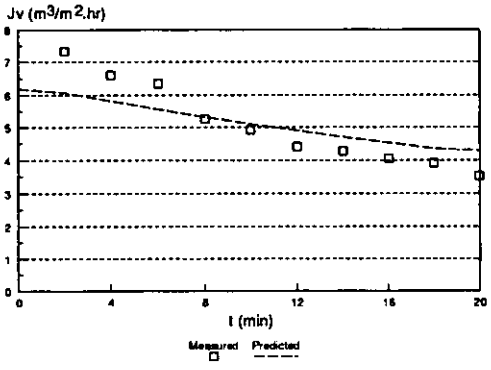

Test H1/4

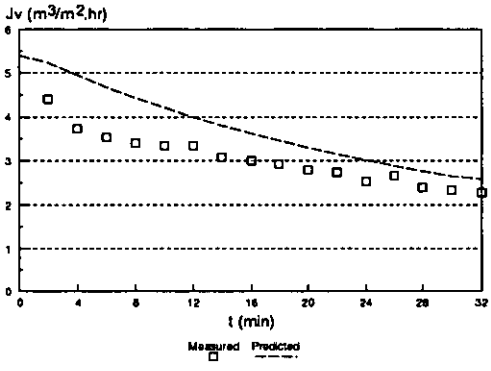

Test H2/1

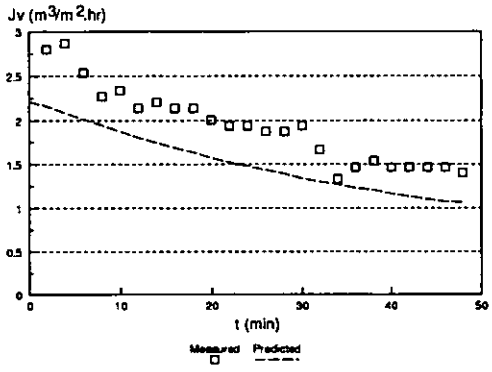

Test H2/2

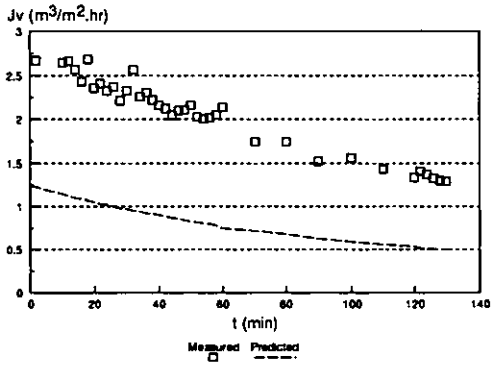

Test H3

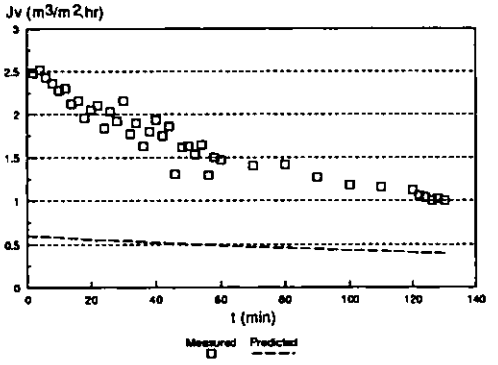

Test H4

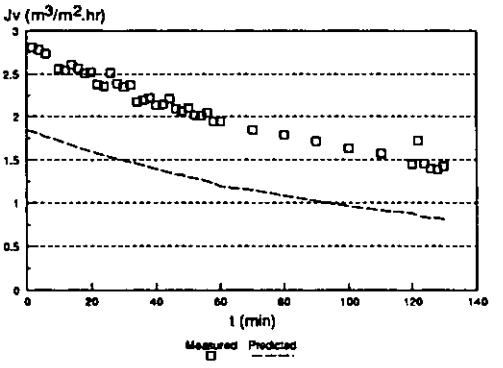

Test H5

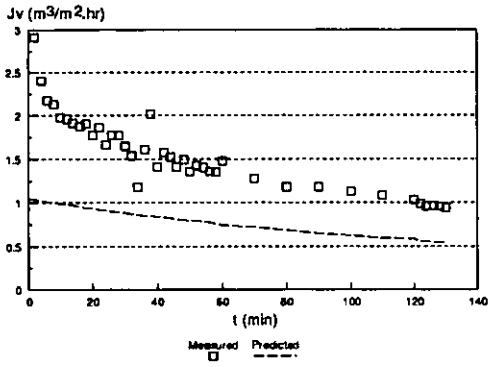

Test H6

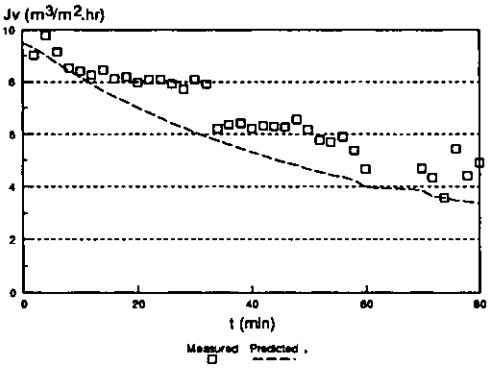

Test I1

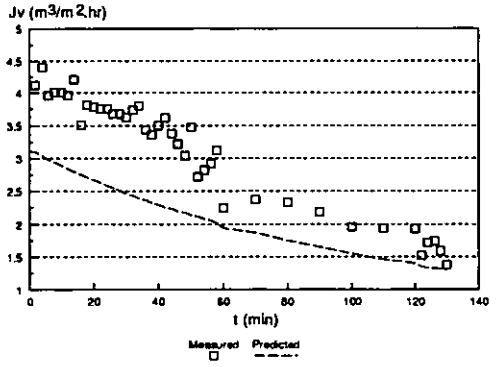

Test I2

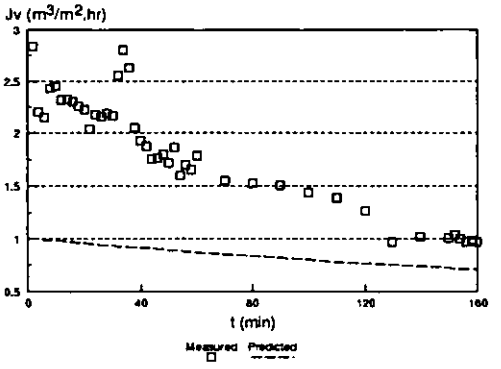

Test I3

Fig 53 Comparisons of measured and predicted permeate flux rate

4.6.4 Discussions on the predictions

a) **A** and **B**

There are differences in the measured and predicted **A**, one cause is the predicted **A** is calculated with averaged $\delta_m \cdot N_m$, the other reason is the C_{pore} used. The C_{pore} used in Eq 4.18a is an independent parameter and assumed to be equal to C_b. However, according to the particle size distribution of latices as shown in Fig 37, some particles are larger than the pores, therefore, C_{pore} should be lower than C_b and the ratio of C_{pore}/C_b should become smaller with the decrease in pore size. If this can be achieved, A_i by Eq 4.18a will be closer to the measured ones. However, this approach was not applicable in this study because $\delta_m \cdot N_m$ used in Eq 4.20b was obtained from Eq 4.14a which means $\delta_m \cdot N_m$ is proportional to C_{pore}, hence, $C_{pore}/(\delta_m N_m)$ in Eq 4.20b is independent of C_{pore} and the change in C_{pore} will not affect A_i at all. Because of high values of A_i, the obtained $\mathbf{d}_i$ from Eq 4.20c was smaller which in turn provided a greater value of **A** of the next run.

Since the **B** in Eq 4.18b is a function of the predicted d_i, the changes in d_i will of course provide differences in **B**.

b) d_i

d_i in Table 19 generally decreases with the runs and they decrease more quickly than those estimated ones in Table 17 which also fluctuate between some tests. The reasons for these are due to:

1) the effect of the pressure distribution test

During the pressure distribution test between each run, some deposit at the pore walls on the downstream side may have been flushed away which would result in the increase of pore size of the following run. This change can be described by Eq 4.13b since it estimates the d_i (Table 17) after the pressure distribution test while Eq 4.20c predicts the d_i (Table 19) before such test and therefore can not take the effect of such test on the pore size into consideration.

2) the values of **A** and **B**

The values of **A** and **B** in estimating d_i in Table 17 were from the experimental data and therefore they are independent to $\mathbf{d}_i$ and operating conditions while those used

to predict d_i in Table 19 were based on the estimated d_{i-1} and operating conditions which brought about a cumulative error and caused smaller values and quicker decrease in d_i in Table 19.

c) **W** and $\mathbf{J_v}$

Table 19 shows that the predictions give fairly close values to the measured ones in **W** or $\mathbf{J_v}$. This indicates that the models are applicable to the predictions of special note is the prediction of the maximum values of **W** and $\mathbf{J_v}$.

Eq 4.19a suggests that the minimum W is zero when t is zero and the maximum W is $1/A$ when t tends to infinity, which means the value of the gradient A in the Standard blocking model will decide the value of W.

Eq 4.19b suggests that the maximum $\mathbf{J_v}$ is $1/(SB)$ when t is zero and the minimum $\mathbf{J_v}$ is zero when t tends to infinity, which means the value of the intercept B in the Standard blocking model will decide the value of $\mathbf{J_v}$.

The so called "steady-state" of $\mathbf{J_v}$ has not been taken into consideration in the prediction. The flux rate is a function of the process time in Eq 4.20b, it decreases with the time, the greater in t, the lower in J_v. This explains why the predicted W has a maximum value $1/A$. But in practice, the flux rate will become steady after a certain time.

It is clear from Fig 53 that the predicted flux rate decreases more slowly than the measured one, this indicates that in addition to the pore shrinkage which is the major cause of flux rate decay, there may be other mechanisms which also increase the flow resistances during the filtration. Therefore, crossflow filtration is a very complicated process and it is difficult to explain the whole process by a single mechanism.

The model can give better prediction if:

1) δ_m, N_m and d_o can be experimentally obtained so that **A** and **B** in Eq 4.18 can be directly determined, and C_{pore} be determined according to d_o. Since δ_m, N_m and C_{pore} are independent to each other, the obtained **A** and **B** from Eq 4.18 will be smaller and d_{i+1} from Eq 4.20 will decrease slower than before.

2) The "steady-state" filtration can be taken into consideration so that the flux rate will not tend to zero when the process time tends to infinity.

4.7 Brief summary

A relatively comprehensive knowledge about the development of particulate membrane fouling has been obtained from this study.

It appears that the membrane fouling during crossflow filtration usually starts inside the membrane if the particles are smaller than the pore size. It is characterised with the shrinkage of membrane pores caused by the particles which are usually supposed to pass through the membrane freely. There are various mechanisms to capture the particles inside the membrane. The matrix structure of the membrane certainly assists such mechanisms to trap the particles, but it has also been found that cylindrical pores are also easily fouled by small particles due to physico-chemical forces [Wilkinson et al, 1981].

The reason why the backflushing was effective in simulated seawater filtration but not effective in fresh seawater filtration, was the tap water used for the former had been filtered by cartridge filter, most of the particles greater than 0.1 μm had been cleared so that the internal pore blocking was not dominant The fresh seawater had not been treated before entering the filter, there were plenty of particles of submicron size which were brought into the pores and retained there to foul the membrane with the aid of lipid. The backflushing can push the deposits off the membrane surface effectively but weakly affect the deposits in the pores due the laminar flow there.

In this study, the deposit layer starts to build up on the membrane surface when the membrane has been partially fouled. However, this layer is in a dynamically unstable condition - it can be wholly or partially removed by simply changing the flow conditions. The absence of a fouling layer on the membrane surface during latex filtration was also due to the lack of a substance which can adhere the solids to the membrane as the lipid did in fresh seawater filtration. The interaction between the latex and membrane was not strong enough to withstand a strong shear force.

It seems that crossflow can effectively reduce the formation of deposit layer on the membrane surface so that if the particles are large enough, membrane fouling can be reduced.

The particle size distribution has been determined by several different sizers. The membrane pore size distribution has only been observed by SEM due to the lack of alternative instruments.

The experimental results showed that the particle deposition process in this study was a type of Standard blocking model. The pore size variation due to deposition was estimated based on that model assisted by the data from a clean membrane resistance test with pure water.

The mathematical model based on the Standard blocking model for predicting the filtration process in terms of permeate cumulative volume or flux rate with process time gave acceptable results. The model can provide better predictions if the membrane characteristics can be experimentally determined and the dependence on time can be further modified. These improvements will be carried out in a future study.

Most practical crossflow filtration operations deal with multi-size particles in fluids, therefore, the existence of particles which are close to or smaller than the membrane pore sizes will inevitably cause internal pore clogging if proper prevention methods have not been taken. Since the membrane itself cannot stop such invasion, and crossflow can only reduce the deposit layer on the surface, it is important to prevent the small particles from, or at least retard their speed of, approaching the membrane surface so as to reduce the amount of particles entering the pores. This can be achieved by means of chemical, physical and mechanical methods as described in § 1.7.3. One of such techniques will be presented in the next chapter.

CHAPTER 5

Crossflow Microfiltration Incorporating Rotating Fluid Flow (Anti-Fouling Technique)

Many cleaning techniques have been briefly described in § 1.7, the last one of these techniques increases the shear stress at the surface of the membrane rather than increasing the velocity of the suspension over the surface of the membrane. However, rotating the membrane surface has certain disadvantages such as the maintenance of an effective fluid seal under pressure in systems containing suspended solids. Also, a low membrane surface area per unit volume of space is usually found.

In addition to increase shear force, the centrifugal field acting on the material suspended in the resulting rotating flow may be a significant body force and increase the permeate flux. High shear and a centrifugal field force can be effected by the use of tangential inlet and exit ports in a filter holder. Tangential inlet conditions are used already in hydrocyclones, which separate solid mixtures in a similar way to centrifuges but without the need for moving parts.

5.1 Test rig and experimental procedures

5.1.1 Test rig

The experiments were carried out on Rig 2 whose layout is shown in Fig 54. The feed tank contained 0.02 m^3 of tap water as suspending medium. The cleaning procedures of the rig and the tap water with the 0.1 μm Millipore cartridge filter were the same as those descirbed in the previous chapters. When the total number of counts of particles above 0.8 μm was less than 200 per ml prior to adding the powdered solids according to the Hiac/Royco sizing equipment, the water was assumed to be clean.

A conventional metal membrane, Pall PSS 5, was used for this study. Its nominal pore size cut-off was 5 μm. It was 0.27 m in length and 0.012 m in diameter. The holder was unconventional in its use of both entry and outlet ports at right angles to the membrane surface as shown in Fig 55. This arrangement produced high turbulence and high pressure drop when compared to the more conventional inlet and outlet in parallel with the membrane surface.

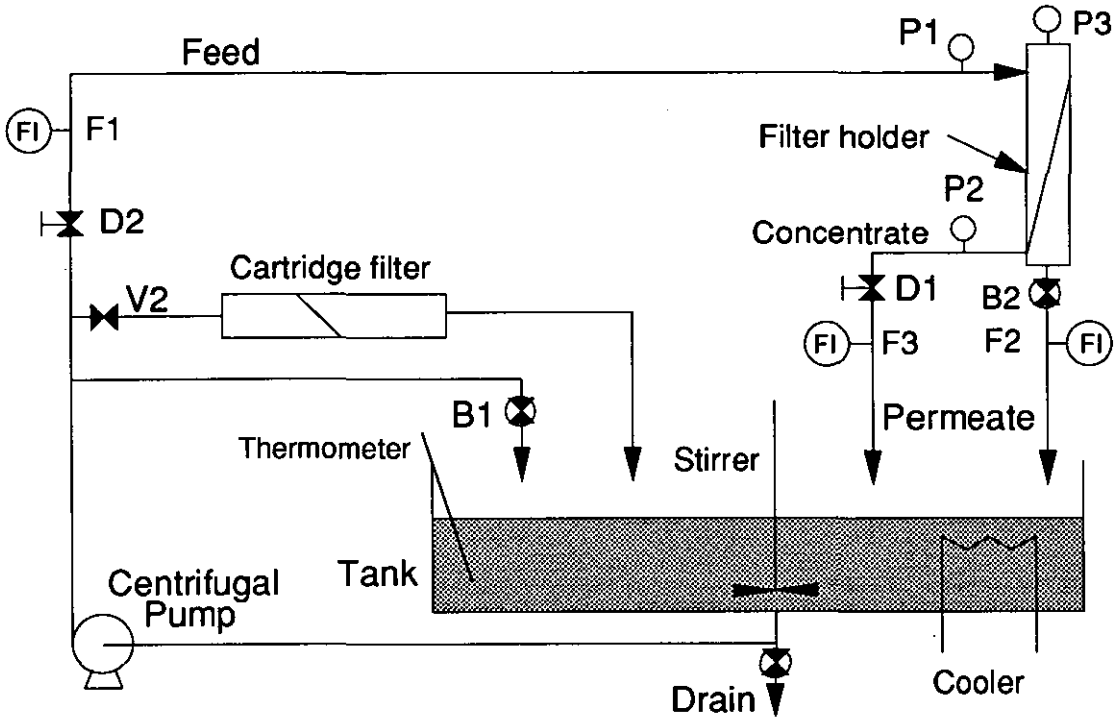

Fig 54 The layout of test rig

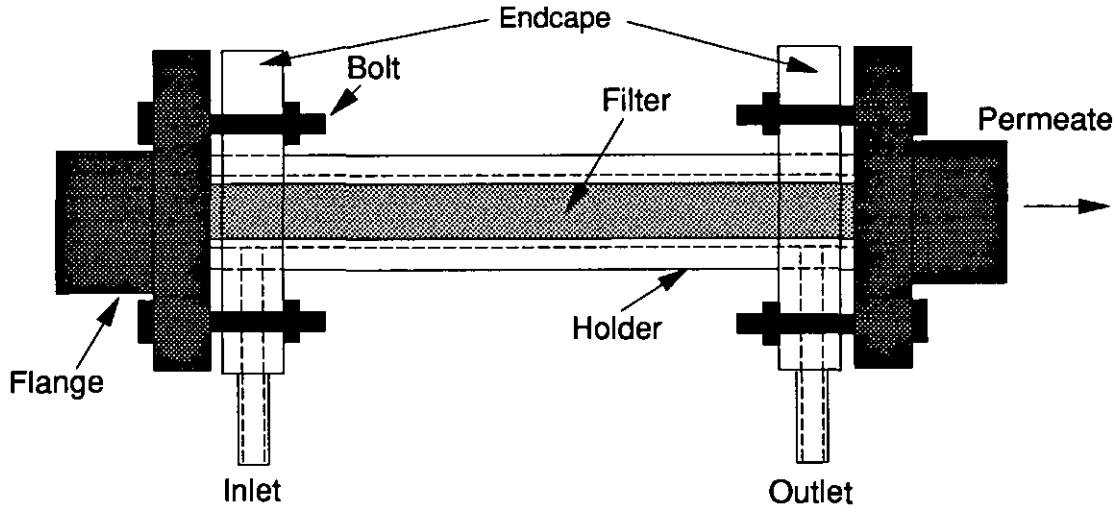

Fig 55 The configuration of filter module

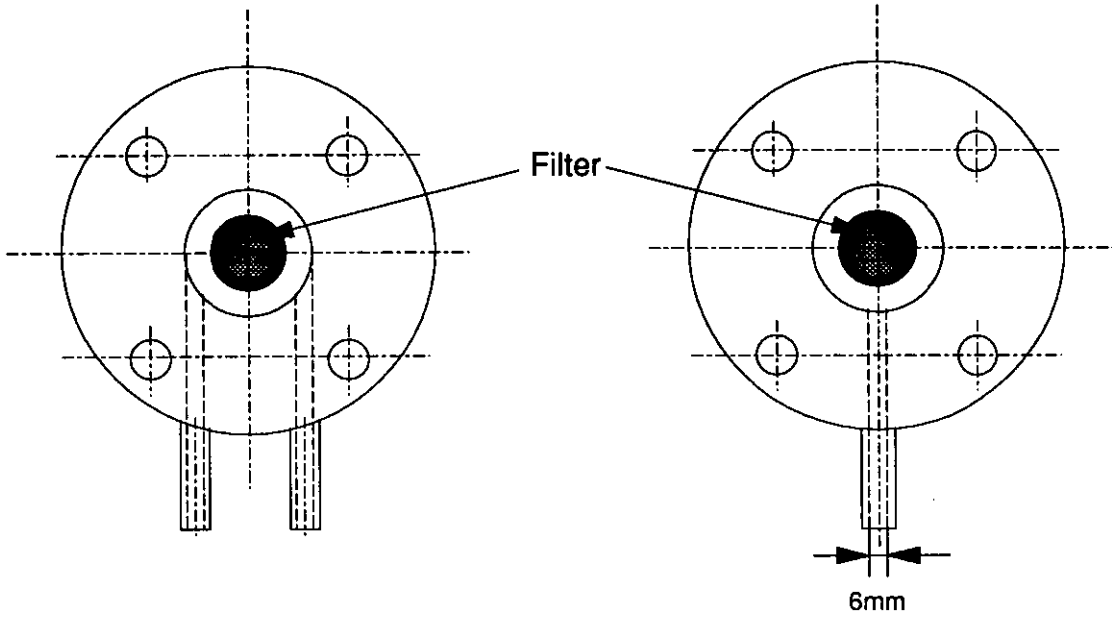

a) Tangential endcaps b) Normal endcap

Fig 56 Endcaps of tangential and normal modules

The filtration was effected on the outer surface of the membrane, in an annular gap of 0.004 m. The use of the outer membrane surface facilitated the centrifugal flow field, by means of tangential inlet and outlet endcaps as shown in Fig 56a which is the end view of Fig 55. Filtration of suspensions containing suspended solids denser than the suspending medium would, therefore, be assisted by the centrifugal flow field.

Fig 56b shows the alternative type of endcap employed, which had the inlet at right angles to the filter tube and is termed "normal" entry.

An additional set of experiments was conducted using a helix formed out of o-ring material wound around the outer surface of the membrane, using a pitch of 0.022m as shown in Fig 57. In this instance the rotating flow, and centrifugal field, was formed by forcing the fluid to rotate around the filter along the spiral flow path. A helix might be preferred to tangential entry because of its relative ease of construction. The endcap employed for helix filtration was the same as that shown in Fig 56b.

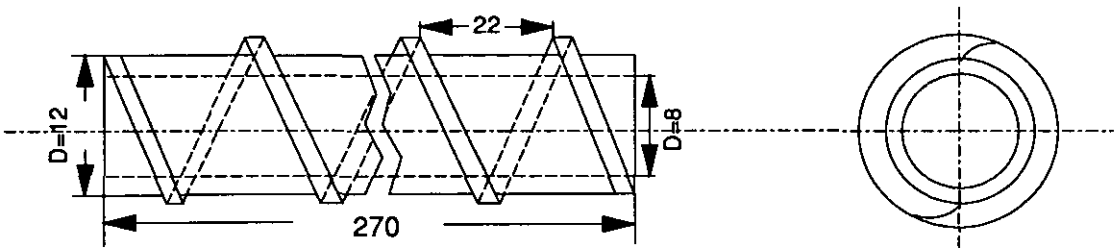

Fig 57 The side view of the filter with helically wound o-ring

5.1.2 Experimental procedures

1) Operating conditions

Membrane resistance was tested only once for a new concentration.

The experiments were run in batch mode. The permeate was sent back to the tank after its flow rate had been measured.

Feed flow rate and pressure into and out of the module were monitored during filtration.

It is usual to estimate the pressure drop across the membrane during filtration by averaging the inlet and outlet pressure as described by Eq 4.4:

$$P_t = \frac{P1 + P2}{2} - P_p \tag{4.4}$$

However, this was not an acceptable practice during filtration using endcaps shown in Fig 56 because of the greater pressure drop associated with normal and tangential entry to the filter holder. Hence a series of tests were conducted to measure the pressure inside the holder at various flow rates. The procedures were the same as those in the pressure distribution tests in Chapter 4. Fig 58 shows the measured inlet pressure with flow rate for the normal and tangential endcaps on the filter holder, plus that for the normal endcap with the wound helix. The pressure causing the fluid to spin can be calculated from Fig 58 by deducting the normal and tangential inlet pressure, at the same flow rate. The difference between the normal and tangential inlet pressure was due to both setting up the spinning flow field in the filter, plus an additional pressure drop due to the presence of the spirally wound o-ring, which increases fluid drag and hence the pressure drop.

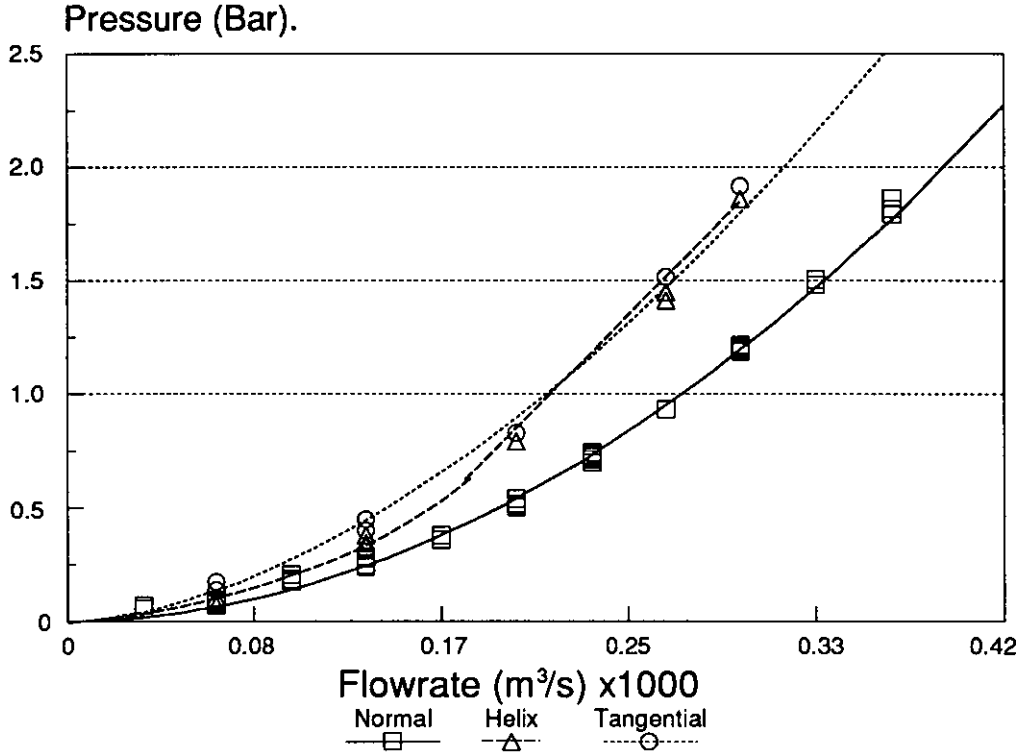

Fig 58 Inlet pressure (P1) as a function of feed flow rate for different endcap types

The pressure inside the filter holder, equivalent to the permeate side under no permeate flow conditions, also depended on the type of inlet holder used, this can be seen in Fig 59. A higher pressure was present in the case of the tangential filter endcap, but the helical insert did not significantly alter the permeate pressure from that given by the normal endcap. The outlet pressure from the filter holders remained independent of filter endcap type, as would be expected, this is also shown on Fig 59.

The pressure drop across the membrane during filtration, i.e. the pressure difference between the feed and permeate sides of the membrane, was calculated from the feed flow rate and the measured pressure. The pressure on the permeate side during filtration was always atmospheric when the permeate valve was fully opened. The pressure on the feed side of the membrane was assumed to be that shown in Fig 59 for a given feed flow rate. The pressure drop across the membrane could be higher than that shown in Fig 59 if the outlet valve is restricted. Under these circumstances both the inlet and outlet pressures were also raised, and by an equivalent amount, over that

shown in Figs 58 and 59. Thus the amount by which these two pressures were raised was added to the filtration (permeate) pressure taken from Fig 59, to give a new value of pressure drop across the membrane.

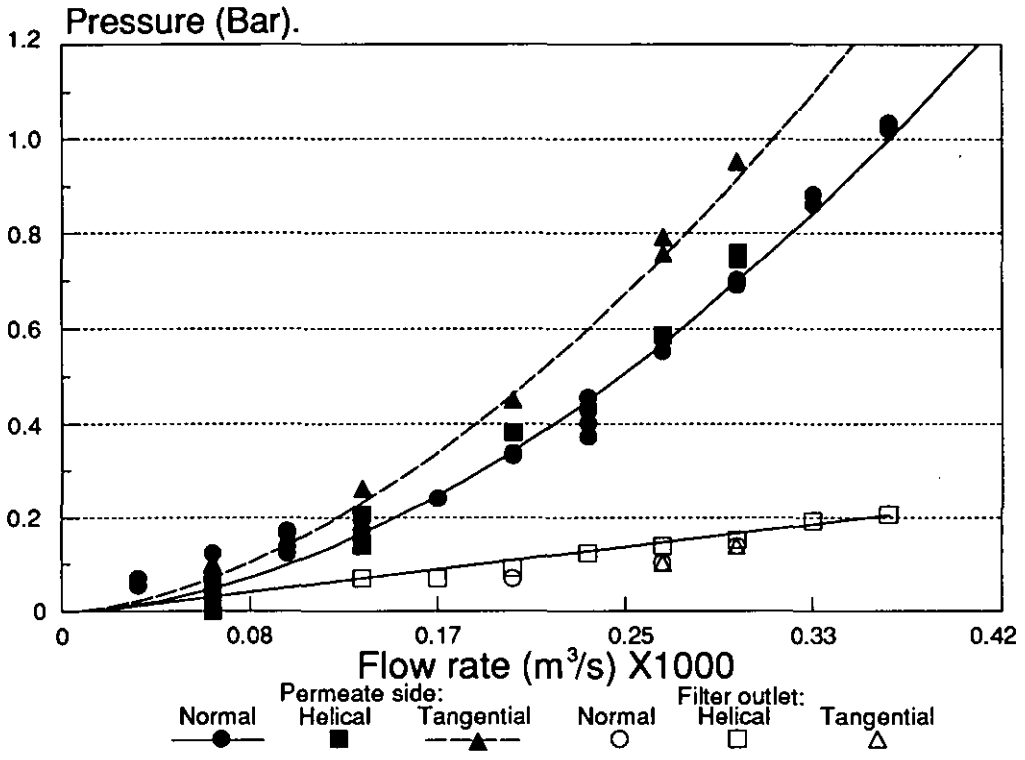

Fig 59 Pressure inside the membrane module (P3) and downstream of the filter (P2) for different endcap types

The centrifugal pump used in this study generated heat, and the original cooling coil was not sufficiently powerful to maintain the temperature which rose from 20 to 32 °C during a 90 minute period experiment. For a limited period in time and an additional cooling unit was employed, a stable temperature of 24 to 26 °C was maintained under these conditions. This experimental run was repeated under conditions of rising temperature, the results are given in Fig 60.

Between the filtrations, the membrane was removed, washed with distilled water and backflushed with compressed air at 2 Bar.

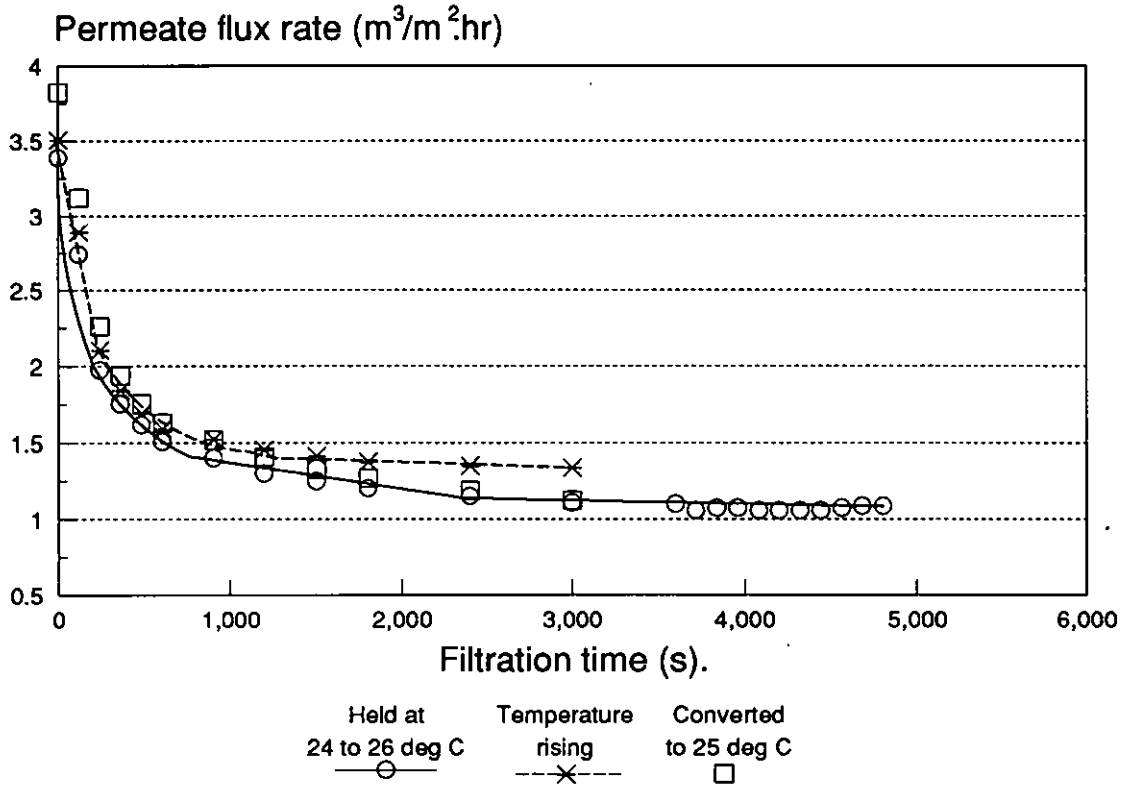

Fig 60 Permeate flux rate decay with time and the effect of variable temperature

2) Particle size distributions and concentrations

Coarse and fine calcium carbonate powders were used, the particle size distribution of the both are given in Fig 61. The concentrations of the coarse powder were 1.5 and 4% by weight, while the concentrations of the fine powder were 1.6 and 3% by weight respectively. Similar operating conditions for filtration were used for each size and concentration.

Samples were taken from the tank every 20 minutes during the run for monitoring the variations in particle size distribution and concentration by weight.

The deposits at the bottom of the filter were also sampled after each test. The particle size distribution was analysed by Malvern Laser Diffractometer, and the concentration was measured by the oven drying method.

The quality of the permeate was monitored by a Turbidity meter at 20 minutes intervals during filtration.

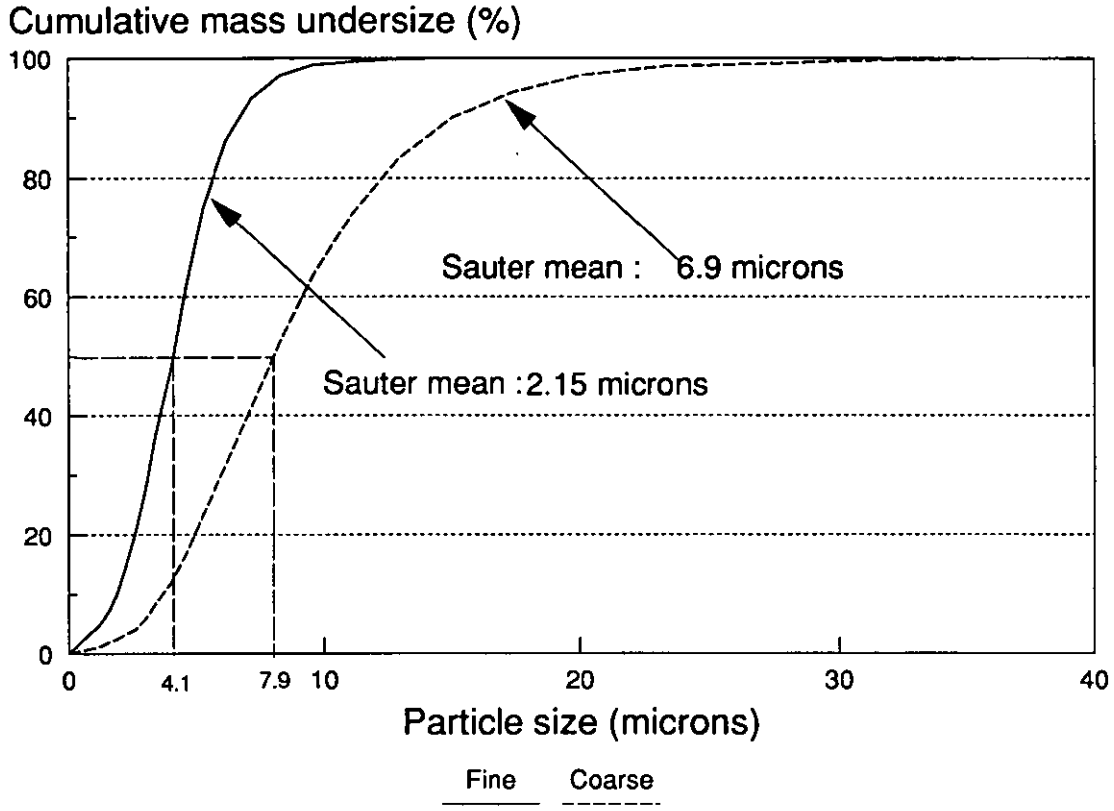

Fig 61 Particle size distributions of fine and coarse powders

5.2 Test results and discussions

The details of the test results are listed in Appendix 5, and tabulated in Tables 20 to 23.

Accurate interpretion of crossflow filtration processes is notoriously difficult due to complex interactions of the following factors: variation in flow resistances, temperature fluctuation, lack of accurate knowledge of the filtration pressure, size and density segregation of deposit on the membrane surface, surface charges, lack of homogeneous membrane, etc. The following procedures were followed in order to eliminate or reduce the degree of some of these variations.

5.2.1 Effect of temperature

Temperature was recorded at the same time as the permeate flux rate.

Variation of permeate flux rate with temperature was corrected using the viscosity difference between water at the measured temperature and a reference temperature taken to be 25 °C. Thus all the flux rates were corrected to that which would have been

obtained at a temperature of 25 °C. This is shown in Fig 60 where the flux rate (J_θ) under conditions of rising temperature has been converted to one equivalent to that at 25 °C (J_{25}) using the following equations:

$$\mu_\theta = 10^{-3} \cdot 10^{(0.201844 - 0.010\theta)} \tag{5.1}$$

$$J_{25} = \frac{\mu}{\mu_{25}} J_\theta \tag{5.2}$$

where subscript θ is the temperature in °C.

A duplicate run is also shown in Fig 60 where the temperature was maintained at 24 to 26 °C. From this figure it can be seen that correcting the experimental data for rising temperature gives a similar result to one obtained under conditions of constant temperature. The very slightly larger values of flux rate after conversion, compared with that obtained by maintaining the temperature, can be explained by the slightly higher initial permeate rate, i.e. the slightly lower membrane resistance, in the experiment in which the temperature increased. This experiment validated the use of Equation 5.2 to correct filtration flux rates in the other filtrations where temperature fluctuation occurred.

5.2.2 Membrane resistance

In membrane studies involving modelling , or comparison, it is a common practice to determine the membrane resistance by using clean water permeate flux rate (J_{water}) against the transmembrane pressure (P_t) in the form of Darcy's law:

$$R_m = \frac{P_t}{\mu \cdot J_{water}} \tag{2.1a}$$

It is often assumed that the membrane resistance remains constant and equal to the clean water value during filtration, thus any increase in resistance during filtration must be due to the deposit. This approach is not valid in conventional filtration for the estimation of filter cloth resistance, and it is unlikely to be accurate in crossflow microfiltration processes in which the suspended particle size is close to or finer than the pore size of the membrane such as those described in the previous and present chapters. Therefore, the membrane resistance under these circumstances must be calculated *in-situ*, just as it must be for conventional filtration.

In conventional constant pressure filtration the square of the volume of permeate (W^2) is proportional to the filtration time, and the filter medium resistance can be calculated from the experimental results by some simple algebraic manipulation. In crossflow filtration no such simple relation between time and permeate volume exists, thus an alternative method must be used to calculate the *in-situ* membrane resistance. Such a method is to consider the initial stage of filtration, taking a tangent to the volume permeate against time curve to provide a value for J_{water}, which is then used in Eq 2.1a to provide a value for membrane resistance. An example of this for one filtration is shown in Fig 62.

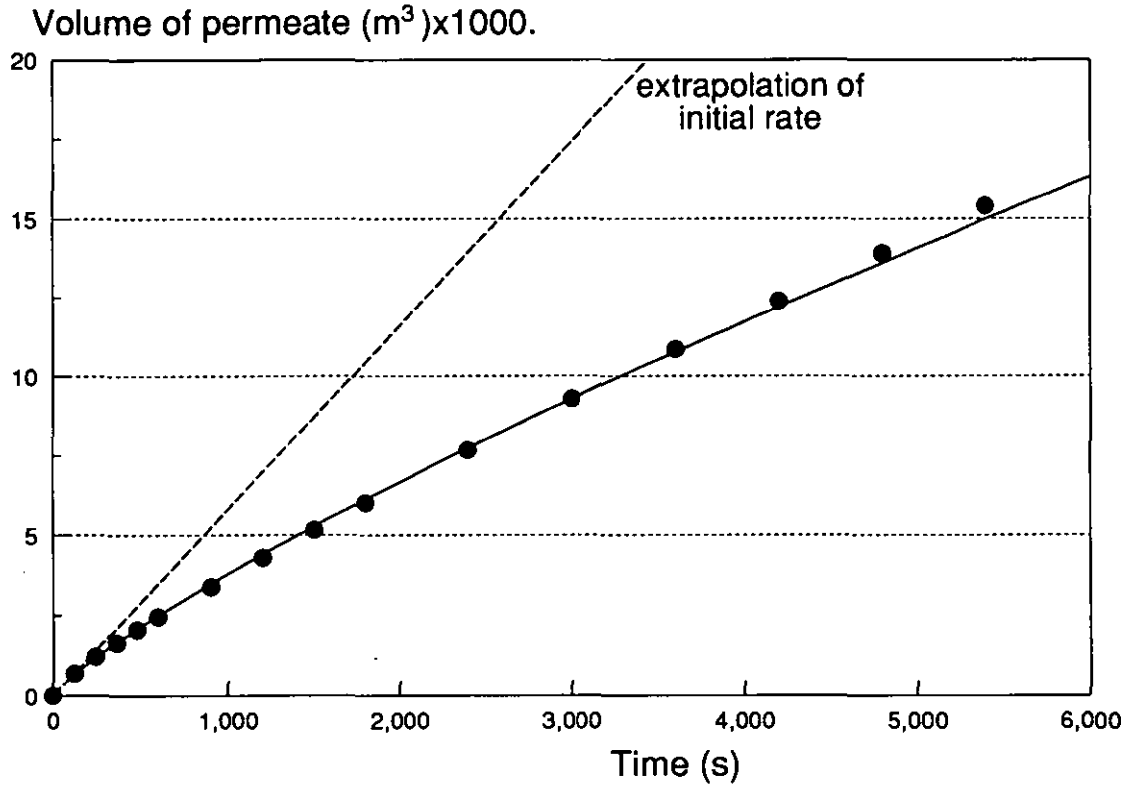

Fig 62 Cumulative permeate volume with time and use of initial rate for membrane resistance

Membrane resistances were calculated for all the filtrations by this method, these are given in Tables 20 and 21 for the coarse powder, and Tables 22 and 23 for the fine powder at different concentrations.

Table 20
Membrane resistance at 1.5% solid concentration (Coarse powders)

U	J_e	P_t	R_m	R_C	P_t^+	File
m/s	$m^3/m^2 \cdot hr$	Bar	$10^9\ m^{-1}$	$10^9\ m^{-1}$	Bar	code
Helical endcap						
1.52	0.290	0.204	2.4	2.4	0.162	HF
2.08	0.416	0.441	3.1	4.0	0.337	HE
2.65	0.551	0.492	2.1	4.0	0.422	HC
2.65	0.543	0.492	2.3	3.8	0.409	HD
3.22	0.757	0.667	1.9	4.1	0.588	HA
3.22	0.639	0.667	2.1	4.9	0.580	HB
3.22	0.596	0.667	2.0	5.6	0.594	HG
Normal endcap						
0.66	0.343	0.170	1.1	2.2	0.166	NN
0.66	0.287	0.176	1.4	2.8	0.164	NG
0.66	0.427	0.269	1.2	3.0	0.259	NO
0.66	0.489	0.476	1.5	5.1	0.446	NP
0.91	0.527	0.282	1.1	2.5	0.276	NK
0.91	0.363	0.299	1.6	4.0	0.273	NF
0.91	0.567	0.343	1.2	2.9	0.331	NL
0.91	0.653	0.557	1.5	4.3	0.518	NM
1.16	0.578	0.456	1.8	3.5	0.402	ND
1.16	0.465	0.456	1.8	4.8	0.410	NE
1.16	0.438	0.456	1.9	5.1	0.407	NH
1.16	0.519	0.640	2.1	6.2	0.567	NI
1.16	0.565	0.847	2.5	7.6	0.736	NJ
1.41	0.608	0.624	1.8	5.1	0.564	NC
1.66	0.694	0.880	2.1	6.5	0.782	NA
1.66	0.680	0.880	2.1	6.7	0.784	NB
Tangential endcap						
0.66	0.452	0.231	1.3	2.1	0.216	TE
1.00	0.650	0.461	1.7	3.1	0.410	TD
1.00	0.677	0.720	2.2	5.0	0.620	TN
1.00	0.600	0.581	1.7	4.8	0.526	TM
1.00	0.572	0.461	1.9	3.6	0.403	TL
1.33	0.818	0.839	2.3	4.7	0.714	TI
1.33	0.814	0.749	1.9	4.4	0.666	TH
1.33	0.792	0.977	2.3	6.0	0.843	TK
1.33	0.849	0.750	1.8	4.2	0.672	TC
1.33	0.961	0.977	2.0	4.8	0.856	TJ
1.49	0.940	0.963	1.8	5.1	0.869	TF
1.49	0.962	1.018	2.2	5.0	0.878	TG
1.49	1.020	0.949	1.8	4.5	0.851	TB
1.49	1.091	0.966	2.6	3.4	0.772	TA

Table 21

Membrane resistance at 4% solid concentration (Coarse powders)

U	J_e	P_t	R_m	R_C	P_t^+	File
m/s	$m^3/m^2 \cdot hr$	Bar	$10^9\ m^{-1}$	$10^9\ m^{-1}$	Bar	code
Normal endcap						
0.99	0.563	0.534	2.6	3.8	0.429	NV
0.99	0.616	1.086	3.5	8.4	0.886	NW
1.41	0.622	0.694	3.4	4.1	0.516	NR
1.66	0.709	0.914	3.5	5.2	0.696	NQ
1.66	0.644	0.949	3.0	6.9	0.780	NS
1.66	0.781	1.066	3.4	5.9	0.833	NT
1.66	0.833	1.204	3.6	5.6	0.919	NU
Tangential						
0.99	0.559	0.461	2.4	3.2	0.375	TR
1.16	0.634	0.597	2.4	4.0	0.495	TQ
1.33	0.781	0.750	2.6	3.8	0.599	TP
1.33	0.739	0.750	2.5	4.3	0.616	TS
1.33	0.812	0.856	2.7	4.4	0.691	TT
1.33	0.811	0.994	3.3	4.9	0.760	TU
1.49	0.955	0.963	2.7	4.1	0.771	TO
1.49	0.918	1.052	3.1	4.7	0.820	TV
1.49	1.043	1.121	3.1	4.2	0.860	TW
1.49	0.879	1.156	3.8	5.1	0.853	TX

Table 22
Membrane resistance at 1.6% solid concentration (Fine powders)

U	J_e	P_t	R_m	R_C	P_t^+	File
m/s	$m^3/m^2 \cdot hr$	Bar	$10^9\ m^{-1}$	$10^9\ m^{-1}$	Bar	code
Normal endcap						
1.16	0.592	0.560	2.4	4.0	0.461	NC
1.16	0.589	0.526	1.7	4.3	0.474	NJ
1.16	0.634	0.657	2.0	5.0	0.582	NK
1.16	0.696	0.795	2.2	5.5	0.693	NL
1.41	0.653	0.781	2.3	5.8	0.678	NB
1.41	0.731	0.746	2.1	4.8	0.647	NG
1.41	0.776	0.846	2.2	5.1	0.729	NH
1.41	0.842	0.984	2.4	5.5	0.833	NI
1.45	0.838	0.967	2.4	5.4	0.820	NF
1.47	0.824	0.932	2.3	5.2	0.799	NE
1.50	0.786	0.856	2.2	5.2	0.740	ND
1.65	0.802	0.841	2.2	4.8	0.719	NA
Tangential endcap						
1.16	0.73	0.597	2.0	3.5	0.513	TA
1.16	0.742	0.600	1.9	3.6	0.523	TG
1.16	0.756	0.676	1.9	4.1	0.594	TH
1.16	0.817	0.676	1.8	3.8	0.601	TI
1.16	0.816	0.763	1.9	4.4	0.677	TJ
1.32	0.836	0.739	2.0	4.0	0.638	TC
1.32	0.875	0.739	2.2	3.6	0.623	TD
1.32	0.914	0.805	2.0	4.0	0.698	TE
1.32	0.939	0.960	2.3	4.6	0.816	TF
1.45	1.022	0.917	2.1	4.0	0.790	TM
1.46	0.953	0.889	2.2	4.1	0.753	TL
1.47	0.937	0.894	2.1	4.4	0.774	TB
1.48	0.936	0.902	2.2	4.3	0.767	TK

Table 23

Membrane resistance at 3% solid concentration (Fine powders)

U	J_e	P_t	R_m	R_C	P_t^+	File
m/s	$m^3/m^2 \cdot hr$	Bar	$10^9\ m^{-1}$	$10^9\ m^{-1}$	Bar	code
Normal endcap						
1.16	0.627	0.560	2.4	3.6	0.459	NO
1.16	0.607	0.540	2.3	3.7	0.449	NU
1.16	0.677	0.674	2.4	4.3	0.558	NV
1.16	0.749	0.795	2.7	4.5	0.645	NW
1.32	0.72	0.675	2.6	3.8	0.543	NN
1.41	0.742	0.746	2.5	4.3	0.612	NR
1.41	0.777	0.829	2.4	4.8	0.693	NS
1.41	0.886	0.967	2.7	4.7	0.783	NT
1.46	0.827	1.018	3.0	5.3	0.814	NQ
1.47	0.876	0.931	2.9	4.3	0.735	NP
1.5	0.822	0.873	2.7	4.4	0.702	NM
Tangential endcap						
1.16	0.689	0.600	2.3	3.6	0.494	TU
1.16	0.736	0.676	2.3	3.9	0.562	TY
1.16	0.788	0.831	2.6	4.6	0.682	TZ
1.32	0.792	0.753	2.5	3.9	0.611	TT
1.32	0.792	0.753	2.5	4.0	0.617	TV
1.32	0.85	0.805	2.5	3.9	0.654	TW
1.32	0.895	0.960	2.8	4.4	0.764	TX
1.45	0.871	0.917	2.7	4.4	0.742	TS
1.47	0.879	0.899	2.7	4.2	0.722	TR
1.48	0.888	0.902	2.6	4.2	0.727	TQ

Also shown in these Tables is the deposit resistance (R_C) which was calculated by applying the Darcy's law after equilibrium had been reached. The two resistances due to the membrane and the deposit are assumed to be additive, thus:

$$P_t = \mu(R_m + R_C)J_e \tag{5.3}$$

where subscript *e* refers to equilibrium status.

It should be noted that R_m is assumed to be a constant but R_C is a function of filtration time until the equilibrium flux rate is achieved. Darcy's law is then applied to determine the equilibrium value of the deposit resistance using a rearranged form of Eq 5.3.

In order to compare the effects of filtration in or without a rotating flow field, any effect due to the variable nature of the membrane resistance must be removed. The lowest membrane resistance in Tables 20 to 23 is 1×10^9 (m^{-1}), thus the data for the remaining filtrations have been "normalised" to this membrane resistance, which means $R_m^+ = 10^9\ m^{-1}$. The most straightforward way of achieving this normalisation is to consider the pressure drops as being additive:

$$P_t = \Delta P_m + \Delta P_c \tag{5.4}$$

where subscript ***m*** refers to the resistance caused by membrane and its variations.

By rearranging and substituting in Darcy's law gives:

$$\Delta P_c = \left(1 - \frac{\Delta P_m}{P_t}\right) P_t \tag{5.5a}$$

$$\Delta P_m = \left(\frac{R_m}{R_m + R_c}\right) P_t \tag{5.5b}$$

$$\Delta P_m^+ = \left(\frac{R_m^+}{R_m^+ + R_c}\right) P_t \tag{5.5b}$$

The combination of Eq 5.3 to 5.5 provides the following expression for total pressure drop across the membrane and deposit based on the normalised membrane resistance (R_m^+), this is the corrected membrane pressure (P_t^+) in Tables 20 to 23:

$$P_t^+ = \Delta P_c + \Delta P_m^+ \tag{5.6a}$$

$$P_t^+ = P_t\left(1-\left(\frac{R_m}{R_m+R_c}\right)+\left(\frac{R_m^+}{R_m^++R_c}\right)\right) \tag{5.6b}$$

The pressure across the membrane as those shown in Figs 63 (low solids concentration) and 64 (high solids concentration) are the corrected values, i.e. these should be the flux rates achieved if the membrane resistance was consistently $1x10^9$ m^{-1}.

5.2.3 Effect of filtration pressure

The equilibrium permeate flux rate was clearly pressure dependent, up to a pressure across the membrane of 1 Bar. The rate of increase in flux rate with pressure was, however, decreasing and it was possible that the system became pressure independent at higher pressure. Equilibrium permeate flux rates were higher when using the tangential endcaps, i.e. with rotating flow, despite the difference in particle sizes and concentrations tested as shown in Figs 63 and 64. The helical module also provided increased values of equilibrium permeate flux rate over normal module, for a given pressure as shown in Fig 63a.

5.2.4 Effect of shear rate

Figs 65a and 66a show that flux rate was substantially independent of shear rate at constant pressure for the normal module. There was however, an underlying relation between flux rate and transmembrane pressure. Figs 65b and 66b are for the tangential module and some flux rate dependency with crossflow velocity can be observed.

There is some degree of spread on the experimental results shown in Figs 65 and 66 but, nevertheless, it is evident that the membrane endcaps did have a considerable influence on the filtration behaviour of this material. If the flux rate was shear rate independent, over this limited region, then the additional flux rate given by the helical or tangential mode of operation must be due to the centrifugal force field.

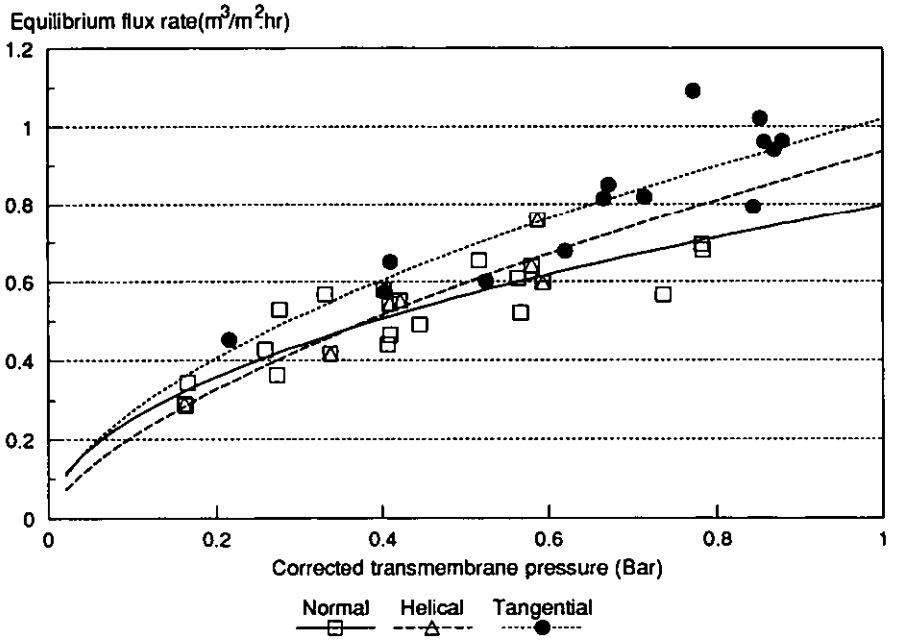

Fig 63a Equilibrium permeate flux rate with pressure using different endcaps (1.5% coarse powder)

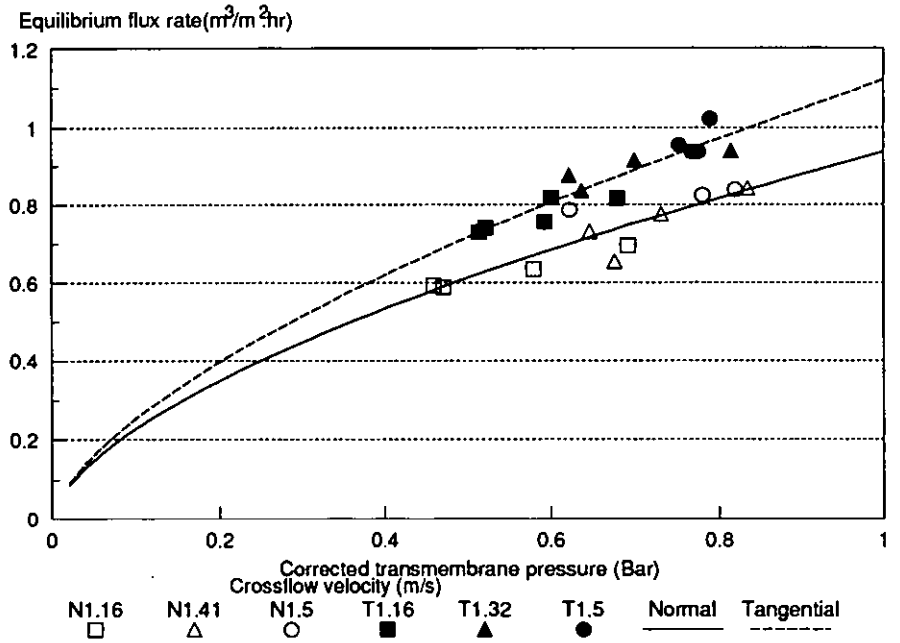

Fig 63b Equilibrium permeate flux rate with pressure using different endcaps (1.6% fine powder)

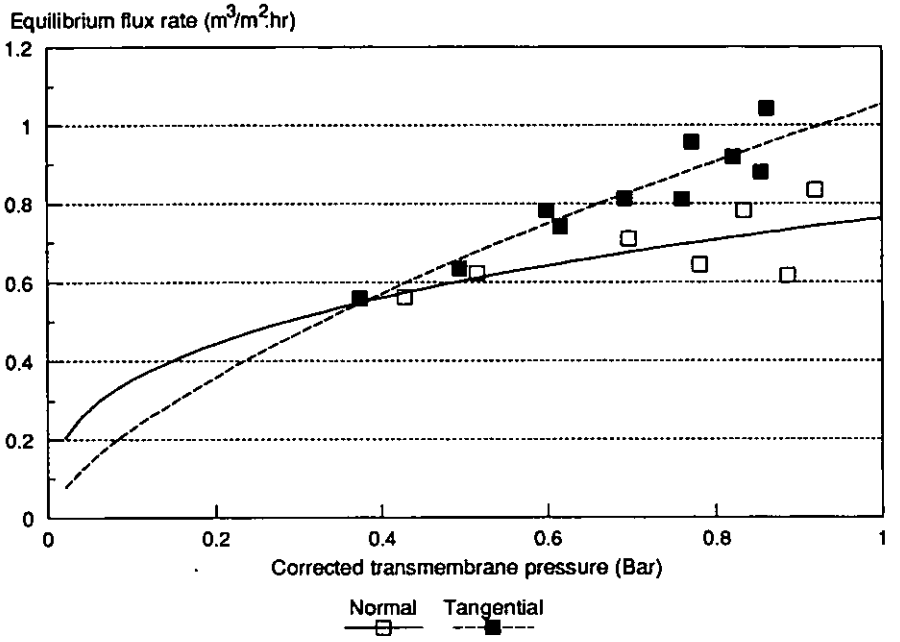

Fig 64a Equilibrium permeate flux rate with pressure using different endcaps (4% coarse powder)

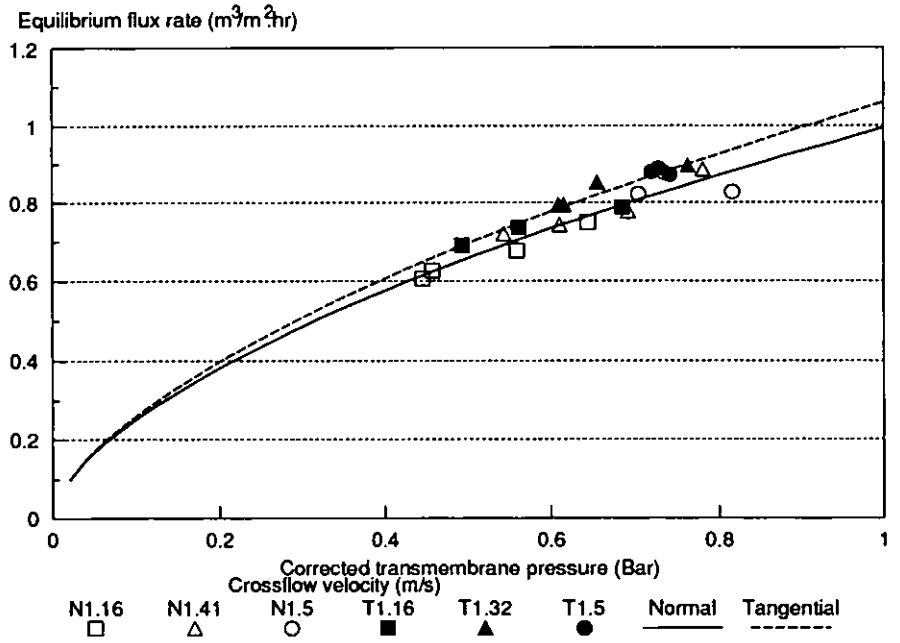

Fig 64b Equilibrium permeate flux rate with pressure using different endcaps (3% fine powder)

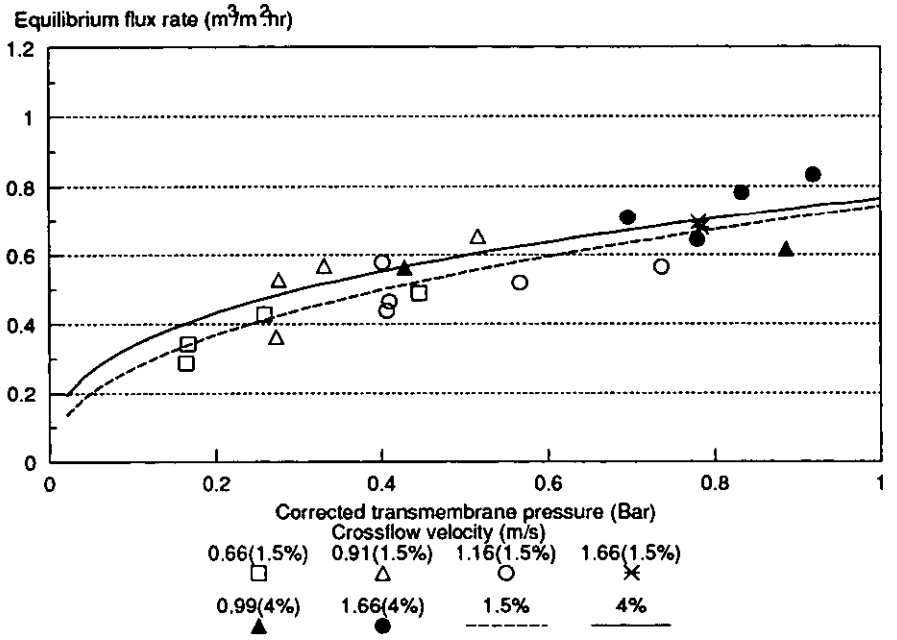

Fig 65a Equilibrium permeate flux rate with pressure at various crossflow velocities using normal endcaps (coarse powder)

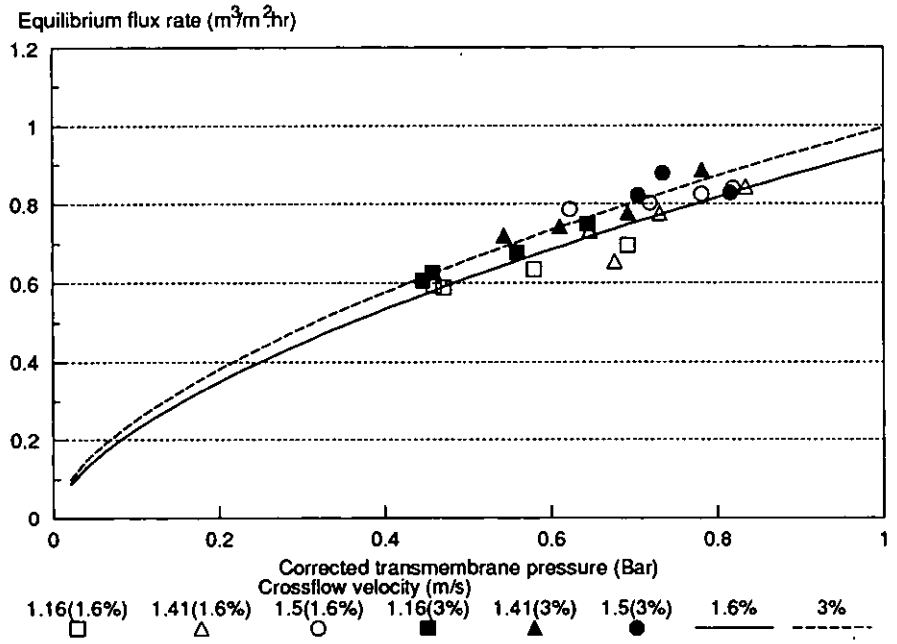

Fig 65b Equilibrium permeate flux rate with pressure at various crossflow velocities using normal endcaps (fine powder)

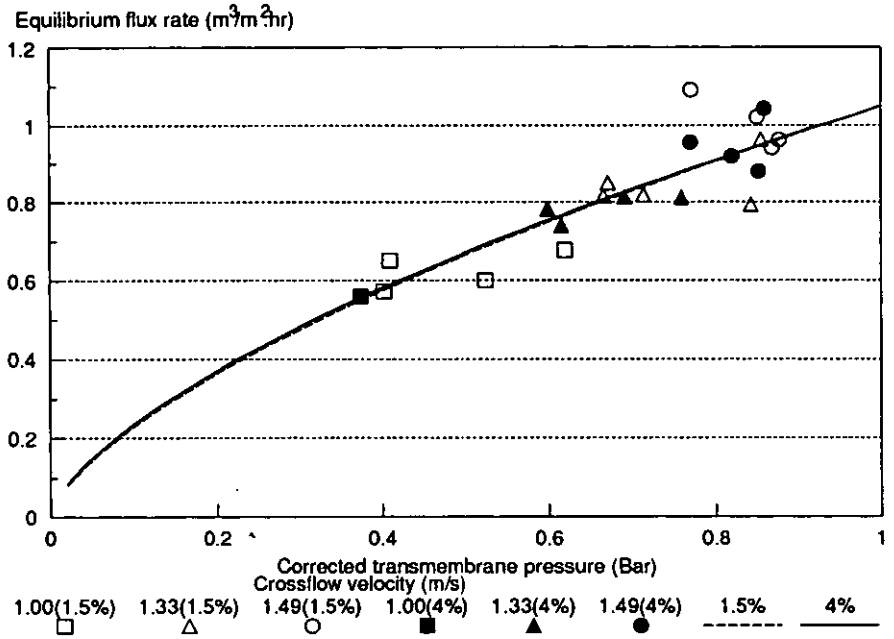

Fig 66a Equilibrium permeate flux rate with pressure at various crossflow velocities using tangential endcaps (coarse powder)

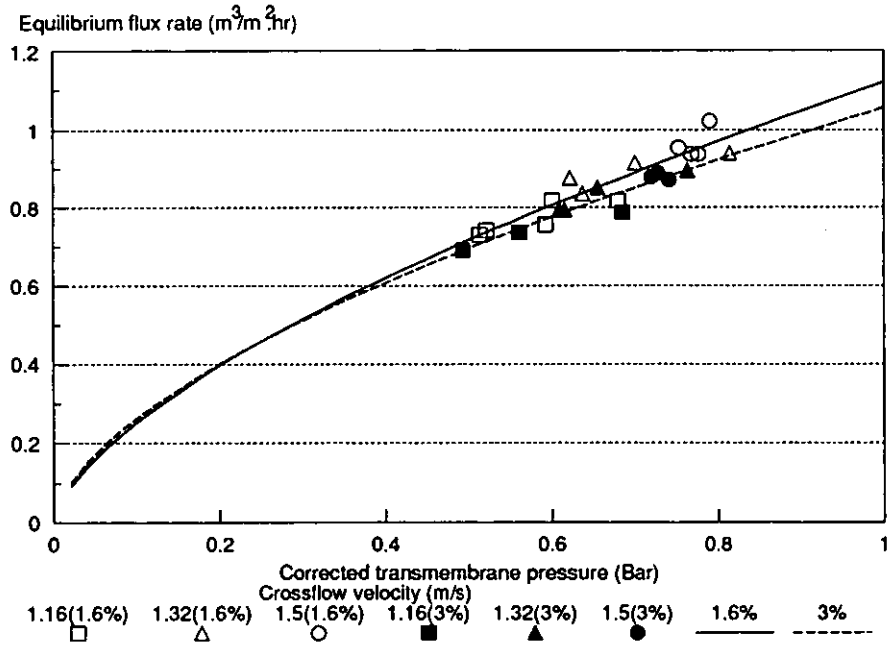

Fig 66b Equilibrium permeate flux rate with pressure at various crossflow velocities using tangential endcaps (fine powder)

Flux rate is usually a function of crossflow velocity or shear rate, the lack of such a relation in the case of the normal module could have been due to the very high turbulence induced by having entry at right angles to the axis flow, in addition to the relatively short filter tube length. Another reason for this effect could have been the large amount of fines which were smaller than the nominal membrane pore size. Thus a substantial part of the deposit resistance was due to material depositing inside the membrane structure and therefore, protected from the shear induced by the crossflow.

5.2.5 Effect of particle size, concentration and centrifugal acceleration

In the particle-fluid systems the distinction between free and hindered systems is usually drawn, based on the solid concentration of dispersion. The threshold between them is often assumed to be approximately 1% by volume, but it is a function of the suspended material. The concentrations of different particle sizes employed in the study were chosen to be below and above this threshold, to test the application of centrifugally induced anti-fouling of this membrane under both of these operating conditions. Particles influenced by a centrifugal field force and under free and hindered conditions are shown schematically in Fig 67.

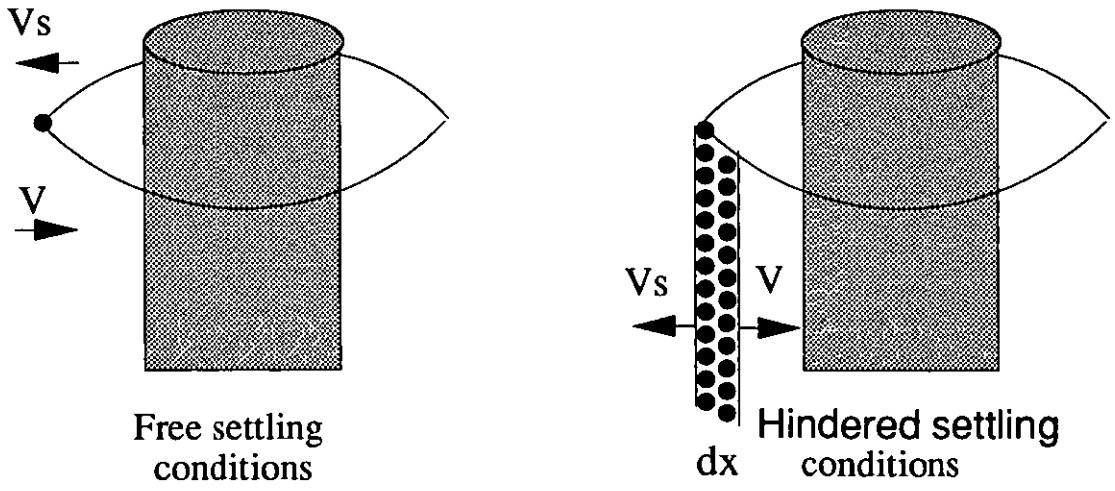

Fig 67 Schematic diagram of particles in stationary orbit around filter due to balance of centrifugal field and liquid drag force

1) Free dispersions

The drag force (F_D) on a freely dispersed particle can be calculated from Stokes law:

$$F_D = -3\pi\mu d_s \frac{dx}{dt} \qquad (5.7a)$$

where x is the radial position (m)

F_D is the drag force per unit volume ($N \cdot m^{-3}$)

dx/dt is the relative radial velocity of the particle ($m \cdot s^{-1}$).

Note that F_D is a function of the radial position. The buoyed centrifugal force (F_C) for an assuming spherical particle at distance x is:

$$F_C = \frac{\pi}{6} d_s^3 (\rho_s - \rho) x\, \omega^2 \qquad (5.7b)$$

where ω is angular velocity (s^{-1})

F_C is the buoyed centrifugal force ($N \cdot m^{-3}$)

ρ_s and ρ are solid and liquid densities respectively.

If the resultant force of F_C and F_D on the particle(s) is zero, i.e. $F_C/F_D = 1$, and if inertia and gravitational body forces can be neglected, then equating Eqs 5.7a and 5.7b gives:

$$J_v \equiv \frac{dx}{dt} = \frac{d_s^2 (\rho_s - \rho) x\, \omega^2}{18\mu} \qquad (5.7c)$$

The above equation can be used to estimate the liquid flux rate towards the membrane that must be exceeded before particles move in the direction of the membrane. At lower flux rate particles will move outwards, if they are denser than the supporting fluid, due to the action of the centrifugal field force. Thus this represents the minimum flux rate that should be obtained from a membrane incorporating centrifugal separation.

It is extremely difficult to estimate the angular velocity inside a centrifugal separator in order to apply Eq 5.7c. Conservation of angular momentum is sometimes used in hydrocyclone investigations, but it is often found necessary to introduce empirical coefficients into the equations. An alternative approach is to estimate the centrifugal acceleration at the membrane surface using a rearranged form of Eq 5.7c:

$$x\, \omega^2 = \frac{18\mu J_v}{d_s^2 (\rho_s - \rho)} \qquad (5.8)$$

2) Hindered dispersions

In hindered dispersions a force balance can be constructed over a laminar layer of suspension, instead of considering individual particles. The centrifugal field force is again balanced by the liquid drag force, if there is no net particle motion and the forces due to inertia and gravity can be ignored, then:

$$C\,x\,\omega^2(\rho_s-\rho)S\,dx - C\,F_D\,S\,dx = 0 \tag{5.9}$$

where S is the area of the laminar layer (m^2)

C is the solid volume fraction concentration.

A liquid force balance results in the following:

$$\frac{dP}{dx} = CF_D = C\,x\,\omega^2(\rho_s-\rho) \tag{5.10}$$

where dP/dx is the dynamic liquid pressure gradient.

This can be related to solid concentration and velocities by a modified form of Darcy's law:

$$\frac{dP}{dx} = -\frac{\mu}{p_s}(1-C)(V-V_s) \tag{5.11a}$$

where p_s is the permeability of the deposit layer (m^2)

V and V_s are the radial velocities of liquid and solids respectively ($m \cdot s^{-1}$).

If the particle layer remains in a stationary orbit, i.e. does not move towards or foul the membrane, then the solid velocity is zero, i.e. $V_s = 0$. Therefore:

$$\frac{dP}{dx} = -\frac{\mu}{p_s}(1-C)V \tag{5.11b}$$

Combining Eq 5.11b with Eq 5.10 and rearranging provides:

$$J_v = V = \frac{C\,x\,\omega^2(\rho_s-\rho)p_s}{\mu(1-C)} \tag{5.11c}$$

Rearranging Eq 5.11c for the centrifugal acceleration at the membrane surface:

$$x\,\omega^2 = \frac{\mu(1-C)J_v}{C\,(\rho_s-\rho)p_s} \tag{5.12}$$

p_s can be calculated from various models, one such is Happel and Brenner [1965]:

$$p_s = \frac{(2-3C^{1/3}+3C^{5/3}-2C^2)}{(3+2C^{5/3})}\frac{d_s^2}{12C} \tag{5.13}$$

If the permeate flux rate is dominated by the flow resistance through the most concentrated laminar layer, which likely to be adjacent to the membrane surface, and this layer is assumed to have a porosity of 50% then the permeability of this layer is $1.4x10^{-13}$ (m^2) by Eq 5.13.

Figs 63 and 64 also show that solid concentration did not significantly affect the permeate flux rate, over the limited range investigated.

Fig 68 is the relation between the equilibrium permeate flux rate and corrected transmembrane pressure with tangential endcap at different axial velocites and particle sizes at low and high solid concentration, respectively. In both cases, the permeate flux rate of the fine powder at low velocity is higher than that of the coarse, but lower at higher velocity.

5.2.6 Comparison of models and rotating velocities

The increase in permeate flux rate over that obtained in the absence of rotating flow can be deduced from Figs 65 and 66. At an axial velocity of 1.33 and 1.49 m/s the increase in permeate flux rate is 0.13 and 0.23 $m^3/m^2 \cdot hr$, respectively. Table 24 shows the centrifugal acceleration averaged over the full membrane length, based on Eqs 5.8 and 5.12 for the two models for free and hindered dispersions, respectively. Also shown in Table 24 is the equivalent rotating speed of the membrane to achieve the same rotating flow condition if the membrane had been rotated instead of the fluid. These were both calculated by assuming that the additional permeate flux was due to the fouling solids entering the stationary orbit. Thus Eqs 5.8 and 5.12 were used with J as the increase in permeate flux and not the total permeate flux.

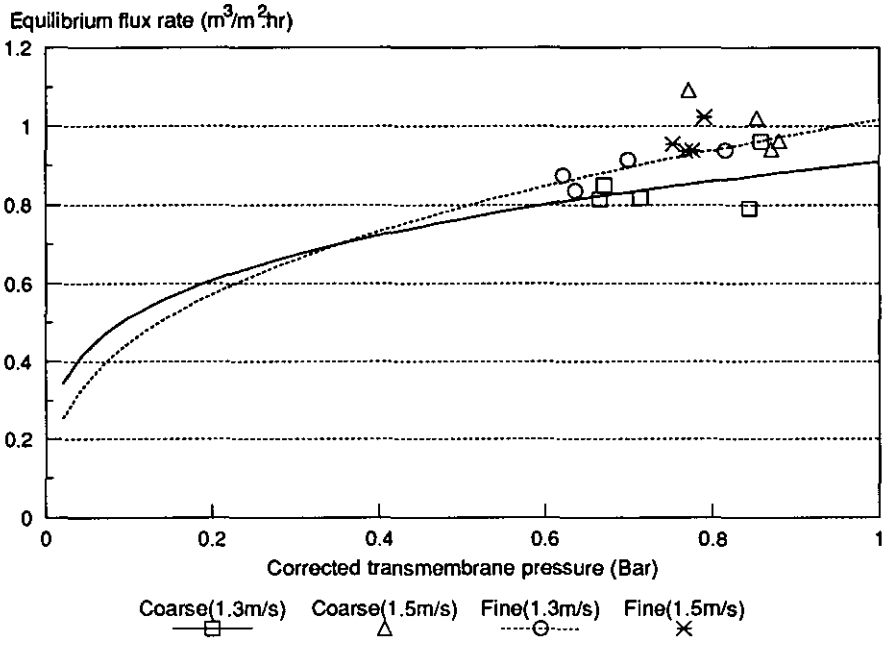

Fig 68a Permeate flux rate with tangential endcaps at different particle sizes (1.5%)

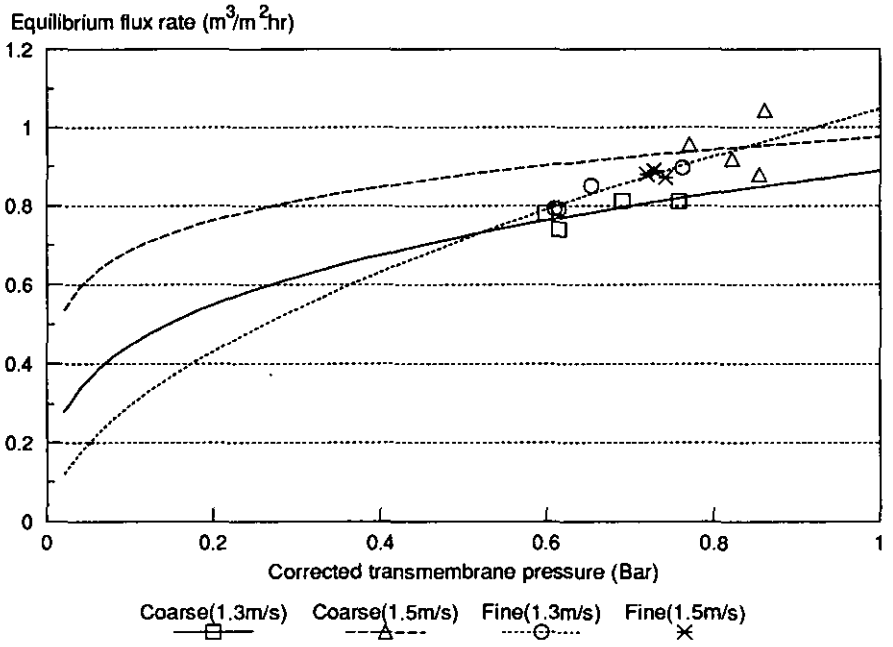

Fig 68b Permeate flux rate with tangential endcaps at different particle sizes (3%)

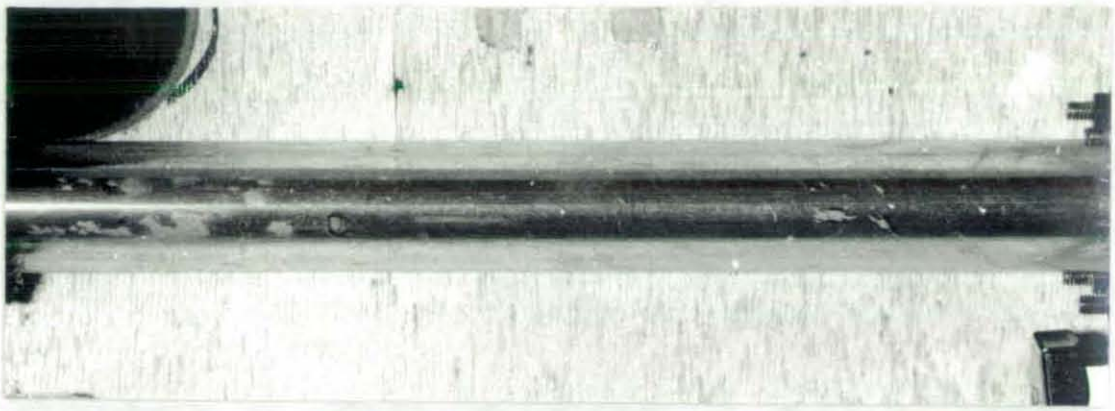

(a) Clean filter

(b) Normal filter

(c) Tangential filter

Fig 69 The deposits on the filter with different endcaps

Table 24
Conditions of membrane surface according to models
based on free and hindered dispersions

Axial flow velocity	Additional permeate flux rate	Free dispersion		Hindered dispersion	
		Centrifugal acceleration	Rotating speed	Centrifugal acceleration	Rotating speed
(m/s)	(m^3/m^2•hr)	(m/s^2)	(rpm)	(m/s^2)	(rpm)
1.33	0.130	7.4	475	141	2070
1.49	0.230	13.2	632	250	2760

It is possible to estimate the angular velocity and acceleration at the membrane surface by considering the geometry of the membrane filter holder, and from a knowledge of the entry condition. The principle of conservation of angular momentum is:

$$U\ x = Constant \tag{5.14}$$

where U is the tangential velocity at a radial position x.

Eq 5.14 is valid for frictionless conditions and is often modified by the inclusion of a fractional power exponent on the radial position term to account for energy losses. Using the filter system described in Figs 56 and 57, the centrifugal acceleration at the membrane surface ($x\omega^2$) is in the range 19000 to 8400 (m/s^2) over the range of inlet velocities employed in this work.

It is evident from Table 24 that if the dispersion concentration is sufficiently high for hindered conditions to pertain, a substantial angular velocity is required in order to decrease the fouling effect. It is reasonable to deduce that a hindered system existed because a deposit was observed on the surface of the membrane surface as shown in Fig 69 despite the differences in the types of endcaps, particle sizes, solid concentrations, and operating conditions.

The centrifugal accelerations in Table 24, deduced from the operating data, are considerably lower than the theoretical values. The deduced acceleration are also the average values over the full surface of the membrane and, clearly, are affected by frictional losses within the filter module. Visual observation confirmed that the suspensions rotated rapidly at the filter inlet, but it decayed to only a slight rotation

towards the base of the module where the exit was located. The discrepancy between theoretical and deduced centrifugal acceleration, and the information obtained by visual observation suggest that very careful design of the filter module must be made in order to maximise the benefit due to rotating flow.

5.2.7 Depth of the deposit

The average depth of the deposit on the membrane surface can be calculated from the membrane deposit resistance shown in Tables 20 to 23, the deposit permeability estimated from Eq 5.13, and

$$x_l = R_c p_s \tag{5.15}$$

Deposit resistance can be seen to vary from 2.1 to 8.4 x10^9 m^{-1}, in Tables 20 to 23. The deposit depth corresponding to these resistances were 0.05 to 1.2 mm, respectively. A deposit of approximately 1 mm was measured, with a significantly tapering shape; less deep at the feed end, much thicker at the outlet as shown in Fig 69. Calculated values of deposit permeability, resistance and, therefore, thickness appear to be in reasonable agreement with visual observation.

5.2.8 Energy efficiency

It is clear that the permeate flux rates were enhanced by the use of rotating flow on the membrane surface. The effectiveness of this technique can be evaluated by considering the energy input required by the normal and tangential filters. Both filter systems used the same experimental rig, thus Bernoulli's equation can be applied using the filter module entry and exit conditions of pressure and velocity. By neglecting energy terms due to internal, mechanical and static pressure, Bernoulli's equation for energy per unit mass can be written as:

$$\frac{\Delta P}{\rho} + \frac{U^2}{2} = A \tag{5.16}$$

Multiplying Eq 5.16 by the mass flow rate gives the rate of energy change with time, i.e. the power used by the system.

The pressure drop of the filter module and the fluid velocity in the module feed pipe were used in Eq 5.16 to calculate the power requirement for the equilibrium flux rate given in Tables 20 to 23. The results are plotted in Figs 70 and 71 for low and high solid concentrations respectively.

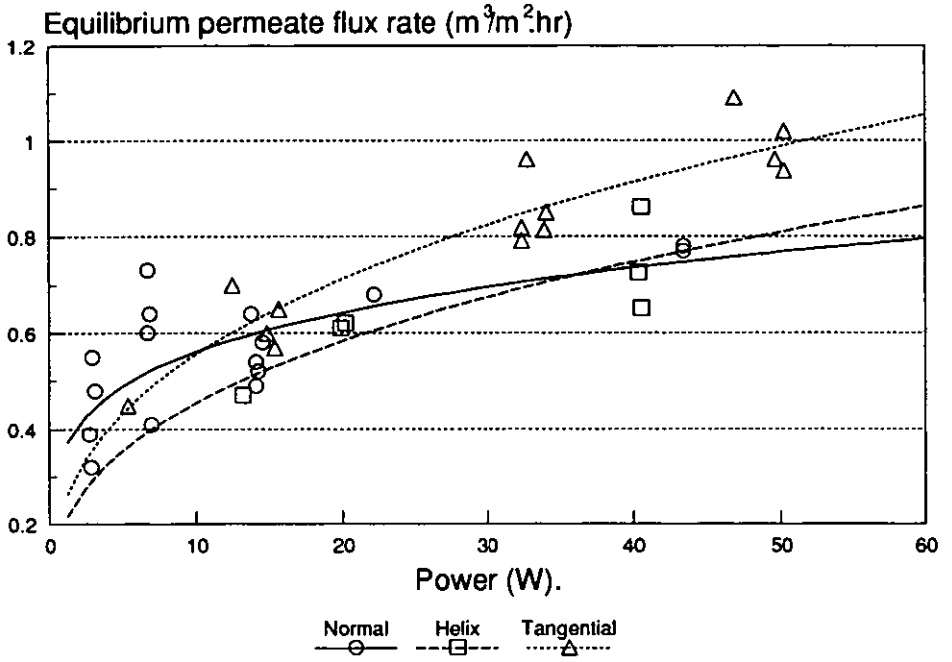

Fig 70a Equilibrium flux rate as a function of power requirement (1.5% coarse powder)

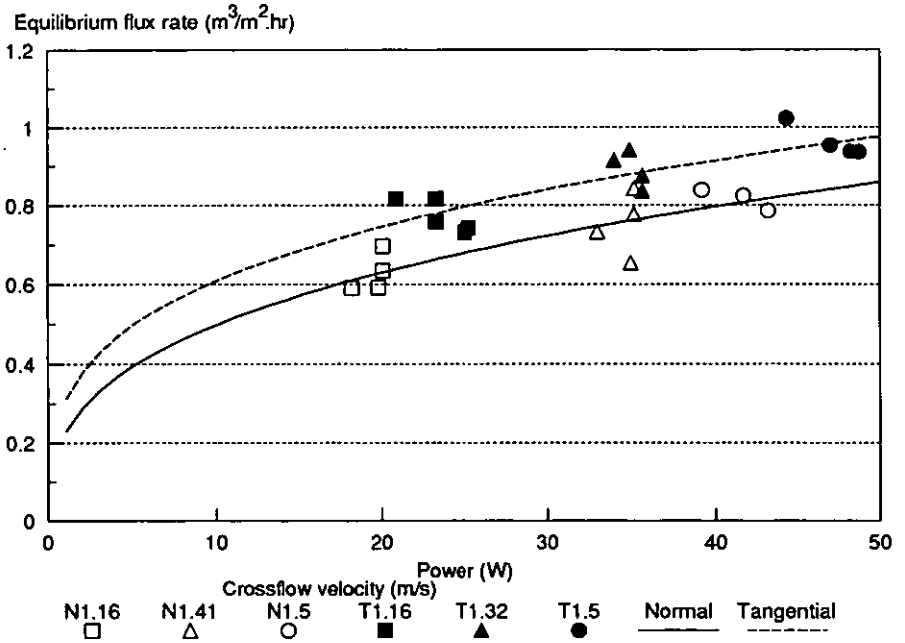

Fig 70b Equilibrium flux rate as a function of power requirement (1.6% fine powder)

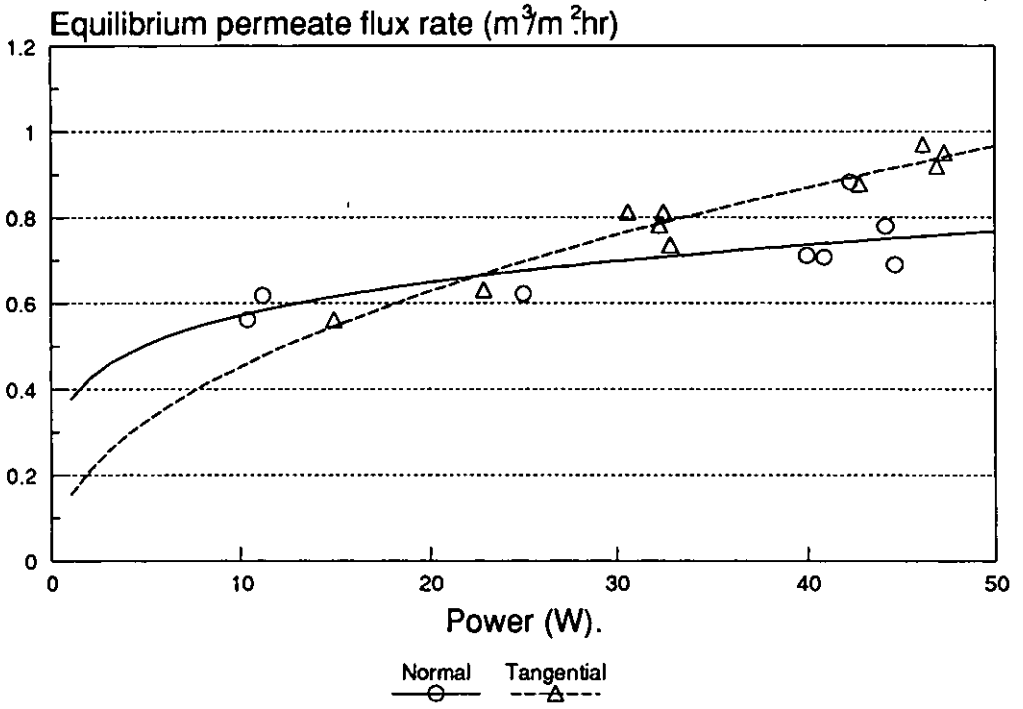

Fig 71a Equilibrium flux rate as a function of power requirement (3% coarse powder)

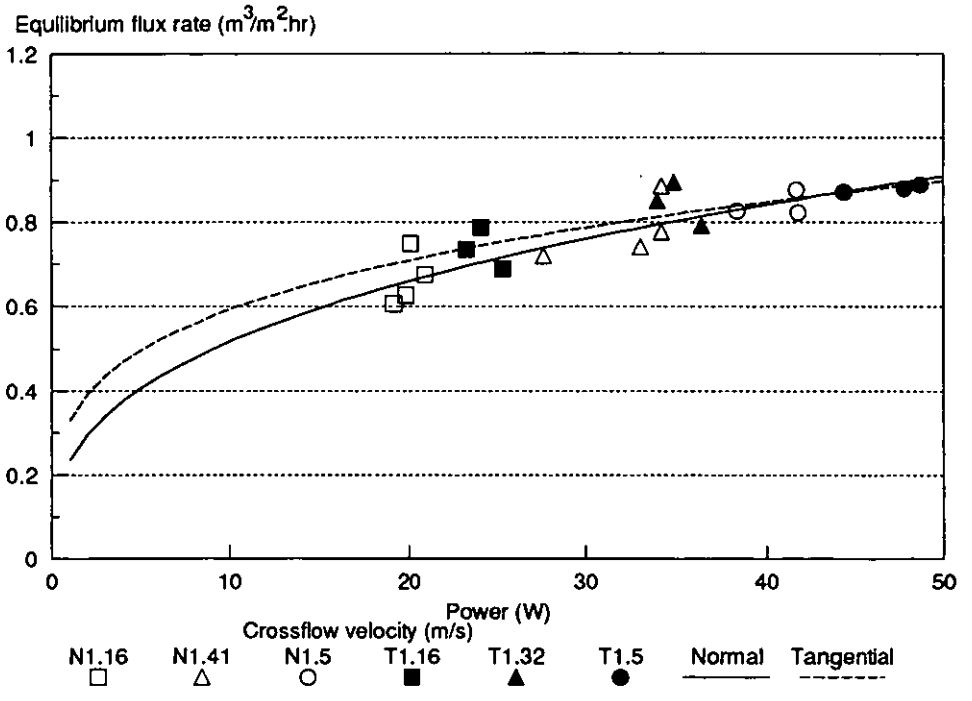

Fig 71b Equilibrium flux rate as a function of power requirement (4% fine powder)

Figs 70 and 71 demonstrate that for the coarse powder, at high power inputs or for high equilibrium flux rates, it was more energy efficient to the filter with tangential endcaps, at low flux rates or power inputs, the normal filtration was more efficient; for the fine powder, filtration with tangential endcaps is always more efficient than with the normal ones.

A common alternative method of comparing energy requirement for crossflow filtration is to calculate the energy required to produce 1 m^3 of permeate. This can be estimate from Figs 70 and 71. For example, Fig 67a shows the values for the flux rate of 0.82 and 0.68 $m^3/m^2 \cdot hr$ for the tangential and normal filtration respectively at the same power input of 30 W. Thus the time taken to produce 1 m^3 of permeate on this filter (0.01 m^{-2}) would be 122 and 147 hours, respectively. The energy required would therefore be 3.66 and 4.41 $kW \cdot hr/m^3$ for the tangential and normal respectively. Thus the extra energy required by the normal filter is 20% compared to the tangential one.

5.3 Brief summary

The above test results show that membrane fouling can be reduced by the incorporation of rotating fluid flow on the surface of a filter membrane. This has some advantages over the alternatively strategy of rotating the membrane mechanically. These are principally the removal of the necessity of a mechanical seal operating under pressure, at high rotation speeds within particulate suspensions, and the easier application of this technique to narrow diameter membrane tubes. The last advantage is important when high values of membrane surface area per unit volume of space are required.

The use of a helical insert, instead of tangential inlet and outlet ports, also induced rotating flow, and is more attractive in terms of membrane surface area per unit volume. However, the helical insert did lead to an additional pressure loss due to fluid drag on the increased surface area inside the filter module, and therefore further improvement on the design is needed to optimize the advantages of this system.

The experimental results indicate that this technique is efficient in terms of the energy required for separation, with energy saving of as much as 20% or so.

CHAPTER 6

Conclusions and Recommendations

During crossflow microfiltration there are many resistances to the permeate flow, these were qualitatively described in § 1.7.1. A universal filtration theory that adequately accounts for the importance of each of these resistances in every filtration undertaken is unlikely to be developed. The filtration engineer has, therefore, to exercise some discretion over the mathematical modelling based on his observation of experimental data. In microfiltration film models, which were developed for ultrafiltration, are often found to be inapplicable. Cake filtration models are often found to be applicable but only when in-situ membrane and cake resistances can be calculated and, of course, when filter cakes are formed on the surface of the crossflow microfilter. If cakes are not formed, it may be possible to model the flux decay and equilibrium flux period by filter blocking models.

In this study a real process fluid, seawater, was filtered on several different types of microfiltration membranes. Manufacturers claimed that their membrane material would be superior to the others. This was not found to be the case, as all the membranes were prone to foul both internally and externally. External membrane fouling was by means of a cake which built up on the surface of the filter, such a deposit could be mechanically removed by backflushing with air or filtered water. Thus good average filtration flux rates could be maintained under such circumstances. After each backflush, however, a small amount of retained fines could enter the membrane thus long term flux decay is inevitable. Ensuring a surface only deposit with all membranes meant the use of filter aids to raise the suspended solids content of the seawater to one sufficient to initiate a cake. If a filter cake did not form on the filter surface, penetration of the membrane was possible with severe consequences on filtration performance.

The photographs of membranes used for seawater filtration by SEM showed that an organic material (lipid) acts as a binder on the inorganic debris. If such material enters the membrane structure, irreversible fouling follows. Hence there is a paradox that effective crossflow microfiltration is only possible when filtering concentrated suspensions of solid material, using periodic backflushing. This is quite the opposite of effective dead-end microfiltration on cartridge filters when rapid blocking and

increasing pressure drop occurs under such operating conditions. Crossflow micro-filtration was considered to be an improvement on cartridge filtration for seawater filtration duty and this is clearly the case only under the conditions described above. When filtering low suspended solids, cartridge filtration is preferable. Thus the two technologies are complementary: crossflow filtration at a very coarse particle size, say 3 to 10 microns, followed by fine filtration in cartridges. During an algae bloom period, the crossflow filters would protect the cartridge filters, during other periods the latter filter would perform adequately. The seawater filtration work demonstrated that crossflow membrane fouling could be due to particulates, organisms or a mixture of both, and could be effected inside or on top of the filter.

Modelling such a system is beyond the scope of present understanding of the process. Most theories predict the "equilibrium" flux rate and how it varies with operating conditions such as flow rate and transmembrane pressure. Few, if any, models consider the deposition of solids inside the membrane matrix. This was obviously a significant effect in the seawater filtration study. Some work on blocking models did exist for conventional filtration and for non-Newtonian fluid crossflow filtration, mainly due to Grace (1956) and Hermia (1982). An investigation of this was conducted using latex particles, prepared during this study, of various surface properties. The membrane studied was an acrylonitrile type (Versapor) of nominal rating between 0.45 and 1.2 microns. The actual pore opening sizes were in considerable excess of these nominal ratings and, therefore, internal blocking or fouling was apparent. The models, coupled with a mass balance on the deposited solids, were capable of modelling the flux decline period as well as the initial and equilibrium fluxes. Thus this approach is an important step forward when modelling filtration processes, involving low suspended solids concentrations, in which the flux decline period is a substantial part of the filtration cycle. The models show considerable promise but further work is needed to enable them to be applied with confidence and with minimal amount of laboratory testing. One noticeable factor which would assist in the full characterisation of the membrane material used would be the provision of a Coulter porometer. Such an instrument provides an effective pore size distribution of the membrane material and this could be very important when combined with the particle

size distribution of the fouling material. Such a facility was not available in this study, hence a nominal pore size was used in the modelling work and the results illustrated in Fig 53 could be improved if the above approach is adopted.

The Standard blocking model predicting flux decay described in Chapter 4 shows better accuracy when correlating the 0.45 μm membrane performance than the 1.2 μm membrane performance. One point worthy of note was that during the operation of the filter, the calibration of the flow and pressures were checked several times by switching off the permeate valve. This might have had the effect of dislodging particles which, presumably, is more likely with the coarser membranes. The calibration check was later found to be unnecessary and should not be repeated in future runs investigating the permeate decay period due to internal membrane fouling.

Backflushing has been shown to be an effective means of membrane cleaning when solids can be prevented from entering the membrane structure. Another mechanical means was investigated in Chapter 5, which should also have relevance to the filtration of suspensions of low solid content. The importance of a centrifugal force field on the filtration was shown to reduce the cake resistance and was, apparently, efficient in terms of energy consumption. The design and practical operation of such a technique probably limits it to filtration on the internal surface of a tubular crossflow microfilter. In this study it was used on the outer surface of such a filter, but a module containing only a limited number of tubes could be constructed. It is recommended that this technique be investigated further, but specially for the filtration of a dispersed phase lighter than the suspending medium.

Finally, as the membrane fouling can be due to chemical, physical, and biological means, it would be appropriate to test anti-fouling techniques which can combine these phenomena. For example, microfiltration incorporating rotating flow and electrical (DC) cleaning: the foulant is physically discouraged from entering the membrane and the periodic application of a DC field is used to generate a local acid environment within the membrane to chemically, or biochemically, remove the trapped species.

ALPHABETIC

A,a,b,B	the constants, their values varied according to the applied formulae
C	concentration ($kg \cdot m^{-3}$)
CF	crossflow
d	diameter (m)
D	diffusion coefficient ($m^2 \cdot s^{-1}$)
D/x	mass transfer coefficient represented by ***k*** later ($m^1 \cdot s^{-1}$)
D_e	eddy diffusivity function
(e/d)	equivalent roughness of the wall
f	Fanning friciton factor
F	force (N)
F_g	CP modulus C_g/C_b (in Eq 2.14b)
H	height (m)
ID	internal diameter (m)
J	flux rate [usually in ($m^3 \cdot m^{-2} \cdot hr^{-1}$)]
j_D	Colburn ***j*** factor (mass transfer in Eq 2.31)
k	mass transfer coefficient ($m \cdot s^{-1}$)
k_{cr}	crowding factor (the inverse of the maximum volume fraction of the particles in Eq 4.3)
k_d	distribution coefficient for the solute
L	length (m)
m	mass (kg)
m_b	number of bursts per unit area (m^{-2})
M	molecular weight ($kg \cdot mol^{-1}$)
MF	microfiltration
N	number of total particles one the surface at time T_t (m^{-2})
N_o	original number particles per unit area (m^{-2})
N_s	number of particles between bursts (m^{-2})
n	compressibility factor or power index of non-Newtonian fluid
Nu	Nusselt number
p	permeability (m^2)
P	applied pressure (Pa, Bar or psi)
Pr	Prandtl number
Q	permeate flow rate ($m^3 \cdot s^{-1}$)

q	compressibility factor (in Eq 2.21)
r	specific resistance (m^{-2})
r_h	half channel height (m)
R	gas constant
R	membrane resistance (with subscript) (m^{-1})
Re	Reynolds number
RO	reverse osmosis
s(C)	function of concentration C (in Eq 2.24)
s_o	original conditon of s(C) (in Eq 2.24)
S	surface area of the membrane (m^2)
S_a	pore area available for transporting particles (m^2)
S_B	fraction of surface cleared by turbulence burst (m^2)
Sc	Schmidt number
S(C)	sedimentation coefficient
S_D	total cross sectional area of the pore (m^2)
SEM	Scanning Electron Micrograph
Sh	Sherwood number
S_s/v_s	ratio of particle surface area to volume (specific surface) (m^{-1})
St	Stanton number
t	processing time (s)
T	absolute temperature (K)
TB	turbulent burst
T_t	set time interval in turbulent burst model (s)
U, u	axial flow velocity ($m \cdot s^{-1}$)
u_B	superficial liquid velocity ($m \cdot s^{-1}$)
U_{max}	maximum undisturbed fluid flow velocity at the entrance to a porous channel ($m \cdot s^{-1}$)
$\overline{U}$	average axial velocity ($m \cdot s^{-1}$)
UF	ultrafiltration
v	volume of the pore (m^3)
v_1, v_0	partial specific volumes of the solute and solvent
V	radial flow velocity ($m \cdot s^{-1}$)
W	volume of the permeate (m^3)
x	distance from the membrane or filter (m)
y	axial distance (m)
z	reflection coefficient in Eq 2.16 or distace or lateral distance in the turbulent burst model

SUPERSCRIPTS

+	normalized value
-	average
*	wall friction
·	rate
°	notes to $\Delta P - \Delta \Pi = 0$

SUBSCRIPTS

B	burst
b	bulk flow
C	centrifugal
c	cake layer
D	drag
e	equilibrium status
f	foulant
g	gel layer
h	equivalent hydraulic
L	lift force or velocity
l	boundary layer
latex	latex
m	membrane
o	original condition
pore	pore
r	ratio
rela	relative
s	particle
seed	latex seed
t	total or transmembrane
v	permeate
w	wall
W	van der Waals force
water	clean water
σ	surface tension force
ζ	zeta potential

GREEK

α	dimensionless funtion of n in Table 5b
β	parameter in equation 2.56c
γ	fluid shear rate at the membrane surface (s^{-1})
Δ	difference
μ	dynamic viscosity of the liquid (Pa•s)
δ	membrane or cake thickness (m)
σ	surface tension coefficient ($N•m^{-1}$)
κ	$2m^2/(m+1)(m+2)$ $m=f(F_g)$ (in Eq 2.14b)
$f\{\beta\}$	result of a numerical integration involving the undisturbed velocity profile and the Green's function.
τ	shear stress ($N•m^{-2}$)
η	efficiency
υ	partial molecular volume
ε	porosity
ρ	density ($kg•m^{-3}$)
Π	osmotic pressure (Pa)
λ	correction factor for the drag force on a spherical particle in a concentration suspension
ν	kinematic viscosity ($m^2•s^{-1}$)
θ	temperature in °C
ω	angular velocity ($rad•s^{-1}$)
ζ	zeta potential (V)

Abdel-Ghani M S, Jones R E, Wilson F G (1988) "Crossflow Membrane Filtration of Seawater" Filt & Sep Mar/Apr pp105-109

Afonso M D, Pinho M N (1991) "Membrane Separation Processes in Pulp and PaperProduction" Filt & Sep Jan/Feb pp42-44

Aggarwal J K, Hollinsworth M A, Mayhew Y R, (1972) "Experimental Friction Functions for Turbulent Flow with Suctions in a Porous Tube" Intl J Heat Mass Transfer, 15 pp1585-1602

Altena F W, Belfort G, (1984) "Lateral Migration of Spherical Particles in Porous Flow Channels: Application to Membrane Filtration" Chem Eng Commun, 39(2) pp343-355

Antonia R A (1981) "Conditional Sampling in Turbulent Measurement" Ann Rev Fluid Mech 13 pp131-156

Applegate L E, Sacklinger C T (1984) "Avoiding Iron Fouling in Reverse Osmosis Desalination Plants" Filt & Sepa Nov/Dec pp411-413

Asaadi M (1990) "Fouling Behaviour and Radioactive Retention Properties of Inorganic Crossflow Microfiltration Membrane" Ph D Thesis Dept. Chem. Eng., Feb., Imperial College, London.

Ashehov I (1925) "Preparation of Graded Collodion Membrane" C R Soc Bio 92 pp362-363

Bailey R (1991) "Porous Aluminium Membrane Technology" Filt & Sep Jul/Aug pp226

Baker R J, Fane A G, Fell C J D, Yoo B Y (1985) "Factors Affecting Flux in Crossflow Filtration" Desalination, 53 pp81-93

Baller H W , Porter M C (1980) "Selection of Microporous Membranes for Optimum Separation" Filt & Sep Jul/Aug pp347-352

Baranetzky J (1872) "Diosmotishe Untersuchunger" Pogg Ann 147 pp195-245

Bechhold H (1907) "Kolloidstudien mit der Filterationesmethode" Z Phys Chem 60 pp257-38

Bedwell W B, S F Yates, I M Drubaker, S Üban (1988) "Crossflow Microfiltration - Fouling Mechanisms Studies" Sep Sci & Tech 23(6 & 7) pp531-548

Belfort G (1986) "Fluid Mechanics and Cross-Flow Membrane Filtration" <<Advances in Solid-Liquid Separation>> pp165-189

Belfort G (1989) "Fluid Mechanics in Membrane Filtration: Recent Developments" J Membrane Sci 40 pp123-147

Belfort G, Altena F W (1983) "Toward an Inductive Understanding of Membrane Fouling" Desalination 47 pp105-127

Belfort G, Mark B (1979) "Artficial Particulate Fouling of Hyperfiltration Membrane - II Analysis and Protection from Fouling" Desalination 28(1) pp13-30

Belfort G, Nagata N (1985) "Fluid Mechanics and Crossflow Filtration: Some Thoughts" Desalination, 53 pp57-79

Bennett C, Myers J (1982) <<Momentum Heat and Mass Transfer>>, McGraw-Hill, New York, NY, pp560-587

Berman A S (1958) "Effects of Porous Boundaries on the Flow of Fluids in Systems with Various Geometries" Proc 2nd Intl Congr Peaceful Use of Atomic Energy, paper #P/720, pp351-358

Bernard M, Largeteau D (1990) "Selection of Membrane Structure: Comparative Performance of Micro Porous and Micro Perforated Membranes Tangential Flow Microfiltration of Skimmed Milk and Whey" Proceedings 5th World Filtration Congr v3 pp128-132 Nice, France

Bhattacharya I N, Das S C, Panda D (1988) "Settling and Filtration Characteristics of Manganese Nodule Leach Slurry" The Chem Engr J 38 pp143-148

Bhattacharyya D, Grieves R B (1979) "Charged Membrane Ultrafiltration of Heavy Metals from Non-Ferrous Metals" J Water Pollut Control Fed 51(1) pp176-186

Bhattacharyya D, Jumnwan A B, Grieves R B, Harris L R (1979) "Ultrafiltration Characteristics of Oil-Detergent-Water Systems: Membrane Fouling Mechanisms" Sep Sci & Tech 14(6) pp529-549

Bigelow S L, Gemberling A (1907) "Collodion Membranes" J Am Chem Soc 29 pp1576-1589

Bird R B, Stewart W E, Lightfoot E N (1960) <<Transport Phenomena>>, Wiley & Sons, New York, USA

Blake N J (1990) <<A Study of Crossflow Filtration Using Dilute Suspensions of Monodisperse Spherical Particles>> PhD Thesis University of London

Blatt W F, Dravid A, Michaels A S, Nelson L (1970) "Solute Polarization and Cake Formation in Membrane Ultrafiltration: Causes, Consequences, and Control Techniques" <<Membrane Science and Technology - Industrial, Biological, and Waste Treatment Processes>> pp47-97 Flinn J E ed., Plenum press, New York-London

Blosse P T (1982) "The New Attraction in Membrane Filters" Process Eng Sept., pp34-37

Bogard D G (1982) <<Investigation of Burst Structures in Turbulent Channel Flows through Simultaneous Flow Visualization and Velocity Measurement>> PhD Thesis Purdue University USA

Boonthanon S, Hwan L S Vigneswaran S Aim R B Mora J C (1991) "Application of Pulsating Cleaning Technique in Crossflow Microfiltration" Filt & Sep May/Jun pp199-201

Borre E, Zievers J F, Schmidt H (1988) " Apparatus for Particle Separation by Crossflow Filtration " US Patent 4741881 3 May 7p

Boudier G, Bauer J M, Alary J A (1990) "New Generations of Metal and Composite Porous Tubes" Proceedings 5th World Filtration Congr v1 pp118-122 Nice France

Bowen W R, Sabani H (1992) "Pulsed Electrokinetic Cleaning of Cellulose Nitrate Microfiltration Membrane" Ind Eng Chem Res 31(2) pp515-523

Brenner H (1966) "Hydrodynamic Resistance of Particles at Small Reynolds Nembers" Advan Chem Engng, 6 pp287-438

Brian P L T (1965) "Concentration Polarization in Reverse Osmosis Desalination with Variable Flux and Incomplete Salt Rejection" Ind & Eng Chem - Fundam 4(4) pp439-445

Brock T D (1983) "Membrane Filtration" Sci Tech, p40 Madison, Wis..

Brodkey R S, McKelvey K N, Hershey H C, S G Nychas (1978) "Mass Transfer at the Wall as a Result of Coherent Structures in a Turbulently Flowing Liquid" Intl J Heat Mass Transfer, 21 pp593-603

Brosh A, Winograd Y (1974) "Experimental Study of Tubulent Flow in a Tube with Wall Suction" paper No 74-HT-BB J Heat Transfer v96 Ser C n3 Trans ASME, Aug pp338-342

Brown W (1915) "On the Preparation of Collodion Membranes of Differential Permeability" Biochem J 9 pp591-617

Brown W (1917) "Further Contributions to the Technique of Preparing Membranes for Dialysis" Biochem J 11 pp40-57

Bundy R D, Weissberg H L (1970) "Experimental Study of Fully Developed Laminar Flow in a Porous Pipes with Wall Injection" Physics of Fluids, 13pp2613-2625

Butcher C (1990) "Microfiltration" The Chem Engr Feb. 469 pp50-53

Cabassud C, Aim R B (1986) "Evaluation of a Membrane Bioreactor with a Crossflow Microfiltration Unit" 3rd World Cong of Chem Eng pp288-291

Calderbank P H, Moo-Young M B (1961) "The Continuous Phase Heat and Mass Transfer Properties of Dispersions" Chem Eng Sci, 16 pp39-54

Campbell J A, Hanratty T J (1982) "Mass Transfer between a Turbulent Fluid and a Solid Boundary: Linear Theory" AIChE J, 28 pp988-993

Campbell J A, Hanratty T J (1983) "Mechanism of Turbulent Mass Transfer at a Solid Boundary" AIChE J, 29 pp215-229

Carlberg B L (1979) "How to Treat Seawater for Injection System" J Pet Tech June pp67-71

Carter A J (1982) "An Experimental Study of Crossflow Filtration and the Design of a Prototype Crossflow Filter" M Phil Thesis Loughborough University of Technology

Carter J W, Hoyland G (1976) "Build up of Rust Fouling Layers on Membrane in Reverse Osmosis Flow Systems and Its Calculation" 5th Intl Symp on Fresh Water from the Sea v4 pp21-29 16-20 May, Alghero Italy

Cartwright P S (1985) "Membrane Fouling - Causes and Remedial Action " << Particle and Multiphase Processes>> v2 pp140-143 Contamination Analysis & Control, Proceedings of Intl Symp Worksho Miami U S A

Cartwright P S "Membrane Technologies for Pollution Control - A System Primer" FilTech '91 pp105-125 Karlsruhe Germany

Castino F, Friedman L I, Solomon B A, Colton C K, Lysaght M J (1978) "The Filtration of Plasma from Whole Blood: A Novel Approach to Clinical Detoxification" <<Artificial Kidney, Artificial Liver, and Artificial Cells>> p489 Chang T M ed, Plenum, New York

Charpin J, Bergez P, Vain F, Barnier H, Maurel A, Martinet J M (1988) "Inorganic Membranes: Preparation, Characterization, Specific Applications" Ind Ceramics 8(1) pp23-27

Chatterjee S G, Belfort G (1986) "Fluid Flow in an Idealized Spiral Wound Membrane Module" J Membrane Sci 28(2) pp191-208

Cheryan M (1980) <<UF Membrane & Applications, Polymer Sci & Tech>>, Vol 13 Plenum Press p343

Cheryan M, Nichlos D J (1980) "Food Process System" in <<Food Process Engineering>> pp572-577 P Link et al ed. Appli Sci Pub Ltd , London

Chien S, Lose S A, Bryan C A (1971) "Hemolysis during Filtration through Micropores: A Scanning Electron Microscope and Hemorheologic Correlation" Microvascular Research 3(2) pp183-203

Chilton T H, Colburn A (1934) "Mass Transfer (Absortion) Coefficients Prediction from Data on Heat Transfer and Fluid Frictions" Ind Eng Chem, 26 pp1183-1187

Chudacek M W, Fane A G(1984) "The Dynamics of Polarization in Unstirred and Stirred Ultrafiltration" J Membrane Sci, 21 pp145-160

Churchill S W (1977) "Comprehensive Correlating Equations for Heat Mass and Momentum Transfer in Fully Developed Flow in Smooth Tubes" IEChE Fundam, 16(1) pp109-116

Clark A, Markland E (1971) "Flow Visualization in the Turbulent Boundary Layer" J Hydr Div ASCE 97 (Part II) pp1653-1664

Cleaver J W, Yates B (1973) "Mechanism of Detachment of Colloidal Particles from a Flat Substrate in a Turbulent Flow" J of Colloid and Interface Sci 44(3) pp464-474

Cleaver J W, Yates B (1976) "The Effect of Re-Entrainment on Particle Deposition" Chem Eng Sci 31 pp147-151

Cowieson D (1992) "Composite Membrane for Cost-Effective Large Applications" Filt & Sep Sept/Oct pp381-384

Cox R G, Brenner H (1968) "The Lateral Migration of Solid Particles in Poiseuille Flow - I Theory" Chem Engng Sci, 23 pp147-173

Cox R G, Mason S G (1971) "Suspened Particles in Fluid Flow through Tubes" Ann Rev Fluid Mech, 3 pp291-316

Cubine J K, Randolf S G (1973) "Offshore Treating Facilities for Seawater Injection" Petroleum Engr Aug pp38-40

Culkin B, Armando A D (1992) "New Separation System Extends the Use of Membranes" Filt & Sep Sept/Oct pp376-378

Cumming I W, Holdich R G, Freund M "The Filtration of Slurries Using Crossflow Microfiltration " FilTech '91 pp41-49 Karlsruhe, Germany

Dahlheimer J A, Thomas D G, Kraus K A (1970) "Hyperfiltration Application of Woven Fiber Hoses to Hyperfiltration of Salts and Crossflow Filtration of Suspended Solids" Ind Eng Chem Proc Des Dev 9(4) pp566-569

Davidson A P, Thomas M P, Azubike D C, Gallagher P M (1990) "Novel Ceramic/Metal-Mesh Composite Inorganic Membrane Filters" Proceedings 5th World Filtration Congr v3 pp235-241 Nice, France

Davies J C "Membranes in Chromatography" The 1987 5th Annual Membrane Technology/Planning Conf pp408-422 21-23 Oct Cambridge, Matt., USA

Davis M A, Jones A G, Trindale H (1974) "A Rapid and Accurate Method for Sizing Radiocolloids" J Nuclear Medicines 15(11) pp923-928

Davis R H, Birdsell S A (1987) "Hydrodynamic Model and Experiments for Crossflow Microfiltration " Chem Eng Comm 49 pp217-234

Davis R H, Sherwood J D (1990) "A Similarity Solution for Steady-State Crossflow Microfiltration" Chem Eng Sci 45(11) pp3203-3209

de Bruyne R "A New Series of Metal Fibre Filter Media" FilTech Europa'89 pp18-25 Karlsruhe, Germany

de Bruyne R, Verschaeve R (1990) "New Developments with Sintered Metal Fibre Porous Structure as Filter Media Membrane Supports" Proceedings 5th World Filtration Congr v1 pp123-133 Nice France

Deissler R G, Taylor M F (1959) "Analysis of turbulent Flow and Heat Transfer in Noncircular Passages" NASA Tech Report n R-31 18p

Dejmek P, Funeteg B, Hallstrom B, Winge L (1974) "Turbulence Promoters in Ultrafiltration of Whey Protein Concentrate" J Food Sci 39 pp1014-1017

Dejmek P (1975) "Concentration Polarization in Ultrafiltration of Macromolecules" Ph D Thesis, Univ of Lund, Sweden

Drioli E, Molinari R (1990) "Membrane Processing of Musts, Wines and Alcoholic Beverages" Proceedings 5th World Filtration Congr v1 pp50-57 Nice France

Druin M L, Loft J T, Plovan S G (1974) "Novel Open-Celled Microporous Film" US Patent 3801404 2 Apr

Ebner H (1981) "Continuous Microfiltration of Vinegar" Chem Ing Tech 53(1) pp25-31

Eckstein E C, Bailey D G, Shapiro A H (1977) "Self-Diffusion of Particles in Shear Flow of a Suspension" J Fluid Mech 79(1) pp191-208

Edyvean R G J, Sneddon A D (1985) "The Filtration of Plakton from Seawater" Filt & Sep May/Jun pp184-189

Edyvean R G J, Lynch J L (1989) "The Effect of Organic Fouling on the Life of Cartridge Filters" Filtech'89 pp10-17 Karlsruhe, Germany

Eggereth A H (1921) "The Preparation and Standarization of Collodion Membrane" J Biol Chem 48 pp203-221

Einstein H A, Li H (1956) "The Viscous Sublayer along a Smooth Boundary" J Eng Mech, Div Soc Civil Eng, 82, EM2(Apr) pp293

Elford W J (1931) "A New Series of Graded Collodion Membranes Suitable for General Bacteriological Use, Especially in Filterable Virus Studies" J Pathol Bacteriol 34 pp505-521

Eriksson P (1980) Ph D Thesis, Chem Eng Dept, Lund Univ, Sweden

Fane A G, Fell C J D, Nor M T (1982) "Ultrafiltration in the Presence of Suspended Matter" <<IChemE Symp Ser 73>> C1

Fane A G (1984) "Ultrafiltration of Suspensions" J Membrane Sci, 20(1984) pp249-259

Fane A G, Fell C J D, Hodgson P H H, Leslie G, Marshall K C (1991) "Microfiltration of Biomass and Biofluids : Effects of Membrane Morphology and Operating Conditions" Filt & Sep Sep/Oct pp332-340

Faxén H (1922a) Ark Mat Astron Fusik 17 p27

Faxén H (1922b) "The Resistance to Motion of a Solid Sphere in a Viscous Liquid Enclosed between Parallel Walls" Ann Physik 68 pp89-119

Férry J D (1936) "Ultrafilter Membranes and Ultrafiltration" Chem Revs 18 pp373-455

Fick A (1895) "Üeber Diffusion" Pogg Ann 94 pp59-86

Finningan S M, Howell J A (1989) "The Effect of Pulsatile Flow on Ultrafiltration Fluxes in a Baffled Tubular Membrane System" Chem Eng Res Des 67 pp278-282

Fleischer R L, Price P B, Walker R M (1963) "Methods of Forming Fine Holes of Near Atomic Dimensions" Rev Sci Instr 34 pp510-512

Fleischer R L, Price P B, Symes E M (1964) "A Novel Filter for Biological Studies" Science 143 pp249-250

Fleischer R L, Price P B, Walker R M (1969) "Nuclear Tracks in Solids" Sci Amer 220 p30

Flottmann T, Tretzel J (1990) "Micro/Ultrafiltration Membranes with a Fixed Pore Size Formed through Irradiation with Pulsed Laser and Process for Manufacturing the Same" US Patent 4923608 8 May 11p

Forström R J, Bartelt K, Blackshear P L Jr, Wood T (1975) "Formed Elements Deposition onto Filtering Walls" Trans Am Soc Artif Intern Organs, 21 pp602-607

Freeman M P (1976) <<Colloid and Interface Science>> Vol 5 p133 Academic Press

Galowin L S, Desantis M J (1971) "Theoretical Analysis of Laminar Pipe Flow in a Porous Wall Cylinder" J of Dynamic Systems., Measurement and Control, Trans ASME, Ser G. 93 June, pp102-108

Galowin L S, Fletcher L S, DeSantis M J (1974) "Investigation of Laminar Flow in a Porous Pipes with Variable Wall Suctions" AIAA J, 12(11) pp1585-1589

Gekas V, Hallström B (1987) "Mass Transfer in the Membrane Concentration Polarization Layer under Turbulent Cross Flow - 1 Critical Literature Review and Adaptation of Existing Sherwood Correlations to Membrane Operations" J Membrane Sci, 30 pp153-170

Gelman C (1965) "Microporous Membrane Technology: Part I. Historical Development and Applications" Anal Chem 37(6) pp29-34

Gilliand E, Sherwood T (1934) "Diffusion of Vapors into Air Streams" Ind Eng Chem, 26 pp516-523

Gillot J, Brinkman G, Garcera D (1984) "New Ceramic Filter Media for Crossflow Microfiltration and Ultrafiltration" Filtra'84 Conference, Paris

Gillot J, Garcera D, Soria R, Brinkman G (1990) "New Developments in the Membralox Micro- and Ultrafiltration Membranes" Proceedings 5th World Filtration Congr v1 pp155-158 Nice France

Gnielinski V (1975) "Neue Gleichungen für den Wärme- und den Stoffübergang in Turbulent Durchströmten Rohren und Kanälen" Forsch. Ind-Wes., 41(1) pp8-16

Goetz A (1947) "Materials, Techniques, and Testing Methods for the Sanitation (Bacterial Decontamination) of Small-Scale Water Supplies in the Field Used in Germany during and after the War" Final Report 1312, Joint Intelligience Objectives Agency, Washington, D C

Goetz A, Tsuneishi N (1951) "Application of Molecular Filter Membranes to the Bacteriological Analysis of Water" J Am Water Works Assoc., 43(12) pp943-967

Goldsmith R L (1971) "Macromolecular Ultrafiltration with Microporous Membranes" Ind Eng Chem Fundam, 10(1) pp113-120

Goldsmith H L, Mason S G (1967) "The Microrheology of Dispersions" <<Rheology - Theory and Applications>>, Vol 4 pp86-250 Eirich F R ed Academic press, New York, USA

Goodwin J W, Hearn J, Ho C C, Ottewill R (1974) "Studies on the Preparation and Characterisation on Monodisperse Polystyrene Latixes" Coll Polym Sci 252 pp464-471

Gore R W (1976) "Process for Producing Porous Products" US Patent 3953566 27 April

Gore R W (1976) "Very Highly Stretched Polytetrafluoroethylene and Process therefore" US Patent 3962153 8 June

Grabska-Winnicka D, Winnicki T (1991) "Membrane Separation in Biological Sewage Treatment Processes" Desalination 83 p243

Grace H P (1956) "Structure and Performance of Filter Media" AIChE J 2 (3) pp307-336

Graetz L (1885) "Über die Wärmeleitungsfähikeit von Flüssigkeiten" Ann de Physik, 25 pp335-337

Grass A J (1971) << Structural Features of Turbulent Flow over Smooth and Rough Boundaries >> J Fluid Mech 50(2) pp233-255

Green G, Belfort G (1980) "Fouling of Ultrafiltration Membrane: Lateral Migration and the Particle Trajectory Model" Desalination, 35 pp129-147

Greiner G (1986) "Membrane Process for Boiler Feedwater Treatment: State of Development" VGB Kraftwerkstechnik 66(4) pp395-399

Gröber H, Erk S, Grigull V (1961) <<Fundanmentals of Heat Transfer>>, McGraw-Hill, New York, NY, p233

Gutman R G (1977) "The Design of Membrane Separation Plant" The Chem Engr July pp510-523

Gutman R G (1987) <<Membrane Filtration - The technology of Pressure-Driven Crossflow Processes>> Adam Hilger, Bristol, UK

Haarstrick A, Rau U, Wagner F (1990) "Crossflow Filtration as a Method of Separating Fungal Cells and Purifying the Polysaccharide Produced" Proceedings 5th World Filtration Congr v1 pp342-347 Nice, France

Hanemaaijer J H (1985) "Microfiltration in Whey Processing" Desalination 53 pp143-155

Hannah O T, Sandall O C (1972) "Developed Turbulence Transport in Ducts for Large Prandtl or Schmidt Numbers" AIChE J, 18 pp527-533

Hannah O T, Sandall O C, Mazet P R (1981) "Heat and Mass Transfer in Turbulent Flow under Conditions of Drag Reduction"" AIChE. J, 27(4) pp693-697

Happel J, Brenner H (1965) <<Low Reynolds Number Hydrodynamics>> Prentice-Hall, Englewood Cliffs, N J U S A

Harriott P (1962) "A Review of Mass Transfer to Interface" Can J Chem Eng, Apr pp60-69

Harriott P, Hamilton R M (1965) "Solid-Liquid Mass Transfer in Turbulent Pipe Flow" Chem Eng Sci, 20 pp1073-1078

Hayes J F, Dunkerley J A, Muller L L, Griffin A T (1974) "Studies on Whey Processing by Ultrafiltration II - Improving Permeation Rates by Preventing Fouling" Austr J Dairy Tech 29(3) pp132-140

Henry J D Jr (1972) "Cross Flow Filtration" in Recent Development in Separation Science, Vol II, pp205-225 Lin NN ed., Chem Rubber Company, Ohio, USA

Hermia J (1982) "Constant Pressure Blocking Filtration Laws - Application to Power-Law Non-Newtonian Fluids" Trans IChemE, 60 pp183-187

Hiddink J, de Boer R, Nooy P F C (1980) "Reverse Osmosis of Dairy Liquids" J Dairy Sci 63 pp204-214

Ho B P, Leal L G (1974) "Inertial Migration of Rigid Spheres in Two-Dimensional Unidirectional Flows" J Fluid Mech, 65(2) pp365-400

Holdich R G, Boston J S (1990) "Microfiltration Using a Dynamically Formed Membrane" Filt & Sep May/Jun pp184-187

Holdich R G, Zhang G M, Boston J S (1990) "Crossflow Filtration of Seawater" Proceedings 5th World Filtration Congr v1 pp518-522 Nice, France

Holdich R G, Zhang G M (1991) "Seawater Crossflow Filtration" Filtech'91 pp19-27 Karlsruhe, Germany

Hoogland M R, Fell C J D, Fane A G, Jones D A R (1990) "The Optimun Design of Crossflow Filtration Elements for Mineral Slurry Processes" Proceeding 5th World Filtration Congr v1 pp604-610 Nice, France

Hopfenberg H B, Palmer J A, Felder R M (1973) "Specific Solute-Membrane Interactions Producing Flux-Limiting Effects with Ultrafiltration Membranes" 166th National Meeting of American Chemical Society, Aug 27-31 Chicago, USA

Howell J A, Velicangil O (1980) "Theoretical Considerations of Membrane Fouling and Its Treatment with Immobilized Enzymes for Protein Ultrafiltration" in <<Polymer Science and Technology>>, 13 pp217-229 A R Cooper ed.

Hsieh H P, Bhave R R, Fleming H L (1988) "Microporous Alumina Membranes" J Membrane Sci 39 pp221-241

Hunt J W, Treffry-Goalley K, Flemmer R L C, Raal J D, Buckley C A (1987a) "A Mathematical Model of Steady-State Crossflow Microfiltration in a Woven Hose Support" Desalination 61 pp187-200

Hunt J W, Brouckert C J, Raal J D, Treffry-Goalley K, Buckley C A (1987b) "The Unsteady-State Modelling of Crossflow Microfiltration" Desalination 64 pp431-442

Hughmark G A (1971) "Heat and Mass Transfer for Turbulent Pipe Flow" AIChE J 17(4) pp902-909

Ishii K, Hasimoto H (1980) "Lateral Migration of a Spherical particle in Flows in a Circular Tube" J Phys Soc Japan, 48(6) pp2144-2155

Jackson J M, Landolt D (1973) "About the Mechanism of Formation of Iron Hydroxide Fouling Layers on Reverse Osmosis Membranes" Desalination 12 pp361-378

Jaffrin M Y, Gupta B B, Blanpain P (1990) "Membrane Fouling Control by Back-flushing in Microfiltration with Mineral Membranes" Proceedings 5th World Filtration Congr v1 pp479-483 Nice, France

Jaouen P, Bothorel M, Quéméneur F (1990) "Membrane Processes Utilizations in Fishing Industries and Aquacultural Farming" Proceedings 5th World Filtration Congr v1 pp523-535 Nice, France

Japanese Patent Application "Manufacturing of Microfiltering Materials" (Kokai Tokyo Koho) 61-111102 29 May, (1986) 3p

Johnson J N (1986) "Crossflow Microfiltration Using Polypropylene Hollow Fibers" Fluid Filt: Liquid Vol II, ASTM STP 975 pp15-26

Johnson Jr J S et al (1966) in <<Principle of Desalination>> Chpt 8 p345 Academic, New York

Jonsson G, Kristensen S (1980) "Membrane Filtration of NSSC-Waste Liquor" Desalination 32(1-3) pp327-339

Jonsson G (1984) "Boundary Layer Phenomenon during Ultrafiltration of Dextran and Whey Protein Solutions" Desalination 51 pp61-77

Kaiser D (1983) "Filtration of Injection Fluids" Oil, Gas & Petroleum Equipment July pp16-26

Karnis A, Goldsmith H L, Mason S G (1966) "The Kinetic of Flowing Dispersions: I. Concentrated Suspensions of Rigid Particles" J Coll Interface Sci, 22 pp531-553

Karnis A, Goldsmith H L, Mason S G (1966) "The Flow of Suspensions through Tubes V - Inertial Effects" Can J Chem Eng 44(1966) pp181-193

Karpov I N, Zhuzhikov V A (1981) " Mathematical Description of a Process for Separation of Suspensions by Filtration " Theo Found Chem Eng 15(1) pp79-83

Kavanagh P R, Brown D E (1987) "Crossflow Separation of Yeast Cell Suspensions Using a Sintered Stainless Steel Filter Tube" J Chem Tech Biotechnol 38 pp187-200

Kawase Y, Ulbrecht J J (1982) "Turbulent Heat and Mass Transfer in Dilute Polymer Solutions" Chem Eng Sci, 37 pp1039-1046

Kawase Y, Ulbrecht J J (1983) "Turbulent Heat and Mass Transfer in Non-Newtonian Pipe-flow: a Model Based on the Surface Renewal Concept" PCH Physico-Chemical Hydrodynamics, 4(4) pp351-368

Kawase Y, De A (1984) "Turbulent Heat and Mass Transfer in Newtonian and Dilute Polymer Solutions Flowing through Rough Pipes" Intl J Heat Mass Transfer, 27(1) pp140-142

Kays W M (1966) Convective Heat and Mass Transfer, p171 McGraw-Hill, New York NY,

Kesting R E (1971) <<Synthetic Polymer Resins>> pp12-52, 227-270 McGraw-Hill Book Co., NY, USA

Kesting R E (1981) <<Synthetic Polymer Resins>> pp98-104 2nd ed., Puropore, Inc., Tustin Calif., USA

Kilham O "Wine Separation: Membrane, Application" The 1987 5th Annual Membrane Technology/Planning Conf pp190-198 21-23 Oct Cambridge USA

Kimura S, Nakao S I (1975) "Fouling of Cellulose Acetate Tubular Reverse Osmosis Modules Treating the Industrial Water in Tokyo" Desalination 17(3) pp267-288

Kiviniemi L (1972) "A Method for Determing the Number of Stages Required in a Cascade Ultrafiltration Process" Meijeritiet Aikak, 31 pp70-105

Klein W (1982) "Crossflow Microfiltration - a Membrane Process for Concentration of Suspensions" Filt & Sep Mar/Apr pp130-134

Klein W, Hoelz W (1982) "Crossflow Microfiltration in Chemical Processes" The Chem Engr Oct pp369-373

Knibbs R H (1981) "The Development of a High Flux Microfilter with a Wide Range of Applications" FilTech Conf'81, London, U.K.

Knibbs R H (1984) << The Decontamination of α Bearing Waste Streams Using Coprecipitation with Ferric Hydroxide in Conjunction with Ultrafiltration >> AERE-R 10269 Oct.

Koglin B (1985) "Influence of Agglomeration of Filterability of Suspensions " Ger Chem Eng 8 pp217-223

Krieger I M (1972) "Rheology of Monodisperse Latices" Adv Coll Intl Sci 3 p111-136

Kroner K H, Schutte H, Hustedt H, Kula M R (1984) "Crossflow Filtration in the Downstream Processing of Enzymes" Process Biochemistry Apr pp67-74

Lafaille J P, Sanchez V, Mahenc J (1987) "Mass Transfer in Hollow Fiber Ultrafiltration Modules" Intl Chem Eng 27(2) pp258-267

Le M S, Ward P S (1984) "Membrane Techniques and Application in Downstream Processing" Solid-Liquid Separation Practice and the Influence of New Techniques, Leeds (U.K.) 2-5 April

Le S, Howell J A (1984) "An Alternative Model for Ultrafiltration" Chem Eng Res Dev 62 pp373-380

Leal L G (1980) "Particle Motions in a Viscous Fluid" Ann Rev Fluid Mech, 12 pp435-476

Lee C R (1977) PhD Thesis, The Ohio State Univ.

Lee D N, Merson R L (1976) "Chemical Treatments of Cottage Cheese Whey to Reduce Fouling of Ultrafiltration Membrane" J Food Sci 41(4) pp778-786

Leighton D T, Acrivos A (1987) "Measurement of the Shear-Indused Coefficient of Self-Diffusion in Concentrated Suspensions of Spheres" J Fluid Mech 177 p109-133 Chem Eng Sci 41(1986) pp1377-1384

Leonard E F, Vassilief C S (1984) "The Deposition of Rejected Matter in Membrane separation Process" Chem Eng Comm 30 pp209-217

Leveque M A (1928) "Les Lois de la Transmission de la Chaleur par Convection" J Ann Mines 13 pp201-299, 305-362, 381-415

Levich V G (1962) <<Physicochemical Hydrodynamics>>, Prentice Hall, New Jersey

Light W G, Tran T V (1981) "Improvement of Thin-Channel Design for Pressure-Driven Membrane Systems" Ind Eng Chem Proc Des Dev 20 pp33-40

Lin C S, Moulton R W, Putnam G L (1953) "Mass Transfer between Solid Wall and Fluid Streams" Ind Eng Chem, 45(3) pp636-646

Lin I J (1990) "Membrane Performance under the Influence of Magnetic Pretreatment" Proceedings 5th World Filtration Congr v1 pp503-506 Nice, France

Lu W M, Ju S C (1989) "Selective Particle Deposition in Crossflow Filtration" Sep Sci & Tech 24(7 & 8) pp517-540

Madsen R F (1977) <<Hyperfiltration and Ultrafiltraion in Plate and Frame System>> Elsevier Sci Pub Co, New York

Mahenc J, Lafaille J P, Sanchez V (1986) "Estimation of the Performance of Hollow Fiber Ultrafiltration Modules" Intl Ch E, 26(4) pp660-670

Mason E A Lonsdale H K (1990) "Statistical-Mechanical Theory of Membrane Transport" J Membrane Sci 51 pp1-81

Mason E A (1991) "From Pig Bladders and Cracked Jars to Polysulfones: An Historical Perspective on Membrane Transport" J Membrane Sci 60 pp125-145

Matteucci O H, Cima A (1845) "Memoire sur l'endosmose" Ann. Dhim. Phys. 13 pp63-86

Matthews M E (1978) "Performance Characteristics of a Plate and Frame System for Ultrafiltration of Sulphuric Acid Casein Whey" N Z J of Dairy Sci & Tech, 13 pp37-42

Meek R L, Baer A D (1970) "The Periodic Viscous Sublayer in Turbulent Flow" AIChE., 16 pp841-848, p1100

Meunier J P (1990) "Use of Cross Flow Filtration for Processing Beer Yeast and Tank Bottoms" Proceedings 5th World Filtration Congr v1 pp26-28 Nice, France

Metzner A, Friend P (1959) "Heat Transfer to Turbulent Non-Newtonian Fluids" Ind Eng Chem, 51 pp879-882

Michaels A S (1968) " New Separation Techniques for the CPI" Chem Eng Prog 64(12) Dec., pp31-43

Michaels A S (1968) <<Progress in Separation & Purification>> pp234-248 Wiley, New York

Michaels A S, "New Horizons for Membrane Technology" The 1987 5th Annual Membrane Technology/Planning Conf pp336-355 21-23 Oct Cambridge, USA

Mikhlin J A, Weber M E, Turkson A K (1982) "Electrically-aided axial Filtration" J Sep Proc Tech 3(1) pp16-24

Milisic V, Bersillon J L (1986) "Anti-Fouling Techniques in Crossflow Microfiltration" Filt & Sep Nov/Dec pp347-349

Minneci P A, Paulson D J (1988) "Molecularly - Bonded Metal Microfiltration Membrane" J Membrane Sci 39 pp273-283

Mitchell R W (1978) "The Forties Field Seawater Injection System" J Pet Tech June pp877-884

Mitchell R W, Finch E M (1981) "Water Quality Aspects of North Sea Injection Water" J Pet Tech June pp1141-1152

Mizushina T, Ogino F, Oka Y, Fukuda H (1971) "Turbulent Heat and Mass Transfer between Wall and Fluid Streams of Large Prandtl and Schmidt Numbers" Intl J Heat Mass Transfer 14 pp1705-1716

Mueller G (1947a) "Lactose-Fuchsin Plate for Detection of Coli in Drinking Water by Means of Membrane Filters" Z Hyg Infektionskr 127 pp187-190

Mueller G (1947b) "Eine Trinkwassergebundene Ruhrepidemie" Zentralbl Bakteriol Parasitenkd Infektionskr Hyg Abt I Orig 152 pp133-135

Muller L L, Hayes J F, Griffin A T (1973) "Studies on Whey Processing by Ultrafiltration. I. Comparative Performance of Various Ultrafiltration Modules on Whey from Hydrochloric Acid Casein and Cheddar Cheese" Austr J Dairy Tech 28(2) pp70-77

Murkes J, Carlsson C G (1988) <<Crossflow Filtration>> Wiley, Chichester, UK

Nakao S, Nomura S, Kimura S (1990) "Transport Phenomena of the Crossflow Microfiltration Process" Proceeding 5th World Filtration Congr v1 pp564-570 Nice, France

Nakashima T, Shimizu M (1989) "Microfiltration of Oil in Water Emulsion by Porous Glass Membrane" Kagaku Kogaku Ronbunshu 15(3) pp638-644

Noël R, Fermier P (1990) "Integrated Unit Operation Combination to Obtain High Purity Proteins and Pharmaceutical Lactose" Proceedings 5th World Filtration Congr v1 pp468-472 Nice, France

Abbe' Nollet (1748) "Lecons de Physique Experimentale" Hippolyte - Louis Gurein and Louis -Francois Pelatour, Paris

O'Neill M E (1968) <<A Sphere in Contact with a Plane Wall in a Slow Linear Shear Flow>> Chem Eng Sci 23 pp1293-1298

Nonaka M (1986) "A Macro-Kinetic Approach to Membrane Microfiltration" Filtech Conf 86 pp11.49-11.56

Nonogami T, Akimoto N, Shishido M, Hirukawa H (1986) "Liquid Permeation Method" Japanese Patent Application 61-129007 17 June 4p

Notter R H, Sleicher C A (1971) "The Eddy Diffusivity in the Turbulent Boundary Layer near a Wall" Chem Eng Sci, 26 pp161-171

Ogasawara K, Yoshida R, Sakai K (1991) "Effects of Hematocrit on Filtrate Flux of Microporous Glass Membrane for Bovine Blood" J Chem Eng of Japan 24(1) pp118-120

Oliver D R (1962) "Influence of Particles on Radial Migration in the Poiseulle Flow of Suspensions" Nature, 194 pp1269-1271

Ostermann A E (1986) "Advances in Crossflow Microfiltration" Filtech Conf pp11.25-33

Pain A T, Moulin C, Faivre M, Bourbigot M M, Rumeau M (1990) "Iron Removal in Groundwater by Crossflow Micro- and Ultrafiltration" Proceedings 5th World Filtration Congr v1 pp29-35 Nice, France

Palmer J A, HopfenbergH B, Felder R M (1973) "Effluent of Solute-Membrane Interactions on Flux - Limiting Concentration Polarization in Ultrafiltration Processing" J Colloid & Interface Sci 45(2) pp223-234

Paulson D J "An Overview of and Definitions for Membrane Fouling" The 1987 5th Annual Membrane Technology/Planning Conf pp103-123 21-23 Oct Cambridge, USA

Peri C, Setti D (1976) "Whey and Skimmilk Ultrafiltration I - Parameters Affecting Permeation Rate in Sweet Whey Ultrafiltration" Milchwissenschaft, 31(3) pp135-139

Peters T A, Pedersen F S (1990) "MEMCOR - Crossflow Microfiltration with Gas-Backwashing Design and Different Applications for a New Technical Concept" Proceedings 5th World Filtration Congr v1 pp473-478 Nice, France

Pillay V I, Brouckaert C J, Buckley C A, Raal J D (1989) "Predicted Performance Profiles along a Long-Tube Crossflow Microfiltration System" Desalination 71 pp247-264

Pinczewski W, Sideman S (1974) "A Model for Mass (Heat) Transfer in Turbulent Tube Flow: Moderate and High Schmidt (Prandtl) Numbers" Chem Eng Sci, 29 pp1969-1976

Porter J, Billiet C T (1986) "Developments in UK Membrane Technology" Filt & Sep Jul/Aug pp232-235

Porter M C (1972) "Concentration Polarization with Membrane Ultrafiltration" Ind Eng Chem Prod Res Develop, 11(3) pp234-248

Porter M C (1975) "Selecting the Right Membrane" Chem Eng Prog 12(71) pp55-61

Porter M C (1986) "Pressure-Driven Membrane Filtration - A Historical Perspective" 3rd World Cong of Chem Eng, pp451-471

Poyen S, Quemeneur F, Bariou B (1987) "Improvement of the Flux of Permeate in Ultrafiltration by Turbulence Promotors" Intl Chem Eng 27(3) pp441-447

Probstein J R F, Shen J S, Leung W F (1978) "Ultrafiltration of Macromolecular solutions at High Polarization in Laminar Channel Flow" Desalination, 24 pp1-16

Punidadas P, Decloux M (1990) "Experimental Results of Purification of Sugar Solutions by Crossflow Microfiltration on Mineral Membrane" Proceedings 5th World Filtration Congr v3 pp284-291 Nice, France

Rashidi M, Hetsroni G, Banerjee S (1990) << Particle-Turbulence Interaction in a Boundary Layer >> Intl J Multiphase Flow 16(6) pp935-949

Rautenbach R, Holtz H (1980) " Effect of Concentration Dependence of Physical Properties on Ultrafiltration " Ger Chem Eng 3 (1980) pp180-185

Rautenbach R, Schock (1988) "Ultrafiltration of Macromolecular Solutions and Crossflow Microfiltration of Colloidal Suspensions - A Contribution to Permeate Flux Calculations" J Membrane Sci 36 pp231-242

Rivet P (1979) <<Societe Francaise de Filtration Guide de la Separation Liquide-Solide>> Idexpa ed.

Rogers C B, Eaton J K (1989) "The Interaction between Dispersed Particles and Fluid Turbulence in a Flat Plate Turbulent Boundary Layer in Air" Report MD-52 Stanford Univ.

Rubinow S I, Keller J B (1961) "The Transverse Force on a Spinning Sphere Moving in a Viscous Fluid" J Fluid Mech, 11 pp447-459

Ruckenstein E (1967) "On Solid-Liquid Mass Transfer in Turbulent Pipe Flow" Chem Eng Sci pp474-476

Rushton A, Aziz R (1984) " Crossflow Microfiltration of Slurries " <<Solids/Liquids Sepa. Prctice & the Influence of New Techniques>> pp1-15 The Filtr Soc, 2-5 Apr, IChE Yorkshire, UK

Rushton A, Zhang G S (1988) "Separation of Fine Particles from Liquids by Moving Microporous Membrane" PARTEC'88 pp1-19 7-9 Sept Malaysia

Sabuni H A M (1990) PhD Thesis, Univ College of Swansea. UK

Saffman P G (1956) "On the Motion of Small Spheroidical Particles in a Viscous Liquid" J Fluid Mech, 1 pp540-533

Sanarelli G (1891) "Zentralbl. Bakeriol. Parasitenkd" Infektionskr Hyg Abt 1(9) p457

Schiele B, Alt C (1978) "Dynamic Pressure Filtration of Highly Dispersed Suspension by Means of Microporous Membranes" Intl Symp on Solid-Liquid Filtration pp75-88 6-7 June, Antwerp, Belgium

Schmidt S, Wulle E (1988) "Belastung eines Oberflachengewassers durch Abwasser aus Fischaufzuchtgraben" Wasser-Abwasser 129 pp476-483

Schoep A (1911) "Üeber ein neues Ultrafilter" Kolloid Z 8 80-57

Schulz G, Ripperger S (1989) "Concentration Polarization in Crossflow Microfiltration" J Membrane Sci 40 pp173-187

Segré G, Silberberg A (1962) "Behaviour of Macroscopic Rigid Spheres in Poiseuille Flow" J Fluid Mech, 14 pp115-157

Setti D, C Peri C (1976) "Whey and Skimmilk Ultrafiltration I - Parameters Affecting Permeation Rate in Skimmilk Ultrafiltration" Milchwissenschaft, 31(8) pp466-468

Sharma M M, Yortsos Y C (1987) "Transport of Particulate Suspensions in Porous Media: Model Formulation" AIChE J 33(10) pp1636-1643

Shaw D A, T J Hanratty T J (1977) "Influence of Schmidt Number on the Fluctuation of Turbulent Mass Transfer to a Wall" AIChE J, 23 pp160-169

Shen J J S, Probstein R F (1977) "On the Prediction of Limiting Flux in Laminar Ultrafiltration of Macromolecular Solutions " IChE Fundam, 16(4) pp459-465

Shen J J S, Probstein R F (1979) " Turbulence Promotion and Hydrodynamic Optimization in an Ultrafiltration Process" Ind Eng Chem Process Des Dev 18(3) pp547-554

Shirato M, Osasa K, Takaoku Y (1970) "Critical Tracting Condition of Particulate Beds under Permeation" Kagaku Kogaku (34(7) pp773-779

Shishido M, Sawada S, Goto C (1988) "Application of Crossflow Microfiltration to the Separation and Concentration of a Ferric Hydroxide Suspension" pp391-392

Shulman Z P, Pokryvailo N A (1980) "Hydrodynamics and Heat and Mass Transfer of Polymer Solutions" The Luikov Heat and Mass Transfer Institute, Minsk, U S S R

Sims K A, Cheryan M (1986) "Crossflow Microfiltration of Aspergillus Niger Fermentation Broth" Biotechnol Bioeng Symp, 17 pp495-505

Singh R, Laurence R L, (1979a) "Influence of Slip Velocity at a Membrane Surface on Ultrafiltration Performance - I. Channel Flow System" J Heat Mass Transfer 22 pp721-729

Singh R, Laurence R L, (1979b) "Influence of Slip Velocity at a Membrane Surface on Ultrafiltration Performance - II. Tube Flow System" J Heat Mass Transfer 22 pp731-737

Society Belge de Filtration (1975) "La Filtration Industrielle des Liquides" Deuxieme Partie T III, Derouaux Ed. Liege, Belgium

Steadyly H, Laccetti A J (1988) "Microporous Asymmetric Polymide Membrane" US Patent 4770777 13 Sept., 13p

Sumer B M, Deigaard R (1981) << Particle Motions near the Bottom in Turbulent Flow in an Open Channel Pt 2 >> J Fluid Mech 109 pp311-337

Szaniawski A R, Lipinski K, Mazur J, Filary A (1990) "The Evaluation of the Possibilities of Dyehouse Wastewaters Treatment by Membrane Techniques" Proceedings 5th World Filtration Congr v1 pp101-106 Nice, France

Taddei C, Aimer P, Howell J, Scott J A (1990) "Yeast Cell Harvesting from Cider Using Microfiltration" J Chem Tech Biotechnol 47 pp365-376

Tanny G B (1986) "UV/EB Polymerized Breathable Microporous Membranes and Coatings" Gelman Sci Tech Ltd., Rohouot, Israel

Tanny G B, Hauk D, Merin U (1982) "Biotechnical Applications of a Pleated Cross flow Microfiltration Module" Desalination 41(3) pp299-312

Terrill R M (1983) "Laminar Flow in a Porous Tubes" J Fluids Eng, Trans ASME, 105(3) pp303-307

Theodore L (1964) Ph D Dissertation, New York Univ, NY

Trettin D R, Doshi M R (1980) "Limiting Flux in Ultrafiltration of Macromolecular Solutions" Chem Eng Commun, 4 pp507-522

Van den Berg G B Hanemaaijer J H, Smolders C A (1987) " Ultrafiltration of Protein Solutions: the Role of Protein Association in Rejection and Osmotic Pressure" J Membrane Sci, 31 pp307-320

Van den Berg G B, Smolders C A (1988) "Flux Decline in Membrane Process" Filt & sep Mar/Apr pp115-121

van'tHoff J (1887) Z Phys Chem 1 p481 (Translated and reprinted in The <Foundation of the Theory of Dilute Solutions>, Alembic Club Reprint No 19, E & S Livingstone Edingburgh (1961) pp5-42

van't Hoff J (1888) "On the Function of Osmotic Pressure in the Analogy between Solutions and Gases" Phil Mag 26 pp81-104

Vasseur P, Cox R G (1974) "The Lateral Migration of a Spherical Particle in Two-Dimensional Shear Flows" J Fluid Mech, 78 p385

Vassilieff C S, Leonard E F, Stepner T A (1985) "The Mechanisms of Cell Rejection in Membrane Plasmapheresis" Clinic Hemorheology, 5 p7

Vieth W R, Porter J H, Sherwood T K (1963) "Mass Transfer and Chemical Reaction in a Turbulent Boundary Layer" Ind Eng Chem Fundam, 2 pp1-3

Vilker V L, Colton C K, Smith K A (1981a) "Concentration Polarization in Protein Ultrafiltration Part II: Theoretical and Experimental Study of Albumin Ultrafiltered in an Unstirred Cell" AIChE J, 27(4) pp637-645

Vilker V L, Colton C K, Smith K A (1981b) "The Osmotic Pressure of Concentrated Protein Solutions - Effect of Concentration and pH in Saline Solutions of Bovine Serum Albumin" J Coll Interf Sci, 79 pp548-566

Virk P, Suraiya T (1977) in 2nd Intl Conf on Drag Reduction, G3-41, BHRA, Fluid Eng., Cranfield, England

Volkmann J K, Gatten R R, Sargent J R, (1980) "Composition and Origin of Milky Water in the North Sea" J Marine Biol Assoc UK 60 pp759-768

Wakeman R J, Tarleton E S (1987) "Membrane Fouling Prevention in Crossflow Microfiltration by the Use of Electric Fields " Chem Eng Sci 42(4) pp829-842

Wakeman R J, Tarleton E S (1991) "An Experimental Study of Electroacoustic Crossflow Microfiltration " Chem Eng Res Des 69 pp386-397

Wallis G B (1965) Proceedings, Inst of Mech Engrs, 180 pp36-40

Warren D, Crull A, Saxon D (1986) "P-041U Membrane Separation Markets and Technology" Business Communications Co., Stamford, Conn., USA

Watanabe A, Ohtani T, Horikita H, Ohya H, Kimura S (1986) "Recovery of Soluble Proteins from Fish Jelly Processing with Self-Rejecting Dynamic Membranes" Food Eng & Proc Appl 2 pp225-236

Weissberg H L, Berman A S (1955) Proceedings, Heat and Fluid Mech Inst, 14 pp1-30

Weissberg H L (1956) "Velocity Profiles and Friction Factors for Turbulent Pipe Flow with Uniform Wall Suction" Unicorn Carbide Nuclear Co., Report K-1264

Werynski A, Malchesky P S, Sueoka A, Asanuma Y, Smith J W, Kayashima K, Herpy E, Sato H, Nosé Y (1981) "Membrane Plasma Separation: Toward Improved Clinical Operation" Trans Am Soc Artif Intern Organs, 27 pp539-543

White F M (1974) <<Viscous Fluid Flow>> McGraw-Hill, NY, p158

Wilkinson M C, Hearn J, Cope P, Chainey M (1981) "A Microfiltration Technique for Cleaning Polymer Latices" The British Polymer J, 13 June pp82-89

Willis M S, Raviprakash J, Tosun I (1986) " A Continuum Theory for Filtration " Fluid Filtration: Liquid, Vol II, ASTM 975, pp163-175

Winfield B A (1979) "Treatment of Sewage Effluents by Reverse Osmosis -pH Based Studies of the Fouling Layer and Its Removal" Water Research 13(7) pp561-564

Wohl P R, Rubinow S I (1974) "The Transverse Force on a Drop in an Unbounded Parabolic Flow" J Fluid Mech, 62 pp185-207

Wood D, Petty C (1983) "New Model for Turbulent Mass Transfer near a Rigid Interface" AIChE J, 29 pp164-167

Yaeger S "Trends in Semiconductor Ultrapure Water for Final Membranes" The 1987 5th Annual Membrane Technology/Planning Conf pp131-138 21-23 Oct Cambridge, USA

Yan S H, Hill Jr C G, Amundson C H (1979) "Ultrafiltration of Whole Milk" J Dairy Sci, 62(1) pp23-40

Yasminov A A, Gleizer V, Volodin V F, Ryabenko E A (1990) "Intensificztion of Microfiltration Processs in the Ultrafiltration of Fluid" High Purity Substances 4(3) pp476-484

Yoo S S, Hartnett J (1974) "Heat Transfer and Friction Factors for Purely Viscous Non-Newtonian Fluids in Turbulent Pipe Flow" Proceedings of the 5th Intl Heat Transfer Congr, 3-7 Sept., v2 pp218-222 Japanese Soc of Mech Eng, Tokyo, Japan

Yung B P K, Merry H, Bott T R (1989) "The Role of Turbulent Bursts in Particle Re-Entrainment in Aqueous Systems" Chem Eng Sci 44(4) pp873-882

Zawicki I, Malchesky P S, Smith J W, Haraski H, Asanuma Y, Nose Y (1981) "Axial Changes of Blood and Plasma Flow, Pressure, and Cellular Deposition in Capillary Plasma Filters" Artificial Organs 5(1981) pp241-247

Zsigmondy R, Bachmann W (1918) "Üeber neue Filter" Z Anorg Allgem Chem 103 pp119-128

Zydney A L, Colton C K (1984) "A Red Cell Deformation Model for Hemolysis in Crossflow Memebrane Plasmapheresis" Chem Eng Commun 30 pp191-207

Zuk J S, Rucka M (1988) "Resistance of a Gel Layer during Ultrafiltration of Casein Solution" Chem Eng Commun 54 pp85-92

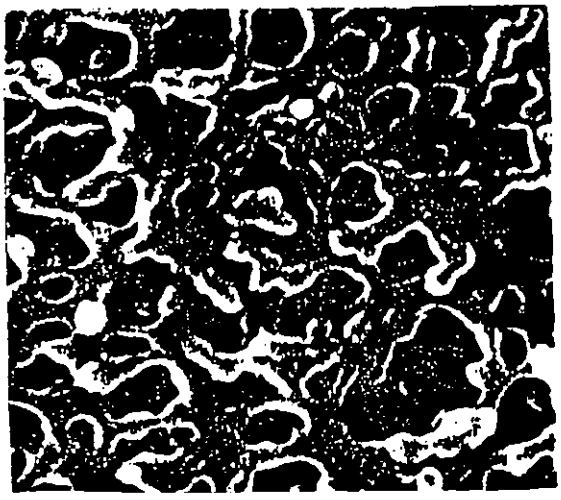

(a) By phase inversion

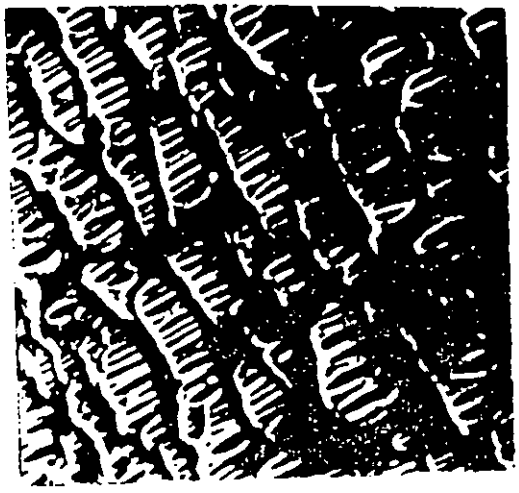

(b) Polypropylene by stretching

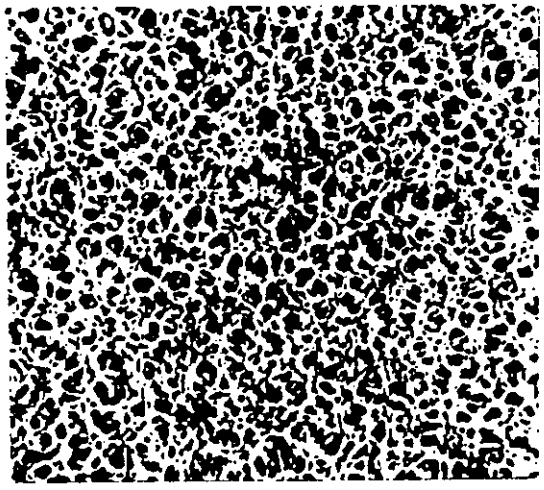

(c) PTFE by stretching

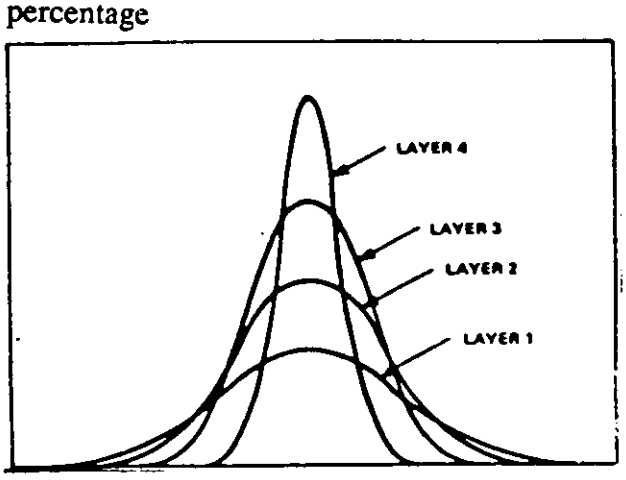

(d) By thermoplast

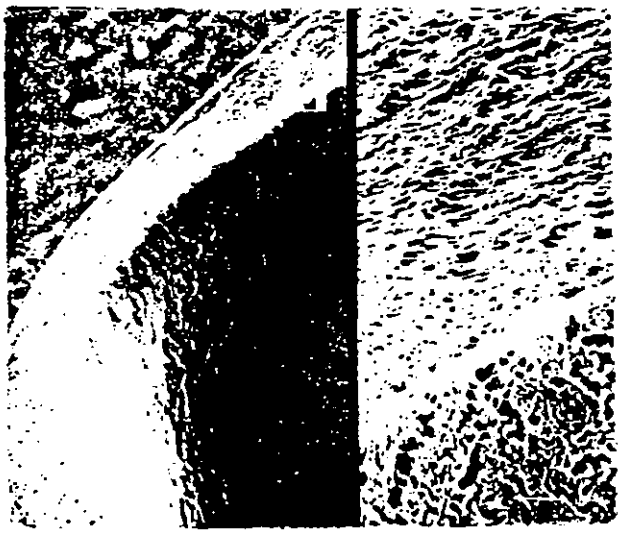

(e) By Thermal inversion

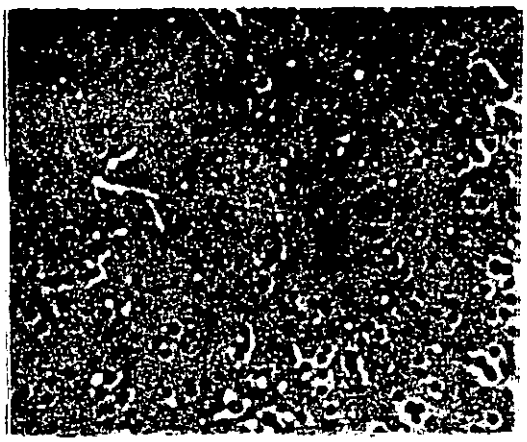

(f) By track-etch

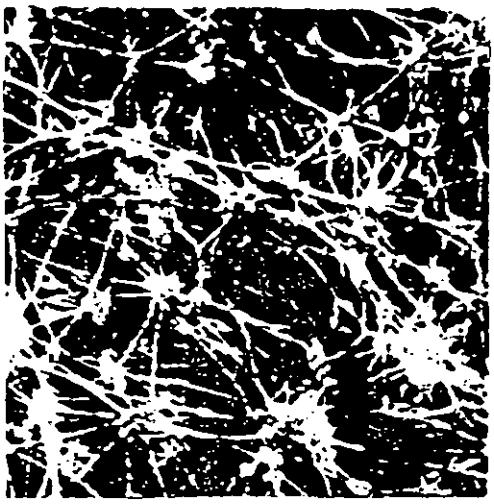

(g) By high-speed

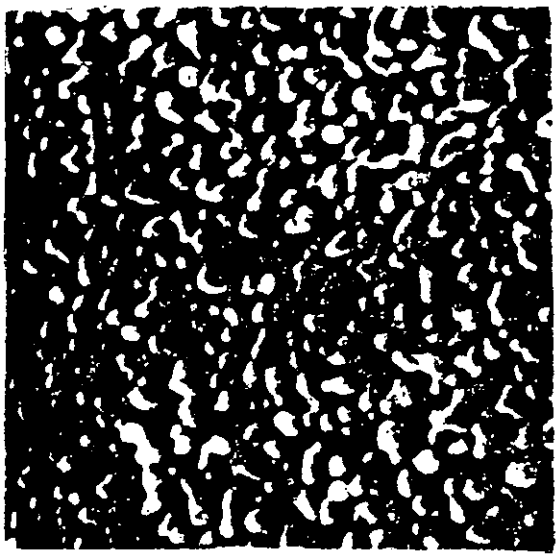

(h) By composite

Fig 1 Polymeric membranes

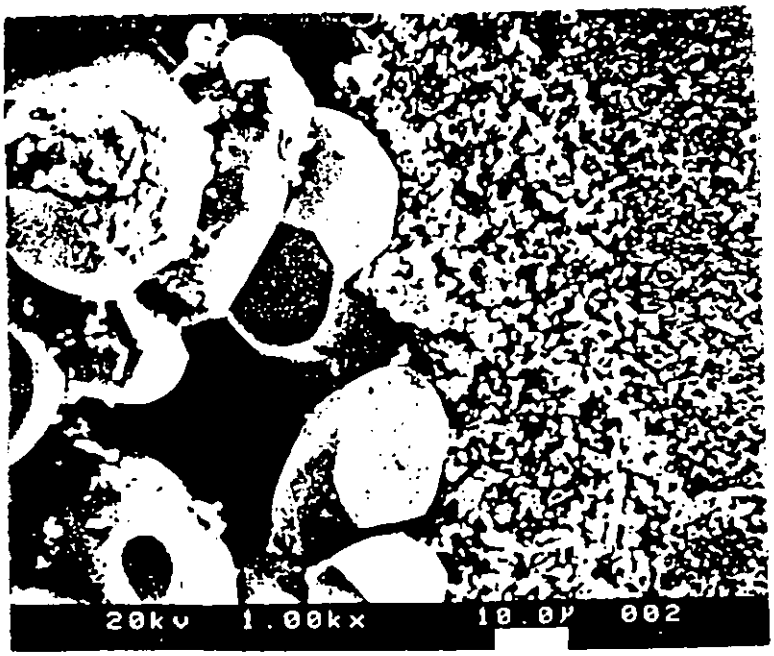

(a) γ-Al_2O_3 membrane

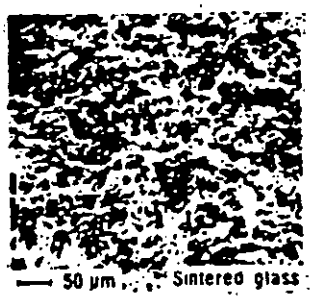

(b) Sintered glass

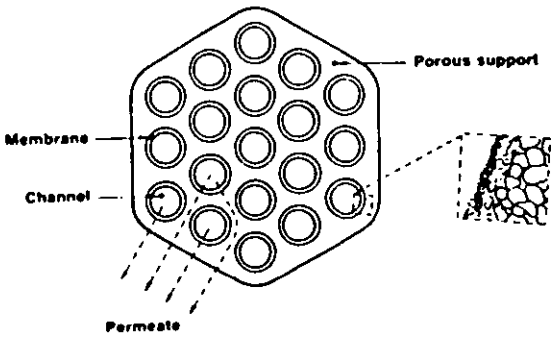

(c) Monolithic module

Fig 2 Ceramic membranes

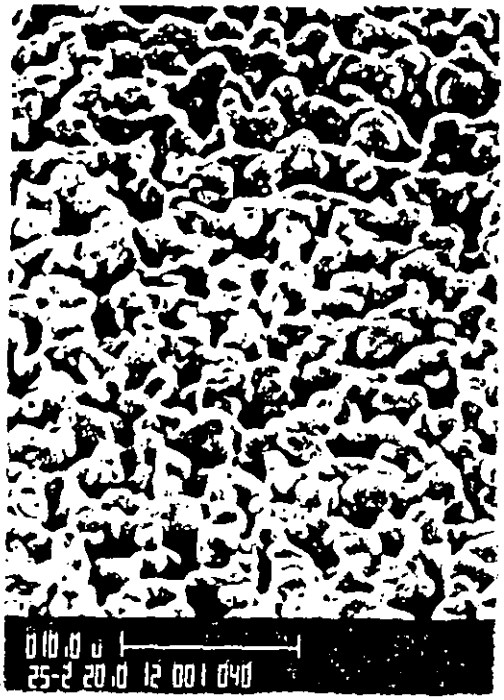

(b) Silver

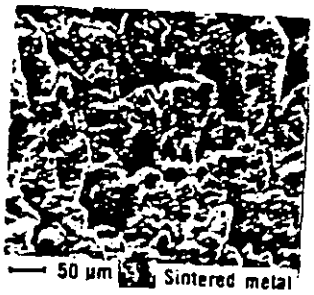

(a) Steel

(d) Zirconia/Inconel

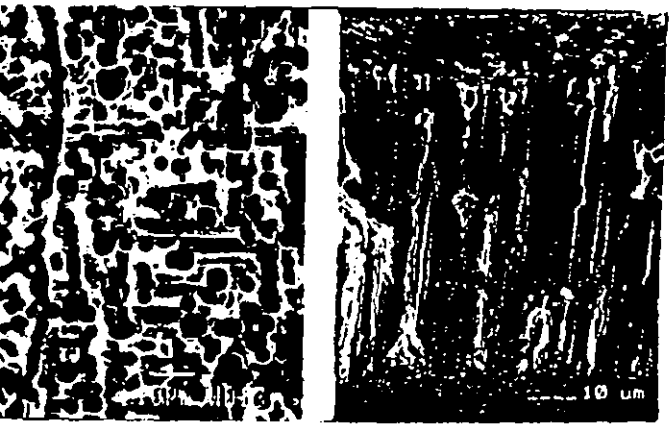

(c) Aluminium

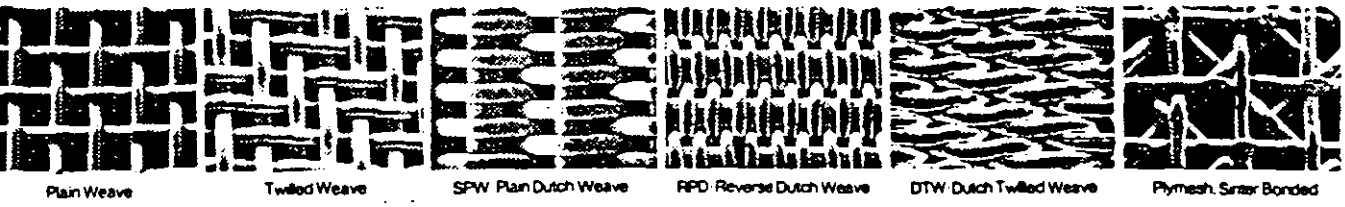

(e) metal meshes

Fig 3 Metal membranes

Mass Transfer Correlations by Gekas & Hallström (1987)

(A) For Turbulent Newtonian Fluids in Pipes or Flat Ducts

Sh equations	Conditions	Authors
1)Based on momentum, mass, heat transfer analogies		
$Sh = 0.023Re^{0.8}Sc^{0.33}$	$Re>10^5$ $Sc>0.5$	Bennett & Mayers (1982)
$Sh = 0.34Re^{0.75}Sc^{0.33}$	$10^4<Re<10^5$, $Sc>0.5$	Bennett & Mayers (1982)
$Sh = (f/2)ReSc \cdot [1+5(Sc-1)\sqrt{f/2}]^{-1}$		Bennett & Mayers (1982)
$Sh = \frac{(f/2)ReSc}{1+5[Sc-1+\ln(1-5Sc)/6]\sqrt{f/2}}$		Bennett & Mayers (1982)
$Sh = 0.021Re^{0.8}Sc^{0.6}$	$0.5<Sc<5$	Kays (1966)
$Sh = 0.0082Re^{0.69}Sc^{0.33}$	gas/liquid dispersions $10^4<Re<10^5$	Calderbank & Young (1961)
$Sh = 0.0012(Re^{0.87}-280)Sc^{0.4}\left[1+\left(\frac{d_h}{L}\right)^{\frac{2}{3}}\right]$		Gnielinski (1975)
(L is channel length)	$1.5<Sc<500$	
$Sh = 3\sqrt{3}Re(f/2)Sc^{1/3}\left(\frac{U_{max}}{\overline{U}}\right)\cdot(2\pi 1.77^3)^{-1}$		Vieth et al (1963)
U_{max} and $\overline{U}$ are the maximum and mean velocity (m/s)		
$Sh = Sh^0 + 0.079ReSc\sqrt{f}\cdot[(1+Sc^{0.8})^{5/6}]^{-1}$	$Re > 10^5$	Churchill (1977)
Sh^0 is valid for $Sc \to 0$, $Re \to 2100$		
$Sh = 0.079ReSc^{1/3}\sqrt{f}$	$Re>10^5$ $Sc>100$	Churchill (1977)
2) Based on eddy diffusivity models		
$Sh = 0.023Re^{0.875}Sc^{0.25}$	$300<Sc<700$	Deissler (1959)
$Sh = 0.0149Re^{0.88}Sc^{0.33}$	$Sc>100$	Notter & Sleicher (1971)
$Sh = 9Re\ Sc^{0.33}\sqrt{f}\cdot(29\pi\sqrt{3})^{-1}$	high Sc number	Lin et al (1953)

Sh equations	Conditions	Authors
3) Based on surface renewal model		
$Sh = 0.107 Re^{0.9} Sc^{0.5}$	0.5< Sc < 100	Einstein & Li (1956)
		Pinczeski & Sideman (1974)
$Sh \propto Re^{0.9} Sc^{0.33}$		Ruckenstein (1967)
$Sh = \frac{0.0097 Re^{0.9} Sc^{0.5}(1.1 + 0.44 Sc^{-1/3} - 0.7 Sc^{-1/6})}{1 + 0.064 Sc^{0.5}(1.1 + 0.44 Sc^{-1/3} - 0.7 Sc^{-1/6})}$		
	10 < Sc < 1000	Pinczeski & Sideman (1974)
$Sh = 0.102 Re^{0.9} Sc^{0.33}$	Sc > 1000	
	For rough pipes	Pinczeski & Sideman (1974)
$Sh = 0.00929 (e/d_h)^{0.15} Re Sc^{0.5} (1.11 + 0.44 Sc^{-1/3} - 0.7 Sc^{-1/6})$		
	Rough pipes	Kawase & Ulbrecht (1982 & 1983)
$Sh = (f/2) Re\, Sc \cdot \{1 + 1.5 Re^{-1.8} Sc^{-0.17} [Sc(f/f_s) - 1]\}^{-1}$		
	Re > 5000	Kawase & Ulbrecht (1982 & 1983)
4) Based on Levich's "Three-Zone" model		
$Sh = 0.0105 (e/d_h)^{0.15} Re Sc^{0.5}$		
	rough pipes	Kawase & Ulbrecht (1982)
5) Based on new turbulence concepts (coherent structures)		
$St^+ = 0.0967 Sc^{-0.7}$	high Sc number	Wood & Petty (1983)
St =(Sh/Re Sc)		
$\overline{k}^+ \propto Sc^{-0.75}$ (linear approach)	high Sc number	Campbell & Hanratty (1982)
$\overline{k}^+ \propto Sc^{-0.7}$ (non-linear approach)	high Sc number	Campbell & Hanratty (1983)
6) Based on experimental data		
$Sh = 0.023 Re^{0.83} Sc^{0.44}$	0.6< Sc <2.5	Gilliand & Sherwood (1934)
$Sh = 0.0096 Re^{0.931} Sc^{0.346}$	10^4<Re<10^5 430<Sc<10^5	Harriott & Hamilton (1965)
$St^* = 0.0889\ Sc^{-0.704}$	high Sc number	Shaw & Hanratty (1977)
$Sh = 0.827\ A^{0.33}\ (f/2)^{0.5}\ Re\ Sc^{0.33}$		Mizushina et al (1971 & 1972)
(experimental testing of an	3000< Re < 80000	
eddy diffusivity based model)	800< Sc < 15000	
	non-porous and porous walls	

(B) For Turbulent Viscoelastic Fluids in Smooth or Rough Pipes

Sh equations	Conditions	Authors
1) Based on surface renewal model		
$Sh = 0.0165 Re^{0.709} Sc^{0.33}$	smooth pipes	Kawase & Ulbrecht (1983)
$Sh = 0.0141 f^{1/2} ReSc^{1/2}(1.11 + 0.44 Sc^{-0.33} - 0.7 Sc^{-1.67})$	rough pipes	Kawase & De [1984)
2) Based on empirical correlation		
$Sh = 0.022 Re^{0.71} Sc^{0.33}$	high Sc number	Virk & Suraiya (1977)
$Sh = 0.0206 Re^{0.725} Sc^{0.33}$	high Sc number	Shulman & Pokryvailo (1980)
$Sh = 0.181 Re^{0.47} Sc^{0.33}$		Cheryan (1980)
3) Based on "Three-Zone" concept		
$Sh = 0.0133 Re^{0.725} Sc^{0.33}$	high Sc number	Kawase & Ulbrecht (1982)
$Sh = 0.0111 f^{1/2} ReSc^{1/2}$	rough pipes	Kawase & Ulbrecht (1982)
$Sh = 0.0179 Re^{0.709} Sc^{0.33}$		Hughmark (1971)
4) Based on periodic viscous sublayer model, Chilton-Colburn analogy		
$Sh = 0.284 Re^{0.418} Sc^{0.4}$	smooth pipes	Meek & Baer (1970)
5) Based on eddy diffusivity model		
$Sh = \sqrt{\frac{f/2}{St}} = a_1 Sc^{2/3} - a_3 \ln Sc + a_4 Sc + u_g^+ + u^+ \{45\}$	high Sc number	Hannah et al (1981)
(a_1,a_3, a_4 constants, u_g central line velocity, u^+ dimensionless velocity)		

(C) For Turbulent Power-law Fluids in Smooth Pipes

Sh equations	Conditions	Authors
$Sh = (0.0118 Re^{0.9} Sc^{0.3})/n$	(n=flow index)	Yoo & Hartnett (1974)
$Sh = 0.023(9350)^{0.8\left(1-\frac{1}{n^n}\right)} Re^{\left(\frac{0.8}{n^n}\right)} Sc^{0.4}$	high Sc number	Gröber et al (1961)
$Sh = \frac{f}{2} Re\, Sc \cdot [1.2 + 5.9 f(Sc-1) Sc^{-1/3}]^{-1}$	high Sc number	Metznar & Friend (1959)
$Sh = 0.075 n^{\frac{1}{3}} \left(\frac{\alpha_1}{2}\right)^{\frac{1}{n}} 8^{-\frac{\alpha_2}{n}} \left(\frac{n}{6n+2}\right)^{\alpha_2 \frac{(4-n)}{6}} Sc^{1/3} Re^{\left(4-2n\alpha_2+\frac{\alpha_2 n}{6n}\right)}$	Levich's Three-zone model	Kawase & Ulbrecht (1982)
(α_1, α_2 are the dimensionless function of n)		

Table A
PTFE and ceramic filter with tap water
and cleaned by air backflushing and nitric acid washing

Time	Fluxrate ($m^3/m^2 \cdot hr$)		
	PTFE		Ceramic
(mins)	before cleaned	after cleaned	after cleaned
0	0.269	0.431	0.776
1	0.259	0.388	0.668
2	0.194	0.366	0.582
3	0.183	0.355	0.528
4	0.145	0.35	0.474
5	0.129	0.345	0.453
6	0.108	0.312	0.431
7	0.108	0.269	0.41
8	0.102	0.269	0.388
9	0.108	0.291	0.377
10	0.086	0.302	0.371
11	0.081	0.302	0.371
12	0.081	0.318	0.366
13	0.075	0.323	0.366
14	0.081	0.345	0.361
15	0.075	0.334	0.361
16	0.097	0.517	0.361
17	0.097	0.496	0.361
18	0.086	0.528	0.361
19	0.097	0.528	0.361
20	0.086	0.528	0.361

Table B
Fariey Metal Tubular Filter (No 97)

Test	Q	ΔP	J_v ($m^3/m^2 \cdot hr$)			C (mg/l)	
	(l/min)	(Bar)	Initial	Before	After	Solids	Lipids
1	4	0	0.724	0.665			
2	8	0.12	1.94	1.753			
3	16	0.26	2.394	2.034			
4	20	0.34	2.738	2.316			
5	12	0	0.908	1.33			
6	12	1.07	5.086	5.852			
7	12	1.69	6.791	6.416			
8	4	0	0.735	0.352	1.248	10	
9	8	0.48	0.822	0.203	0.602	10	
10	16	0.29	1.009	0.25	0.853	10	
11	20	0.55	1.706	0.43	1.33	10	
12	12	0	0.524	0.086	0.469	10	
13	12	0.97	2.472	0.203	0.681	10	
14	12	1.69	2.441	0.227	0.759	10	

Table C
Fariey Metal Tubular Filter (No 98)

Test	Q	ΔP	J_v ($m^3/m^2 \cdot hr$)			C (mg/l)	
	(l/min)	(Bar)	Initial	Before	After	Solids	Lipids
1	4	0	0.563	0.422	0.704		
2	8	0.07	6.181	5.946			
3	16	0.51	2.699	2.691			
4	20	0.24	6.181	5.946			
5	12	0.97	5.273	4.835			
6	12	1.79	6.431	6.165			
7	12	0.07	7.355	7.355			
8	4	0.41	1.001	0.266	2.245	10	
9	8	0.07	3.13	0.563	2.77	10	
10	16	0	1.174	0.035	0.868	10	
11	20	1.03	0.274	0.031	0.532	10	
12	12	1.02	1.174	0.274	2.011	10	
13	12	1.69	0.978	0.297	0.751	10	

Table D
Fariey Metal Tubular Filter (No 99)

Test	Q	ΔP	J_v ($m^3/m^2 \cdot hr$)			C (mg/l)	
	(l/min)	(Bar)	Initial	Before	After	Solids	Lipids
1	4	0.07	1.549	1.58			
2	8	0.12	2.566	2.77			
3	16	0.26	3.233	3.208			
4	20	0.41	4.209	4.109			
5	12	0	1.361	1.291			
6	12	1.07	6.431	6.713			
7	12	1.69	7.902	7.605			
8	4	0	0.766	0.196	1.396	10	
9	8	0.48	2.535	0.211	3.036	10	
10	16	0.29	3.083	0.146	1.314	10	
11	20	0.55	2.817	0.102	0.861	10	
12	12	0	1.048	0.039	0.598	10	
13	12	0.97	1.338	0.074	0.391	10	
14	12	0.9	2.738	0.074	0.282	10	

Table E
Fariey Metal Tubular Filter (No 98)

Test	Q	ΔP	J_v ($m^3/m^2 \cdot hr$)			C (mg/l)	
	(l/min)	(Bar)	Initial	Before	After	Solids	Lipids
1	12	1.16	5.729	4.445	5.322		
2	12	1.16	3.177	0.814	2.677	2	
3	12	1.16	3.146	0.454	1.831	2	5
4	12	1.16	6.738	5.963	6.417		
5	12	1.16	4.461	0.908	2.191	2	
6	12	1.16	1.409	0.282	0.1534	2	10
7	12	1.16	5.874	0.468	5.306		
8	12	1.16	3.35	0.83	2.191	2	
9	12	1.16	2.191	0.125	2.238	2	20

Table F
Enka capillary filter
(at 12 l/min and 0.5 Bar)

Time	J_v ($m^3/m^2 \cdot hr$)						
	Clean	Silica (mg/l)			Silica (2 mg/l)+Lipid (mg/l)		
mins	Water	0.5	1	2	5	10	20
0	1.008	0.888	0.864	0.835	0.763	0.72	0.72
2	1.037	0.821	0.821	0.806	0.706	0.706	0.706
4	0.994	0.806	0.806	0.792	0.662	0.706	0.648
6	0.95	0.763	0.763	0.792	0.662	0.634	0.634
8	0.936	0.763	0.749	0.763	0.662	0.648	0.634
10	0.922	0.763	0.72	0.749	0.662	0.648	0.619
12	0.095	0.72	0.705	0.72	0.662	0.619	0.576
14	0.907	0.706	0.691	0.72	0.662	0.634	0.648
16	0.936	0.835	0.806	0.806	0.72	0.706	0.634
18	0.893	0.749	0.792	0.792	0.662	0.648	0.698
20	0.922	0.806	0.821	0.821	0.677	0.706	0.634
22	0.893	0.749	0.792	0.763	0.648	0.662	0.698
24	0.907	0.778	0.849	0.806	0.706	0.706	0.677
26	0.864	0.778	0.749	0.763	0.648	0.648	0.634
28	0.893	0.821	0.864	0.835	0.72	0.706	0.677
30	0.864	0.778	0.806	0.749	0.691	0.662	0.59

Table G
Ceramic Monolithic Filter

Test	Q	ΔP	J_v ($m^3/m^2 \cdot hr$)			C (mg/l)	
	(l/min)	(Bar)	Initial	Before	After	Solids	Lipids
1	4	0.07	0.081	0.107	0		
2	8	0.07	0.084	0.084	0		
3	16	0.07	0.401	0.441	0.349		
4	20	0.14	0.602	0.564	0.564		
5	4	0.28	1.139	1.053	1.064		
6	8	0.24	1.128	0.989	1.01		
7	12	0.34	0.989	0.806	1.021		
8	16	0.59	2.225	1.612	1.773		
9	16	0.86	2.902	2.601	2.784		
10	12	1.17	4.504	3.6	3.719		
11	4	0.07	0.084	0.03	0	2	
12	8	0.07	0.081	0.018	0	2	
13	16	0.07	0.333	0.296	0.143	2	
14	20	0.21	0.398	408	0.387	2	
15	4	0.28	0.645	0.51	0.523	2	
16	8	0.24	0.508	0.451	0.502	2	
17	12	0.21	0.564	0.451	0.451	2	
18	16	0.56	1.128	0.914	0.85	2	
19	16	0.79	1.494	1.107	1.3	2	
20	12	1.07	2.171	1.58	1.72	2	
21	4	0.07	0.009	0	0	2	5
22	8	0.07	0.09	0.066	0.066	2	5
23	16	0.07	0.296	0.188	0.161	2	5
24	20	0.28	0.478	0.242	0.242	2	5
25	12	0.21	0.457	0.21	0.215	2	5

(to be continued)

Table G
Ceramic Monolithic Filter

Test	Q	ΔP	J_v ($m^3/m^2 \cdot hr$)			C (mg/l)	
	(l/min)	(Bar)	Initial	Before	After	Solids	Lipids
26	8	0.21	0.322	0.183	0.215	2	5
27	4	0.28	0.441	0.263	0.333	2	5
28	16	0.59	0.946	0.516	0.623	2	5
29	16	0.86	1.118	0.849	0.935	2	5
30	12	1.07	1.236	1.021	1.15	2	5
31	4	0.07	0.01	0	0	2	10
32	8	0.07	0.061	0.054	0	2	10
33	16	0.07	0.188	0.14	0	2	10
34	20	0.28	0.339	0.183	0	2	10
35	12	0.2	0.21	0.148	0	2	10
36	8	0.2	0.263	0.14	0	2	10
37	4	0.27	0.247	0.145	0.167	2	10
38	16	0.65	0.382	0.228	0.269	2	10
39	16	0.85	0.392	0.285	0.328	2	10
40	12	1.05	0.575	0.328	0.36	2	10
41	4	0.07	0.072	0.027	0	2	20
42	8	0.07	0.059	0.041	0	2	20
43	16	0.07	0.199	0.126	0	2	20
44	20	0.28	0.296	0.159	0.173	2	20
45	12	0.2	0.199	0.134	0.164	2	20
46	8	0.2	0.142	0.102	0.116	2	20
47	4	0.27	0.18	0.099	0.129	2	20
48	16	0.54	0.301	0.156	0.188	2	20
49	16	0.85	0.306	0.202	0.212	2	20
50	12	1.05	0.301	0.193	0.202	2	20

NOTES

The operating conditions, the permeate cumulative volume and flux rate with process time of all tests in Chapetr 4 are listed in Appendix 4.

Membrane C was used to test different material, and hence its results were not included.

The pore size of membranes J, L and M were 0.2 μm, and that of membrane D was 3 μm. These membranes were only used in clean water test for membrane selection.

Membranes K and A were tested with No 6 latex, and B, E and F with No 11 latex. However, due to the lack of the knowledge of pressure distribution, their results were not consistent, and hence there were no further analysis on these tests. The code of the run with * on the both sides indicate permeate pressure was greater than outlet pressure in that run.

The results of the pressure distribution tests, membrane resistance tests, and permeate flux rate or cumulative volume against processing time based on several filtration models (Cake filtration, Complete blocking, Intermediate blocking and Standard blocking) of membranes G, H and I are shown in the diagrams.

Membrane A 0.45 um Single pass mode

Test	A1		A2/1			A2/2			*A2/3*		
Flow rate	1.33		1.4			1.8			2.5	l/min	
Re	7464		7857			10102			14030		
P1	0.83		0.86			0.94			1.21	Bar	
P2	0.53		0.54			0.50			0.22	Bar	
Pp	0.30		0.30			0.30			0.30	Bar	
Pt	0.68		0.40			0.42			0.41	Bar	
Temp	23.5		23			23			23	C	
Conc	0.201		0.21							mg/l (No 6)	
Time min	Rate l/min	Cumu l	Time min	Rate l/min	Cumu l	Time min	Rate l/min	Cumu l	Time min	Rate l/min	Cumu l
0		0	0		.0	0	0.338	0	0	0.1830	0.000
2	1.615	3.2	2	0.4640	0.9	10	0.2500	3.4	10	0.1500	1.9
4	1.841	6.8	4	0.5270	2.0	20	0.3410	5.8	20	0.2000	3.6
6	1.998	10.4	6	0.5640	2.9	30	0.2340	8.6	30	0.1790	5.4
8	1.751	14.1	8	0.4510	4.0	40	0.2110	10.7	40	0.1720	7.1
10	1.651	17.6	10	0.5170	4.9	50	0.1830	12.5	50	0.1480	8.5
12	1.764	20.8	12	0.4260	5.8				60	0.1130	9.6
14	1.581	24.2	14	0.4390	6.7						
16	1.578	27.6	16	0.4050	7.5						
18	1.815	30.7	18	0.4140	8.4						
20	1.507	34.0	20	0.4730	9.2						
22	1.496	36.9	22	0.4000	10.1						
24	1.449	39.8	24	0.3890	10.9						
26	1.382	42.4	26	0.4010	11.7						
28	1.187	44.9	28	0.408	12.5						
30	1.120	47.2	30	0.3760	13.2						
40	1.045	49.3	40	0.3220	16.7						
			50	0.3230	20.0						
			60	0.338	22.9						

Test	A3/1		A3/2		
Flow rate	2.45		1.18	l/min	
Re	13750		6622		
P1	1.15		0.83	Bar	
P2	0.52		0.60	Bar	
Pp	0.07		0.07	Bar	
Pt	0.77		0.64	Bar	
Temp	23		23	C	
Conc	0.1			mg/l (No 6)	
Time min	Rate l/min	Cumu l	Time min	Rate l/min	Cumu l
0		0.000	0	0.347	0
1	0.223	0.223	1	0.398	0.258
2	0.159	0.419	2	0.168	0.565
3	0.168	0.589	3	0.217	0.729
4	0.182	0.750	4	0.16	0.912
5	0.153	0.930	5	0.149	1.069
6	0.178	1.086	6	0.153	1.222
7	0.16	1.249	7	0.157	1.371
8	0.148	1.401	8	0.145	1.520
9	0.143	1.555	9	0.142	1.663
10	0.16	1.690	10	0.141	1.804
12	0.128	1.974	12	0.14	2.064
14	0.124	2.220	14	0.119	2.323
16	0.118	2.462	16	0.119	2.556
18	0.118	2.688	18	0.114	2.800
20	0.108	2.913	20	0.125	3.029
22	0.107	3.126	22	0.115	3.265
24	0.105	3.338	24	0.111	3.493
26	0.105	3.550	26	0.113	3.708
28	0.107	3.757	28	0.104	3.929
30	0.102	3.963	30	0.108	4.152
32	0.099	4.193	32	0.119	4.379
34	0.128	4.391	34	0.119	4.599
36	0.099	4.617	36	0.101	4.816
38	0.098	4.812	38	0.098	5.012
40	0.096	4.999	40	0.095	5.200
50	0.089	5.884	50	0.09	6.1
60	0.081	6.694			

Membrane B 0.45 um Single pass mode

Test	*B1/1*	*B1/2*	B1/3	B1/4	
Flow rate	2.5	2	1.17	0.83	l/min
Re	14030	11224	6566	4675	
P1	1.21	1.04	0.91	0.87	Bar
P2	0.33	0.47	0.63	0.73	Bar
Pp	0.52	0.52	0.52	0.37	Bar
Pt	0.26	0.24	0.25	0.23	Bar
Temp	22	24	26	14	C
Conc	0.04				mg/l (No 11)

Time (min)	Rate l/min	Cumu l	Time (min)	Rate l/min	Cumu l	Time (min)	Rate l/min	Cumu l	Time (min)	Rate l/min	Cumu l
0		0	0		0	0		0	0	0.6149	0
2	0.2500	0.549	2	0.3361	0.672	2	0.4098	0.820	2	0.6281	1.230
4	0.1888	0.926	4	0.3434	1.359	4	0.5313	1.882	4	0.6845	2.486
6	0.1603	1.247	6	0.3282	2.015	6	0.4666	2.815	6	0.5950	3.855
8	0.1440	1.535	8	0.3296	2.675	8	0.4562	3.728	8	0.6254	5.045
10	0.1374	1.810	10	0.2882	3.251	10	0.4477	4.623	10	0.5563	6.296
12	0.1335	2.077	12	0.2824	3.816	12	0.4382	5.500	12	0.5704	7.408
14	0.1283	2.333	14	0.2732	4.362	14	0.4330	6.366	14	0.5349	8.549
16	0.1258	2.585	16	0.2804	4.923	16	0.4695	7.305	16	0.5287	9.619
18	0.1252	2.835	18	0.2596	5.442	18	0.4263	8.157	18	0.5183	10.677
20	0.1160	3.067	20	0.2651	5.973	20	0.3943	8.946	20	0.5220	11.713
22	0.1967	3.460	22	0.2597	6.492	22	0.4814	9.909	22	0.4837	12.757
24	0.1102	3.681	24	0.2676	7.027	24	0.4254	10.760	24	0.5507	13.725
26	0.1247	3.930	26	0.2655	7.558	26	0.4188	11.597	26	0.5245	14.826
28	0.1052	4.141	28	0.2491	8.056	28	0.4295	12.456	28	0.4902	15.875
30	0.1153	4.371	30	0.2536	8.564	30	0.4156	13.288	30	0.4406	16.855
40	0.0982	5.353	40	0.2264	10.828	40	0.4162	17.450	40	0.4497	21.261
50	0.0987	6.340	50	0.2167	12.994	50	0.4124	21.574	50	0.5562	25.758
60	0.0967	7.308	60	0.2140	15.134	60	0.2668	24.242	60	0.4497	31.319

Test	*B2/1*	B2/2	B2/3	
Flow rate	2.5	1.67	0.83	l/min
Re	14030	9372	4675	
P1	1.21	1.00	0.87	Bar
P2	0.33	0.61	0.73	Bar
Pp	0.37	0.40	0.37	Bar
Pt	0.40	0.41	0.43	Bar
Temp	28	28	28	C
Conc	water			

Time (min)	Rate l/min	Cumu l	Time (min)	Rate l/min	Cumu l	Time (min)	Rate l/min	Cumu l
0		0	0		0	0		0
2	0.72	1.440	2	0.9296	1.859	2	0.7816	1.563
4	0.68	2.800	4	1.1787	4.217	4	0.8743	3.312
6	0.4758	3.752	6	0.9474	6.112	6	0.9119	5.136
8	0.5231	4.798	8	0.9721	8.056	8	0.8820	6.900
10	0.6433	6.084	10	0.9348	9.926	10	0.8483	8.596
12	0.4954	7.075				12	0.8670	10.330
14	0.5151	8.105						
16	0.4913	9.088						
18	0.4923	10.072						
20	0.4085	10.889						

Test	B3/1	B3/2	B3/3	
Flow rate	2.5	2	1.16	l/min
Re	14030	11224	6510	
P1	1.17	1.00	0.91	Bar
P2	0.90	0.41	0.63	Bar
Pp	0.33	0.30	0.37	Bar
Pt	0.70	0.40	0.40	Bar
Temp	25	26	28	C
Conc	0.038			mg/l (No 11)

Time (min)	Rate l/min	Cumu l	Time (min)	Rate l/min	Cumu l	Time (min)	Rate l/min	Cumu l
0		0.000	0		0	0		0
2	0.1789	0.358	2	0.2875	0.5749	2	0.7770	1.554
4	0.1594	0.677	4	0.3151	1.2051	4	1.1386	3.831
6	0.1404	0.957	6	0.3144	1.8339	6	0.9300	5.691
8	0.1381	1.234	8	0.3057	2.4452	8	0.9139	7.519
10	0.1368	1.507	10	0.3263	3.0979	10	0.9649	9.449
12	0.1265	1.760	12	0.3020	3.7019	12	0.9736	11.396
14	0.1116	1.983	14	0.3008	4.3035	14	0.9582	13.313
16	0.1154	2.214	16	0.2894	4.8822	16	0.8730	15.059
18	0.1180	2.450	18	0.3286	5.5394	18	0.8384	16.735
20	0.1225	2.695	20	0.2862	6.1119	20	0.8513	18.438
22	0.1095	2.914	22	0.2751	6.6620	22	0.6639	19.766
24	0.1105	3.135	24	0.2661	7.1942	24	0.7765	21.319
26	0.1106	3.356	26	0.3009	7.7959	26	0.7715	22.862
28	0.1004	3.557	28	0.5681	8.9321	28	0.8090	24.480
30	0.1763	3.910	30	0.2586	9.4492	30	0.8064	26.093

Test	D (3 um)		E1	(1.2 um)	
Flow rate	1.16		1.16		
Re	6510		6510		
P1	1.45		2.07		
P2	0.69		1.31		
Pp	0.55		0.55		
pT	0.52		1.14		
Temp	30		30		
Conc	Water		Water		
Time	Rate	Cumu	Time	Rate	Cumu
(min)	l/min	l	(min)	l/min	l
0	3.45	0	0	3.72	0
10	3.24	33.5	10	3.60	36.6
20	3.24	65.4	20	3.60	72.6
30	3.15	97.8	30	3.60	108.3
40	3.24	129.3	40	3.54	144.3
50	3.15	161.4	50	3.60	180.0
60	3.18	193.2	60	3.60	215.2
70	3.2	225.1	70	3.45	250.9
80	3.2	257.1	80	3.54	285.3
90	3.2	289.1	90	3.42	320.5
100	3.2	321.6	100	3.49	354.6
110	3.3	353.3	110	3.40	389.0
120	3.15	384.8	120	3.40	384.8

Flow rate	*E2/1*		*E2/2*		
Flow rate	2.5		2	l/min	
Re	14030		11224		
P1	1.43		1.01	Bar	
P2	0.59		0.47	Bar	
Pp	0.77		0.53	Bar	
pT	0.23		0.21	Bar	
Temp	26		30	C	
Conc	0.022			mg/l (No 11)	
Time	Rate	Cumu	Time	Rate	Cumu
(min)	l/min	l	(min)	l/min	l
0	0.2624	0	0	0.3289	0
10	0.1981	2.5	10	0.4918	3.6
20	0.2441	4.7	20	0.3845	7.8
30	0.2376	7.0	30	0.3516	11.4
40	0.2157	9.2	40	0.3371	14.8
50	0.2089	11.3	50	0.3390	18.2
60	0.2031	12.4	60	0.3249	19.8

Membrane F 1.2 um Single pass mode

Test	F1		F2			F3	1.2 um
Flow rate	1.15		1.15			1.15	l/min
Re	6454		6454			6454	
P1	0.62		0.62			0.62	Bar
P2	0.48		0.48			0.48	Bar
Pp	0.31		0.31			0.31	Bar
Pt	0.24		0.24			0.24	Bar
Temp	27.5		29			29	C
Conc	0.109		0.022			0.002	mg/l (No 11)
Time (min)	Rate l/min	Cumu l	Time (min)	Rate l/min	Cumu l	Time (min)	Rate l/min	Cumu l
0		0	0	2.096	0	0		0
10	2.479	24.8	2	2.131	4.2	2	1.611	3.2
20	2.45	49.3	4	2.111	8.4	4	1.357	6.2
30	2.166	71	6	2.063	12.5	6	1.334	8.8
35	1.233	83	8	1.992	16.5	8	1.292	11.4
			10	1.974	20.4	10	1.275	14.0
			12	1.841	24.1	12	1.249	16.5
			14	1.721	27.6	14	1.242	19.0
			16	1.721	31.1	16	1.238	21.5
			18	1.706	34.5	18	1.262	24.0
			20	1.695	37.9	20	1.267	26.5
			22	1.678	41.2	22	1.255	29.0
			24	1.621	44.2	24	1.23	31.4
			26	1.381	47.2	26	1.181	33.7
			28	1.3	49.8	28	1.06	35.9
			30	1.256	52.3	30	1.03	38.0
			32	1.19	54.7	32	1.05	40.1
			34	1.173	57.0	34	1.019	42.2
			36	1.126	59.3	36	1.037	44.2
			38	1.146	61.5	38	1.013	46.2
			40	1.066	63.6	40	1.004	48.2
			42	0.942	65.6	42	0.928	50.2
			44	0.927	67.5	44	0.962	51.9
			46	0.896	69.2	46	0.861	53.7
			48	0.866	71.0	48	0.84	55.4
			50	0.858	72.7	50	0.831	57.1
						52	0.834	58.7
						54	0.754	60.3
						56	0.747	61.8
						58	0.749	63.3
						60	0.75	64.8
						62	0.791	66.4
						64	0.788	68.0
						66	0.824	69.5
						68	0.766	71.1
						70	0.79	72.7

Membrane G 1.2 um Single pass mode

Test	G1	G2/1	G2/2	
Flow rate	1.22	1.22	1.22	l/min
Re	6847	6847	6847	
P1	0.54	0.69	0.69	Bar
P2	0.41	0.48	0.48	Bar
Pp	0.26	0.31	0.31	Bar
Pt	0.15	0.16	0.17	Bar
Temp	29	29	29	C
Conc	0.22	0.22		mg/l (No 11)

Time (min)	Rate l/min	Cumu l	Time (min)	Rate l/min	Cumu l	Time (min)	Rate l/min	Cumu l
0		0.0	0		0	0		0
2	5.07	10.1	2	3.05	6.1	2	1.42	2.8
4	5.49	19.7	4	2.26	10.7	4	1.29	5.3
6	4.48	30.2	6	1.51	14.2	6	1.08	7.6
8	5	39.3	8	1.29	16.7	8	0.94	9.6
10	4.68	49.0	10	1.01	18.8	10	0.92	11.3
12	4.61	58.4				12	0.74	12.9
14	4.75	67.9				14	0.75	14.4
						16	0.73	15.9
						18	0.72	17.3
						20	0.71	18.7

Test	G2/3	G2/3	G3/1	G3/2	
Flow rate	1.2	1.22	1.15	1.15	l/min
Re	6734	6847	6454	6454	
P1	0.69	0.69	0.69	0.68	Bar
P2	0.48	0.48	0.48	0.48	Bar
Pp	0.31	0.31	0.31	0.31	Bar
Pt	0.17	0.17	0.2	0.18	Bar
Temp	29	29	29	29	C
Conc			0.22		mg/l (No 11)

Time (min)	Rate l/min	Cumu l	Time (min)	Rate l/min	Cumu l	Time (min)	Rate l/min	Cumu l	Time (min)	Rate l/min	Cumu l
0		0	0			0		0	0		0
2	0.90	1.8	2	0.73	1.5	2	1.27	2.5	2	1.04	2.1
4	0.79	3.5	4	0.67	2.9	4	1.22	4.8	4	0.98	4.0
6	0.76	5.0	6	0.66	4.2	6	1.01	6.9	6	0.86	5.6
8	0.72	6.4	8	0.65	5.5	8	0.89	8.8	8	0.67	7.1
10	0.63	7.7	10	0.62	6.7	10	0.85	10.5	10	0.65	8.5
12	0.59	8.8	12	0.61	7.8	12	0.84	12.2	12	0.67	9.6
14	0.51	9.9	14	0.51	8.9	14	0.82	13.8	14	0.52	10.8
16	0.47	10.9	16	0.43	9.8	16	0.77	15.3	16	0.48	11.8
18	0.47	11.8	18	0.4	10.6	18	0.65	16.7	18	0.46	12.7
20	0.47	12.7	20	0.34	11.3	20	0.62	17.9	20	0.46	13.6
22	0.47	13.6	22	0.31	11.9	22	0.61	19.2	22	0.46	14.5
24	0.42	14.5	24	0.33	12.5	24	0.63	20.3	24	0.44	15.4
26	0.39	15.3	26	0.25	13.1	26	0.50	21.5	26	0.46	16.2
28	0.37	16.0	28	0.27	13.6	28	0.63	22.5	28	0.36	17.1
30	0.36	16.7	30	0.27	14.2	30	0.50	23.5	30	0.38	17.8

Test	G3/3	G3/4	G4/1	G4/2	
Flow rate	1.18	1.18	1.16	1.17	l/min
Re	6641	6641	6510	6566	
P1	0.68	0.68	0.68	0.68	Bar
P2	0.48	0.48	0.48	0.48	Bar
Pp	0.31	0.31	0.31	0.31	Bar
Pt	0.15	0.17	0.19	0.19	Bar
Temp	29	29	29	29	C
Conc			0.196		mg/l (No 11)

Time (min)	Rate l/min	Cumu l	Time (min)	Rate l/min	Cumu l	Time (min)	Rate l/min	Cumu l	Time (min)	Rate l/min	Cumu l
0		0	0		0	0		0	0		
2	0.81	1.6	2	0.56	1.1	2	0.56	1.1	2	0.35	0.7
4	0.74	3.1	4	0.49	2.1	4	0.50	2.1	4	0.32	1.4
6	0.68	4.5	6	0.44	3.0	6	0.47	3.1	6	0.31	1.9
8	0.65	5.7	8	0.34	3.7	8	0.45	3.9	8	0.24	2.5
10	0.50	6.8	10	0.32	4.3	10	0.39	4.7	10	0.24	3.0
12	0.44	7.7	12	0.28	4.9	12	0.26	5.3	12	0.24	3.4
14	0.43	8.6	14	0.24	5.4	14	0.30	5.9	14	0.22	3.9
16	0.40	9.4	16	0.24	5.9	16	0.29	6.5	16	0.21	4.3
18	0.37	10.1	18	0.23	6.4	18	0.25	7.0	18	0.19	4.7
20	0.36	10.8	20	0.23	6.8	20	0.27	7.5	20	0.19	5.0
22	0.34	11.5	22	0.23	7.3	22	0.26	8.0	22	0.12	5.3
24	0.30	12.1	24	0.22	7.7	24	0.22	8.5	24	0.16	5.6
26	0.27	12.7	26	0.20	8.1	26	0.20	8.9	26	0.14	5.9
28	0.27	13.2	28	0.18	8.5	28	0.19	9.3	28	0.13	6.1
30	0.27	13.7	30	0.17	8.8	30	0.17	9.6	30	0.13	6.4
32	0.26	14.3	32	0.17	9.2	32	0.17	10.0	32	0.13	6.7
34	0.26	14.8	34	0.17	9.5	34	0.17	10.3	34	0.13	6.9
36	0.24	15.3	36	0.17	9.9	36	0.21	10.7	36	0.13	7.2
38	0.23	15.7	38	0.17	10.2	38	0.18	11.1	38	0.13	7.4
40	0.23	16.2	40	0.16	10.5	40	0.18	11.4	40	0.13	7.7
			42	0.15	10.8						
			44	0.15	11.1						
			46	0.14	11.4						
			48	0.14	11.7						
			50	0.14	11.9						

Membrane H 0.45 um Single pass mode

Test	H1/1	H1/2	H1/3	H1/4	
Flow rate	1.18	1.18	1.28	1.2	l/min
Re	6622	6622	7183	6734	
P1	0.90	0.90	0.91	0.90	Bar
P2	0.76	0.76	0.76	0.76	Bar
Pp	0.14	0.14	0.14	0.14	Bar
Pt	0.59	0.61	0.64	0.60	Bar
Temp	29	29	29	29	C
Conc	0.245				mg/l (No 11)

Time (min)	Rate l/min	Cumu l	Time (min)	Rate l/min	Cumu l	Time (min)	Rate l/min	Cumu l	Time (min)	Rate l/min	Cumu l
0		0.0	0		0	0		0	0		0
2	2.08	4.2	2	1.78	3.6	2	1.46	2.9	2	1.10	2.2
4	1.96	8.1	4	1.66	6.9	4	1.33	5.6	4	0.99	4.3
6	1.90	11.9	6	1.52	9.9	6	1.24	8.1	6	0.95	6.0
8	1.83	15.5	8	1.42	12.8	8	1.12	10.4	8	0.79	7.7
10	1.78	19.1	10	1.33	15.5	10	1.06	12.5	10	0.74	9.2
12	1.70	22.5	12	1.32	18.1	12	1.02	14.5	12	0.66	10.6
						14	0.95	16.5	14	0.64	11.8
						16	0.92	18.3	16	0.61	13.1
									18	0.59	14.2
									20	0.53	15.3

Test	H2/1	H2/1	
Flow rate	1.22	1.22	l/min
Re	6847	6847	
P1	0.90	0.91	Bar
P2	0.76	0.76	Bar
Pp	0.14	0.14	Bar
Pt	0.62	0.64	Bar
Temp	29	29	C
Conc	0.327		mg/l (No 11)

Time (min)	Rate l/min	Cumu l	Time (min)	Rate l/min	Cumu l
0		0	0		0
2	0.66	1.3	2	0.42	0.8
4	0.56	2.5	4	0.43	1.6
6	0.53	3.6	6	0.38	2.4
8	0.51	4.6	8	0.34	3.1
10	0.5	5.6	10	0.35	3.8
12	0.5	6.6	12	0.32	4.5
14	0.46	7.5	14	0.33	5.1
16	0.45	8.4	16	0.32	5.8
18	0.44	9.3	18	0.32	6.4
20	0.42	10.2	20	0.3	7.0
22	0.41	11.0	22	0.29	7.6
24	0.38	11.8	24	0.29	8.2
26	0.4	12.5	26	0.28	8.7
28	0.36	13.3	28	0.28	9.3
30	0.35	14.0	30	0.29	9.8
32	0.34	14.6	32	0.25	10.3
			34	0.2	10.8
			36	0.22	11.2
			38	0.23	11.7
			40	0.22	12.1
			42	0.22	12.6
			44	0.22	13.0
			46	0.22	13.4
			48	0.21	13.8

Test	H3	H4	H5	H6	
Flow rate	1.17	1.17	1.93	3.08	l/min
Re	6547	6547	10859	17304	
P1	0.90	0.90	1.38	1.86	Bar
P2	0.76	0.76	1.03	1.03	Bar
Pp	0.14	0.14	0.14	0.14	Bar
Pt	0.65	0.61	0.91	0.95	Bar
Temp	25	26	29	29	C
Conc	0.2	0.120	0.12	0.12	mg/l (No 11)

Time (min)	Rate l/min	Cumu l	Time (min)	Rate l/min	Cumu l	Time (min)	Rate l/min	Cumu l	Time (min)	Rate l/min	Cumu l
0		0	0		0	0		0	0	0	0
2	0.401	0.80	2	0.372	0.74	2	0.422	0.84	2	0.437	0.87
4	0.534	1.78	4	0.378	1.48	4	0.417	1.68	4	0.362	1.64
6	0.582	2.78	6	0.365	2.21	6	0.411	2.56	6	0.327	2.32
8	0.459	3.75	8	0.355	2.92	8	0.467	3.35	8	0.320	2.94
10	0.397	4.61	10	0.342	3.62	10	0.384	4.20	10	0.298	3.56
12	0.399	5.39	12	0.345	4.28	12	0.381	4.98	12	0.295	4.14
14	0.385	6.16	14	0.319	4.95	14	0.390	5.74	14	0.288	4.72
16	0.365	6.94	16	0.324	5.56	16	0.385	6.51	16	0.282	5.29
18	0.403	7.66	18	0.295	6.20	18	0.376	7.27	18	0.286	5.84
20	0.354	8.43	20	0.309	6.81	20	0.378	8.00	20	0.267	6.40
22	0.361	9.13	22	0.316	7.39	22	0.357	8.73	22	0.279	6.92
24	0.349	9.85	24	0.276	8.01	24	0.354	9.47	24	0.250	7.47
26	0.356	10.53	26	0.305	8.57	26	0.377	10.18	26	0.267	7.98
28	0.332	11.23	28	0.289	9.20	28	0.358	10.91	28	0.267	8.49
30	0.349	11.95	30	0.325	9.76	30	0.352	11.62	30	0.247	8.99
32	0.385	12.63	32	0.267	10.37	32	0.356	12.30	32	0.231	9.42
34	0.339	13.36	34	0.285	10.88	34	0.327	12.98	34	0.177	9.89
36	0.346	14.04	36	0.246	11.43	36	0.330	13.64	36	0.242	10.37
38	0.333	14.71	38	0.270	11.97	38	0.333	14.29	38	0.304	10.82
40	0.324	15.36	40	0.291	12.50	40	0.321	14.95	40	0.211	11.36
42	0.319	15.99	42	0.263	13.07	42	0.323	15.60	42	0.236	11.80
44	0.308	16.62	44	0.280	13.53	44	0.332	16.24	44	0.228	12.25
46	0.315	17.25	46	0.196	14.06	46	0.314	16.88	46	0.212	12.70
48	0.317	17.89	48	0.243	14.50	48	0.310	17.51	48	0.224	13.11
50	0.324	18.51	50	0.245	14.97	50	0.316	18.12	50	0.204	13.55
52	0.305	19.13	52	0.231	15.46	52	0.303	18.74	52	0.214	13.96
54	0.302	19.74	54	0.247	15.89	54	0.302	19.35	54	0.210	14.38
56	0.304	20.35	56	0.194	16.36	56	0.308	19.94	56	0.204	14.79
58	0.307	20.97	58	0.225	16.77	58	0.293	20.54	58	0.203	15.22
60	0.321	21.54	60	0.221	17.21	60	0.293	21.11	60	0.222	15.61
70	0.261	24.46	70	0.210	19.37	70	0.277	23.92	70	0.191	17.61
80	0.263	26.91	80	0.212	21.38	80	0.268	26.59	80	0.177	19.44
90	0.229	29.39	90	0.191	23.32	90	0.258	29.16	90	0.177	21.18
100	0.233	31.61	100	0.177	25.14	100	0.246	31.63	100	0.170	22.87
110	0.214	33.78	110	0.174	26.86	110	0.237	33.95	110	0.163	24.50
120	0.201	35.91	120	0.167	28.53	120	0.217	36.42	120	0.156	26.05
122	0.212	36.31	122	0.160	28.85	122	0.258	36.86	122	0.148	26.35
124	0.206	36.73	124	0.157	29.16	124	0.219	37.33	124	0.144	26.65
126	0.199	37.13	126	0.150	29.47	126	0.210	37.75	126	0.145	26.93
128	0.195	37.52	128	0.153	29.77	128	0.209	38.18	128	0.144	27.22
130	0.194	37.91	130	0.150	30.07	130	0.214	38.61	130	0.142	27.50

Membrane I 0.45 um Single pass mode

Test	I1	I2	I3	
Flow rate	0.95	1.22	1.28	l/min
Re	5331	6828	7161	
P1	0.76	0.81	0.77	Bar
P2	0.62	0.62	0.62	Bar
Pp	0.41	0.41	0.41	Bar
Pt	0.26	0.23	0.15	Bar
Temp	29	25	25	C
Conc	0.033	0.0293	0.018	mg/l (No 9)

Time (min)	Rate l/min	Cumu l	Time (min)	Rate l/min	Cumu l	Time (min)	Rate l/min	Cumu l
0		0	0		0	0		0
2	1.356	2.71	2	0.619	1.24	2	0.426	0.85
4	1.472	5.44	4	0.660	2.45	4	0.330	1.60
6	1.373	8.19	6	0.594	3.71	6	0.323	2.29
8	1.280	10.83	8	0.601	4.90	8	0.364	2.98
10	1.264	13.35	10	0.600	6.10	10	0.367	3.69
12	1.241	15.89	12	0.594	7.33	12	0.348	4.41
14	1.272	18.35	14	0.630	8.45	14	0.350	5.10
16	1.220	20.85	16	0.527	9.65	16	0.345	5.79
18	1.230	23.26	18	0.572	10.74	18	0.340	6.47
20	1.196	25.71	20	0.567	11.88	20	0.334	7.12
22	1.216	28.12	22	0.565	13.01	22	0.306	7.78
24	1.213	30.52	24	0.564	14.13	24	0.327	8.41
26	1.190	32.90	26	0.550	15.24	26	0.324	9.06
28	1.159	35.30	28	0.551	16.33	28	0.329	9.71
30	1.213	37.65	30	0.545	17.44	30	0.326	10.42
32	1.189	39.79	32	0.559	18.56	32	0.384	11.17
34	0.934	41.94	34	0.570	19.63	34	0.420	11.95
36	0.957	43.84	36	0.516	20.71	36	0.394	12.68
38	0.966	45.73	38	0.503	21.75	38	0.308	13.36
40	0.936	47.64	40	0.526	22.79	40	0.289	13.95
42	0.948	49.52	42	0.543	23.83	42	0.282	14.50
44	0.945	51.41	44	0.508	24.85	44	0.265	15.05
46	0.943	53.34	46	0.482	25.82	46	0.266	15.59
48	0.984	55.21	48	0.456	26.82	48	0.270	16.11
50	0.925	57.06	50	0.520	27.68	50	0.258	16.66
52	0.867	58.84	52	0.409	28.62	52	0.281	17.16
54	0.856	60.60	54	0.423	29.47	54	0.240	17.69
56	0.888	62.27	56	0.439	30.36	56	0.255	18.18
58	0.812	63.85	58	0.468	31.14	58	0.250	18.71
60	0.701	65.37	60	0.338	31.96	60	0.269	19.19
70	0.705	72.14	70	0.356	35.40	70	0.232	21.68
72	0.653	73.39	80	0.351	38.83	80	0.230	23.97
74	0.543	74.86	90	0.329	42.05	90	0.226	26.20
76	0.816	76.06	100	0.294	45.15	100	0.216	28.38
78	0.664	77.62	110	0.291	48.06	110	0.209	30.41
80	0.740	79.10	120	0.289	50.67	120	0.191	32.19
			122	0.230	51.21	130	0.146	33.91
			124	0.258	51.70	140	0.154	35.39
			126	0.261	52.20	150	0.152	36.94
			128	0.239	52.67	152	0.156	37.24
			130	0.207	53.08	154	0.150	37.54
						156	0.145	37.84
						158	0.147	38.13
						160	0.146	38.42

Membrane J, L, M. 0.2 um

Test	J1	J2	J3
Mode	Batch	Batch	Batch
Flow rate	2	2	2
Re	11224	11224	11224
P1	0.69	1.38	2.07
P2	0.14	0.83	1.52
Pp	0.00	0.00	0.21
Pt	0.41	1.1	1.59
P(B/F)	3.72	3.72	3.72
Temp	20	20	25
Conc	water	water	water

Time (min)	Rate l/m^2.hr	Cumu l	B/F sec	Time (min)	Rate l/m^2.hr	Cumu l	B/F sec	Time (min)	Rate l/m^2.hr l	Cumu	B/F sec
0	2880	0		0	2720	0		0	3936	0	
10	2400	36		10	2016	33		10	2912	48	
20	1920	66		20	1728	60		20	2400	86	
30	1600	91		30	1568	84		30	2240	119	
40	1440	113		40	1440	106		40	2016	149	
50	1280	131		50	1312	126		50	1760	178	
60	960	147		60	1216	144		60	1760	203	
70	880	160		70	1184	162		70	1632	228	
80	800	173		80	1120	179		80	1568	251	
90	800	184		90	1120	195		90	1440	274	
100	720	194		100	1040	211		100	1440	295	
110	560	203		110	960	226		110	1440	316	
120	480	210		120	928	240		120	1280	336	
130	384	217		130	960	254		130	1216	354	
140	352	222		140	880	267		140	1120	371	
150	304	227		150	848	280		150	1120	388	
152	304	228		152	832	282		152	1120	391	3
154	304	229		154	832	285		154	1120	395	3
156	304	230		156	832	287		156	1120	398	3
158	304	230		158	832	290		158	1056	401	3
160	304	231		160	864	293		160	1120	401	3
162	304	232	1	162	1152	296	3				
164	304	233	1	172	1380	312					
166	312	234	2	182	996	330					
168	312	235	3	192	996	345					
170	320	236	3	202	948	359					
172	320	236	3	206	892	359	3				

Test	L	*M*	
Mode	Single	Single	
Flow rate	3.6	1.37	l/min
Re	20203	7689	
P1	2.07	0.17	Bar
P2	0.83	0.00	Bar
Pp	0.00	0.00	Bar
Pt	1.45	0.09	Bar
P(B/F)	3.72	///	Bar
Temp	20	25	C
Conc	water	0.012	mg/l (No 6)

Time (min)	Rate l/m^2.hr	Cumu l	B/F sec	Time (min)	Rate l/m^2.hr	Cumu l	Time (min)	Rate l/m^2.hr	Cumu l
0	2100	0.0		0		0	72	38	6.7849
90	480	17.4		2	103	0.234	74	35	6.898
120	270	19.1		4	118	0.5428	76	34	7.0021
180	150	21.0		6	94	0.8962	78	33	7.1043
191	150	21.2	2	8	93	1.1791	80	32	7.2039
193	150	21.3	3	10	90	1.4581	82	35	7.3
195	450	21.4	4	12	63	1.7286	84	32	7.4049
197	450	21.5	5	14	109	1.9169	86	35	7.5005
199	450	21.6	4	16	42	2.2429	88	30	7.6065
201	450	21.8	4	18	121	2.3697	90	30	7.6961
203	450	21.8	4	20	76	2.7315	92	30	7.7848
				22	77	2.9604	94	29	7.8749
				24	71	3.1923	96	29	7.961
				26	67	3.4042	98	29	8.049
				28	70	3.6061	100	28	8.1347
				30	60	3.817	102	28	8.2181
				32	57	3.9983	104	29	8.3013
				34	59	4.17	106	24	8.3873
				36	55	4.3483	108	28	8.4591
				38	46	4.5142	110	27	8.5435
				40	56	4.6523	112	27	8.6257
				42	53	4.8205	114	26	8.706
				44	53	4.979	116	26	8.7854
				46	59	5.1374	118	27	8.8629
				48	48	5.3142	120	25	8.9427
				50	47	5.4581	122	23	9.019
				52	45	5.6002	132	23	9.3622
				54	45	5.7365	142	16	9.7061
				56	35	5.8725	152	32	9.9422
				58	41	5.9769	162	25	10.4192
				60	38	6.1008	172	24	10.8013
				62	38	6.2158	182	22	11.1608
				64	38	6.3309	202	21	11.8257
				66	41	6.4439	222	20	12.4563
				68	37	6.5662	242	19	13.0509
				70	36	6.6764	272	17	13.8937
							302	16	14.6692
							332	16	15.4101

Membrane K 0.45 um Single pass mode

Test	K1	K2	K3	
Flow rate	1.56	1.73	1.73	l/min
Re	8755	9709	9709	
P1	0.83	0.69	0.51	Bar
P2	0.28	0.21	0.21	Bar
Pp	0.00	0.00	0.00	Bar
Pt	0.55	0.45	0.36	Bar
Temp	20	20	24	C
Conc	0.257	0.255	0.252	mg/l (No 6)

Time (min)	Rate l/min	Cumu l	Time (min)	Rate l/min	Cumu l	Time (min)	Rate l/min	Cumu l
0	0.218	0	0		0	0		0
1	0.333	0.218	2	0.2912	0.58	1	0.8193	0.8
2	0.332	0.551	4	0.5379	1.66	2	1.3728	2.2
3	0.345	0.883	6	0.3457	2.35	3	1.5988	3.8
4	0.329	1.228	8	0.4049	3.16	4	1.5501	5.3
5	0.333	1.557	10	0.2920	3.74	6	1.5653	8.5
6	0.334	1.890	12	0.2950	4.33	8	1.6146	11.7
7	0.401	2.224	14	0.2660	4.87	10	1.3425	14.4
8	0.330	2.625	16	0.2489	5.36	12	1.0910	16.6
9	0.319	2.955	18	0.2332	5.83	14	1.0352	18.6
10	0.318	3.274	20	0.2292	6.29	16	1.4362	21.5
11	0.316	3.592	22	0.2255	6.74	18	1.3201	24.2
12	0.342	3.908	24	0.2322	7.20	20	1.2514	26.7
14	0.378	4.250	26	0.2088	7.62	22	1.1434	28.9
16	0.347	5.006	28	0.1935	8.01	24	1.2228	31.4
18	0.283	5.700	30	0.1861	8.38			
20	0.275	6.266	40	0.1527	9.91			
22	0.275	6.816	50	0.1102	11.01			
24	0.286	7.367	60	0.0690	11.70			
26	0.265	7.938	70	0.0610	12.31			
28	0.262	8.468	80	0.0516	12.83			
30	0.279	8.991	90	0.0468	13.29			
32	0.316	9.550	110	0.0364	14.02			
34	0.310	10.181	130	0.0324	14.67			
36	0.316	10.802						
38	0.262	11.434						
40	0.264	11.958						
42	0.238	12.487						
52	0.206	12.962						
62	0.202	15.022						
72	0.186	17.045						
82	0.167	18.909						
92	0.147	20.574						
102	0.127	22.046						
132	0.101	23.314						
152	0.115	25.340						
172	0.132	27.636						
192	0.109	30.274						

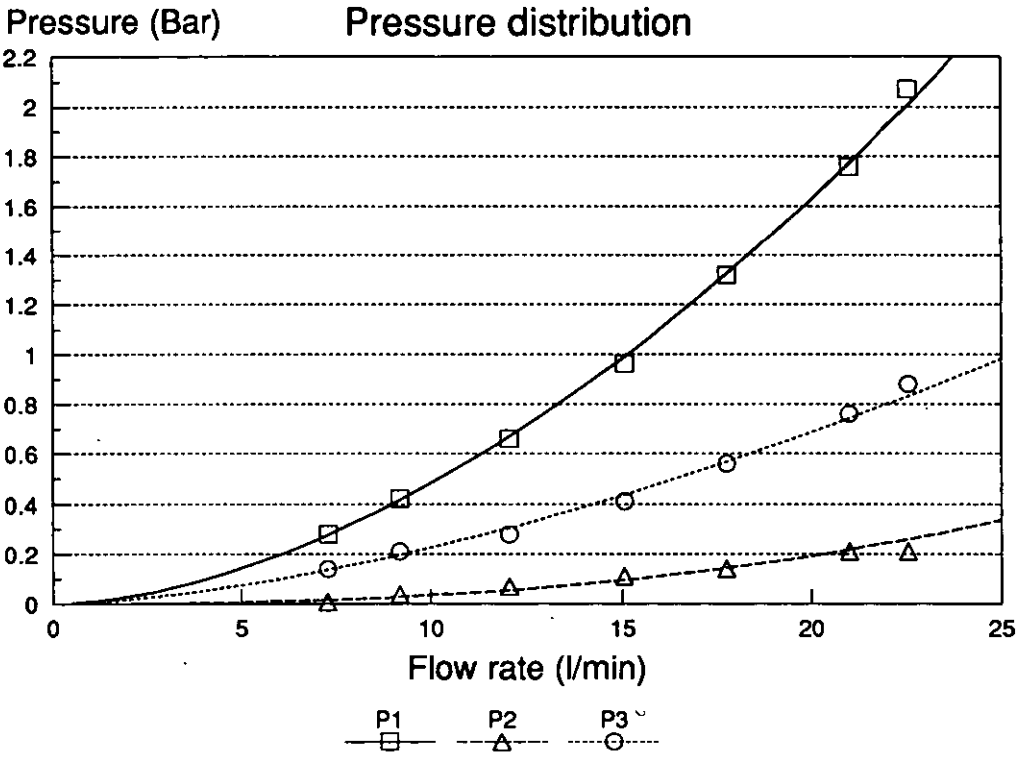

Test G1

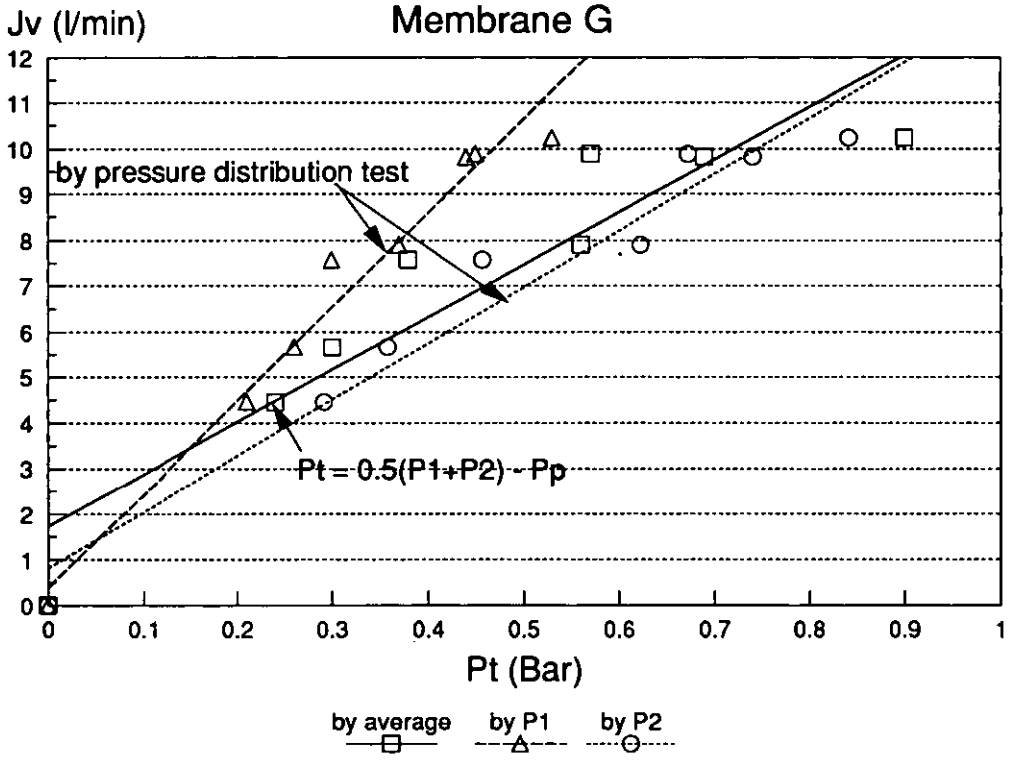

Test G1

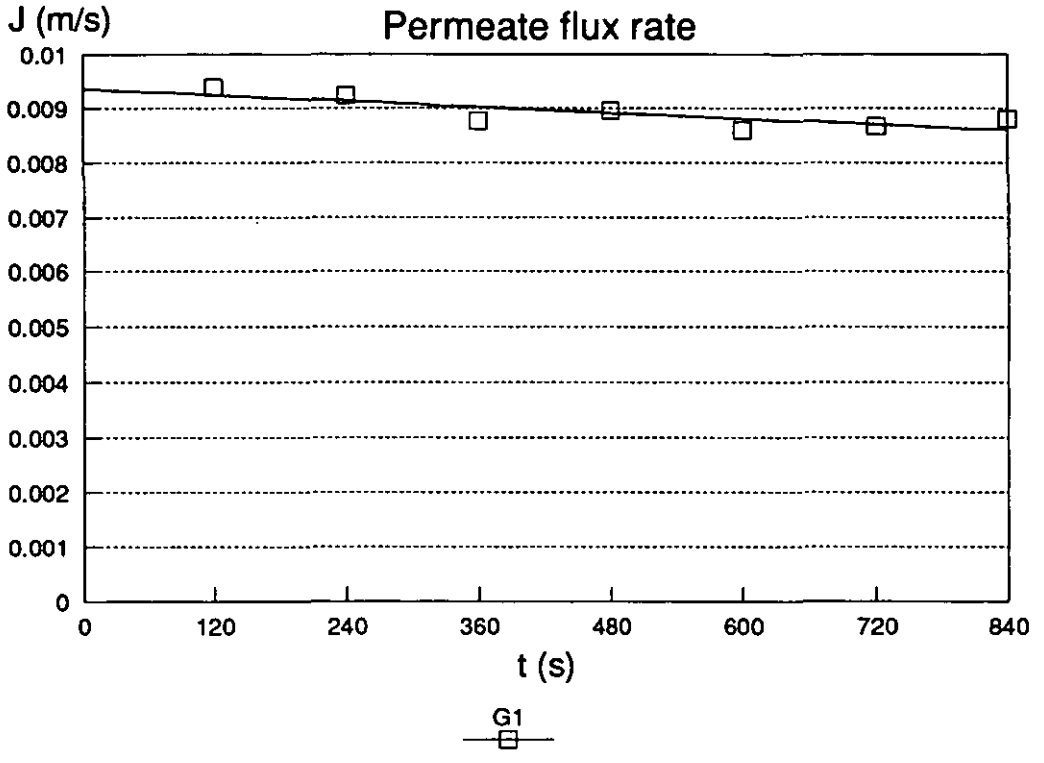

Test G1

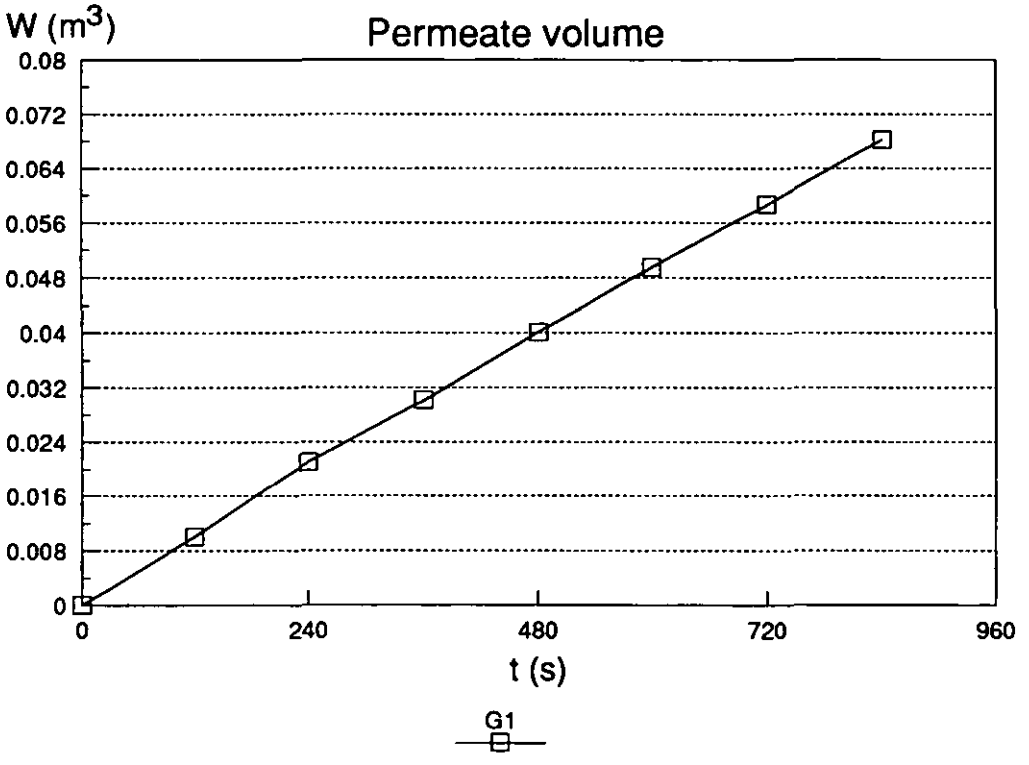

Test G1

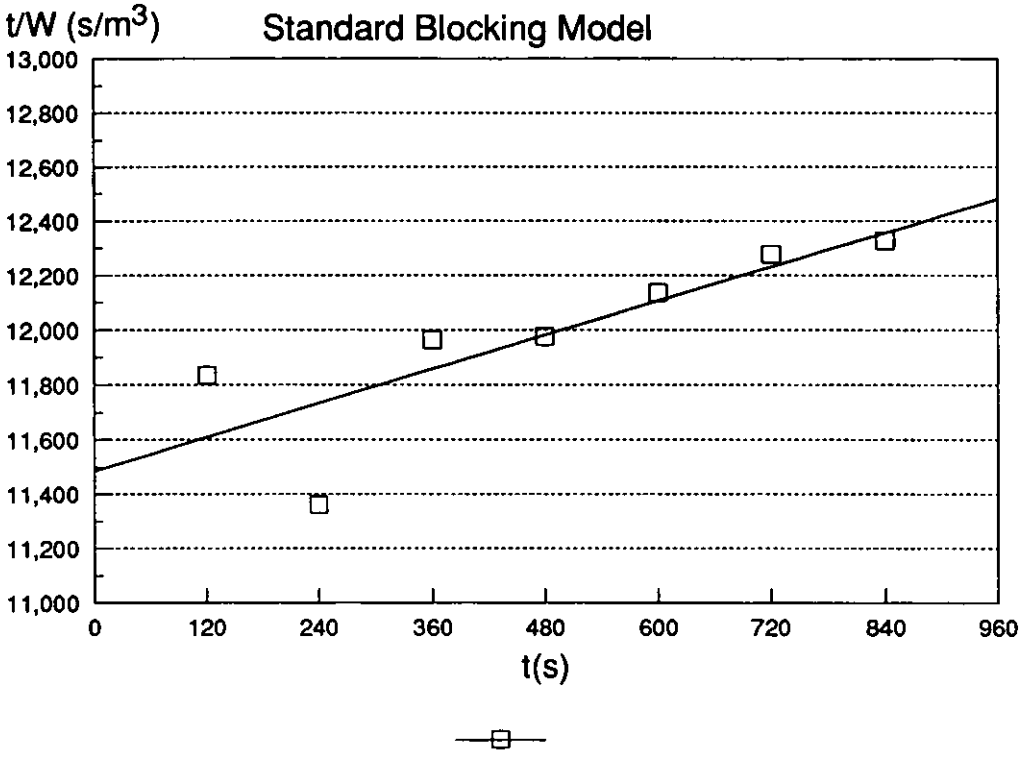
t/W (s/m3)
Standard Blocking Model
13,000
12,800
12,600
12,400
12,200
12,000
11,800
11,600
11,400
11,200
11,000
0
120
240
360
480
600
720
840
960
t(s)
Test G1

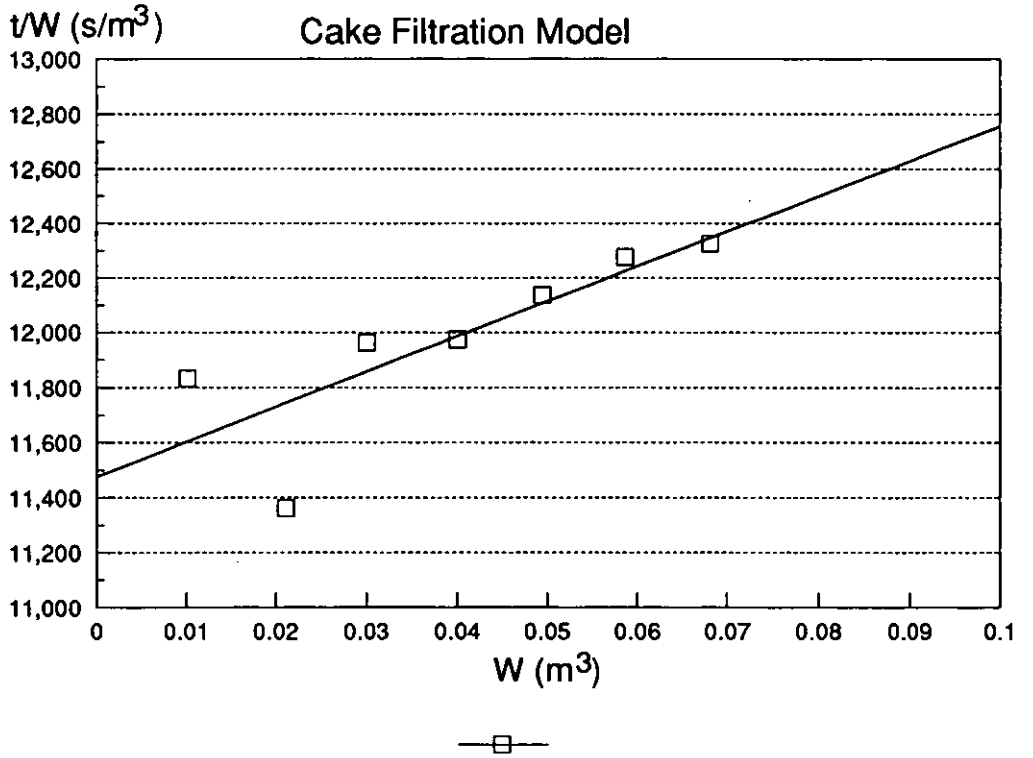
t/W (s/m3)
Cake Filtration Model
13,000
12,800
12,600
12,400
12,200
12,000
11,800
11,600
11,400
11,200
11,000
0
0.01
0.02
0.03
0.04
0.05
0.06
0.07
0.08
0.09
0.1
W (m3)
Test G1

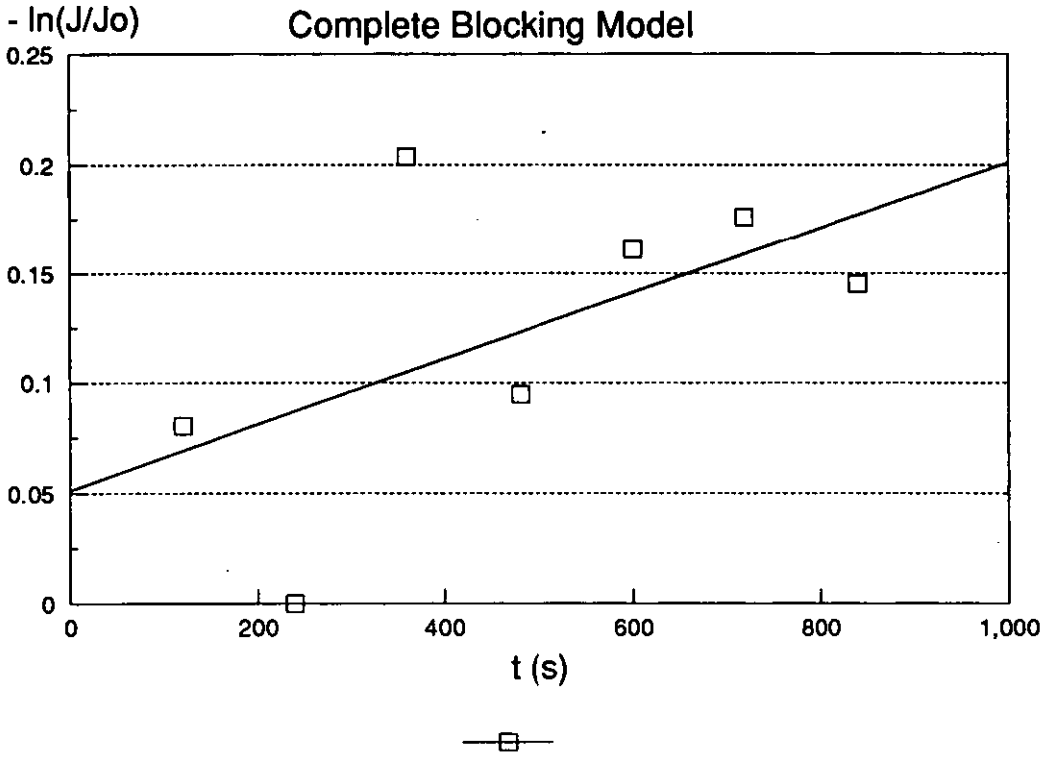
- ln(J/Jo)
Complete Blocking Model
0.25
0.2
0.15
0.1
0.05
0
0
200
400
600
800
1,000
t (s)
Test G1

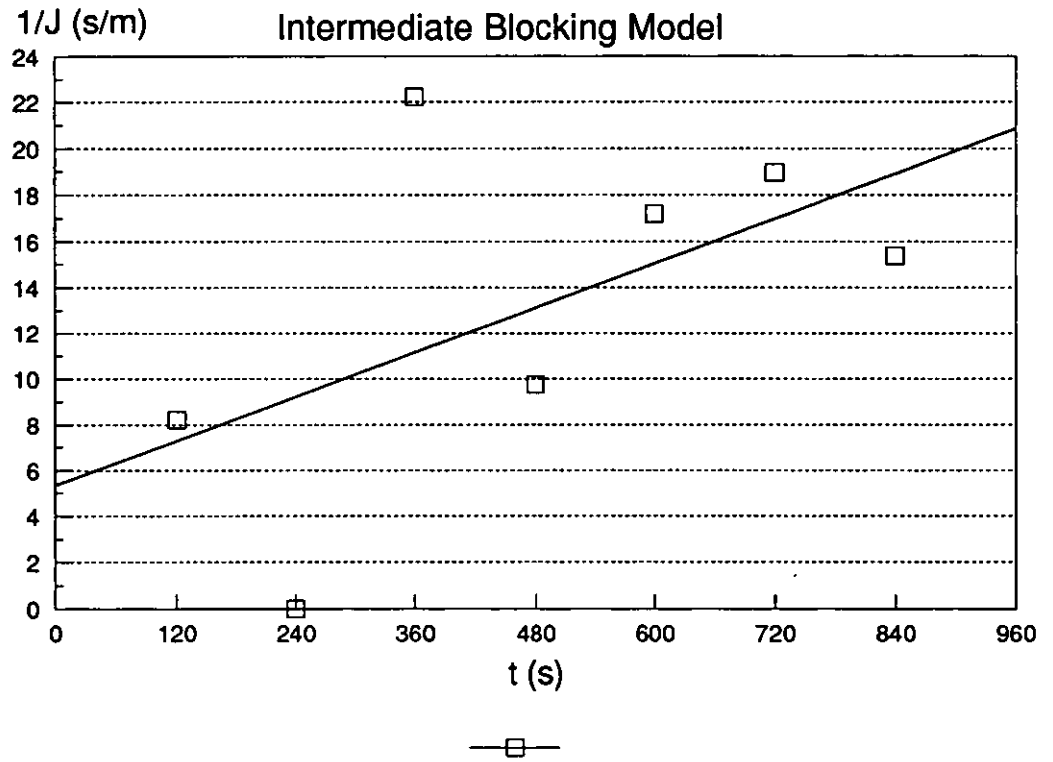
1/J (s/m)
Intermediate Blocking Model
24
22
20
18
16
14
12
10
8
6
4
2
0
0
120
240
360
480
600
720
840
960
t (s)
Test G1

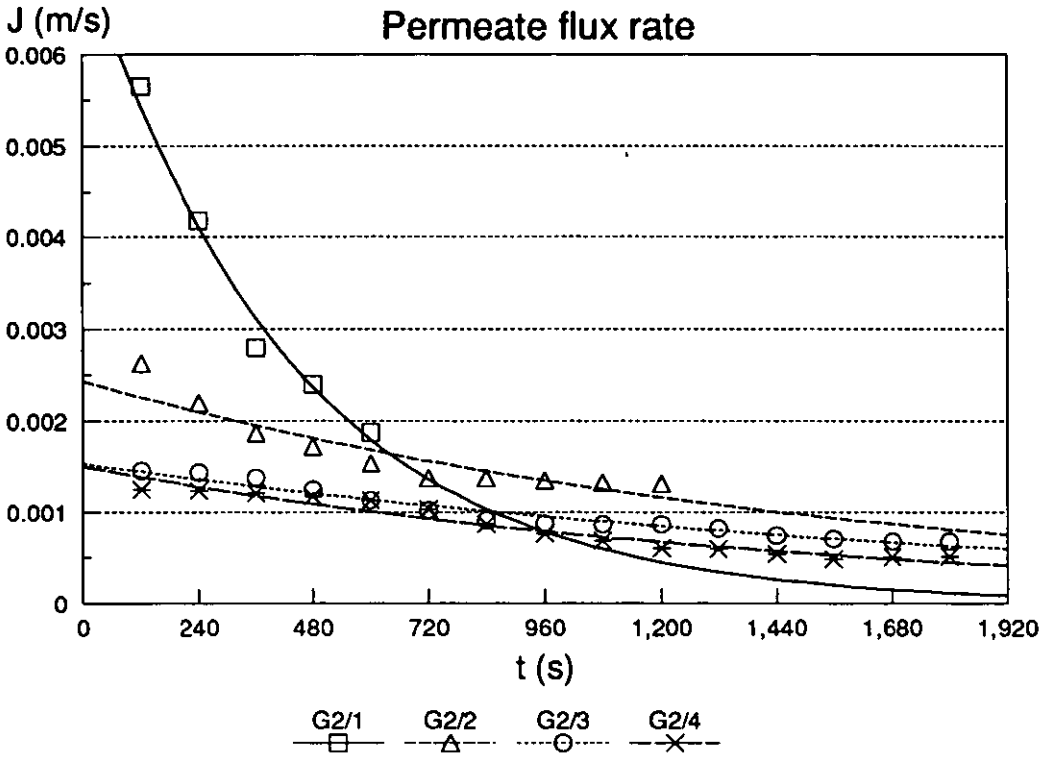

Test G2

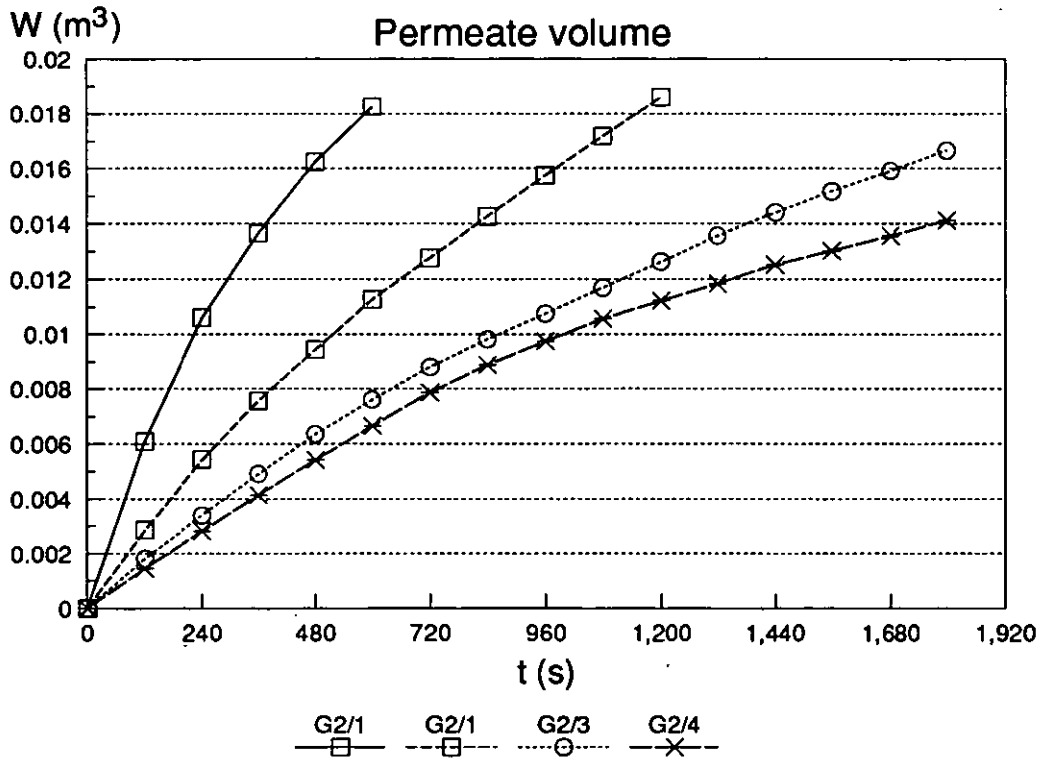

Test G2

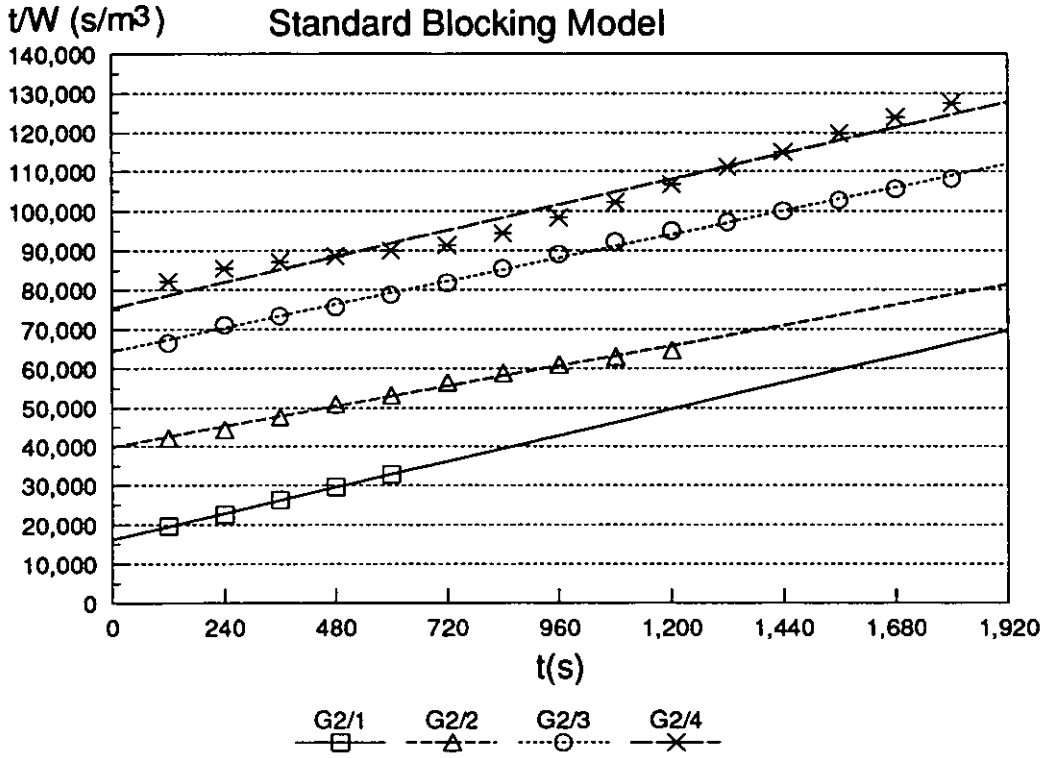

Test G2

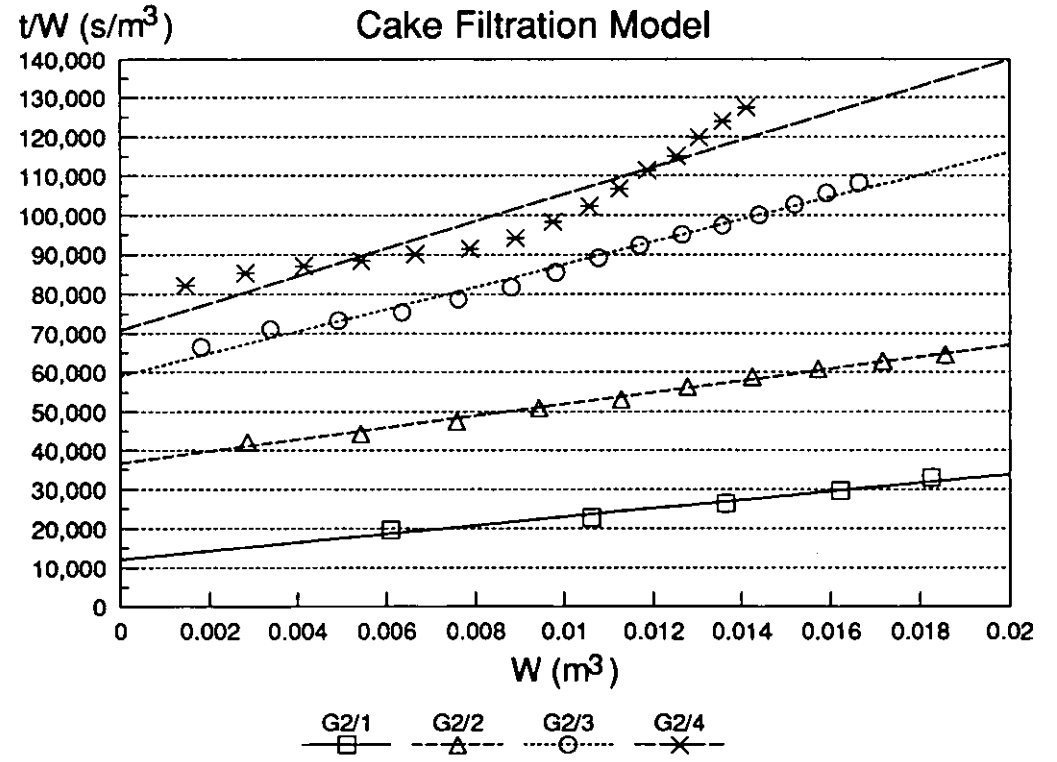

Test G2

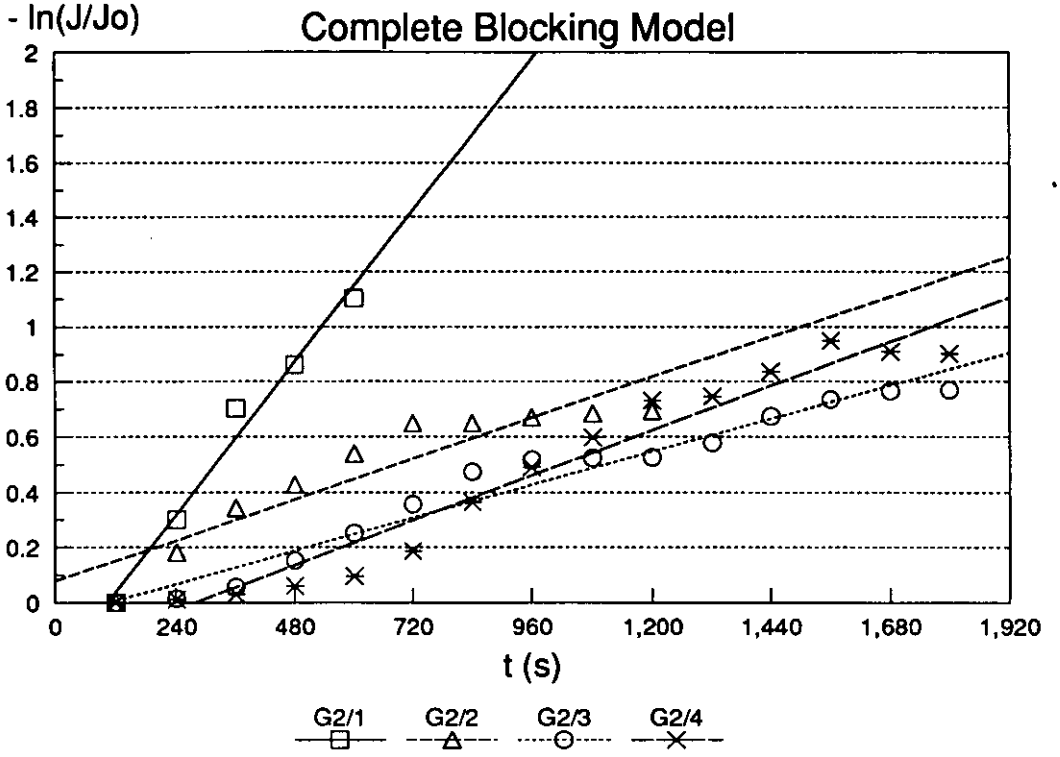

Test G2

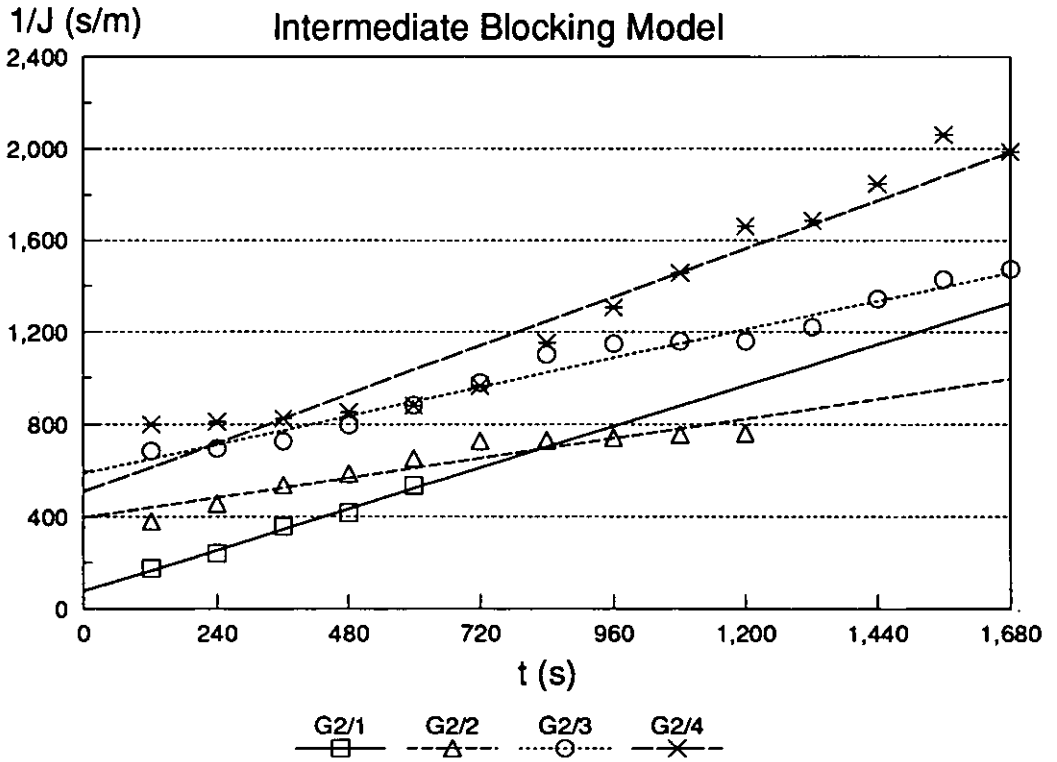

Test G2

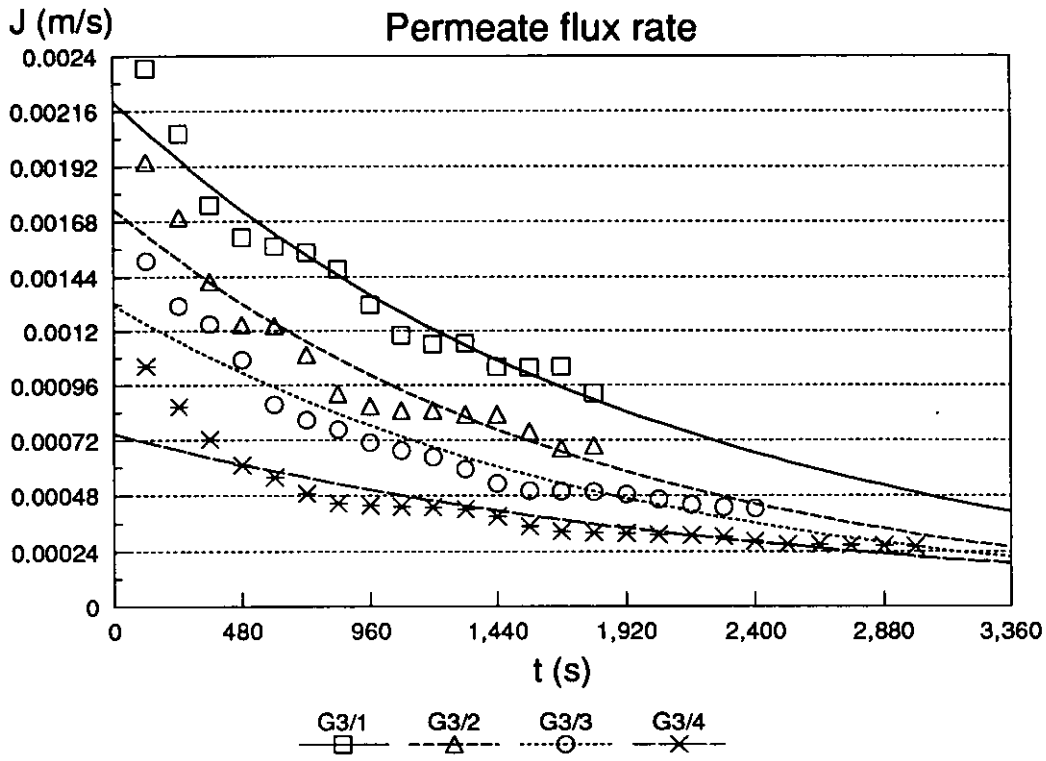

Test G3

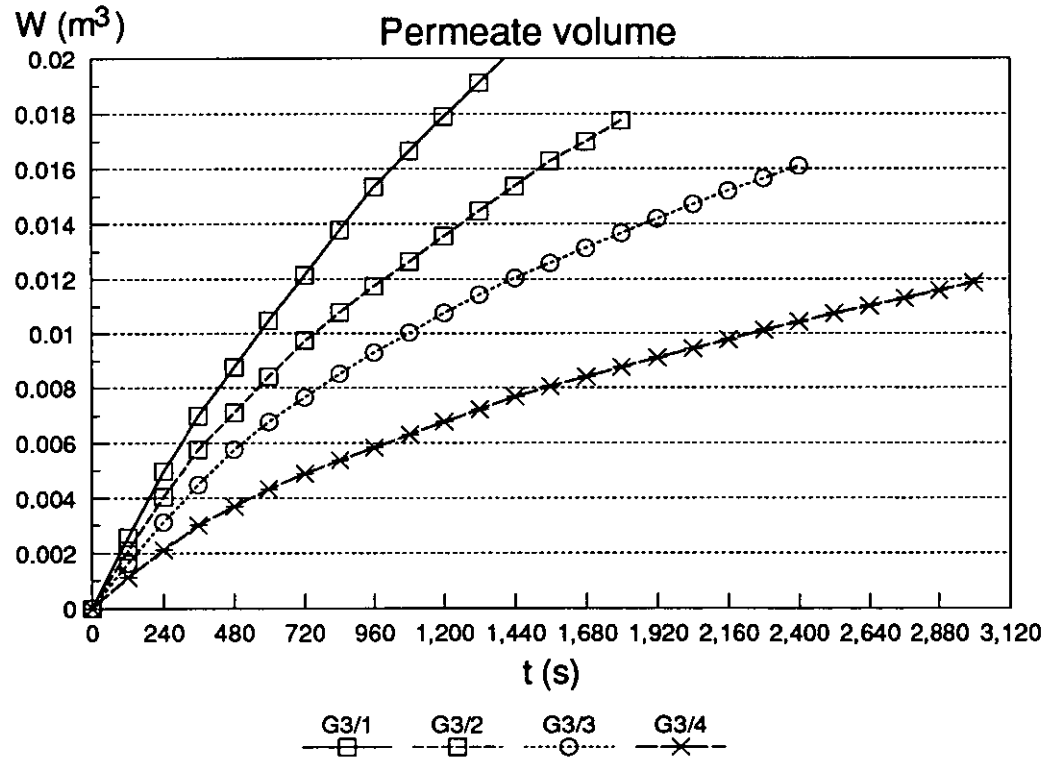

Test G3

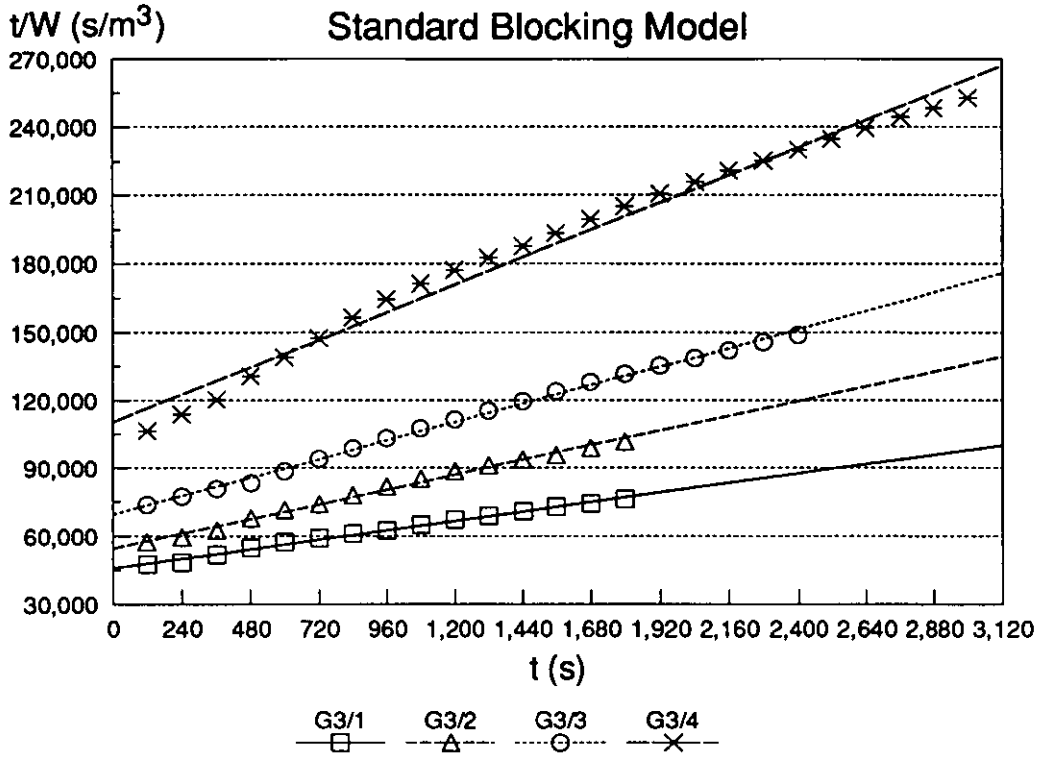

Test G3

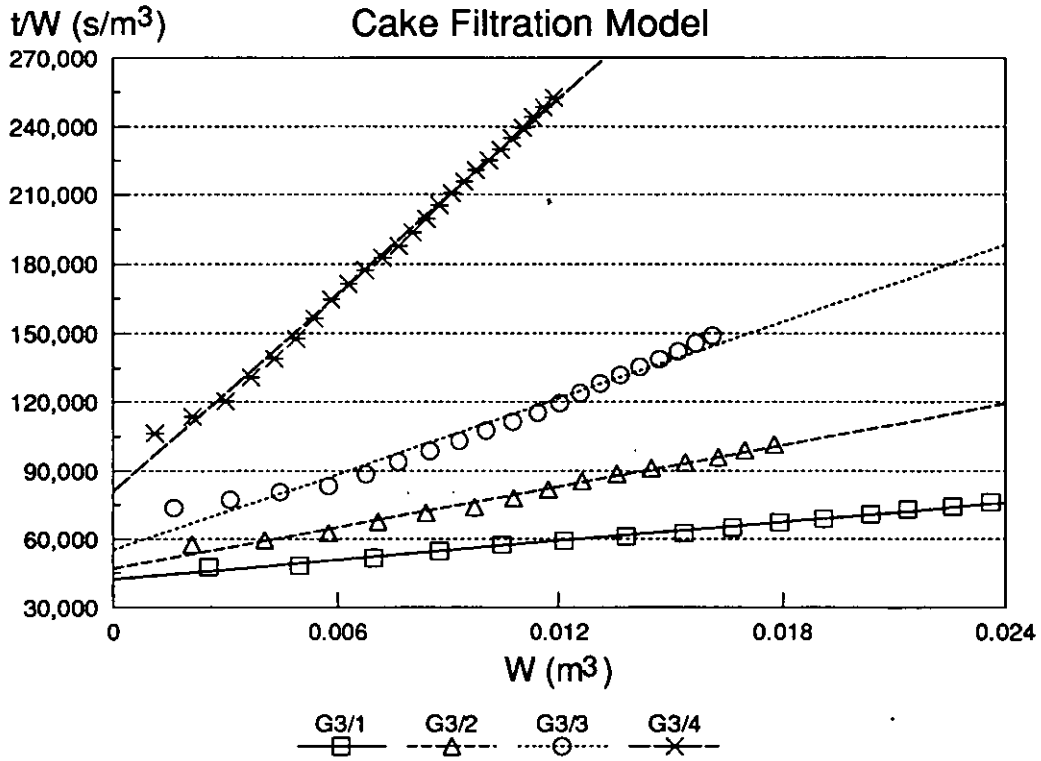

Test G3

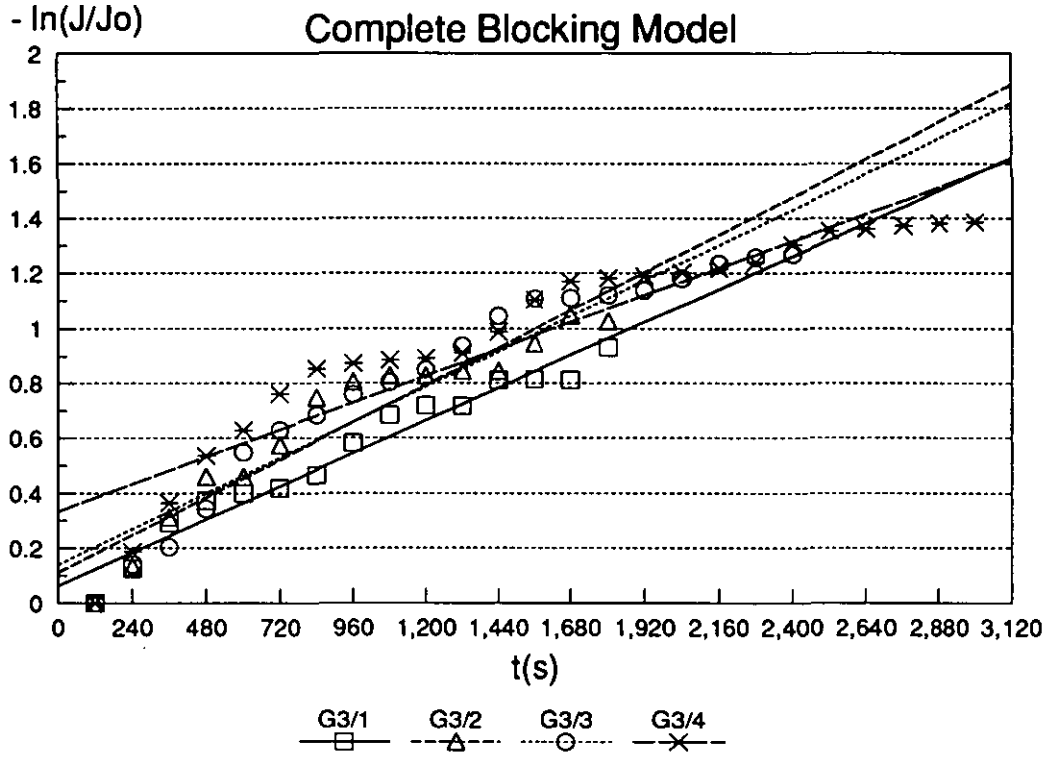

Test G3

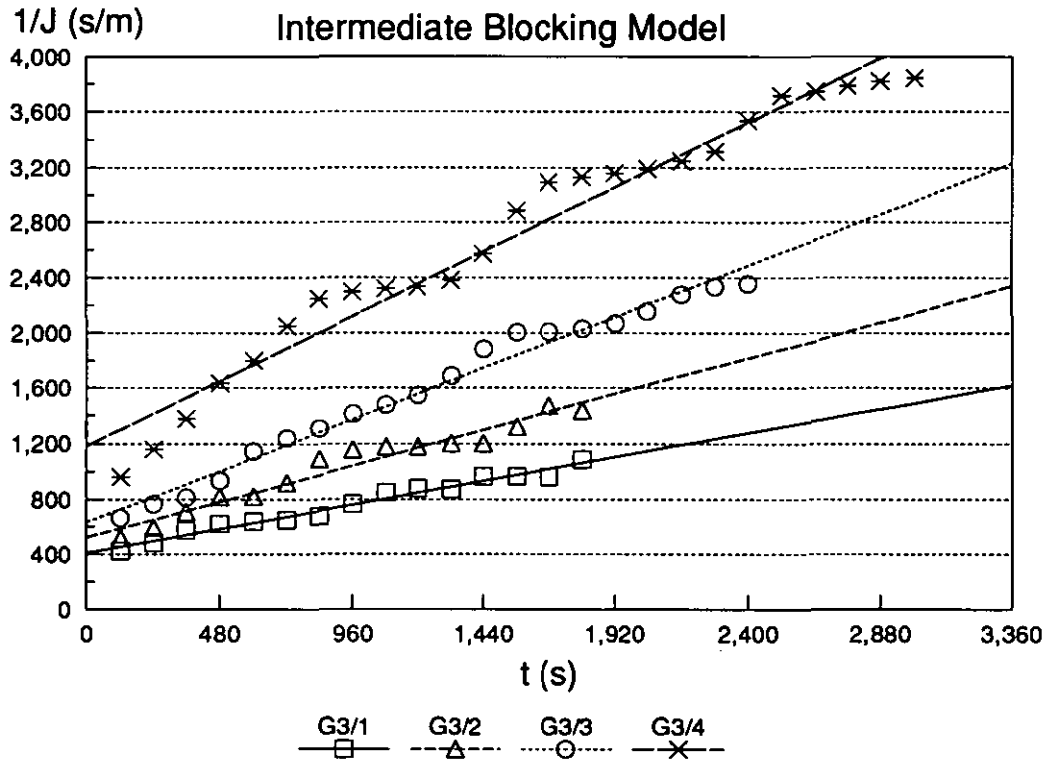

Test G3

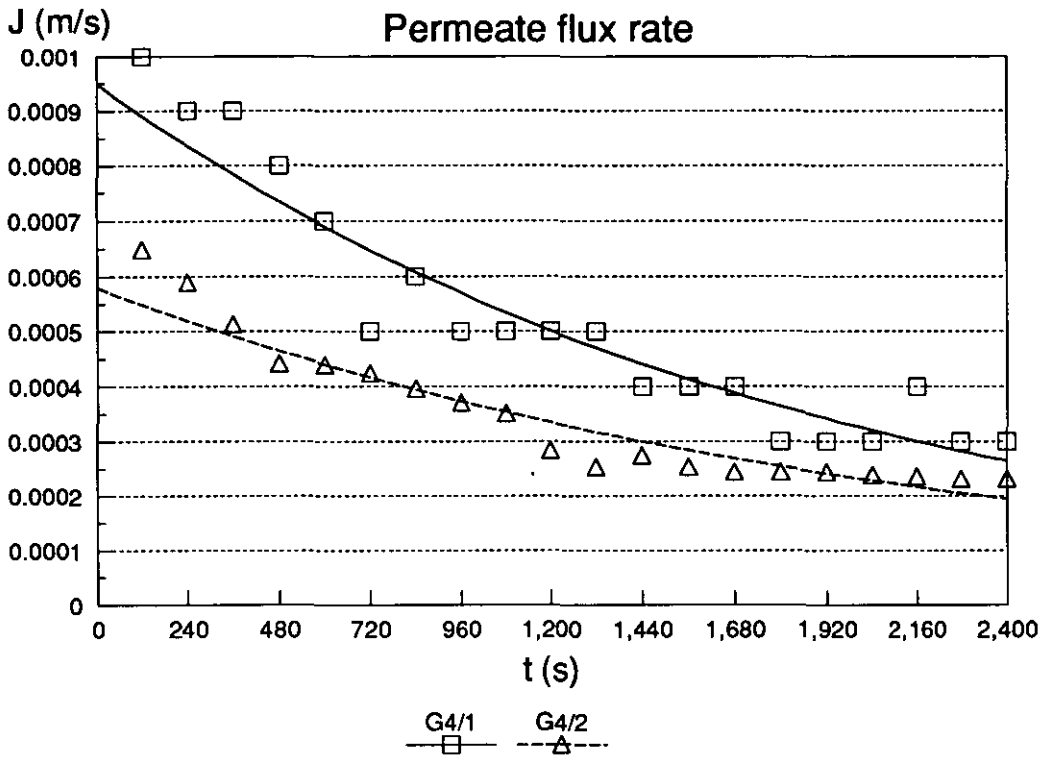

Test G4

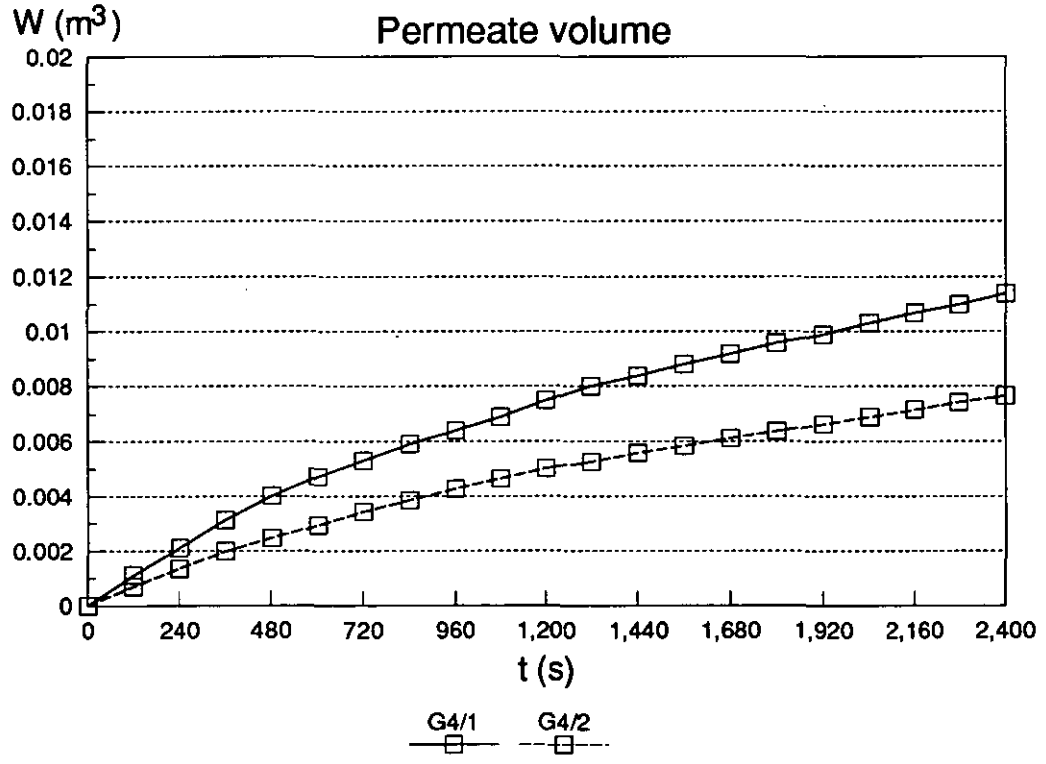

Test G4

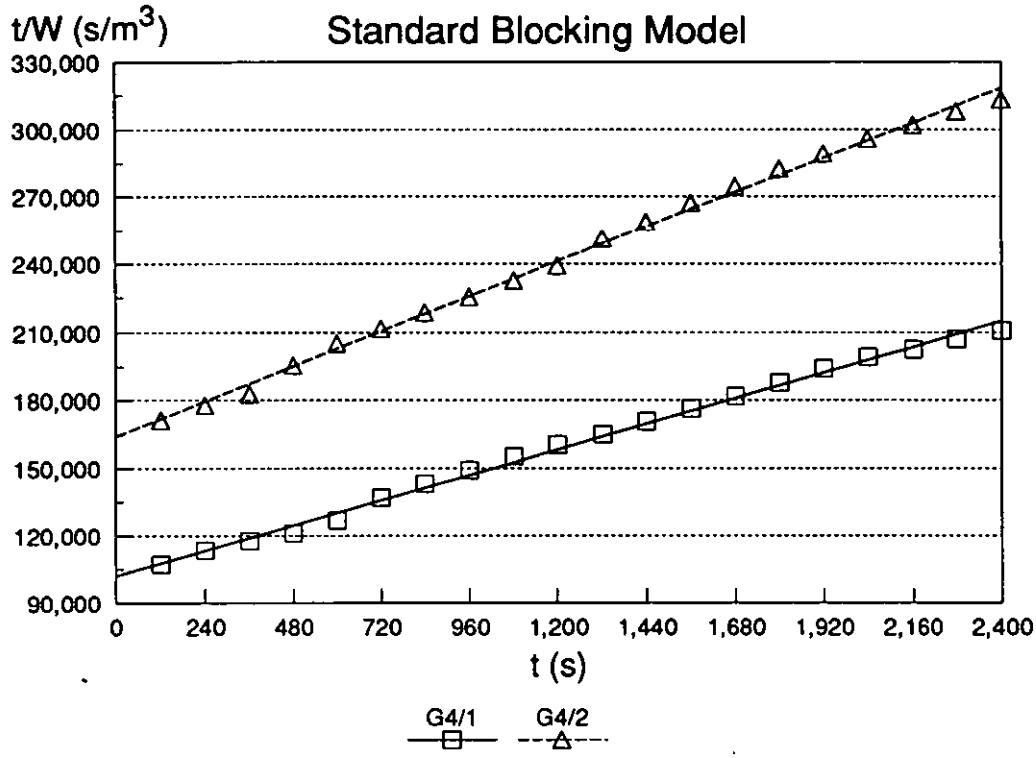

Test G4

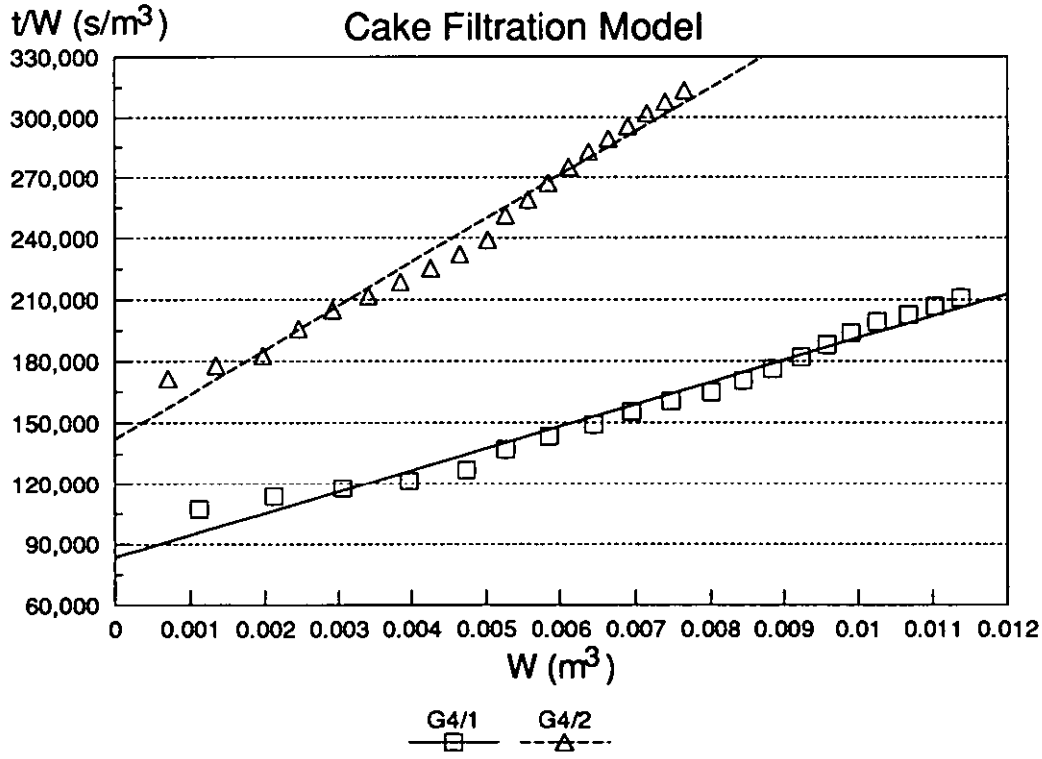

Test G4

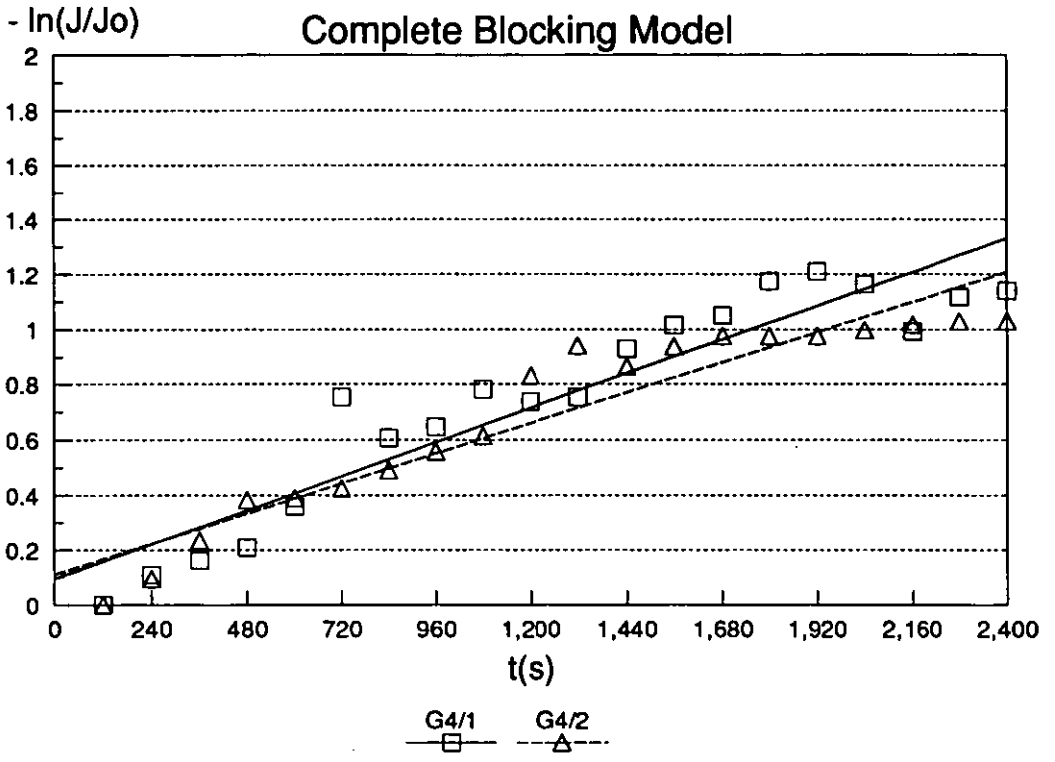

Test G4

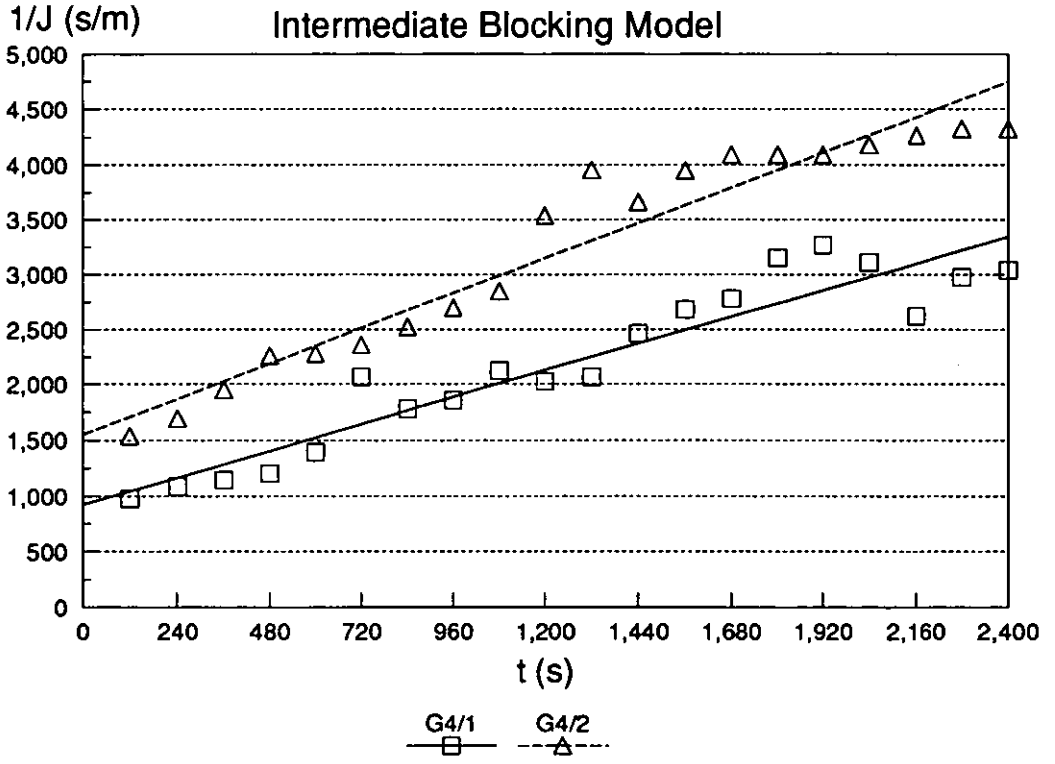

Test G4

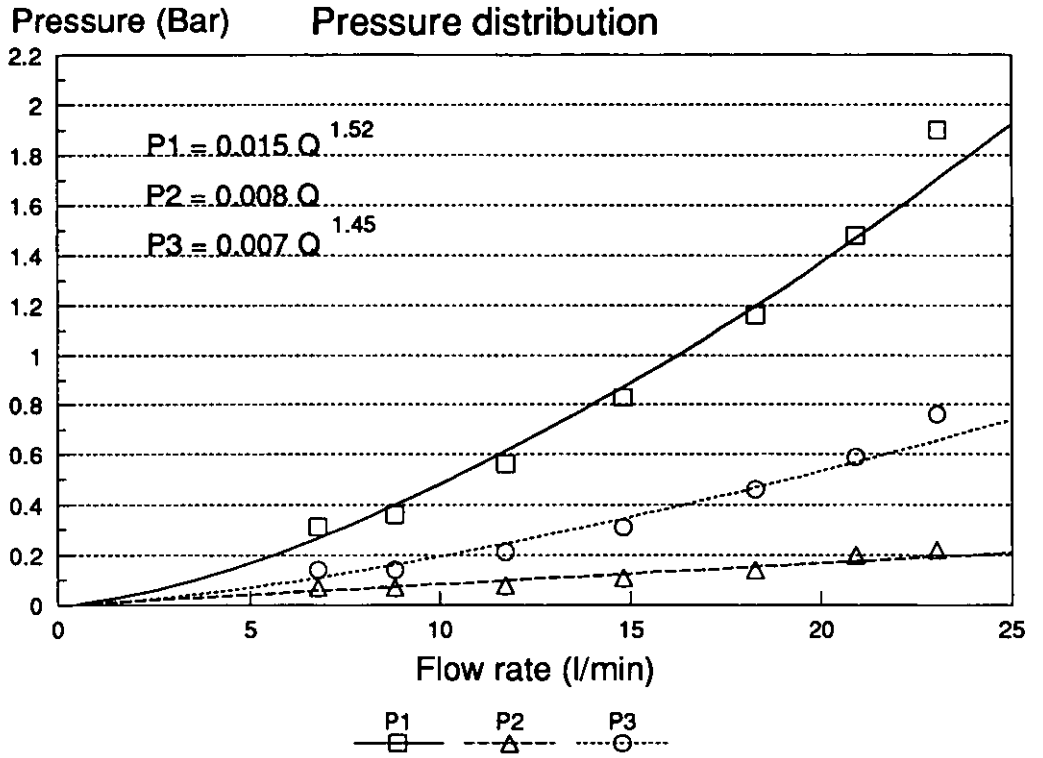

Test H1

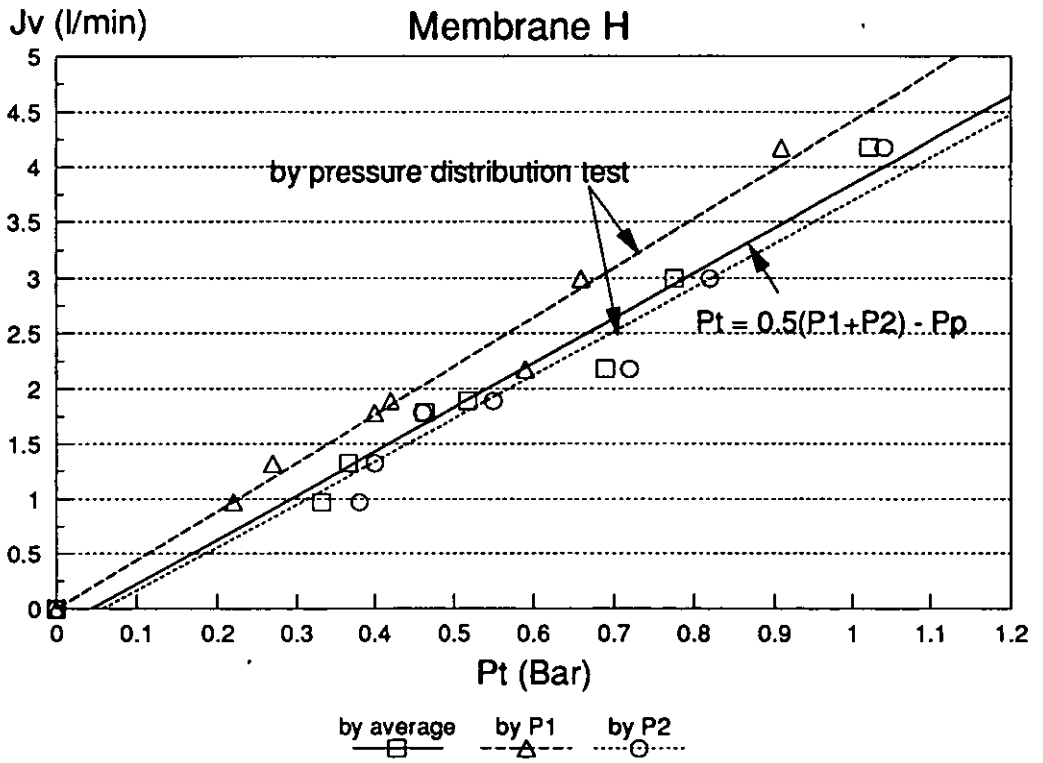

Test H1

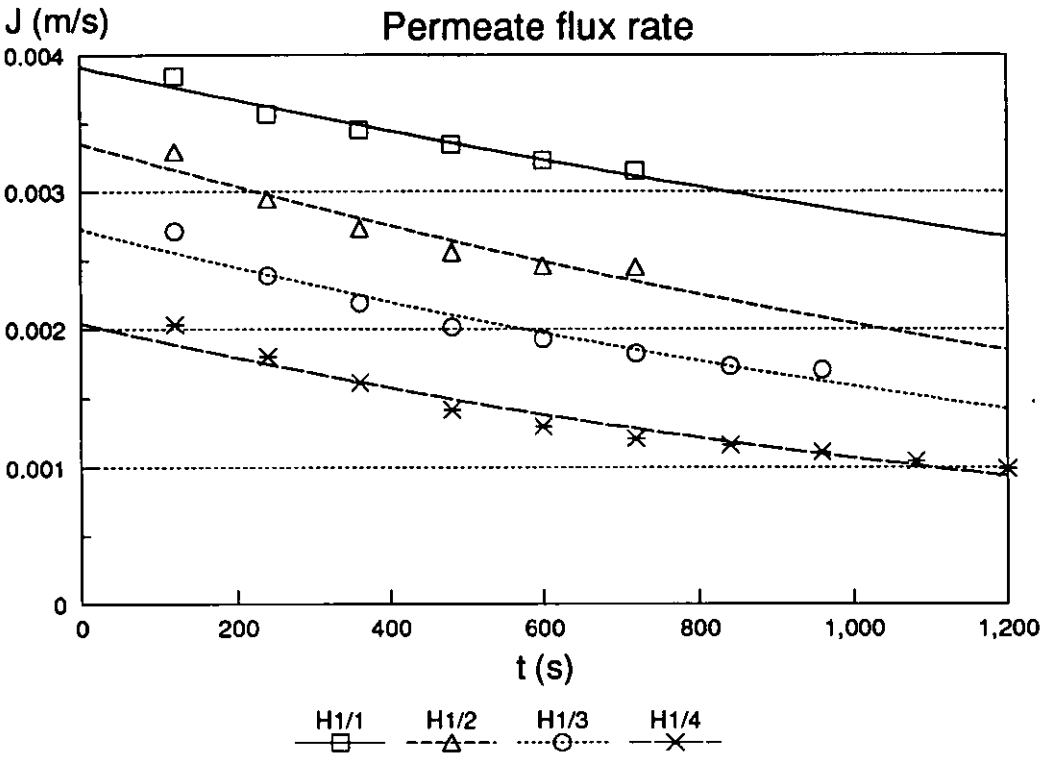

Test H1

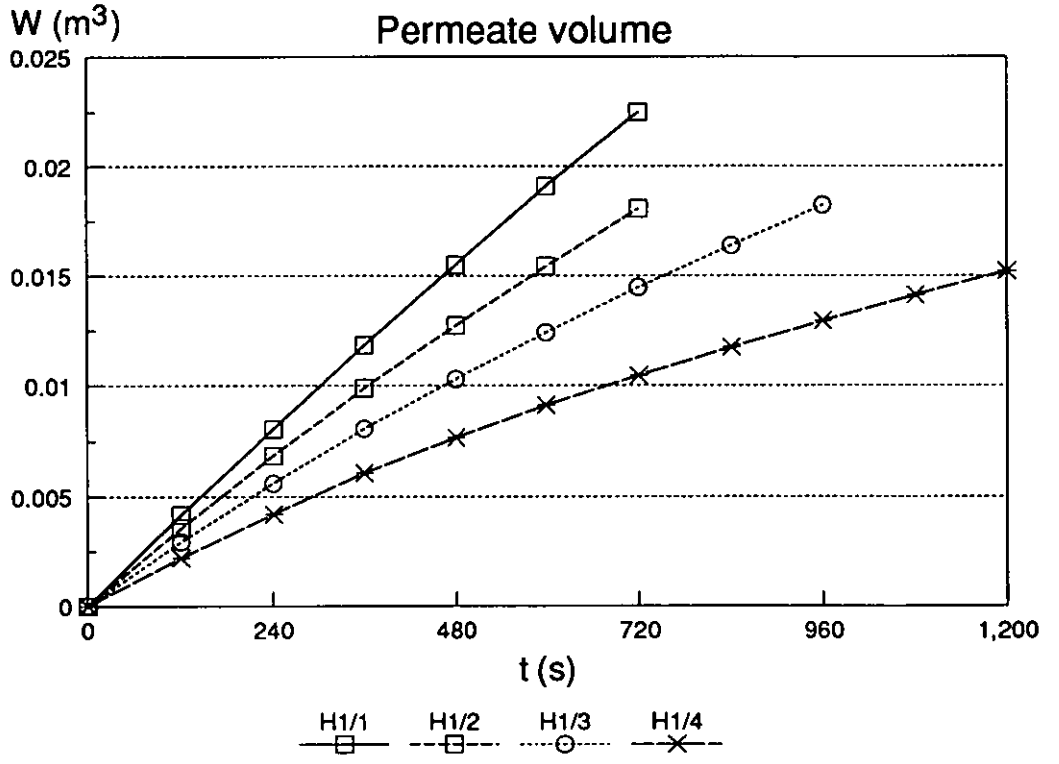

Test H1

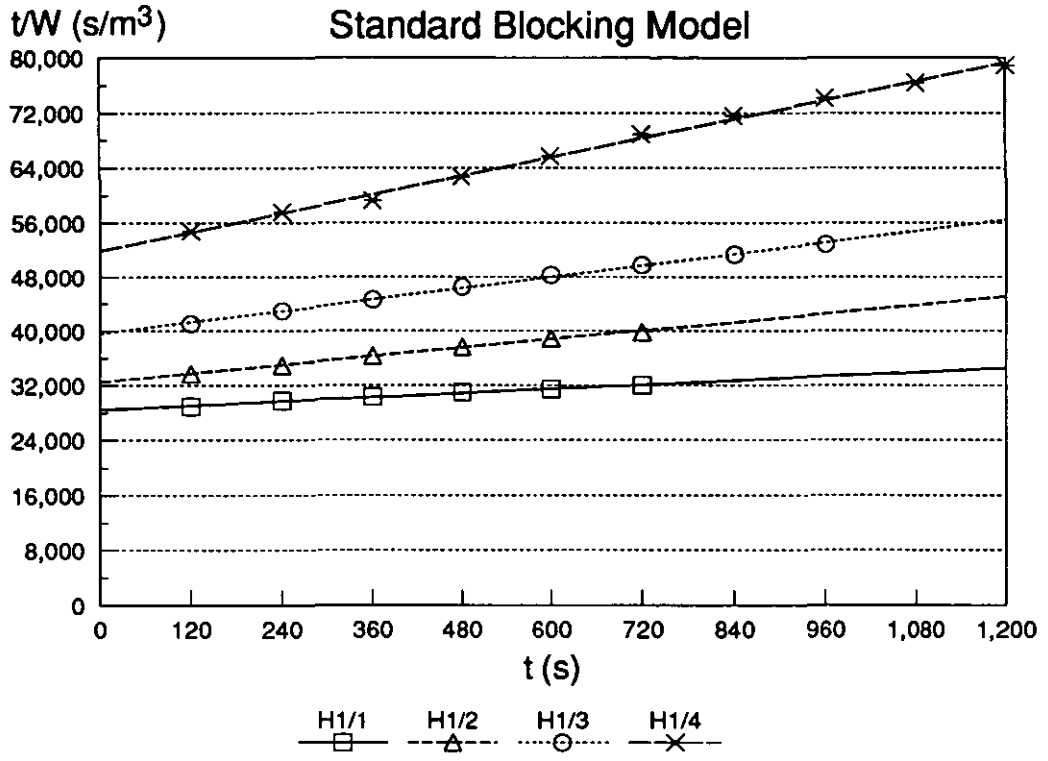

Test H1

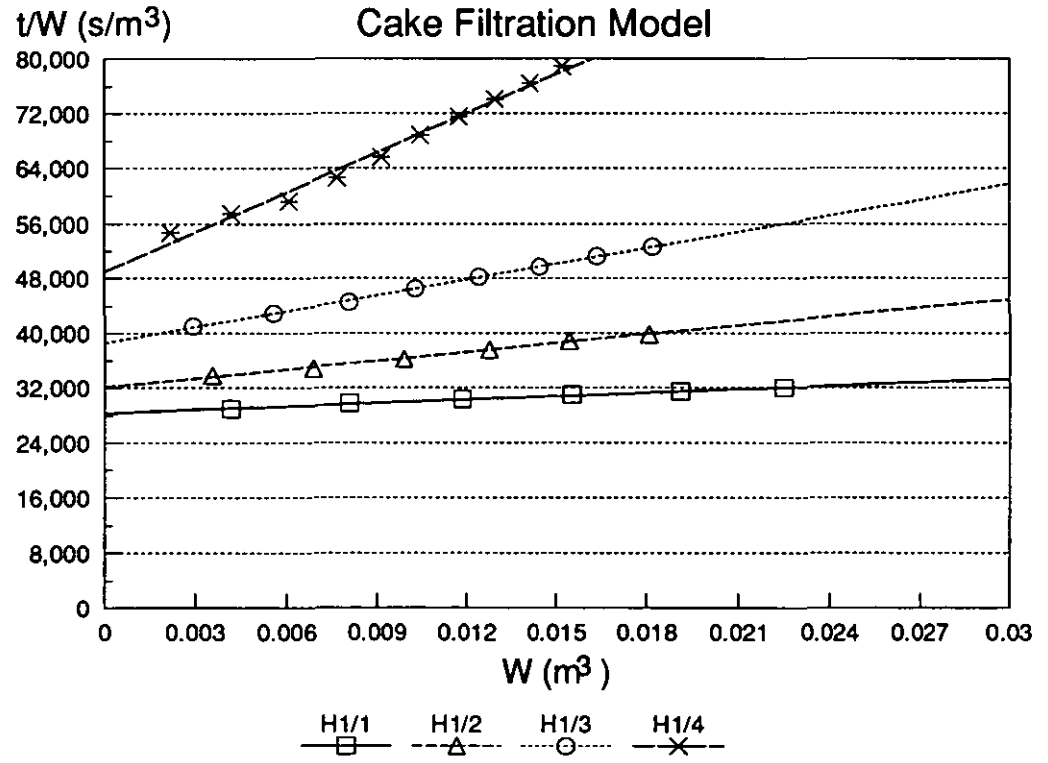

Test H1

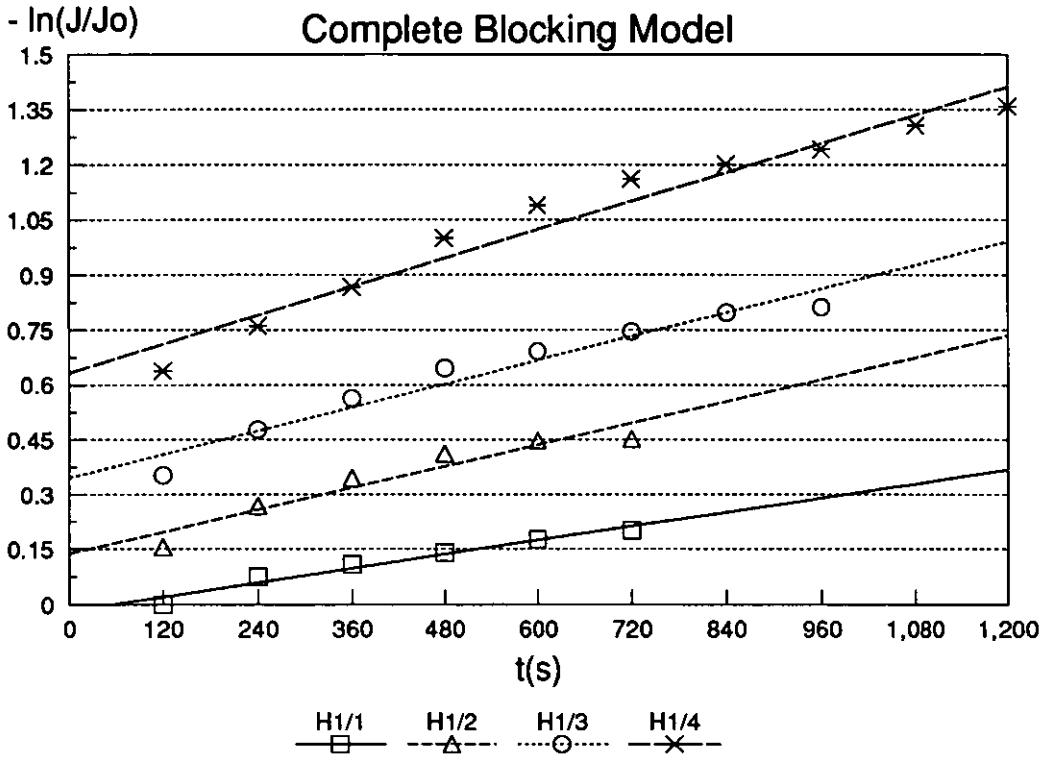

Test H1

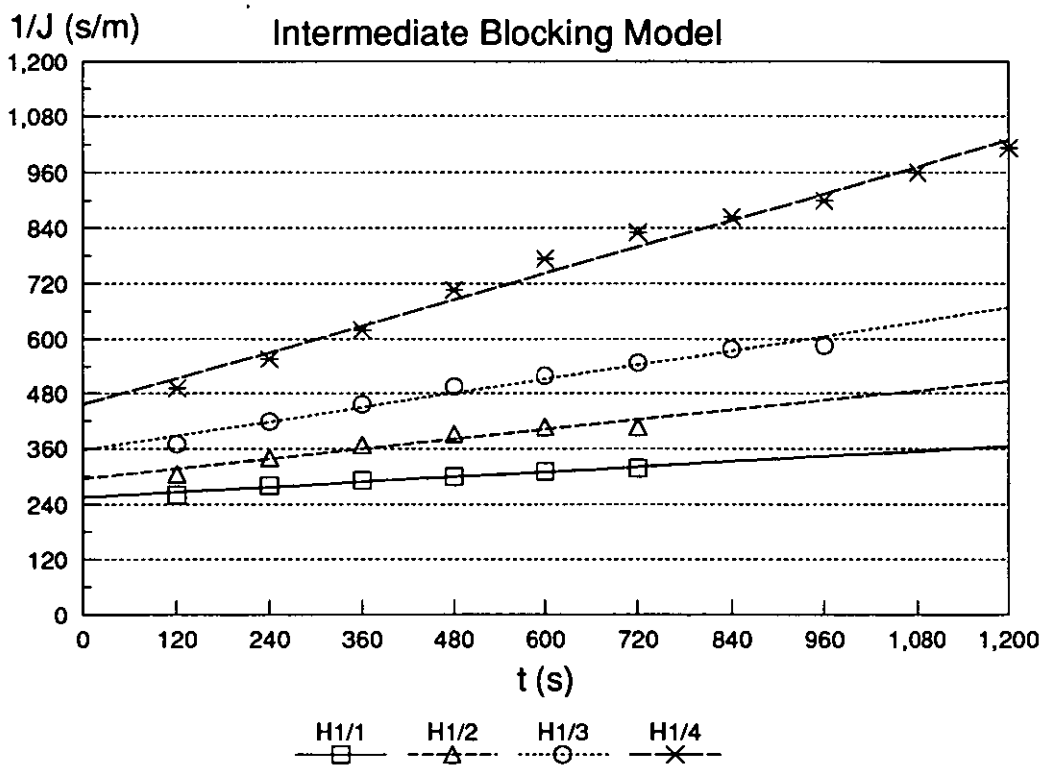

Test H1

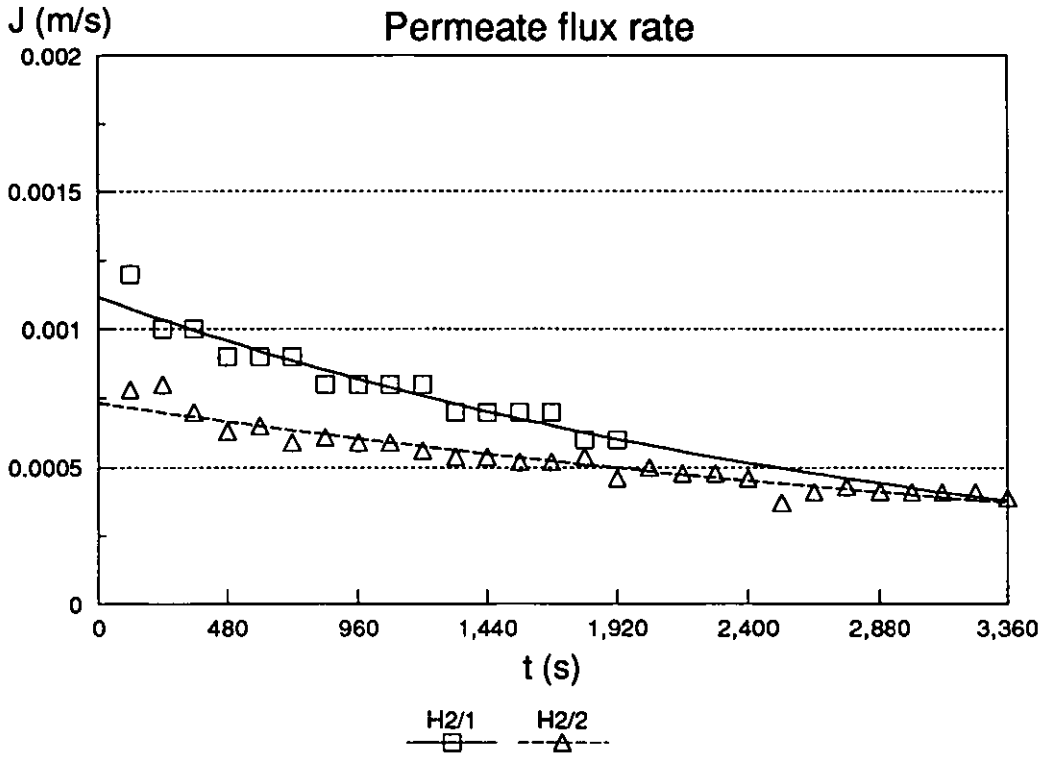

Test H2

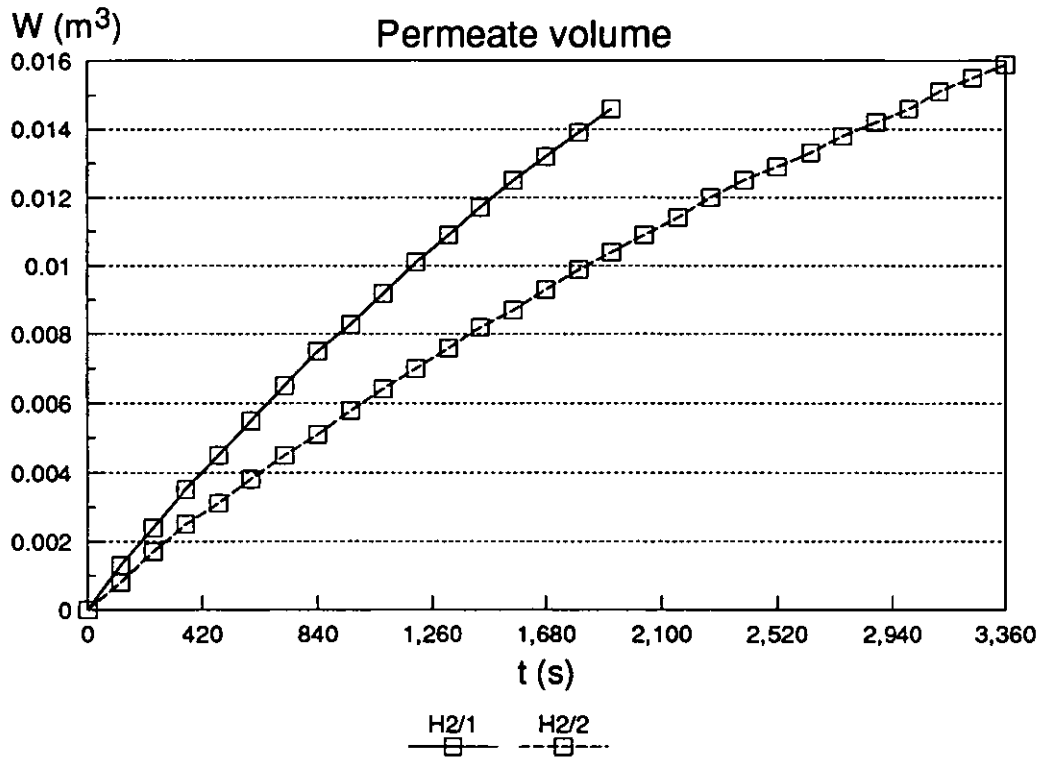

Test H2

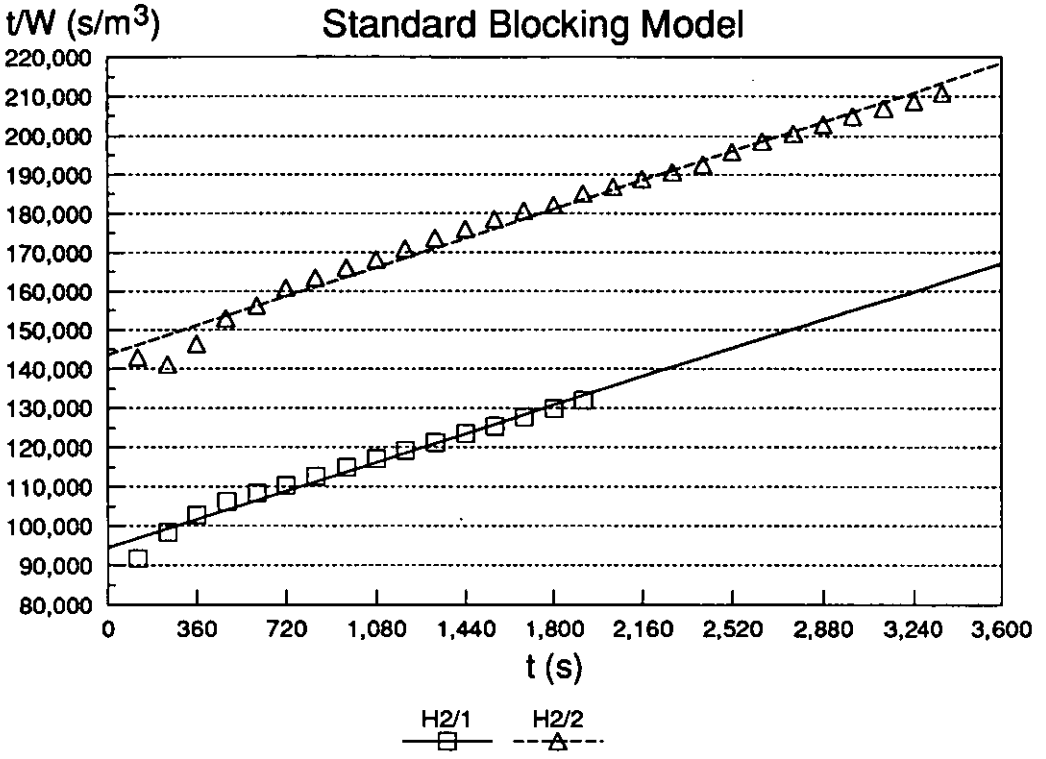

Test H2

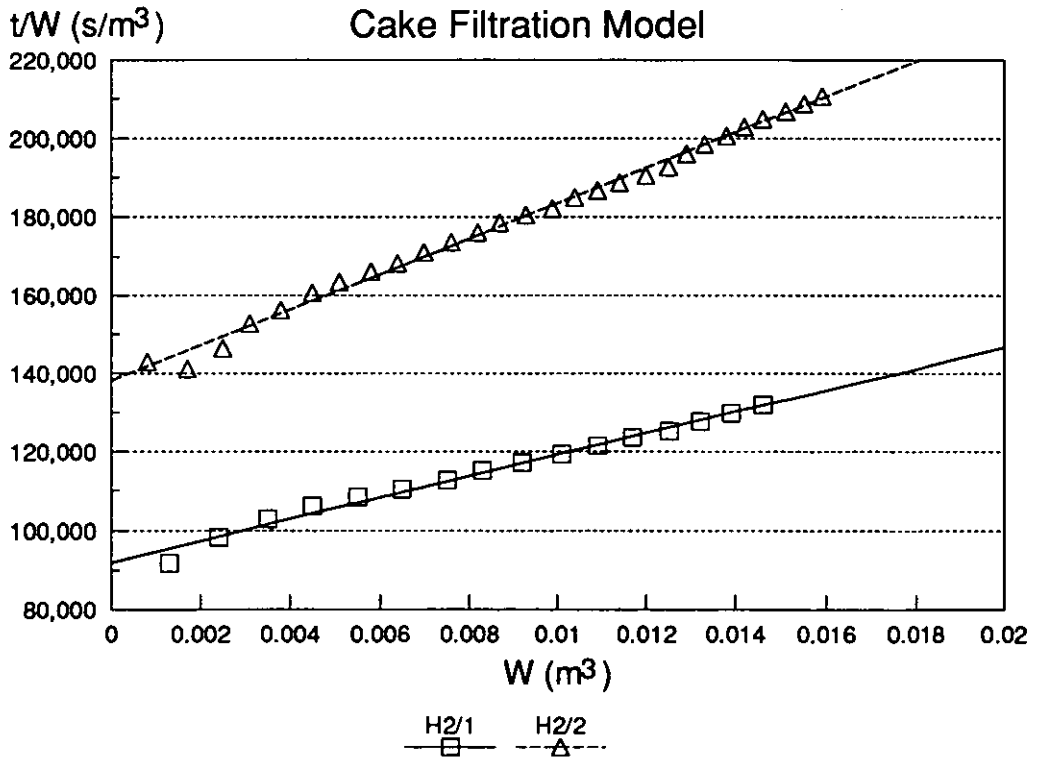

Test H2

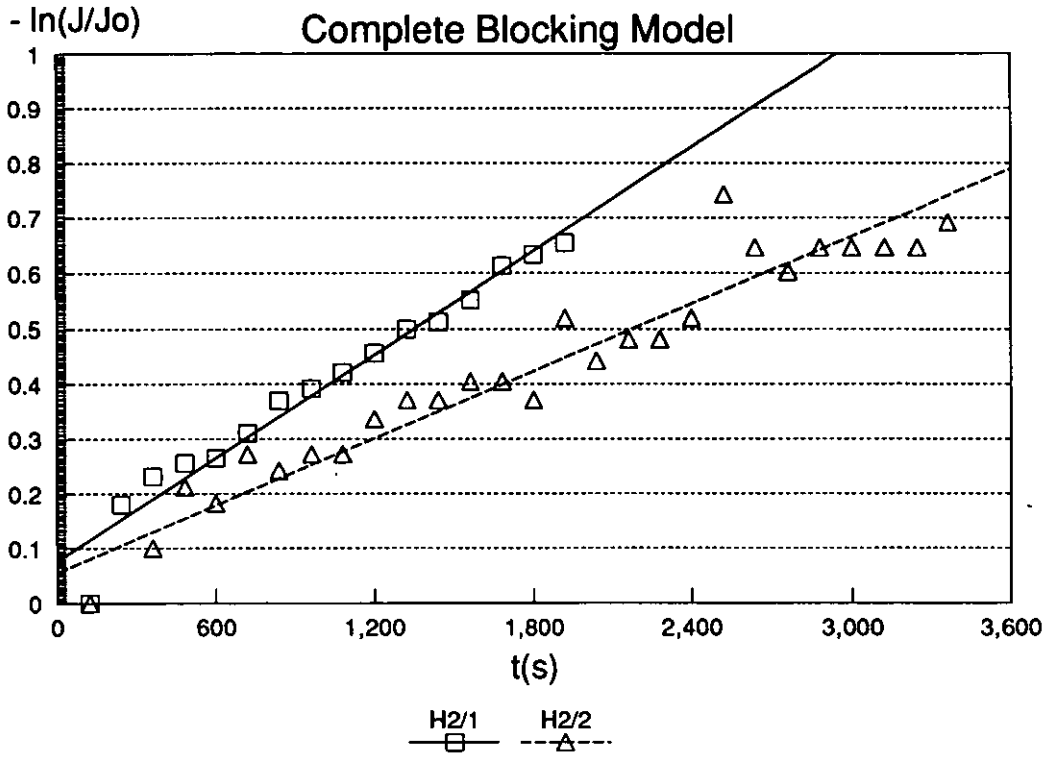

Test H2

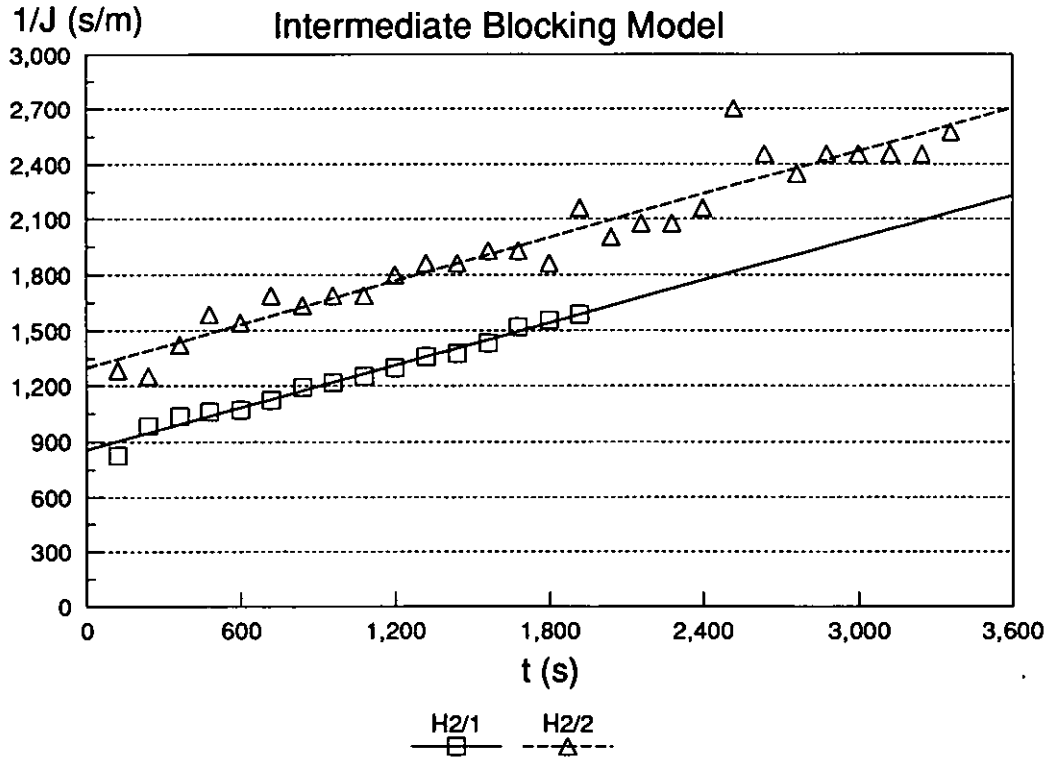

Test H2

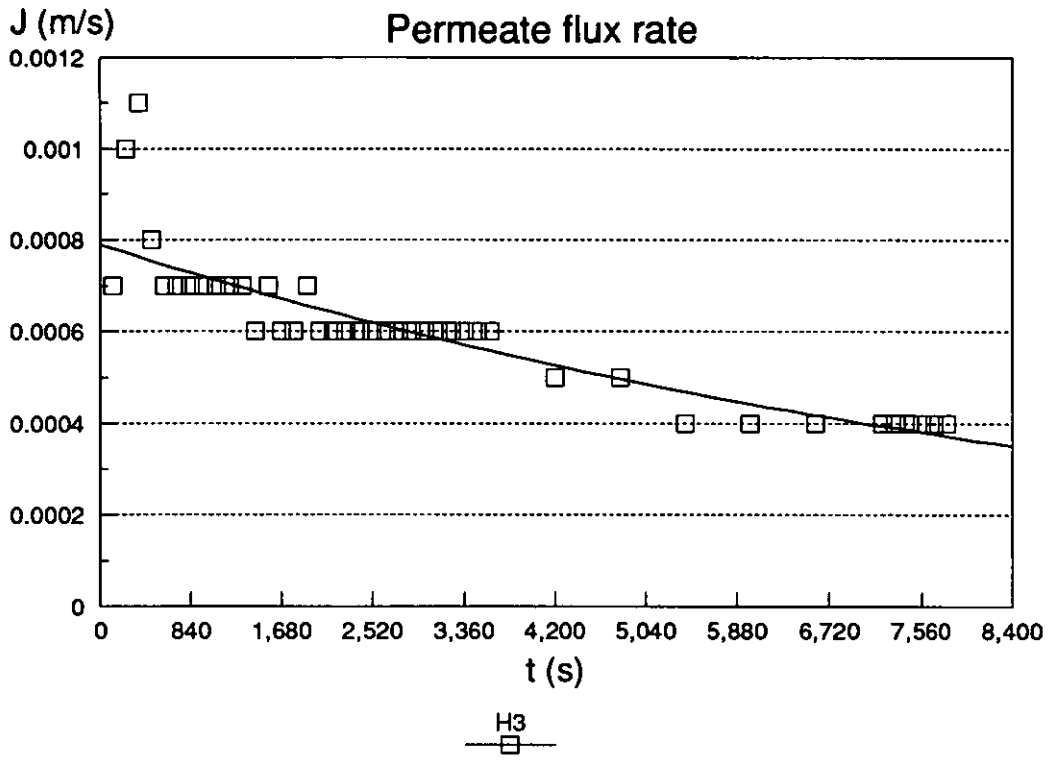

Test H3

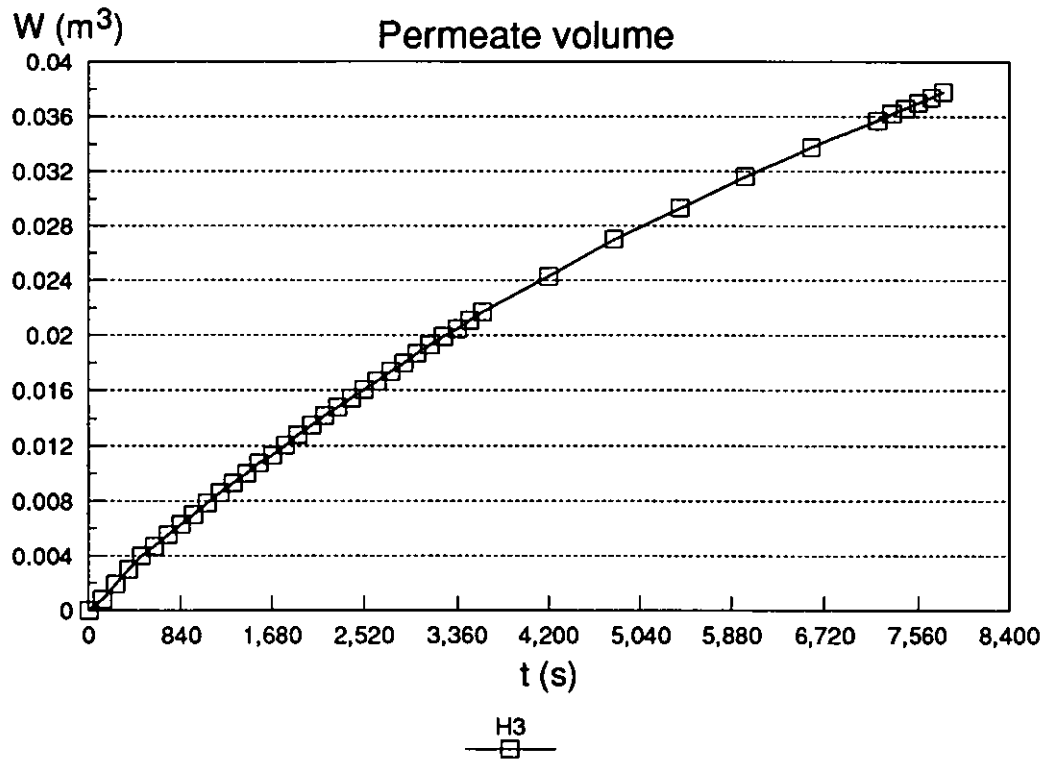

Test H3

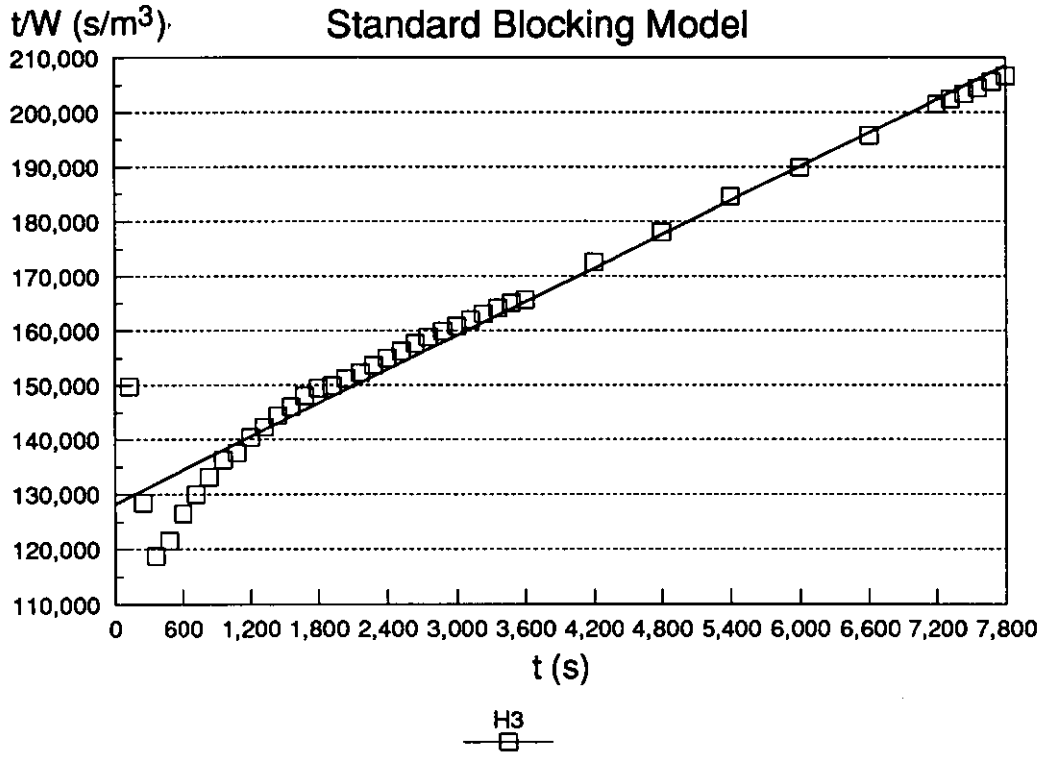

Test H3

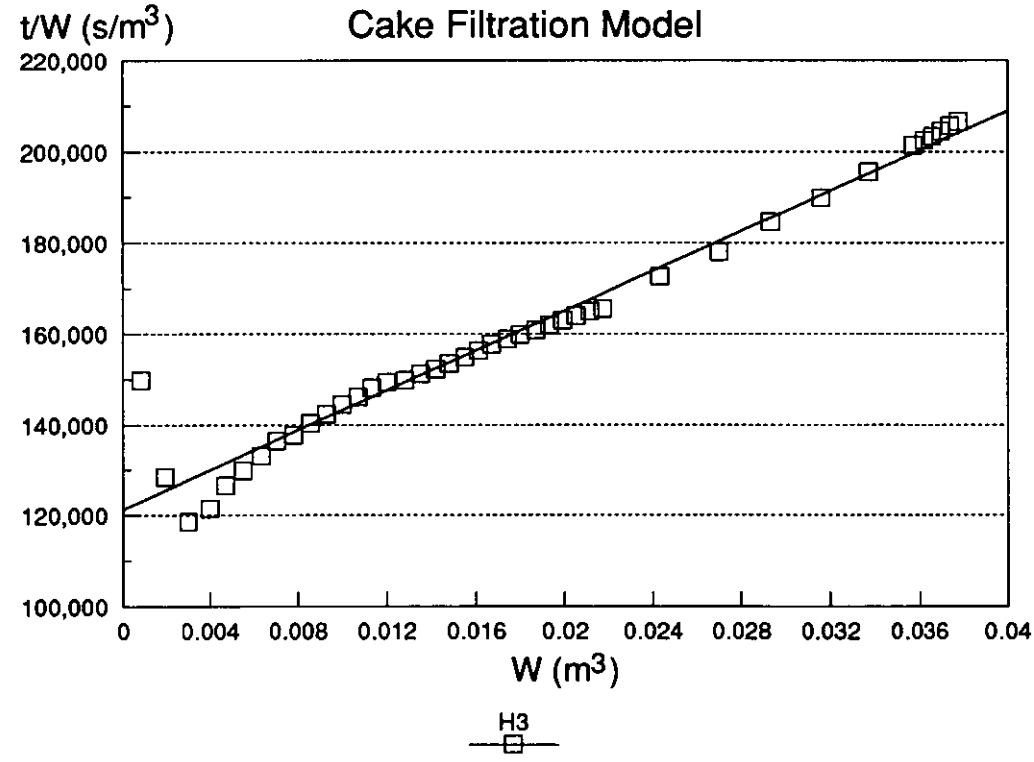

Test H3

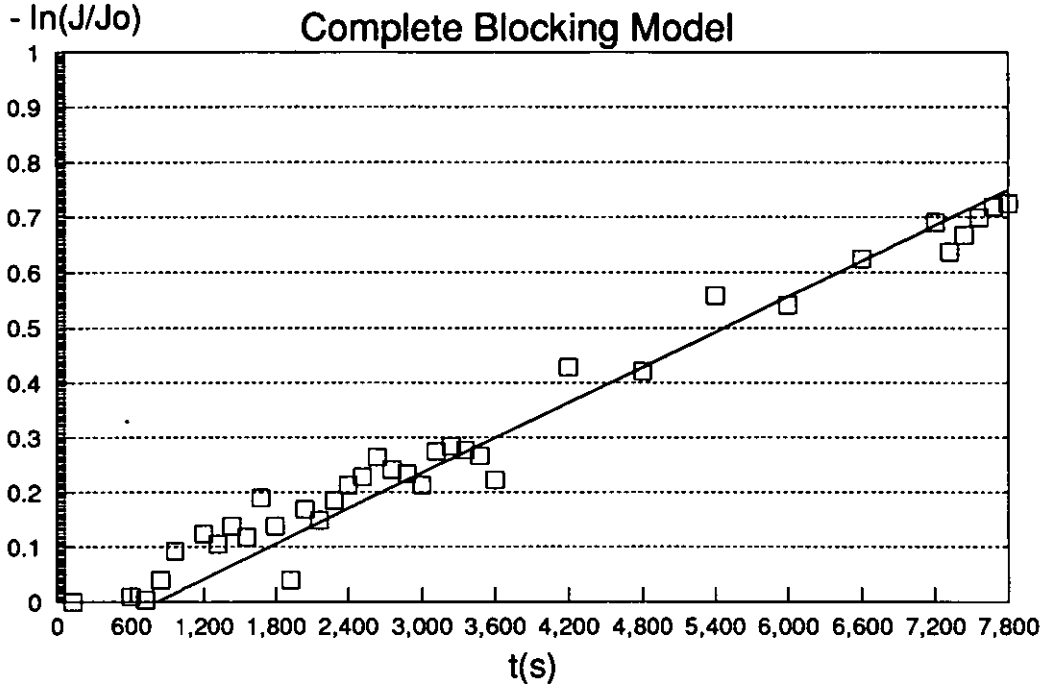

Test H3

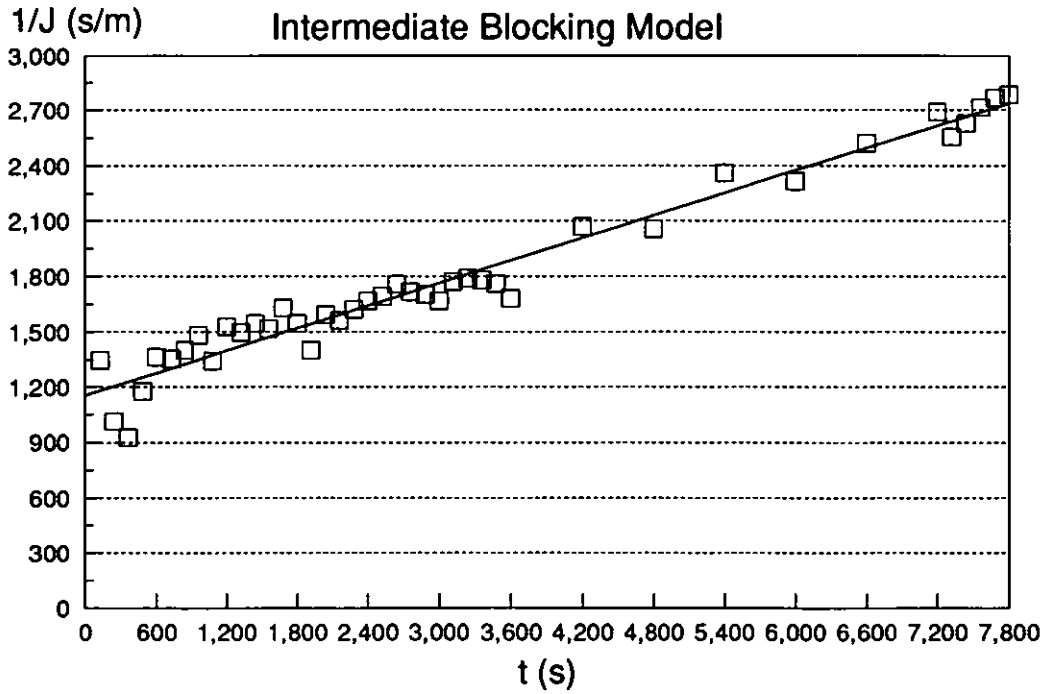

Test H3

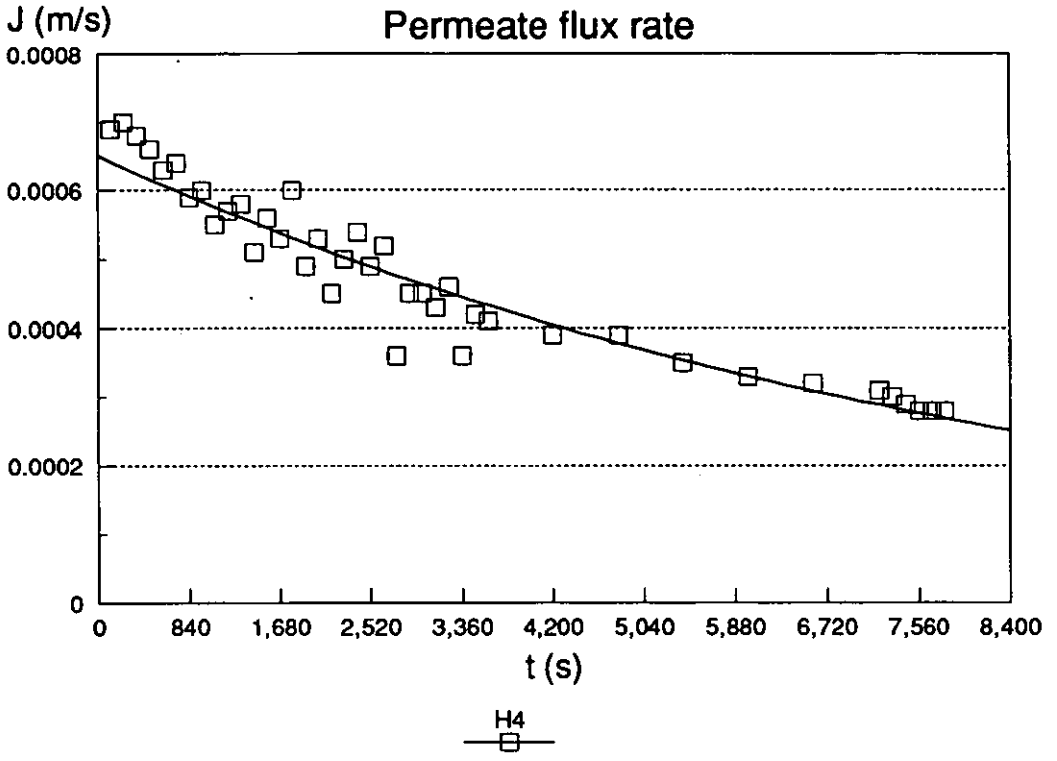

Test H4

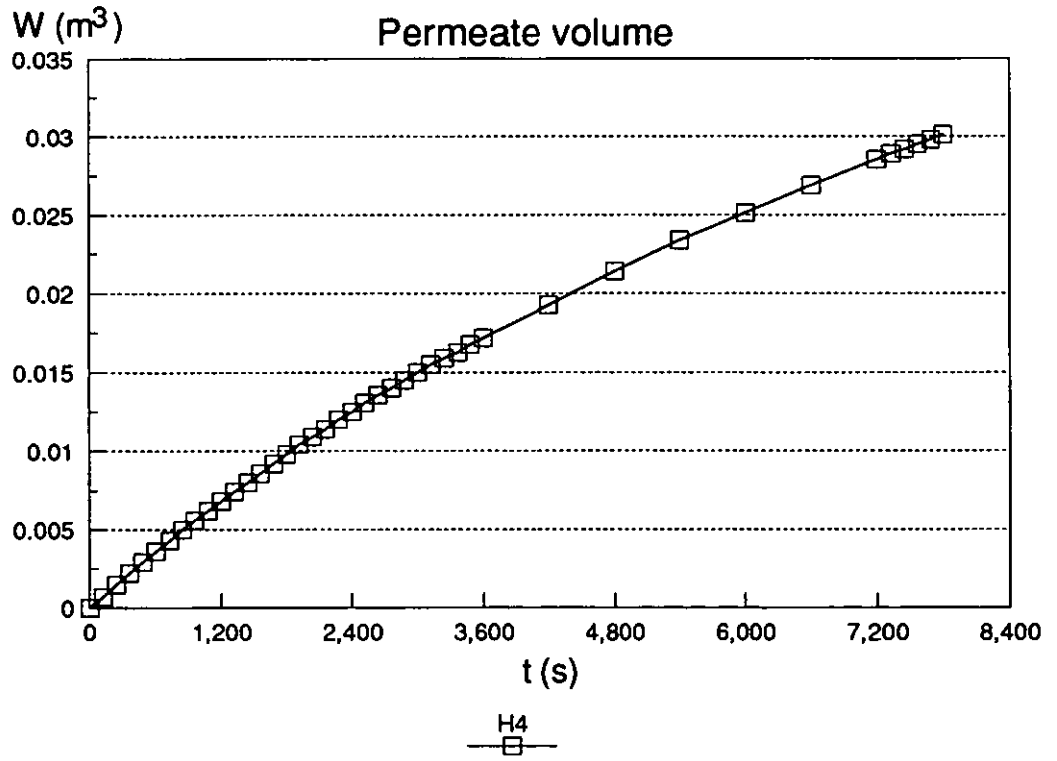

Test H4

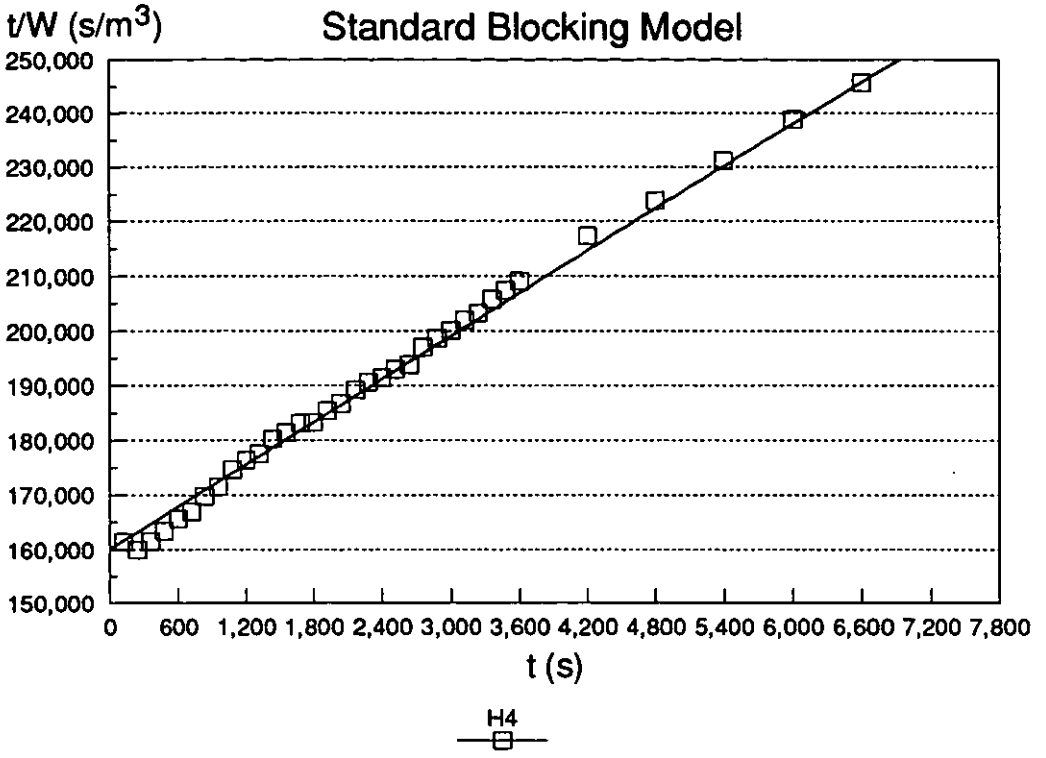

Test H4

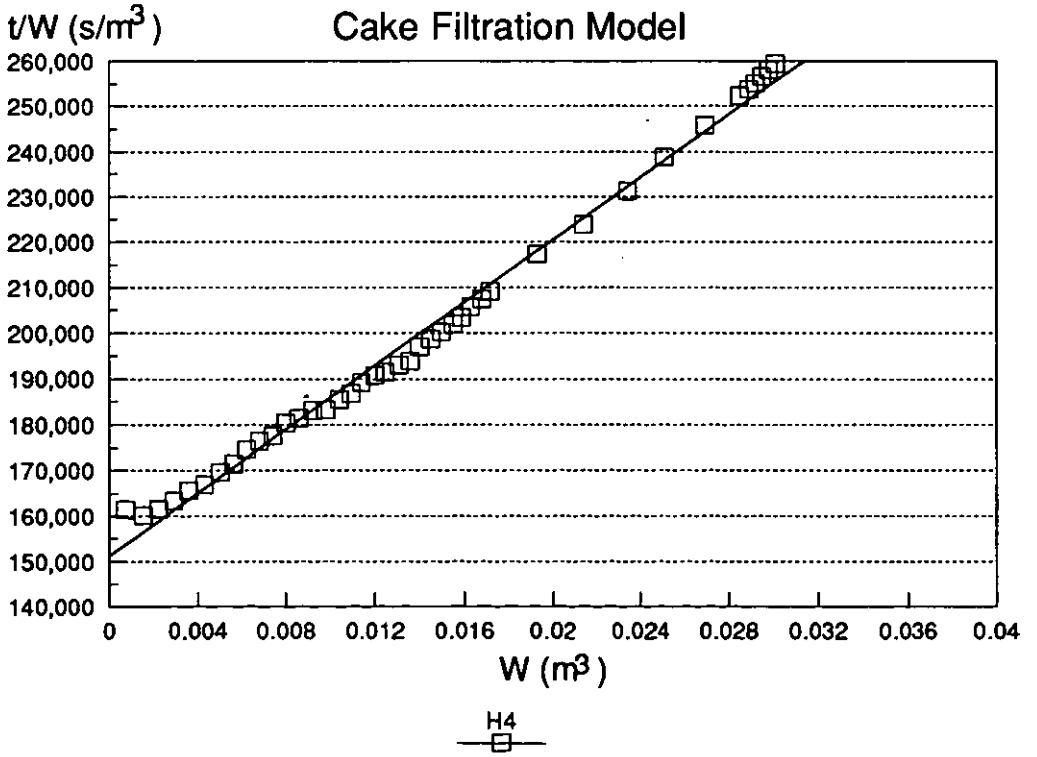

Test H4

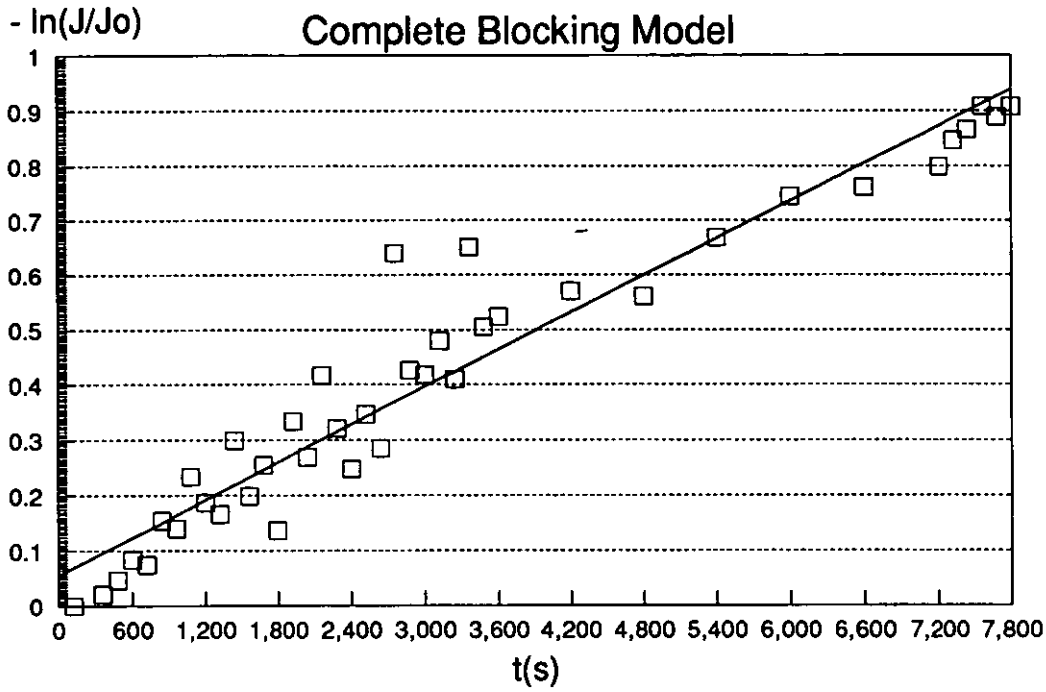

Test H4

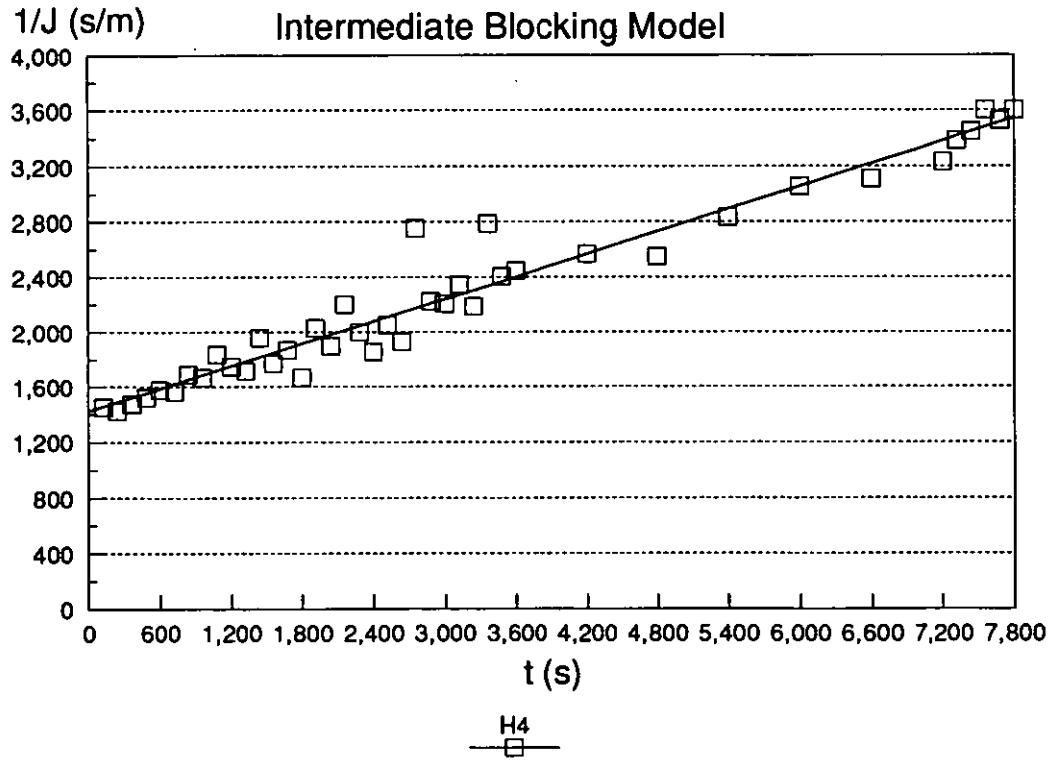

Test H4

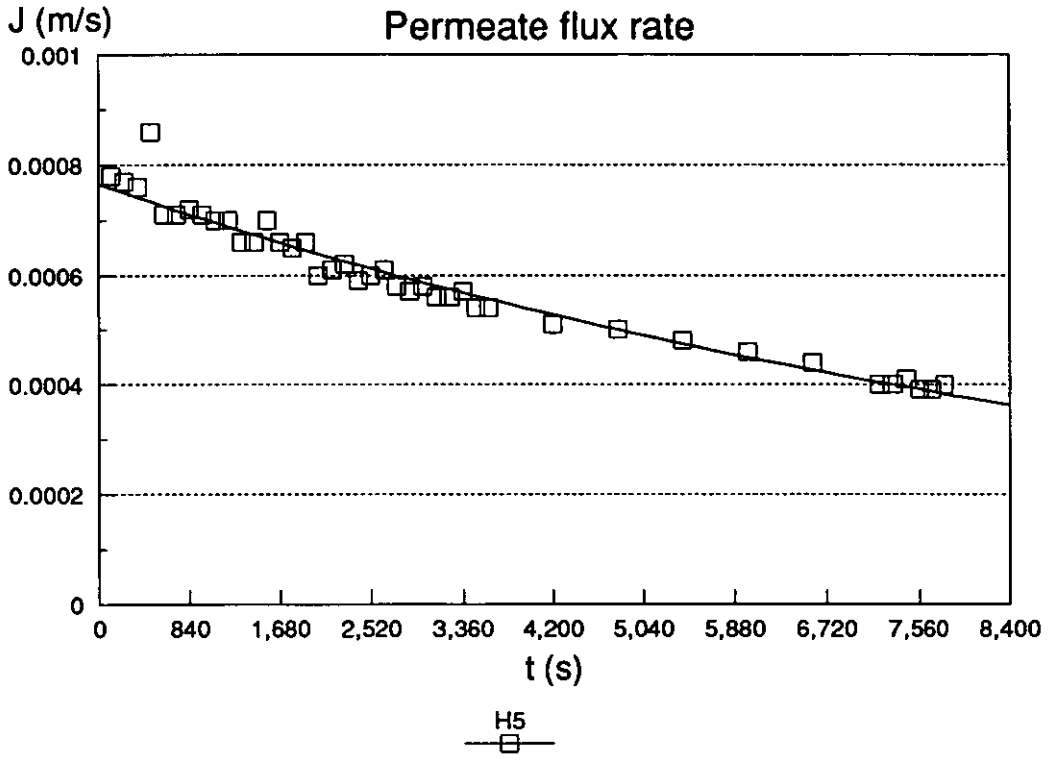

Test H5

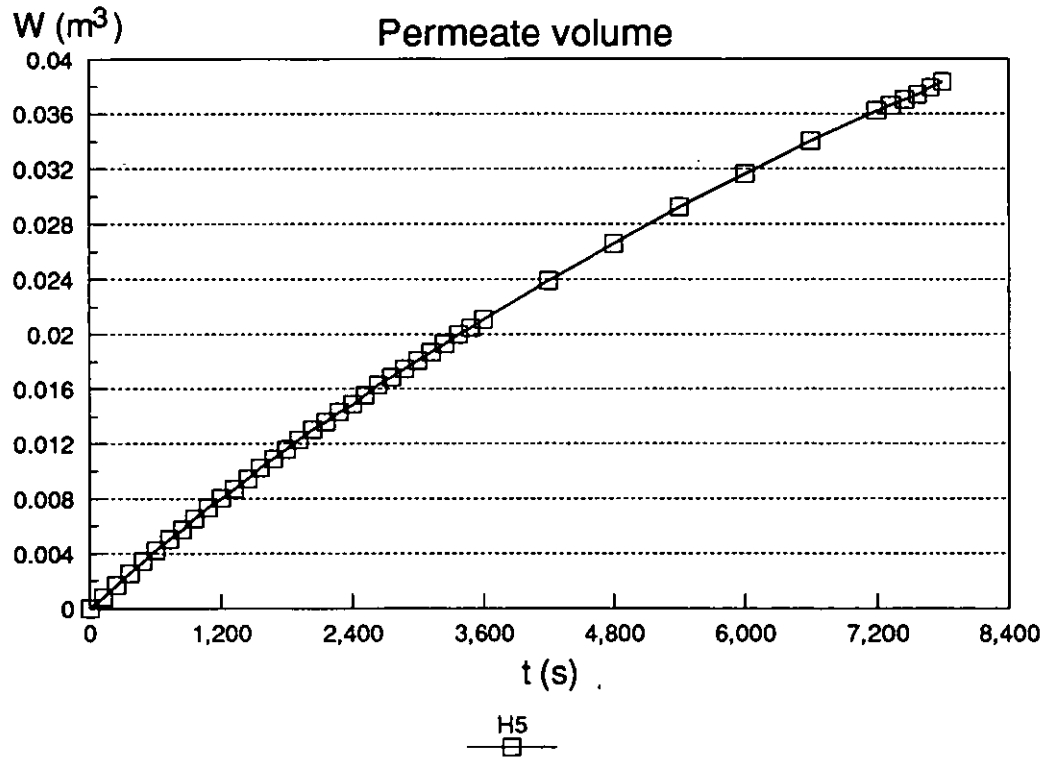

Test H5

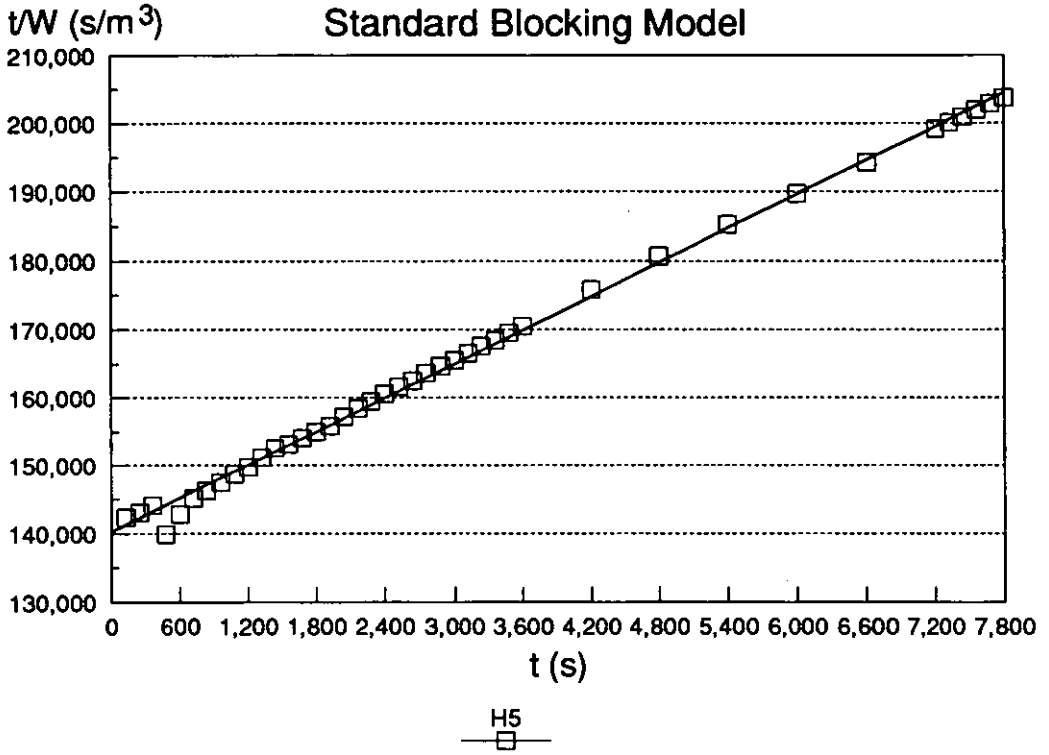

Test H5

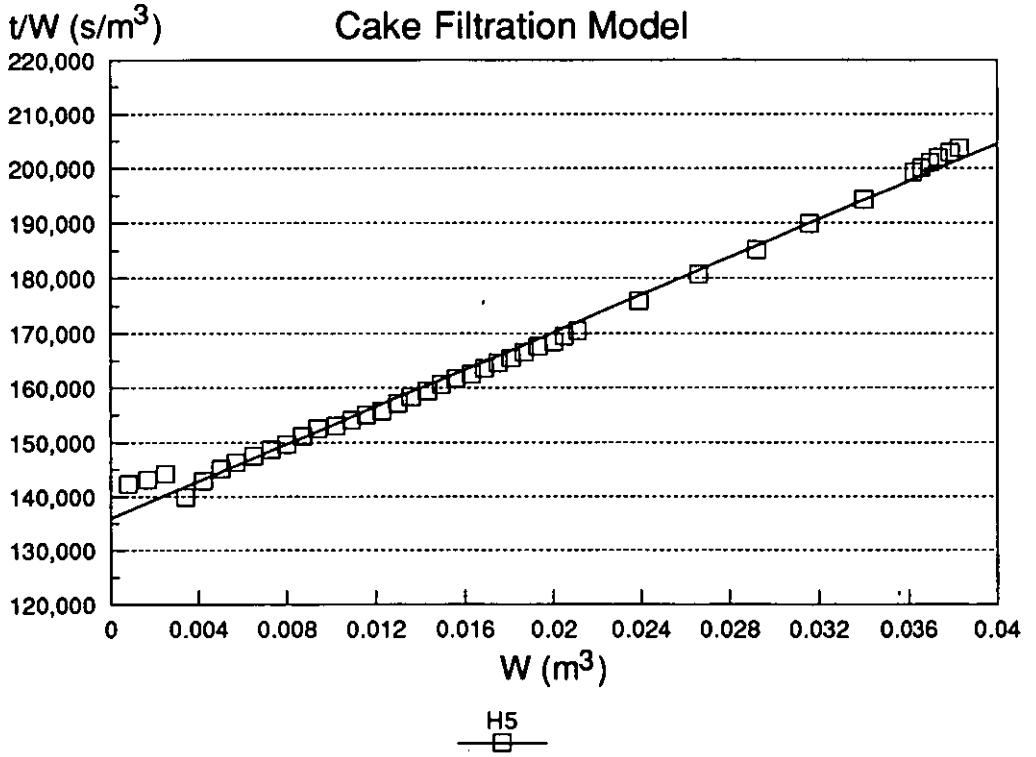

Test H5

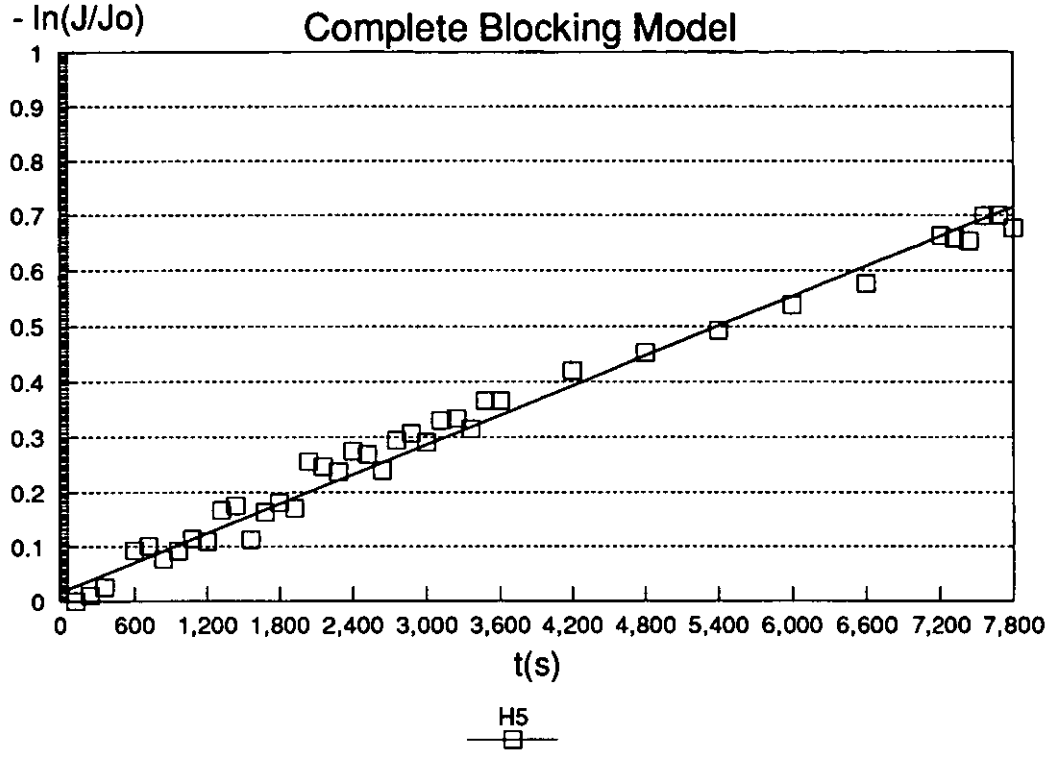

Test H4

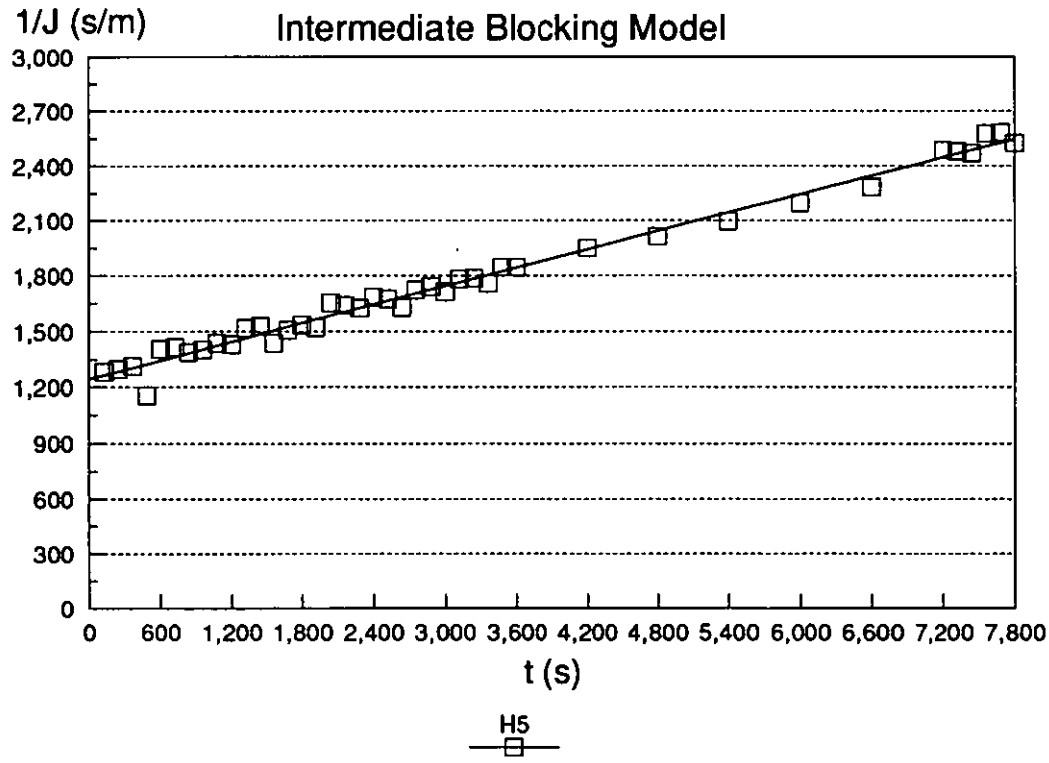

Test H5

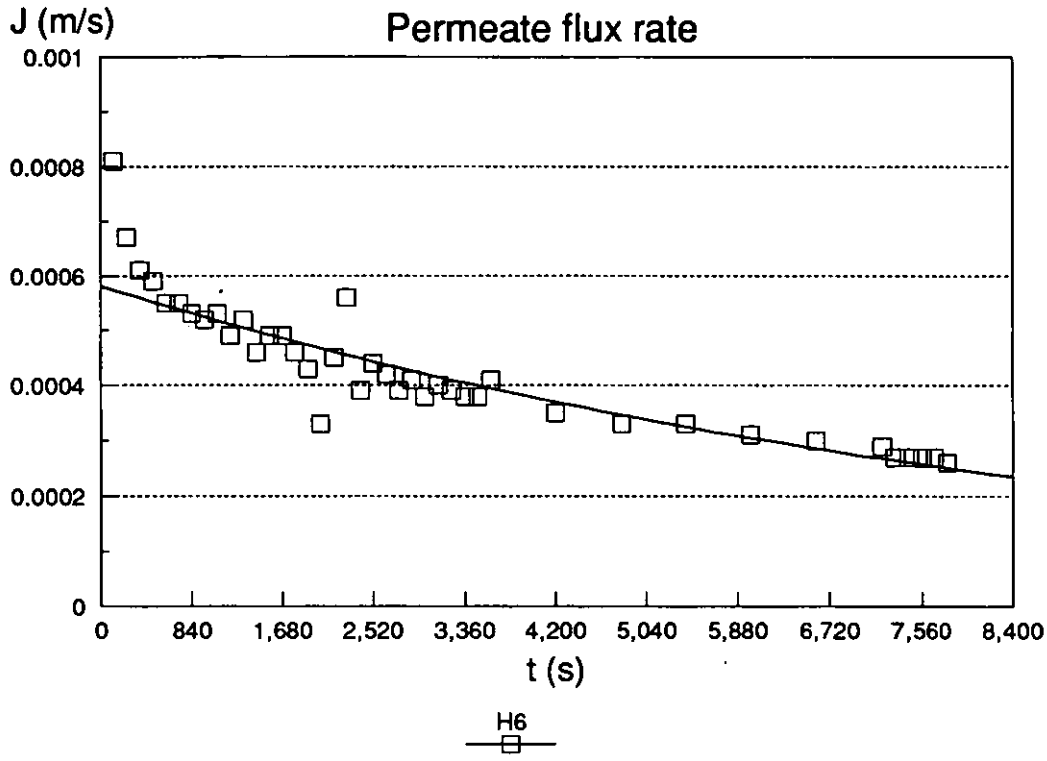

Test H6

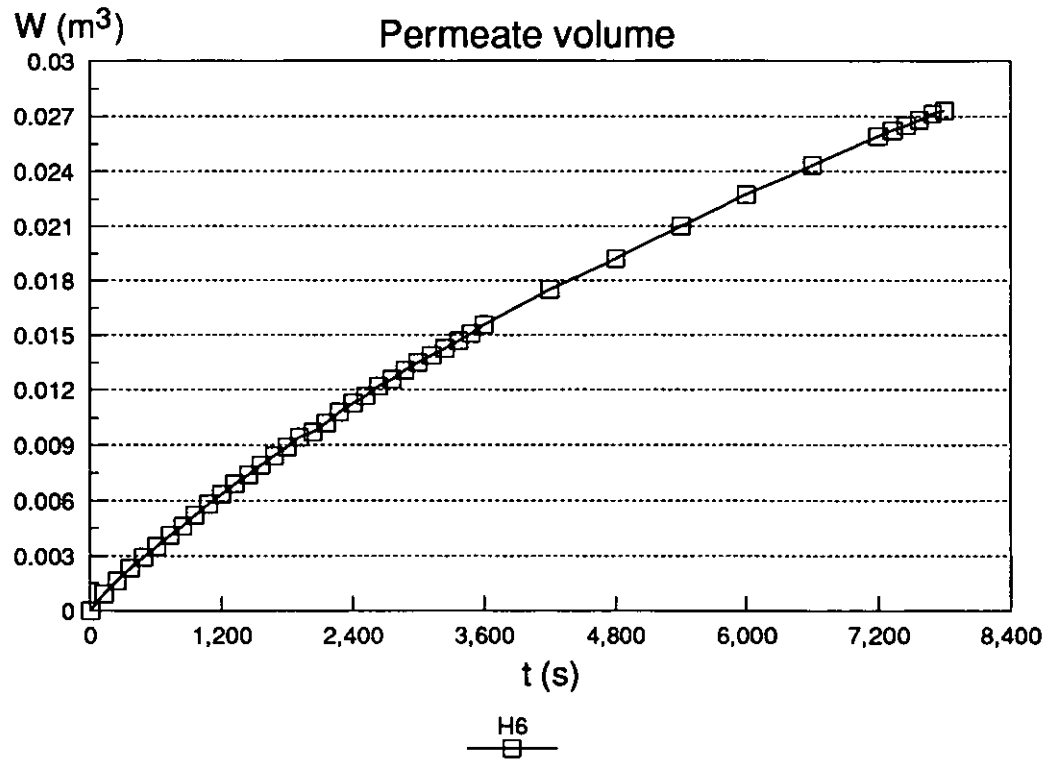

Test H6

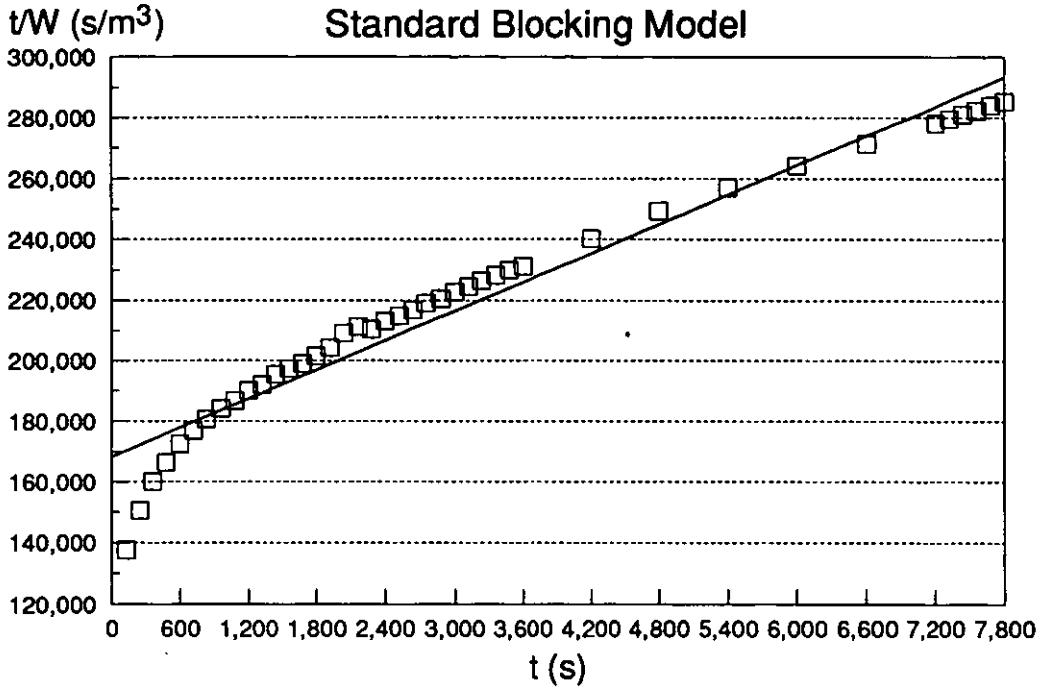

Test H6

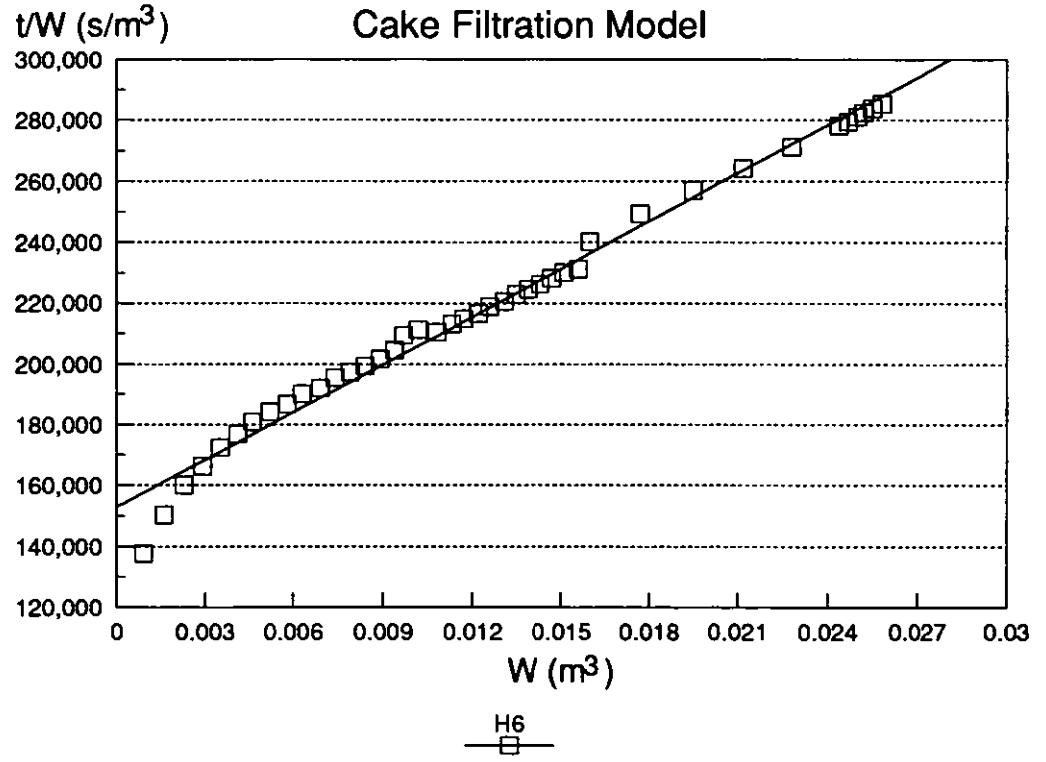

Test H6

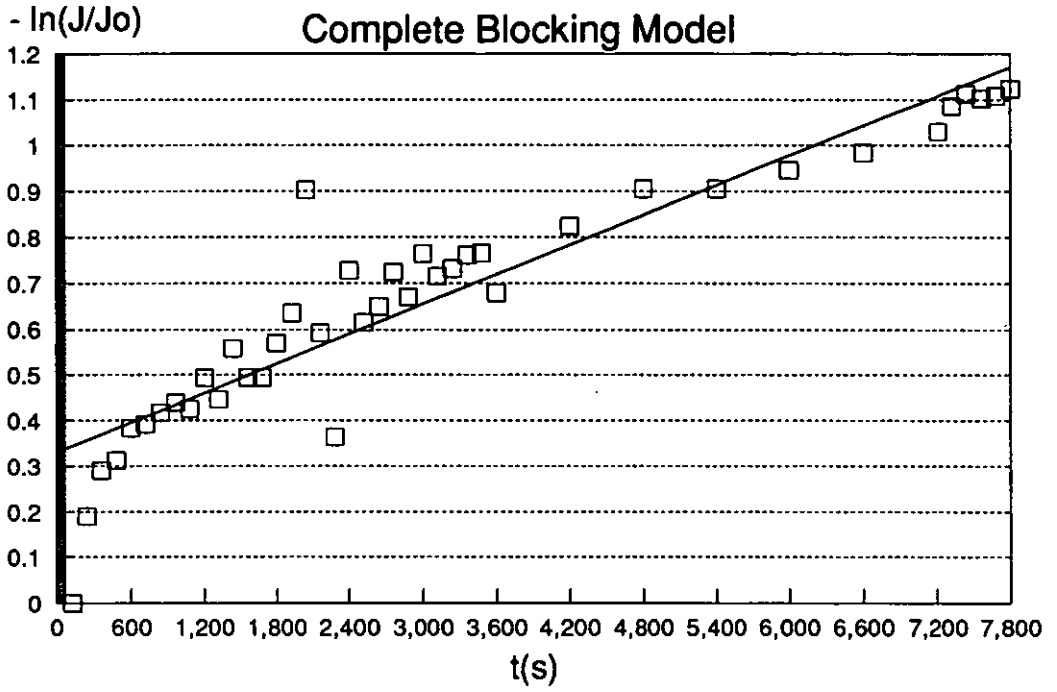

Test H6

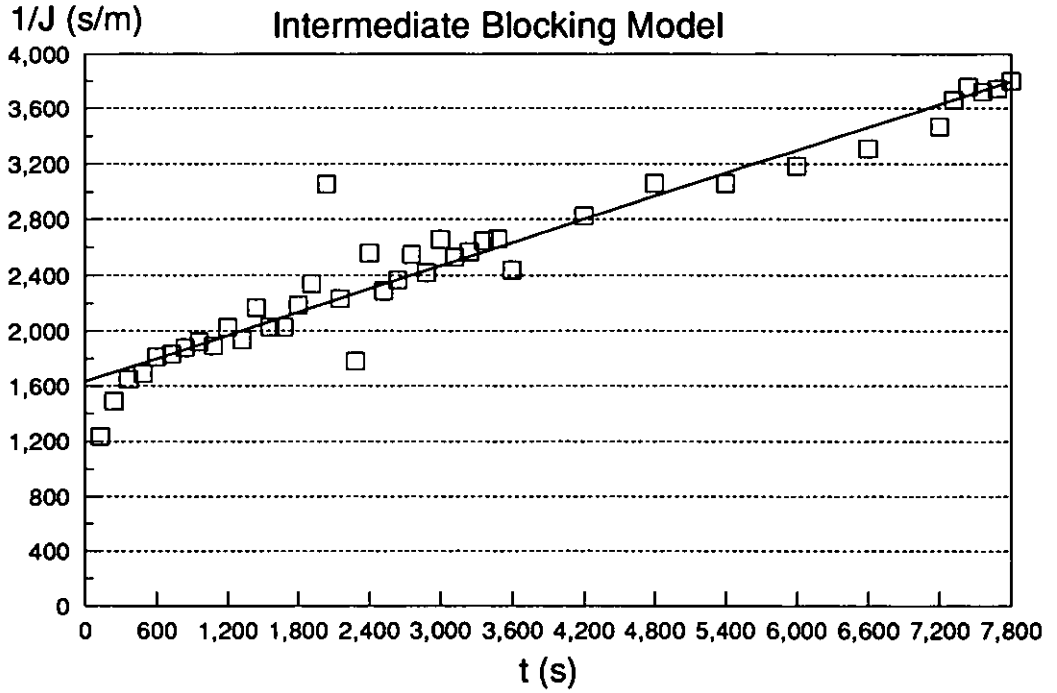

Test H6

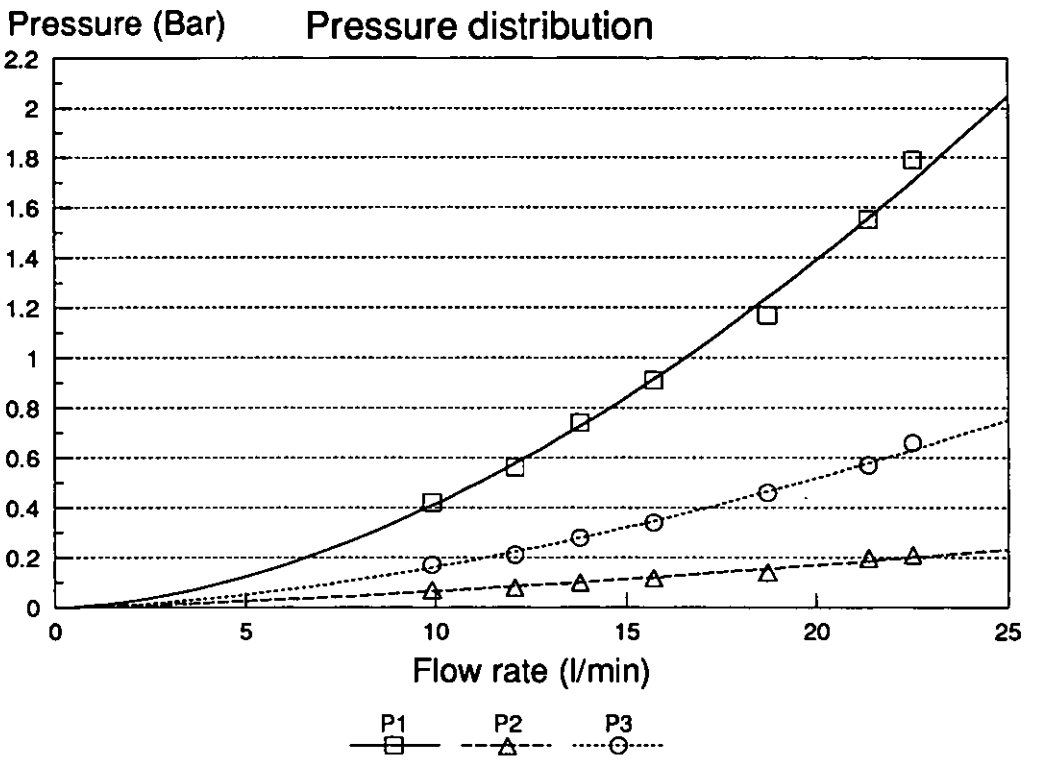

Test I1

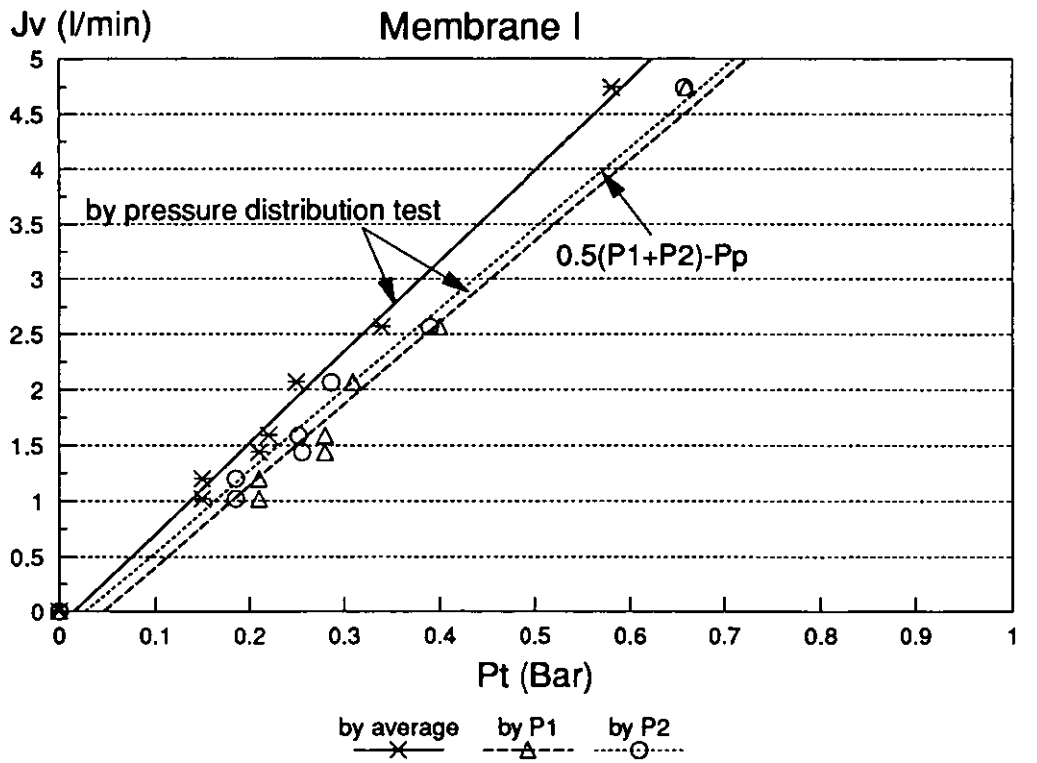

Test I1

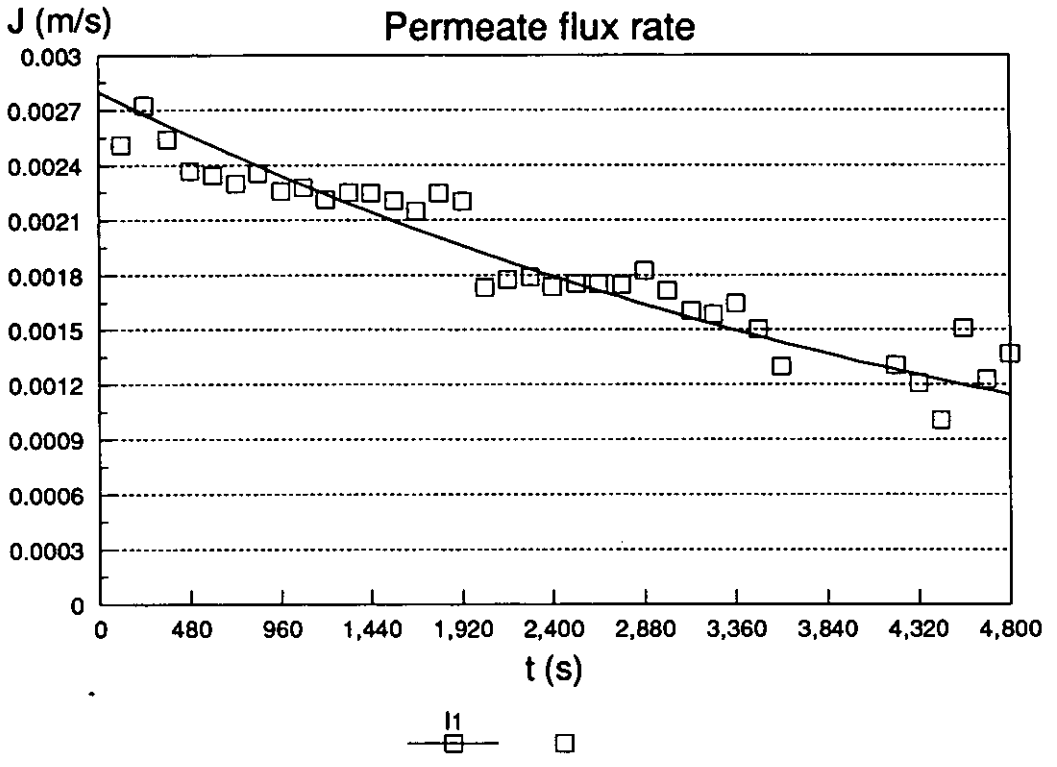

Test I1

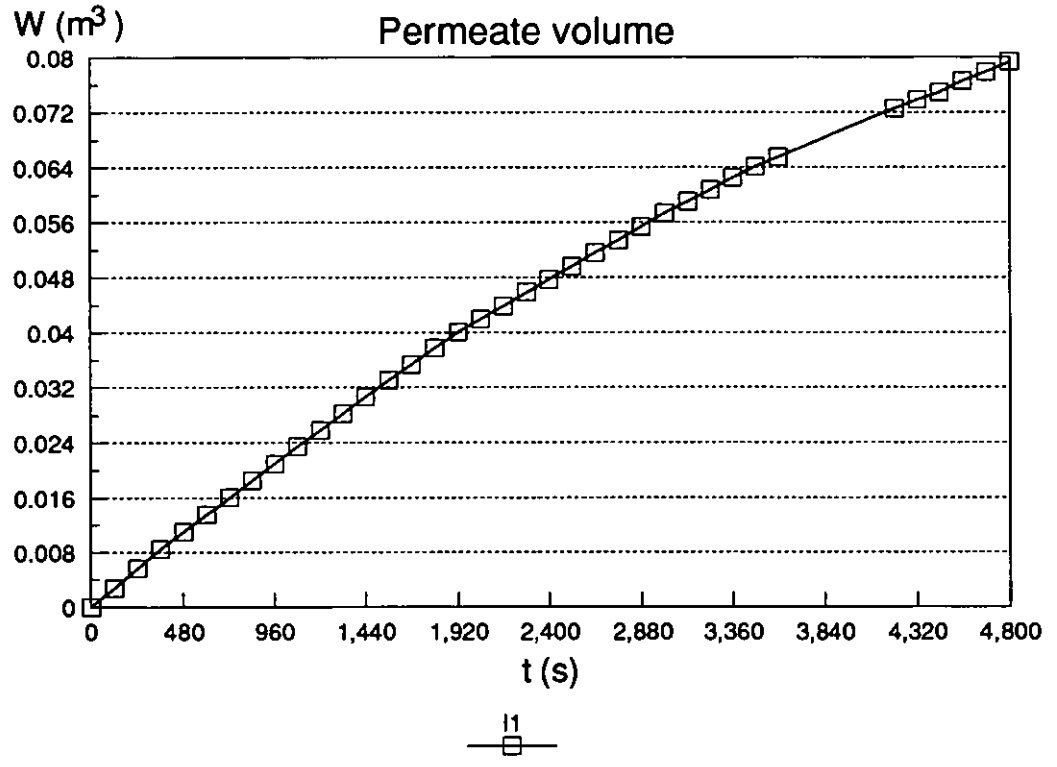

Test I1

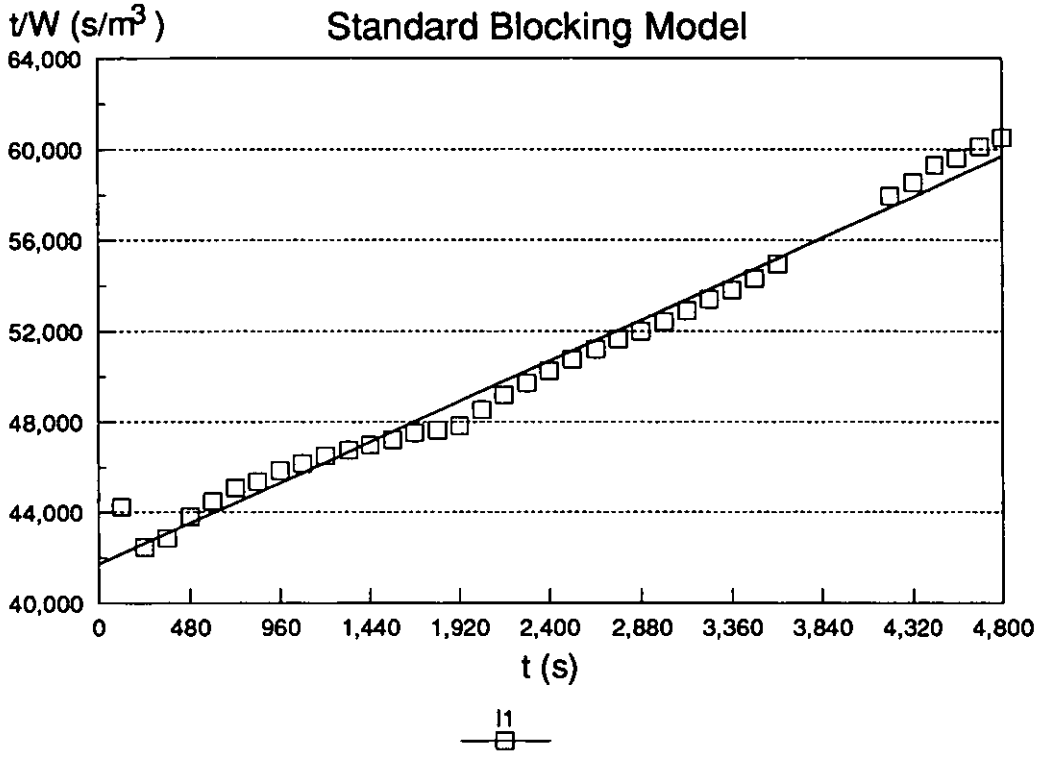

Test I1

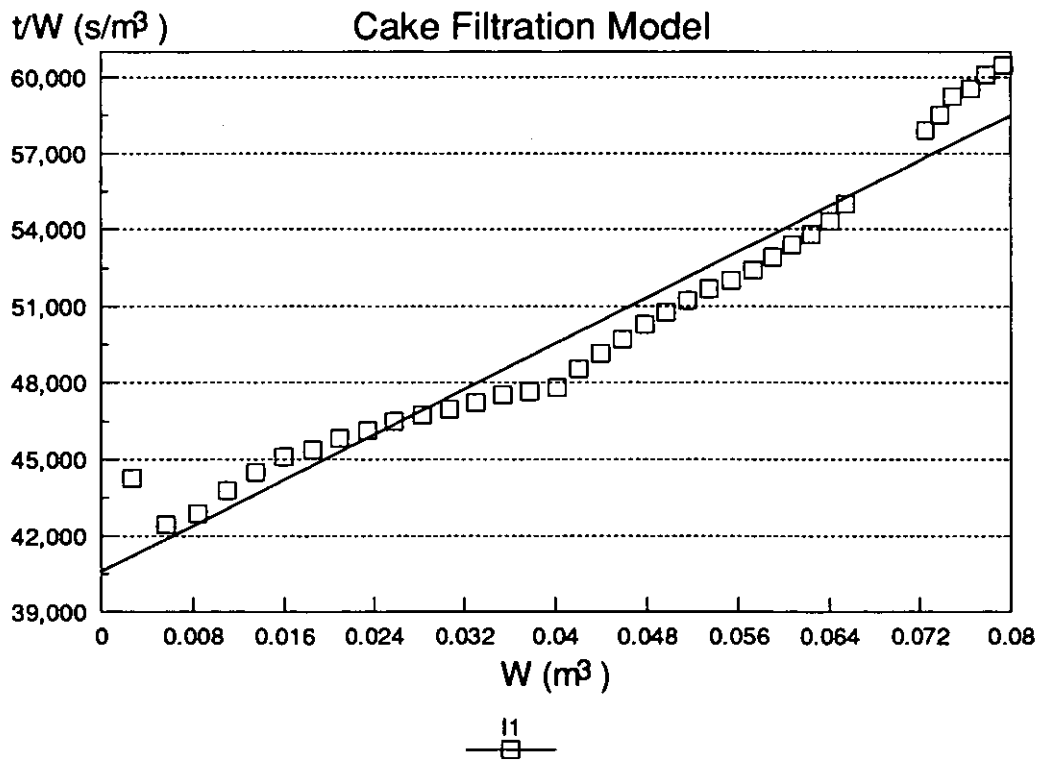

Test I1

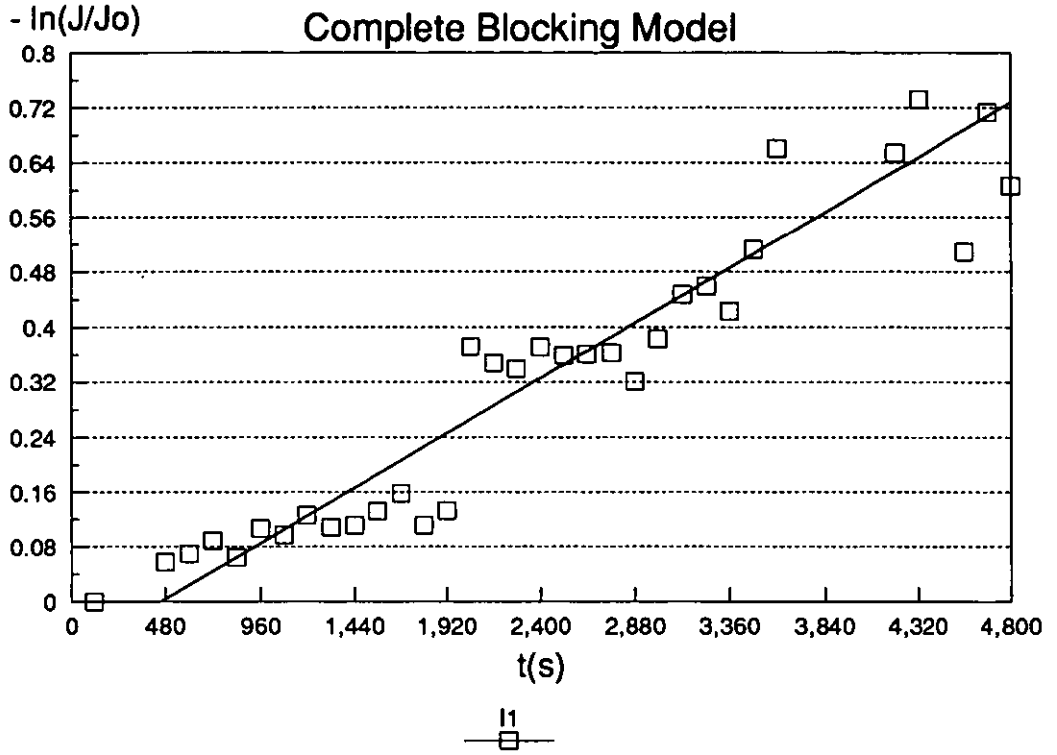

Test I1

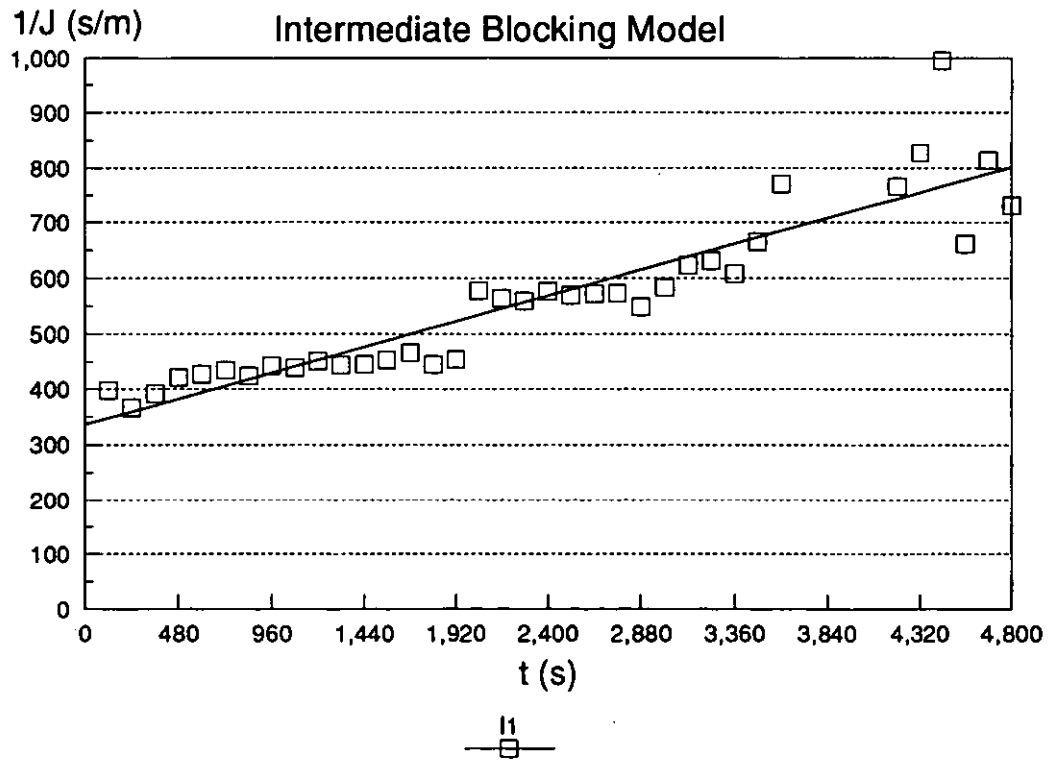

Test I1

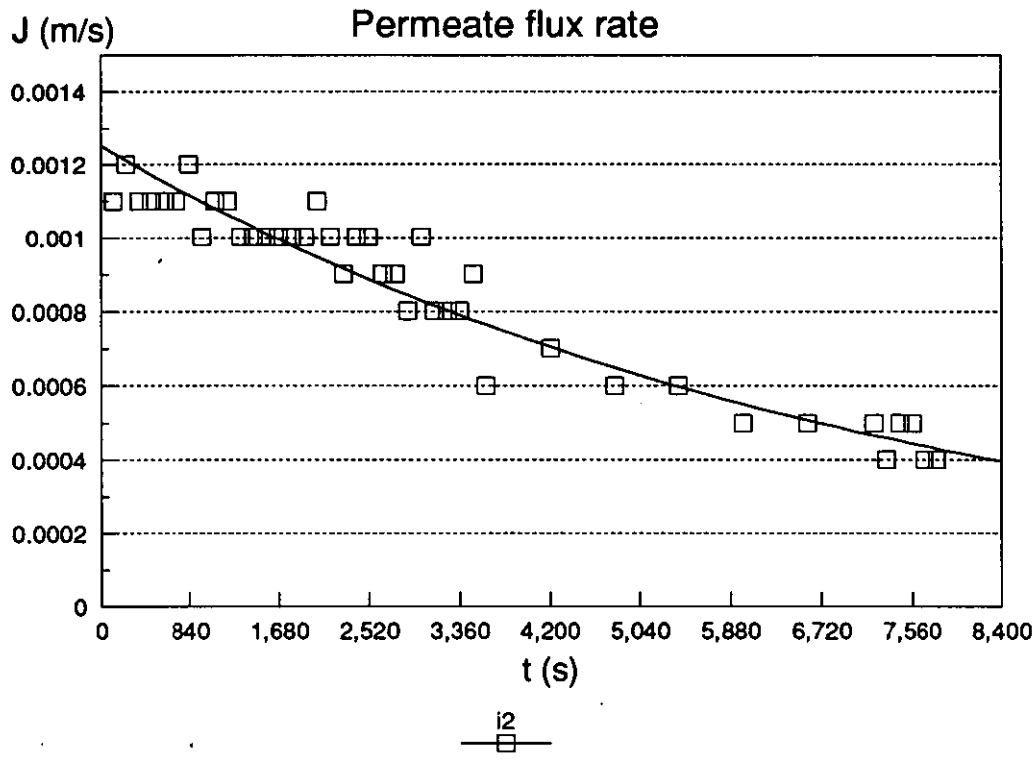

Test I2

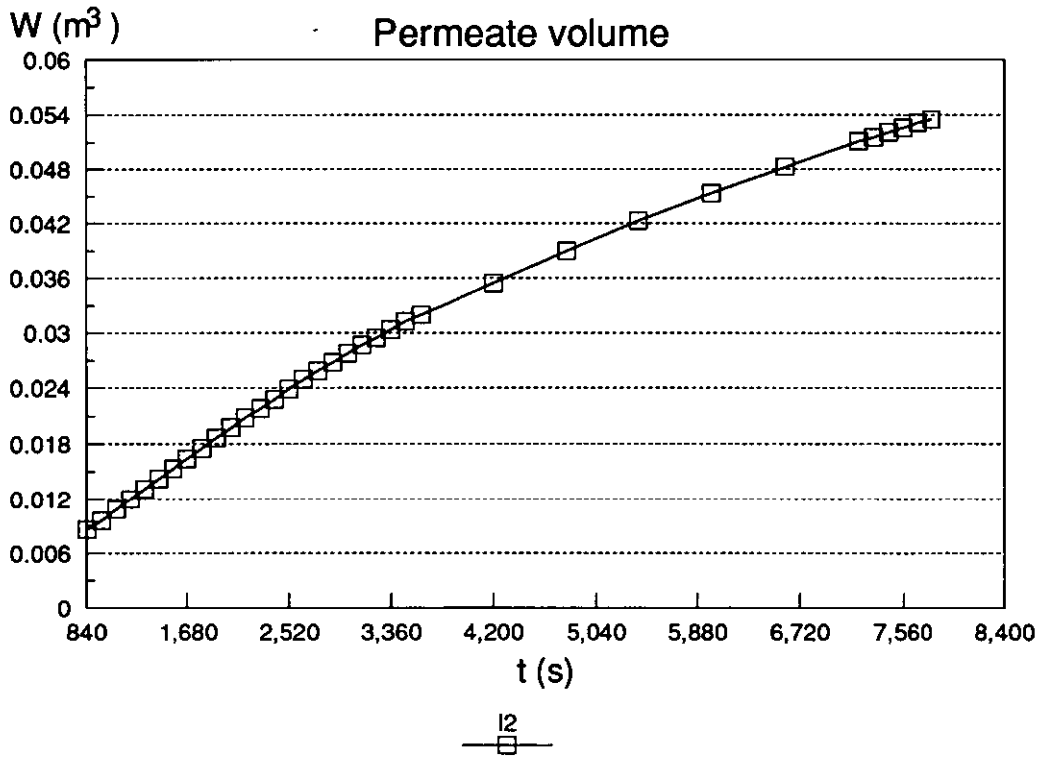

Test I2

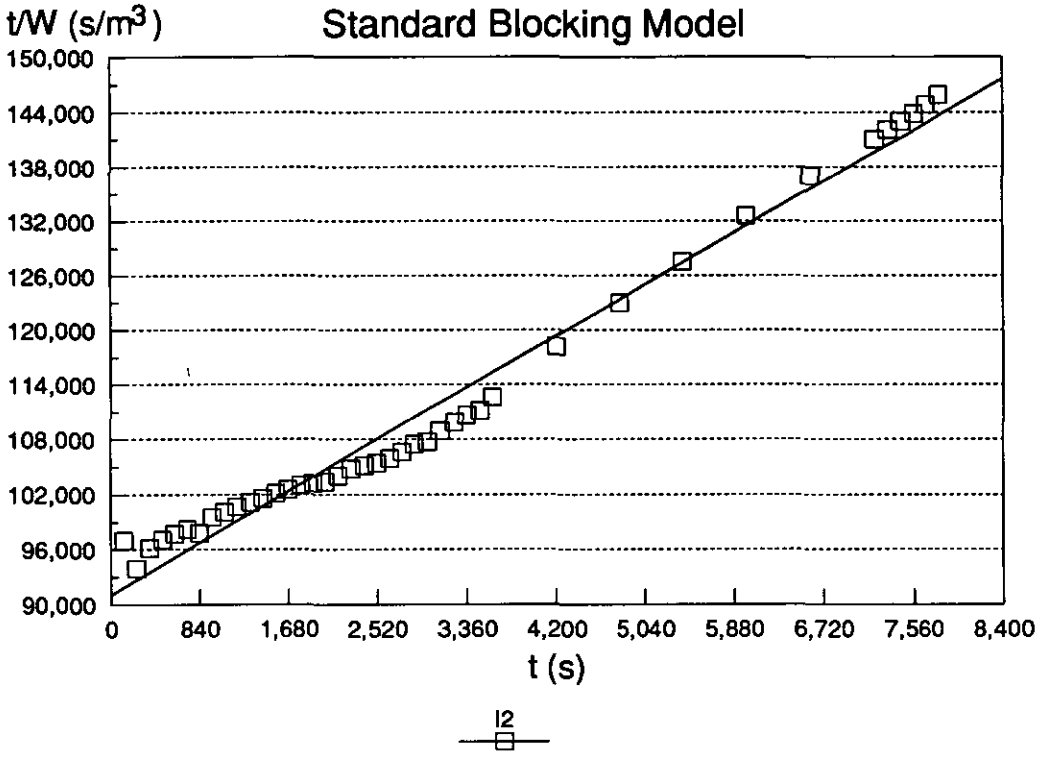

Test I2

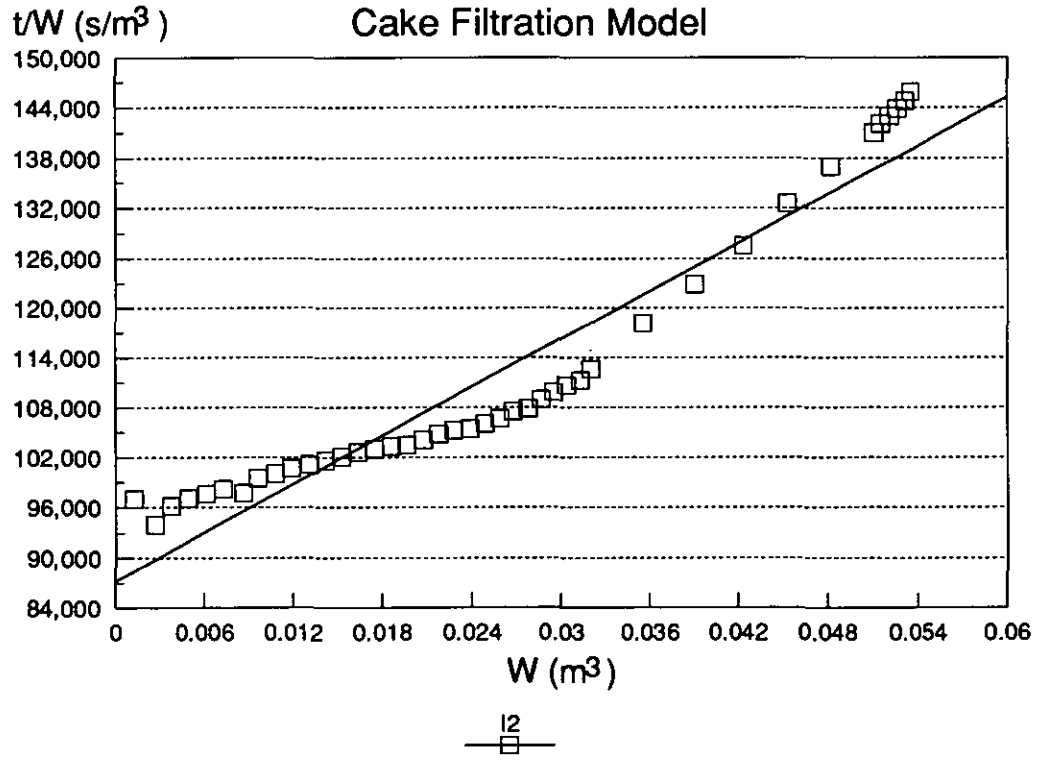

Test I2

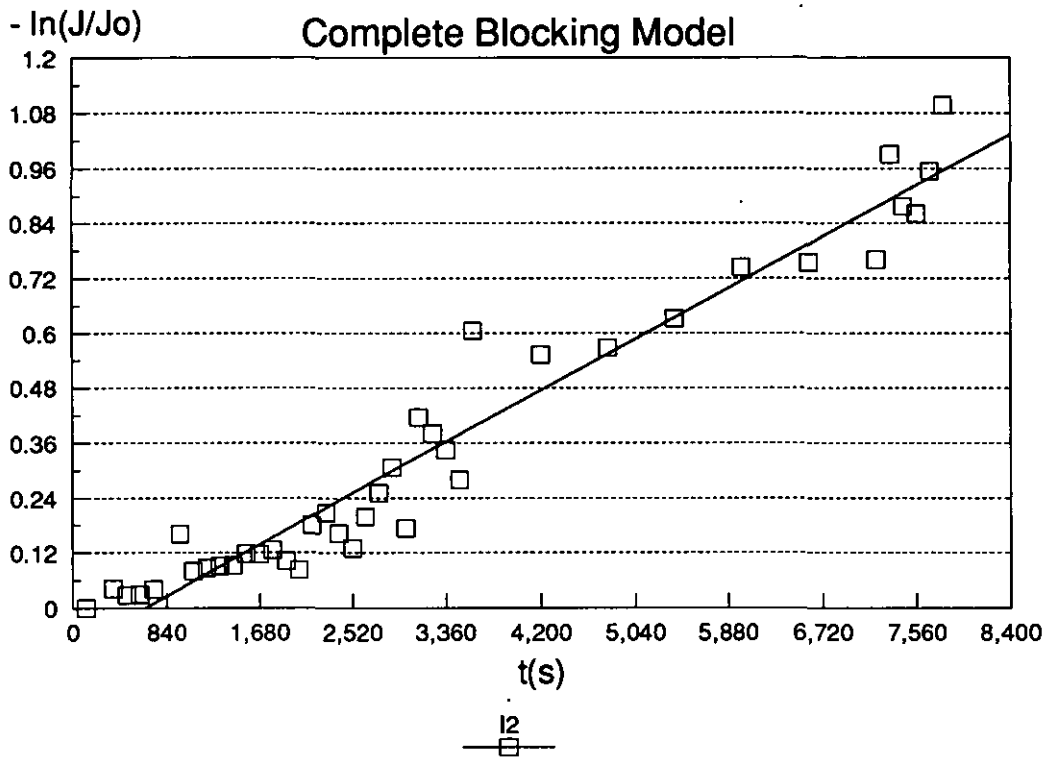

Test I2

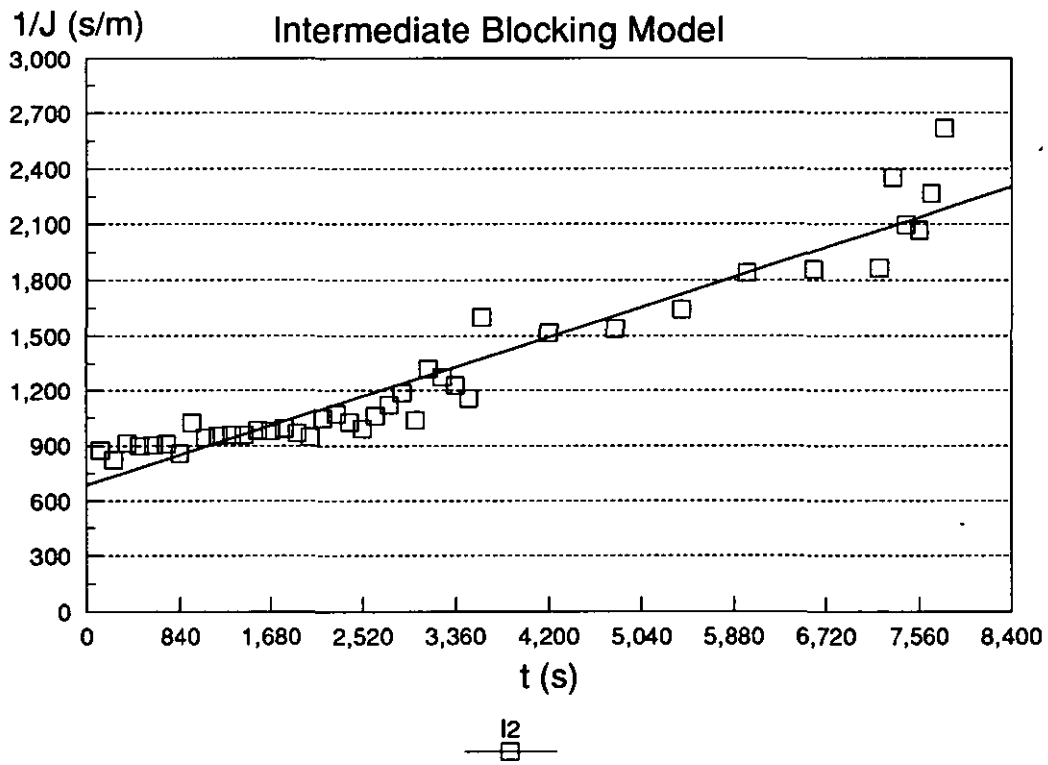

Test I2

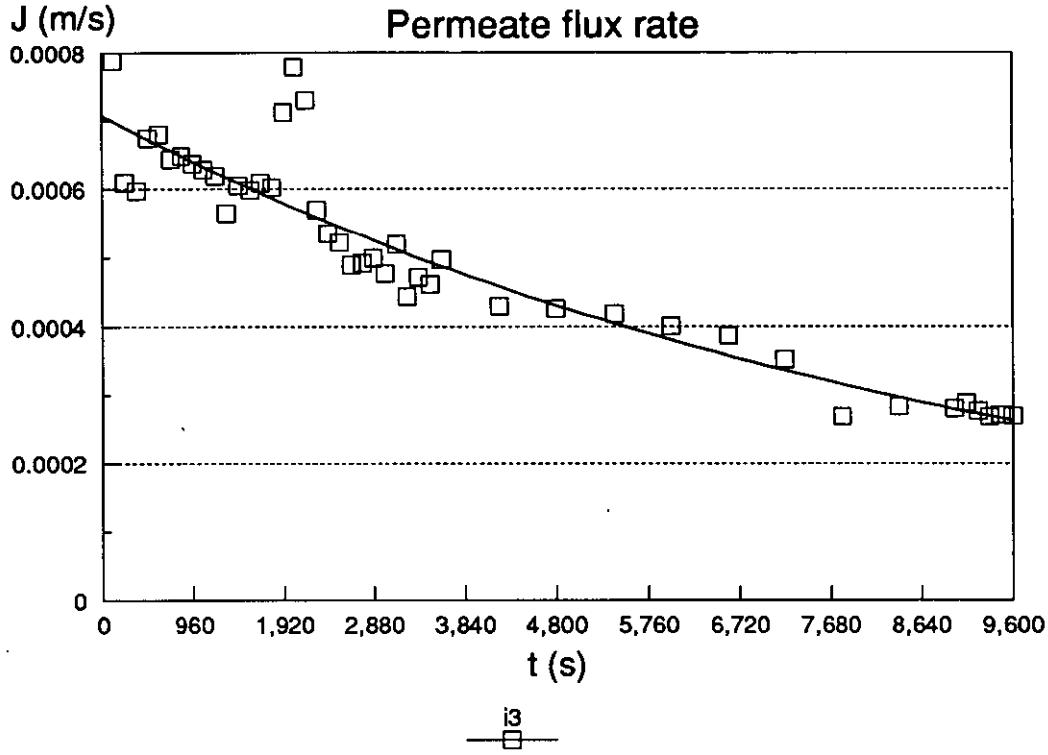

Test I3

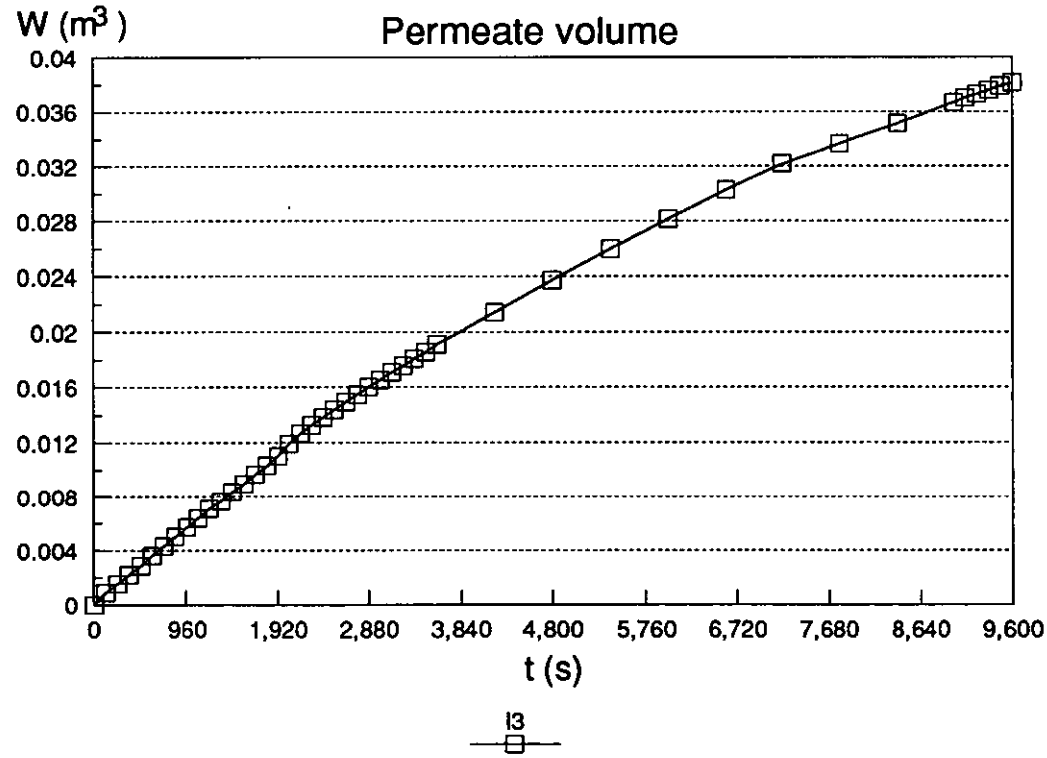

Test I3

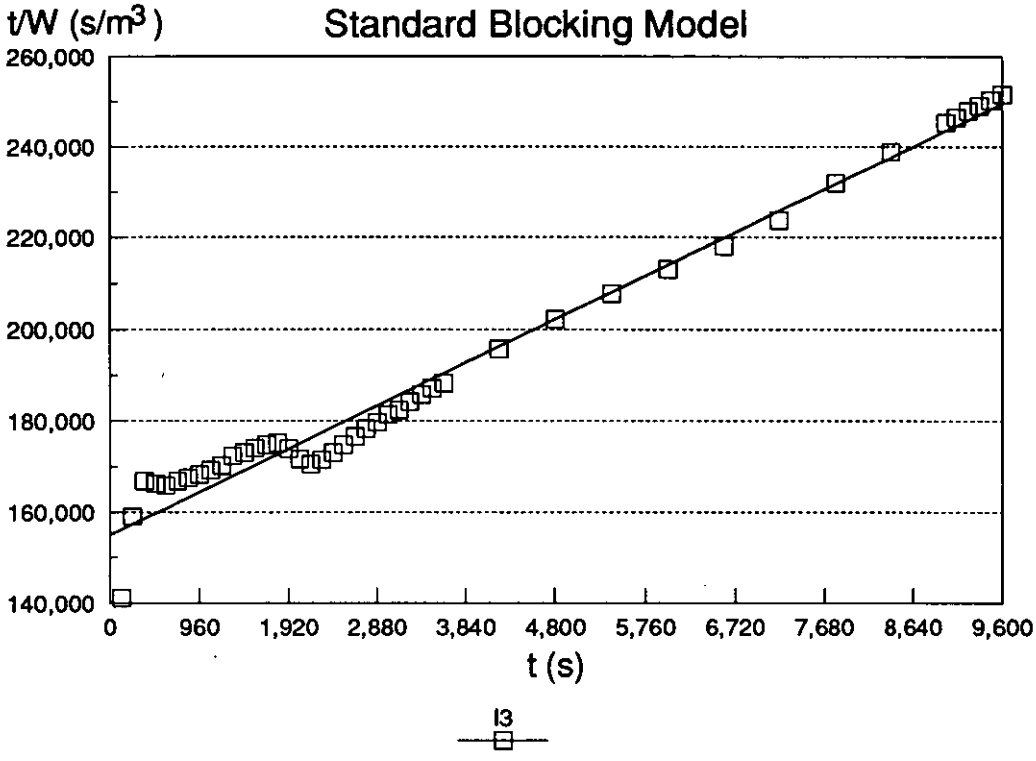

Test I3

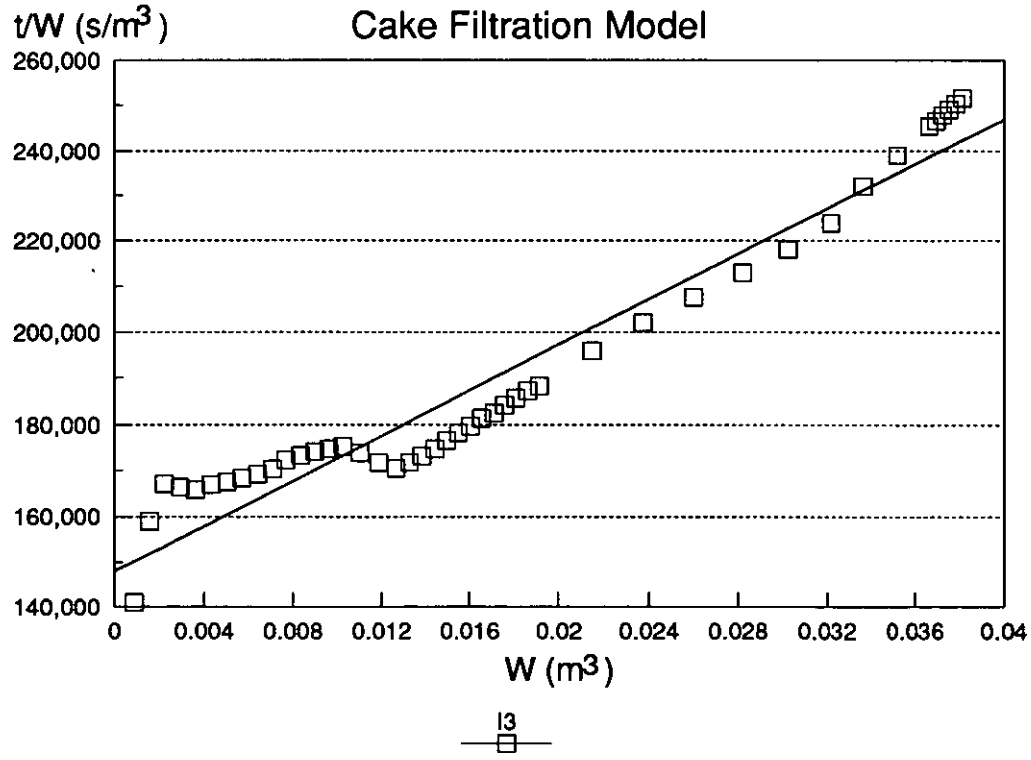

Test I3

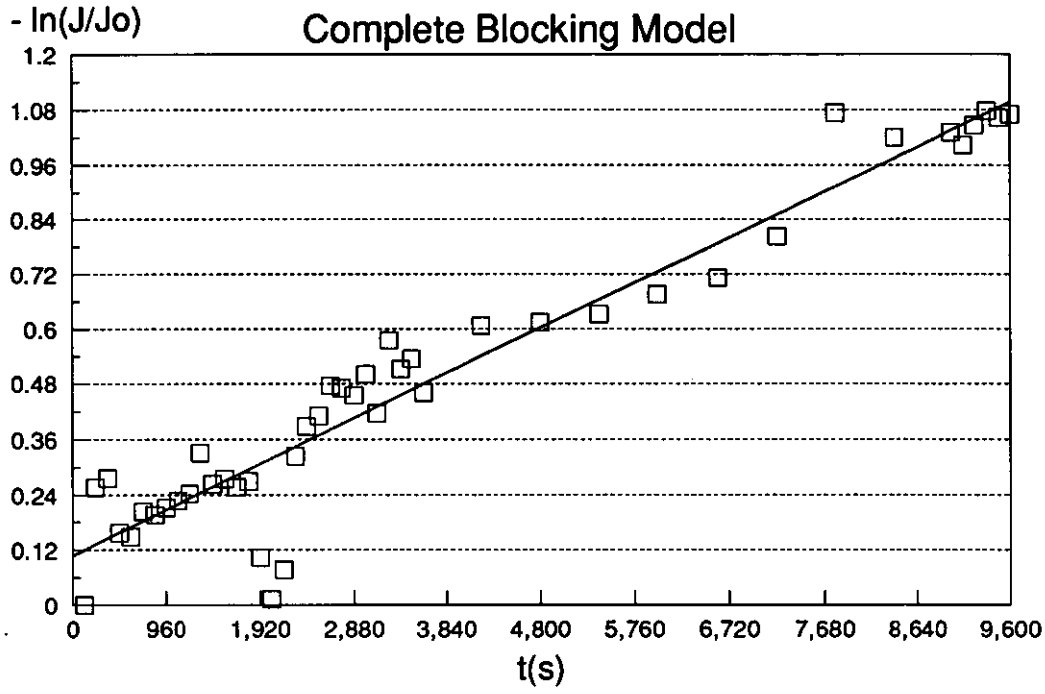

Test I3

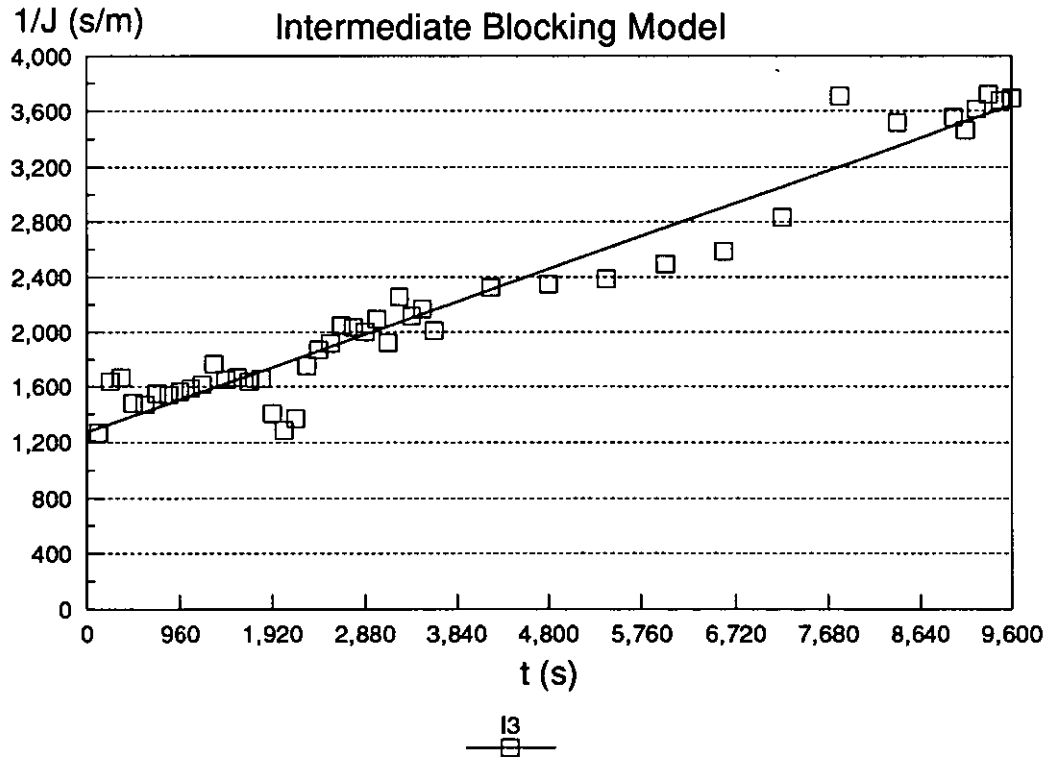

Test I3

Notes

The contents of the files in Appendix 5 refer to Tables 20 to 23 respectively, in which:

NORMAL, ***HELIX*** and ***TANGENTIAL*** refer to the types of the endcap employed;

The first letter in the item "***file***" refers to the size of the powders, ***F*** for fine and ***C*** for coarse;

The second letter again refers to the types of the endcap employed;

The first number refers to the solid concentration, ***1*** refers to low concentration and ***4*** refers to high concentration;

The following two numbers refer to the feed flow rate in ***l/min***;

The last two neumbers refer to the inlet pressure in ***Bar***;

The last letter is the code of this test.

The values in "***Flow rate***" and "***Solid conc***" were measured during the tests. The values in "***Bulk velocity***" corespond to ***U*** in Tables 20 to 23.

The values in the item "***Base pressures (in, filt, out)***" were calculated from Figs *** and *** in ***BAR***. They might be the values in the items "***Inlet pressure***" and "***Outlet pressure***" if they were higher than those displyed by the pressure gauges during the tests.

The values in the item "***Pressure (by inlet, outlet)***" normally equal to the value of per(meate) side, but they may vary if the outlet valve has been throttled.

The values in the item "***Average TMP***" in ***Pa*** refer to the P_t in Tables 20 to 23.

The values in the item "***Membrane resistance***", and those in the last row of items "***Flux corrected***" and "***Deposit res'ce***" refer to R_m, J_c,and R_c in Tables 20 to 23 respectively.

The methods of calculating the values in items "***Flux raw data***", "***Viscosity***" and "***Flux corrected***" have been explained in Chapter 5.

HELIX File: CH11723A

Outer radius:	0.01	m		Flow rate:		17.0	l/m
Inner radius:	0.006	m		P(in)		1.60	Bar
Active length:	0.27	m		P(out)		0.12	Bar
Hydraulic dx4:	0.008	m		Fluid density:		1000	kg/m^3
Solids conc:	1.5	% wt		Viscosity (25C)		0.00089	Pa.s
Membrane area:	0.0101788	m^2		Bulk velocity:		3.22	m/s
Flow area:	8.8E-05	m^2		Re:		28941	
Base press(in,filt,out)			1.60	0.67	0.12	Bar	
Press (by inlet,outlet)			0.67		0.67	Bar	
Average TMP:	0.67	Bar		66712	Pa		

Time	Cum' filtrate	Temp	Flux raw data	Viscosity	Flux corrected	Cum've filtrate	Deposit res'ce
(min)	(l)	('C)	(lmh)	(Pa.s)	(lmh)	(l)	(1/m)
0	0.00	32.5	2829	0.000753	2393	0.00	3.73E-09
2	0.96	32.5	2357	0.000753	1994	0.81	3.76E+08
4	1.60	32.5	1784	0.000753	1510	1.41	1.10E+09
6	2.17	32.5	1639	0.000753	1387	1.90	1.36E+09
8	2.71	32.5	1550	0.000753	1311	2.36	1.55E+09
10	3.22	32.5	1489	0.000753	1260	2.79	1.69E+09
12	3.72	32.5	1444	0.000753	1222	3.21	1.80E+09
14	4.20	32.6	1416	0.000751	1195	3.62	1.88E+09
16	4.68	32.7	1378	0.00075	1161	4.02	1.99E+09
18	5.14	32.9	1350	0.000746	1132	4.41	2.09E+09
20	5.60	33	1366	0.000744	1143	4.80	2.06E+09
22	6.06	33.1	1334	0.000743	1113	5.18	2.16E+09
24	6.50	33.2	1307	0.000741	1088	5.55	2.25E+09
26	6.95	33.2	1295	0.000741	1078	5.92	2.29E+09
28	7.38	33.3	1286	0.000739	1068	6.28	2.33E+09
30	7.82	33.4	1292	0.000738	1071	6.65	2.32E+09
35	8.92	33.5	1267	0.000736	1048	7.55	2.41E+09
40	9.97	33.5	1238	0.000736	1024	8.42	2.51E+09
45	11.02	33.6	1219	0.000734	1006	9.29	2.59E+09
50	12.04	33.8	1194	0.000731	981	10.13	2.71E+09
55	13.04	34	1172	0.000728	958	10.95	2.82E+09
60	14.03	34.1	1142	0.000726	932	11.75	2.95E+09
70	15.95	34.1	1119	0.000726	913	13.32	3.05E+09
80	17.83	34.3	1094	0.000723	888	14.84	3.18E+09
90	19.66	34.5	1072	0.000719	866	16.33	3.31E+09
100	21.46	34.7	1054	0.000716	848	17.79	3.42E+09
110	23.24	35	1034	0.000711	826	19.21	3.57E+09
120	24.97	35	1015	0.000711	811	20.59	3.67E+09
130	26.69	35	1003	0.000711	801	21.96	3.73E+09
140	28.37	35	989	0.000711	790	23.31	3.82E+09
150	30.04	35.2	978	0.000708	778	24.64	3.90E+09
160	31.69	35.3	966	0.000706	766	25.95	3.99E+09
170	33.32	35.5	959	0.000703	757	27.25	4.06E+09
			Rm	1.88E+09	1/m		

HELIX File: CH11723B

Outer radius:	0.01	m		Flow rate:		17.0	l/m
Inner radius:	0.006	m		Inlet pressure:		1.60	Bar
Active length:	0.27	m		Outlet pressure:		0.12	Bar
Hydraulic dx4:	0.008	m		Fluid density:		1000	kg/m^3
Solids conc:	1.5	% wt		Viscosity (25'C):		0.00089	Pa.s
Membrane area:	0.0101788	m^2		Bulk velocity:		3.22	m/s
Flow area:	8.8E-05	m^2		Re:		28941	
Base press. (in,filt,out):		1.60		0.67	0.12	Bar	
Pressure (by inlet,outlet):		0.67			0.67	Bar	
Average TMP:	0.67	Bar		66712	Pa		

Time	Cum' filtrate	Temp	Flux raw data	Viscosity	Flux corrected	Cum've filtrate	Deposit res'ce
(min)	(l)	('C)	(lmh)	(Pa.s)	(lmh)	(l)	(1/m)
0	0.00	23.2	2035	0.000933	2133	0.00	1.07E-07
2	0.69	23.5	1782	0.000926	1855	0.72	3.16E+08
4	1.21	23.8	1432	0.00092	1481	1.29	9.28E+08
6	1.66	24.2	1292	0.000912	1323	1.77	1.29E+09
8	2.09	24.5	1219	0.000905	1240	2.20	1.52E+09
10	2.49	24.9	1165	0.000897	1174	2.61	1.72E+09
12	2.88	25.3	1124	0.000889	1123	3.00	1.90E+09
14	3.25	25.5	1101	0.000885	1095	3.38	2.00E+09
16	3.62	25.7	1071	0.000881	1059	3.74	2.14E+09
18	3.98	26	1047	0.000875	1029	4.10	2.26E+09
20	4.33	26.3	1036	0.000869	1011	4.44	2.34E+09
22	4.68	26.5	1018	0.000865	989	4.78	2.44E+09
24	5.02	27	1005	0.000855	965	5.11	2.55E+09
26	5.36	27.5	994	0.000845	943	5.44	2.66E+09
28	5.70	28	1002	0.000835	941	5.76	2.67E+09
30	6.04	28.5	962	0.000826	893	6.07	2.93E+09
35	6.84	29	846	0.000816	776	6.77	3.68E+09
40	7.48	29.4	934	0.000809	848	7.46	3.19E+09
45	8.43	29.9	1015	0.0008	911	8.21	2.83E+09
50	9.20	30.5	911	0.000789	807	8.94	3.46E+09
55	9.97	31	900	0.00078	789	9.62	3.59E+09
60	10.73	31.5	886	0.000771	768	10.28	3.75E+09
70	12.23	32	876	0.000762	750	11.56	3.89E+09
80	13.70	32.6	864	0.000751	730	12.82	4.05E+09
90	15.16	33.2	850	0.000741	708	14.04	4.24E+09
100	16.59	33.2	834	0.000741	695	15.23	4.37E+09
110	17.99	33.2	824	0.000741	686	16.40	4.44E+09
120	19.38	33.3	816	0.000739	678	17.56	4.52E+09
130	20.76	33.9	809	0.000729	663	18.69	4.67E+09
140	22.13	34.7	805	0.000716	648	19.80	4.83E+09
150	23.49	35.2	804	0.000708	639	20.91	4.93E+09
Membrane resistance:				2.11E+09	1/m		

HELIX			File:	CH11416C	
Outer radius:	0.01	m	Flow rate:	14.0	l/m
Inner radius:	0.006	m	Inlet pressure:	1.11	Bar
Active length:	0.27	m	Outlet pressure:	0.09	Bar
Hydraulic dx4	0.008	m	Fluid density:	1000	kg/m^3
Solids conc:	1.5	% wt	Viscosity (25'C):	0.0009	Pa.s
Membrane ar	0.0102	m^2	Bulk velocity:	2.65	m/s
Flow area:	8.8E-05	m^2	Re:	23834	
Base press. (in,filt,out)	1.11	0.49	0.09	Bar	
Pressure (by inlet,outle	0.49		0.49	Bar	
Average TMP	0.49	Bar	49193	Pa	

Time	Cum' filtrate	Temp	Flux raw data	Viscosity	Flux corrected	Cum've filtrate	Deposit res'ce
(min)	(l)	('C)	(lmh)	(Pa.s)	(lmh)	(l)	(1/m)
0	0.00	23	1525	0.000937	1606	0.00	-2.3E-08
2	0.52	23.2	1348	0.000933	1413	0.54	2.82E+08
4	0.91	24	1115	0.000916	1148	0.98	8.24E+08
6	1.27	24.4	1022	0.000907	1042	1.35	1.12E+09
8	1.61	24.8	960	0.000899	970	1.69	1.36E+09
10	1.93	25.2	901	0.000891	902	2.01	1.61E+09
15	2.68	25.7	842	0.000881	833	2.75	1.91E+09
20	3.35	26.2	791	0.000871	773	3.43	2.22E+09
25	4.02	26.7	781	0.000861	755	4.07	2.33E+09
30	4.68	27.2	775	0.000851	741	4.71	2.41E+09
40	5.99	28.5	771	0.000826	715	5.94	2.57E+09
50	7.29	29.8	765	0.000801	689	7.14	2.75E+09
60	8.59	30.6	760	0.000787	672	8.29	2.87E+09
70	9.87	31.4	750	0.000772	651	9.41	3.03E+09
80	11.13	32.3	743	0.000757	632	10.50	3.19E+09
90	12.39	33	732	0.000744	612	11.56	3.35E+09
100	13.62	33.8	726	0.000731	596	12.58	3.50E+09
110	14.86	34.2	725	0.000724	590	13.59	3.56E+09
120	16.08	34.6	707	0.000718	570	14.57	3.75E+09
130	17.26	35.1	707	0.000709	564	15.53	3.82E+09
140	18.48	31	709	0.00078	621	16.54	3.28E+09
150	19.66	35.6	699	0.000701	551	17.53	3.96E+09
Membrane resistance:				2.07E+09	1/m		

HELIX			File:	CH11416D	
Outer radius:	0.01	m	Flow rate:	14.0	l/m
Inner radius:	0.006	m	Inlet pressure:	1.11	Bar
Active length:	0.27	m	Outlet pressure:	0.09	Bar
Hydraulic dx4	0.008	m	Fluid density:	1000	kg/m^3
Solids conc:	1.5	% wt	Viscosity (25'C):	0.0009	Pa.s
Membrane ar	0.0102	m^2	Bulk velocity:	2.65	m/s
Flow area:	8.8E-05	m^2	Re:	23834	
Base press. (in,filt,out)	1.11	0.49	0.09	Bar	
Pressure (by inlet,outle	0.49		0.49	Bar	
Average TMP	0.49	Bar	49193	Pa	

Time	Cum' filtrate	Temp	Flux raw data	Viscosity	Flux corrected	Cum've filtrate	Deposit res'ce
(min)	(l)	('C)	(lmh)	(Pa.s)	(lmh)	(l)	(1/m)
0	0.00	24.2	1405	0.000912	1439	0.00	1.25E-07
2	0.48	24.7	1208	0.000901	1223	0.49	4.07E+08
4	0.82	25.2	1025	0.000891	1026	0.87	9.28E+08
6	1.17	25.6	983	0.000883	975	1.21	1.10E+09
8	1.49	26	3099	0.000875	3046	1.89	-1.2E+09
10	3.27	26.4	2118	0.000867	2062	2.76	-7.0E+08
15	4.00	26.8	835	0.000859	805	3.97	1.81E+09
20	4.69	27.5	794	0.000845	754	4.64	2.09E+09
25	5.35	28	778	0.000835	730	5.27	2.24E+09
30	6.01	28.7	768	0.000822	709	5.88	2.37E+09
35	6.65	29.4	751	0.000809	683	6.47	2.55E+09
40	7.29	30	734	0.000798	658	7.03	2.74E+09
50	8.52	30.7	716	0.000785	632	8.13	2.94E+09
60	9.72	31.7	697	0.000767	601	9.17	3.21E+09
70	10.89	32.5	690	0.000753	584	10.18	3.38E+09
80	12.06	33	686	0.000744	574	11.16	3.47E+09
90	13.21	33.7	680	0.000733	559	12.12	3.62E+09
100	14.36	34.2	673	0.000724	547	13.06	3.76E+09
110	15.49	34.2	668	0.000724	543	13.99	3.80E+09
Membrane resistance:			2E+09	1/m			

HELIX			File:	CH11113E	
Outer radius:	0.01	m	Flow rate:	11.0	l/m
Inner radius:	0.006	m	Inlet pressure:	0.90	Bar
Active length:	0.27	m	Outlet pressure:	0.07	Bar
Hydraulic dx4:	0.008	m	Fluid density:	1000	kg/m^3
Solids conc:	1.5	% wt	Viscosity (25'C):	0.0009	Pa.s
Membrane area	0.0102	m^2	Bulk velocity:	2.08	m/s
Flow area:	8.8E-05	m^2	Re:	18727	
Base press. (in,filt,out):	0.70	0.34	0.06	Bar	
Pressure (by inlet,outlet	0.53		0.35	Bar	
Average TMP:	0.44	Bar	44063	Pa	

Time	Cum've filtrate	Temp	Flux raw data	Viscosity	Flux corrected	Cum've filtrate	Deposit res'ce
(min)	(l)	('C)	(lmh)	(Pa.s)	(lmh)	(l)	(1/m)
0	0.00	22	887	0.000959	956	0.00	1.30E-08
2	0.30	22.2	788	0.000955	845	0.32	4.07E+08
4	0.53	22.9	705	0.000939	744	0.59	8.85E+08
6	0.78	23.5	715	0.000926	744	0.85	8.83E+08
8	1.02	23.9	671	0.000918	692	1.09	1.18E+09
10	1.23	24.2	633	0.000912	648	1.32	1.48E+09
15	1.77	25	612	0.000895	616	1.85	1.72E+09
20	2.27	25.8	581	0.000879	574	2.36	2.07E+09
25	2.76	26.5	577	0.000865	560	2.84	2.20E+09
30	3.25	27.2	562	0.000851	537	3.30	2.43E+09
40	4.19	28.5	545	0.000826	505	4.19	2.77E+09
50	5.10	29.5	543	0.000807	492	5.03	2.92E+09
60	6.03	30.5	542	0.000789	481	5.86	3.07E+09
70	6.94	31.5	532	0.000771	460	6.66	3.34E+09
80	7.83	32.4	523	0.000755	444	7.42	3.59E+09
90	8.71	33	523	0.000744	437	8.17	3.69E+09
100	9.61	33.6	519	0.000734	428	8.91	3.83E+09
110	10.48	34.2	512	0.000724	416	9.62	4.03E+09
Membrane resistance:			3E+09	1/m			

HELIX File: CH10806F

Outer radius:	0.01	m	Flow rate:	8.0	l/m
Inner radius:	0.006	m	Inlet pressure:	0.38	Bar
Active length:	0.27	m	Outlet pressure:	0.03	Bar
Hydraulic dx4	0.008	m	Fluid density:	1000	kg/m^3
Solids conc:	1.5	% wt	Viscosity (25'C):	0.0009	Pa.s
Membrane ar	0.0102	m^2	Bulk velocity:	1.52	m/s
Flow area:	8.8E-05	m^2	Re:	13619	

Base press. (in,filt,out)	0.38	0.20	0.03	Bar	
Pressure (by inlet,outle	0.20		0.20	Bar	
Average TMP	0.20	Bar	20444	Pa	

Time (min)	Cum' filtrate (l)	Temp ('C)	Flux raw data (lmh)	Viscosity (Pa.s)	Flux corrected (lmh)	Cum've filtrate (l)	Deposit res'ce (1/m)
0	0.00	26	597	0.000875	587	0.00	6.33E-08
2	0.20	26.6	537	0.000863	521	0.20	2.97E+08
4	0.36	27	450	0.000855	432	0.36	8.41E+08
6	0.51	27.5	444	0.000845	422	0.51	9.18E+08
8	0.67	27.6	478	0.000843	453	0.65	6.94E+08
10	0.83	28	483	0.000835	454	0.81	6.89E+08
15	1.24	28.7	463	0.000822	428	1.18	8.72E+08
20	1.62	29	444	0.000816	407	1.54	1.04E+09
25	1.99	29.6	439	0.000805	397	1.88	1.12E+09
30	2.36	30.2	424	0.000794	379	2.21	1.29E+09
40	3.07	31	405	0.00078	355	2.83	1.54E+09
50	3.74	31.7	371	0.000767	319	3.40	1.97E+09
60	4.33	32.6	388	0.000751	328	3.95	1.85E+09
70	5.05	33.4	409	0.000738	339	4.51	1.72E+09
80	5.72	34	385	0.000728	315	5.07	2.03E+09
90	6.36	34.5	376	0.000719	304	5.59	2.19E+09
100	6.99	35	370	0.000711	295	6.10	2.32E+09
110	7.61	35.5	367	0.000703	290	6.60	2.41E+09

Membrane resistance: 2.35E+09 1/m

HELIX File: CH11723G

Outer radius:	0.01	m	Flow rate:	17.0	l/m
Inner radius:	0.006	m	Inlet pressure:	1.60	Bar
Active length:	0.27	m	Outlet pressure:	0.12	Bar
Hydraulic dx4	0.008	m	Fluid density:	1000	kg/m^3
Solids conc:	1.5	% wt	Viscosity (25'C):	0.0009	Pa.s
Membrane ar	0.01018	m^2	Bulk velocity:	3.22	m/s
Flow area:	8.8E-05	m^2	Re:	28941	

Base press. (in,filt,out):	1.60	0.67	0.12	Bar
Pressure (by inlet,outlet	0.67		0.67	Bar
Average TMP	0.67	Bar	66712	Pa

Time (min)	Cum' filtrate (l)	Temp ('C)	Flux raw data (lmh)	Viscosity (Pa.s)	Flux corrected (lmh)	Cum've filtrate (l)	Deposit res'ce (1/m)
0	0.00	23	2172	0.000937	2287	0.00	6.07E-08
2	0.74	23.5	1753	0.000926	1824	0.78	4.99E+08
4	1.19	24.1	1254	0.000914	1288	1.30	1.53E+09
6	1.59	24.4	1144	0.000907	1167	1.72	1.89E+09
8	1.97	24.6	1094	0.000903	1110	2.11	2.08E+09
10	2.33	25	1014	0.000895	1020	2.47	2.44E+09
15	3.17	25.7	966	0.000881	956	3.31	2.74E+09
20	3.97	26.5	925	0.000865	899	4.09	3.04E+09
25	4.74	27.2	895	0.000851	856	4.84	3.29E+09
30	5.49	27.9	862	0.000837	811	5.54	3.58E+09
40	6.93	29	840	0.000816	771	6.89	3.87E+09
50	8.34	30	817	0.000798	732	8.16	4.18E+09
60	9.71	31.2	797	0.000776	695	9.37	4.51E+09
70	11.04	31.8	782	0.000765	672	10.53	4.72E+09
80	12.36	32.5	767	0.000753	649	11.65	4.97E+09
90	13.64	33	753	0.000744	630	12.74	5.17E+09
100	14.91	33.7	742	0.000733	611	13.79	5.40E+09
110	16.16	34.4	736	0.000721	596	14.81	5.58E+09

Membrane resistance: 1.97E+09 1/m

NORMAL File: CN10804N

Outer radius:	0.01	m	Flow rate:	8.0	l/m
Inner radius:	0.006	m	Inlet pressure:	0.26	Bar
Active length:	0.27	m	Outlet pressure:	0.06	Bar
Hydraulic dx4	0.008	m	Fluid density:	1000	kg/m^3
Solids conc:	1.5	% wt	Viscosity (25'C):	0.0009	Pa.s
Membrane ar	0.0102	m^2	Bulk velocity:	0.66	m/s
Flow area:	0.0002	m^2	Re:	5961	

Base press. (in,filt,out)	0.23	0.15	0.06	Bar	
Pressure (by inlet,outle	0.19		0.15	Bar	
Average TMP	0.17	Bar	16951	Pa	

Time (min)	Cum' filtrate (l)	Temp ('C)	Flux raw data (lmh)	Viscosity (Pa.s)	Flux corrected (lmh)	Cum've filtrate (l)	Deposit res'ce (1/m)
0	0.00	22	941	0.000959	1014	0.00	4.18E-08
2	0.32	22.5	788	0.000948	840	0.34	2.35E+08
4	0.53	23	612	0.000937	645	0.60	6.46E+08
6	0.73	23.3	529	0.000931	554	0.80	9.37E+08
8	0.89	23.5	496	0.000926	516	0.98	1.09E+09
10	1.07	23.9	488	0.000918	504	1.15	1.14E+09
15	1.47	24.6	473	0.000903	480	1.57	1.26E+09
20	1.87	25.5	459	0.000885	456	1.97	1.38E+09
25	2.25	26.1	444	0.000873	435	2.35	1.50E+09
30	2.63	26.8	428	0.000859	413	2.71	1.64E+09
40	3.34	28.1	415	0.000833	388	3.39	1.82E+09
50	4.03	29.4	408	0.000809	371	4.03	1.96E+09
60	4.73	30.2	409	0.000794	365	4.65	2.00E+09
70	5.42	31	409	0.00078	358	5.27	2.06E+09
80	6.11	31.7	407	0.000767	351	5.87	2.13E+09
90	6.80	32.5	415	0.000753	351	6.46	2.13E+09
100	7.52	33	420	0.000744	352	7.06	2.12E+09
110	8.23	33.6	416	0.000734	343	7.63	2.20E+09

Membrane resistance: 1.13E+09 1/m

NORMAL File: CN10804G

Outer radius:	0.01	m	Flow rate:	8.0	l/m
Inner radius:	0.006	m	Inlet pressure:	0.28	Bar
Active length:	0.27	m	Outlet pressure:	0.06	Bar
Hydraulic dx4	0.008	m	Fluid density:	1000	kg/m^3
Solids conc:	1.5	% wt	Viscosity (25'C):	0.0009	Pa.s
Membrane ar	0.01018	m^2	Bulk velocity:	0.66	m/s
Flow area:	0.0002	m^2	Re:	5961	

Base press. (in,filt,out):	0.23	0.15	0.06	Bar
Pressure (by inlet,outlet	0.20		0.15	Bar
Average TMP	0.18	Bar	17641	Pa

Time (min)	Cum' filtrate (l)	Temp ('C)	Flux raw data (lmh)	Viscosity (Pa.s)	Flux corrected (lmh)	Cum've filtrate (l)	Deposit res'ce (1/m)
0	0.00	30	973	0.000798	872	0.00	-9.3E-08
2	0.33	30.3	830	0.000792	739	0.30	2.46E+08
4	0.56	30.4	653	0.00079	580	0.52	6.87E+08
6	0.77	30.5	561	0.000789	497	0.70	1.03E+09
8	0.94	30.6	500	0.000787	442	0.86	1.33E+09
10	1.11	30.7	468	0.000785	413	1.01	1.52E+09
15	1.50	30.8	440	0.000783	387	1.35	1.71E+09
20	1.86	31	416	0.00078	364	1.66	1.90E+09
25	2.20	31.3	406	0.000774	353	1.97	2.00E+09
30	2.55	31.5	397	0.000771	344	2.26	2.09E+09
40	3.22	31.8	387	0.000765	332	2.84	2.21E+09
50	3.86	32	375	0.000762	321	3.39	2.34E+09
60	4.49	32.3	367	0.000757	312	3.93	2.45E+09
70	5.10	32.5	360	0.000753	304	4.45	2.54E+09
80	5.71	32.6	353	0.000751	298	4.96	2.63E+09
90	6.30	32.7	347	0.00075	293	5.46	2.70E+09
100	6.89	32.9	344	0.000746	288	5.96	2.76E+09
110	7.47	33	343	0.000744	287	6.45	2.78E+09

Membrane resistance: 1.36E+09 1/m

NORMAL File: CN10806O

Outer radius:	0.01	m	Flow rate:	8.0	l/m
Inner radius:	0.006	m	Inlet pressure:	0.38	Bar
Active length:	0.27	m	Outlet pressure:	0.14	bar
Hydraulic dx4	0.008	m	Fluid density:	1000	kg/m^3
Solids conc:	1.5	% wt	Viscosity (25'C):	0.0009	Pa.s
Membrane ar	0.01018	m^2	Bulk velocity:	0.66	m/s
Flow area:	0.0002	m^2	Re:	5961	

Base press. (in,filt,out):	0.23	0.15	0.06	Bar	
Pressure (by inlet,outlet	0.30		0.23	Bar	
Average TMP	0.27	Bar	26885	Pa	

Time (min)	Cum' filtrate (l)	Temp ('C)	Flux raw data (lmh)	Viscosity (Pa.s)	Flux corrected (lmh)	Cum've filtrate (l)	Deposit res'ce (1/m)
0	0.00	30	1666	0.000798	1493	0.00	8.95E-08
2	0.57	30.6	1376	0.000787	1216	0.51	2.77E+08
4	0.93	30.7	997	0.000785	879	0.86	8.48E+08
6	1.24	30.8	867	0.000783	763	1.14	1.16E+09
8	1.52	31	788	0.00078	690	1.39	1.41E+09
10	1.78	31.2	704	0.000776	614	1.61	1.74E+09
15	2.36	31.9	663	0.000764	569	2.11	1.97E+09
20	2.90	32	627	0.000762	537	2.58	2.16E+09
25	3.42	32.2	604	0.000758	515	3.02	2.31E+09
30	3.93	32.6	582	0.000751	491	3.45	2.48E+09
40	4.90	33.1	572	0.000743	478	4.27	2.58E+09
50	5.87	33.8	558	0.000731	459	5.07	2.74E+09
60	6.80	34.3	562	0.000723	456	5.84	2.76E+09
70	7.77	34.4	570	0.000721	462	6.62	2.71E+09
80	8.73	35	561	0.000711	448	7.39	2.83E+09
90	9.68	35.5	554	0.000703	437	8.14	2.93E+09
100	10.61	35.6	549	0.000701	433	8.88	2.98E+09
110	11.54	36	547	0.000695	427	9.62	3.03E+09

Membrane resistance: 1.21E+09 1/m

NORMAL File: CN10809P

Outer radius:	0.01	m	Flow rate:	8.0	l/m
Inner radius:	0.006	m	Inlet pressure:	0.59	Bar
Active length:	0.27	m	Outlet pressure:	0.34	Bar
Hydraulic dx4	0.008	m	Fluid density:	1000	kg/m^3
Solids conc:	1.5	% wt	Viscosity (25'C):	0.0009	Pa.s
Membrane ar	0.01018	m^2	Bulk velocity:	0.66	m/s
Flow area:	0.0002	m^2	Re:	5961	

Base press. (in,filt,out):	0.23		0.15	0.06	Bar
Pressure (by inlet,outlet	0.51			0.44	Bar
Average TMP	0.48	Bar	47575	Pa	

Time (min)	Cum' filtrate (l)	Temp ('C)	Flux raw data (lmh)	Viscosity (Pa.s)	Flux corrected (lmh)	Cum've filtrate (l)	Deposit res'ce (1/m)
0	0.00	21.6	1968	0.000968	2141	0.00	-4.1E-08
2	0.67	22.1	1614	0.000957	1735	0.73	3.50E+08
4	1.10	22.5	1149	0.000948	1224	1.23	1.12E+09
6	1.45	22.9	983	0.000939	1038	1.61	1.59E+09
8	1.76	23.2	892	0.000933	935	1.95	1.93E+09
10	2.05	23.5	800	0.000926	833	2.25	2.35E+09
15	2.71	24.3	742	0.00091	758	2.92	2.73E+09
20	3.31	25.1	686	0.000893	688	3.54	3.16E+09
25	3.88	25.7	654	0.000881	648	4.10	3.45E+09
30	4.42	26	642	0.000875	631	4.64	3.58E+09
40	5.51	27.5	634	0.000845	602	5.69	3.83E+09
50	6.57	28.5	621	0.000826	576	6.69	4.07E+09
60	7.62	29.6	607	0.000805	549	7.64	4.34E+09
70	8.63	30.6	592	0.000787	523	8.55	4.63E+09
80	9.63	31.5	589	0.000771	510	9.43	4.79E+09
90	10.63	32.2	591	0.000758	503	10.29	4.87E+09
100	11.63	32.8	590	0.000748	496	11.14	4.97E+09
110	12.63	33.5	592	0.000736	489	11.97	5.06E+09

Membrane resistance: 1.50E+09 1/m

NORMAL File: CN11107K

Outer radius:	0.01	m	Flow rate:	11.0	l/m
Inner radius:	0.006	m	Inlet pressure:	0.45	Bar
Active length:	0.27	m	Outlet pressure:	0.08	Bar
Hydraulic dx4	0.008	m	Fluid density:	1000	kg/m^3
Solids conc:	1.5	% wt	Viscosity (25'C):	0.0009	Pa.s
Membrane ar	0.01018	m^2	Bulk velocity:	0.91	m/s
Flow area:	0.0002	m^2	Re:	8196	

Base press. (in,filt,out):	0.44	0.28	0.08	Bar
Pressure (by inlet,outlet	0.29		0.28	Bar
Average TMP	0.28	Bar	28215	Pa

Time (min)	Cum' filtrate (l)	Temp ('C)	Flux raw data (lmh)	Viscosity (Pa.s)	Flux corrected (lmh)	Cum've filtrate (l)	Deposit res'ce (1/m)
0	0.00	26	1796	0.000875	1765	0.00	-1.0E-07
2	0.61	26.4	1462	0.000867	1424	0.60	2.58E+08
4	0.99	26.6	1052	0.000863	1019	1.01	7.88E+08
6	1.32	26.8	941	0.000859	908	1.34	1.02E+09
8	1.63	27	868	0.000855	834	1.64	1.20E+09
10	1.91	27.2	793	0.000851	758	1.91	1.43E+09
15	2.57	27.6	750	0.000843	711	2.53	1.60E+09
20	3.18	28	713	0.000835	669	3.11	1.77E+09
25	3.78	28.4	698	0.000828	649	3.67	1.85E+09
30	4.37	28.7	685	0.000822	632	4.22	1.93E+09
40	5.52	29.4	676	0.000809	614	5.27	2.02E+09
50	6.66	29.7	657	0.000803	593	6.30	2.13E+09
60	7.75	30.5	642	0.000789	569	7.28	2.27E+09
70	8.84	30.8	637	0.000783	561	8.24	2.31E+09
80	9.92	31.2	632	0.000776	551	9.18	2.38E+09
90	10.98	31.6	627	0.000769	542	10.11	2.43E+09
100	12.04	32	623	0.000762	533	11.02	2.49E+09
110	13.10	32.4	621	0.000755	527	11.93	2.53E+09

Membrane resistance: 1.08E+09 1/m

NORMAL File: CN11107F

Outer radius:	0.01	m	Flow rate:	11.0	l/m
Inner radius:	0.006	m	Inlet pressure:	0.48	Bar
Active length:	0.27	m	Outlet pressure:	0.08	Bar
Hydraulic dx4	0.008	m	Fluid density:	1000	kg/m^3
Solids conc:	1.5	% wt	Viscosity (25'C):	0.0009	Pa.s
Membrane ar	0.01018	m^2	Bulk velocity:	0.91	m/s
Flow area:	0.0002	m^2	Re:	8196	

Base press. (in,filt,out):	0.44	0.28	0.08	Bar
Pressure (by inlet,outlet	0.32		0.28	Bar
Average TMP	0.30	Bar	29940	Pa

Time (min)	Cum' filtrate (l)	Temp ('C)	Flux raw data (lmh)	Viscosity (Pa.s)	Flux corrected (lmh)	Cum've filtrate (l)	Deposit res'ce (1/m)
0	0.00	16.8	1054	0.001081	1281	0.00	8.03E-08
2	0.36	17.2	877	0.001071	1055	0.43	3.36E+08
4	0.60	17.5	648	0.001064	774	0.74	1.03E+09
6	0.80	18.1	576	0.001049	679	0.99	1.40E+09
8	0.99	18.4	533	0.001042	624	1.21	1.66E+09
10	1.16	18.9	494	0.00103	572	1.42	1.95E+09
15	1.57	19.6	471	0.001014	536	1.88	2.19E+09
20	1.96	20.6	451	0.00099	502	2.33	2.44E+09
25	2.34	21.5	443	0.00097	483	2.74	2.61E+09
30	2.71	22.2	428	0.000955	459	3.14	2.82E+09
40	3.43	23.5	426	0.000926	444	3.91	2.97E+09
50	4.15	24.8	424	0.000899	429	4.65	3.13E+09
60	4.87	26	420	0.000875	413	5.36	3.32E+09
70	5.58	27	415	0.000855	398	6.05	3.49E+09
80	6.28	27.8	411	0.000839	388	6.72	3.63E+09
90	6.97	28.7	408	0.000822	377	7.37	3.78E+09
100	7.66	29.4	405	0.000809	368	8.00	3.91E+09
110	8.35	30	405	0.000798	363	8.63	3.99E+09

Membrane resistance: 1.58E+09 1/m

NORMAL File: CN11108L

Outer radius:	0.01	m	Flow rate:	11.0	l/m
Inner radius:	0.006	m	Inlet pressure:	0.52	Bar
Active length:	0.27	m	Outlet pressure:	0.14	Bar
Hydraulic dx4	0.008	m	Fluid density:	1000	kg/m^3
Solids conc:	1.5	% wt	Viscosity (25'C):	0.0009	Pa.s
Membrane ar	0.01018	m^2	Bulk velocity:	0.91	m/s
Flow area:	0.0002	m^2	Re:	8196	

Base press. (in,filt,out):	0.44	0.28	0.08	Bar
Pressure (by inlet,outlet	0.36		0.33	Bar
Average TMP	0.34	Bar	34332	Pa

Time (min)	Cum' filtrate (l)	Temp ('C)	Flux raw data (lmh)	Viscosity (Pa.s)	Flux corrected (lmh)	Cum've filtrate (l)	Deposit res'ce (1/m)
0	0.00	24.5	1886	0.000905	1919	0.00	1.59E-08
2	0.64	25	1491	0.000895	1500	0.65	3.37E+08
4	1.01	25.3	1079	0.000889	1077	1.09	9.42E+08
6	1.37	25.5	990	0.000885	985	1.44	1.14E+09
8	1.68	25.8	902	0.000879	891	1.76	1.39E+09
10	1.98	26	855	0.000875	840	2.05	1.55E+09
15	2.70	26.5	810	0.000865	787	2.74	1.73E+09
20	3.36	27.1	766	0.000853	734	3.39	1.95E+09
25	4.00	27.5	747	0.000845	710	4.00	2.06E+09
30	4.63	28	727	0.000835	683	4.59	2.18E+09
40	5.85	29	714	0.000816	655	5.72	2.33E+09
50	7.05	29.8	703	0.000801	633	6.82	2.45E+09
60	8.23	30.5	696	0.000789	617	7.87	2.55E+09
70	9.41	31.3	687	0.000774	598	8.90	2.67E+09
80	10.57	31.7	680	0.000767	586	9.91	2.75E+09
90	11.72	32.3	677	0.000757	575	10.89	2.82E+09
100	12.86	32.7	677	0.00075	570	11.87	2.85E+09
110	14.01	33	678	0.000744	567	12.84	2.87E+09

Membrane resistance: 1.21E+09 1/m

NORMAL File: CN11111M

Outer radius:	0.01	m	Flow rate:	11.0	l/m
Inner radius:	0.006	m	Inlet pressure:	0.74	Bar
Active length:	0.27	m	Outlet pressure:	0.34	Bar
Hydraulic dx4	0.008	m	Fluid density:	1000	kg/m^3
Solids conc:	1.5	% wt	Viscosity (25'C):	0.0009	Pa.s
Membrane ar	0.01018	m^2	Bulk velocity:	0.91	m/s
Flow area:	0.0002	m^2	Re:	8196	

Base press. (in,filt,out):	0.44	0.28	0.08	Bar
Pressure (by inlet,outlet	0.58		0.54	Bar
Average TMP	0.56	Bar	55712	Pa

Time (min)	Cum' filtrate (l)	Temp ('C)	Flux raw data (lmh)	Viscosity (Pa.s)	Flux corrected (lmh)	Cum've filtrate (l)	Deposit res'ce (1/m)
0	0.00	27.7	2725	0.000841	2576	0.00	-3.1E-08
2	0.92	28	2181	0.000835	2047	0.87	3.77E+08
4	1.48	28.3	1486	0.00083	1386	1.46	1.25E+09
6	1.93	28.5	1263	0.000826	1172	1.89	1.75E+09
8	2.34	28.6	1162	0.000824	1076	2.27	2.03E+09
10	2.72	28.8	1056	0.00082	973	2.62	2.40E+09
15	3.59	29.2	995	0.000813	909	3.42	2.68E+09
20	4.41	29.7	947	0.000803	855	4.17	2.93E+09
25	5.20	30	918	0.000798	823	4.88	3.11E+09
30	5.97	30.5	889	0.000789	788	5.56	3.31E+09
40	7.46	31.2	868	0.000776	757	6.87	3.50E+09
50	8.91	31.8	850	0.000765	731	8.13	3.68E+09
60	10.35	32.5	839	0.000753	710	9.35	3.83E+09
70	11.76	32.9	830	0.000746	695	10.55	3.94E+09
80	13.16	33.5	822	0.000736	680	11.71	4.07E+09
90	14.55	33.8	816	0.000731	670	12.86	4.15E+09
100	15.93	34.1	811	0.000726	661	13.99	4.22E+09
110	17.30	34.5	808	0.000719	653	15.10	4.29E+09

Membrane resistance: 1.46E+09 1/m

NORMAL File: CN11411D

Outer radius:	0.01	m	Flow rate:	14.0	l/m
Inner radius:	0.006	m	Inlet pressure:	0.76	Bar
Active length:	0.27	m	Outlet pressure:	0.11	Bar
Hydraulic dx4	0.008	m	Fluid density:	1000	kg/m^3
Solids conc:	1.5	% wt	Viscosity (25'C):	0.0009	Pa.s
Membrane ar	0.01018	m^2	Bulk velocity:	1.16	m/s
Flow area:	0.0002	m^2	Re:	10432	

Base press. (in,filt,out):	0.72	0.43	0.11	Bar
Pressure (by inlet,outlet	0.48		0.43	Bar
Average TMP	0.46	Bar	45571	Pa

Time (min)	Cum' filtrate (l)	Temp ('C)	Flux raw data (lmh)	Viscosity (Pa.s)	Flux corrected (lmh)	Cum've filtrate (l)	Deposit res'ce (1/m)
0	0.00	24	1643	0.000916	1691	0.00	-3.6E-08
2	0.56	24.7	1343	0.000901	1360	0.57	4.43E+08
4	0.91	25.2	985	0.000891	986	0.97	1.30E+09
6	1.23	25.5	878	0.000885	873	1.29	1.70E+09
8	1.51	25.7	806	0.000881	797	1.57	2.04E+09
10	1.77	26	754	0.000875	741	1.83	2.33E+09
15	2.40	26.5	709	0.000865	688	2.44	2.65E+09
20	2.97	27	668	0.000855	642	3.00	2.97E+09
25	3.54	27.5	651	0.000845	618	3.54	3.15E+09
30	4.08	28	629	0.000835	590	4.05	3.39E+09
40	5.14	29	611	0.000816	560	5.02	3.67E+09
50	6.15	29.7	591	0.000803	534	5.95	3.94E+09
60	7.14	30.4	582	0.00079	517	6.84	4.13E+09
70	8.13	31	584	0.00078	511	7.71	4.19E+09
80	9.12	31.5	576	0.000771	499	8.57	4.34E+09
90	10.08	32	561	0.000762	480	9.40	4.59E+09
100	11.03	32.5	622	0.000753	526	10.26	4.02E+09
110	12.19	32.8	687	0.000748	578	11.31	3.50E+09

Membrane resistance: 1.82E+09 1/m

NORMAL File: CN11411E

Outer radius:	0.01	m	Flow rate:	14.0	l/m
Inner radius:	0.006	m	Inlet pressure:	0.76	Bar
Active length:	0.27	m	Outlet pressure:	0.11	Bar
Hydraulic dx4	0.008	m	Fluid density:	1000	kg/m^3
Solids conc:	1.5	% wt	Viscosity (25'C):	0.0009	Pa.s
Membrane ar	0.01018	m^2	Bulk velocity:	1.16	m/s
Flow area:	0.0002	m^2	Re:	10432	

Base press. (in,filt,out):	0.72	0.43	0.11	Bar	
Pressure (by inlet,outlet	0.48		0.43	Bar	
Average TMP	0.46	Bar	45571	Pa	

Time (min)	Cum' filtrate (l)	Temp ('C)	Flux raw data (lmh)	Viscosity (Pa.s)	Flux corrected (lmh)	Cum've filtrate (l)	Deposit res'ce (1/m)
0	0.00	17.3	1411	0.001069	1694	0.00	5.81E-08
2	0.48	17.5	1167	0.001064	1394	0.57	3.89E+08
4	0.79	18.2	842	0.001047	991	0.98	1.29E+09
6	1.05	18.5	745	0.00104	870	1.29	1.72E+09
8	1.30	19	703	0.001028	811	1.58	1.97E+09
10	1.53	19.4	648	0.001018	742	1.84	2.33E+09
15	2.07	20.8	612	0.000986	678	2.45	2.72E+09
20	2.57	21	587	0.000981	648	3.01	2.93E+09
25	3.06	21.7	578	0.000966	627	3.55	3.08E+09
30	3.55	22.5	563	0.000948	600	4.07	3.31E+09
40	4.50	23.8	553	0.00092	572	5.06	3.56E+09
50	5.42	25	545	0.000895	548	6.01	3.79E+09
60	6.34	26.4	538	0.000867	524	6.92	4.05E+09
70	7.25	27.2	531	0.000851	508	7.80	4.24E+09
80	8.15	28	527	0.000835	494	8.65	4.40E+09
90	9.04	28.8	523	0.00082	482	9.48	4.56E+09
100	9.92	29.7	521	0.000803	470	10.28	4.72E+09
110	10.80	30	519	0.000798	465	11.09	4.79E+09

Membrane resistance: 1.81E+09 1/m

NORMAL File: CN11411H

Outer radius:	0.01	m	Flow rate:	14.0	l/m
Inner radius:	0.006	m	Inlet pressure:	11.0	psig
Active length:	0.27	m	Outlet pressure:	1.7	psig
Hydraulic dx4	0.008	m	Fluid density:	1000	kg/m^3
Solids conc:	1.5	% wt	Viscosity (25'C):	0.0009	Pa.s
Membrane ar	0.01018	m^2	Bulk velocity:	1.16	m/s
Flow area:	0.0002	m^2	Re:	10432	
Base press. (in,filt,out):	10.4	6.3	1.7		
Pressure (by inlet,outlet	6.9		6.3		
Average TMP	6.6	psig	45571	Pa	

Time (min)	Cum' filtrate (l)	Temp ('C)	Flux raw data (lmh)	Viscosity (Pa.s)	Flux corrected (lmh)	Cum've filtrate (l)	Deposit res'ce (1/m)
0	0.00	16.4	1298	0.001091	1592	0.00	-7.2E-08
2	0.44	16.8	1072	0.001081	1302	0.54	4.30E+08
4	0.73	17.1	783	0.001074	944	0.92	1.32E+09
6	0.97	17.5	689	0.001064	823	1.22	1.80E+09
8	1.19	18	661	0.001052	781	1.49	2.00E+09
10	1.42	18.5	599	0.00104	699	1.74	2.46E+09
15	1.91	19.1	562	0.001025	648	2.32	2.81E+09
20	2.37	20	546	0.001004	616	2.85	3.06E+09
25	2.83	20.8	533	0.000986	591	3.36	3.27E+09
30	3.28	21.6	519	0.000968	564	3.85	3.52E+09
40	4.15	22.9	509	0.000939	538	4.79	3.78E+09
50	5.01	24.2	501	0.000912	513	5.68	4.06E+09
60	5.85	25.2	496	0.000891	497	6.54	4.25E+09
70	6.69	26.1	490	0.000873	480	7.36	4.47E+09
80	7.51	27.1	485	0.000853	465	8.17	4.68E+09
90	8.34	27.8	484	0.000839	456	8.95	4.80E+09
100	9.16	28.6	481	0.000824	446	9.71	4.96E+09
110	9.97	29.3	480	0.000811	438	10.46	5.09E+09

Membrane resistance: 1.93E+09 1/m

NORMAL File: CN11414I

Outer radius:	0.01	m	Flow rate:	14.0	l/m
Inner radius:	0.006	m	Inlet pressure:	0.97	Bar
Active length:	0.27	m	Outlet pressure:	0.28	Bar
Hydraulic dx4	0.008	m	Fluid density:	1000	kg/m^3
Solids conc:	1.5	% wt	Viscosity (25'C):	0.0009	Pa.s
Membrane ar	0.01018	m^2	Bulk velocity:	1.16	m/s
Flow area:	0.0002	m^2	Re:	10432	

Base press. (in,filt,out):	0.72	0.43	0.11	Bar
Pressure (by inlet,outlet	0.68		0.60	Bar
Average TMP	0.64	Bar	63972	Pa

Time (min)	Cum' filtrate (l)	Temp ('C)	Flux raw data (lmh)	Viscosity (Pa.s)	Flux corrected (lmh)	Cum've filtrate (l)	Deposit res'ce (1/m)
0	0.00	18.3	1750	0.001044	2054	0.00	-4.2E-08
2	0.59	18.9	1416	0.00103	1638	0.70	5.33E+08
4	0.96	19.6	1001	0.001014	1140	1.17	1.68E+09
6	1.27	20.1	879	0.001002	989	1.53	2.26E+09
8	1.56	20.4	811	0.000995	907	1.85	2.66E+09
10	1.82	20.7	747	0.000988	829	2.15	3.10E+09
15	2.44	21	710	0.000981	783	2.83	3.41E+09
20	3.03	22.2	676	0.000955	725	3.47	3.85E+09
25	3.59	22.9	651	0.000939	687	4.07	4.18E+09
30	4.13	23.6	632	0.000924	657	4.64	4.47E+09
40	5.20	24.5	622	0.000905	633	5.73	4.72E+09
50	6.24	26	609	0.000875	598	6.77	5.11E+09
60	7.26	26.8	600	0.000859	579	7.77	5.35E+09
70	8.28	27.8	594	0.000839	560	8.74	5.60E+09
80	9.28	28.7	590	0.000822	544	9.68	5.82E+09
90	10.28	29	584	0.000816	535	10.59	5.96E+09
100	11.26	29.3	576	0.000811	525	11.49	6.12E+09
110	12.23	29.5	573	0.000807	519	12.38	6.21E+09

Membrane resistance: 2.10E+09 1/m

NORMAL File: CN11417J

Outer radius:	0.01	m	Flow rate:	14.0	l/m
Inner radius:	0.006	m	Inlet pressure:	1.17	Bar
Active length:	0.27	m	Outlet pressure:	0.48	Bar
Hydraulic dx4	0.008	m	Fluid density:	1000	kg/m^3
Solids conc:	1.5	% wt	Viscosity (25'C):	0.0009	Pa.s
Membrane ar	0.01018	m^2	Bulk velocity:	1.16	m/s
Flow area:	0.0002	m^2	Re:	10432	

Base press. (in,filt,out):	0.72	0.43	0.11	Bar
Pressure (by inlet,outlet	0.89		0.80	Bar
Average TMP	0.85	Bar	84661	Pa

Time (min)	Cum' filtrate (l)	Temp ('C)	Flux raw data (lmh)	Viscosity (Pa.s)	Flux corrected (lmh)	Cum've filtrate (l)	Deposit res'ce (1/m)
0	0.00	26	2299	0.000875	2259	0.00	-1.3E-07
2	0.78	26.1	1827	0.000873	1792	0.77	6.59E+08
4	1.24	26.2	1267	0.000871	1240	1.28	2.08E+09
6	1.64	26.3	1120	0.000869	1093	1.68	2.70E+09
8	2.00	26.4	1017	0.000867	990	2.03	3.24E+09
10	2.33	26.5	926	0.000865	900	2.35	3.82E+09
15	3.10	26.8	878	0.000859	847	3.09	4.21E+09
20	3.82	27.2	831	0.000851	795	3.79	4.66E+09
25	4.51	27.5	719	0.000845	683	4.41	5.83E+09
30	5.04	27.7	762	0.000841	720	5.01	5.40E+09
40	6.45	28.4	781	0.000828	726	6.24	5.33E+09
50	7.69	28.8	722	0.00082	665	7.42	6.05E+09
60	8.90	29.4	707	0.000809	643	8.53	6.35E+09
70	10.09	29.8	699	0.000801	629	9.61	6.55E+09
80	11.27	29.8	690	0.000801	621	10.67	6.66E+09
90	12.43	30.5	672	0.000789	595	11.70	7.06E+09
100	13.55	31	654	0.00078	573	12.69	7.43E+09
110	14.65	31.2	648	0.000776	565	13.69	7.57E+09

Membrane resistance: 2.53E+09 1/m

NORMAL File: CN11715C

Outer radius:	0.01	m	Flow rate:	17.0	l/m
Inner radius:	0.006	m	Inlet pressure:	1.06	Bar
Active length:	0.27	m	Outlet pressure:	0.15	Bar
Hydraulic dx4	0.008	m	Fluid density:	1000	kg/m^3
Solids conc:	1.5	% wt	Viscosity (25'C):	0.0009	Pa.s
Membrane ar	0.01018	m^2	Bulk velocity:	1.41	m/s
Flow area:	0.0002	m^2	Re:	12667	

Base press. (in,filt,out):	1.06	0.62	0.15	Bar
Pressure (by inlet,outlet	0.62		0.62	Bar
Average TMP	0.62	Bar	62351	Pa

Time (min)	Cum' filtrate (l)	Temp ('C)	Flux raw data (lmh)	Viscosity (Pa.s)	Flux corrected (lmh)	Cum've filtrate (l)	Deposit res'ce (1/m)
0	0.00	16.8	1929	0.001081	2343	0.00	-1.1E-07
2	0.65	17.2	1551	0.001071	1866	0.79	4.58E+08
4	1.05	17.6	1100	0.001061	1312	1.33	1.41E+09
6	1.40	18	988	0.001052	1167	1.75	1.81E+09
8	1.72	18.6	909	0.001037	1059	2.13	2.18E+09
10	2.02	19	845	0.001028	976	2.48	2.51E+09
15	2.73	19.6	811	0.001014	923	3.28	2.76E+09
20	3.39	20.5	773	0.000993	863	4.04	3.08E+09
25	4.04	21.5	753	0.00097	821	4.75	3.32E+09
30	4.67	22.5	731	0.000948	778	5.43	3.61E+09
40	5.90	23.8	718	0.00092	742	6.72	3.87E+09
50	7.11	25.2	706	0.000891	707	7.95	4.15E+09
60	8.29	26.5	700	0.000865	680	9.13	4.39E+09
70	9.48	27.5	697	0.000845	662	10.27	4.56E+09
80	10.66	28.5	689	0.000826	639	11.37	4.79E+09
90	11.82	29.3	686	0.000811	625	12.44	4.94E+09
100	12.99	30	688	0.000798	616	13.49	5.03E+09
110	14.15	30.6	687	0.000787	608	14.54	5.12E+09

Membrane resistance: 1.79E+09 1/m

NORMAL File: CN12023A

Outer radius:	0.01	m	Flow rate:	20.0	l/m
Inner radius:	0.006	m	Inlet pressure:	1.55	Bar
Active length:	0.27	m	Outlet pressure:	0.18	Bar
Hydraulic dx4	0.008	m	Fluid density:	1000	kg/m^3
Solids conc:	1.5	% wt	Viscosity (25'C):	0.0009	Pa.s
Membrane ar	0.01018	m^2	Bulk velocity:	1.66	m/s
Flow area:	0.0002	m^2	Re:	14902	
Base press. (in,filt,out):	1.48	0.84	0.18	Bar	
Pressure (by inlet,outlet	0.92		0.84	Bar	
Average TMP	0.88	Bar	88027	Pa	

Time (min)	Cum' filtrate (l)	Temp ('C)	Flux raw data (lmh)	Viscosity (Pa.s)	Flux corrected (lmh)	Cum've filtrate (l)	Deposit res'ce (1/m)
0	0.00	13	2181	0.00118	2891	0.00	-1.1E-08
2	0.74	14	1753	0.001153	2271	0.98	5.61E+08
4	1.19	15.2	1258	0.001122	1585	1.64	1.69E+09
6	1.59	15.5	1123	0.001114	1406	2.14	2.17E+09
8	1.95	16.2	1034	0.001096	1273	2.60	2.61E+09
10	2.30	16.5	963	0.001089	1178	3.01	2.98E+09
15	3.10	17.8	917	0.001056	1089	3.97	3.40E+09
20	3.85	18.6	875	0.001037	1020	4.87	3.77E+09
25	4.58	19.5	849	0.001016	969	5.71	4.07E+09
30	5.29	20.5	834	0.000993	931	6.52	4.32E+09
40	6.70	22.2	822	0.000955	882	8.06	4.68E+09
50	8.08	23.8	810	0.00092	838	9.51	5.03E+09
60	9.45	25.1	808	0.000893	810	10.91	5.27E+09
70	10.82	26.5	800	0.000865	778	12.26	5.58E+09
80	12.17	27	795	0.000855	763	13.57	5.72E+09
90	13.52	27.8	796	0.000839	750	14.85	5.86E+09
100	14.87	28.9	785	0.000818	722	16.10	6.17E+09
110	16.18	30	775	0.000798	694	17.27	6.50E+09

Membrane resistance: 2.05E+09 1/m

NORMAL File: CN12023B

Outer radius:	0.01	m	Flow rate:	20.0	l/m
Inner radius:	0.006	m	Inlet pressure:	1.55	Bar
Active length:	0.27	m	Outlet pressure:	0.18	Bar
Hydraulic dx4	0.008	m	Fluid density:	1000	kg/m^3
Solids conc:	1.5	% wt	Viscosity (25'C):	0.0009	Pa.s
Membrane ar	0.01018	m^2	Bulk velocity:	1.66	m/s
Flow area:	0.0002	m^2	Re:	14902	
Base press. (in,filt,out):	1.48	0.84	0.18	Bar	
Pressure (by inlet,outlet	0.92		0.84	Bar	
Average TMP	0.88	Bar	87980	Pa	

Time (min)	Cum' filtrate (l)	Temp ('C)	Flux raw data (lmh)	Viscosity (Pa.s)	Flux corrected (lmh)	Cum've filtrate (l)	Deposit res'ce (1/m)
0	0.00	18	2434	0.001052	2876	0.00	-4.9E-08
2	0.83	18.6	1942	0.001037	2263	0.98	5.59E+08
4	1.32	19.2	1348	0.001023	1550	1.62	1.77E+09
6	1.74	19.5	1172	0.001016	1338	2.11	2.37E+09
8	2.11	20	1075	0.001004	1213	2.55	2.83E+09
10	2.47	20.5	1043	0.000993	1163	2.95	3.04E+09
15	3.35	21.2	988	0.000977	1085	3.90	3.41E+09
20	4.15	22	922	0.000959	993	4.78	3.91E+09
25	4.92	22.6	892	0.000946	948	5.61	4.20E+09
30	5.66	23.2	862	0.000933	904	6.39	4.50E+09
40	7.11	24.7	833	0.000901	844	7.87	4.97E+09
50	8.49	26.2	812	0.000871	794	9.26	5.41E+09
60	9.86	27	809	0.000855	777	10.60	5.57E+09
70	11.23	28	796	0.000835	747	11.89	5.87E+09
80	12.57	28.9	784	0.000818	721	13.14	6.17E+09
90	13.89	29.5	777	0.000807	704	14.34	6.36E+09
100	15.20	30.4	774	0.00079	687	15.52	6.57E+09
110	16.52	31	776	0.00078	680	16.70	6.66E+09

Membrane resistance: 2.06E+09 1/m

TANGENTIAL File: CT10807E

Outer radius:	0.01	m	Flow rate:	8.0	l/m
Inner radius:	0.006	m	Inlet pressure:	0.45	Bar
Active length:	0.27	m	Outlet pressure:	0.03	Bar
Hydraulic dx4	0.008	m	Fluid density:	1000	kg/m^3
Solids conc:	1.5	% wt	Viscosity (25'C):	0.0009	Pa.s
Membrane ar	0.01018	m^2	Bulk velocity:	0.66	m/s
Flow area:	0.0002	m^2	Re:	5961	

Base press. (in,filt,out):	0.45	0.23	0.03	Bar
Pressure (by inlet,outlet	0.23		0.23	Bar
Average TMP	0.23	Bar	23084	Pa

Time (min)	Cum' filtrate (l)	Temp ('C)	Flux raw data (lmh)	Viscosity (Pa.s)	Flux corrected (lmh)	Cum've filtrate (l)	Deposit res'ce (1/m)
0	0.00	31.6	1341	0.000769	1158	0.00	-7.7E-08
2	0.46	31.7	1224	0.000767	1055	0.39	1.32E+08
4	0.83	31.8	1068	0.000765	918	0.73	3.52E+08
6	1.18	31.9	958	0.000764	822	1.02	5.51E+08
8	1.48	32	864	0.000762	739	1.29	7.61E+08
10	1.77	32.1	792	0.00076	676	1.53	9.58E+08
15	2.42	32.3	749	0.000757	637	2.08	1.10E+09
20	3.04	32.5	716	0.000753	606	2.61	1.23E+09
25	3.64	32.6	689	0.000751	582	3.12	1.33E+09
30	4.21	32.7	654	0.00075	551	3.60	1.48E+09
40	5.30	33	630	0.000744	527	4.51	1.61E+09
50	6.34	33.1	604	0.000743	504	5.38	1.74E+09
60	7.35	33.4	585	0.000738	485	6.22	1.87E+09
70	8.33	33.5	568	0.000736	470	7.03	1.97E+09
80	9.28	33.6	554	0.000734	457	7.82	2.06E+09
90	10.21	33.7	549	0.000733	452	8.59	2.10E+09

Membrane resistance: 1.34E+09 1/m

TANGENTIAL File: CT11213D

Outer radius:	0.01	m	Flow rate:	12.0	l/m
Inner radius:	0.006	m	Inlet pressure:	0.90	Bar
Active length:	0.27	m	Outlet pressure:	0.07	Bar
Hydraulic dx4	0.008	m	Fluid density:	1000	kg/m^3
Solids conc:	1.5	% wt	Viscosity (25'C):	0.0009	Pa.s
Membrane ar	0.01018	m^2	Bulk velocity:	0.99	m/s
Flow area:	0.0002	m^2	Re:	8941	

Base press. (in,filt,out):	0.90	0.46	0.07	Bar	
Pressure (by inlet,outlet	0.46		0.46	Bar	
Average TMP	0.46	Bar	46054	Pa	

Time (min)	Cum' filtrate (l)	Temp ('C)	Flux raw data (lmh)	Viscosity (Pa.s)	Flux corrected (lmh)	Cum've filtrate (l)	Deposit res'ce (1/m)
0	0.00	33	2185	0.000744	1828	0.00	1.96E-08
2	0.74	33.2	1880	0.000741	1566	0.62	2.84E+08
4	1.28	33.3	1466	0.000739	1218	1.09	8.51E+08
6	1.74	33.4	1325	0.000738	1098	1.49	1.13E+09
8	2.17	33.5	1262	0.000736	1044	1.85	1.28E+09
10	2.59	33.5	1195	0.000736	988	2.19	1.44E+09
15	3.59	33.8	1135	0.000731	932	3.01	1.63E+09
20	4.52	33.9	1074	0.000729	880	3.78	1.83E+09
25	5.42	34	1039	0.000728	850	4.51	1.96E+09
30	6.28	34.2	992	0.000724	807	5.21	2.15E+09
40	7.94	34.5	957	0.000719	773	6.55	2.32E+09
50	9.53	35	921	0.000711	736	7.83	2.52E+09
60	11.07	35.2	890	0.000708	708	9.06	2.69E+09
70	12.55	35.5	861	0.000703	680	10.23	2.87E+09
80	13.99	35.5	837	0.000703	661	11.37	3.00E+09
90	15.39	35.7	827	0.0007	650	12.48	3.08E+09

Membrane resistance: 1.70E+09 1/m

TANGENTIAL File: CT11217N

Outer radius:	0.01	m	Flow rate:	12.0	l/m
Inner radius:	0.006	m	Inlet pressure:	1.14	Bar
Active length:	0.27	m	Outlet pressure:	0.34	Bar
Hydraulic dx4	0.008	m	Fluid density:	1000	kg/m^3
Solids conc:	1.5	% wt	Viscosity (25'C):	0.0009	Pa.s
Membrane ar	0.01018	m^2	Bulk velocity:	0.99	m/s
Flow area:	0.0002	m^2	Re:	8941	

Base press. (in,filt,out):	0.90	0.46	0.07	Bar
Pressure (by inlet,outlet	0.70		0.74	Bar
Average TMP	0.72	Bar	71916	Pa

Time (min)	Cum' filtrate (l)	Temp ('C)	Flux raw data (lmh)	Viscosity (Pa.s)	Flux corrected (lmh)	Cum've filtrate (l)	Deposit res'ce (1/m)
0	0.00	27	2303	0.000855	2212	0.00	7.94E-08
2	0.78	27.5	1901	0.000845	1805	0.75	4.94E+08
4	1.29	27.7	1403	0.000841	1326	1.28	1.46E+09
6	1.73	28	1253	0.000835	1176	1.71	1.93E+09
8	2.14	28.3	1174	0.00083	1094	2.09	2.24E+09
10	2.53	28.5	1104	0.000826	1024	2.45	2.54E+09
15	3.45	29	1055	0.000816	968	3.29	2.82E+09
20	4.32	29.5	1007	0.000807	913	4.09	3.12E+09
25	5.16	30	982	0.000798	880	4.85	3.31E+09
30	5.99	30.6	953	0.000787	843	5.58	3.56E+09
40	7.59	31.8	925	0.000765	796	6.97	3.90E+09
50	9.13	32.3	902	0.000757	767	8.30	4.13E+09
60	10.65	32.8	893	0.000748	751	9.59	4.27E+09
70	12.16	33.4	883	0.000738	732	10.84	4.43E+09
80	13.64	33.9	867	0.000729	711	12.07	4.63E+09
90	15.10	34.4	854	0.000721	692	13.26	4.82E+09
100	16.54	35.1	849	0.000709	677	14.42	4.97E+09

Membrane resistance: 2.19E+09 1/m

TANGENTIAL File: CT11215M

Outer radius:	0.01	m	Flow rate:	12.0	l/m
Inner radius:	0.006	m	Inlet pressure:	1	Bar
Active length:	0.27	m	Outlet pressure:	0.21	Bar
Hydraulic dx4	0.008	m	Fluid density:	1000	kg/m^3
Solids conc:	1.5	% wt	Viscosity (25'C):	0.0009	Pa.s
Membrane ar	0.01018	m^2	Bulk velocity:	0.99	m/s
Flow area:	0.0002	m^2	Re:	8941	

Base press. (in,filt,out):	0.90	0.46	0.07	Bar
Pressure (by inlet,outlet	0.56		0.60	Bar
Average TMP	0.58	Bar	58123	Pa

Time (min)	Cum' filtrate (l)	Temp ('C)	Flux raw data (lmh)	Viscosity (Pa.s)	Flux corrected (lmh)	Cum've filtrate (l)	Deposit res'ce (1/m)
0	0.00	17	1858	0.001076	2246	0.00	1.75E-09
2	0.63	17.5	1606	0.001064	1920	0.76	2.97E+08
4	1.09	17.7	1279	0.001059	1522	1.35	8.30E+08
6	1.50	17.9	1069	0.001054	1266	1.82	1.35E+09
8	1.82	18.1	932	0.001049	1099	2.22	1.82E+09
10	2.13	18.3	856	0.001044	1004	2.58	2.16E+09
15	2.83	19	793	0.001028	916	3.39	2.53E+09
20	3.48	19.5	729	0.001016	832	4.13	2.97E+09
25	4.07	20	689	0.001004	778	4.82	3.29E+09
30	4.65	20.5	661	0.000993	737	5.46	3.57E+09
40	5.75	22.3	644	0.000952	689	6.67	3.94E+09
50	6.83	23.3	631	0.000931	660	7.81	4.19E+09
60	7.89	24.3	624	0.00091	637	8.91	4.40E+09
70	8.95	25.3	621	0.000889	620	9.98	4.58E+09
80	10.00	26	619	0.000875	608	11.02	4.70E+09
90	11.05	26.5	618	0.000865	600	12.05	4.78E+09

Membrane resistance: 1.74E+09 1/m

TANGENTIAL File: CT11213L

Outer radius:	0.01	m	Flow rate:	12.0	l/m
Inner radius:	0.006	m	Inlet pressure:	0.90	Bar
Active length:	0.27	m	Outlet pressure:	0.07	Bar
Hydraulic dx4	0.008	m	Fluid density:	1000	kg/m^3
Solids conc:	1.5	% wt	Viscosity (25'C):	0.0009	Pa.s
Membrane ar	0.01018	m^2	Bulk velocity:	0.99	m/s
Flow area:	0.0002	m^2	Re:	8941	

Base press. (in,filt,out):	0.90	0.46	0.07	Bar	
Pressure (by inlet,outlet	0.46		0.46	Bar	
Average TMP	0.46	Bar	46054	Pa	

Time (min)	Cum' filtrate (l)	Temp ('C)	Flux raw data (lmh)	Viscosity (Pa.s)	Flux corrected (lmh)	Cum've filtrate (l)	Deposit res'ce (1/m)
0	0.00	20.8	1488	0.000986	1648	0.00	8.68E-08
2	0.50	21.3	1275	0.000975	1397	0.56	3.39E+08
4	0.87	21.8	1063	0.000963	1150	0.99	8.15E+08
6	1.23	22.2	943	0.000955	1012	1.36	1.18E+09
8	1.51	22.5	806	0.000948	859	1.68	1.73E+09
10	1.77	22.8	795	0.000942	841	1.96	1.81E+09
15	2.45	23.6	777	0.000924	807	2.66	1.96E+09
20	3.09	24.5	740	0.000905	753	3.32	2.24E+09
25	3.70	25	717	0.000895	721	3.95	2.42E+09
30	4.31	25.8	705	0.000879	696	4.55	2.58E+09
40	5.50	27	688	0.000855	661	5.70	2.81E+09
50	6.64	28.1	671	0.000833	629	6.79	3.05E+09
60	7.78	29	666	0.000816	610	7.85	3.20E+09
70	8.90	30.5	661	0.000789	586	8.86	3.41E+09
80	10.02	30.8	658	0.000783	579	9.85	3.47E+09
90	11.13	31.3	657	0.000774	572	10.82	3.55E+09

Membrane resistance: 1.88E+09 1/m

TANGENTIAL File: CT11623I

Outer radius:	0.01	m	Flow rate:	16.0	l/m
Inner radius:	0.006	m	Inlet pressure:	1.55	Bar
Active length:	0.27	m	Outlet pressure:	0.21	Bar
Hydraulic dx4	0.008	m	Fluid density:	1000	kg/m^3
Solids conc:	1.5	% wt	Viscosity (25'C):	0.0009	Pa.s
Membrane ar	0.01018	m^2	Bulk velocity:	1.33	m/s
Flow area:	0.0002	m^2	Re:	11922	

Base press. (in,filt,out):	1.47	0.75	0.11	Bar	
Pressure (by inlet,outlet	0.83		0.85	Bar	
Average TMP	0.84	Bar	83916	Pa	

Time (min)	Cum' filtrate (l)	Temp ('C)	Flux raw data (lmh)	Viscosity (Pa.s)	Flux corrected (lmh)	Cum've filtrate (l)	Deposit res'ce (1/m)
0	0.00	29.5	2779	0.000807	2520	0.00	-6.8E-09
2	0.94	29.7	2314	0.000803	2088	0.85	4.64E+08
4	1.57	30	1680	0.000798	1506	1.46	1.51E+09
6	2.08	30.1	1481	0.000796	1324	1.94	2.03E+09
8	2.58	30.3	1432	0.000792	1274	2.39	2.19E+09
10	3.05	30.5	1348	0.000789	1194	2.80	2.49E+09
15	4.18	31	1286	0.00078	1127	3.79	2.78E+09
20	5.24	31.5	1231	0.000771	1066	4.72	3.06E+09
25	6.26	31.7	1188	0.000767	1024	5.60	3.28E+09
30	7.25	32.1	1146	0.00076	979	6.45	3.53E+09
40	9.18	32.9	1119	0.000746	938	8.08	3.79E+09
50	11.05	33.6	1089	0.000734	898	9.64	4.05E+09
60	12.87	34.2	1066	0.000724	867	11.14	4.28E+09
70	14.66	34.6	1047	0.000718	844	12.59	4.46E+09
80	16.43	35	1037	0.000711	828	14.01	4.59E+09
90	18.18	35.3	1035	0.000706	821	15.40	4.65E+09

Membrane resistance: 2.25E+09 1/m

TANGENTIAL File: CT11621H

Outer radius:	0.01	m	Flow rate:	16.0	l/m
Inner radius:	0.006	m	Inlet pressure:	1.47	Bar
Active length:	0.27	m	Outlet pressure:	0.11	Bar
Hydraulic dx4	0.008	m	Fluid density:	1000	kg/m^3
Solids conc:	1.5	% wt	Viscosity (25'C):	0.0009	Pa.s
Membrane ar	0.01018	m^2	Bulk velocity:	1.33	m/s
Flow area:	0.0002	m^2	Re:	11922	

Base press. (in,filt,out):	1.47	0.75	0.11	Bar
Pressure (by inlet,outlet	0.75		0.75	Bar
Average TMP	0.75	Bar	74895	Pa

Time (min)	Cum' filtrate (l)	Temp ('C)	Flux raw data (lmh)	Viscosity (Pa.s)	Flux corrected (lmh)	Cum've filtrate (l)	Deposit res'ce (1/m)
0	0.00	25	2715	0.000895	2730	0.00	7.00E-08
2	0.92	25.5	2207	0.000885	2194	0.93	4.52E+08
4	1.50	25.6	1577	0.000883	1564	1.56	1.38E+09
6	1.99	25.7	1420	0.000881	1405	2.07	1.74E+09
8	2.46	25.8	1347	0.000879	1330	2.53	1.95E+09
10	2.91	26.1	1259	0.000873	1234	2.97	2.24E+09
15	3.96	26.7	1204	0.000861	1164	3.98	2.49E+09
20	4.95	27.5	1144	0.000845	1086	4.94	2.80E+09
25	5.90	27.9	1104	0.000837	1039	5.84	3.01E+09
30	6.82	28.5	1074	0.000826	997	6.70	3.22E+09
40	8.63	29.5	1051	0.000807	953	8.36	3.45E+09
50	10.39	30.5	1028	0.000789	910	9.94	3.70E+09
60	12.12	31.5	1012	0.000771	876	11.45	3.92E+09
70	13.82	32.5	999	0.000753	846	12.91	4.12E+09
80	15.51	32.8	989	0.000748	831	14.33	4.22E+09
90	17.18	33.5	984	0.000736	814	15.73	4.35E+09

Membrane resistance: 1.85E+09 1/m

TANGENTIAL File: CT11625K

Outer radius:	0.01	m	Flow rate:	16.0	l/m
Inner radius:	0.006	m	Inlet pressure:	1.69	Bar
Active length:	0.27	m	Outlet pressure:	0.34	Bar
Hydraulic dx4	0.008	m	Fluid density:	1000	kg/m^3
Solids conc:	1.5	% wt	Viscosity (25'C):	0.0009	Pa.s
Membrane ar	0.01018	m^2	Bulk velocity:	1.33	m/s
Flow area:	0.0002	m^2	Re:	11922	

Base press. (in,filt,out):	1.47	0.75	0.11	Bar
Pressure (by inlet,outlet	0.97		0.99	Bar
Average TMP	0.98	Bar	97709	Pa

Time (min)	Cum' filtrate (l)	Temp ('C)	Flux raw data (lmh)	Viscosity (Pa.s)	Flux corrected (lmh)	Cum've filtrate (l)	Deposit res'ce (1/m)
0	0.00	30	3153	0.000798	2826	0.00	-1.1E-07
2	1.07	30.5	2557	0.000789	2266	0.96	5.77E+08
4	1.74	30.7	1820	0.000785	1605	1.62	1.77E+09
6	2.30	31	1621	0.00078	1420	2.13	2.31E+09
8	2.84	31.2	1518	0.000776	1323	2.59	2.65E+09
10	3.33	31.4	1408	0.000772	1222	3.03	3.06E+09
15	4.51	31.7	1343	0.000767	1157	4.04	3.36E+09
20	5.61	32.2	1270	0.000758	1082	4.98	3.76E+09
25	6.66	32.5	1217	0.000753	1030	5.88	4.06E+09
30	7.68	32.8	1169	0.000748	983	6.73	4.37E+09
40	9.64	33.5	1132	0.000736	936	8.36	4.71E+09
50	11.52	34	1085	0.000728	887	9.91	5.10E+09
60	13.32	34.3	1042	0.000723	846	11.38	5.46E+09
70	15.05	34.6	1014	0.000718	818	12.79	5.72E+09
80	16.76	35	1001	0.000711	799	14.16	5.91E+09
90	18.45	35.2	995	0.000708	792	15.51	5.99E+09

Membrane resistance: 2.33E+09 1/m

TANGENTIAL File: CT11621C

Outer radius:	0.01	m	Flow rate:	16.0	l/m
Inner radius:	0.006	m	Inlet pressure:	1.47	Bar
Active length:	0.27	m	Outlet pressure:	0.11	Bar
Hydraulic dx4	0.008	m	Fluid density:	1000	kg/m^3
Solids conc:	1.5	% wt	Viscosity (25'C):	0.0009	Pa.s
Membrane ar	0.01018	m^2	Bulk velocity:	1.33	m/s
Flow area:	0.0002	m^2	Re:	11922	
Base press. (in,filt,out):	1.47	0.75	0.11		
Pressure (by inlet,outlet	0.75		0.75		
Average TMP	0.75	Bar	74950	Pa	

Time (min)	Cum' filtrate (l)	Temp ('C)	Flux raw data (lmh)	Viscosity (Pa.s)	Flux corrected (lmh)	Cum've filtrate (l)	Deposit res'ce (1/m)
0	0.00	25.7	2890	0.000881	2860	0.00	6.65E-08
2	0.98	26	2447	0.000875	2405	0.97	3.35E+08
4	1.66	26.5	1861	0.000865	1808	1.69	1.03E+09
6	2.24	26.6	1634	0.000863	1583	2.26	1.42E+09
8	2.77	26.7	1506	0.000861	1457	2.78	1.70E+09
10	3.27	27.1	1412	0.000853	1353	3.25	1.97E+09
15	4.45	27.6	1353	0.000843	1282	4.37	2.17E+09
20	5.56	28.2	1288	0.000831	1203	5.42	2.43E+09
25	6.63	28.5	1238	0.000826	1149	6.42	2.63E+09
30	7.66	29.2	1189	0.000813	1086	7.37	2.89E+09
40	9.66	30.2	1153	0.000794	1028	9.16	3.15E+09
50	11.57	31	1113	0.00078	975	10.86	3.42E+09
60	13.43	31.8	1082	0.000765	931	12.48	3.66E+09
70	15.25	32.5	1057	0.000753	894	14.03	3.88E+09
80	17.02	32.9	1036	0.000746	868	15.52	4.05E+09
90	18.76	33.5	1026	0.000736	849	16.98	4.19E+09

Membrane resistance: 1.77E+09 1/m

TANGENTIAL File: CT11625J

Outer radius:	0.01	m	Flow rate:	16.0	l/m
Inner radius:	0.006	m	Inlet pressure:	1.69	Bar
Active length:	0.27	m	Outlet pressure:	0.34	Bar
Hydraulic dx4	0.008	m	Fluid density:	1000	kg/m^3
Solids conc:	1.5	% wt	Viscosity (25'C):	0.0009	Pa.s
Membrane ar	0.01018	m^2	Bulk velocity:	1.33	m/s
Flow area:	0.0002	m^2	Re:	11922	

Base press. (in,filt,out):	1.47	0.75	0.11	Bar
Pressure (by inlet,outlet	0.97		0.99	Bar
Average TMP	0.98	Bar	97709	Pa

Time (min)	Cum' filtrate (l)	Temp ('C)	Flux raw data (lmh)	Viscosity (Pa.s)	Flux corrected (lmh)	Cum've filtrate (l)	Deposit res'ce (1/m)
0	0.00	24.7	3223	0.000901	3264	0.00	6.73E-08
2	1.09	25	2654	0.000895	2669	1.11	4.50E+08
4	1.80	25.5	1787	0.000885	1777	1.86	1.69E+09
6	2.31	25.7	1482	0.000881	1467	2.41	2.47E+09
8	2.81	25.8	1458	0.000879	1439	2.90	2.56E+09
10	3.30	26.1	1379	0.000873	1352	3.38	2.85E+09
15	4.44	26.7	1317	0.000861	1273	4.49	3.16E+09
20	5.53	27.2	1253	0.000851	1198	5.54	3.48E+09
25	6.57	27.7	1212	0.000841	1146	6.53	3.73E+09
30	7.59	28.4	1173	0.000828	1091	7.48	4.02E+09
40	9.56	29.5	1148	0.000807	1041	9.29	4.31E+09
50	11.48	30.5	1122	0.000789	994	11.02	4.61E+09
60	13.36	31.5	1110	0.000771	961	12.68	4.83E+09

Membrane resistance: 2.02E+09 1/m

TANGENTIAL File: CT11828F

Outer radius:	0.01	m	Flow rate:	18.0	l/m
Inner radius:	0.006	m	Inlet pressure:	1.90	Bar
Active length:	0.27	m	Outlet pressure:	0.13	Bar
Hydraulic dx4	0.008	m	Fluid density:	1000	kg/m^3
Solids conc:	1.5	% wt	Viscosity (25'C):	0.0009	Pa.s
Membrane ar	0.01018	m^2	Bulk velocity:	1.49	m/s
Flow area:	0.0002	m^2	Re:	13412	

Base press. (in,filt,out):	1.80	0.91	0.13	Bar
Pressure (by inlet,outlet	1.01		0.91	Bar
Average TMP	0.96	Bar	96282	Pa

Time (min)	Cum' filtrate (l)	Temp ('C)	Flux raw data (lmh)	Viscosity (Pa.s)	Flux corrected (lmh)	Cum've filtrate (l)	Deposit res'ce (1/m)
0	0.00	19.5	3147	0.001016	3592	0.00	-5.2E-09
2	1.07	20.2	2589	0.001	2908	1.22	4.25E+08
4	1.76	20.7	1831	0.000988	2033	2.06	1.39E+09
6	2.31	21.1	1607	0.000979	1768	2.70	1.86E+09
8	2.85	21.5	1533	0.00097	1671	3.29	2.08E+09
10	3.35	22	1416	0.000959	1526	3.83	2.45E+09
15	4.53	22.8	1348	0.000942	1426	5.08	2.75E+09
20	5.64	23.6	1280	0.000924	1329	6.25	3.08E+09
25	6.70	24.5	1208	0.000905	1229	7.33	3.47E+09
30	7.69	25.3	1180	0.000889	1179	8.35	3.70E+09
40	9.70	26.7	1166	0.000861	1128	10.31	3.95E+09
50	11.64	27.7	1127	0.000841	1065	12.17	4.29E+09
60	13.53	28.8	1105	0.00082	1018	13.94	4.57E+09
70	15.39	29.8	1096	0.000801	987	15.64	4.77E+09
80	17.25	30.6	1088	0.000787	962	17.29	4.94E+09
90	19.08	31.4	1083	0.000772	940	18.90	5.10E+09

Membrane resistance: 1.81E+09 1/m

TANGENTIAL File: CT11829G

Outer radius:	0.01	m	Flow rate:	18.0	l/m
Inner radius:	0.006	m	Inlet pressure:	1.97	Bar
Active length:	0.27	m	Outlet pressure:	0.17	Bar
Hydraulic dx4	0.008	m	Fluid density:	1000	kg/m^3
Solids conc:	1.5	% wt	Viscosity (25'C):	0.0009	Pa.s
Membrane ar	0.01018	m^2	Bulk velocity:	1.49	m/s
Flow area:	0.0002	m^2	Re:	13412	

Base press. (in,filt,out):	1.80	0.91	0.13	Bar
Pressure (by inlet,outlet	1.08		0.96	Bar
Average TMP	1.02	Bar	101794	Pa

Time (min)	Cum' filtrate (l)	Temp ('C)	Flux raw data (lmh)	Viscosity (Pa.s)	Flux corrected (lmh)	Cum've filtrate (l)	Deposit res'ce (1/m)
0	0.00	24.5	3095	0.000905	3149	0.00	7.92E-08
2	1.05	25	2687	0.000895	2702	1.07	3.60E+08
4	1.82	25.5	2061	0.000885	2049	1.87	1.17E+09
6	2.45	25.7	1778	0.000881	1760	2.52	1.72E+09
8	3.03	26	1663	0.000875	1634	3.10	2.02E+09
10	3.58	26.5	1547	0.000865	1503	3.63	2.39E+09
15	4.87	27	1461	0.000855	1403	4.86	2.71E+09
20	6.06	27.7	1387	0.000841	1311	6.01	3.06E+09
25	7.22	28.3	1351	0.00083	1260	7.10	3.27E+09
30	8.35	28.8	1300	0.00082	1197	8.14	3.55E+09
40	10.53	29.9	1253	0.0008	1126	10.11	3.92E+09
50	12.60	30.9	1205	0.000781	1058	11.97	4.31E+09
60	14.62	31.5	1196	0.000771	1036	13.74	4.44E+09
70	16.66	32.4	1197	0.000755	1015	15.48	4.58E+09
80	18.68	32.8	1177	0.000748	989	17.18	4.76E+09
90	20.65	33.5	1163	0.000736	962	18.84	4.96E+09

Membrane resistance: 2.18E+09 1/m

TANGENTIAL File: CT11828B

Outer radius:	0.01	m	Flow rate:	18.0	l/m
Inner radius:	0.006	m	Inlet pressure:	1.90	Bar
Active length:	0.27	m	Outlet pressure:	0.10	Bar
Hydraulic dx4	0.008	m	Fluid density:	1000	kg/m^3
Solids conc:	1.5	% wt	Viscosity (25'C):	0.0009	Pa.s
Membrane ar	0.01018	m^2	Bulk velocity:	1.49	m/s
Flow area:	0.0002	m^2	Re:	13412	
Base press. (in,filt,out):	1.80	0.91	0.13	Bar	
Pressure (by inlet,outlet	1.01		0.89	Bar	
Average TMP	0.95	Bar	94898	Pa	

Time (min)	Cum' filtrate (l)	Temp ('C)	Flux raw data (lmh)	Viscosity (Pa.s)	Flux corrected (lmh)	Cum've filtrate (l)	Deposit res'ce (1/m)
0	0.00	21.8	3307	0.000963	3581	0.00	-3.4E-08
2	1.12	22.5	2724	0.000948	2902	1.21	4.18E+08
4	1.85	23	2007	0.000937	2114	2.07	1.24E+09
6	2.48	23.3	1842	0.000931	1926	2.75	1.53E+09
8	3.10	23.7	1692	0.000922	1753	3.38	1.86E+09
10	3.63	24.1	1548	0.000914	1589	3.94	2.24E+09
15	4.94	24.9	1497	0.000897	1509	5.26	2.45E+09
20	6.17	25.5	1428	0.000885	1420	6.50	2.72E+09
25	7.36	26.3	1381	0.000869	1347	7.67	2.96E+09
30	8.51	27.1	1334	0.000853	1278	8.79	3.22E+09
40	10.75	28.5	1299	0.000826	1206	10.89	3.52E+09
50	12.92	28.7	1259	0.000822	1162	12.90	3.72E+09
60	15.02	29.6	1232	0.000805	1114	14.83	3.95E+09
70	17.10	30.4	1210	0.00079	1075	16.69	4.17E+09
80	19.13	31.4	1191	0.000772	1034	18.48	4.40E+09
90	21.14	31.8	1186	0.000765	1020	20.22	4.48E+09

Membrane resistance: 1.79E+09 1/m

TANGENTIAL File: CT31828A

Outer radius:	0.01	m	Flow rate:	18.0	l/m
Inner radius:	0.006	m	Inlet pressure:	1.90	Bar
Active length:	0.27	m	Outlet pressure:	0.14	Bar
Hydraulic dx4	0.008	m	Fluid density:	1000	kg/m^3
Solids conc:	3	% wt	Viscosity (25'C):	0.0009	Pa.s
Membrane ar	0.01018	m^2	Bulk velocity:	1.49	m/s
Flow area:	0.0002	m^2	Re:	13412	

Base press. (in,filt,out):	1.80	0.91	0.13	Bar
Pressure (by inlet,outlet	1.01		0.92	Bar
Average TMP	0.97	Bar	96622	Pa

Time (min)	Cum' filtrate (l)	Temp ('C)	Flux raw data (lmh)	Viscosity (Pa.s)	Flux corrected (lmh)	Cum've filtrate (l)	Deposit res'ce (1/m)
0	0.00	25.5	2568	0.000885	2553	0.00	-4.1E-08
2	0.87	25.8	2134	0.000879	2107	0.87	5.40E+08
4	1.45	26.2	1676	0.000871	1640	1.50	1.42E+09
6	2.01	26.5	1624	0.000865	1577	2.05	1.58E+09
8	2.55	26.8	1573	0.000859	1518	2.57	1.74E+09
10	3.08	27.3	1498	0.000849	1429	3.07	2.01E+09
15	4.33	27.8	1445	0.000839	1363	4.26	2.23E+09
20	5.53	28.6	1395	0.000824	1292	5.38	2.49E+09
25	6.70	29.3	1356	0.000811	1235	6.45	2.72E+09
30	7.83	30	1315	0.000798	1178	7.48	2.98E+09
40	10.04	31	1289	0.00078	1129	9.43	3.22E+09
50	12.20	32	1274	0.000762	1091	11.32	3.42E+09

Membrane resistance: 2.55E+09 1/m

NORMAL File: CN41212V

Outer radius:	0.01	m	Flow rate:	12.0	l/m
Inner radius:	0.006	m	Inlet pressure:	0.83	Bar
Active length:	0.27	m	Outlet pressure:	0.21	Bar
Hydraulic dx4	0.008	m	Fluid density:	1000	kg/m^3
Solids conc:	4	% wt	Viscosity (25'C):	0.0009	Pa.s
Membrane ar	0.01018	m^2	Bulk velocity:	0.99	m/s
Flow area:	0.0002	m^2	Re:	8941	

Base press. (in,filt,out):	0.52	0.33	0.09	Bar	
Pressure (by inlet,outlet	0.63		0.44	Bar	
Average TMP	0.53	Bar	53439	Pa	

Time (min)	Cum' filtrate (l)	Temp ('C)	Flux raw data (lmh)	Viscosity (Pa.s)	Flux corrected (lmh)	Cum've filtrate (l)	Deposit res'ce (1/m)
0	0.00	25	1387	0.000895	1395	0.00	-6.9E-08
2	0.47	25.5	1115	0.000885	1108	0.47	6.67E+08
4	0.76	25.7	822	0.000881	813	0.80	1.85E+09
6	1.03	26	774	0.000875	761	1.07	2.15E+09
8	1.28	26.3	719	0.000869	702	1.31	2.55E+09
10	1.52	26.6	687	0.000863	666	1.55	2.83E+09
15	2.10	27.2	684	0.000851	654	2.11	2.93E+09
20	2.68	27.8	682	0.000839	643	2.66	3.02E+09
25	3.25	28.4	680	0.000828	632	3.20	3.11E+09
30	3.83	28.9	677	0.000818	623	3.73	3.20E+09
40	4.98	29.6	677	0.000805	613	4.78	3.30E+09
50	6.13	30.5	679	0.000789	602	5.81	3.40E+09
60	7.28	31.1	679	0.000778	593	6.82	3.49E+09
70	8.43	31.8	676	0.000765	582	7.82	3.61E+09
80	9.58	32.3	672	0.000757	571	8.79	3.72E+09
90	10.71	32.7	669	0.00075	563	9.76	3.81E+09

Membrane resistance: 2.58E+09 1/m

NORMAL File: CN41221W

Outer radius:	0.01	m	Flow rate:	12.0	l/m
Inner radius:	0.006	m	Inlet pressure:	1.45	Bar
Active length:	0.27	m	Outlet pressure:	0.69	Bar
Hydraulic dx4	0.008	m	Fluid density:	1000	kg/m^3
Solids conc:	4	% wt	Viscosity (25'C):	0.0009	Pa.s
Membrane ar	0.01018	m^2	Bulk velocity:	0.99	m/s
Flow area:	0.0002	m^2	Re:	8941	

Base press. (in,filt,out):	0.52	0.33	0.09	Bar
Pressure (by inlet,outlet	1.25		0.92	Bar
Average TMP	1.09	Bar	108611	Pa

Time (min)	Cum' filtrate (l)	Temp ('C)	Flux raw data (lmh)	Viscosity (Pa.s)	Flux corrected (lmh)	Cum've filtrate (l)	Deposit res'ce (1/m)
0	0.00	24.6	2093	0.000903	2124	0.00	-2.1E-07
2	0.71	25	1662	0.000895	1672	0.72	9.33E+08
4	1.13	25.5	1142	0.000885	1135	1.20	3.00E+09
6	1.49	25.7	1017	0.000881	1006	1.56	3.83E+09
8	1.82	26	975	0.000875	958	1.89	4.19E+09
10	2.15	26.3	922	0.000869	900	2.21	4.69E+09
15	2.91	27	881	0.000855	846	2.95	5.21E+09
20	3.64	28	840	0.000835	789	3.64	5.84E+09
25	4.34	28.4	819	0.000828	762	4.30	6.17E+09
30	5.03	29.2	807	0.000813	737	4.94	6.49E+09
40	6.39	30.4	798	0.00079	708	6.16	6.89E+09
50	7.74	31.4	786	0.000772	682	7.34	7.29E+09
60	9.06	32	776	0.000762	664	8.48	7.58E+09
70	10.37	32.9	770	0.000746	645	9.59	7.90E+09
80	11.67	33.5	761	0.000736	629	10.67	8.19E+09
90	12.95	34	754	0.000728	616	11.73	8.44E+09

Membrane resistance: 3.45E+09 1/m

NORMAL File: CN41718R

Outer radius:	0.01	m	Flow rate:	17.0	l/m
Inner radius:	0.006	m	Inlet pressure:	1.21	Bar
Active length:	0.27	m	Outlet pressure:	0.14	Bar
Hydraulic dx4	0.008	m	Fluid density:	1000	kg/m^3
Solids conc:	4	% wt	Viscosity (25'C):	0.0009	Pa.s
Membrane ar	0.01018	m^2	Bulk velocity:	1.41	m/s
Flow area:	0.0002	m^2	Re:	12667	

Base press. (in,filt,out):	1.06	0.62	0.15	Bar
Pressure (by inlet,outlet	0.77		0.62	Bar
Average TMP	0.69	Bar	69473	Pa

Time (min)	Cum' filtrate (l)	Temp ('C)	Flux raw data (lmh)	Viscosity (Pa.s)	Flux corrected (lmh)	Cum've filtrate (l)	Deposit res'ce (1/m)
0	0.00	29.3	1514	0.000811	1379	0.00	-3.2E-08
2	0.51	29.5	1297	0.000807	1176	0.47	5.86E+08
4	0.88	29.7	1041	0.000803	939	0.83	1.59E+09
6	1.22	29.9	988	0.0008	887	1.14	1.88E+09
8	1.55	30.1	946	0.000796	846	1.43	2.14E+09
10	1.86	30.3	895	0.000792	796	1.71	2.48E+09
15	2.61	30.8	877	0.000783	771	2.37	2.68E+09
20	3.35	31	865	0.00078	757	3.02	2.79E+09
25	4.08	31.5	846	0.000771	733	3.65	3.00E+09
30	4.78	31.9	829	0.000764	711	4.27	3.19E+09
40	6.19	32.6	824	0.000751	696	5.46	3.34E+09
50	7.58	33	808	0.000744	676	6.62	3.53E+09
60	8.93	33.5	792	0.000736	655	7.75	3.75E+09
70	10.27	34	784	0.000728	641	8.85	3.91E+09
80	11.59	34.5	780	0.000719	630	9.93	4.04E+09
90	12.91	35	778	0.000711	622	10.99	4.14E+09

Membrane resistance: 3.40E+09 1/m

NORMAL File: CN42024Q

Outer radius:	0.01	m	Flow rate:	20.0	l/m
Inner radius:	0.006	m	Inlet pressure:	1.62	Bar
Active length:	0.27	m	Outlet pressure:	0.18	Bar
Hydraulic dx4	0.008	m	Fluid density:	1000	kg/m^3
Solids conc:	4	% wt	Viscosity (25'C):	0.0009	Pa.s
Membrane ar	0.01018	m^2	Bulk velocity:	1.66	m/s
Flow area:	0.0002	m^2	Re:	14902	

Base press. (in,filt,out):	1.48	0.84	0.18	Bar
Pressure (by inlet,outlet	0.98		0.84	Bar
Average TMP	0.91	Bar	91429	Pa

Time (min)	Cum' filtrate (l)	Temp ('C)	Flux raw data (lmh)	Viscosity (Pa.s)	Flux corrected (lmh)	Cum've filtrate (l)	Deposit res'ce (1/m)
0	0.00	20	1576	0.001004	1778	0.00	1.20E-07
2	0.53	20.5	1356	0.000993	1512	0.60	6.10E+08
4	0.92	21.2	1069	0.000977	1173	1.06	1.79E+09
6	1.26	21.5	987	0.00097	1076	1.44	2.26E+09
8	1.59	21.8	943	0.000963	1021	1.80	2.57E+09
10	1.90	22.3	909	0.000952	973	2.13	2.87E+09
15	2.67	23.1	902	0.000935	947	2.95	3.04E+09
20	3.43	24.1	884	0.000914	907	3.74	3.33E+09
25	4.17	24.8	868	0.000899	877	4.49	3.56E+09
30	4.90	25.6	859	0.000883	852	5.23	3.77E+09
40	6.36	26.8	854	0.000859	824	6.65	4.02E+09
50	7.80	28.4	846	0.000828	787	8.01	4.36E+09
60	9.23	29.5	837	0.000807	759	9.33	4.65E+09
70	10.64	30.4	831	0.00079	738	10.60	4.89E+09
80	12.05	31.1	829	0.000778	724	11.84	5.04E+09
90	13.45	32	828	0.000762	709	13.05	5.23E+09

Membrane resistance: 3.47E+09 1/m

NORMAL File: CN42025S

Outer radius:	0.01	m	Flow rate:	20.0	l/m
Inner radius:	0.006	m	Inlet pressure:	1.69	Bar
Active length:	0.27	m	Outlet pressure:	0.18	Bar
Hydraulic dx4	0.008	m	Fluid density:	1000	kg/m^3
Solids conc:	4	% wt	Viscosity (25'C):	0.0009	Pa.s
Membrane ar	0.01018	m^2	Bulk velocity:	1.66	m/s
Flow area:	0.0002	m^2	Re:	14902	

Base press. (in,filt,out):	1.48	0.84	0.18	Bar
Pressure (by inlet,outlet	1.05		0.84	Bar
Average TMP	0.95	Bar	94877	Pa

Time (min)	Cum' filtrate (l)	Temp ('C)	Flux raw data (lmh)	Viscosity (Pa.s)	Flux corrected (lmh)	Cum've filtrate (l)	Deposit res'ce (1/m)
0	0.00	21.2	1922	0.000977	2109	0.00	-1.8E-07
2	0.65	21.8	1577	0.000963	1707	0.72	7.15E+08
4	1.07	22.2	1177	0.000955	1263	1.22	2.03E+09
6	1.45	22.8	1095	0.000942	1158	1.63	2.49E+09
8	1.81	23.3	1057	0.000931	1105	2.01	2.76E+09
10	2.17	23.7	1039	0.000922	1077	2.38	2.91E+09
15	3.05	24.6	1032	0.000903	1047	3.29	3.08E+09
20	3.92	25.3	1019	0.000889	1018	4.16	3.25E+09
25	4.78	26	1002	0.000875	985	5.01	3.46E+09
30	5.62	26.7	988	0.000861	956	5.83	3.66E+09
40	7.29	28.2	981	0.000831	916	7.42	3.95E+09
50	8.95	29.5	971	0.000807	881	8.95	4.23E+09
60	10.59	30.5	877	0.000789	777	10.35	5.20E+09
70	11.92	31.5	784	0.000771	679	11.59	6.38E+09
80	13.25	32.5	780	0.000753	660	12.72	6.66E+09
90	14.57	33.5	778	0.000736	644	13.83	6.90E+09

Membrane resistance: 3.03E+09 1/m

NORMAL File: CN42027T

Outer radius:	0.01	m	Flow rate:	20.0	l/m
Inner radius:	0.006	m	Inlet pressure:	1.83	Bar
Active length:	0.27	m	Outlet pressure:	0.28	Bar
Hydraulic dx4	0.008	m	Fluid density:	1000	kg/m^3
Solids conc:	4	% wt	Viscosity (25'C):	0.0009	Pa.s
Membrane ar	0.01018	m^2	Bulk velocity:	1.66	m/s
Flow area:	0.0002	m^2	Re:	14902	

Base press. (in,filt,out):	1.48	0.84	0.18	Bar
Pressure (by inlet,outlet	1.19		0.94	Bar
Average TMP	1.07	Bar	106601	Pa

Time (min)	Cum' filtrate (l)	Temp ('C)	Flux raw data (lmh)	Viscosity (Pa.s)	Flux corrected (lmh)	Cum've filtrate (l)	Deposit res'ce (1/m)
0	0.00	17.8	1808	0.001056	2146	0.00	8.96E-08
2	0.61	18.4	1471	0.001042	1722	0.73	8.25E+08
4	1.00	18.9	1084	0.00103	1254	1.23	2.38E+09
6	1.35	19.5	1010	0.001016	1153	1.64	2.89E+09
8	1.68	19.9	971	0.001007	1098	2.02	3.20E+09
10	2.01	20.2	942	0.001	1058	2.39	3.44E+09
15	2.80	21.4	928	0.000972	1014	3.27	3.74E+09
20	3.58	22.3	911	0.000952	975	4.11	4.02E+09
25	4.35	23.2	904	0.000933	948	4.93	4.23E+09
30	5.12	24.2	903	0.000912	925	5.72	4.42E+09
40	6.65	25.7	901	0.000881	892	7.26	4.71E+09
50	8.17	27.2	901	0.000851	861	8.75	5.00E+09
60	9.70	28.5	900	0.000826	835	10.19	5.25E+09
70	11.23	29.6	900	0.000805	814	11.59	5.48E+09
80	12.76	30.5	900	0.000789	797	12.95	5.66E+09
90	14.28	31.4	900	0.000772	781	14.29	5.85E+09

Membrane resistance: 3.35E+09 1/m

NORMAL File: CN42029U

Outer radius:	0.01	m	Flow rate:	20.0	l/m
Inner radius:	0.006	m	Inlet pressure:	1.97	Bar
Active length:	0.27	m	Outlet pressure:	0.41	Bar
Hydraulic dx4	0.008	m	Fluid density:	1000	kg/m^3
Solids conc:	4	% wt	Viscosity (25'C):	0.0009	Pa.s
Membrane ar	0.01018	m^2	Bulk velocity:	1.66	m/s
Flow area:	0.0002	m^2	Re:	14902	

Base press. (in,filt,out):	1.48	0.84	0.18	Bar
Pressure (by inlet,outlet	1.33		1.08	Bar
Average TMP	1.20	Bar	120394	Pa

Time (min)	Cum' filtrate (l)	Temp ('C)	Flux raw data (lmh)	Viscosity (Pa.s)	Flux corrected (lmh)	Cum've filtrate (l)	Deposit res'ce (1/m)
0	0.00	26.3	2335	0.000869	2279	0.00	-1.8E-07
2	0.79	26.6	1900	0.000863	1842	0.77	8.45E+08
4	1.29	26.9	1402	0.000857	1349	1.31	2.45E+09
6	1.74	27.2	1319	0.000851	1261	1.76	2.87E+09
8	2.18	27.5	1261	0.000845	1198	2.17	3.21E+09
10	2.60	27.7	1209	0.000841	1142	2.57	3.54E+09
15	3.62	28.4	1189	0.000828	1106	3.52	3.78E+09
20	4.62	29	1166	0.000816	1069	4.45	4.03E+09
25	5.60	29.5	1150	0.000807	1043	5.34	4.22E+09
30	6.57	30	1137	0.000798	1020	6.22	4.40E+09
40	8.49	31	1128	0.00078	988	7.92	4.65E+09
50	10.39	31.7	1115	0.000767	961	9.57	4.88E+09
60	12.28	32.5	1105	0.000753	935	11.18	5.12E+09
70	14.14	33.1	1097	0.000743	916	12.75	5.30E+09
80	16.00	33.6	1089	0.000734	899	14.29	5.47E+09
90	17.84	34.2	1086	0.000724	883	15.80	5.63E+09

Membrane resistance: 3.56E+09 1/m

TANGENTIAL File: CT41213R

Outer radius:	0.01	m	Flow rate:	12.0	l/m
Inner radius:	0.006	m	Inlet pressure:	0.90	Bar
Active length:	0.27	m	Outlet pressure:	0.07	Bar
Hydraulic dx4	0.008	m	Fluid density:	1000	kg/m^3
Solids conc:	4	% wt	Viscosity (25'C):	0.0009	Pa.s
Membrane ar	0.01018	m^2	Bulk velocity:	0.99	m/s
Flow area:	0.0002	m^2	Re:	8941	

Base press. (in,filt,out):	0.90	0.46	0.07	Bar
Pressure (by inlet,outlet	0.46		0.46	Bar
Average TMP	0.46	Bar	46054	Pa

Time (min)	Cum' filtrate (l)	Temp ('C)	Flux raw data (lmh)	Viscosity (Pa.s)	Flux corrected (lmh)	Cum've filtrate (l)	Deposit res'ce (1/m)
0	0.00	28.9	1432	0.000818	1317	0.00	-6.7E-08
2	0.49	29.1	1276	0.000814	1168	0.45	3.01E+08
4	0.87	29.4	1091	0.000809	992	0.81	7.73E+08
6	1.23	29.6	1037	0.000805	938	1.14	9.51E+08
8	1.57	29.7	994	0.000803	897	1.45	1.10E+09
10	1.90	29.8	964	0.000801	868	1.75	1.22E+09
15	2.71	30.3	920	0.000792	819	2.47	1.43E+09
20	3.46	30.6	860	0.000787	761	3.14	1.72E+09
25	4.17	31	826	0.00078	724	3.77	1.93E+09
30	4.86	31.5	803	0.000771	695	4.37	2.11E+09
40	6.22	32	786	0.000762	673	5.53	2.26E+09
50	7.53	32.5	761	0.000753	644	6.64	2.46E+09
60	8.80	33	738	0.000744	617	7.71	2.67E+09
70	10.03	33.5	717	0.000736	593	8.74	2.88E+09
80	11.23	33.8	697	0.000731	572	9.73	3.07E+09
90	12.40	34.2	687	0.000724	559	10.69	3.20E+09

Membrane resistance: 2.36E+09 1/m

TANGENTIAL File: CT41417Q

Outer radius:	0.01	m	Flow rate:	14.0	l/m
Inner radius:	0.006	m	Inlet pressure:	1.17	Bar
Active length:	0.27	m	Outlet pressure:	0.09	Bar
Hydraulic dx4	0.008	m	Fluid density:	1000	kg/m^3
Solids conc:	4	% wt	Viscosity (25'C):	0.0009	Pa.s
Membrane ar	0.01018	m^2	Bulk velocity:	1.16	m/s
Flow area:	0.0002	m^2	Re:	10432	

Base press. (in,filt,out):	1.17	0.60	0.09	Bar
Pressure (by inlet,outlet	0.59		0.60	Bar
Average TMP	0.60	Bar	59704	Pa

Time (min)	Cum' filtrate (l)	Temp ('C)	Flux raw data (lmh)	Viscosity (Pa.s)	Flux corrected (lmh)	Cum've filtrate (l)	Deposit res'ce (1/m)
0	0.00	27.6	1800	0.000843	1705	0.00	1.35E-08
2	0.61	28	1551	0.000835	1456	0.58	4.04E+08
4	1.05	28.2	1272	0.000831	1189	1.03	1.03E+09
6	1.47	28.4	1209	0.000828	1125	1.42	1.22E+09
8	1.87	28.6	1141	0.000824	1057	1.79	1.45E+09
10	2.25	28.8	1074	0.00082	990	2.14	1.71E+09
15	3.15	29.3	1046	0.000811	953	2.96	1.86E+09
20	4.02	29.8	999	0.000801	899	3.75	2.11E+09
25	4.84	30.3	942	0.000792	838	4.48	2.44E+09
30	5.62	30.6	897	0.000787	793	5.17	2.72E+09
40	7.13	31.5	868	0.000771	751	6.48	3.00E+09
50	8.57	32.2	837	0.000758	713	7.73	3.28E+09
60	9.97	32.7	814	0.00075	686	8.91	3.51E+09
70	11.33	33.1	796	0.000743	664	10.06	3.70E+09
80	12.67	33.6	782	0.000734	645	11.17	3.88E+09
90	13.98	34	775	0.000728	634	12.25	3.99E+09

Membrane resistance: 2.36E+09 1/m

TANGENTIAL File: CT41621P

Outer radius:	0.01	m	Flow rate:	16.0	l/m
Inner radius:	0.006	m	Inlet pressure:	1.47	Bar
Active length:	0.27	m	Outlet pressure:	0.11	Bar
Hydraulic dx4	0.008	m	Fluid density:	1000	kg/m^3
Solids conc:	4	% wt	Viscosity (25'C):	0.0009	Pa.s
Membrane ar	0.01018	m^2	Bulk velocity:	1.33	m/s
Flow area:	0.0002	m^2	Re:	11922	

Base press. (in,filt,out):	1.47	0.75	0.11	Bar
Pressure (by inlet,outlet	0.75		0.75	Bar
Average TMP	0.75	Bar	74950	Pa

Time (min)	Cum' filtrate (l)	Temp ('C)	Flux raw data (lmh)	Viscosity (Pa.s)	Flux corrected (lmh)	Cum've filtrate (l)	Deposit res'ce (1/m)
0	0.00	29.5	2113	0.000807	1915	0.00	7.17E-08
2	0.72	29.9	1871	0.0008	1681	0.65	3.68E+08
4	1.27	30	1568	0.000798	1405	1.17	9.58E+08
6	1.78	30.2	1480	0.000794	1321	1.64	1.19E+09
8	2.27	30.4	1414	0.00079	1256	2.07	1.38E+09
10	2.74	30.6	1335	0.000787	1180	2.49	1.64E+09
15	3.86	30.8	1280	0.000783	1126	3.46	1.85E+09
20	4.91	31.2	1215	0.000776	1059	4.39	2.13E+09
25	5.92	31.5	1168	0.000771	1012	5.27	2.36E+09
30	6.89	32	1116	0.000762	955	6.10	2.65E+09
40	8.76	32.5	1078	0.000753	912	7.69	2.90E+09
50	10.55	33.2	1041	0.000741	866	9.20	3.19E+09
60	12.29	33.7	1013	0.000733	834	10.64	3.42E+09
70	13.99	34	994	0.000728	812	12.04	3.58E+09
80	15.66	34.5	978	0.000719	790	13.40	3.76E+09
90	17.31	34.7	970	0.000716	781	14.73	3.84E+09

Membrane resistance: 2.64E+09 1/m

TANGENTIAL File: CT41621S

Outer radius:	0.01	m	Flow rate:	16.0	l/m
Inner radius:	0.006	m	Inlet pressure:	1.47	Bar
Active length:	0.27	m	Outlet pressure:	0.11	Bar
Hydraulic dx4	0.008	m	Fluid density:	1000	kg/m^3
Solids conc:	4	% wt	Viscosity (25'C):	0.0009	Pa.s
Membrane ar	0.01018	m^2	Bulk velocity:	1.33	m/s
Flow area:	0.0002	m^2	Re:	11922	

Base press. (in,filt,out):	1.47	0.75	0.11	Bar
Pressure (by inlet,outlet	0.75		0.75	Bar
Average TMP	0.75	Bar	74950	Pa

Time (min)	Cum' filtrate (l)	Temp ('C)	Flux raw data (lmh)	Viscosity (Pa.s)	Flux corrected (lmh)	Cum've filtrate (l)	Deposit res'ce (1/m)
0	0.00	20	1789	0.001004	2018	0.00	-1.6E-07
2	0.61	20.5	1549	0.000993	1728	0.68	4.21E+08
4	1.05	21	1262	0.000981	1391	1.21	1.13E+09
6	1.46	21.4	1187	0.000972	1296	1.67	1.39E+09
8	1.86	21.8	1136	0.000963	1229	2.10	1.61E+09
10	2.23	22.2	1081	0.000955	1159	2.50	1.85E+09
15	3.14	23	1053	0.000937	1109	3.47	2.05E+09
20	4.02	24	1019	0.000916	1049	4.38	2.31E+09
25	4.87	24.7	981	0.000901	993	5.25	2.58E+09
30	5.68	25.5	946	0.000885	941	6.07	2.87E+09
40	7.28	26.8	924	0.000859	891	7.62	3.17E+09
50	8.82	28	900	0.000835	845	9.09	3.48E+09
60	10.33	29.2	884	0.000813	807	10.49	3.76E+09
70	11.82	30.2	871	0.000794	777	11.84	4.00E+09
80	13.29	31	863	0.00078	756	13.14	4.18E+09
90	14.74	31.8	860	0.000765	739	14.41	4.33E+09

Membrane resistance: 2.50E+09 1/m

TANGENTIAL File: CT41623T

Outer radius:	0.01	m	Flow rate:	16.0	l/m
Inner radius:	0.006	m	Inlet pressure:	1.59	Bar
Active length:	0.27	m	Outlet pressure:	0.21	Bar
Hydraulic dx4	0.008	m	Fluid density:	1000	kg/m^3
Solids conc:	4	% wt	Viscosity (25'C):	0.0009	Pa.s
Membrane ar	0.01018	m^2	Bulk velocity:	1.33	m/s
Flow area:	0.0002	m^2	Re:	11922	

Base press. (in,filt,out):	1.47	0.75	0.11	Bar	
Pressure (by inlet,outlet	0.86		0.85	Bar	
Average TMP	0.86	Bar	85640	Pa	

Time (min)	Cum' filtrate (l)	Temp ('C)	Flux raw data (lmh)	Viscosity (Pa.s)	Flux corrected (lmh)	Cum've filtrate (l)	Deposit res'ce (1/m)
0	0.00	20.5	1931	0.000993	2154	0.00	-1.7E-07
2	0.66	20.7	1658	0.000988	1841	0.73	4.55E+08
4	1.13	21.2	1328	0.000977	1457	1.29	1.28E+09
6	1.56	21.6	1245	0.000968	1354	1.77	1.58E+09
8	1.97	22	1199	0.000959	1292	2.22	1.79E+09
10	2.37	22.5	1156	0.000948	1232	2.64	2.01E+09
15	3.34	23.5	1122	0.000926	1168	3.66	2.26E+09
20	4.27	24.5	1082	0.000905	1101	4.62	2.57E+09
25	5.18	25.2	1055	0.000891	1056	5.54	2.79E+09
30	6.06	26.1	1028	0.000873	1008	6.41	3.05E+09
40	7.79	27.5	1012	0.000845	960	8.08	3.33E+09
50	9.49	28.8	995	0.00082	917	9.68	3.62E+09
60	11.17	30	984	0.000798	882	11.20	3.87E+09
70	12.83	31	976	0.00078	855	12.68	4.07E+09
80	14.48	32	970	0.000762	830	14.10	4.28E+09
90	16.12	32.8	967	0.000748	812	15.50	4.43E+09

Membrane resistance: 2.68E+09 1/m

TANGENTIAL File: CT41625U

Outer radius:	0.01	m	Flow rate:	16.0	l/m
Inner radius:	0.006	m	Inlet pressure:	1.72	Bar
Active length:	0.27	m	Outlet pressure:	0.34	Bar
Hydraulic dx4	0.008	m	Fluid density:	1000	kg/m^3
Solids conc:	4	% wt	Viscosity (25'C):	0.0009	Pa.s
Membrane ar	0.01018	m^2	Bulk velocity:	1.33	m/s
Flow area:	0.0002	m^2	Re:	11922	

Base press. (in,filt,out):	1.47	0.75	0.11	Bar
Pressure (by inlet,outlet	1.00		0.99	Bar
Average TMP	0.99	Bar	99433	Pa

Time (min)	Cum' filtrate (l)	Temp ('C)	Flux raw data (lmh)	Viscosity (Pa.s)	Flux corrected (lmh)	Cum've filtrate (l)	Deposit res'ce (1/m)
0	0.00	27.1	2095	0.000853	2007	0.00	1.94E-07
2	0.71	27.4	1791	0.000847	1704	0.68	5.94E+08
4	1.22	27.7	1430	0.000841	1352	1.20	1.62E+09
6	1.68	27.9	1337	0.000837	1258	1.64	1.99E+09
8	2.12	28.2	1285	0.000831	1201	2.06	2.24E+09
10	2.55	28.5	1241	0.000826	1151	2.46	2.48E+09
15	3.60	29	1205	0.000816	1105	3.42	2.73E+09
20	4.60	29.8	1165	0.000801	1049	4.33	3.05E+09
25	5.57	30	1136	0.000798	1018	5.21	3.24E+09
30	6.53	30.6	1104	0.000787	976	6.05	3.53E+09
40	8.38	31.4	1082	0.000772	939	7.68	3.80E+09
50	10.20	32.2	1056	0.000758	900	9.24	4.11E+09
60	11.97	32.8	1038	0.000748	872	10.74	4.35E+09
70	13.72	33.4	1021	0.000738	847	12.20	4.58E+09
80	15.43	33.9	1006	0.000729	824	13.61	4.79E+09
90	17.13	34.4	1002	0.000721	811	15.00	4.92E+09

Membrane resistance: 3.34E+09 1/m

TANGENTIAL File: CT41828O

Outer radius:	0.01	m	Flow rate:	18.0	l/m
Inner radius:	0.006	m	Inlet pressure:	1.90	Bar
Active length:	0.27	m	Outlet pressure:	0.13	Bar
Hydraulic dx4	0.008	m	Fluid density:	1000	kg/m^3
Solids conc:	4	% wt	Viscosity (25'C):	0.0009	Pa.s
Membrane ar	0.01018	m^2	Bulk velocity:	1.49	m/s
Flow area:	0.0002	m^2	Re:	13412	

Base press. (in,filt,out):	1.80	0.91	0.13	Bar
Pressure (by inlet,outlet	1.01		0.91	Bar
Average TMP	0.96	Bar	96277	Pa

Time (min)	Cum' filtrate (l)	Temp ('C)	Flux raw data (lmh)	Viscosity (Pa.s)	Flux corrected (lmh)	Cum've filtrate (l)	Deposit res'ce (1/m)
0	0.00	23	2293	0.000937	2415	0.00	8.52E-08
2	0.78	23.3	1987	0.000931	2078	0.82	4.36E+08
4	1.35	23.7	1612	0.000922	1671	1.46	1.20E+09
6	1.87	24	1504	0.000916	1548	2.00	1.51E+09
8	2.37	24.3	1440	0.00091	1471	2.51	1.72E+09
10	2.85	24.6	1372	0.000903	1392	3.00	1.97E+09
15	4.00	25.3	1315	0.000889	1313	4.15	2.25E+09
20	5.08	26	1270	0.000875	1248	5.23	2.51E+09
25	6.15	26.6	1251	0.000863	1213	6.28	2.66E+09
30	7.20	27.2	1225	0.000851	1171	7.29	2.85E+09
40	9.27	28.3	1195	0.00083	1113	9.23	3.14E+09
50	11.26	29.4	1165	0.000809	1059	11.07	3.44E+09
60	13.22	30.2	1152	0.000794	1028	12.84	3.63E+09
70	15.17	30.8	1139	0.000783	1002	14.56	3.79E+09
80	17.09	31.7	1128	0.000767	972	16.24	3.99E+09
90	18.99	32.3	1123	0.000757	955	17.87	4.11E+09

Membrane resistance: 2.69E+09 1/m

TANGENTIAL File: CT41829V

Outer radius:	0.01	m	Flow rate:	18.0	l/m
Inner radius:	0.006	m	Inlet pressure:	2	Bar
Active length:	0.27	m	Outlet pressure:	0.21	Bar
Hydraulic dx4	0.008	m	Fluid density:	1000	kg/m^3
Solids conc:	4	% wt	Viscosity (25'C):	0.0009	Pa.s
Membrane ar	0.01018	m^2	Bulk velocity:	1.49	m/s
Flow area:	0.0002	m^2	Re:	13412	
Base press. (in,filt,out):	1.80	0.91	0.13	Bar	
Pressure (by inlet,outlet	1.11		0.99	Bar	
Average TMP	1.05	Bar	105243	Pa	

Time (min)	Cum' filtrate (l)	Temp ('C)	Flux raw data (lmh)	Viscosity (Pa.s)	Flux corrected (lmh)	Cum've filtrate (l)	Deposit res'ce (1/m)
0	0.00	18	1958	0.001052	2314	0.00	-2.0E-07
2	0.66	18.3	1632	0.001044	1915	0.79	6.38E+08
4	1.11	19.2	1252	0.001023	1439	1.35	1.86E+09
6	1.51	19.5	1169	0.001016	1334	1.82	2.25E+09
8	1.90	20.5	1127	0.000993	1258	2.26	2.57E+09
10	2.28	21	1088	0.000981	1200	2.68	2.85E+09
15	3.19	21.3	1065	0.000975	1166	3.68	3.02E+09
20	4.09	22.4	1042	0.00095	1113	4.65	3.31E+09
25	4.96	23	1030	0.000937	1085	5.58	3.47E+09
30	5.83	24	1025	0.000916	1055	6.49	3.66E+09
40	7.57	25.4	1026	0.000887	1022	8.25	3.88E+09
50	9.31	26.8	1030	0.000859	993	9.96	4.08E+09
60	11.06	27.8	1034	0.000839	974	11.63	4.21E+09
70	12.82	28.8	1036	0.00082	955	13.27	4.36E+09
80	14.58	29.7	1036	0.000803	935	14.87	4.52E+09
90	16.34	30.5	1036	0.000789	918	16.44	4.66E+09

Membrane resistance: 3.07E+09 1/m

TANGENTIAL File: CT41830W

Outer radius:	0.01	m	Flow rate:	18.0	l/m
Inner radius:	0.006	m	Inlet pressure:	2.07	Bar
Active length:	0.27	m	Outlet pressure:	0.28	Bar
Hydraulic dx4	0.008	m	Fluid density:	1000	kg/m^3
Solids conc:	4	% wt	Viscosity (25'C):	0.0009	Pa.s
Membrane ar	0.01018	m^2	Bulk velocity:	1.49	m/s
Flow area:	0.0002	m^2	Re:	13412	
Base press. (in,filt,out):	1.80	0.91	0.13		
Pressure (by inlet,outlet	1.18		1.06		
Average TMP	1.12	Bar	112139	Pa	

Time (min)	Cum' filtrate (l)	Temp ('C)	Flux raw data (lmh)	Viscosity (Pa.s)	Flux corrected (lmh)	Cum've filtrate (l)	Deposit res'ce (1/m)
0	0.00	19.1	2122	0.001025	2445	0.00	-1.2E-07
2	0.72	19.5	1765	0.001016	2014	0.83	6.61E+08
4	1.20	20	1356	0.001004	1530	1.43	1.85E+09
6	1.64	20.3	1270	0.000997	1424	1.93	2.22E+09
8	2.06	20.7	1218	0.000988	1353	2.40	2.50E+09
10	2.47	21.1	1191	0.000979	1310	2.85	2.68E+09
15	3.47	22	1181	0.000959	1273	3.95	2.85E+09
20	4.47	23	1167	0.000937	1229	5.01	3.06E+09
25	5.45	23.7	1153	0.000922	1194	6.04	3.24E+09
30	6.43	24.5	1138	0.000905	1158	7.04	3.44E+09
40	8.35	25.9	1132	0.000877	1115	8.96	3.69E+09
50	10.27	27.2	1128	0.000851	1078	10.82	3.92E+09
60	12.18	28.5	1125	0.000826	1043	12.62	4.15E+09

Membrane resistance: 3.09E+09 1/m

TANGENTIAL File: CT41830X

Outer radius:	0.01	m	Flow rate:	18.0	l/m
Inner radius:	0.006	m	Inlet pressure:	2.07	Bar
Active length:	0.27	m	Outlet pressure:	0.34	Bar
Hydraulic dx4	0.008	m	Fluid density:	1000	kg/m^3
Solids conc:	4	% wt	Viscosity (25'C):	0.0009	Pa.s
Membrane ar	0.01018	m^2	Bulk velocity:	1.49	m/s
Flow area:	0.0002	m^2	Re:	13412	
Base press. (in,filt,out):	1.80	0.91	0.13	Bar	
Pressure (by inlet,outlet	1.18		1.13	Bar	
Average TMP	1.16	Bar	115588	Pa	

Time (min)	Cum' filtrate (l)	Temp ('C)	Flux raw data (lmh)	Viscosity (Pa.s)	Flux corrected (lmh)	Cum've filtrate (l)	Deposit res'ce (1/m)
0	0.00	27.3	2164	0.000849	2064	0.00	1.79E-07
2	0.73	27.5	1810	0.000845	1718	0.70	7.60E+08
4	1.23	27.7	1393	0.000841	1317	1.22	2.14E+09
6	1.68	27.9	1306	0.000837	1228	1.65	2.57E+09
8	2.11	28.1	1262	0.000833	1182	2.06	2.82E+09
10	2.54	28.4	1214	0.000828	1129	2.45	3.12E+09
15	3.56	28.7	1174	0.000822	1084	3.39	3.41E+09
20	4.53	29	1139	0.000816	1044	4.29	3.69E+09
25	5.49	29.8	1127	0.000801	1015	5.16	3.90E+09
30	6.44	30.3	1110	0.000792	988	6.01	4.11E+09
40	8.31	31	1097	0.00078	961	7.67	4.33E+09
50	10.16	31.7	1085	0.000767	935	9.27	4.56E+09
60	12.00	32.2	1077	0.000758	917	10.85	4.72E+09
70	13.82	32.7	1067	0.00075	899	12.39	4.89E+09
80	15.62	33.1	1062	0.000743	886	13.90	5.02E+09
90	17.42	33.5	1063	0.000736	879	15.40	5.09E+09

Membrane resistance: 3.78E+09 1/m

NORMAL File: FN11414C

Outer radius:	0.01	m	Flow rate:	14.0	l/m
Inner radius:	0.006	m	Inlet pressure:	0.97	Bar
Active length:	0.27	m	Outlet pressure:	0.12	Bar
Hydraulic dx4	0.008	m	Fluid density:	1000	kg/m^3
Solids conc:	1.6	% wt	Viscosity (25'C):	0.0009	Pa.s
Membrane ar	0.01018	m^2	Bulk velocity:	1.16	m/s
Flow area:	0.0002	m^2	Re:	10440	

Base press. (in,filt,out):	0.72	0.43	0.11	Bar
Pressure (by inlet,outlet	0.68		0.44	Bar
Average TMP	0.56	Bar	56041	Pa

Time (min)	Cum' filtrate (l)	Temp ('C)	Flux raw data (lmh)	Viscosity (Pa.s)	Flux corrected (lmh)	Cum've filtrate (l)	Deposit res'ce (1/m)
0	0.00	27.2	1641	0.000851	1569	0.00	-2.2E-07
2	0.56	27	1311	0.000855	1259	0.53	5.93E+08
4	0.89	27	965	0.000855	927	0.90	1.67E+09
6	1.21	26.9	943	0.000857	908	1.21	1.75E+09
8	1.53	26.9	925	0.000857	891	1.52	1.83E+09
10	1.84	26.8	862	0.000859	832	1.81	2.13E+09
15	2.55	26.7	814	0.000861	787	2.50	2.39E+09
20	3.22	26.7	765	0.000861	740	3.15	2.70E+09
25	3.85	26.6	725	0.000863	703	3.76	2.97E+09
30	4.45	26.5	693	0.000865	673	4.34	3.21E+09
40	5.61	26.5	676	0.000865	657	5.47	3.34E+09
50	6.74	26.3	657	0.000869	641	6.57	3.49E+09
60	7.84	26.1	640	0.000873	627	7.65	3.61E+09
70	8.92	26	628	0.000875	618	8.70	3.71E+09
80	9.97	25.7	610	0.000881	603	9.74	3.85E+09
90	10.98	25.5	595	0.000885	592	10.75	3.97E+09

Membrane resistance: 2.41E+09 1/m

NORMAL File: FN11413J

Outer radius:	0.01	m	Flow rate:	14.0	l/m
Inner radius:	0.006	m	Inlet pressure:	0.90	Bar
Active length:	0.27	m	Outlet pressure:	0.12	Bar
Hydraulic dx4	0.008	m	Fluid density:	1000	kg/m^3
Solids conc:	1.6	% wt	Viscosity (25'C):	0.0009	Pa.s
Membrane ar	0.01018	m^2	Bulk velocity:	1.16	m/s
Flow area:	0.0002	m^2	Re:	10432	

Base press. (in,filt,out):	0.72	0.43	0.11	Bar
Pressure (by inlet,outlet	0.61		0.44	Bar
Average TMP	0.52	Bar	52593	Pa

Time (min)	Cum' filtrate (l)	Temp ('C)	Flux raw data (lmh)	Viscosity (Pa.s)	Flux corrected (lmh)	Cum've filtrate (l)	Deposit res'ce (1/m)
0	0.00	22	1886	0.000959	2032	0.00	-2.6E-08
2	0.64	22.5	1503	0.000948	1601	0.69	4.70E+08
4	1.02	23	1061	0.000937	1117	1.15	1.43E+09
6	1.36	23.5	974	0.000926	1014	1.51	1.75E+09
8	1.68	24	884	0.000916	910	1.84	2.15E+09
10	1.96	24.5	792	0.000905	805	2.13	2.66E+09
15	2.62	25	753	0.000895	757	2.79	2.94E+09
20	3.24	26	714	0.000875	702	3.41	3.31E+09
25	3.83	27	690	0.000855	662	3.99	3.61E+09
30	4.41	28	675	0.000835	634	4.54	3.85E+09
40	5.55	27.8	670	0.000839	632	5.61	3.87E+09
50	6.68	27	653	0.000855	627	6.68	3.91E+09
60	7.77	26.2	636	0.000871	622	7.74	3.95E+09
70	8.84	28.1	632	0.000833	592	8.77	4.25E+09
80	9.91	27.5	622	0.000845	590	9.77	4.26E+09
90	10.95	27	613	0.000855	589	10.77	4.28E+09

Membrane resistance: 1.74E+09 1/m

NORMAL File: FN11416K

Outer radius:	0.01	m	Flow rate:	14.0	l/m
Inner radius:	0.006	m	Inlet pressure:	1.07	Bar
Active length:	0.27	m	Outlet pressure:	0.21	Bar
Hydraulic dx4	0.008	m	Fluid density:	1000	kg/m^3
Solids conc:	1.6	% wt	Viscosity (25'C):	0.0009	Pa.s
Membrane ar	0.01018	m^2	Bulk velocity:	1.16	m/s
Flow area:	0.0002	m^2	Re:	10432	

Base press. (in,filt,out):	0.72	0.43	0.11	Bar
Pressure (by inlet,outlet	0.66		0.53	Bar
Average TMP	0.66	Bar	65696	Pa

Time (min)	Cum' filtrate (l)	Temp ('C)	Flux raw data (lmh)	Viscosity (Pa.s)	Flux corrected (lmh)	Cum've filtrate (l)	Deposit res'ce (1/m)
0	0.00	27	2356	0.000855	2263	0.00	4.62E-08
2	0.80	27.4	1877	0.000847	1786	0.77	5.22E+08
4	1.27	27.8	1259	0.000839	1187	1.27	1.77E+09
6	1.65	27.7	1003	0.000841	948	1.63	2.72E+09
8	1.95	27.7	879	0.000841	831	1.94	3.37E+09
10	2.25	27.6	865	0.000843	819	2.22	3.45E+09
15	2.98	27.4	828	0.000847	788	2.90	3.66E+09
20	3.65	27	781	0.000855	750	3.55	3.95E+09
25	4.31	26.9	756	0.000857	728	4.18	4.13E+09
30	4.94	26.8	727	0.000859	701	4.78	4.36E+09
40	6.15	26.5	706	0.000865	686	5.96	4.50E+09
50	7.33	26	683	0.000875	671	7.11	4.64E+09
60	8.47	25.7	663	0.000881	656	8.24	4.79E+09
70	9.58	25.5	647	0.000885	643	9.34	4.93E+09
80	10.67	25.2	636	0.000891	637	10.42	5.00E+09
90	11.74	25	631	0.000895	634	11.50	5.03E+09

Membrane resistance: 1.96E+09 1/m

NORMAL File: FN11418L

Outer radius:	0.01	m	Flow rate:	14.0	l/m
Inner radius:	0.006	m	Inlet pressure:	1.21	Bar
Active length:	0.27	m	Outlet pressure:	0.34	Bar
Hydraulic dx4	0.008	m	Fluid density:	1000	kg/m^3
Solids conc:	1.6	% wt	Viscosity (25'C):	0.0009	Pa.s
Membrane ar	0.01018	m^2	Bulk velocity:	1.16	m/s
Flow area:	0.0002	m^2	Re:	10440	

Base press. (in,filt,out):	0.72	0.43	0.11	Bar
Pressure (by inlet,outlet	0.93		0.66	Bar
Average TMP	0.79	Bar	79489	Pa

Time (min)	Cum' filtrate (l)	Temp ('C)	Flux raw data (lmh)	Viscosity (Pa.s)	Flux corrected (lmh)	Cum've filtrate (l)	Deposit res'ce (1/m)
0	0.00	27.7	2640	0.000841	2495	0.00	-2.1E-07
2	0.90	27.5	2036	0.000845	1933	0.85	6.24E+08
4	1.38	27.4	1320	0.000847	1256	1.39	2.12E+09
6	1.79	27.3	1148	0.000849	1095	1.79	2.75E+09
8	2.16	27.2	1061	0.000851	1015	2.14	3.13E+09
10	2.51	27.1	981	0.000853	940	2.48	3.55E+09
15	3.33	26.7	928	0.000861	897	3.26	3.83E+09
20	4.09	26.6	878	0.000863	851	4.00	4.15E+09
25	4.82	26.5	849	0.000865	825	4.71	4.35E+09
30	5.53	26.3	814	0.000869	795	5.39	4.60E+09
40	6.89	26	793	0.000875	779	6.73	4.73E+09
50	8.21	25.6	762	0.000883	756	8.03	4.94E+09
60	9.47	25.3	737	0.000889	736	9.30	5.14E+09
70	10.71	25.1	722	0.000893	724	10.53	5.25E+09
80	11.92	24.9	705	0.000897	710	11.75	5.40E+09
90	13.10	24.7	696	0.000901	705	12.95	5.45E+09

Membrane resistance: 2.15E+09 1/m

NORMAL File: FN11720B

Outer radius:	0.01	m	Flow rate:	17.0	l/m
Inner radius:	0.006	m	Inlet pressure:	1.38	Bar
Active length:	0.27	m	Outlet pressure:	0.14	Bar
Hydraulic dx4	0.008	m	Fluid density:	1000	kg/m^3
Solids conc:	1.6	% wt	Viscosity (25'C):	0.0009	Pa.s
Membrane ar	0.01018	m^2	Bulk velocity:	1.41	m/s
Flow area:	0.0002	m^2	Re:	12693	

Base press. (in,filt,out):	1.07	0.63	0.15	Bar
Pressure (by inlet,outlet	0.94		0.62	Bar
Average TMP	0.78	Bar	78091	Pa

Time (min)	Cum' filtrate (l)	Temp ('C)	Flux raw data (lmh)	Viscosity (Pa.s)	Flux corrected (lmh)	Cum've filtrate (l)	Deposit res'ce (1/m)
0	0.00	27.7	2476	0.000841	2340	0.00	1.19E-07
2	0.84	27.7	1979	0.000841	1870	0.79	5.65E+08
4	1.34	27.7	1390	0.000841	1314	1.33	1.76E+09
6	1.78	27.7	1215	0.000841	1149	1.75	2.33E+09
8	2.17	27.6	1111	0.000843	1052	2.13	2.75E+09
10	2.54	27.6	997	0.000843	945	2.46	3.32E+09
15	3.35	27.2	931	0.000851	890	3.24	3.66E+09
20	4.12	27	896	0.000855	861	3.98	3.87E+09
25	4.87	26.7	881	0.000861	852	4.71	3.93E+09
30	5.61	26.5	853	0.000865	829	5.42	4.10E+09
40	7.04	26	818	0.000875	804	6.81	4.30E+09
50	8.39	25.7	779	0.000881	771	8.14	4.58E+09
60	9.69	25.5	759	0.000885	754	9.44	4.73E+09
70	10.96	25.2	736	0.000891	737	10.70	4.90E+09
80	12.18	26.8	696	0.000859	672	11.90	5.59E+09
90	13.32	26.5	672	0.000865	653	13.02	5.81E+09

Membrane resistance: 2.25E+09 1/m

NORMAL File: FN11719G

Outer radius:	0.01	m	Flow rate:	17.0	l/m
Inner radius:	0.006	m	Inlet pressure:	1.31	Bar
Active length:	0.27	m	Outlet pressure:	0.14	Bar
Hydraulic dx4	0.008	m	Fluid density:	1000	kg/m^3
Solids conc:	1.6	% wt	Viscosity (25'C):	0.0009	Pa.s
Membrane ar	0.01018	m^2	Bulk velocity:	1.41	m/s
Flow area:	0.0002	m^2	Re:	12693	

Base press. (in,filt,out):	1.07	0.63	0.15	Bar
Pressure (by inlet,outlet	0.87		0.62	Bar
Average TMP	0.75	Bar	74643	Pa

Time (min)	Cum' filtrate (l)	Temp ('C)	Flux raw data (lmh)	Viscosity (Pa.s)	Flux corrected (lmh)	Cum've filtrate (l)	Deposit res'ce (1/m)
0	0.00	27.8	2531	0.000839	2387	0.00	-3.4E-08
2	0.86	27.8	1964	0.000839	1851	0.81	6.10E+08
4	1.33	27.6	1299	0.000843	1231	1.33	1.98E+09
6	1.74	27.6	1155	0.000843	1094	1.73	2.49E+09
8	2.12	27.6	1081	0.000843	1024	2.09	2.81E+09
10	2.47	27.5	1014	0.000845	963	2.42	3.12E+09
15	3.32	27.3	971	0.000849	926	3.22	3.32E+09
20	4.12	27.2	931	0.000851	890	3.99	3.54E+09
25	4.90	27	901	0.000855	866	4.74	3.71E+09
30	5.65	26.8	866	0.000859	836	5.46	3.91E+09
40	7.11	26.6	839	0.000863	814	6.86	4.08E+09
50	8.50	26.4	810	0.000867	789	8.22	4.27E+09
60	9.85	26.2	787	0.000871	770	9.54	4.43E+09
70	11.17	26	766	0.000875	753	10.83	4.57E+09
80	12.45	25.8	748	0.000879	738	12.10	4.71E+09
90	13.70	25.6	737	0.000883	731	13.34	4.78E+09

Membrane resistance: 2.11E+09 1/m

NORMAL File: FN11721H

Outer radius:	0.01	m	Flow rate:	17.0	l/m
Inner radius:	0.006	m	Inlet pressure:	1.45	Bar
Active length:	0.27	m	Outlet pressure:	0.21	Bar
Hydraulic dx4	0.008	m	Fluid density:	1000	kg/m^3
Solids conc:	1.6	% wt	Viscosity (25'C):	0.0009	Pa.s
Membrane ar	0.01018	m^2	Bulk velocity:	1.41	m/s
Flow area:	0.0002	m^2	Re:	12693	

Base press. (in,filt,out):	1.07	0.63	0.15	Bar
Pressure (by inlet,outlet	1.01		0.69	Bar
Average TMP	0.85	Bar	84643	Pa

Time (min)	Cum' filtrate (l)	Temp ('C)	Flux raw data (lmh)	Viscosity (Pa.s)	Flux corrected (lmh)	Cum've filtrate (l)	Deposit res'ce (1/m)
0	0.00	28.4	2763	0.000828	2570	0.00	-4.4E-08
2	0.94	28.2	2134	0.000831	1994	0.87	6.42E+08
4	1.45	28.1	1412	0.000833	1322	1.43	2.10E+09
6	1.90	28	1268	0.000835	1190	1.86	2.57E+09
8	2.31	27.9	1184	0.000837	1114	2.25	2.90E+09
10	2.70	27.8	1104	0.000839	1041	2.62	3.26E+09
15	3.62	27.6	1056	0.000843	1000	3.48	3.48E+09
20	4.49	27.4	1008	0.000847	960	4.31	3.73E+09
25	5.33	27.3	969	0.000849	925	5.11	3.95E+09
30	6.13	27.2	927	0.000851	886	5.88	4.22E+09
40	7.69	26.8	902	0.000859	871	7.37	4.33E+09
50	9.20	26.6	874	0.000863	847	8.83	4.52E+09
60	10.65	26.3	843	0.000869	823	10.24	4.71E+09
70	12.06	26	814	0.000875	800	11.62	4.91E+09
80	13.42	25.7	790	0.000881	781	12.96	5.08E+09
90	14.74	25.4	778	0.000887	776	14.28	5.14E+09

Membrane resistance: 2.22E+09 1/m

NORMAL File: FN11723I

Outer radius:	0.01	m	Flow rate:	17.0	l/m
Inner radius:	0.006	m	Inlet pressure:	1.59	Bar
Active length:	0.27	m	Outlet pressure:	0.34	Bar
Hydraulic dx4	0.008	m	Fluid density:	1000	kg/m^3
Solids conc:	1.6	% wt	Viscosity (25'C):	0.0009	Pa.s
Membrane ar	0.01018	m^2	Bulk velocity:	1.41	m/s
Flow area:	0.0002	m^2	Re:	12693	

Base press. (in,filt,out):	1.07	0.63	0.15	Bar
Pressure (by inlet,outlet	1.15		0.82	Bar
Average TMP	0.98	Bar	98436	Pa

Time (min)	Cum' filtrate (l)	Temp ('C)	Flux raw data (lmh)	Viscosity (Pa.s)	Flux corrected (lmh)	Cum've filtrate (l)	Deposit res'ce (1/m)
0	0.00	27.6	2888	0.000843	2735	0.00	-1.2E-07
2	0.98	27.5	2258	0.000845	2143	0.93	6.70E+08
4	1.53	27.4	1514	0.000847	1441	1.54	2.18E+09
6	2.01	27.2	1348	0.000851	1289	2.00	2.72E+09
8	2.45	27	1259	0.000855	1209	2.42	3.06E+09
10	2.86	26.9	1172	0.000857	1128	2.82	3.46E+09
15	3.84	26.5	1119	0.000865	1087	3.76	3.68E+09
20	4.76	26.2	1064	0.000871	1041	4.66	3.95E+09
25	5.64	26	1026	0.000875	1008	5.53	4.16E+09
30	6.50	25.7	982	0.000881	972	6.37	4.40E+09
40	8.14	25.2	960	0.000891	961	8.01	4.48E+09
50	9.76	27.5	947	0.000845	899	9.59	4.95E+09
60	11.36	26.9	935	0.000857	900	11.11	4.95E+09
70	12.93	26.4	899	0.000867	876	12.62	5.15E+09
80	14.41	25.8	860	0.000879	849	14.08	5.39E+09
90	15.84	25.5	847	0.000885	842	15.52	5.45E+09

Membrane resistance: 2.43E+09 1/m

NORMAL File: FN11824F

Outer radius:	0.01	m	Flow rate:	17.5	l/m
Inner radius:	0.006	m	Inlet pressure:	1.62	Bar
Active length:	0.27	m	Outlet pressure:	0.28	Bar
Hydraulic dx4	0.008	m	Fluid density:	1000	kg/m^3
Solids conc:	1.6	% wt	Viscosity (25'C):	0.0009	Pa.s
Membrane ar	0.01018	m^2	Bulk velocity:	1.45	m/s
Flow area:	0.0002	m^2	Re:	13069	

Base press. (in,filt,out):	1.13	0.66	0.15	Bar
Pressure (by inlet,outlet	1.15		0.78	Bar
Average TMP	0.97	Bar	96667	Pa

Time (min)	Cum' filtrate (l)	Temp ('C)	Flux raw data (lmh)	Viscosity (Pa.s)	Flux corrected (lmh)	Cum've filtrate (l)	Deposit res'ce (1/m)
0	0.00	27.6	2872	0.000843	2721	0.00	1.97E-07
2	0.97	28	2281	0.000835	2141	0.92	6.49E+08
4	1.55	28	1547	0.000835	1452	1.53	2.09E+09
6	2.02	27.9	1340	0.000837	1260	1.99	2.78E+09
8	2.46	27.8	1271	0.000839	1198	2.41	3.04E+09
10	2.89	27.7	1189	0.000841	1124	2.80	3.41E+09
15	3.87	27.5	1130	0.000845	1073	3.74	3.68E+09
20	4.80	27.4	1081	0.000847	1029	4.63	3.94E+09
25	5.70	27.3	1043	0.000849	995	5.49	4.15E+09
30	6.57	27.1	1000	0.000853	958	6.31	4.41E+09
40	8.25	26.8	969	0.000859	935	7.92	4.58E+09
50	9.86	26.5	926	0.000865	900	9.47	4.85E+09
60	11.39	26.2	891	0.000871	872	10.98	5.08E+09
70	12.88	25.9	871	0.000877	858	12.44	5.20E+09
80	14.35	25.7	853	0.000881	844	13.89	5.33E+09
90	15.78	25.5	843	0.000885	838	15.31	5.38E+09

Membrane resistance: 2.40E+09 1/m

NORMAL File: FN11824E

Outer radius:	0.01	m	Flow rate:	17.7	l/m
Inner radius:	0.006	m	Inlet pressure:	1.62	Bar
Active length:	0.27	m	Outlet pressure:	0.21	Bar
Hydraulic dx4	0.008	m	Fluid density:	1000	kg/m^3
Solids conc:	1.6	% wt	Viscosity (25'C):	0.0009	Pa.s
Membrane ar	0.01018	m^2	Bulk velocity:	1.47	m/s
Flow area:	0.0002	m^2	Re:	13219	

Base press. (in,filt,out):	1.16	0.68	0.15	Bar
Pressure (by inlet,outlet	1.14		0.73	Bar
Average TMP	0.93	Bar	93198	Pa

Time (min)	Cum' filtrate (l)	Temp ('C)	Flux raw data (lmh)	Viscosity (Pa.s)	Flux corrected (lmh)	Cum've filtrate (l)	Deposit res'ce (1/m)
0	0.00	27.8	2870	0.000839	2706	0.00	-1.7E-08
2	0.97	27.7	2256	0.000841	2132	0.92	6.24E+08
4	1.53	27.6	1521	0.000843	1440	1.52	2.04E+09
6	2.01	27.5	1357	0.000845	1288	1.99	2.55E+09
8	2.45	27.4	1260	0.000847	1199	2.41	2.92E+09
10	2.86	27.3	1186	0.000849	1131	2.80	3.23E+09
15	3.86	27.3	1062	0.000849	1013	3.71	3.88E+09
20	4.66	27.1	997	0.000853	955	4.55	4.25E+09
25	5.55	26.9	1026	0.000857	988	5.37	4.04E+09
30	6.40	26.7	985	0.000861	952	6.20	4.27E+09
40	8.06	26.5	954	0.000865	927	7.79	4.45E+09
50	9.64	26.1	915	0.000873	897	9.34	4.68E+09
60	11.16	25.9	884	0.000877	871	10.84	4.89E+09
70	12.64	25.7	857	0.000881	848	12.29	5.09E+09
80	14.07	25.5	834	0.000885	829	13.72	5.25E+09
90	15.47	25.3	825	0.000889	824	15.12	5.30E+09

Membrane resistance: 2.32E+09 1/m

NORMAL File: FN11822D

Outer radius:	0.01	m	Flow rate:	18.0	l/m
Inner radius:	0.006	m	Inlet pressure:	1.52	Bar
Active length:	0.27	m	Outlet pressure:	0.16	Bar
Hydraulic dx4	0.008	m	Fluid density:	1000	kg/m^3
Solids conc:	1.6	% wt	Viscosity (25'C):	0.0009	Pa.s
Membrane ar	0.01018	m^2	Bulk velocity:	1.50	m/s
Flow area:	0.0002	m^2	Re:	13444	
Base press. (in,filt,out):	1.20	0.70	0.16	Bar	
Pressure (by inlet,outlet	1.01		0.70	Bar	
Average TMP	0.86	Bar	85575	Pa	

Time (min)	Cum' filtrate (l)	Temp ('C)	Flux raw data (lmh)	Viscosity (Pa.s)	Flux corrected (lmh)	Cum've filtrate (l)	Deposit res'ce (1/m)
0	0.00	22.3	2470	0.000952	2643	0.00	-5.6E-08
2	0.84	23.1	1946	0.000935	2044	0.90	6.40E+08
4	1.32	23.6	1334	0.000924	1386	1.48	1.98E+09
6	1.74	24	1213	0.000916	1248	1.93	2.44E+09
8	2.14	24.6	1162	0.000903	1180	2.34	2.71E+09
10	2.53	25.1	1098	0.000893	1101	2.72	3.06E+09
15	3.45	26.2	1062	0.000871	1039	3.63	3.37E+09
20	4.33	27.3	1030	0.000849	983	4.49	3.69E+09
25	5.20	27.5	997	0.000845	946	5.31	3.92E+09
30	6.02	27.1	951	0.000853	912	6.10	4.15E+09
40	7.62	26.6	916	0.000863	888	7.62	4.32E+09
50	9.13	26.1	880	0.000873	863	9.11	4.50E+09
60	10.60	25.6	835	0.000883	828	10.54	4.78E+09
70	11.96	25.1	809	0.000893	812	11.93	4.93E+09
80	13.35	26.7	810	0.000861	783	13.28	5.18E+09
90	14.71	26.3	805	0.000869	786	14.62	5.16E+09

Membrane resistance: 2.18E+09 1/m

NORMAL File: FN12021A

Outer radius:	0.01	m	Flow rate:	20.0	l/m
Inner radius:	0.006	m	Inlet pressure:	1.48	Bar
Active length:	0.27	m	Outlet pressure:	0.18	Bar
Hydraulic dx4	0.008	m	Fluid density:	1000	kg/m^3
Solids conc:	1.6	% wt	Viscosity (25'C):	0.0009	Pa.s
Membrane ar	0.01018	m^2	Bulk velocity:	1.65	m/s
Flow area:	0.0002	m^2	Re:	14871	
Base press. (in,filt,out):	1.47	0.84	0.18	Bar	
Pressure (by inlet,outlet	0.84		0.84	Bar	
Average TMP	0.84	Bar	84197	Pa	

Time (min)	Cum' filtrate (l)	Temp ('C)	Flux raw data (lmh)	Viscosity (Pa.s)	Flux corrected (lmh)	Cum've filtrate (l)	Deposit res'ce (1/m)
0	0.00	24.8	2512	0.000899	2538	0.00	-3.9E-08
2	0.85	25.2	2029	0.000891	2031	0.86	5.59E+08
4	1.38	25.7	1521	0.000881	1505	1.46	1.53E+09
6	1.88	26	1344	0.000875	1321	1.94	2.06E+09
8	2.29	26.5	1175	0.000865	1141	2.36	2.74E+09
10	2.68	27	1146	0.000855	1101	2.74	2.92E+09
15	3.65	26.7	1120	0.000861	1084	3.67	3.00E+09
20	4.58	26.5	1070	0.000865	1039	4.57	3.23E+09
25	5.46	26.4	1022	0.000867	996	5.43	3.46E+09
30	6.32	26.2	974	0.000871	953	6.25	3.72E+09
40	7.94	26	936	0.000875	920	7.84	3.93E+09
50	9.49	25.7	865	0.000881	856	9.35	4.40E+09
60	10.88	25.5	813	0.000885	808	10.76	4.79E+09
70	12.25	25.3	807	0.000889	806	12.13	4.80E+09
80	13.62	25.1	810	0.000893	813	13.50	4.74E+09
90	15.00	26	816	0.000875	802	14.87	4.84E+09

Membrane resistance: 2.24E+09 1/m

TANGENTIAL File: FT11417A

Outer radius:	0.01	m	Flow rate:	14.0	l/m
Inner radius:	0.006	m	Inlet pressure:	1.17	Bar
Active length:	0.27	m	Outlet pressure:	0.09	Bar
Hydraulic dx4	0.008	m	Fluid density:	1000	kg/m^3
Solids conc:	1.7	% wt	Viscosity (25'C):	0.0009	Pa.s
Membrane ar	0.01018	m^2	Bulk velocity:	1.16	m/s
Flow area:	0.0002	m^2	Re:	10440	

Base press. (in,filt,out):	1.17	0.60	0.09	Bar
Pressure (by inlet,outlet	0.60		0.60	Bar
Average TMP	0.60	Bar	60044	Pa

Time (min)	Cum' filtrate (l)	Temp ('C)	Flux raw data (lmh)	Viscosity (Pa.s)	Flux corrected (lmh)	Cum've filtrate (l)	Deposit res'ce (1/m)
0	0.00	25.5	2023	0.000885	2012	0.00	-9.4E-08
2	0.69	25.5	1783	0.000885	1773	0.68	2.71E+08
4	1.21	25.5	1379	0.000885	1371	1.22	9.40E+08
6	1.62	25.5	1189	0.000885	1182	1.65	1.41E+09
8	2.02	25.5	1129	0.000885	1122	2.04	1.60E+09
10	2.39	25.5	1078	0.000885	1072	2.41	1.76E+09
15	3.30	25.5	498	0.000885	495	3.08	6.17E+09
20	3.23	25.5	424	0.000885	421	3.47	7.60E+09
25	4.02	25.5	472	0.000885	469	3.84	6.62E+09
30	4.03	25.5	575	0.000885	571	4.28	5.07E+09
40	5.48	25.5	812	0.000885	808	5.45	3.00E+09
50	6.79	25.3	770	0.000889	769	6.79	3.25E+09
60	8.09	25.1	765	0.000893	768	8.09	3.26E+09
70	9.38	24.9	757	0.000897	763	9.39	3.29E+09
80	10.66	25	738	0.000895	743	10.67	3.44E+09
90	11.89	25	726	0.000895	730	11.92	3.53E+09

Membrane resistance: 2.01E+09 1/m

TANGENTIAL File: FT11417G

Outer radius:	0.01	m	Flow rate:	14.0	l/m
Inner radius:	0.006	m	Inlet pressure:	1.17	Bar
Active length:	0.27	m	Outlet pressure:	0.09	Bar
Hydraulic dx4	0.008	m	Fluid density:	1000	kg/m^3
Solids conc:	1.7	% wt	Viscosity (25'C):	0.0009	Pa.s
Membrane ar	0.01018	m^2	Bulk velocity:	1.16	m/s
Flow area:	0.0002	m^2	Re:	10440	

Base press. (in,filt,out):	1.17	0.60	0.09	Bar
Pressure (by inlet,outlet	0.60		0.60	Bar
Average TMP	0.60	Bar	60044	Pa

Time (min)	Cum' filtrate (l)	Temp ('C)	Flux raw data (lmh)	Viscosity (Pa.s)	Flux corrected (lmh)	Cum've filtrate (l)	Deposit res'ce (1/m)
0	0.00	25	2120	0.000895	2132	0.00	7.46E-08
2	0.72	26.3	1787	0.000869	1744	0.72	4.23E+08
4	1.21	26.3	1372	0.000869	1339	1.25	1.13E+09
6	1.65	26.3	1256	0.000869	1226	1.68	1.40E+09
8	2.06	26.3	1190	0.000869	1162	2.09	1.59E+09
10	2.46	26.3	1103	0.000869	1076	2.47	1.86E+09
15	3.37	26.2	1034	0.000871	1011	3.35	2.11E+09
20	4.21	26.1	960	0.000873	941	4.18	2.40E+09
25	5.00	26	914	0.000875	898	4.96	2.61E+09
30	5.76	25.9	880	0.000877	867	5.71	2.77E+09
40	7.24	25.7	855	0.000881	846	7.16	2.89E+09
50	8.66	25.6	820	0.000883	813	8.57	3.08E+09
60	10.02	25.5	790	0.000885	785	9.93	3.26E+09
70	11.34	25.4	769	0.000887	766	11.24	3.39E+09
80	12.63	25.3	749	0.000889	748	12.53	3.51E+09
90	13.89	25.1	739	0.000893	742	13.79	3.56E+09

Membrane resistance: 1.90E+09 1/m

TANGENTIAL File: FT11418H

Outer radius:	0.01	m	Flow rate:	14.0	l/m
Inner radius:	0.006	m	Inlet pressure:	1.21	Bar
Active length:	0.27	m	Outlet pressure:	0.21	Bar
Hydraulic dx4	0.008	m	Fluid density:	1000	kg/m^3
Solids conc:	1.7	% wt	Viscosity (25'C):	0.0009	Pa.s
Membrane ar	0.01018	m^2	Bulk velocity:	1.16	m/s
Flow area:	0.0002	m^2	Re:	10440	

Base press. (in,filt,out):	1.17	0.60	0.09	Bar
Pressure (by inlet,outlet	0.63		0.72	Bar
Average TMP	0.68	Bar	67630	Pa

Time (min)	Cum' filtrate (l)	Temp ('C)	Flux raw data (lmh)	Viscosity (Pa.s)	Flux corrected (lmh)	Cum've filtrate (l)	Deposit res'ce (1/m)
0	0.00	26.2	2439	0.000871	2386	0.00	-1.1E-08
2	0.83	26.2	2034	0.000871	1990	0.81	3.80E+08
4	1.38	26.2	1500	0.000871	1467	1.40	1.20E+09
6	1.85	26.2	1355	0.000871	1326	1.87	1.53E+09
8	2.30	26.2	1296	0.000871	1267	2.31	1.69E+09
10	2.72	26.2	1206	0.000871	1180	2.72	1.95E+09
15	3.73	26.1	1148	0.000873	1126	3.70	2.14E+09
20	4.67	26.1	1067	0.000873	1046	4.62	2.45E+09
25	5.54	26	993	0.000875	976	5.48	2.76E+09
30	6.36	26	936	0.000875	920	6.29	3.05E+09
40	7.92	26	901	0.000875	886	7.82	3.24E+09
50	9.41	26	861	0.000875	846	9.29	3.48E+09
60	10.84	26	828	0.000875	813	10.69	3.70E+09
70	12.22	26	800	0.000875	787	12.05	3.88E+09
80	13.56	26	779	0.000875	765	13.37	4.05E+09
90	14.86	26	769	0.000875	756	14.66	4.12E+09

Membrane resistance: 1.91E+09 1/m

TANGENTIAL File: FT11418I

Outer radius:	0.01	m	Flow rate:	14.0	l/m
Inner radius:	0.006	m	Inlet pressure:	1.21	Bar
Active length:	0.27	m	Outlet pressure:	0.21	Bar
Hydraulic dx4	0.008	m	Fluid density:	1000	kg/m^3
Solids conc:	1.7	% wt	Viscosity (25'C):	0.0009	Pa.s
Membrane ar	0.01018	m^2	Bulk velocity:	1.16	m/s
Flow area:	0.0002	m^2	Re:	10440	

Base press. (in,filt,out):	1.17	0.60	0.09	Bar	
Pressure (by inlet,outlet	0.63		0.72	Bar	
Average TMP	0.68	Bar	67630	Pa	

Time (min)	Cum' filtrate (l)	Temp ('C)	Flux raw data (lmh)	Viscosity (Pa.s)	Flux corrected (lmh)	Cum've filtrate (l)	Deposit res'ce (1/m)
0	0.00	26.5	2640	0.000865	2565	0.00	-5.6E-08
2	0.90	26.5	2137	0.000865	2076	0.87	4.19E+08
4	1.45	26.5	1536	0.000865	1493	1.48	1.28E+09
6	1.94	26.5	1370	0.000865	1331	1.95	1.65E+09
8	2.38	26.5	1282	0.000865	1246	2.39	1.88E+09
10	2.81	26.4	1200	0.000867	1168	2.80	2.12E+09
15	3.80	26.3	1141	0.000869	1113	3.77	2.32E+09
20	4.74	26.3	1086	0.000869	1060	4.69	2.52E+09
25	5.65	26.3	1045	0.000869	1020	5.57	2.69E+09
30	6.52	26.2	993	0.000871	971	6.42	2.92E+09
40	8.17	26.1	960	0.000873	941	8.04	3.07E+09
50	9.77	26.1	927	0.000873	909	9.61	3.24E+09
60	11.32	26	897	0.000875	882	11.13	3.39E+09
70	12.82	25.9	867	0.000877	854	12.60	3.56E+09
80	14.26	25.8	838	0.000879	828	14.03	3.73E+09
90	15.66	25.7	825	0.000881	817	15.42	3.80E+09

Membrane resistance: 1.78E+09 1/m

TANGENTIAL File: FT11418J

Outer radius:	0.01	m	Flow rate:	14.0	l/m
Inner radius:	0.006	m	Inlet pressure:	1.24	Bar
Active length:	0.27	m	Outlet pressure:	0.34	Bar
Hydraulic dx4	0.008	m	Fluid density:	1000	kg/m^3
Solids conc:	1.7	% wt	Viscosity (25'C):	0.0009	Pa.s
Membrane ar	0.01018	m^2	Bulk velocity:	1.16	m/s
Flow area:	0.0002	m^2	Re:	10440	

Base press. (in,filt,out):	1.17	0.60	0.09	Bar
Pressure (by inlet,outlet	0.67		0.86	Bar
Average TMP	0.76	Bar	76251	Pa

Time (min)	Cum' filtrate (l)	Temp ('C)	Flux raw data (lmh)	Viscosity (Pa.s)	Flux corrected (lmh)	Cum've filtrate (l)	Deposit res'ce (1/m)
0	0.00	26.1	2800	0.000873	2745	0.00	-4.0E-08
2	0.95	26.1	2314	0.000873	2269	0.93	3.94E+08
4	1.57	26.1	1650	0.000873	1618	1.59	1.30E+09
6	2.07	26.1	1429	0.000873	1402	2.10	1.80E+09
8	2.54	26.1	1341	0.000873	1315	2.56	2.04E+09
10	2.98	26.1	1213	0.000873	1189	2.99	2.45E+09
15	3.98	26	1144	0.000875	1124	3.97	2.70E+09
20	4.92	26	1091	0.000875	1072	4.90	2.92E+09
25	5.83	26	1037	0.000875	1020	5.79	3.17E+09
30	6.68	25.9	1002	0.000877	987	6.64	3.34E+09
40	8.38	25.8	964	0.000879	952	8.28	3.53E+09
50	9.95	25.7	902	0.000881	892	9.85	3.89E+09
60	11.44	25.6	869	0.000883	862	11.34	4.09E+09
70	12.90	25.6	846	0.000883	839	12.78	4.25E+09
80	14.31	25.5	825	0.000885	820	14.19	4.39E+09
90	15.70	25.4	819	0.000887	816	15.58	4.42E+09

Membrane resistance: 1.87E+09 1/m

TANGENTIAL File: FT11621C

Outer radius:	0.01	m	Flow rate:	16.0	l/m
Inner radius:	0.006	m	Inlet pressure:	1.45	Bar
Active length:	0.27	m	Outlet pressure:	0.11	Bar
Hydraulic dx4	0.008	m	Fluid density:	1000	kg/m^3
Solids conc:	1.7	% wt	Viscosity (25'C):	0.0009	Pa.s
Membrane ar	0.01018	m^2	Bulk velocity:	1.33	m/s
Flow area:	0.0002	m^2	Re:	11942	

Base press. (in,filt,out):	1.47	0.75	0.11	Bar
Pressure (by inlet,outlet	0.72	0.00	0.75	Bar
Average TMP	0.74	Bar	73902	Pa

Time (min)	Cum' filtrate (l)	Temp ('C)	Flux raw data (lmh)	Viscosity (Pa.s)	Flux corrected (lmh)	Cum've filtrate (l)	Deposit res'ce (1/m)
0	0.00	25	2457	0.000895	2471	0.00	-5.7E-08
2	0.83	25	2042	0.000895	2054	0.84	4.09E+08
4	1.39	25	1500	0.000895	1508	1.44	1.29E+09
6	1.85	25	1305	0.000895	1312	1.92	1.78E+09
8	2.27	25	1217	0.000895	1223	2.35	2.06E+09
10	2.68	25	1142	0.000895	1148	2.75	2.32E+09
15	3.63	25	1090	0.000895	1097	3.71	2.53E+09
20	4.53	25	1040	0.000895	1046	4.61	2.75E+09
25	5.39	25	1000	0.000895	1006	5.48	2.94E+09
30	6.22	25	960	0.000895	966	6.32	3.14E+09
40	7.83	25	932	0.000895	937	7.93	3.30E+09
50	9.38	25	902	0.000895	907	9.50	3.48E+09
60	10.89	24.9	878	0.000897	885	11.02	3.61E+09
70	12.36	24.8	877	0.000899	886	12.52	3.61E+09
80	13.87	27	877	0.000855	843	13.99	3.90E+09
90	15.34	26.9	868	0.000857	836	15.41	3.95E+09

Membrane resistance: 2.02E+09 1/m

TANGENTIAL File: FT11621D

Outer radius:	0.01	m	Flow rate:	16.0	l/m
Inner radius:	0.006	m	Inlet pressure:	1.45	Bar
Active length:	0.27	m	Outlet pressure:	0.11	Bar
Hydraulic dx4	0.008	m	Fluid density:	1000	kg/m^3
Solids conc:	1.7	% wt	Viscosity (25'C):	0.0009	Pa.s
Membrane ar	0.01018	m^2	Bulk velocity:	1.33	m/s
Flow area:	0.0002	m^2	Re:	11942	

Base press. (in,filt,out):	1.47	0.75	0.11	Bar
Pressure (by inlet,outlet	0.72		0.75	Bar
Average TMP	0.74	Bar	73902	Pa

Time (min)	Cum' filtrate (l)	Temp ('C)	Flux raw data (lmh)	Viscosity (Pa.s)	Flux corrected (lmh)	Cum've filtrate (l)	Deposit res'ce (1/m)
0	0.00	25	2310	0.000895	2323	0.00	6.29E-08
2	0.78	25	1922	0.000895	1933	0.79	4.33E+08
4	1.30	25	1447	0.000895	1455	1.36	1.28E+09
6	1.77	25	1322	0.000895	1330	1.84	1.60E+09
8	2.20	25	1254	0.000895	1261	2.27	1.80E+09
10	2.62	25	1177	0.000895	1183	2.69	2.07E+09
15	3.60	25	1125	0.000895	1131	3.67	2.26E+09
20	4.52	24.9	1075	0.000897	1084	4.61	2.45E+09
25	5.42	25.6	1047	0.000883	1039	5.51	2.65E+09
30	6.30	25.6	1010	0.000883	1002	6.38	2.83E+09
40	7.99	25.4	977	0.000887	974	8.05	2.97E+09
50	9.62	25.2	939	0.000891	940	9.67	3.15E+09
60	11.18	24.9	920	0.000897	927	11.26	3.23E+09
70	12.74	26.6	910	0.000863	882	12.79	3.50E+09
80	14.27	26.2	892	0.000871	873	14.28	3.56E+09
90	15.76	25.6	882	0.000883	875	15.76	3.55E+09

Membrane resistance: 2.15E+09 1/m

TANGENTIAL File: FT11621E

Outer radius:	0.01	m	Flow rate:	16.0	l/m
Inner radius:	0.006	m	Inlet pressure:	1.48	Bar
Active length:	0.27	m	Outlet pressure:	0.21	Bar
Hydraulic dx4	0.008	m	Fluid density:	1000	kg/m^3
Solids conc:	1.7	% wt	Viscosity (25'C):	0.0009	Pa.s
Membrane ar	0.01018	m^2	Bulk velocity:	1.33	m/s
Flow area:	0.0002	m^2	Re:	11942	

Base press. (in,filt,out):	1.47	0.75	0.11	Bar
Pressure (by inlet,outlet	0.76		0.85	Bar
Average TMP	0.80	Bar	80454	Pa

Time (min)	Cum' filtrate (l)	Temp ('C)	Flux raw data (lmh)	Viscosity (Pa.s)	Flux corrected (lmh)	Cum've filtrate (l)	Deposit res'ce (1/m)
0	0.00	25	2709	0.000895	2725	0.00	5.72E-08
2	0.92	25	2210	0.000895	2223	0.92	4.49E+08
4	1.50	25	1611	0.000895	1620	1.58	1.36E+09
6	2.01	25	1483	0.000895	1491	2.10	1.65E+09
8	2.51	25	1354	0.000895	1362	2.59	1.99E+09
10	2.93	25	1251	0.000895	1258	3.03	2.32E+09
15	3.99	25	1217	0.000895	1224	4.09	2.44E+09
20	5.00	25	1161	0.000895	1168	5.10	2.65E+09
25	5.96	24.9	1118	0.000897	1127	6.07	2.82E+09
30	6.89	24.9	1070	0.000897	1078	7.01	3.04E+09
40	8.68	25	1034	0.000895	1040	8.80	3.23E+09
50	10.40	24.8	999	0.000899	1009	10.54	3.38E+09
60	12.07	25.5	979	0.000885	973	12.22	3.58E+09
70	13.72	25.5	965	0.000885	959	13.86	3.66E+09
80	15.35	25.5	954	0.000885	948	15.48	3.73E+09
90	16.96	26.9	949	0.000857	914	17.06	3.95E+09

Membrane resistance: 1.99E+09 1/m

TANGENTIAL File: FT11624F

Outer radius:	0.01	m	Flow rate:	16.0	l/m
Inner radius:	0.006	m	Inlet pressure:	1.66	Bar
Active length:	0.27	m	Outlet pressure:	0.34	Bar
Hydraulic dx4	0.008	m	Fluid density:	1000	kg/m^3
Solids conc:	1.7	% wt	Viscosity (25'C):	0.0009	Pa.s
Membrane ar	0.01018	m^2	Bulk velocity:	1.33	m/s
Flow area:	0.0002	m^2	Re:	11942	

Base press. (in,filt,out):	1.47	0.75	0.11	Bar
Pressure (by inlet,outlet	0.93		0.99	Bar
Average TMP	0.96	Bar	95971	Pa

Time (min)	Cum' filtrate (l)	Temp ('C)	Flux raw data (lmh)	Viscosity (Pa.s)	Flux corrected (lmh)	Cum've filtrate (l)	Deposit res'ce (1/m)
0	0.00	25.6	2888	0.000883	2865	0.00	-2.1E-07
2	0.98	25.6	2266	0.000883	2248	0.97	6.20E+08
4	1.54	25.6	1591	0.000883	1578	1.62	1.84E+09
6	2.06	25.6	1492	0.000883	1480	2.14	2.11E+09
8	2.55	25.6	1400	0.000883	1389	2.63	2.40E+09
10	3.01	25.6	1296	0.000883	1285	3.08	2.78E+09
15	4.09	25.5	1233	0.000885	1225	4.14	3.02E+09
20	5.10	25.4	1167	0.000887	1163	5.16	3.30E+09
25	6.07	25.4	1122	0.000887	1118	6.13	3.53E+09
30	7.00	25.4	1082	0.000887	1078	7.06	3.74E+09
40	8.82	25.3	1045	0.000889	1044	8.86	3.94E+09
50	10.55	25.3	998	0.000889	997	10.59	4.23E+09
60	12.21	25.2	969	0.000891	970	12.26	4.41E+09
70	13.84	25.1	952	0.000893	955	13.89	4.51E+09
80	15.44	25.1	939	0.000893	942	15.50	4.61E+09
90	17.03	25	934	0.000895	939	17.10	4.63E+09

Membrane resistance: 2.26E+09 1/m

TANGENTIAL File: FT11825M

Outer radius:	0.01	m	Flow rate:	17.5	l/m
Inner radius:	0.006	m	Inlet pressure:	1.72	Bar
Active length:	0.27	m	Outlet pressure:	0.21	Bar
Hydraulic dx4	0.008	m	Fluid density:	1000	kg/m^3
Solids conc:	1.7	% wt	Viscosity (25'C):	0.0009	Pa.s
Membrane ar	0.01018	m^2	Bulk velocity:	1.45	m/s
Flow area:	0.0002	m^2	Re:	13069	

Base press. (in,filt,out):	1.72	0.88	0.13	Bar
Pressure (by inlet,outlet	0.88		0.96	Bar
Average TMP	0.92	Bar	91711	Pa

Time (min)	Cum' filtrate (l)	Temp ('C)	Flux raw data (lmh)	Viscosity (Pa.s)	Flux corrected (lmh)	Cum've filtrate (l)	Deposit res'ce (1/m)
0	0.00	25.4	3029	0.000887	3018	0.00	7.56E-08
2	1.03	25.8	2545	0.000879	2513	1.02	4.12E+08
4	1.73	26.4	1900	0.000867	1850	1.76	1.29E+09
6	2.32	26.1	1653	0.000873	1621	2.35	1.77E+09
8	2.85	26	1536	0.000875	1509	2.88	2.05E+09
10	3.36	25.9	1427	0.000877	1406	3.38	2.35E+09
15	4.54	25.7	1329	0.000881	1315	4.53	2.65E+09
20	5.61	25.5	1251	0.000885	1244	5.62	2.92E+09
25	6.67	25.3	1190	0.000889	1189	6.65	3.15E+09
30	7.63	25.1	1142	0.000893	1146	7.64	3.35E+09
40	9.57	26.7	1120	0.000861	1083	9.53	3.66E+09
50	11.43	26.3	1071	0.000869	1046	11.34	3.86E+09
60	13.21	25.7	1042	0.000881	1031	13.10	3.95E+09
70	14.97	25.3	1026	0.000889	1024	14.84	3.99E+09
80	16.69	25	1015	0.000895	1021	16.58	4.01E+09
90	18.41	25	1016	0.000895	1022	18.31	4.00E+09

Membrane resistance: 2.05E+09 1/m

TANGENTIAL File: FT11825L

Outer radius:	0.01	m	Flow rate:	17.6	l/m
Inner radius:	0.006	m	Inlet pressure:	1.74	Bar
Active length:	0.27	m	Outlet pressure:	0.14	Bar
Hydraulic dx4	0.008	m	Fluid density:	1000	kg/m^3
Solids conc:	1.7	% wt	Viscosity (25'C):	0.0009	Pa.s
Membrane ar	0.01018	m^2	Bulk velocity:	1.46	m/s
Flow area:	0.0002	m^2	Re:	13144	
Base press. (in,filt,out):	1.74	0.88	0.13	Bar	
Pressure (by inlet,outlet	0.88		0.90	Bar	
Average TMP	0.89	Bar	88896	Pa	

Time (min)	Cum' filtrate (l)	Temp ('C)	Flux raw data (lmh)	Viscosity (Pa.s)	Flux corrected (lmh)	Cum've filtrate (l)	Deposit res'ce (1/m)
0	0.00	26.2	2789	0.000871	2729	0.00	6.71E-08
2	0.95	26.2	2286	0.000871	2237	0.93	4.83E+08
4	1.55	25.9	1700	0.000877	1675	1.59	1.38E+09
6	2.10	25.9	1543	0.000877	1520	2.13	1.75E+09
8	2.60	25.8	1449	0.000879	1431	2.63	1.99E+09
10	3.08	25.7	1371	0.000881	1356	3.10	2.22E+09
15	4.23	25.5	1305	0.000885	1297	4.23	2.42E+09
20	5.30	25.2	1235	0.000891	1236	5.30	2.65E+09
25	6.32	26.3	1196	0.000869	1167	6.32	2.94E+09
30	7.33	26	1144	0.000875	1124	7.30	3.13E+09
40	9.23	25.5	1097	0.000885	1090	9.17	3.30E+09
50	11.05	25	1061	0.000895	1067	11.00	3.42E+09
60	12.83	26.8	1043	0.000859	1006	12.76	3.76E+09
70	14.58	26.5	1017	0.000865	988	14.45	3.87E+09
80	16.28	26	983	0.000875	966	16.11	4.00E+09
90	17.92	25.8	965	0.000879	953	17.74	4.09E+09

Membrane resistance: 2.20E+09 1/m

TANGENTIAL File: FT11825B

Outer radius:	0.01	m	Flow rate:	17.7	l/m
Inner radius:	0.006	m	Inlet pressure:	1.76	Bar
Active length:	0.27	m	Outlet pressure:	0.13	Bar
Hydraulic dx4	0.008	m	Fluid density:	1000	kg/m^3
Solids conc:	1.7	% wt	Viscosity (25'C):	0.0009	Pa.s
Membrane ar	0.01018	m^2	Bulk velocity:	1.47	m/s
Flow area:	0.0002	m^2	Re:	13219	

Base press. (in,filt,out):	1.76	0.89	0.13	Bar
Pressure (by inlet,outlet	0.90		0.89	Bar
Average TMP	0.89	Bar	89356	Pa

Time (min)	Cum' filtrate (l)	Temp ('C)	Flux raw data (lmh)	Viscosity (Pa.s)	Flux corrected (lmh)	Cum've filtrate (l)	Deposit res'ce (1/m)
0	0.00	25.5	2943	0.000885	2926	0.00	-9.4E-08
2	1.00	25.5	2504	0.000885	2489	0.99	3.61E+08
4	1.70	25.5	1881	0.000885	1870	1.73	1.16E+09
6	2.27	25.5	1570	0.000885	1561	2.31	1.80E+09
8	2.76	25.5	1370	0.000885	1362	2.81	2.36E+09
10	3.20	25.5	1196	0.000885	1189	3.24	3.01E+09
15	4.19	25.5	1134	0.000885	1127	4.23	3.29E+09
20	5.13	25.5	1088	0.000885	1081	5.16	3.51E+09
25	6.03	25.5	1053	0.000885	1047	6.06	3.70E+09
30	6.91	25.3	1029	0.000889	1028	6.94	3.80E+09
40	8.65	25.2	1013	0.000891	1014	8.68	3.88E+09
50	10.35	25	997	0.000895	1003	10.39	3.95E+09
60	12.03	25.6	980	0.000883	972	12.06	4.14E+09
70	13.68	25.4	961	0.000887	957	13.70	4.23E+09
80	15.29	25.1	942	0.000893	945	15.31	4.32E+09
90	16.87	25	932	0.000895	937	16.91	4.37E+09

Membrane resistance: 2.06E+09 1/m

TANGENTIAL File: FT11826K

Outer radius:	0.01	m	Flow rate:	17.8	l/m
Inner radius:	0.006	m	Inlet pressure:	1.77	Bar
Active length:	0.27	m	Outlet pressure:	0.13	Bar
Hydraulic dx4	0.008	m	Fluid density:	1000	kg/m^3
Solids conc:	1.7	% wt	Viscosity (25'C):	0.0009	Pa.s
Membrane ar	0.01018	m^2	Bulk velocity:	1.48	m/s
Flow area:	0.0002	m^2	Re:	13294	

Base press. (in,filt,out):	1.77	0.90	0.13	Bar
Pressure (by inlet,outlet	0.90		0.90	Bar
Average TMP	0.90	Bar	90161	Pa

Time (min)	Cum' filtrate (l)	Temp ('C)	Flux raw data (lmh)	Viscosity (Pa.s)	Flux corrected (lmh)	Cum've filtrate (l)	Deposit res'ce (1/m)
0	0.00	21.2	2514	0.000977	2759	0.00	-2.0E-08
2	0.85	22.9	2197	0.000939	2319	0.94	4.18E+08
4	1.49	23	1705	0.000937	1795	1.63	1.18E+09
6	2.01	23.1	1440	0.000935	1513	2.20	1.81E+09
8	2.47	23.6	1330	0.000924	1381	2.69	2.20E+09
10	2.91	24	1365	0.000916	1405	3.16	2.12E+09
15	4.09	25.5	1378	0.000885	1370	4.34	2.23E+09
20	5.25	26.1	1341	0.000873	1315	5.47	2.42E+09
25	6.36	25.8	1271	0.000879	1255	6.56	2.64E+09
30	7.41	25.7	1159	0.000881	1147	7.58	3.10E+09
40	9.31	25.3	1076	0.000889	1075	9.47	3.45E+09
50	11.06	25	1028	0.000895	1034	11.26	3.68E+09
60	12.80	27.1	1024	0.000853	982	12.97	3.99E+09
70	14.53	26.8	1001	0.000859	966	14.62	4.09E+09
80	16.20	26.5	967	0.000865	939	16.23	4.27E+09
90	17.81	26	953	0.000875	936	17.82	4.29E+09

Membrane resistance: 2.20E+09 1/m

NORMAL File : FN31417O

Outer radius:	0.01	m	Flow rate:	14.0	l/m
Inner radius:	0.006	m	Inlet pressure:	1.20	Bar
Active length:	0.27	m	Outlet pressure:	0.16	Bar
Hydraulic dx4	0.008	m	Fluid density:	1000	kg/m^3
Solids conc:	3	% wt	Viscosity (25'C):	0.0009	Pa.s
Membrane ar	0.01018	m^2	Bulk velocity:	1.50	m/s
Flow area:	0.0002	m^2	Re:	13444	

Base press. (in,filt,out):	1.20	0.70	0.16	Bar
Pressure (by inlet,outlet	1.05		0.70	Bar
Average TMP	0.87	Bar	87299	Pa

Time (min)	Cum' filtrate (l)	Temp ('C)	Flux raw data (lmh)	Viscosity (Pa.s)	Flux corrected (lmh)	Cum've filtrate (l)	Deposit res'ce (1/m)
0	0.00	21.8	2001	0.000963	2166	0.00	0.00E+00
2	0.68	22.4	1634	0.00095	1744	0.73	6.57E+08
4	1.11	22.8	1215	0.000942	1286	1.25	1.86E+09
6	1.50	23.3	1140	0.000931	1192	1.67	2.22E+09
8	1.88	23.7	1104	0.000922	1144	2.07	2.43E+09
10	2.25	24.3	1076	0.00091	1100	2.45	2.63E+09
15	3.16	25.6	1064	0.000883	1055	3.36	2.86E+09
20	4.06	26.8	1054	0.000859	1017	4.24	3.07E+09
25	4.95	27.8	1047	0.000839	987	5.09	3.24E+09
30	5.83	28.9	1032	0.000818	949	5.91	3.48E+09
40	7.58	28.7	1001	0.000822	924	7.50	3.65E+09
50	9.23	27.5	953	0.000845	905	9.05	3.79E+09
60	10.81	27.3	913	0.000849	871	10.56	4.04E+09
70	12.33	26.5	878	0.000865	853	12.02	4.18E+09
80	13.79	25.9	843	0.000877	830	13.45	4.37E+09
90	15.19	25.4	825	0.000887	822	14.85	4.44E+09

Membrane resistance: 2.72E+09 1/m

NORMAL File: FN31414U

Outer radius:	0.01	m	Flow rate:	14.0	l/m
Inner radius:	0.006	m	Inlet pressure:	0.93	Bar
Active length:	0.27	m	Outlet pressure:	0.11	Bar
Hydraulic dx4	0.008	m	Fluid density:	1000	kg/m^3
Solids conc:	3	% wt	Viscosity (25'C):	0.0009	'Pa.s
Membrane ar	0.01018	m^2	Bulk velocity:	1.16	m/s
Flow area:	0.0002	m^2	Re:	10440	
Base press. (in,filt,out):	0.72	0.43	0.11	Bar	
Pressure (by inlet,outlet	0.65		0.43	Bar	
Average TMP	0.54	Bar	53972	Pa	

Time (min)	Cum' filtrate (l)	Temp ('C)	Flux raw data (lmh)	Viscosity (Pa.s)	Flux corrected (lmh)	Cum've filtrate (l)	Deposit res'ce (1/m)
0	0.00	26	1621	0.000875	1593	0.00	-2.5E-08
2	0.55	26.4	1329	0.000867	1294	0.54	5.27E+08
4	0.90	26.5	979	0.000865	951	0.92	1.54E+09
6	1.21	26.4	895	0.000867	872	1.23	1.89E+09
8	1.51	26.4	855	0.000867	833	1.52	2.09E+09
10	1.79	26.3	813	0.000869	793	1.80	2.30E+09
15	2.47	26.1	783	0.000873	768	2.46	2.45E+09
20	3.12	26	753	0.000875	740	3.10	2.63E+09
25	3.75	25.8	727	0.000879	718	3.72	2.78E+09
30	4.36	25.7	690	0.000881	682	4.31	3.05E+09
40	5.51	25.5	664	0.000885	660	5.45	3.23E+09
50	6.61	25.3	648	0.000889	648	6.56	3.33E+09
60	7.71	25.2	644	0.000891	645	7.65	3.36E+09
70	8.80	25.6	633	0.000883	628	8.73	3.51E+09
80	9.85	25.4	616	0.000887	614	9.79	3.65E+09
90	10.88	25.3	608	0.000889	607	10.82	3.71E+09

Membrane resistance: 2.28E+09 1/m

NORMAL File: FN31416V

Outer radius:	0.01	m	Flow rate:	14.0	l/m
Inner radius:	0.006	m	Inlet pressure:	1.10	Bar
Active length:	0.27	m	Outlet pressure:	0.21	Bar
Hydraulic dx4	0.008	m	Fluid density:	1000	kg/m^3
Solids conc:	3	% wt	Viscosity (25'C):	0.0009	Pa.s
Membrane ar	0.01018	m^2	Bulk velocity:	1.16	m/s
Flow area:	0.0002	m^2	Re:	10440	

Base press. (in,filt,out):	0.72	0.43	0.11	Bar
Pressure (by inlet,outlet	0.82		0.53	Bar
Average TMP	0.67	Bar	67421	Pa

Time (min)	Cum' filtrate (l)	Temp ('C)	Flux raw data (lmh)	Viscosity (Pa.s)	Flux corrected (lmh)	Cum've filtrate (l)	Deposit res'ce (1/m)
0	0.00	25.5	1886	0.000885	1875	0.00	-6.7E-08
2	0.64	26	1512	0.000875	1486	0.64	6.35E+08
4	1.03	26.5	1080	0.000865	1049	1.07	1.91E+09
6	1.37	26.5	953	0.000865	926	1.40	2.48E+09
8	1.67	26.4	881	0.000867	858	1.70	2.87E+09
10	1.97	26.2	874	0.000871	855	1.99	2.89E+09
15	2.71	26	856	0.000875	841	2.71	2.98E+09
20	3.42	25.9	827	0.000877	815	3.42	3.16E+09
25	4.11	25.7	801	0.000881	793	4.10	3.31E+09
30	4.78	25.5	777	0.000885	773	4.76	3.46E+09
40	6.09	25	763	0.000895	768	6.07	3.50E+09
50	7.37	25.9	744	0.000877	733	7.34	3.78E+09
60	8.62	25.4	722	0.000887	720	8.57	3.89E+09
70	9.82	25.1	711	0.000893	713	9.79	3.95E+09
80	11.03	26.6	704	0.000863	682	10.97	4.24E+09
90	12.21	26.5	697	0.000865	677	12.13	4.29E+09

Membrane resistance: 2.42E+09 1/m

NORMAL File: FN31418W

Outer radius:	0.01	m	Flow rate:	14.0	l/m
Inner radius:	0.006	m	Inlet pressure:	1.21	Bar
Active length:	0.27	m	Outlet pressure:	0.34	Bar
Hydraulic dx4	0.008	m	Fluid density:	1000	kg/m^3
Solids conc:	3	% wt	Viscosity (25'C):	0.0009	Pa.s
Membrane ar	0.01018	m^2	Bulk velocity:	1.16	m/s
Flow area:	0.0002	m^2	Re:	10440	
Base press. (in,filt,out):	0.72	0.43	0.11	Bar	
Pressure (by inlet,outlet	0.93		0.66	Bar	
Average TMP	0.79	Bar	79489	Pa	

Time (min)	Cum' filtrate (l)	Temp ('C)	Flux raw data (lmh)	Viscosity (Pa.s)	Flux corrected (lmh)	Cum've filtrate (l)	Deposit res'ce (1/m)
0	0.00	26	2060	0.000875	2025	0.00	-1.9E-07
2	0.70	26	1649	0.000875	1621	0.69	6.60E+08
4	1.12	26	1177	0.000875	1157	1.16	1.98E+09
6	1.50	25.9	1088	0.000877	1072	1.54	2.35E+09
8	1.86	25.9	1039	0.000877	1024	1.89	2.59E+09
10	2.20	25.8	982	0.000879	970	2.23	2.88E+09
15	3.02	25.8	943	0.000879	931	3.04	3.11E+09
20	3.80	25.7	908	0.000881	898	3.81	3.32E+09
25	4.56	25.6	880	0.000883	873	4.56	3.49E+09
30	5.30	25.6	858	0.000883	851	5.29	3.65E+09
40	6.75	25.5	836	0.000885	831	6.72	3.80E+09
50	8.13	25.4	807	0.000887	804	8.11	4.02E+09
60	9.48	25.2	787	0.000891	788	9.46	4.15E+09
70	10.81	25.5	772	0.000885	767	10.78	4.34E+09
80	12.10	25.4	757	0.000887	754	12.07	4.46E+09
90	13.37	25.3	750	0.000889	749	13.34	4.51E+09

Membrane resistance: 2.65E+09 1/m

NORMAL File : FN31617N

Outer radius:	0.01	m	Flow rate:	16.0	l/m
Inner radius:	0.006	m	Inlet pressure:	1.20	Bar
Active length:	0.27	m	Outlet pressure:	0.16	Bar
Hydraulic dx4	0.008	m	Fluid density:	1000	kg/m^3
Solids conc:	3	% wt	Viscosity (25'C):	0.0009	Pa.s
Membrane ar	0.01018	m^2	Bulk velocity:	1.50	m/s
Flow area:	0.0002	m^2	Re:	13444	

Base press. (in,filt,out):	1.20	0.70	0.16	Bar
Pressure (by inlet,outlet	1.05		0.70	Bar
Average TMP	0.87	Bar	87299	Pa

Time (min)	Cum' filtrate (l)	Temp ('C)	Flux raw data (lmh)	Viscosity (Pa.s)	Flux corrected (lmh)	Cum've filtrate (l)	Deposit res'ce (1/m)
0	0.00	21.8	2001	0.000963	2166	0.00	0.00E+00
2	0.68	22.4	1634	0.00095	1744	0.73	6.57E+08
4	1.11	22.8	1215	0.000942	1286	1.25	1.86E+09
6	1.50	23.3	1140	0.000931	1192	1.67	2.22E+09
8	1.88	23.7	1104	0.000922	1144	2.07	2.43E+09
10	2.25	24.3	1076	0.00091	1100	2.45	2.63E+09
15	3.16	25.6	1064	0.000883	1055	3.36	2.86E+09
20	4.06	26.8	1054	0.000859	1017	4.24	3.07E+09
25	4.95	27.8	1047	0.000839	987	5.09	3.24E+09
30	5.83	28.9	1032	0.000818	949	5.91	3.48E+09
40	7.58	28.7	1001	0.000822	924	7.50	3.65E+09
50	9.23	27.5	953	0.000845	905	9.05	3.79E+09
60	10.81	27.3	913	0.000849	871	10.56	4.04E+09
70	12.33	26.5	878	0.000865	853	12.02	4.18E+09
80	13.79	25.9	843	0.000877	830	13.45	4.37E+09
90	15.19	25.4	825	0.000887	822	14.85	4.44E+09

Membrane resistance: 2.72E+09 1/m

NORMAL File : FN31719R

Outer radius:	0.01	m	Flow rate:	17.0	l/m
Inner radius:	0.006	m	Inlet pressure:	1.31	Bar
Active length:	0.27	m	Outlet pressure:	0.16	Bar
Hydraulic dx4	0.008	m	Fluid density:	1000	kg/m^3
Solids conc:	3	% wt	Viscosity (25'C):	0.0009	Pa.s
Membrane ar	0.01018	m^2	Bulk velocity:	1.50	m/s
Flow area:	0.0002	m^2	Re:	13444	

Base press. (in,filt,out):	1.20	0.70	0.16	Bar
Pressure (by inlet,outlet	1.05		0.70	Bar
Average TMP	0.87	Bar	87299	Pa

Time (min)	Cum' filtrate (l)	Temp ('C)	Flux raw data (lmh)	Viscosity (Pa.s)	Flux corrected (lmh)	Cum've filtrate (l)	Deposit res'ce (1/m)
0	0.00	21.8	2001	0.000963	2166	0.00	0.00E+00
2	0.68	22.4	1634	0.00095	1744	0.73	6.57E+08
4	1.11	22.8	1215	0.000942	1286	1.25	1.86E+09
6	1.50	23.3	1140	0.000931	1192	1.67	2.22E+09
8	1.88	23.7	1104	0.000922	1144	2.07	2.43E+09
10	2.25	24.3	1076	0.00091	1100	2.45	2.63E+09
15	3.16	25.6	1064	0.000883	1055	3.36	2.86E+09
20	4.06	26.8	1054	0.000859	1017	4.24	3.07E+09
25	4.95	27.8	1047	0.000839	987	5.09	3.24E+09
30	5.83	28.9	1032	0.000818	949	5.91	3.48E+09
40	7.58	28.7	1001	0.000822	924	7.50	3.65E+09
50	9.23	27.5	953	0.000845	905	9.05	3.79E+09
60	10.81	27.3	913	0.000849	871	10.56	4.04E+09
70	12.33	26.5	878	0.000865	853	12.02	4.18E+09
80	13.79	25.9	843	0.000877	830	13.45	4.37E+09
90	15.19	25.4	825	0.000887	822	14.85	4.44E+09

Membrane resistance: 2.72E+09 1/m

NORMAL File : FN31721S

Outer radius:	0.01	m	Flow rate:	17.0	l/m
Inner radius:	0.006	m	Inlet pressure:	1.41	Bar
Active length:	0.27	m	Outlet pressure:	0.21	Bar
Hydraulic dx4	0.008	m	Fluid density:	1000	kg/m^3
Solids conc:	3	% wt	Viscosity (25'C):	0.0009	Pa.s
Membrane ar	0.01018	m^2	Bulk velocity:	1.50	m/s
Flow area:	0.0002	m^2	Re:	13444	

Base press. (in,filt,out):	1.20	0.70	0.16	Bar
Pressure (by inlet,outlet	1.05		0.70	Bar
Average TMP	0.87	Bar	87299	Pa

Time (min)	Cum' filtrate (l)	Temp ('C)	Flux raw data (lmh)	Viscosity (Pa.s)	Flux corrected (lmh)	Cum've filtrate (l)	Deposit res'ce (1/m)
0	0.00	21.8	2001	0.000963	2166	0.00	0.00E+00
2	0.68	22.4	1634	0.00095	1744	0.73	6.57E+08
4	1.11	22.8	1215	0.000942	1286	1.25	1.86E+09
6	1.50	23.3	1140	0.000931	1192	1.67	2.22E+09
8	1.88	23.7	1104	0.000922	1144	2.07	2.43E+09
10	2.25	24.3	1076	0.00091	1100	2.45	2.63E+09
15	3.16	25.6	1064	0.000883	1055	3.36	2.86E+09
20	4.06	26.8	1054	0.000859	1017	4.24	3.07E+09
25	4.95	27.8	1047	0.000839	987	5.09	3.24E+09
30	5.83	28.9	1032	0.000818	949	5.91	3.48E+09
40	7.58	28.7	1001	0.000822	924	7.50	3.65E+09
50	9.23	27.5	953	0.000845	905	9.05	3.79E+09
60	10.81	27.3	913	0.000849	871	10.56	4.04E+09
70	12.33	26.5	878	0.000865	853	12.02	4.18E+09
80	13.79	25.9	843	0.000877	830	13.45	4.37E+09
90	15.19	25.4	825	0.000887	822	14.85	4.44E+09

Membrane resistance: 2.72E+09 1/m

NORMAL File : FN31723T

Outer radius:	0.01	m	Flow rate:	17.0	l/m
Inner radius:	0.006	m	Inlet pressure:	1.55	Bar
Active length:	0.27	m	Outlet pressure:	0.34	Bar
Hydraulic dx4	0.008	m	Fluid density:	1000	kg/m^3
Solids conc:	3	% wt	Viscosity (25'C):	0.0009	Pa.s
Membrane ar	0.01018	m^2	Bulk velocity:	1.50	m/s
Flow area:	0.0002	m^2	Re:	13444	
Base press. (in,filt,out):	1.20	0.70	0.16	Bar	
Pressure (by inlet,outlet	1.05		0.70	Bar	
Average TMP	0.87	Bar	87299	Pa	

Time (min)	Cum' filtrate (l)	Temp ('C)	Flux raw data (lmh)	Viscosity (Pa.s)	Flux corrected (lmh)	Cum've filtrate (l)	Deposit res'ce (1/m)
0	0.00	21.8	2001	0.000963	2166	0.00	0.00E+00
2	0.68	22.4	1634	0.00095	1744	0.73	6.57E+08
4	1.11	22.8	1215	0.000942	1286	1.25	1.86E+09
6	1.50	23.3	1140	0.000931	1192	1.67	2.22E+09
8	1.88	23.7	1104	0.000922	1144	2.07	2.43E+09
10	2.25	24.3	1076	0.00091	1100	2.45	2.63E+09
15	3.16	25.6	1064	0.000883	1055	3.36	2.86E+09
20	4.06	26.8	1054	0.000859	1017	4.24	3.07E+09
25	4.95	27.8	1047	0.000839	987	5.09	3.24E+09
30	5.83	28.9	1032	0.000818	949	5.91	3.48E+09
40	7.58	28.7	1001	0.000822	924	7.50	3.65E+09
50	9.23	27.5	953	0.000845	905	9.05	3.79E+09
60	10.81	27.3	913	0.000849	871	10.56	4.04E+09
70	12.33	26.5	878	0.000865	853	12.02	4.18E+09
80	13.79	25.9	843	0.000877	830	13.45	4.37E+09
90	15.19	25.4	825	0.000887	822	14.85	4.44E+09

Membrane resistance: 2.72E+09 1/m

NORMAL File: FN31824Q

Outer radius:	0.01	m	Flow rate:	17.6	l/m
Inner radius:	0.006	m	Inlet pressure:	1.66	Bar
Active length:	0.27	m	Outlet pressure:	0.34	Bar
Hydraulic dx4	0.008	m	Fluid density:	1000	kg/m^3
Solids conc:	3	% wt	Viscosity (25'C):	0.0009	Pa.s
Membrane ar	0.01018	m^2	Bulk velocity:	1.46	m/s
Flow area:	0.0002	m^2	Re:	13144	
Base press. (in,filt,out):	1.15	0.67	0.15	Bar	
Pressure (by inlet,outlet	1.18		0.86	Bar	
Average TMP	1.02	Bar	101829	Pa	

Time (min)	Cum' filtrate (l)	Temp ('C)	Flux raw data (lmh)	Viscosity (Pa.s)	Flux corrected (lmh)	Cum've filtrate (l)	Deposit res'ce (1/m)
0	0.00	25.1	2292	0.000893	2300	0.00	-1.8E-07
2	0.78	25.7	1882	0.000881	1862	0.78	7.02E+08
4	1.28	26.4	1364	0.000867	1328	1.32	2.18E+09
6	1.70	26.8	1252	0.000859	1208	1.75	2.70E+09
8	2.13	26.6	1222	0.000863	1184	2.16	2.81E+09
10	2.53	26.5	1161	0.000865	1128	2.55	3.10E+09
15	3.51	26.1	1129	0.000873	1107	3.50	3.22E+09
20	4.45	25.8	1081	0.000879	1068	4.42	3.44E+09
25	5.34	25.6	1032	0.000883	1024	5.31	3.72E+09
30	6.20	25.4	988	0.000887	984	6.16	3.99E+09
40	7.85	25	971	0.000895	976	7.82	4.05E+09
50	9.49	26.7	958	0.000861	927	9.44	4.42E+09
60	11.10	26	920	0.000875	904	10.99	4.61E+09
70	12.62	25.5	874	0.000885	869	12.49	4.91E+09
80	14.07	25	854	0.000895	858	13.96	5.01E+09
90	15.51	26.4	849	0.000867	827	15.39	5.32E+09

Membrane resistance: 2.98E+09 1/m

NORMAL File: FN31824P

Outer radius:	0.01	m	Flow rate:	17.7	l/m
Inner radius:	0.006	m	Inlet pressure:	1.62	Bar
Active length:	0.27	m	Outlet pressure:	0.21	Bar
Hydraulic dx4	0.008	m	Fluid density:	1000	kg/m^3
Solids conc:	3	% wt	Viscosity (25'C):	0.0009	Pa.s
Membrane ar	0.01018	m^2	Bulk velocity:	1.47	m/s
Flow area:	0.0002	m^2	Re:	13219	

Base press. (in,filt,out):	1.16	0.68	0.15	Bar
Pressure (by inlet,outlet	1.14	0.00	0.73	Bar
Average TMP	0.93	Bar	93198	Pa

Time (min)	Cum' filtrate (l)	Temp ('C)	Flux raw data (lmh)	Viscosity (Pa.s)	Flux corrected (lmh)	Cum've filtrate (l)	Deposit res'ce (1/m)
0	0.00	28.9	2389	0.000818	2197	0.00	1.20E-07
2	0.81	28.7	1932	0.000822	1784	0.75	6.61E+08
4	1.31	28.5	1384	0.000826	1284	1.27	2.03E+09
6	1.75	28.3	1268	0.00083	1182	1.68	2.45E+09
8	2.17	28.2	1222	0.000831	1142	2.08	2.64E+09
10	2.58	28	1168	0.000835	1096	2.46	2.87E+09
15	3.56	27.7	1126	0.000841	1064	3.37	3.04E+09
20	4.49	27.3	1079	0.000849	1030	4.26	3.24E+09
25	5.39	27	1042	0.000855	1001	5.12	3.42E+09
30	6.26	26.8	997	0.000859	962	5.96	3.67E+09
40	7.93	26.1	963	0.000873	944	7.57	3.80E+09
50	9.52	25.7	925	0.000881	916	9.15	4.00E+09
60	11.07	25.2	907	0.000891	908	10.70	4.06E+09
70	12.60	27.4	903	0.000847	859	12.20	4.45E+09
80	14.13	26.8	900	0.000859	868	13.66	4.37E+09
90	15.65	26.3	897	0.000869	876	15.14	4.31E+09

Membrane resistance: 2.86E+09 1/m

NORMAL File: FN31823M

Outer radius:	0.01	m	Flow rate:	18.0	l/m
Inner radius:	0.006	m	Inlet pressure:	1.55	Bar
Active length:	0.27	m	Outlet pressure:	0.16	Bar
Hydraulic dx4	0.008	m	Fluid density:	1000	kg/m^3
Solids conc:	3	% wt	Viscosity (25'C):	0.0009	Pa.s
Membrane ar	0.01018	m^2	Bulk velocity:	1.50	m/s
Flow area:	0.0002	m^2	Re:	13444	
Base press. (in,filt,out):	1.20	0.70	0.16	Bar	
Pressure (by inlet,outlet	1.05		0.70	Bar	
Average TMP	0.87	Bar	87299	Pa	

Time (min)	Cum' filtrate (l)	Temp ('C)	Flux raw data (lmh)	Viscosity (Pa.s)	Flux corrected (lmh)	Cum've filtrate (l)	Deposit res'ce (1/m)
0	0.00	21.8	2001	0.000963	2166	0.00	-1.7E-07
2	0.68	22.4	1634	0.00095	1744	0.73	6.57E+08
4	1.11	22.8	1215	0.000942	1286	1.25	1.86E+09
6	1.50	23.3	1140	0.000931	1192	1.67	2.22E+09
8	1.88	23.7	1104	0.000922	1144	2.07	2.43E+09
10	2.25	24.3	1076	0.00091	1100	2.45	2.63E+09
15	3.16	25.6	1064	0.000883	1055	3.36	2.86E+09
20	4.06	26.8	1054	0.000859	1017	4.24	3.07E+09
25	4.95	27.8	1047	0.000839	987	5.09	3.24E+09
30	5.83	28.9	1032	0.000818	949	5.91	3.48E+09
40	7.58	28.7	1001	0.000822	924	7.50	3.65E+09
50	9.23	27.5	953	0.000845	905	9.05	3.79E+09
60	10.81	27.3	913	0.000849	871	10.56	4.04E+09
70	12.33	26.5	878	0.000865	853	12.02	4.18E+09
80	13.79	25.9	843	0.000877	830	13.45	4.37E+09
90	15.19	25.4	825	0.000887	822	14.85	4.44E+09

Membrane resistance: 2.72E+09 1/m

TANGENTIAL File: FT41417U

Outer radius:	0.01	m	Flow rate:	14.0	l/m
Inner radius:	0.006	m	Inlet pressure:	1.17	Bar
Active length:	0.27	m	Outlet pressure:	0.09	Bar
Hydraulic dx4	0.008	m	Fluid density:	1000	kg/m^3
Solids conc:	3.4	% wt	Viscosity (25'C):	0.0009	Pa.s
Membrane ar	0.01018	m^2	Bulk velocity:	1.16	m/s
Flow area:	0.0002	m^2	Re:	10440	
Base press. (in,filt,out):	1.17	0.60	0.09	Bar	
Pressure (by inlet,outlet	0.60		0.60	Bar	
Average TMP	0.60	Bar	60044	Pa	

Time (min)	Cum' filtrate (l)	Temp ('C)	Flux raw data (lmh)	Viscosity (Pa.s)	Flux corrected (lmh)	Cum've filtrate (l)	Deposit res'ce (1/m)
0	0.00	24.7	1718	0.000901	1740	0.00	-8.9E-08
2	0.58	25.2	1489	0.000891	1491	0.59	3.89E+08
4	1.01	25.7	1199	0.000881	1187	1.04	1.08E+09
6	1.40	26.2	1120	0.000871	1095	1.43	1.37E+09
8	1.77	26.7	1085	0.000861	1049	1.80	1.53E+09
10	2.13	27.1	1048	0.000853	1004	2.14	1.70E+09
15	3.01	28.2	1024	0.000831	956	2.98	1.91E+09
20	3.87	29.5	985	0.000807	893	3.76	2.21E+09
25	4.69	29.1	944	0.000814	864	4.50	2.36E+09
30	5.47	28.7	894	0.000822	825	5.22	2.58E+09
40	6.96	28.2	853	0.000831	797	6.60	2.75E+09
50	8.36	27.8	809	0.000839	763	7.92	2.98E+09
60	9.70	27.2	769	0.000851	735	9.19	3.18E+09
70	10.97	26.8	736	0.000859	710	10.42	3.37E+09
80	12.20	26.5	713	0.000865	693	11.61	3.52E+09
90	13.39	26.1	703	0.000873	689	12.78	3.55E+09

Membrane resistance: 2.33E+09 1/m

TANGENTIAL File: FT41418Y

Outer radius:	0.01	m	Flow rate:	14.0	l/m
Inner radius:	0.006	m	Inlet pressure:	1.21	Bar
Active length:	0.27	m	Outlet pressure:	0.21	Bar
Hydraulic dx4	0.008	m	Fluid density:	1000	kg/m^3
Solids conc:	3.4	% wt	Viscosity (25'C):	0.0009	Pa.s
Membrane ar	0.01018	m^2	Bulk velocity:	1.16	m/s
Flow area:	0.0002	m^2	Re:	10440	
Base press. (in,filt,out):	1.17	0.60	0.09	Bar	
Pressure (by inlet,outlet	0.63		0.72	Bar	
Average TMP	0.68	Bar	67630	Pa	

Time (min)	Cum' filtrate (l)	Temp ('C)	Flux raw data (lmh)	Viscosity (Pa.s)	Flux corrected (lmh)	Cum've filtrate (l)	Deposit res'ce (1/m)
0	0.00	25.7	1991	0.000881	1970	0.00	1.94E-07
2	0.68	26.1	1694	0.000873	1661	0.67	4.31E+08
4	1.15	26.8	1346	0.000859	1299	1.17	1.20E+09
6	1.59	27.2	1268	0.000851	1212	1.60	1.45E+09
8	2.01	27.7	1230	0.000841	1163	2.00	1.61E+09
10	2.42	28	1186	0.000835	1113	2.39	1.78E+09
15	3.42	29.4	1140	0.000809	1036	3.30	2.09E+09
20	4.36	28.9	1081	0.000818	993	4.16	2.28E+09
25	5.25	28.7	1030	0.000822	951	4.98	2.48E+09
30	6.10	28.4	978	0.000828	909	5.77	2.70E+09
40	7.74	28.2	933	0.000831	871	7.28	2.92E+09
50	9.27	27.6	880	0.000843	834	8.73	3.15E+09
60	10.73	27.2	841	0.000851	804	10.12	3.36E+09
70	12.12	26.8	805	0.000859	777	11.46	3.56E+09
80	13.46	26.5	769	0.000865	748	12.75	3.79E+09
90	14.73	26.2	752	0.000871	736	14.01	3.88E+09

Membrane resistance: 2.31E+09 1/m

TANGENTIAL File: FT41420Z

Outer radius:	0.01	m	Flow rate:	14.0	l/m
Inner radius:	0.006	m	Inlet pressure:	1.38	Bar
Active length:	0.27	m	Outlet pressure:	0.34	Bar
Hydraulic dx4	0.008	m	Fluid density:	1000	kg/m^3
Solids conc:	3.4	% wt	Viscosity (25'C):	0.0009	Pa.s
Membrane ar	0.01018	m^2	Bulk velocity:	1.16	m/s
Flow area:	0.0002	m^2	Re:	10440	

Base press. (in,filt,out):	1.17	0.60	0.09	Bar	
Pressure (by inlet,outlet	0.81		0.86	Bar	
Average TMP	0.83	Bar	83147	Pa	

Time (min)	Cum' filtrate (l)	Temp ('C)	Flux raw data (lmh)	Viscosity (Pa.s)	Flux corrected (lmh)	Cum've filtrate (l)	Deposit res'ce (1/m)
0	0.00	25.7	2214	0.000881	2191	0.00	-3.0E-09
2	0.75	26.2	1853	0.000871	1813	0.74	5.33E+08
4	1.26	26.7	1431	0.000861	1384	1.29	1.49E+09
6	1.72	27.3	1342	0.000849	1280	1.74	1.82E+09
8	2.17	27.7	1296	0.000841	1225	2.16	2.02E+09
10	2.60	28.3	1254	0.00083	1168	2.57	2.24E+09
15	3.66	29.4	1219	0.000809	1108	3.53	2.50E+09
20	4.67	28.9	1170	0.000818	1075	4.46	2.65E+09
25	5.64	28.7	1120	0.000822	1034	5.35	2.86E+09
30	6.57	28.3	1056	0.00083	984	6.21	3.14E+09
40	8.33	27.7	1007	0.000841	952	7.85	3.33E+09
50	9.99	27.5	941	0.000845	893	9.42	3.72E+09
60	11.52	27.1	887	0.000853	850	10.90	4.03E+09
70	13.00	26.7	852	0.000861	824	12.32	4.24E+09
80	14.41	26.5	819	0.000865	795	13.69	4.49E+09
90	15.78	26.1	803	0.000873	788	15.03	4.56E+09

Membrane resistance: 2.56E+09 1/m

TANGENTIAL File: FT41621T

Outer radius:	0.01	m	Flow rate:	16.0	l/m
Inner radius:	0.006	m	Inlet pressure:	1.48	Bar
Active length:	0.27	m	Outlet pressure:	0.11	Bar
Hydraulic dx4	0.008	m	Fluid density:	1000	kg/m^3
Solids conc:	3.4	% wt	Viscosity (25'C):	0.0009	Pa.s
Membrane ar	0.01018	m^2	Bulk velocity:	1.33	m/s
Flow area:	0.0002	m^2	Re:	11942	
Base press. (in,filt,out):	1.47	0.75	0.11	Bar	
Pressure (by inlet,outlet	0.75		0.75	Bar	
Average TMP	0.75	Bar	75281	Pa	

Time (min)	Cum' filtrate (l)	Temp ('C)	Flux raw data (lmh)	Viscosity (Pa.s)	Flux corrected (lmh)	Cum've filtrate (l)	Deposit res'ce (1/m)
0	0.00	27.6	2129	0.000843	2017	0.00	2.27E-07
2	0.72	27.9	1830	0.000837	1721	0.68	4.32E+08
4	1.24	28.4	1470	0.000828	1367	1.21	1.20E+09
6	1.72	28.8	1380	0.00082	1272	1.66	1.47E+09
8	2.18	29.3	1321	0.000811	1203	2.08	1.70E+09
10	2.62	29.5	1252	0.000807	1135	2.47	1.96E+09
15	3.66	29	1193	0.000816	1094	3.42	2.12E+09
20	4.64	28.7	1130	0.000822	1043	4.32	2.35E+09
25	5.58	28.2	1071	0.000831	1001	5.19	2.55E+09
30	6.46	27.8	1008	0.000839	950	6.02	2.83E+09
40	8.15	27.2	967	0.000851	925	7.61	2.97E+09
50	9.74	26.6	909	0.000863	881	9.14	3.24E+09
60	11.23	26	863	0.000875	848	10.61	3.47E+09
70	12.67	25.6	831	0.000883	825	12.03	3.64E+09
80	14.05	25.2	802	0.000891	803	13.41	3.81E+09
90	15.39	25	787	0.000895	792	14.76	3.89E+09

Membrane resistance: 2.52E+09 1/m

TANGENTIAL File: FT41621V

Outer radius:	0.01	m	Flow rate:	16.0	l/m
Inner radius:	0.006	m	Inlet pressure:	1.48	Bar
Active length:	0.27	m	Outlet pressure:	0.11	Bar
Hydraulic dx4	0.008	m	Fluid density:	1000	kg/m^3
Solids conc:	3.4	% wt	Viscosity (25'C):	0.0009	Pa.s
Membrane ar	0.01018	m^2	Bulk velocity:	1.33	m/s
Flow area:	0.0002	m^2	Re:	11942	
Base press. (in,filt,out):	1.47	0.75	0.11	Bar	
Pressure (by inlet,outlet	0.75		0.75	Bar	
Average TMP	0.75	Bar	75281	Pa	

Time (min)	Cum' filtrate (l)	Temp ('C)	Flux raw data (lmh)	Viscosity (Pa.s)	Flux corrected (lmh)	Cum've filtrate (l)	Deposit res'ce (1/m)
0	0.00	21	1878	0.000981	2071	0.00	-1.2E-07
2	0.64	21.6	1654	0.000968	1799	0.70	3.71E+08
4	1.12	22.2	1342	0.000955	1440	1.25	1.07E+09
6	1.55	22.6	1237	0.000946	1315	1.72	1.41E+09
8	1.96	23.2	1203	0.000933	1261	2.16	1.58E+09
10	2.36	24	1161	0.000916	1195	2.57	1.80E+09
15	3.34	24.8	1142	0.000899	1153	3.57	1.95E+09
20	4.30	26.3	1115	0.000869	1088	4.52	2.21E+09
25	5.23	27.5	1084	0.000845	1030	5.42	2.48E+09
30	6.14	28.7	1060	0.000822	979	6.27	2.74E+09
40	7.93	28.4	1033	0.000828	961	7.91	2.83E+09
50	9.65	27.6	980	0.000843	928	9.52	3.02E+09
60	11.25	27	927	0.000855	890	11.06	3.25E+09
70	12.79	26.4	879	0.000867	856	12.54	3.48E+09
80	14.24	25.8	822	0.000879	812	13.95	3.80E+09
90	15.58	25.3	793	0.000889	792	15.32	3.96E+09

Membrane resistance: 2.45E+09 1/m

TANGENTIAL File: FT41626W

Outer radius:	0.01	m	Flow rate:	16.0	l/m
Inner radius:	0.006	m	Inlet pressure:	1.48	Bar
Active length:	0.27	m	Outlet pressure:	0.21	Bar
Hydraulic dx4	0.008	m	Fluid density:	1000	kg/m^3
Solids conc:	3.4	% wt	Viscosity (25'C):	0.0009	Pa.s
Membrane ar	0.01018	m^2	Bulk velocity:	1.33	m/s
Flow area:	0.0002	m^2	Re:	11942	

Base press. (in,filt,out):	1.47	0.75	0.11	Bar
Pressure (by inlet,outlet	0.76		0.85	Bar
Average TMP	0.80	Bar	80454	Pa

Time (min)	Cum' filtrate (l)	Temp ('C)	Flux raw data (lmh)	Viscosity (Pa.s)	Flux corrected (lmh)	Cum've filtrate (l)	Deposit res'ce (1/m)
0	0.00	28	2304	0.000835	2162	0.00	2.26E-07
2	0.78	28.4	1971	0.000828	1833	0.73	4.50E+08
4	1.34	28.2	1528	0.000831	1428	1.29	1.29E+09
6	1.82	28	1376	0.000835	1291	1.75	1.69E+09
8	2.27	27.8	1304	0.000839	1230	2.18	1.90E+09
10	2.70	27.7	1241	0.000841	1173	2.58	2.12E+09
15	3.74	27.5	1188	0.000845	1128	3.56	2.30E+09
20	4.72	27	1132	0.000855	1087	4.50	2.48E+09
25	5.67	26.9	1107	0.000857	1066	5.41	2.58E+09
30	6.60	26.5	1063	0.000865	1033	6.30	2.74E+09
40	8.37	26.1	1017	0.000873	997	8.02	2.93E+09
50	10.05	25.5	961	0.000885	956	9.68	3.17E+09
60	11.63	25.3	916	0.000889	915	11.27	3.42E+09
70	13.16	25	894	0.000895	900	12.80	3.52E+09
80	14.67	26.6	881	0.000863	854	14.29	3.85E+09
90	16.14	26.3	871	0.000869	850	15.74	3.87E+09

Membrane resistance: 2.51E+09 1/m

TANGENTIAL File: FT41624X

Outer radius:	0.01	m	Flow rate:	16.0	l/m
Inner radius:	0.006	m	Inlet pressure:	1.66	Bar
Active length:	0.27	m	Outlet pressure:	0.34	Bar
Hydraulic dx4	0.008	m	Fluid density:	1000	kg/m^3
Solids conc:	3.4	% wt	Viscosity (25'C):	0.0009	Pa.s
Membrane ar	0.01018	m^2	Bulk velocity:	1.33	m/s
Flow area:	0.0002	m^2	Re:	11942	

Base press. (in,filt,out):	1.47	0.75	0.11	Bar
Pressure (by inlet,outlet	0.93		0.99	Bar
Average TMP	0.96	Bar	95971	Pa

Time (min)	Cum' filtrate (l)	Temp ('C)	Flux raw data (lmh)	Viscosity (Pa.s)	Flux corrected (lmh)	Cum've filtrate (l)	Deposit res'ce (1/m)
0	0.00	28	2455	0.000835	2304	0.00	1.02E-07
2	0.83	27.8	2094	0.000839	1974	0.78	4.69E+08
4	1.42	27.7	1649	0.000841	1559	1.38	1.34E+09
6	1.95	27.6	1533	0.000843	1452	1.89	1.65E+09
8	2.46	27.4	1446	0.000847	1376	2.37	1.89E+09
10	2.93	27.2	1350	0.000851	1291	2.82	2.20E+09
15	4.06	26.8	1293	0.000859	1248	3.90	2.38E+09
20	5.13	26.3	1221	0.000869	1191	4.94	2.62E+09
25	6.14	26.2	1161	0.000871	1136	5.92	2.89E+09
30	7.10	26	1108	0.000875	1089	6.87	3.13E+09
40	8.95	25.5	1071	0.000885	1065	8.69	3.27E+09
50	10.73	25	1040	0.000895	1045	10.48	3.38E+09
60	12.48	27.4	1023	0.000847	973	12.20	3.84E+09
70	14.20	26.5	970	0.000865	942	13.82	4.06E+09
80	15.77	26	914	0.000875	898	15.38	4.39E+09
90	17.30	25.6	902	0.000883	895	16.90	4.42E+09

Membrane resistance: 2.81E+09 1/m

TANGENTIAL File: FT41825S

Outer radius:	0.01	m	Flow rate:	17.5	l/m
Inner radius:	0.006	m	Inlet pressure:	1.72	Bar
Active length:	0.27	m	Outlet pressure:	0.21	Bar
Hydraulic dx4	0.008	m	Fluid density:	1000	kg/m^3
Solids conc:	3.5	% wt	Viscosity (25'C):	0.0009	Pa.s
Membrane ar	0.01018	m^2	Bulk velocity:	1.45	m/s
Flow area:	0.0002	m^2	Re:	13069	
Base press. (in,filt,out):	1.72	0.88	0.13	Bar	
Pressure (by inlet,outlet	0.88		0.96	Bar	
Average TMP	0.92	Bar	91711	Pa	

Time (min)	Cum' filtrate (l)	Temp ('C)	Flux raw data (lmh)	Viscosity (Pa.s)	Flux corrected (lmh)	Cum've filtrate (l)	Deposit res'ce (1/m)
0	0.00	26.4	2385	0.000867	2322	0.00	2.31E-07
2	0.81	26.7	2007	0.000861	1941	0.79	5.24E+08
4	1.36	27.2	1562	0.000851	1493	1.37	1.48E+09
6	1.87	27.8	1460	0.000839	1377	1.86	1.83E+09
8	2.35	28.3	1386	0.00083	1292	2.31	2.12E+09
10	2.81	28.7	1310	0.000822	1210	2.73	2.45E+09
15	3.91	28.4	1254	0.000828	1166	3.74	2.64E+09
20	4.94	28	1186	0.000835	1113	4.71	2.89E+09
25	5.92	27.8	1140	0.000839	1075	5.64	3.09E+09
30	6.87	27.6	1082	0.000843	1025	6.53	3.37E+09
40	8.67	27.1	1037	0.000853	994	8.24	3.56E+09
50	10.39	26.8	991	0.000859	956	9.89	3.81E+09
60	12.03	26.4	951	0.000867	926	11.49	4.01E+09
70	13.62	26.2	916	0.000871	896	13.04	4.24E+09
80	15.14	25.8	889	0.000879	877	14.54	4.38E+09
90	16.63	25.6	878	0.000883	871	16.02	4.43E+09

Membrane resistance: 2.66E+09 1/m

TANGENTIAL File: FT41826R

Outer radius:	0.01	m	Flow rate:	17.7	l/m
Inner radius:	0.006	m	Inlet pressure:	1.76	Bar
Active length:	0.27	m	Outlet pressure:	0.14	Bar
Hydraulic dx4	0.008	m	Fluid density:	1000	kg/m^3
Solids conc:	3.5	% wt	Viscosity (25'C):	0.0009	Pa.s
Membrane ar	0.01018	m^2	Bulk velocity:	1.47	m/s
Flow area:	0.0002	m^2	Re:	13219	
Base press. (in,filt,out):	1.76	0.89	0.13	Bar	
Pressure (by inlet,outlet	0.90		0.90	Bar	
Average TMP	0.90	Bar	89873	Pa	

Time (min)	Cum' filtrate (l)	Temp ('C)	Flux raw data (lmh)	Viscosity (Pa.s)	Flux corrected (lmh)	Cum've filtrate (l)	Deposit res'ce (1/m)
0	0.00	27.6	2387	0.000843	2261	0.00	-1.2E-07
2	0.81	27.6	2021	0.000843	1914	0.77	4.85E+08
4	1.37	27.5	1576	0.000845	1497	1.35	1.37E+09
6	1.88	27.2	1432	0.000851	1369	1.83	1.75E+09
8	2.34	27.1	1330	0.000853	1274	2.28	2.08E+09
10	2.78	26.9	1254	0.000857	1207	2.70	2.34E+09
15	3.83	26.5	1207	0.000865	1172	3.71	2.49E+09
20	4.83	26.3	1141	0.000869	1114	4.68	2.76E+09
25	5.77	26	1085	0.000875	1067	5.60	3.00E+09
30	6.67	25.7	1031	0.000881	1020	6.49	3.26E+09
40	8.39	25.2	1005	0.000891	1006	8.21	3.34E+09
50	10.08	27.8	988	0.000839	932	9.85	3.82E+09
60	11.74	26.8	968	0.000859	934	11.43	3.81E+09
70	13.36	26.3	931	0.000869	909	13.00	3.99E+09
80	14.90	25.7	893	0.000881	884	14.52	4.18E+09
90	16.39	25.2	878	0.000891	879	16.01	4.21E+09

Membrane resistance: 2.68E+09 1/m

TANGENTIAL File: FT41826Q

Outer radius:	0.01	m	Flow rate:	17.8	l/m
Inner radius:	0.006	m	Inlet pressure:	1.77	Bar
Active length:	0.27	m	Outlet pressure:	0.13	Bar
Hydraulic dx4	0.008	m	Fluid density:	1000	kg/m^3
Solids conc:	3.4	% wt	Viscosity (25'C):	0.0009	Pa.s
Membrane ar	0.01018	m^2	Bulk velocity:	1.48	m/s
Flow area:	0.0002	m^2	Re:	13294	

Base press. (in,filt,out):	1.77	0.90	0.13	Bar
Pressure (by inlet,outlet	0.90		0.90	Bar
Average TMP	0.90	Bar	90161	Pa

Time (min)	Cum' filtrate (l)	Temp ('C)	Flux raw data (lmh)	Viscosity (Pa.s)	Flux corrected (lmh)	Cum've filtrate (l)	Deposit res'ce (1/m)
0	0.00	24.5	2264	0.000905	2304	0.00	-1.5E-07
2	0.77	25	1947	0.000895	1958	0.78	4.66E+08
4	1.32	25.7	1555	0.000881	1539	1.37	1.31E+09
6	1.82	26	1447	0.000875	1422	1.88	1.63E+09
8	2.30	26.5	1394	0.000865	1354	2.35	1.85E+09
10	2.77	26.9	1336	0.000857	1286	2.80	2.09E+09
15	3.89	28	1295	0.000835	1215	3.86	2.36E+09
20	4.97	28.4	1243	0.000828	1156	4.86	2.62E+09
25	6.00	27.9	1191	0.000837	1121	5.83	2.79E+09
30	6.99	27.5	1130	0.000845	1073	6.76	3.03E+09
40	8.87	26.7	1086	0.000861	1050	8.56	3.15E+09
50	10.67	26	1037	0.000875	1019	10.31	3.33E+09
60	12.39	25.6	995	0.000883	987	12.02	3.52E+09
70	14.05	25	985	0.000895	990	13.69	3.50E+09
80	15.73	27.2	983	0.000851	940	15.33	3.83E+09
90	17.39	29.3	975	0.000811	888	16.88	4.20E+09

Membrane resistance: 2.64E+09 1/m

Appendix 6 Relevant Published Papers

<<Crossflow Filtration of Seawater>>
Holdich R G, Zhang G M, Boston J S
Filt & Sep Mar/Apr (1991) pp117-120

<<Seawater Crossflow Filtration>>
Holdich R G, Zhang G M
Filtech'91 pp19-27 Karlsruhe, Germany

<<Crossflow Microfiltration Incorporating Rotational Fluid Flow>>
Holdich R G, Zhang G M
Trans IChemE v70 Part A Sept(1992) pp527-536

Crossflow Filtration of Seawater

By R G Holdich, G M Zhang and J Boston

Department of Chemical Engineering, University of Technology, Loughborough, Leicestershire, LE11 3TU

This paper was presented to the Vth World Filtration Congress, Nice, France, June 1990

Oil is often recovered by means of water flood and the North Sea Oil industry uses filtered seawater for this purpose. Both space and weight are at a premium on offshore oil platforms, hence filtration techniques making use of smaller and light-weight apparatus are of particular interest to this industry. Crossflow filtration has these advantages over deep bed and cartridge filtration. Other uses for filtered seawater include desalination and cooling water duties, where the required flows are also large. Crossflow filters using membranes in sheet, tubular and capillary form have been tested for this duty. Simulated seawater test suspensions have been used, including an investigation of the affect of fish oils (lipids) on the filtrate flux rate. This was found to be a major contributor to flux decline. Flux rates in excess of 2 $m^3.m^{-2}.hr^{-1}$ were achieved with most of the membranes, even under highly fouling test conditions, indicating that this technology could be usefully applied in the oil industry.

The crossflow filtration of seawater has been under investigation at Loughborough University[1] and other research establishments[2,3], for some years. The oil industry uses seawater filtered at 2μm; 98% removal of particulates above this size is usually required[3]. Clearly, this specification assumes a constant feed suspension and an alternative specification requires less than 2000 particles per ml. greater than 2 μm and absolute filtration at 5 μm. The solids need to be removed from the water to prevent deposition and blockage, within the pores of the oil reservoir rock during the water flood as well as to protect injection equipment. The volume of water required in the water flood can be as high as 2600 $m^3.hr^{-1}$ (400 000 barrels of water per day), for a field and is rarely less than 650 $m^3.hr^{-1}$. Deep bed or cartridge filters are used at present.

Nature of seawater. North Sea seawater used in reservoir injection is reasonably clean, containing between 0.2 and 0.8 $mg.l^{-1}$ of suspended solids and it is usually pumped up from a depth of 200 ft (61m).

The major contaminants are clays, sand, bacteria and plankton which are usually filtered out in the deep bed or cartridge filters. The seawater solids loading is highly seasonal; *blooms* of plankton occur in the spring and autumn and during these periods the suspended solids content is increased considerably. It has been reported that the major cause of fouling of the seawater filter cartridges is due to the lipid content of plankton[4] which is released into suspension when the organisms are crushed by the pumps and filters. The resulting lipid concentration can rise to as high as 20 $mg.l^{-1}$ during a bloom period. The lipids are fatty materials which act as a glue; sticking the suspended solids to the filter surface thus encouraging blockage[4].

Experimental

Challenge suspensions. Figure 1 shows the particle size distribution of suspended solids measured in seawater[2] and the size distribution of the silica material used to make the challenge suspensions for the laboratory tests. The lipid tests used fish lipid concentrate capsules with eicosapentaenoic and docosahexaenoic acids, purchased from *Boots the Chemists Ltd.*

Membrane types and rigs. The initial rig was constructed out of PVC and was designed to accommodate the sheet membrane in a plate and frame fashion[1]. The membrane dimensions on each plate are 0.2 × 1m (width × height). Gelman Sciences *Versapor* membranes have been extensively investigated using this rig. The use of PVC enabled a light-weight filter, resistant to chemical attack, to be built — these are important considerations in offshore use.

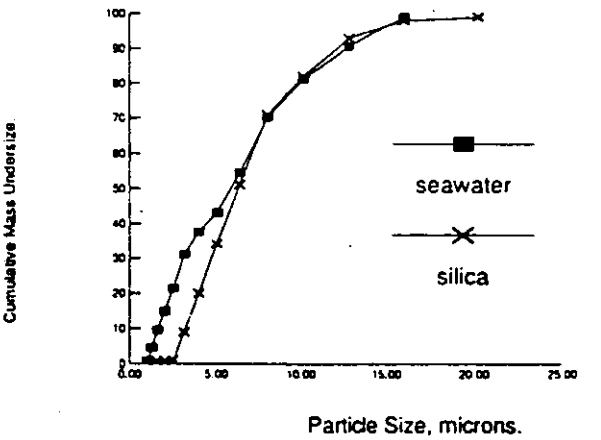

Fig 1. Size distribution of solids in seawater and silica.

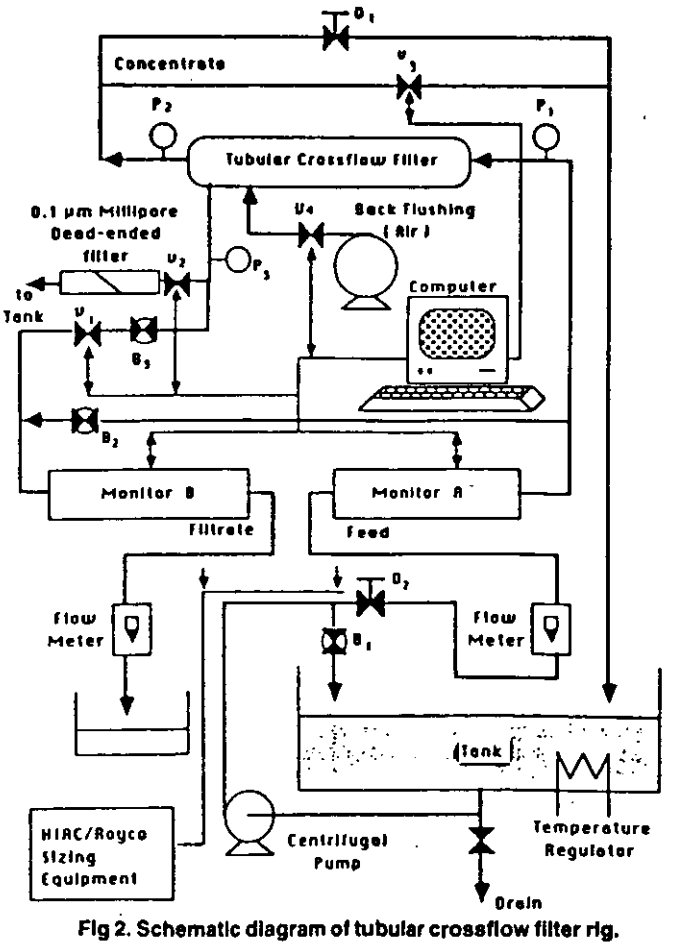

Fig 2. Schematic diagram of tubular crossflow filter rig.

The second rig, developed much later, was built to commodate both tubular and capillary membrane odules. This is shown schematically in Fig 2. Both rigs ve electronically controlled solenoid valves, described follows:

V_1 is responsible for controlling permeate flow from the filter.
V_2 is used to control the flow through the rig clean-up filter (Millipore 0.1μm cartridge).
V_3 controls the outlet pressure from the filter.
V_4 is responsible for controlling the filter backflush.

ne clean-up filter was only used to remove suspended aterial from the tap-water prior to commencing an periment. During crossflow filtration V_2 was closed.

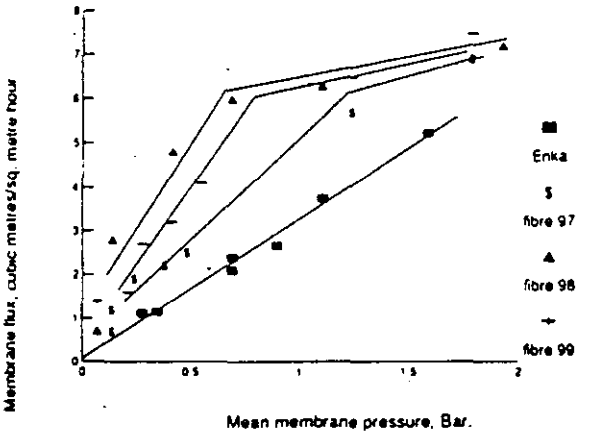

Fig 3. Water flux rates in tubular and capillary membranes.

Backflushing with compressed air was employed to ean most of the membranes and the period between, nd duration of, backflushes was controlled by the com- uter program. Particle monitors were also developed nd employed on the filter feed and filtrate lines to neck the quality of the water.

An Enka 1.8 mm capillary membrane and tubular etal fibre membranes were tested using the above rig. he clean water flux rates for these membranes are iven in Fig 3. The fluxes shown were obtained from uns using a variety of crossflow rates ranging from 4 to 0 l/min through the filter (8 500 < Re < 42 500). This fig- re demonstrates that, up to a flux rate of $6 m^3.m^{-2}.hr^{-1}$, ne permeate rate which is a unique function of mem- rane pressure, was independent of crossflow velocity. his can be true only when filtering clean water. The embrane resistance (R_m) can be calculated from a re- rranged form of Darcy's Law as follows:

$$J = \left(\frac{1}{\mu R_m}\right) \Delta P$$

here J is the flux rate, μ is the viscosity and ΔP is the ean membrane pressure.

For the Versapor 3000 sheet membrane, the mem- rane flux increased linearly with mean membrane ressure; from 2.1 to 9.2 $m^3.m^{-2}.hr^{-1}$ on increasing the ressure from 0.4 to 0.8 Bar.

igh solids suspension. During a bloom period the con- entration of suspended solids in seawater can rise as igh as 10 $mg.l^{-1}$, therefore, the initial series of mem- rane tests were devised using this concentration of sil- a suspended in tap water. The membrane flux rate and etention efficiency were investigated. The flux rates btained from the three metal fibre membranes are nown in Fig 4. Backflushing with compressed air at 3.5 ar was used to clean the membranes at both flow rates nown.

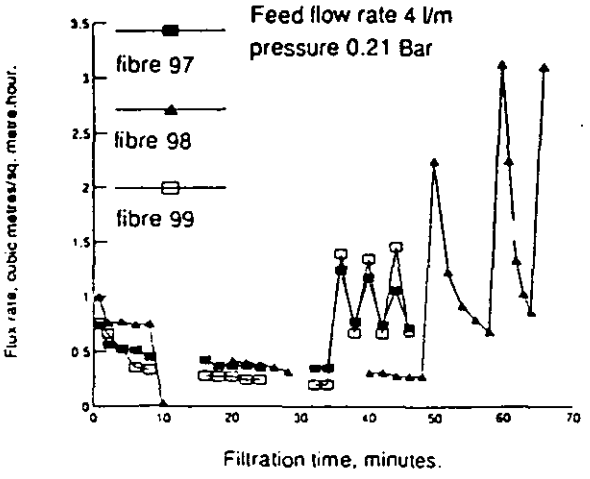

Fig 4a. Flux rates with metal fibre filters. (Re of 8 500).

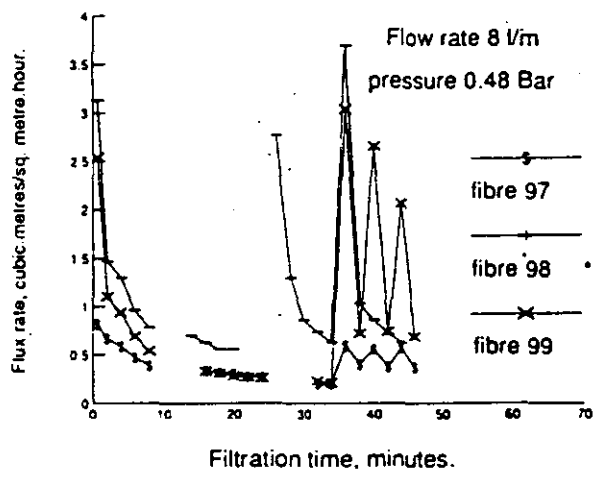

Fig 4b. Flux rates with metal fibre filters. (Re of 42 500).

The particle retention was measured by taking a sample stream from both the filter feed and filtrate through a model 346BCL Hiac Royco particle detector and counter. This enabled the number of particles in suspension, down to a particle size of 0.72 μm, to be measured. The retention efficiencies are tabulated below.

Filter No	Flow rate	Retention efficiency (%) in grade (μm)			
(-)	(l/min)	>3	3 - 2	2 - 1.1	1.1 - 0.72
97	4	100	100	99.9	99.9
97	8	100	100	99.9	99.9
98	4	100	99.7	99.7	99.7
98	8	100	99.9	99.9	99.9
99	4	100	100	100	99.9
99	8	100	100	99.9	99.9

Table 1. Particle retention efficiencies of metal fibre filters.

The flux obtained from the Versapor 3 000 membrane, operating on a similar challenge suspension is shown in Fig 5. Once again, backflushing was performed using compressed air at 3.5 Bar. The duration of the reverse flow was 1 s.

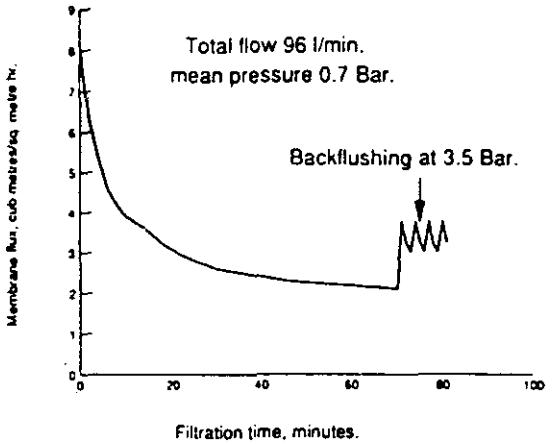

Fig 5. Flux from the Versapor 3000 membrane.

Lipid containing suspensions. The above tests indicate a reasonable flux rate, sufficient for offshore use. Thus these membranes were subjected to challenge suspensions containing lipids (fish oil). The literature suggests that lipid containing suspensions represent the most fouling fluids that the membranes will have to operate on.

Tubular metal membranes. These membranes were tested at a mean membrane pressure of 1.2 Bar and flow rate of 12 l/min (Re of 25 500). Three lipid concentrations were tested: 5, 10 and 20 mg.l^{-1}. Before the lipid was added to the membrane system the flux rate obtained during the filtration of clean water, and 2 mg.l^{-1} silica suspended in clean water, was checked. The lipid was added to the system after the second filtration, hence the suspended solids concentration during the lipid tests was also 2 mg.l^{-1}. This is still a relatively high concentration of solids for offshore seawater filtration. The results are shown in Fig 6.

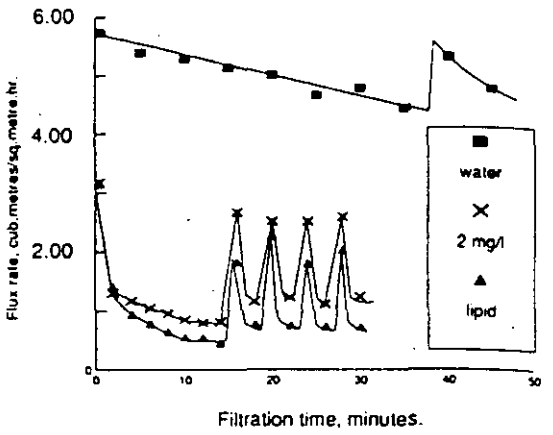

Fig 6a. Permeate flux rate at 5 mg/l of lipid.

These figures show that the *clean* water flux rate, operating at a mean membrane pressure of 1.2 Bar, is between 5 and 7 m^3.m^{-2}.hr^{-1}. Increasing the lipid concentration decreased the membrane flux rate and caused the flux to decay more rapidly after backflush. Backflushing with compressed air at 3.5 Bar restored acceptable membrane flux rates, even on filtering a suspension containing 2 mg.l^{-1} of silica and 20 mg.l^{-1} of lipids.

After each of the above tests the membrane was removed from the filter holder and washed in solvent to dissolve the fish oil, in accordance with the technique given by reference 4. The masses of fish oil measured on the filter, and the measured concentration of oil in the feed, are shown in Table 2.

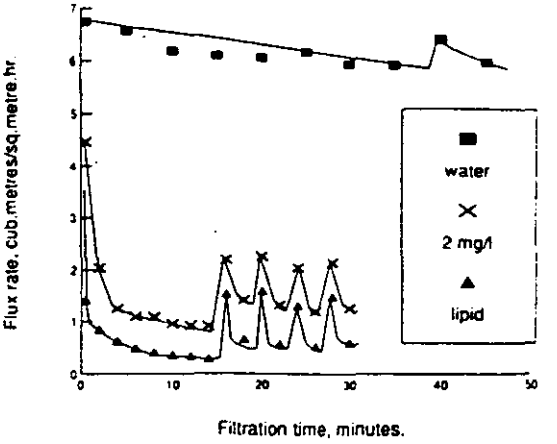

Fig 6b. Permeate flux rate at 10 mg/l of lipid.

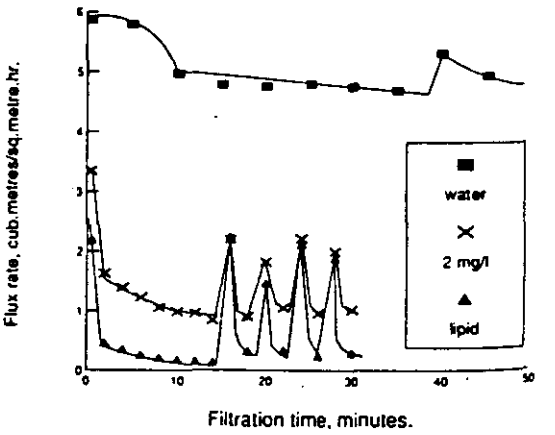

Fig 6c. Permeate flux rate at 20 mg/l of lipid.

Nominal lipid concentration in feed (mg.l^{-1})	Measured lipid concentration in feed (mg.l^{-1})	Measured lipid mass on filter (mg)
5	5	34.8
10	13	81.9
20	25	192.4

Table 2. Lipid concentration in the feed and sticking to the filter.

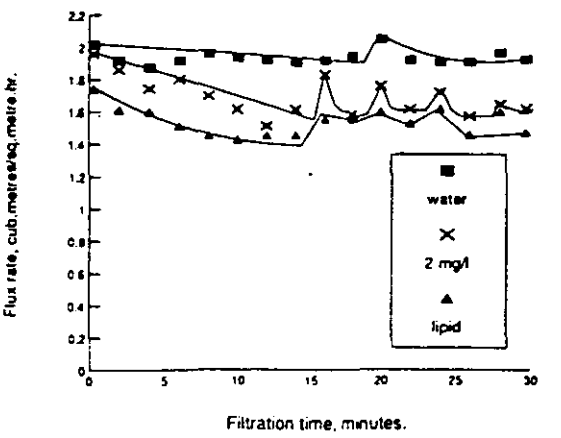

Fig 7. Permeate flux rate at 5 mg/l of lipid.

Enka capillary. Figure 7 shows the results for the same test suspension used with the Enka polypropylene membrane at a lipid concentration of 5 mg.l^{-1} and a mean membrane pressure of 0.7 Bar. This membrane is

ed at 0.2μm pore size and is made out of a hydrophobic material. Before use the membrane has to be , with a low surface tension liquid, for example, A. and backflushing with air cannot be employed for mbrane cleaning because it would be necessary to et the membrane after backflushing. A water backsh was therefore employed using a pump delivering a kflush pulse of 2.8 Bar.

Comparing Figs. 3, 6 & 7 shows that the clean water x rate is lower for the Enka membrane than for the tal fibre ones, but the average flux rate during the filtion of a lipid containing suspension is similar.

rsapor 3000. Figure 8 shows the flux obtained from riable lipid concentration test suspensions challeng- this membrane at 80 l.min^{-1} feed flow rate and mean mbrane pressure of 0.7 Bar. Also shown on this fig- are the flux rates using tap-water and a 2 mg.l^{-1} sil- concentration.

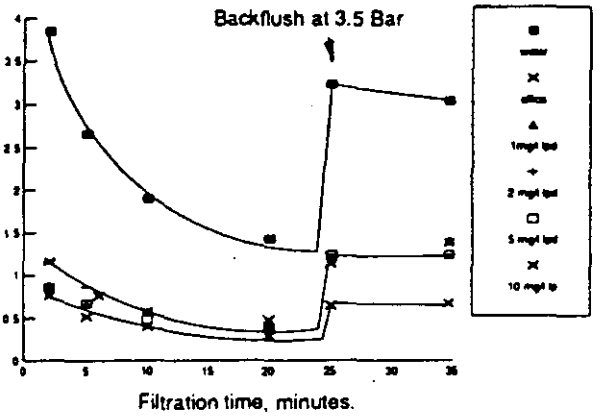

Fig 8. Permeate flux rate at variable lipid concentration

mparison of membrane types. The three different embrane types: tubular, capillary and sheet, give simr flux rates when operating on lipid containing, and ghly fouling suspensions. Backflushing with air or ater was successful in maintaining reasonable permee flux rates. The most appropriate membrane for seater filtration for offshore oil-production depends on ner factors which may be important. The most impornt of these are summarised below:

Membrane packing density. — To provide 650 m^3.hr^{-1}, approximately 400 m^2 of membrane area is required; sheet membrane can be packed most tightly and tubular membrane the least so.

Cost. — Metal fibre tube is the most expensive whilst polymer is the least expensive.

Convenience. — Capillary membrane modules can be easily replaced on the rig, requiring minimal labour. On the other hand sheet membrane is time consuming to replace.

Operating pressure. — Increasing the membrane pressure increases flux. The polymer membranes are limited to pressures of around 2 Bar whilst the metal tubes can operate up to 10 Bar.

Membrane antifouling techniques, such as cleaning the membrane with a D.C. current can be applied to metal membranes.

Coarse filtration, prior to membrane filtration, can be avoided with the metal tubular membranes, thus saving further space and weight on an oil rig.

There is evidence to suggest that the flow distribution in the plate and frame membrane filter is poor, with *dead* areas in the feed channels towards the periphery of the filter plate.

In addition, chemical resistance to both seawater and membrane cleaning fluids must be considered.

Filter unit size. The required 400 m^2 of membrane area could be provided by a series of membrane modules operating in parallel. To provide an indication of the overall filter unit size this can be calculated for the Enka membranes as follows. The largest module commercially available has 10 m^2 membrane area, therefore 40 modules would be required. The dimensions of such a module are (width by height): 0.15 × 1.0 m. Allowing for access space around the modules and for extra modules to act as standby units, a typical crossflow filter unit would be 1 m long, 2.5 m high and 2 m wide. This would require a floor area of 2 m^2. The materials of construction are polymeric are hence light-weight and the resulting filter unit is, therefore, both compact and light-weight.

Conclusions

Seawater is a relatively clean process fluid to filter, for most of the year. Under these circumstances flux rates of up to 5m^3.m^2.hr^{-1} can be achieved, with a membrane pressure drop of 1 to 2 Bar. During a *bloom* period, however, flux rates could easily fall below 1 m^3.m^{-2}.hr^{-1}. Under these conditions frequent cleaning is needed in order to maintain a flux rate of between 1 and 2 m^3.m^{-2}.hr^{-1}. This cleaning can be achieved by backflushing the membrane with air or water.

Under the conditions reported above the polymer membranes were *not* more seriously affected by the presence of oils in water than the metal membranes and flux rates during the filtration of oil containing suspensions appears to be fairly independent of membrane type. This can be explained by the formation of a dynamic or secondary membrane on the surface of the fixed membrane, consisting of the suspended material within the water. After this has formed, further filtration is controlled by the resistance and rejection capabilities, of this dynamic membrane.

The choice of the most appropriate membrane type for the crossflow filtration of seawater does not, therefore, depend on flux and rejection capabilities, but on a multitude of other factors such as ease of cleaning, membrane packing density and robustness.

Acknowledgements

The authors of this paper wish to record their gratitude for a Science and Engineering Research Council grant to support a project of which this work formed a part. The project is administered through the Marine Technology Directorate Ltd, and is also supported by the following: BP Exploration, Texaco, Amoco, Chevron, Occidental, Elf, Marathon, Hamilton Brothers and Unocal.

References

1. Carter, A. J., An Experimental Study of Crossflow Filtration and the Design of a Prototype Crossflow Filter, M. Phil. Thesis, Loughborough University of Technology (1982).
2. Knibbs, R. H., The Development of a High Flux Microfilter with a Wide Range of Applications, Filtech 81, London (1981), Filtration Society, pp 59,68.
3. Abdel-Ghani, M. S., Jones, R. E. and Wilson, F. G., Crossflow Membrane Filtration of Seawater, Filtration and Separation (1988), pp 105,109.
4. Edyvean, G. J. and Lynch, J. L., The Effect of Organic Fouling on the Life of Cartridge Filters, Filtech 89, Karlsruhe (1989), Filtration Society, pp 10,17.

SEAWATER CROSSFLOW FILTRATION

R.G. Holdich and G.M. Zhang, Department of Chemical Engineering,
University of Technology, Loughborough, Leics. LE11 3TU.

Filtered seawater is used in the offshore oil industry for both topside duties such as cooling and for injection into oil reservoirs to displace the crude oil. It is filtered to prevent damage to equipment and blockage of the reservoir. The required filtrate rate can be substantial. Various crossflow filter designs and geometries for this duty have been studied, both in the laboratory and at a seawater test centre. Organic fouling of both microfiltration and ultrafiltration membranes was apparent, with high average flux rates obtained only when it was possible to mechanically remove the fouling layer. The calculated membrane resistance was also shown to increase with fouling and was dependent on hydrodynamic conditions. Thus membrane resistance must be determined *in-situ* when modelling similar crossflow filtration systems.

INTRODUCTION

There are several industries which use seawater, one of the largest being North Sea oil production. Oil lies within the pore spaces of a rock, normally sandstone, and water is used to displace oil from the reservoir by pumping under considerable pressure. The seawater is often filtered to remove suspended material which would otherwise "filter" out within the rock formation. This would eventually lead to clogging of the reservoir. Some production platforms now employ Reverse Osmosis (R.O.) on the injection water to reduce the concentration of sulphate ions present, thus reducing the precipitation of barium sulphate in the rock formation.

Filtration is also employed to protect equipment which uses seawater on the oil platform: R.O., water sealed pumps, cooling, etc. On some platforms over 50% of the water drawn up from the sea is used for duties other than injection. The total flow of filtered water can be over 750 $m^3.h^{-1}$. Fine filtration is achieved at present by means of deep bed or cartridge filters. These perform quite adequately over a large part of the year but frequently become clogged by the seasonal algal blooms. On an offshore platform space and weight are at a premium and any new technology which could reduce these and overcome the seasonal variation is beneficial.

Water used for cooling water duties is at present filtered on 80 μm coarse screens, whereas the injection water is filtered so that less than 2 to 3 thousand particles per ml greater than 2 μm are present.

laboratory trials

The initial trials have been reported elsewhere (1), and were conducted to identify membrane types which might be suitable for further tests. Some of the factors of major importance which were assessed included particle retention size, filtrate flux rate, chemical compatibility with seawater. Various different geometries were evaluated, including capillary, tubular and flat sheet membranes. A brief description of the membranes used in this phase is included in the appendix.

The first problem with any laboratory test is to identify a suitable challenge suspension for the filters; one representative of the end use. The challenge suspensions employed were as follows:

i) tap-water,
ii) silica solids all sub 20 μm with d_{50} of 7 μm in tap-water,
iii) above plus lipids, and
iv) seawater algae suspensions.

Solids concentrations up to 10 $mg.l^{-1}$, and the lipid concentrations to 20 $mg.l^{-1}$ were used. The presence of lipid material has been identified as the major cause of membrane fouling in seawater filtration (2), and concentrations up to 20 $mg.l^{-1}$ are very high. Filtration performance of the most suitable membranes, using the first three test suspensions, are summarised in the appendix.

Tests were conducted with membrane types other than those shown, such as a dynamic membrane system (3), a tubular sintered metal powder membrane and a polymer depth filter. The last two types of filter both suffered from irreversible clogging of the media, a consequence of the depth filtration mechanism. All the membranes in the appendix produced a filtrate of acceptable quality in terms of number of particles above 2 μm. Filtrate fluxes were reasonably similar under similar flow conditions due, possibly, to the formation of a dynamic or secondary membrane, and further tests at a seawater test facility went ahead with the metal and ceramic filters. The polypropylene membrane was not tested because it needed wetting prior to use and could not be allowed to dry out during operation. This was thought to be an unacceptable operating complication in this industrial process.

Further laboratory studies were conducted on a small (0.05 by 0.51 m), sheet membrane system to investigate the effect of increasing membrane resistance during filtration, and different flow conditions. Versapor 0.2 μm membrane and Bekaert "3 AL 3" metal membrane were used, and a challenge suspension containing *Dunaliella tertiolecta* (CCAP 19/6B); a seawater algae cultured from a Norwegian Fjord. The challenge suspension concentration was approximately 1 $mg.l^{-1}$, and the size distribution is shown in Figure 1.

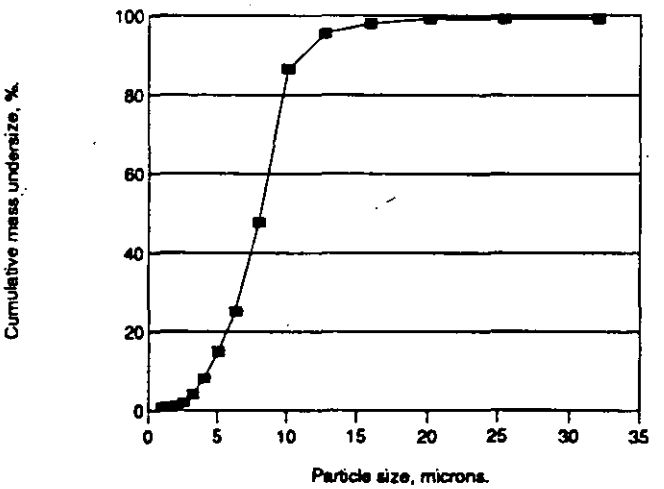

Figure 1 Filtered tap-water with seawater algae - size distribution

Membrane resistance during filtration was calculated according to the "cake" filtration theory as applied to microfiltration:

$$J = \frac{\Delta P}{\mu(R_c + R_m)} \quad (1)$$

where J is filtration flux, ΔP is transmembrane pressure, μ is viscosity and R_m and R_c are membrane and deposit resistance, respectively. The membrane resistances, determined *in-situ*, for the metal membrane are shown in Table 1

Table 1 Metal membrane resistances during crossflow filtration

Challenge suspension	membrane resistance (m^{-1})
filtered tap-water	$(0.3 \text{ to } 1.0)10^{10}$
2 $mg.l^{-1}$ silica	$(0.5 \text{ to } 2.2)10^{10}$
10 $mg.l^{-1}$ silica	$(6 \text{ to } 13)10^{10}$
as above plus algae	$(6 \text{ to } 11)10^{10}$

The polymer membrane results are given in Table 2. The challenge suspensions were tap-water filtered at 0.2 µm, and filtered water plus algae at a concentration of 1 $mg.l^{-1}$.

Table 2 Polymer membrane resistances during crossflow filtration

Challenge suspension	Reynolds number (-)	Membrane pressure (Bar)	Membrane resistance (m^{-1})
filtered tap-water	2500	0.6	$5.1x10^{11}$
filtered tap-water	2500	1.7	$9.4x10^{11}$
filtered tap-water	2500	2.2	$10.1x10^{11}$
filtered tap-water	2500	2.8	$11x10^{11}$
filtered tap-water	7500	0.6	$5.9x10^{11}$
filtered tap-water	7500	1.1	$7.8x10^{11}$
filtered tap-water	7500	1.7	$9.1x10^{11}$
filtered tap-water	7500	2.2	$8.8x10^{11}$
filtered tap-water	12400	0.3	$1.0x10^{11}$
filtered tap-water	12400	1.0	$1.8x10^{11}$
filtered tap-water	12400	1.5	$2.1x10^{11}$
filtered tap-water	12400	2.1	$2.1x10^{11}$
with algae	12400	0.28	$3.2x10^{11}$
with algae	10000	0.34	$4.4x10^{11}$
with algae	7500	0.48	$6.4x10^{11}$
with algae	2500	0.55	$9.7x10^{11}$

Filtrate fluxes during the algae suspension filtrations are shown in Figures 2 and 3 for the metal and polymer membranes, respectively.

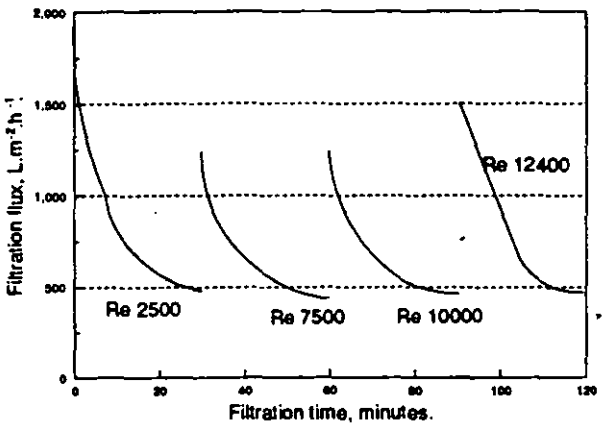

Figure 2 Filtration of seawater algae on metal membrane

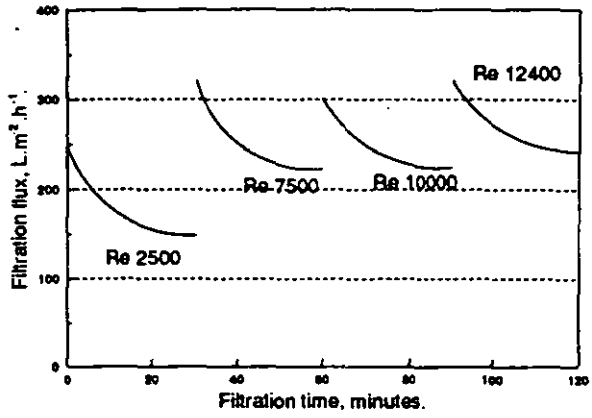

Figure 3 Filtration of seawater algae on 0.2 µm polymer membrane

The presence of algae did not affect the metal membrane resistance. The polymer membrane resistance in the presence of algae is significantly greater than without it, Table 2. It is also noticeable that increasing pressure increased the polymer membrane resistance, and increasing the shear rate on the surface decreased it. Clearly, some suspended material remained after filtering the tap-water which then deposited on the membrane surface. All the above resistances are membrane resistances ***only***, i.e not including the cake or deposit resistance. It is this deposit which must mechanically combine with the membrane to provide a new membrane resistance. Membrane resistance cannot, therefore, be assumed to be constant and equal to that given by a clean water permeation test. It must be determined ***in-situ***, a similar situation to that of classical cake filtration. Further evidence of the intimate relation between the membrane and deposit, and of the reason for the different membrane resistance performance of these two filters, is shown in Figures 7 and 8. Further discussion is left until that Section.

seawater trials

The membrane filters that showed promise during the initial laboratory trials were taken to a seawater test facility for further trials. These ran over late August and September 1990. This was not a bloom period. Nine samples of seawater were taken throughout the trial period, and the Coulter Counter analyses for these are shown in Table 3.

Table 3 Seawater Particle Size Distribution and Solid Concentration during trial period

	Concentration ($mg.l^{-1}$)	Cumulative mass % less than size in microns:				
		32	20	10	5	1.3
1	0.7	88	81	76	68	20
2	1.3	98	88	69	42	6
3	1.5	98	93	76	45	6
4	4.7	91	84	48	14	2
5	0.8	99	95	85	69	13
6	1.1	86	70	52	28	8
7	0.9	89	82	63	43	11
8	2.2	92	78	54	34	4
9	0.9	92	83	63	46	14

Variation in the trial fluid is inevitable when undertaking field trials, but the variation between samples shown above is not substantial. Meaningful comparisons between the filter performance can, therefore, be made.

During all the trials a mean transmembrane pressure of 1.1 Bar was maintained. It was not possible to test under identical conditions of Reynolds (Re) number, however. The flux curves shown in Figures 4 to 6 were obtained by continually monitoring the filtrate rate by a "litre meter" connected to a chart recorder. Backflushing at pressures up to 5 Bar was tested during the trials but it was found to be ineffective in all cases except in the presence of a membrane precoat, this will be discussed later. Chemical cleaning of the membranes was also investigated, both on site and back in the laboratory, but this was also discovered to have little effect in restoring the initial membrane flux. The chemical cleaners used were solutions of 5% citric acid, Ultrasil 50 and Ultrasil 11. Thus the fouling was deemed to be irreversible.

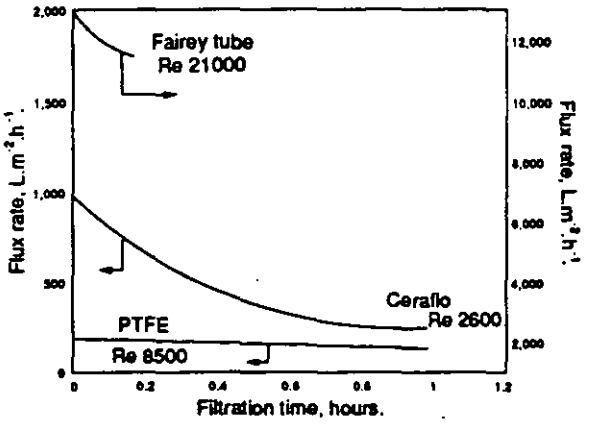

Figure 4 Filtrate flux rate for various membranes

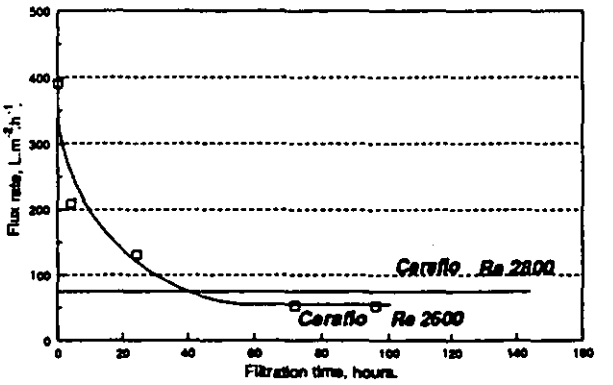

Figure 5 Ceramic membrane flux over several days

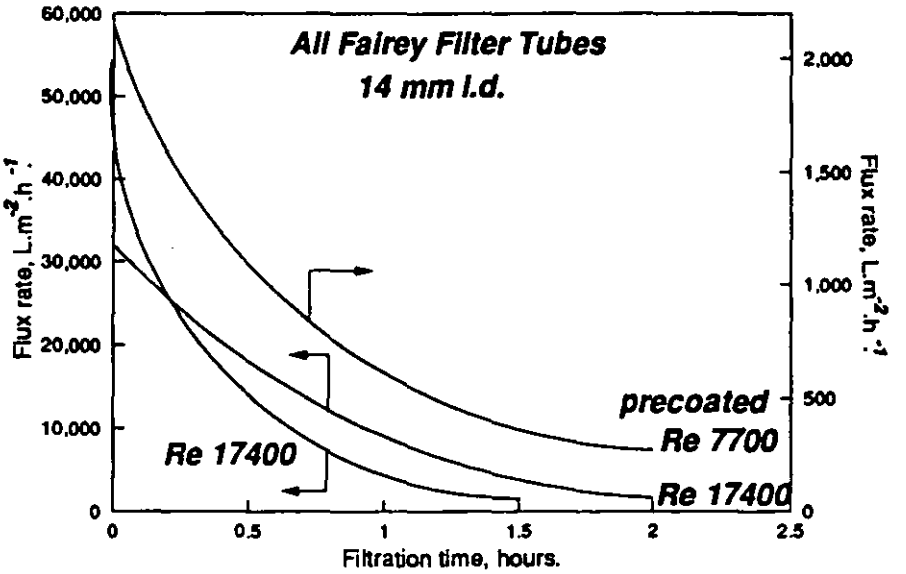

Figure 6 Filtrate flux rate for metal membrane with and without precoat

Figure 6 shows the effect of mixing dicalite speedplus with seawater, filtering at a concentration of 0.5 $g.l^{-1}$ and then introducing seawater at a solids content of 1 $mg.l^{-1}$, i.e a precoated filtration. After precoating the flux then decayed in the same manner as the other filtrations shown. After 2 hours, however, a backflush resulted in a flux rate in excess of 30,000 $l.m^{-2}.h^{-1}$, which subsequently decayed to 400 $l.m^{-2}h^{-1}$. Backflushing was not effective in restoring flux in any other filtration. Clearly, the precoat protected the metal membrane from intrusion of fine

suspended material and irreversible fouling. A new metal membrane filter tube, without precoat, is also shown in Figure 6, flux decaying from over 50,000 to 400 $l.m^{-2}.h^{-1}$. Backflushing did not restore the flux in this instance.

DISCUSSION

Comparison between the above figures and the appendix shows that average fluxes in excess of 1000 $l.m^{-2}.h^{-1}$ can be achieved in the presence of inorganic material using backflushing. Similar flux rates have been claimed for other membranes operating on seawater (4). At low concentration of inorganic material backflushing is ineffective and fluxes reduce to below 100 $l.m^{-2}.h^{-1}$. Scanning Electron Microscope (SEM) photographs of the fouled membranes from the seawater algae runs were taken to determine the form of the fouling present on the membrane surface. These are reproduced in the figures below.

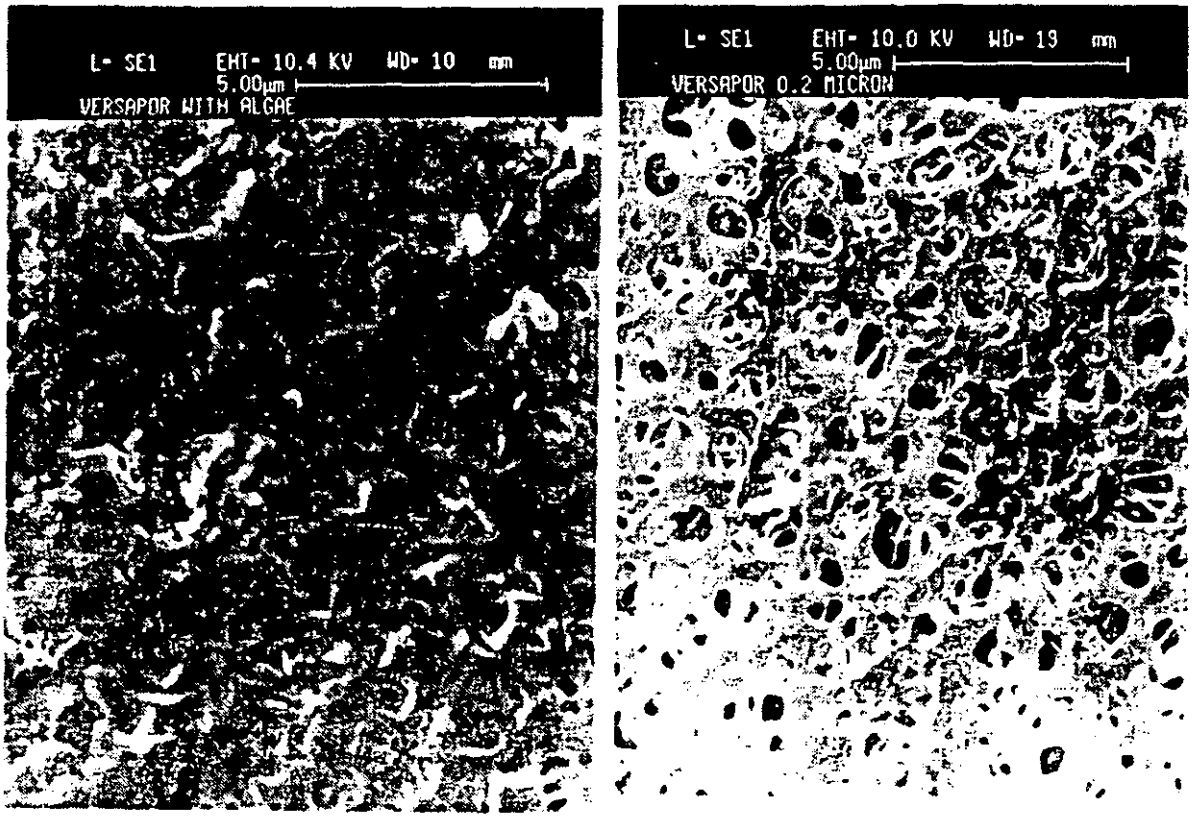

Figure 7 Versapor membrane filter clogged with algae - and clean

It is apparent that the fouling on the surface of the polymer membrane is of the form of a contiguous gel coating. This blocks all but the largest of the surface pores, and severely restricts flow through those remaining open. The surface porosity of the clean metal membrane is much higher than the polymer, but the presence of low concentrations of inorganic material will clog this membrane with the algal products acting as a binder. In both instances it is likely to be the material released by lysing the algal cells that forms a gel layer. When fouling is a problem during microfiltration a finer membrane is often suggested, so that material is too coarse to enter the surface pores and can easily be dislodged. This strategy does not succeed in this instance because the fouling is due to an organic gel of molecular weight proportions (fatty acids). There is also anecdotal evidence that seawater flux rates of 50 $l.m^{-2}.h^{-1}$ occur with fine Ultrafiltration membranes.

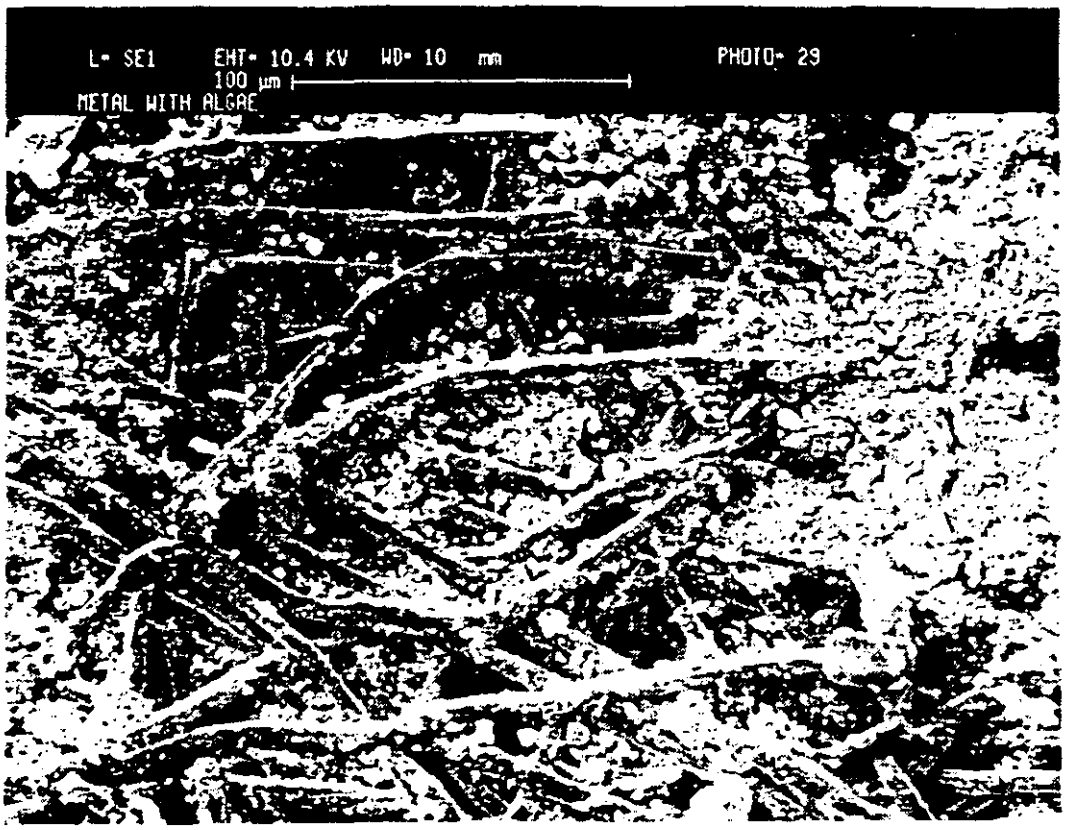

Figure 8 Metal membrane filter clogged with algae and solids

These photographs assist in the interpretation of results included in Tables 1 and 2. Large flow paths remain open in the metal membrane both in the presence of algae and without it. The membrane resistances are, therefore, similar and fluxes in the order of 400 $l.m^{-2}.h^{-1}$ result. Such large flow paths never existed with the polymer membrane, and clogging easily occurs, giving membrane resistances an order of magnitude greater than for the metal membrane and flux rates approximately one half. Polymer membrane resistance decreased with shear, or Reynolds number, but irreversible fouling occurred with both membranes.

CONCLUSIONS

Average seawater fluxes in excess of 1000 $l.m^{-2}.h^{-1}$ can be sustained if it is possible to dislodge the surface deposit. This could be achieved in two ways. Firstly, by the use of a precoat, which could prove expensive or unacceptable from environmental standards. Secondly, by the use of an open structured membrane with surface pores which are too wide for the gel layer to form a strong mechanical bridge on. Under these circumstances the use of backflushing, or a mechanical means of membrane cleaning, would be effective for restoring flux. Fine material would, however, pass the filter. There is considerable variation between the operating companies as to the level at which filtration should occur, but it is likely that injection water not subject to R.O. will only be relatively coarsely filtered, say 10 µm. A crossflow filter could be used for this and, under these circumstances, the coarse filtration stage could be removed. Should fine filtration be required a small cartridge filtration stage could be used to polish the filtrate. The coarse crossflow filtration stage would protect the cartridge filters during a period of algal bloom, when the suspended solids content rises and, paradoxically, efficiency of crossflow filtration improves.

Filter geometry does not appear to be significant in determining flux rates, nor does filter type. This is a consequence of the dynamic or secondary fouling layer. Thus the choice of filter type can be made on the basis of other operating criteria, such as: membrane packing density,

replacement ease, ruggedness and cost. A plate and frame crossflow filter containing sheet membrane is one of the most suitable designs. Very careful attention to flow distribution is required with this type of filter, however.

It is often the case that crossflow filtration is tested as a means of filtering a process suspension that is otherwise difficult to filter. This leads to poor results and, therefore, rejection of the technique. This is sometimes due to a poor understanding or control of the process, or unjustifiably high expectations. This work has shown that good filtration performance can be achieved when filtering suspensions of high mineral content using a mechanical membrane cleaning technique. Suspensions of low mineral content facilitate the penetration of the membrane with organic material which causes irreversible fouling. Strategies have been suggested to prevent such fouling. These strategies are now being investigated.

ACKNOWLEDGEMENTS

The authors of this paper wish to record their gratitude for a Science and Engineering Research Council grant to support a project of which this work formed a part. The project is administered through the Marine Technology Directorate Ltd, and is also sponsored by the following: BP Exploration, Texaco, Amoco, Chevron, Occidental, Elf, Marathon, Hamilton Brothers and Unocal.

REFERENCES

1. Holdich, R.G., Zhang, G.M. and Boston J. "Crossflow Filtration of Seawater", World Filtration Congress, Nice, France (1990), pp 518, 522.

2. Edyvean, G.J. and Lynch, J.L. "The effect of organic fouling on the life of cartridge filter", Filtech 89, Karlsruhe (1989), Filtration Society, pp 10, 17.

3. Holdich, R.G. and Boston, J. "Microfiltration using a dynamically formed membrane ", Filtration and Separation, 27 (1990), pp 184, 187.

4. Goodboy, K.P. and Louy, G.C. "Operational results of crossflow microfiltration for produced and seawater injection", Water Management Offshore, Aberdeen (1989), IBC Technical Services Ltd.

APPENDIX Results of laboratory crossflow filtrations

Reynolds number	Membrane pressure (Bar)	Concentration of: silica ($mg.l^{-1}$)	lipid	Sustainable flux rate using an air backflush at 3.5 Bar ($l.m^{-2}h^{-1}$)
Metal fibre tube membrane, 3 µm absolute, 0.01 m i.d:				
8500	0.2	10	0	1000
42500	0.5	10	0	1500
25500	1.2	0	0	5200
25500	1.2	2	0	1800
25500	1.2	2	5	1000
25500	1.2	0	0	5600
25500	1.2	2	0	1800
25500	1.2	2	10	800
25500	1.2	0	0	5200
25500	1.2	2	0	1300
25500	1.2	2	20	500
Polypropylene 42 capillaries per module, 0.2 µm absolute, 0.0018 m i.d:				
6000	0.7	0	0	2000 B/F at 2.8 Bar
6000	0.7	2	0	1600 B/F at 2.8 Bar
6000	0.7	2	5	1500 B/F at 2.8 Bar
Acrylonitrile sheet membrane, 3 µm absolute:				
13000	0.7	0	0	2500
13000	0.7	2	1	900
13000	0.7	2	2	900
13000	0.7	2	5	900
13000	0.7	2	10	500
Ceramic 19 capillaries per module, 1 µm absolute, 0.0027 m i.d:				
5000	1.2	0	0	4000
5000	0.9	0	0	2700
5000	0.6	0	0	1800
5000	0.3	0	0	1000
5000	1.1	2	0	1600
5000	0.2	2	0	440
5000	1.1	2	5	1000
5000	1.1	2	10	320
5000	1.1	2	20	300

CROSSFLOW MICROFILTRATION INCORPORATING ROTATIONAL FLUID FLOW

R. G. HOLDICH and G. M. ZHANG

Chemical Engineering Department, University of Technology, Loughborough, Leicestershire, UK

Crossflow microfiltration filtrate flux rates have been enhanced by the incorporation of rotational fluid flow around the surface of the filter membrane. The rotational fluid flow induced a centrifugal field force on the suspended material which acted in the opposite direction to the liquid drag, thus membrane fouling was reduced. The rotation was induced by means of filter module holder geometry, and by means of a helical insert causing the flow to rotate. Experimental results show that an energy saving of 20% is possible using this system compared with one in which no rotational flow existed.

INTRODUCTION

Crossflow filtration is employed to minimise deposition of suspended, or dissolved, material at the surface of the retaining membrane in micro- or ultra-filtration, respectively. The rate of permeate production (flux) often declines rapidly; increasing the crossflow velocity reduces but does not eliminate the flux decline. In some instances, however, the permeate flux rate is unaffected by the crossflow velocity when above a certain threshold. Thus the mechanisms involved in crossflow filtration are likely to be complex, with the relative importance of shear, diffusion, particle size, etc. depending upon the experimental conditions used. A variety of membrane resistances during filtration have been reviewed[1].

Considerable research effort has been directed towards techniques which can reduce the rate of permeate flux decline other than by increasing the crossflow velocity, these include:

- electric fields[2,3]
- acoustics and electro-acoustics[4]
- backflushing
- turbulence promoters[5]
- pulsatile feed flow[6]
- baffles[7]
- abrasive particulate material added[8]
- rotating the membrane or a surface near to the membrane[9,10].

The last of these techniques increases the shear stress at the surface of the membrane by moving the membrane surface, or a surface close to it, rather than increasing the velocity of the suspension over the surface of the membrane. In addition to increased shear, the centrifugal field acting on the material suspended in the resulting rotational flow may be a significant force in increasing the permeate flux.

Rotating the membrane surface has certain mechanical disadvantages such as the maintenance of an effective fluid seal under pressure in systems containing suspended solids. Also, a low membrane surface area per unit volume of space is usually found. High shear and a centrifugal field force can be effected by the use of tangential inlet and exit ports in a filter holder. Tangential inlet conditions are used already in hydrocyclones, which separate solid mixtures in a similar way to centrifuges but without the need for moving parts.

Helical inserts inside an annular gap have been used to induce rotational flow of a gas, with a consequent increase in heat transfer coefficients, in the Australian metallurgical industry[11]. Some turbulence promoters can be used to induce rotational flow in pipes or crossflow filters, but the use of this type of flow to enhance mass transfer during filtration has received little attention in the literature.

Experimental results are presented for the crossflow filtration of a mineral material using the filter in a conventional way, and for the filtration of a suspension in which the flow is made to rotate by means of both a helical insert inside an annular gap and by introducing the slurry at right angles, and off-set, to the cylindrical membrane surface. The latter uses an inlet geometry similar to that of a hydrocyclone. Methods are described to evaluate the effects of variable temperature and membrane resistance in order to compare the results from the different filtrations. Deposition of solids at the membrane surface is reduced by means of the angular velocity at that surface, thus this is calculated using two separate models for free and hindered dispersions. Comparison with the value of angular velocity based on the principle of conservation of angular momentum shows that there is considerable scope to enhance the performance of the separator. Finally, the paper considers the energy involved in creating this type of flow field and compares the energy efficiency of the separations provided by the different types of crossflow filtration geometries.

EXPERIMENTAL TECHNIQUES AND PROCEDURES

A conventional, so-called, metal membrane was used in this experimental study: Pall PSS 5, with a nominal pore size cut-off of 5 μm. The filter was 0.27 m in length and 6 mm in radius. The membrane holder was unconventional in its use of both entry and outlet ports at right

0263-8762/92/$05.00 + 0.00

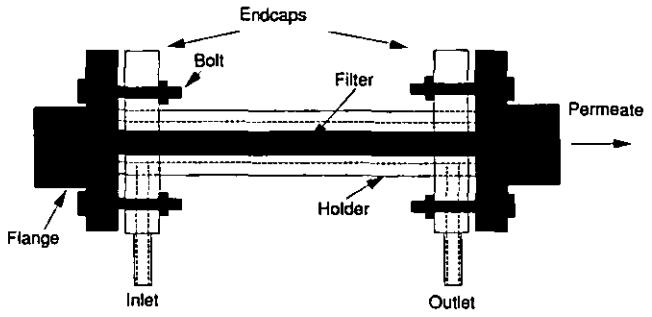

Figure 1. Crossflow filter in membrane holder and endcaps with flow at right angle to filter.

angles (normal) to the membrane surface, Figure 1. These endcaps are referred to as 'normal' entry and exit. A diagram of the normal endcaps is given in Figure 2(a). This arrangement produced high turbulence and high pressure drop when compared to the more conventional inlet and outlet in parallel with the membrane surface. 'Helical' filtration was facilitated by winding a helix around the cylindrical membrane with a pitch of 22 mm, and employing the normal endcaps. The filtration was effected on the outer surface of the membrane, in an annular gap of 4 mm. The use of the outer membrane surface facilitated the centrifugal flow field by means of tangential inlet and outlet endcaps, Figure 2(b). In this context 'tangential' entry is used to indicate that the feed suspension is introduced at right angles, and off-set, to the cylindrical membrane surface. Filtration of suspensions containing suspended solids denser than the suspending medium would, therefore, be assisted by the centrifugal flow field. The suspending medium was prefiltered water. In the separation of a dispersed phase lighter than the suspending medium, oil in water for example, the filtration would have to be conducted on an inner

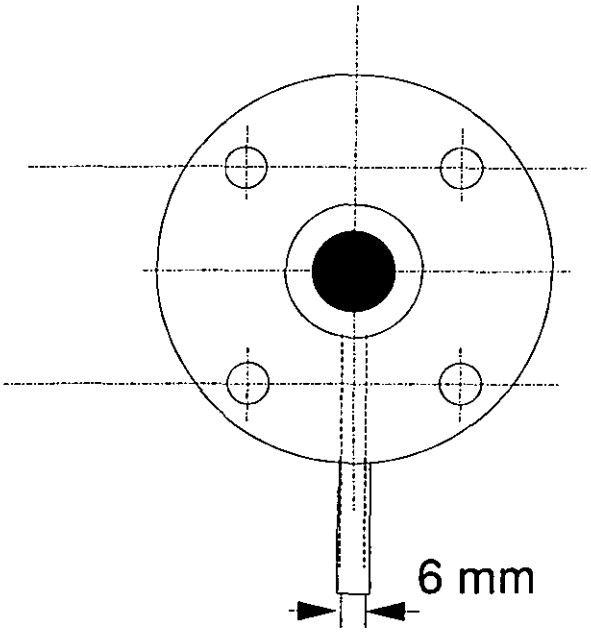

Figure 2a. Endcap showing entry and exit flow normal to filter membrane.

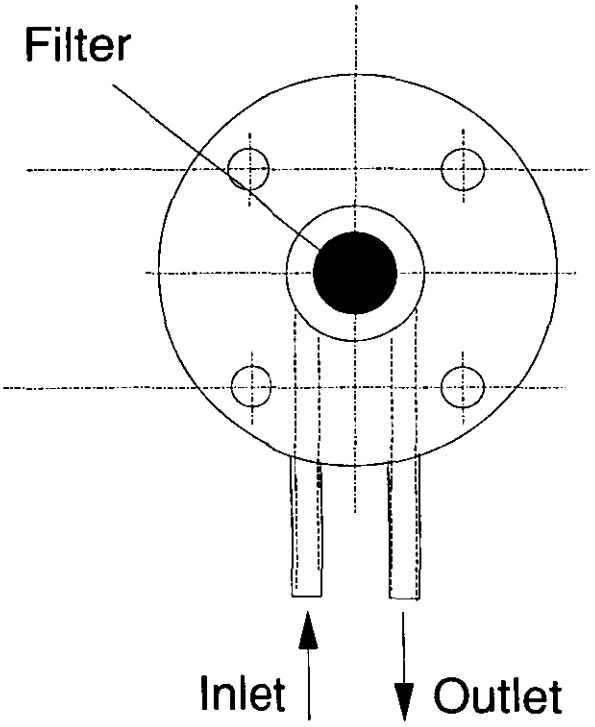

Figure 2b. Endcap showing entry and exit flow tangential to filter membrane.

membrane surface in order to reduce the dispersed phase concentration at the membrane surface. A helix might be preferred to tangential entry as a means of effecting rotational flow because of its relative ease of construction.

A schematic diagram of the equipment is shown in Figure 3. The feed tank contained 0.02 m^3 of water, which was cleaned by means of the 0.1 μm cartridge filter. The cleanlinesss of this water was checked with a Hiac Royco model 346 BCL, and the total number of counts of particles above 0.8 μm was less than 200 per ml prior to adding the powdered solids. Calcium carbonate was used, the Sauter mean diameter of the particle size distribution was 6.9 μm. The suspensions were made up to concentrations of 1.5 and 4% by weight. Flow rate and

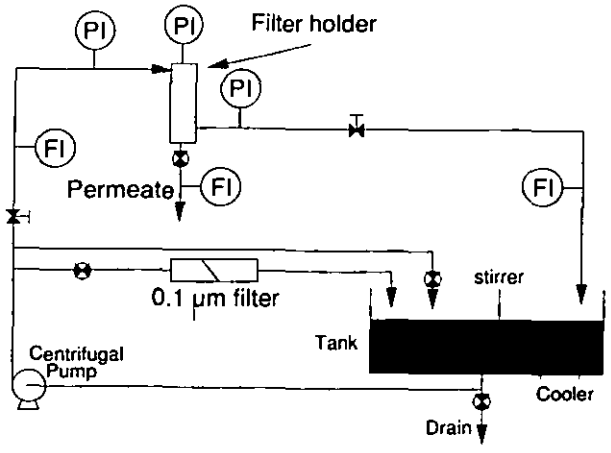

Figure 3. Schematic diagram of the crossflow filter experimental equipment.

pressure into and out of the filter were monitored during filtration.

It is usual to estimate the pressure drop across the membrane during filtration by averaging the inlet and outlet pressures. This was not an acceptable practice during filtration using the endcaps shown, because of the greater pressure drop associated with normal and tangential entry to the filter holder. Hence a series of tests were conducted to measure the pressure inside the filter holder at various flow rates. For these tests the permeate valve was closed and no permeate flowed. Figure 4 shows the measured inlet pressure with flow rate for the normal and tangential endcaps on the filter holder, plus that for the normal endcap with the wound helix. The pressure causing the fluid to spin can be calculated from Figure 4 by deducting the normal from the tangential inlet pressure, at the same flow rate. The difference between the normal and helical inlet pressures was due to both setting up the spinning flow field in the filter, plus an additional pressure drop due to the presence of the spirally wound o-ring, which increases fluid drag and hence the pressure drop.

The pressure inside the filter holder, equivalent to the permeate side under no permeate flow conditions, also depended on the type of intlet holder used. This can be seen in Figure 5. A higher pressure was present in the case of the tangential filter endcap, but the helical insert did not significantly alter the permeate pressure from that given by the normal endcap. The outlet pressure from the filter holder remained independent of filter endcap type, as would be expected. This is also shown on Figure 5.

The pressure drop across the membrane, i.e. the pressure difference between the feed and permeate sides of the membrane, during filtration was calculated from the feed flow rate and the measured pressures. The pressure in the permeate during filtration was always atmospheric when the permeate valve was fully open. The pressure on the feed side of the membrane was assumed to be that shown in Figure 5 for a given feed flow rate. The pressure drop across the membrane could be higher than that shown in Figure 5 if the valve after the filter holder was restricted. Under these circumstances both the inlet and outlet

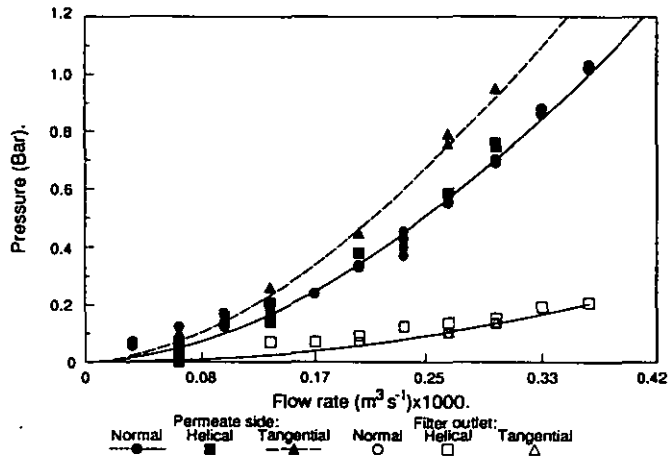

Figure 5. Pressures inside the membrane module and downstream of the filter for different endcap and filter types.

pressures were also raised, and by an equivalent amount, over that shown in Figures 4 and 5. Thus the amount by which these two pressures were raised was added to the filtration (permeate) pressure taken from Figure 5, to give a new value of pressure drop across the membrane.

The centrifugal pump used in this study generated heat, and a cooling coil was employed. The cooling coil was not sufficiently powerful to maintain the temperature and this rose from 20 to 32°C, during an experiment of 90 minutes duration. For a limited period in time an additional cooling unit was employed, and under these conditions a stable temperature of 24 to 26°C was maintained. This experimental run was repeated under conditions of rising temperature, the results are given in Figure 6.

Between filtrations the membrane was removed, washed and cleaned with compressed air.

RESULTS AND DISCUSSION

Accurate interpretation of crossflow filtration processes is notoriously difficult. This is often due to complex interactions of the following: variation in membrane

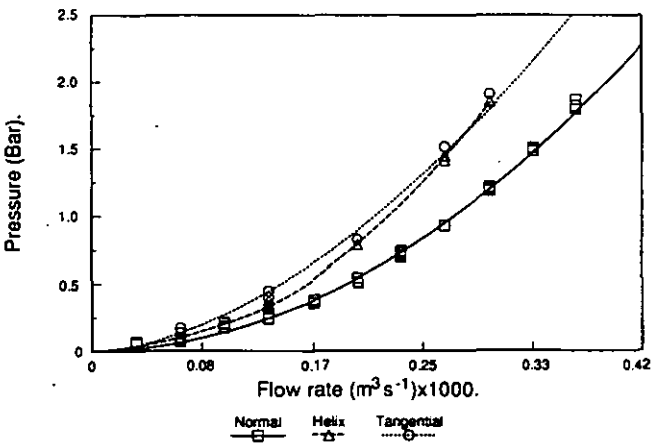

Figure 4. Inlet pressures as a function of feed flow rate for different endcap and filter types.

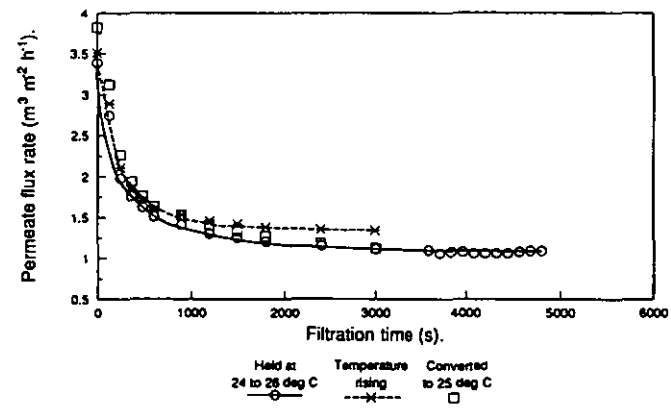

Figure 6. Permeate flux rate decay with time and the effect of variable temperature.

resistance, temperature fluctuation, lack of accurate knowledge of the filtration pressure, size and density segregation of deposit on the membrane surface, surface charges, lack of homogeneous membrane, etc. The following procedures were followed in order to eliminate some of these variations.

Variation of permeate flux rate with temperature was corrected using the viscosity difference between water at the measured temperature and a reference temperature taken to be 25°C. Thus all the flux rates were corrected to that which would have been obtained at a temperature of 25°C. This is shown in Figure 6, where the flux rate (J_θ) under conditions of rising temperature has been converted to one equivalent to that at 25°C (J_{25}) using the following equation:

$$J_{25} = \frac{\mu_\theta}{\mu_{25}} J_\theta \tag{1}$$

where μ_θ and μ_{25} are viscosity at the measured temperature and at 25°C respectively.

A duplicate run is also shown in Figure 6, where the temperature was maintained at 24 to 26°C. From this figure it can be seen that correcting the experimental data for rising temperature gives a similar result to one obtained under conditions of constant temperature. The very slightly larger values of flux rate after conversion, compared with that obtained by maintaining the temperature, can be explained by the slightly higher initial permeate rate, i.e. the slightly lower membrane resistance, in the experiment in which the temperature increased. This experiment validated the use of equation (1) to correct filtration flux rates in the other filtrations where temperature fluctuation occurred.

Membrane resistance

In membrane studies involving modelling, or comparison, it is common for the membrane resistance to be determined by the use of the clean water permeation rate (J_w). The membrane resistance is given by Darcy's law:

$$R_m = \frac{\Delta P}{\mu J_w} \tag{2}$$

where ΔP is the pressure across the membrane and R_m is the membrane resistance. It is often assumed that the membrane resistance remains constant and equal to the clean water value during filtration, thus any increase in resistance during filtration must be due to the deposit. This approach is not valid in conventional cake filtration for the estimation of filter cloth resistance, and it is unlikely to be accurate in microfiltrations in which the suspended particle size is close to, or finer than, the pore size of the membrane, such as in this study. Under these circumstances the membrane resistance must be calculated *in situ*, just as it must be for conventional filtration. This approach is adopted in order to permit comparison of deposit resistance formed under different flow conditions given by the module inlet geometries. It is inevitable that some of the suspended solids will penetrate the membrane initially, this amount of material will vary from experiment to experiment. Thus the filter medium resistance will also vary from experiment to experiment and a technique to quantify the *in situ* deposit resistance is required.

In conventional constant pressure filtration the square of the volume of filtrate produced is proportional to filtration time, and the filter medium resistance can be calculated from the experimental results by some simple algebraic manipulation. In crossflow filtration no such simple relation between time and filtrate volume exists, thus an alternative method must be used to calculate the *in situ* membrane resistance. Such a method is to consider the initial stages of filtration, taking a tangent to the volume filtrate against time curve to provide a value for J_w, which is then used in equation (2) to provide a value for membrane resistance. An example of this for one filtration is shown in Figure 7. Membrane resistances were calculated for all the filtrations by this method, these are given in Tables 1 and 2.

Also shown in these tables are deposit resistance which were calculated by applying that Darcy's law after equilibrium was reached. The two resistances due to the membrane and the deposit are assumed to be additive, thus:

$$\Delta P_{total} = \mu(R_m + R_{deposit})J_e \tag{3}$$

where J_e is the equilibrium flux rate.

It should be noted that R_m is assumed to be a constant, but $R_{deposit}$ is a function of filtration time until the equilibrium flux rate is achieved. Darcy's law is then applied to determine the equilibrium value of the deposit resistance using a rearranged form of equation (3).

It should also be noted that the values of membrane resistance in Tables 1 and 2 include a contribution due to the solids that initially penetrate the membrane surface. They are, therefore, much higher than the membrane resistances that would have been obtained by means of clean water permeation tests.

It is the intention of this work to be able to compare the effects of filtering in a rotating flow field and without such a field. In order to conduct this comparison, any effect due to the variable nature of the membrane resistance must be removed. The lowest membrane resistance in Tables 1 and 2 is $1 \times 10^9\ m^{-1}$, thus the data for the remaining filtrations has been 'normalised' to this membrane resistance. The most straightforward way of

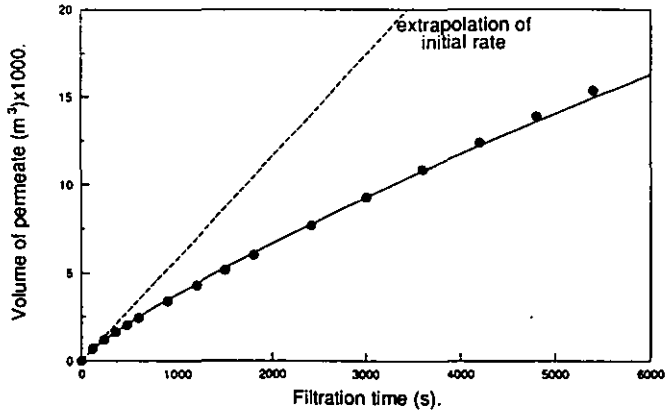

Figure 7. Cumulative filtrate volume with time and use of initial rate for membrane resistance.

Table 1. Table of membrane resistances during crossflow filtration at 1.5% solid concentration.

Crossflow velocity	Equilibrium permeate flux rate	Membrane resistance	Deposit resistance	Corrected trans-membrane pressure
($m\ s^{-1}$)	($m^3\ m^{-2}\ h^{-1}$)	(m^{-1}) × 10^9	(m^{-1}) × 10^9	(Bar)
Normal endcap:				
0.66	0.388	1	1.9	0.172
0.66	0.322	1.2	2.5	0.172
0.66	0.481	1.1	2.7	0.264
0.66	0.548	1.3	4.5	0.456
0.91	0.596	1	2.2	0.283
0.91	0.410	1.4	3.5	0.278
0.91	0.638	1.1	2.6	0.338
0.91	0.734	1.3	3.8	0.533
1.16	0.489	1.7	4.6	0.414
1.16	0.542	1.6	4.1	0.417
1.16	0.523	1.6	4.3	0.418
1.16	0.583	1.9	5.5	0.575
1.16	0.636	2.3	6.7	0.742
1.41	0.680	1.5	4.2	0.532
1.66	0.779	1.8	5.8	0.804
1.66	0.767	1.8	5.9	0.804
Helical endcap:				
1.52	0.325	1.5	1.4	0.130
2.08	0.469	2.7	3.1	0.327
2.65	0.617	1.8	3.3	0.413
2.65	0.610	2.0	3.1	0.399
3.22	0.860	1.8	3.7	0.623
3.22	0.655	2.0	5.1	0.621
3.22	0.725	2.0	4.5	0.615
Tangential endcap:				
0.66	0.450	1.3	2.1	0.220
1.00	0.650	1.7	3.1	0.411
1.00	0.700	2.2	4.8	0.615
1.00	0.600	1.8	4.8	0.521
1.00	0.569	1.9	3.6	0.403
1.33	0.818	2.3	4.7	0.713
1.33	0.814	1.9	4.4	0.664
1.33	0.792	2.3	6.0	0.848
1.33	0.850	1.8	4.2	0.671
1.33	0.960	2.0	4.8	0.860
1.49	0.936	1.8	5.1	0.872
1.49	0.960	2.2	5.0	0.879
1.49	1.090	2.6	3.4	0.767
1.49	1.019	1.8	4.6	0.866

Table 2. Table of membrane resistances during crossflow filtration at 4% solid concentration.

Crossflow velocity	Equilibrium permeate flux rate	Membrane resistance	Deposit resistance	Corrected trans-membrane pressure
($m\ s^{-1}$)	($m^3\ m^{-2}\ h^{-1}$)	(m^{-1}) × 10^9	(m^{-1}) × 10^9	(Bar)
Normal endcap:				
1.00	0.561	2.6	3.8	0.426
1.00	0.617	3.5	8.4	0.879
1.41	0.622	3.4	4.1	0.517
1.66	0.711	3.4	5.1	0.685
1.66	0.706	3.5	5.2	0.696
1.66	0.689	3.0	6.2	0.774
1.66	0.778	3.4	5.9	0.833
1.66	0.883	3.6	5.6	0.917
Tangential endcap:				
1.00	0.561	2.3	3.2	0.379
1.16	0.631	2.4	4.0	0.495
1.33	0.782	2.6	3.8	0.603
1.33	0.735	2.5	4.4	0.619
1.33	0.812	2.7	4.5	0.690
1.33	0.812	3.3	4.9	0.762
1.49	0.952	2.7	4.1	0.771
1.49	0.919	3.1	4.6	0.819
1.49	0.970	3.1	4.1	0.861
1.49	0.877	3.8	5.1	0.854

achieving this normalisation is to consider the pressure drops as being additive:

$$\Delta P_{total} = \Delta P_{medium} + \Delta P_{deposit} \quad (4)$$

which can be rearranged to give:

$$\Delta P_{deposit} = \Delta P_{total}\left(1 - \frac{\Delta P_{medium}}{\Delta P_{total}}\right) \quad (5)$$

where equation (3) can be used for the relation between total pressure drop and the constituent resistances. Combining the above equations provides the following expression for total pressure drop across the membrane and deposit based on the reference membrane resistance (R_m^*). This is the corrected membrane pressure (ΔP^*) in Tables 1 and 2:

$$\Delta P^* = \Delta P\left(1 - \left(\frac{R_m}{R_m + R_{deposit}}\right) + \left(\frac{R_m^*}{R_m^* + R_{deposit}}\right)\right) \quad (6)$$

The reference membrane resistance used in equation (6) was $1 \times 10^9\ m^{-1}$.

The pressures across the membrane shown in Figures 8 and 9 are corrected values, i.e. these should be the flux rates achieved if the membrane resistance was consistently $1 \times 10^9\ m^{-1}$.

Effect of filtration pressure

The equilibrium flux rates were clearly pressure dependent, up to a pressure across the membrane of 1 bar. The rate of increase in flux with pressure was, however, decreasing and it is possible that the system becomes pressure independent at higher pressures. Equilibrium flux rates were higher when using the tangential endcaps, i.e. with rotational flow, at both the solid concentrations tested. The helical arrangement also provided increased values of equilibrium flux rate over normal entry, for a given pressure.

Effect of shear rate

A comparison of Figures 8 and 9 shows that solid concentration did not significantly affect filtrate flux rate, over the limited range investigated. Figures 10 and 11 are for the combined 1.5 and 4% solid concentrations, and show the effect of increasing crossflow velocity, and pressure, on the equilibrium flux rate. The flux rate was substantially independent of shear at constant pressure for the normal filter holder, Figure 10. There was, however, an underlying relation between flux rate and transmembrane pressure. Figure 11 is for the tangential filter

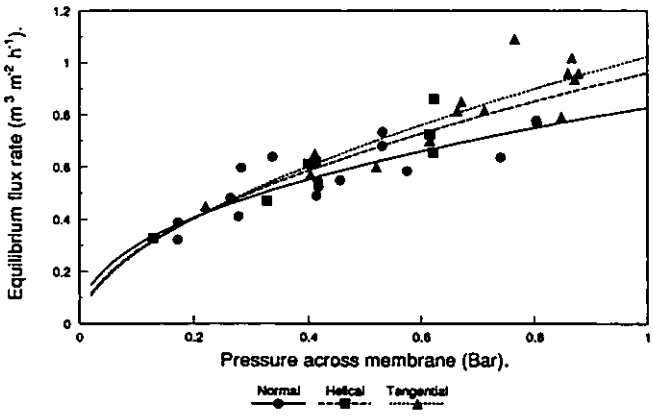

Figure 8. Equilibrium flux rates with pressure for the 1.5% solid suspension using various module endcaps and filter types.

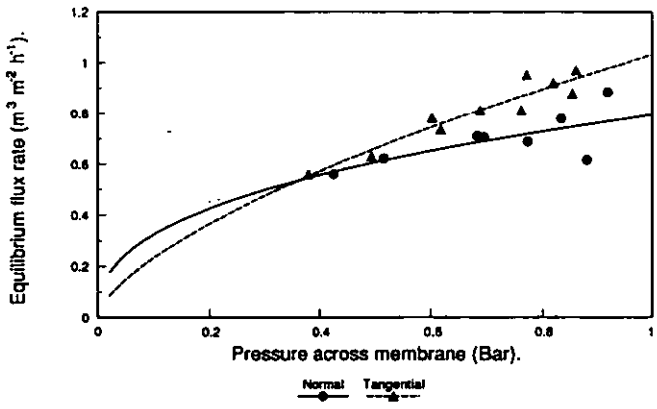

Figure 9. Equilibrium flux rates with pressure for the 4% solid suspension using various module endcaps and filter types.

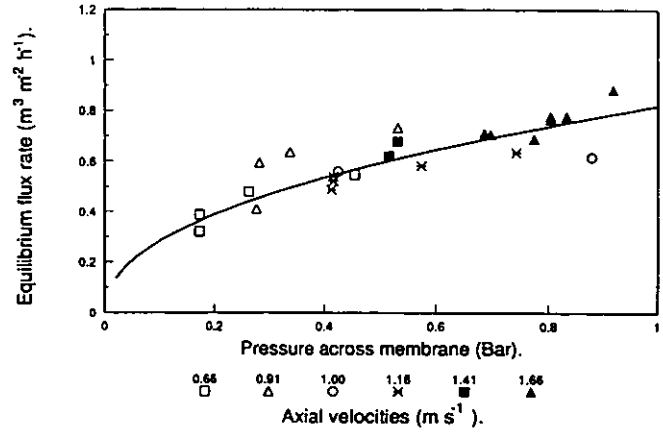

Figure 10. Equilibrium flux rates with pressure at various crossflow velocities using the normal module endcap.

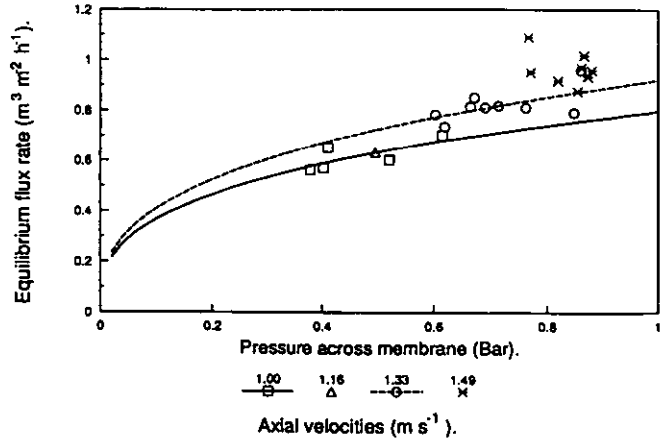

Figure 11. Equilibrium flux rates with pressure at various crossflow velocities using the tangential module endcap.

holder and some flux rate dependency with crossflow velocity can be observed.

Flux rate is usually a function of crossflow velocity or shear rate. The lack of such a relation in the case of the normal filter holder could have been due to the very high turbulence induced by having entry at right angles to the axial flow, in addition to the relatively short filter tube length. Another reason for this effect could have been the large amount of fines which were smaller than the nominal membrane size. Thus a substantial part of the deposit resistance could be due to fine material migrating into the membrane structure and, therefore, protected from the shear induced by the crossflow. Visible inspection of the filter showed that a deposit cake was formed in all the filtrations.

There is some degree of spread on the experimental results shown in Figures 10 and 11 but, nevertheless, it is evident that the membrane endcaps did have a considerable influence on the filtration behaviour of this material. If the flux rate was shear rate independent, over this limited region, then the additional flux given by the helical or tangential mode of operation must be due to the centrifugal force field.

Effect of solid concentration and centrifugal acceleration

In fluid particle systems the distinction between free and hindered systems is usually drawn, based on the solid concentration of the dispersion. The threshold between free and hindered dispersions is often assumed to be approximately 1% by volume, but it is a function of the suspended material. The two concentrations employed in this study were chosen to be below and above this threshold, to test the application of centrifugally induced anti-fouling of this membrane under both of these operating conditions.

i) Free dispersions

Equating the liquid drag force with the buoyed centrifugal force provides the following equation for radial velocity of a particle, if inertia and gravitational body forces can be neglected and Stokes law is valid:

$$J = \frac{dr}{dt} = \frac{x^2(\rho_s - \rho)r\omega^2}{18\mu} \tag{7}$$

where μ is liquid viscosity, x is particle diameter, dr/dt is the radial velocity of the particle, r is radial position, ω is angular velocity, and ρ_s and ρ are solid and liquid densities respectively.

Equation (7) can be used to estimate the liquid flow rate towards the membrane that must be exceeded before particles move in the direction of the membrane. At lower flow rates particles will move outwards, if they are denser than the supporting fluid, due to the action of the centrifugal field force. Thus this represents the minimum flux rate that should be obtained from a membrane incorporating centrifugal separation.

It is extremely difficult to estimate the angular velocity inside a centrifugal separator in order to apply equation (7). Conservation of angular momentum is sometimes used in hydrocyclone investigations, but it is often found necessary to introduce empirical coefficients into the equations. An alternative approach is to estimate the centrifugal acceleration at the membrane surface using a rearranged form of equation (7):

$$r\omega^2 = \frac{18\mu J}{x^2(\rho_s - \rho)} \tag{8}$$

ii) Hindered dispersions

In hindered dispersions a force balance can be constructed over a laminar layer of the suspension, instead of considering individual particles. The centrifugal field force is again balanced by the liquid drag force. If there is no net particle motion and forces due to inertia and gravity can be ignored, then:

$$Cr\omega^2(\rho_s - \rho)A\,dr - CF_D A\,dr = 0 \tag{9}$$

where C is the solid volume fraction concentration, F_D is the drag force per unit volume and A is the area of the laminar layer.

A liquid force balance results in the following:

$$\frac{dP}{dr} = CF_D \tag{10}$$

where dP/dr is the dynamic liquid pressure gradient. This can be related to solid concentration and velocities by a modified form of Darcy's law:

$$\frac{dP}{dr} = -\frac{\mu}{k}(1 - C)(v_l - v_s)$$

where k is the permeability of the layer of solids, v_l and v_s are the liquid and solid velocities respectively. If the particle layer remains in a stationary orbit, i.e. does not move towards or foul the membrane, then the solid velocity is zero and combining the above equations provides:

$$J = v_l = \frac{Cr\omega^2(\rho_s - \rho)k}{\mu(1 - C)} \tag{11}$$

Rearranging equation (11) for the centrifugal acceleration at the membrane surface:

$$r\omega^2 = \frac{\mu(1 - C)J}{C(\rho_s - \rho)k} \tag{12}$$

The permeability of a layer of solids can be calculated from various models, one such is Happel and Brenner[12]:

$$k = \frac{(2 - 3C^{1/3} + 3C^{5/3} - 2C^2)}{(3 + 2C^{5/3})}\,\frac{x^2}{12C} \tag{13}$$

If the filtrate flux rate is dominated by the resistance to flow through the most concentrated laminar layer, which is likely to be adjacent to the membrane surface, and this layer is assumed to have a porosity of 50% then the permeability of this layer is 1.4×10^{-13} m^2 by equation (13).

iii) Conservation of angular momentum

It is possible to estimate the angular velocity and acceleration at the membrane surface by considering the geometry of the membrane filter holder, and from a knowledge of the entry condition. The principle of conservation of angular momentum is:

$$v_l r = constant \tag{14}$$

where v_i is the tangential velocity at a radial position r. Equation (14) is valid for frictionless conditions and is often modified by the inclusion of a fractional power exponent on the radial position term to account for energy losses. Using the filter system described in Figures 1 and 2, the centrifugal acceleration at the membrane surface ($r\omega^2$) is in the range 8400 to 19000 ms^{-2} over the range of inlet velocities employed in this work.

Comparison of models and rotational velocities

The increase in filtrate flux over that obtained in the absence of rotational flow can be deduced from Figures 10 and 11. At an axial velocity of 1.33 and 1.49 $m\,s^{-1}$ the increase in filtrate flux is 0.13 and 0.23 $m^3\,m^{-2}\,h^{-1}$, respectively. Table 3 shows the centrifugal acceleration averaged over the full membrane length, based on equations (8) and (12) for the two models for free and hindered dispersions, respectively. Also shown in Table 3 is the equivalent rotational speed of the membrane to achieve the same rotational flow condition if the membrane had been rotated instead of the fluid. These were both calculated by assuming that the additional filtrate flux was due to the fouling solids entering stationary orbit. Thus equations (8) and (12) were used with J as the increase in filtrate flux and not the total filtrate flux.

It is evident from Table 3 that if the dispersion concentration is sufficiently high for hindered conditions to pertain, a substantial angular velocity is required in order to decrease the fouling effect. It is reasonable to deduce that a hindered system existed because a deposit was observed on the surface of the membrane filter.

The theoretical centrifugal acceleration on the membrane surface at the filter inlet was calculated to be 8400 to 19000 $m\,s^{-2}$ by means of conservation of angular momentum. The centrifugal accelerations in Table 3, deduced from operating data, are considerably lower than the theoretical values. The deduced accelerations are average values over the full surface of the membrane and, clearly, are affected by frictional losses within the filter module. Visual observation confirmed that the suspension rotated rapidly at the filter inlet, but that this decayed to only a slight rotation towards the base of the module. The discrepancy between theoretical and deduced centrifugal acceleration, and the information obtained by visual observation suggests that very careful design of the filter module must be made in order to maximise the benefit due to rotational flow. This is now being studied with the assistance of computational fluid dynamics software.

Depth of membrane deposit

The average depth of the deposit on the membrane surface can be calculated from the membrane deposit resistances shown in Tables 1 and 2, the deposit permeability estimated from equation (13) and the following relation between resistance, permeability and depth (l_d):

$$l_d = R_{deposit}k$$

Deposit resistance can be seen to vary from 1.4 to $8.4 \times 10^9\ m^{-1}$, in Tables 1 and 2. The deposit depths corresponding to these resistances were 0.2 to 1.2 mm, respectively. A deposit of approximately 1 mm was measured, with a significantly tapering shape: less deep at the feed end, much thicker at the outlet. Calculated values of deposit permeability, resistance and, therefore, thickness appear to be in reasonable agreement with visual observation.

Energy efficiency

It is clear that filtrate flux rates were enhanced by the use of rotational flow on the membrane surface. The effectiveness of this technique can be evaluated by considering the energy input required by the normal and tangential filters. Both filter systems used the same experimental rig, thus Bernoulli's equation can be applied using the filter module entry and exit conditions of pressure and velocity. Neglecting energy terms due to internal, mechanical and static pressure Bernoulli's equation for energy per unit mass can be written as:

$$\frac{\Delta P}{\rho} + \frac{v^2}{2} = \textit{energy per unit mass} \qquad (15)$$

Multiplying equation (15) by the mass flow rate gives the rate of energy change with time, i.e. power used by the system.

The pressure drop of the filter module and the fluid velocity in the module feed pipe were used in equation (15) to calculate the power requirement for the equilibrium flux rates given in Tables 1 and 2. The results are plotted in Figures 12 and 13 for the 1.5 and 4% solid suspensions respectively.

Both Figures 12 and 13 demonstrate that it was more energy efficient to filter using the tangential endcaps, at high power inputs or for high equilibrium flux rates. At low flux rates or power inputs normal filtration was more efficient.

A common alternative method of comparing energy requirement for crossflow filtration is to calculate the energy required to produce 1 m^3 of permeate. This can be estimated from Figures 12 and 13 for the two different

Table 3. Table of conditions on membrane surface according to models based on free and hindered dispersions.

Axial velocity	Additional filtrate flux	Free dispersion:		Hindered dispersion:	
		centrifugal acceleration	rotational speed	centrifugal acceleration	rotational speed
($m\,s^{-1}$)	($m^3\,m^{-2}\,h^{-1}$)	($m\,s^{-2}$)	(rpm)	($m\,s^{-2}$)	(rpm)
1.33	0.130	7.4	475	141	2070
1.49	0.230	13.2	632	250	2760

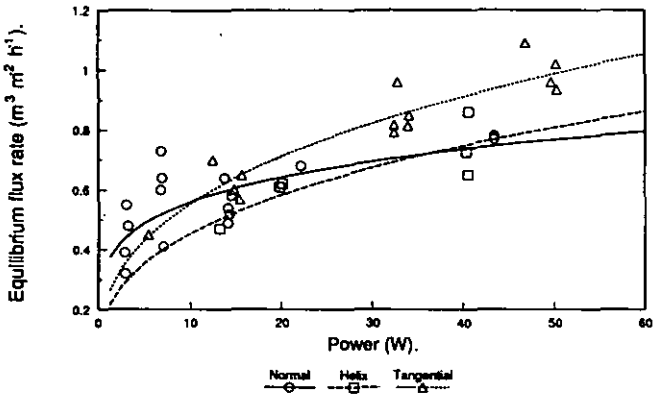

Figure 12. Equilibrium flux rates as a function of power requirement for the 1.5% solids suspension.

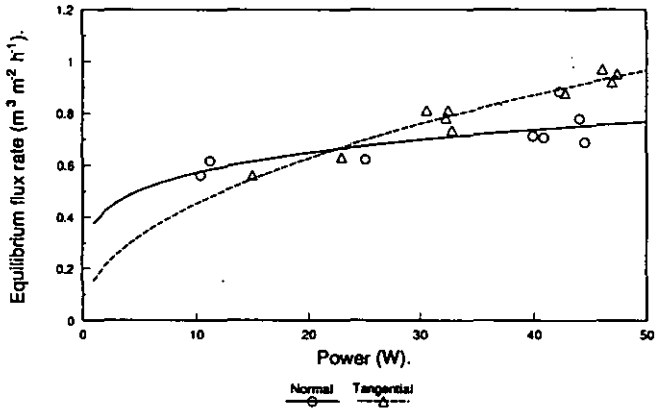

Figure 13. Equilibrium flux rates as a function of power requirement for the 4% solids suspension.

concentrations employed. For example, Figure 12 shows values for the flux rate of 0.82 and 0.68 $m^3\ m^{-2}\ h^{-1}$ for the tangential and normal filtration respectively at the same power input of 30 W. Thus the time taken to produce 1 m^3 of permeate on this filter (0.01 m^2) would be 122 and 147 hours, respectively. The energy required would therefore be 3.66 and 4.41 kWh m^{-3} for the tangential and normal filters respectively. Thus the extra energy required by the normal filter is 20% compared to the tangential.

Under conditions of low power input, i.e. low pressures across the membrane and consequent lower fluxes, the normal filter is more energy efficient than the tangential. This would be expected of a system in which a centrifugal force field is being used to assist in membrane cleaning; this force is dependent on the angular velocity to the second power, and angular velocity diminishes in proportion with the applied pressure.

CONCLUSIONS

It has been shown that microfiltration membrane fouling can be reduced by the incorporation of rotating fluid flow on the surface of a filter membrane. This has some advantages over the alternative strategy of rotating the membrane mechanically. These are principally the removal of the necessity of a mechanical seal operating under pressure, at high rotational speeds within particulate suspensions, and the easier application of this technique to narrow diameter membrane tubes. The last advantage is important when high values of membrane surface area per unit volume of space are required. The use of a helical insert, instead of tangential inlet and outlet ports, also induced rotational flow, and is more attractive in terms of membrane surface area per unit volume. Helical inserts did, however, lead to additional pressure losses due to fluid drag on the increased surface area inside the filter module. There is still a considerable amount of work required to optimise the membrane holder, and helical insert, in order to enhance the centrifugal field force and shear but to minimise the pressure losses in the system.

This anti-fouling technique could also be applied to suspensions in which the dispersed phase is less dense than the continuous phase, such as oil in water. Under such circumstances the filtration would have to be effected on the internal surface of the membrane of circular, or similar, cross section. The experimental results indicate that the technique is efficient in terms of the energy required for separation, with energy savings of 20% achieved.

NOMENCLATURE

A	Area, m^2
C	Solid concentration by volume fraction
F_D	Drag force per unit volume, $N\ m^{-3}$
F_d	Drag force on single particle, N
J	Filtrate flux rate, $m^3\ m^{-2}\ h^{-1}$
J_w	Filtrate flux rate with clean membrane, $m^3\ m^{-2}\ h^{-1}$
k	Permeability, m^2
l_d	Depth of deposit on filter, m
P	Pressure, Pa
ΔP	Pressure drop, Pa
ΔP^*	Corrected trans-membrane pressure drop, equation (6), Pa
R_m	Membrane resistance, m^{-1}
R_m^*	Fixed membrane resistance of 1×10^9, m^{-1}
r	Radial position, m
t	Time, s
v_t	Tangential velocity, $m\ s^{-1}$
v_l	Liquid velocity towards membrane, $m\ s^{-1}$
v_s	Solid velocity towards membrane, $m\ s^{-1}$
x	Particle diameter, m

Greek letters

μ	Liquid viscosity, Pa s
ρ	Liquid density, $kg\ m^{-3}$
ρ_s	Solid density, $kg\ m^{-3}$
ω	Angular velocity, s^{-1}

Subscripts

25	At 25°C
e	At equilibrium
m	Membrane
θ	At some temperature, °C

REFERENCES

1. van den Berg, G. B. and Smolders, C. A., 1988, Flux decline in membrane processes, *Filtration and Separation*, 25(2): 115.
2. Bowen, W. R. and Sabani, H., 1992, Pulsed electrokinetic cleaning of cellulose nitrate microfiltration membranes, *Ind Eng Chem Res*, 31(2): 512.
3. Wakeman, R. J. and Tarleton, E. S., 1987, Membrane fouling prevention in crossflow microfiltration by the use of electric fields, *Chem Eng Sci*, 42(4): 829.

4. Wakeman, R. J. and Tarleton, E. S., 1991, An experimental study of electroacoustic crossflow microfiltration, *Chem Eng Res Des*, 69: 386.
5. Dejmek, P., Funeteg, B., Hallstrom, B. and Winge, L., 1974, Turbulence promoters in ultrafiltration of whey protein concentrate, *J Food Science*, 39: 1014.
6. Boonthanon, S., Hwan, L. S., Vigneswaran, S., Ben Aim, R. and Mora, J. C., 1991, Application of pulsatile cleaning techniques in crossflow microfiltration, *Filtration and Separation*, 28(3): 199.
7. Finnigan, S. M. and Howell, J. A., 1989, The effect of pulsatile flow on ultrafiltration fluxes in a baffled tubular membrane system, *Chem Eng Res Des*, 67: 278.
8. Milisic, V. and Bersillon, J. L., 1986, Anti-fouling techniques in crossflow microfiltration, *Filtration and Separation*, 23(6): 347.
9. Murkes, J. and Carlsson, C. G., 1988, *Crossflow Filtration* (Wiley, Chichester).
10. Rushton, A. and Zhang, G. S., 1988, Rotary microporous filtration, *Desalination*, 70: 379.
11. Dave, N. and Gray, N. B., 1989, Modelling of annular swirled flow lances with helical inserts, *Trans Inst Mining & Met*, 98: C178.
12. Happel, J. and Brenner, H., 1965, *Low Reynolds number hydrodynamics* (Prentice-Hall, Englewood Cliffs, N. J.).

ACKNOWLEDGEMENTS

The authors of this paper wish to record their gratitude for a Science and Engineering Research Council grant to support a project of which this work formed a part.

ADDRESS

Correspondence concerning this paper should be addressed to Dr R. G. Holdich, Department of Chemical Engineering, University of Technology, Loughborough, Leicestershire, LE11 3TU.

The manuscript was received 27 March 1992 and accepted for publication after revision 14 July 1992.